



Determining Thermal Capacitance for Protected Area Network Design in Palau

NOAA Technical Memorandum CRCP 12



CITATION:

Skirving, W.J., S.F. Heron, C.R. Steinberg, C. McLean, B.A.A. Parker, C.M. Eakin, M.L. Heron, A.E. Strong, and L.F. Arzayus. 2010. *Determining Thermal Capacitance for Protected Area Network Design in Palau*. Silver Spring, MD: NOAA Coral Reef Conservation Program. NOAA Technical Memorandum CRCP 12. 317 pp.

AUTHOR AFFILIATIONS:

¹NOAA/NESDIS Coral Reef Watch, Silver Spring, MD, USA

²Australian Institute of Marine Science, Townsville, QLD, Australia

³Australian Coastal Ocean Radar Network, James Cook University, QLD, Australia

⁴I.M. Systems Group, Rockville, MD, USA

⁵NOAA/OAR Office of Ocean Exploration and Research, Silver Spring, MD, USA

FOR MORE INFORMATION:

For more information about this report or to request a copy, please contact NOAA's Coral Reef Conservation Program at 301-713-3155 or write to: NOAA Coral Reef Conservation Program; NOAA/NOS/OCRM; 1305 East West Highway; Silver Spring, MD 20910 or visit www.coralreef.noaa.gov.

DISCLAIMER:

This publication does not constitute an endorsement of any commercial product or intend to be an opinion beyond scientific or other results obtained by the National Oceanic and Atmospheric Administration (NOAA). No reference shall be made to NOAA, or this publication furnished by NOAA, in any advertising or sales promotion which would indicate or imply that NOAA recommends or endorses a proprietary product mentioned herein, or which has as its purpose an interest to cause directly or indirectly the advertised product to be used or purchased because of this publication.

Cover photograph courtesy of Dr. William J. Skirving.

Determining Thermal Capacitance for Protected Area Network Design in Palau

Authors:

William J. Skirving¹

Scott F. Heron¹

Craig R. Steinberg²

Cary McLean²

Britt-Anne A. Parker^{1,4}

C. Mark Eakin¹

Mal L. Heron³

Alan E. Strong¹

Luis F. Arzayus⁵

National Oceanic and Atmospheric Administration

In cooperation with the Australian Institute of Marine Science and
The Nature Conservancy.

January 2010

NOAA Technical Memorandum CRCP 12

United States Department of
Commerce

National Oceanic and
Atmospheric Administration

National Ocean Service

Gary Locke
Secretary

Dr. Jane Lubchenco
Administrator

David Kennedy
Acting Assistant Administrator

Acknowledgements

NOAA would like to thank its partners in this project, the Australian Institute of Marine Science (AIMS) and The Nature Conservancy (TNC), without whom this project would not have been possible.

There are many individuals who contributed to the success of this project. The field work had many helpers, so thanks go to: Debbie, Kyle and Luke McLean; the team at the Palau International Coral Reef Center (PICRC), in particular Steven Victor; Pat Colin and his team at the Coral Reef Research Foundation (CRRF); David Hinchley, Andrew Smith and the rest of the Palau TNC team; and the many various departments of the Palau Federal and Koror State Governments, with special thanks to Andrew Bauman. Thanks also to Bob Richmond from the University of Guam for loaning us a couple of current meters. Thanks to the NOAA National Ocean Service (NOS) team who worked very closely with us to produce the satellite derived bathymetry and thanks to Joe Metzger from Naval Research Laboratory (NRL) for helping with the low-frequency currents. Special thanks to Jessica Pejsa for her assistance in the administration of this project. Lastly, while NOAA and AIMS were the major sources of funds for this project, this work could not have been undertaken without a significant injection of funds from the Michael and Andrea Banks Nature Fund via The Nature Conservancy.

Determining Thermal Capacitance for Protected Area Network Design in Palau

NOAA Technical Memorandum CRCP 12

Table of Contents

Acknowledgements.....	iv
Table of Contents.....	v
Table of Figures.....	vi
Table of Tables.....	vii
Executive Summary.....	viii
Introduction.....	1
Causes of Mass Coral Bleaching In Palau.....	2
Mass Coral Bleaching.....	2
Bleaching Weather.....	2
Physical Processes and Spatial Variability of SST During a Bleaching Event.....	3
Effects of Hydrodynamic Mixing.....	3
The Physics of Ocean Heat Content and Distribution.....	4
Insolation.....	4
Absorption.....	4
Dynamic Mixing by Currents.....	5
Mixing due to Wind Stress.....	5
Mixing due to Wave Breaking.....	6
Stratification of Ocean Water.....	7
Hydrodynamic Modeling for a Bleaching Event.....	8
Constructing a Model for Palau.....	9
Hydrodynamic Data Collection.....	9
The Hydrodynamic Model.....	10
Bathymetry.....	11
Low-Frequency Circulation.....	12
Tidal Elevation.....	15
Other Defined Parameters.....	15
Output.....	15
Vertical Temperature Profile.....	21
Modeling Heat-stress Patterns During a Bleaching Event.....	23
Potential Use as a Planning Tool.....	24
Recommendations.....	26
Bibliography.....	28
Appendix 1: Palau Oceanographic Data Array Report.....	31
Appendix 2: Seasonal Variations of the Ocean Surface Circulation in the Vicinity of Palau.....	283
Appendix 3: Satellite Bathymetry Use in Numerical Models of Ocean Thermal Stress.....	298

Table of Figures

Figure 1	Accumulated thermal coral stress for Palau based on the Degree Heating Week (DHW) product for the period 1985 to 2004.	1
Figure 2	Average SST for 16-18th February for the Southern GBR region.	3
Figure 3	Horizontal surge velocity versus depth for a typical wind wave.	7
Figure 4	Landsat image of Palau showing the Lagoon box, Malakal Harbour box, and the Rock Islands box.	10
Figure 5	(a) Final bathymetry dataset for model domain. (b) Bathymetry data to a depth of 50 m, showing lagoon features.	12
Figure 6	(a) Map of the western equatorial Pacific Ocean. (b) Schematic representation of the surface features reported in literature.	13
Figure 7	Surface features described by Heron <i>et al.</i> (2006).	14
Figure 8	Schematic diagram of the seasonal variation in the currents around Palau.	14
Figure 9	Time-series of sea-level measurements in Malakal Harbour used in the hydrodynamic model.	16
Figure 10	Scatter-plot of Malakal Tide Gauge sea-level values and model output versus measured values.	17
Figure 11	Surface velocity vectors at model time 0.5 days.	18
Figure 12	Sea-surface elevation, referenced to the long-term mean sea-level, at model time 0.5 days.	19
Figure 13	Scaled current speed and direction at the location of instrument A8 (Lighthouse Channel).	20
Figure 14	Scaled current speed and direction at the location of instrument A13 (Toachel Mid).	21
Figure 15	Scaled model output against measured current speed for location A8 (Lighthouse Channel).	22
Figure 16	Plot of the heat balance parameters: incoming total short wave radiation, longwave outgoing, sensible heat flux, and Latent Heat Flux.	22
Figure 17	Development of the surface heat layer over a 14-day period.	23
Figure 18	Vertical temperature profile on the 14th day of modeling.	24
Figure 19	Final output from the Palau model of thermal capacitance, expressed as surface cooling degree-weeks.	25

Table of Tables

Table 1	Correlations between the elevations at the Malakal Harbour Tide Gauge grid point and the eastern boundary grid point for varying time lags.	17
---------	--	----

Executive Summary

During the latter half of 1998, Palau experienced unprecedented bleaching that resulted in significant mortality and the loss of significant proportions of one of the few remaining pristine coral reefs in the world. Prior to 1998 and since 1998, little to no coral bleaching has been observed. These observations were consistent with data from the National Oceanic and Atmospheric Administration (NOAA) Coral Reef Watch (CRW) satellite Degree Heating Week (DHW) product. The DHW satellite product clearly shows that the 1998 accumulated thermal stress easily surpassed the critical DHW equals 4 threshold for coral bleaching and is the only year to have done so since 1985. This is consistent with field observations of bleaching.

The Nature Conservancy (TNC) and the Palau Government joined forces to design and implement a protected areas network (PAN) for Palau's coral reef ecosystem. A PAN is best described as a series of marine protected areas (MPAs). They recognized bleaching as being potentially one of the major future threats to the Palau coral reef ecosystem. However, with only one poorly documented bleaching event on record, it is difficult to gain enough experience to be able to build resilience to these events into the PAN.

In parallel with this effort to design a PAN for Palau, NOAA and the Australian Institute of Marine Science (AIMS) were collaborating on the use of hydrodynamic models to predict heat stress during a bleaching event. In 2003, it was decided to combine these efforts and for NOAA and AIMS to produce a heat stress model for Palau for use in the PAN planning as an attempt to identify factors that might confer resilience to climate change.

For the model to be constructed, NOAA and AIMS needed:

- 1) The bathymetry of Palauan waters: Due to a lack of available conventional data, NOAA derived the bathymetry from a combination of Landsat data and *in situ* bathymetry transects taken with a depth sounder from a small boat. This produced a chart with 250 meter horizontal resolution and precision of ± 1 meter vertically.
- 2) Low-frequency currents: A combination of the Navy Research Laboratory's Layered Ocean Model and NOAA's Ocean Surface Current Analyses – Real time product were used to determine the seasonal low-frequency currents around Palau.
- 3) High-frequency currents: Tide gauge data collected in and around Palau was used to prescribe the sea surface elevation changes that induce tidal currents. Field data collected over a period of 5 months were used to calibrate and validate the currents.
- 4) Vertical temperature profile: This was derived by modeling a column of water with homogeneous temperature and applying a diurnal cycle of solar radiation for a period of two weeks.
- 5) Validation data: These included an intensive field deployment of current meters, temperature loggers, salinity loggers and tide gauges. This deployment has been documented in the Palau Oceanographic Array Data Report (Appendix 1).

Using the bathymetry, low-frequency currents and sea surface elevation as boundary conditions, a high resolution (250 m) two-dimensional hydrodynamic model of the Palau region was developed using the Princeton Ocean Model. This provided currents for the development of a heat stress map. The field validation data were used to assess the accuracy of the model and showed that the model performed remarkably well, given the extremely large range of currents driven by tides within Palau.

The Simpson and Hunter (1974) parameterization was used to distinguish between stratified and well-mixed water by combining currents with bathymetric data. This information was then used in conjunction

with the vertical temperature profile to determine the reduction in surface temperature due to mixing and thus the likely spatial distribution of sea surface temperature during a bleaching event. In fact, this model is best interpreted as a measure of thermal capacitance. The warmer regions in the model represent areas with a low thermal capacitance meaning that a given amount of solar energy heats these regions faster than the cooler regions in the model, which have a high thermal capacitance and resist temperature change.

The result of this is that the cooler regions in this model represent regions of mild temperatures (*i.e.*, normally experiencing less thermal stress) whereas the warmer regions represent those areas in the model that will experience more extreme temperatures (*i.e.*, greater thermal stress). The final product was an accumulation of sea surface temperature reductions over a tidal cycle (one month). Those regions shown as cool were most likely to experience greatest cooling at the surface due to mixing and hence represent the regions with high thermal capacitance. This provides the organisms that live there with a mild climate, characterized by relatively small temperature ranges. In contrast, the warm regions portray those locations that likely experience little to no mixing and hence represent low thermal capacitance. The organisms that live in these regions experience an extreme climate, characterized by relatively large temperature ranges.

A chart of this type can be extremely useful when designing a PAN. In general, most PANs are currently designed so as to provide protection to “representative bioregions,” meaning that, as much as possible, every type of bioregion within the ecosystem of interest should be equally represented within the PAN. However, it is important to recognize that an ecosystem is not only made up of different species but also of organisms within each species that can have unique physiological characteristics. When designing a PAN, it is relatively straight forward to map bioregions on the basis of species composition; however the genetic (phenotypic) variability within each species is not represented by these techniques. With respect to a changing climate, the phenotypes that result in varied physiological characteristics are likely to correspond to different thermal capacitances throughout the region. While we may not know what these characteristics are, the relevant characteristics for resilience against climate change are more likely to be better protected if representative samples of each thermal region within the thermal capacitance map are protected.

The innovative techniques and methodologies presented in this report represent the beginning of a new era in MPA/PAN design. To aid in the ongoing evolution of this work, a list of recommendations to continue the development of these techniques is provided at the end of the report.

Introduction

During the latter half of 1998, Palau experienced unprecedented bleaching that resulted in significant mortality and the loss of significant proportions of one of the few remaining pristine coral reefs in the world (Wilkinson 2000). Prior to 1998 and since 1998, little to no coral bleaching has been observed. Figure 1 is a plot of accumulated thermal stress for Palau, as measured by the National Oceanic and Atmospheric Administration (NOAA) Coral Reef Watch's Degree Heating Week (DHW) satellite product. These data were retrospectively derived using the AVHRR Pathfinder data set (Kilpatrick *et al.* 2001), and using the methodology described in Eakin *et al.* (2009). A DHW value of 4 or more indicates significant bleaching (Liu *et al.* 2003 and Skirving *et al.* 2006). Note the DHW equals 4 threshold is indicated by a line in Figure 1. The accumulated thermal stress in 1998 easily surpassed that mark and is the only year to have done so since 1985. Note also that the heat stress for 1998 lies within the latter half of the year, as do most of the other small peaks.

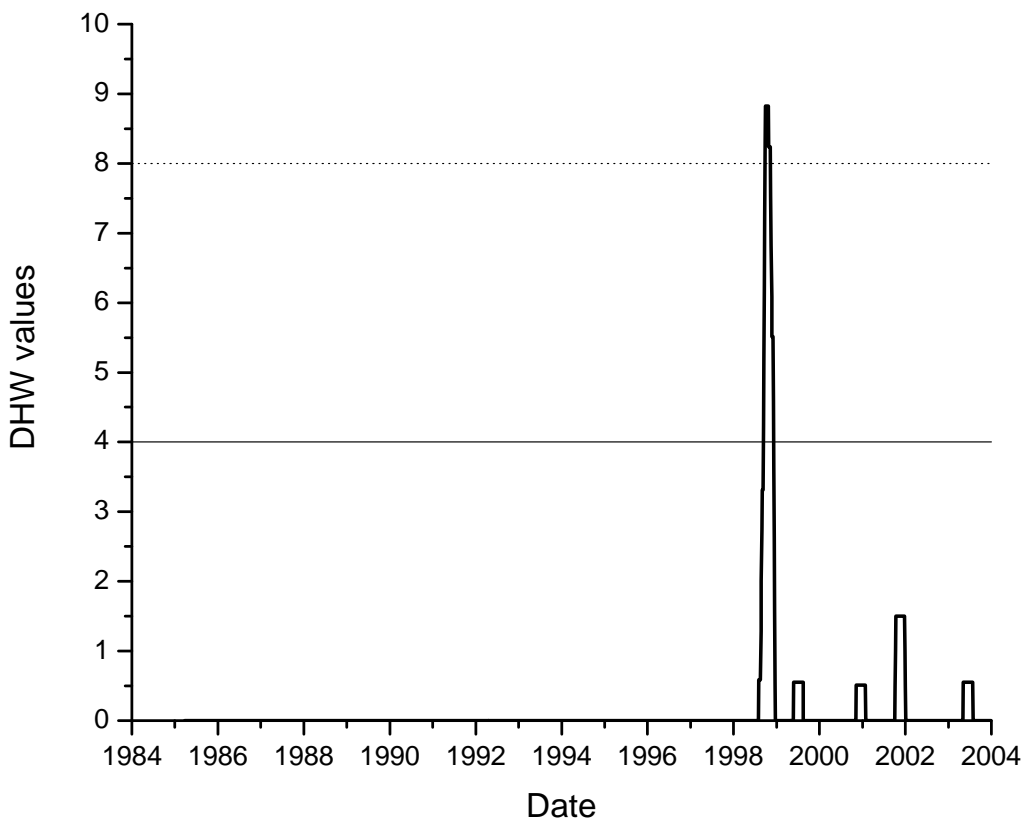


Figure 1 Accumulated thermal coral stress for Palau based on the Degree Heating Week (DHW) product derived from Pathfinder data for the period 1985 to 2004.

The Nature Conservancy (TNC) and the Palau Government joined forces to design and implement a protected areas network (PAN) for Palau's coral reef ecosystem. Punctuated by the 1998 event, they recognized bleaching as one of the major future threats to the Palau coral reef ecosystem. With only one poorly documented bleaching event to go by, it is difficult to gain enough information to build resilience to bleaching events into the PAN.

In parallel with the effort to design a PAN in Palau, NOAA and the Australian Institute of Marine Science (AIMS) were collaborating on the use of hydrodynamic models to predict heat stress during a bleaching event. In 2003, it was decided to combine these efforts and for NOAA and AIMS to produce a heat stress model for Palau for use in the PAN planning, in an attempt to include resilience to climate change.

This report is adapted from the final report for the NOAA/AIMS/TNC collaboration on the development of a model that describes spatial patterns of heat stress for Palau. It includes a description of the data collection, a description of the hydrodynamic model, and how this model was used to derive patterns of heat stress for Palau.

Causes of Mass Coral Bleaching in Palau

Mass Coral Bleaching

Coral bleaching is a generalized stress response by zooxanthellae and is not necessarily related to any one stressor (Glynn 1993). However, mass coral bleaching events are well correlated with thermal stress (*e.g.*, Dennis and Wicklund 1993; Drollet *et al.* 1994; Winter *et al.* 1998; Hoegh-Guldberg 1999; McField 1999; and Berkelmans 2002). High temperatures damage the photosynthetic pathway, which leads to a breakdown of the photosynthetic process (Jones *et al.* 1998). After the thermal threshold is surpassed, the normally robust photosystem can be overwhelmed by significant amounts of light, eventually causing the formation of reactive oxygen molecules that destabilize the relationship between corals and their algal symbionts (Hoegh-Guldberg 1999; Downs *et al.* 2002). Therefore, although light is an important factor in the coral bleaching story, it is not normally a stressor until water temperatures have exceeded certain limits (Berkelmans 2002).

Bleaching Weather

Skirving and Guinotte (2001) investigated the origin of the hot water that caused the Great Barrier Reef (GBR) to bleach during 1998. They noted that a combination of low wind speed and neap tides was correlated with generally high sea surface temperatures (SST). They also noted that, during these periods of higher sea surface temperature, there were correlations between shallow bathymetry and locally-cooler SST, and between deep water and locally-warmer SST.

These correlations led them to conclude that the hot water was a result of *in situ* heating from solar radiation, and that the effect of this heating was amplified by a lack of hydrodynamic mixing. The idea that SST anomalies leading to coral bleaching are mostly a result of *in situ* heating has since been supported by many field observations (Wilkinson 1998, 2000; Berkelmans *et al.* 2004; Bird *et al.* 2004; Skirving *et al.* 2004).

Very few mass coral bleaching events in the world are a result of advected hot water (Skirving 2004). Little to no wind, clear sunny skies and weak ocean currents characterize these events. Most observed bleaching events incorporate at least a few weeks of these conditions. Climate is likely to modulate the frequency of these weather events, but more research is necessary to investigate direct links between climate states (*e.g.*, ENSO), *in situ* heating, and coral bleaching.

Physical Processes and Spatial Variability of SST during a Bleaching Event

Effects of Hydrodynamic Mixing

During a bleaching event, spatial patterns of SST are quite complex and have a scale of hundreds to tens-of-thousands of meters. Figure 2, adapted from Skirving and Guinotte (2001), is an SST image of the southern Great Barrier Reef during the 1998 bleaching event. It clearly shows the high complexity that existed in the spatial patterns of SST during this event.

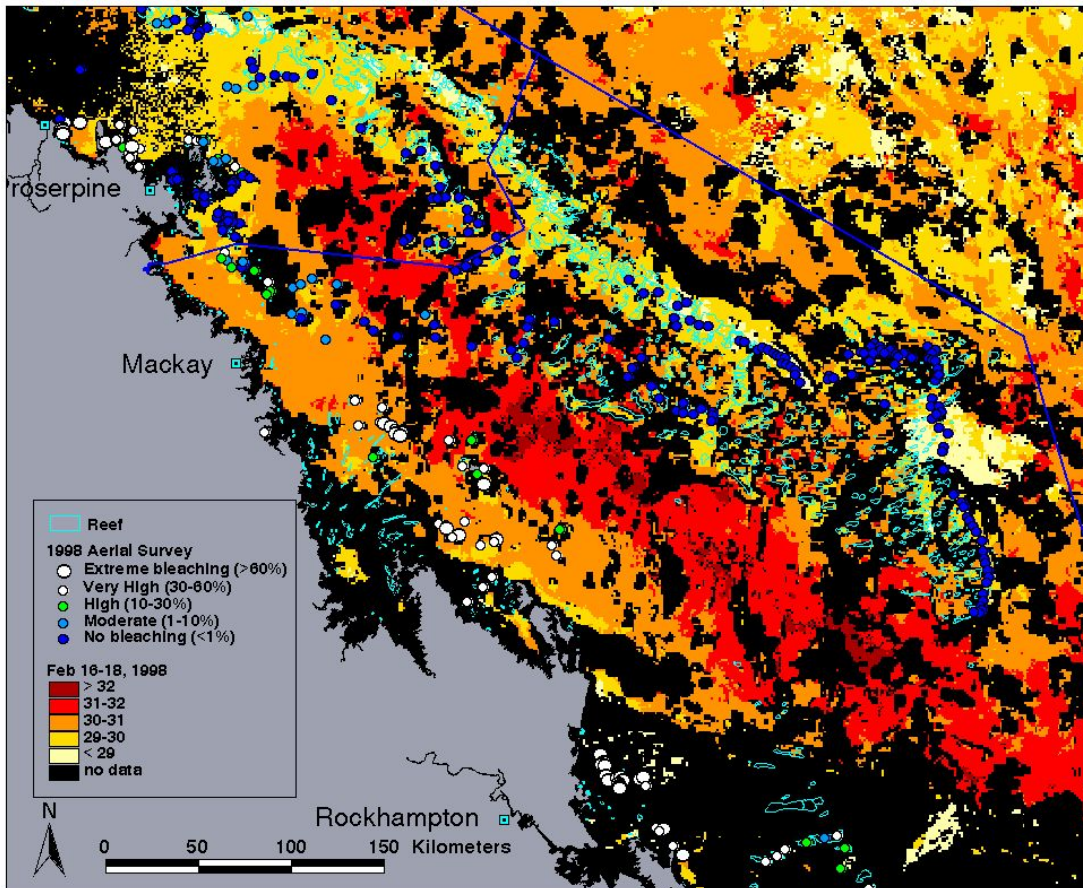


Figure 2 Average SST for 16-18th February for the Southern GBR region. Reefs and bleaching are also depicted (adapted from Skirving and Guinotte 2001).

Given the existence of bright sunny skies (*i.e.*, no cloud) and given that at reef scales, solar radiation is homogeneous in space, hydrodynamic mixing is the most likely mechanism that could create such a complex SST pattern (Skirving and Guinotte 2001; Skirving 2004; Skirving *et al.* 2004). Solar energy is mainly absorbed within the top few meters of the surface of the sea. As warmer water is more buoyant than cooler water of the same salinity, during a bleaching event the warmer water will remain at the top of the water column unless there is a mechanical process to mix it down.

There are four mechanisms that can vertically mix the water column: wind, low-frequency currents (*e.g.*, East Australian current, Gulf Stream, *etc.*), high-frequency currents (*e.g.*, tides) and swell waves. Given that winds are typically low during a bleaching event, swell waves and currents are the only mechanisms

available for vertical mixing. Since the water at the surface is warmer than the water below it, any vertical mixing will induce cooling at the surface and warming at depth. The deeper the mixing, the cooler the surface will become. Therefore, during a bleaching event, patterns of SST are related to a combination of the depth of water and strength of the currents (Skirving *et al.* 2004; Heron and Skirving 2004). Waves can also mix the water column; however, during most bleaching events there is little to no wind to create wind-waves for mixing. Waves can be a factor where reefs are exposed to swell generated well outside the region.

The Physics of Ocean Heat Content and Distribution

During daylight hours there is a net flow of heat into the ocean. The insolation flux is in the form of electromagnetic radiation that is absorbed in the upper layer of the ocean. The resulting warm layer may be mixed down through the water column by dynamic processes driven by currents and waves. The outflow of heat through the surface dominates at night. It is driven by energy loss due to latent heat and heat loss via conduction as a result of the temperature difference between the sea and the air. This temperature difference will also drive heat loss via radiation, and during a bleaching event with low winds, this will often be the dominant component of the night-time heat loss. The combination of these fluxes gives a diurnal variation that sets the climatological mean for the sea surface temperature. When the fluxes change, temperature can vary significantly from the climatological mean and produce conditions stressful to corals. Specific physical processes affecting the flux and distribution of heat in the ocean include the characteristics of the incident solar radiation, the absorption in the water column, and mixing processes.

Insolation

Solar radiation is the primary source of ocean heat content. The solar radiation spectrum at the bottom of the atmosphere peaks in the visible range of wavelengths and has absorption bands due to the composition of the atmosphere. The main control on the energy arriving at the sea surface is exerted by the aerosol and water vapor content of the atmosphere. As such, the type of air mass above a coral reef will have considerable influence over the amount of surface solar radiation. A clear sky with relatively low humidity and low aerosol content, such as can occur over the Red Sea and parts of the Great Barrier Reef, will provide maximum insolation. This is reflected in the extreme SSTs often recorded in these regions. Conversely, regions that experience dust storms, high humidity, and cloudy conditions will experience lower insolation with the same sun angles, resulting in lower SSTs and SST variability.

Absorption

The absorptive properties of seawater define the depth-distribution of solar energy that is transferred directly to the water. A good model for the absorption of solar energy in the upper layer of the ocean is the exponential

$$I = I_0 \exp(-\alpha z) \quad (1)$$

where I_0 is the radiation intensity incident at the surface, α is an absorption coefficient equal to the inverse of the e-folding depth, and z is the depth. Equation (1) works for a single absorbing constituent in the water, and for an absorption coefficient which has no variation with depth. This is often not the case. For example, if there is buoyant biomass then there will be an enhanced absorption layer near the surface; also, turbidity due to resuspension of benthic sediments is usually greater at the bottom of the water column, also enhancing absorption. Under these conditions the absorption has to be calculated by integration across layers of water. At the bottom of the i^{th} thin layer of thickness Δz the intensity is I_i where

$$I_i = I_{i-1} (1 - \alpha_i (z_i) \Delta z) \quad (2)$$

The intensity of solar radiation at depth z_k is

$$I(z_k) = I_0 \prod_{i=1}^k (1 - \alpha_i (z_i) \Delta z) \quad (3)$$

Typically, $\alpha \approx 0.5$ and solar insolation is effective in heating the upper two meters of the water column. If there is no vertical mixing in the water column, then corals within the first two meters from the surface may be susceptible to heat stress and bleaching.

Dynamic Mixing by Currents

Vertical mixing of the water column alters the distribution of heat. Ocean currents have a tendency to induce mixing under most conditions. In shallow water where coral reefs are most-often located, we can expect a boundary layer shear flow due to friction at the bottom of the water column. This is the basic response to ocean currents onto which we can add the effects of surface wind stress, stratification and wave-induced mixing. The only laminar flow is found in the viscous layer at the bottom, and eddy diffusion prevails throughout the water column.

Mixing due to currents is driven by the vertical shear in the horizontal velocity of the water in the column and is carried out by eddies in the vertical plane. A commonly assumed model for the vertical eddy viscosity is the linear model given by

$$N_z = k u_* (H - z) \quad (4)$$

which leads to the logarithmic bottom-friction layer

$$u(z) = \frac{u_*}{k} \ln \left(\frac{H - z}{z_0} \right) \quad (5)$$

where z is the distance from the surface (positive downwards), H is the water depth, z_0 is the thickness of the viscous layer, u_* is the friction velocity and k is the von Karman constant.

Mixing of the vertical column due to bottom friction is strongest near the bottom where velocity shears are greatest. However with strong currents and shallow water this can impact the mixing of the upper solar heated layer. One important thing about this simple theory of mixing in the logarithmic boundary layer is that it gives us a reference frame for thinking about turbulent mixing in the water column when velocity shears are caused by other phenomena.

Mixing due to Wind Stress

Vertical mixing of ocean waters can also be induced by winds. Wind at the ocean surface produces momentum transfer to the water, and hence a wind stress velocity at the surface. The kinetic energy at the surface is transferred down through the column by eddy diffusion. If we assume that the vertical eddy viscosity is controlled by the stress at the surface and grows linearly with depth then we have a mathematical form similar to the bottom friction layer with

$$N'_z = k u'_* z \quad (6)$$

where z is the distance from the water surface (positive downwards), and u'_* is the stress velocity at the surface.

The actual eddy viscosity in the water column is a combination of N'_z and N_z ; the velocity profile is a combination of the bottom boundary layer and the surface boundary layer. This leads to complications in numerical modeling of the currents and various schemes have been suggested for combining the eddy viscosity terms. It is clear that the velocity shears induced by wind at the surface of the water have a significant role in the vertical mixing of the surface solar heated layer.

Mixing due to Wave Breaking

Ocean waters are also vertically mixed by breaking waves. In the open ocean, most of the wave energy is conserved and not lost to mixing processes. It is only when the waves become non-linear that they lose energy to turbulence. It is the process of wave breaking that dominates the transfer of wave energy to mixing. At reef fronts the transfer is almost complete with only a remnant of wave energy being reflected back to the ocean, some of it transferring to a forward bore in the breaking wave, and a significant fraction going into turbulence at the breaker location. For a propagating surface gravity wave, most of the energy is in the upper part of the water column. This is illustrated in Figure 3 where we show the depth profile of the horizontal surge velocity for a wave with 1 m amplitude (trough to crest) and 6 s period. This is a typical oceanic wind wave and the graph shows how the velocity decreases rapidly with depth. If there is any non-linearity or breaking then the associated energy becomes available for mixing.

The kinetic energy density for a wave with amplitude a , angular frequency ω and water depth d is given by

$$KE(z) = \frac{1}{2} \rho (u^2 + w^2) \quad (7)$$

where u and w are the horizontal and vertical depth-dependent particle velocities, respectively, averaged over one cycle:

$$u^2 = \frac{\pi a^2 g^2 k^2 \cosh^2(k(d+z))}{\omega^2 \cosh^2(kd)} \quad (8)$$

$$w^2 = \frac{\pi a^2 g^2 k^2 \sinh^2(k(d+z))}{\omega^2 \cosh^2(kd)} \quad (9)$$

This wave energy is generally not available for mixing on shelf waters. However, when a wave encounters a reef front it loses most of its energy and provides a dominant mixing effect for the solar heated layer near the surface. This effect is so dominant that it is difficult to think there would be coral bleaching on the windward side of a reef except in flat-calm conditions. Waves breaking on the reef front also send pulses of water forward across the reef flat. This pulsing bore is also well-mixed and we would expect mitigation of bleaching on the parts of the reef flat that are flushed with this water. The physical processes of wave breaking on the reef front and the subsequent pulsing of water across the reef flat have a strong mitigating effect on coral bleaching.

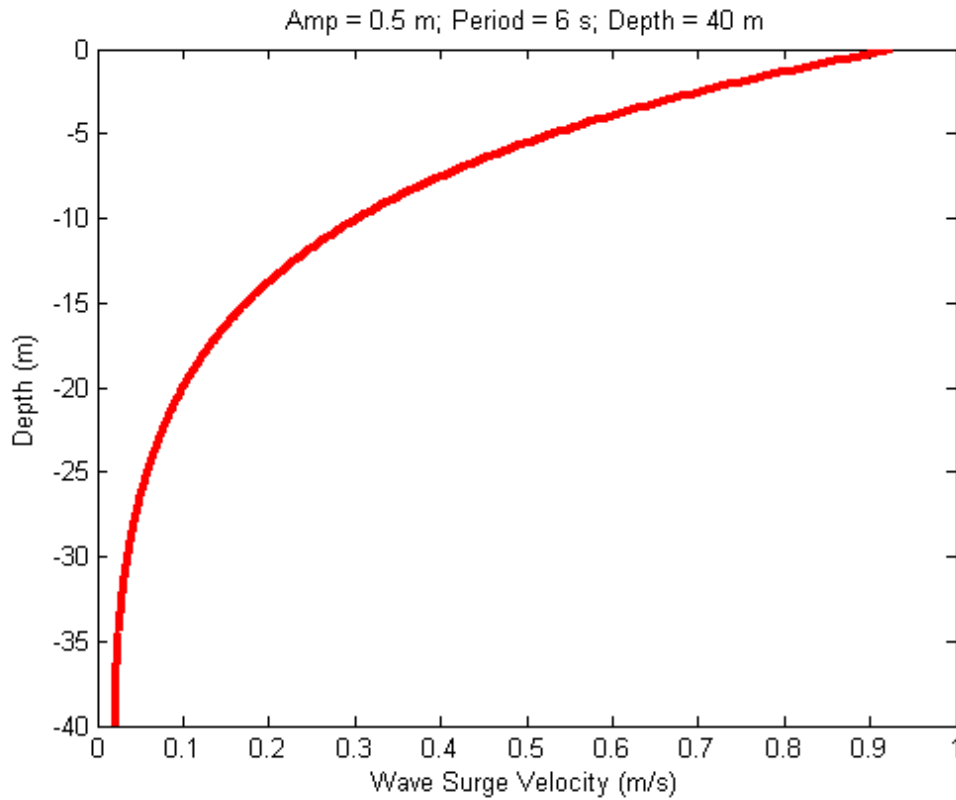


Figure 3 Horizontal surge velocity versus depth for a typical wind wave. Most of the wave energy is in the top few meters. The vertical surge velocity profile follows the same curve near the surface but departs and goes to zero at the bottom of the water column, set to 40 m here.

Stratification of Ocean Water

Horizontal stratification imposes an impediment to mixing, and therefore heat transfer. This is due to the potential energy of the stratification. The Richardson number compares the energy of stratification and the turbulent kinetic energy and provides us with an index to measure the severity of the stratification.

Under high Richardson number conditions there is likely to be a strong vertical shear at the boundary between the stratified layers and the turbulent kinetic energy works to erode the stratified layer. Following the approach of Simpson and Hunter (1974), de Silva Samarasinghe (1989), and others, we consider the rate of loss of potential energy to be equal to some small fraction per second, σ , of the turbulent kinetic energy as

$$\frac{\partial}{\partial t}(PE) = -\sigma(KE) \quad (10)$$

which can be written as

$$\frac{\partial}{\partial t} \left\{ \int_0^h gz(\rho - \bar{\rho}) dz \right\} + \sigma \bar{\rho} \int_0^h N_z \left(\frac{\partial u}{\partial z} \right)^2 dz = 0 \quad (11)$$

per unit area of the water column, where h is the water depth, $\bar{\rho}$ is the mean water density in the column of depth h , and N_z is the vertical eddy viscosity. Simpson and Hunter (1974) found $\sigma = 0.0037 \text{ s}^{-1}$ in the Irish Sea; Hearn (1985) derived a similar value.

Stratification is an important phenomenon for coral bleaching. When the sun heats the surface layer, the density of that layer is reduced and there is an inherent stability caused by the density stratification, which is conducive to further heating of this layer. Current shears are likely to be enhanced at the boundary between stratified layers and equations (10) and (11) become important in estimating the impact of the solar heating. If there is wind stress driving currents in the warm surface layer then there is likely to be an enhanced mixing at the boundary of the stratification. Thus, while the formation of stratification by solar heating of the upper layer is conducive to shallow-water coral bleaching, it can also set up strong current shear zones which can assist mixing. The effects of solar heating and turbulent mixing are finely balanced here.

Another form of stratification is the thin surface layer that is evaporatively cooled by water vapor flux from the ocean to the atmosphere. This is a thin layer of the order of millimeters, with a regeneration time constant of several seconds if it is destroyed, for example by a micro-breaker. This layer is unstable in the water column and promotes mixing. When we put this micro-layer mixing in the context of solar insolation on the order of a meter depth below the surface it is quickly lost in the scales of energy transfer and penetration depth. A more significant effect of the “skin layer” is that it is this layer that provides the infrared radiation used by satellite radiometers to measure the surface temperature. The skin layer reduces the brightness temperature by up to about half a degree (perhaps more in tropical waters). This is not a random error, but is a variable offset in the measured temperature that depends on the nature of the skin layer. The skin layer has little impact on coral bleaching because it is so thin that it does not contain much heat energy.

Hydrodynamic Modeling for a Bleaching Event

As each of the physical processes discussed above influences the transfer of heat into and within the water column, they can thus affect the potential for coral bleaching to occur. As mentioned previously, winds are effectively absent during a mass bleaching event, which leaves swell waves and currents as the only mechanisms capable of altering the spatial patterns of SST. Swell waves are very effective mixers where they exist and can mix the water when they impinge on a reef. However, they are not capable of cooling an entire reef and will not be available for every reef since not all reefs are exposed to swell waves and not all bleaching events have swell.

This leaves currents as the dominant mechanism for altering spatial patterns of SST. The vertical temperature profile is determined by heating from above via incoming solar radiation and cooling from below via upwelling, breaking internal waves, and cold-water intrusions. Currents then mix water vertically via bottom friction and 3D mixing behind reefs and islands. Advection can provide horizontal mixing associated with these currents in some situations. The spatial pattern of mixing interacts with the spatial pattern of vertical temperature profiles to create patterns of low to high SST during a bleaching event.

Constructing a Model for Palau

In order to produce a heat stress model for Palau for use in PAN planning, the following information was needed:

- a. Calibration and Validation Data for the model: Due to a dearth of hydrodynamic data for the Palau region, almost all data needed to be acquired within this project.
- b. The Bathymetry of Palauan waters: Due to a lack of hydrographic data, NOAA derived the bathymetry from a combination of Landsat data and bathymetry transects taken with a depth sounder from a small boat. This produced a chart with 250 meter horizontal resolution and a root mean square (rms) precision of 1 meter vertically.
- c. Low-frequency currents: A combination of the Navy Research Laboratory's (NRL) Layered Ocean Model (NLOM) and NOAA's Ocean Surface Current Analyses – Real time (OSCAR) product were used to derive the seasonal low-frequency currents around Palau.
- d. High-frequency currents: Tide gauge data collected in and around Palau was used to prescribe the sea surface elevation changes that induce tidal currents. Field data collected over a period of 5 months were used to calibrate and validate the currents.
- e. Vertical temperature profile: This was derived by modeling a patch of water with a homogeneous temperature and applying a diurnal cycle of solar radiation for a period of two weeks.

Hydrodynamic Data Collection

An extensive study of oceanographic parameters in Palauan waters was undertaken during the period August 2003 – January 2004. The timing of the deployment was selected to coincide with the time of year during which bleaching events have been observed. Sixty-two instruments were deployed in and near the Palau lagoon to record currents, temperatures, sea-levels, salinities, and weather conditions. This number of instruments is unusually high for a region of this size; the largess of the deployment was fueled by a desire to maximize coverage and the fortuitous availability of instruments from AIMS, the University of Guam, the Coral Reef Research Foundation in Palau, and the Palau International Coral Reef Research Center. The deployment is the most-extensive *in situ* ocean study ever performed in Palau. The data have been made freely available and are described in the Palau Oceanographic Array Data Report (Appendix 1).

For the purpose of the broader project, *i.e.*, to study SST patterns leading to coral heat stress, the Palau lagoon was partitioned into three study areas; the Lagoon box, the Malakal Harbour box and the Rock Islands box. The extent of the Lagoon box, illustrated by the orange line in Figure 4, was primarily described by environmental boundaries (island or reef barriers). This suggests that the majority of water movement in and out of the box is through the channels at the boundaries. Hydrodynamic models of the lagoon circulation can be constrained at the boundaries by the measured flow through these channels. Current-measuring instruments were placed in the major channels; sea-level monitors were deployed on reef flats across the box; salinity meters were placed in an east-west transect across the lagoon; and temperature sensors were positioned in vertical profiles throughout the box (for details, see Appendix 1).

The Malakal Harbour and Rock Islands boxes were defined as sub-regions of the Lagoon box, as shown in Figure 4. These regions, like the Lagoon box, are bounded by islands and/or reefs, again providing a sensible boundary for hydrodynamic models.

These regions are of particular interest for economic, environmental, and scientific purposes. Instruments were deployed at the boundaries of and within each of these boxes. As for the Lagoon box, instruments

were placed at boundary locations of major water movement. Data from these will aid in future modeling efforts for these regions. Detailed maps of individual instrument deployments are provided in Appendix 1.

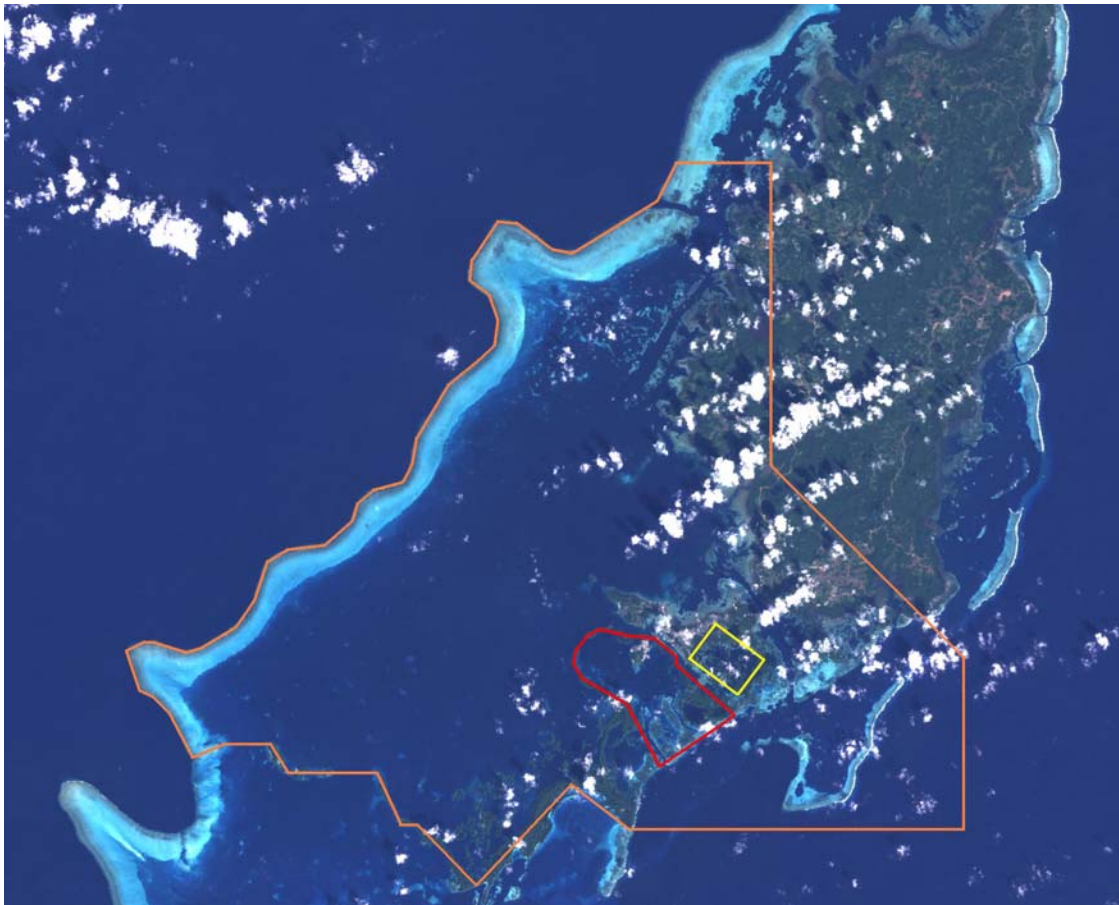


Figure 4 Landsat image of Palau showing the Lagoon box (orange), Malakal Harbour box (red) and the Rock Islands box (yellow).

All instruments were recovered with the exception of one temperature logger. Two of the instruments recorded data intermittently and one recorded no data due to power supply difficulties. Despite these setbacks, the dataset from the recovered instruments provided a broad description of Palauan waters and proved to be invaluable during the modeling phase of this project.

The Hydrodynamic Model

The hydrodynamic model was designed specifically to produce a map of accumulated heat stress for Palau. However, the output may also be useful for other applications; *e.g.*, particle tracking and connectivity modeling. The model code, commonly known as the Princeton Ocean Model (POM) (described in Blumberg and Mellor 1987), was employed for this study. POM is a terrain-following (σ -coordinate) model with a staggered horizontal finite-difference scheme (Arakawa C-grid). A rectilinear horizontal grid was selected for the Palau model.

For the heat-stress map, the desired output from the hydrodynamic model is a two-dimensional map of time-varying currents. To achieve this, a suite of initial- and boundary- conditions was required to drive the model calculations. As the region of interest for Palau consists entirely of islands surrounded by open ocean, the extremities of the model domain were “open” – *i.e.*, there were no land boundaries. Open boundaries require the definition of parameters to constrain the flow. Most numerical model applications have at least one or two “closed” boundaries; this simplifies the model setup and also aids in accurately constraining the model output. Four open boundaries presented a challenge to the modeling process and increased the importance of precision in defining the constraints. The steps involved in determining model bathymetry, investigating low-frequency circulation in the region, and modeling of tidal variations, are described in detail below.

Bathymetry

An accurate description of bathymetry is paramount for the success of a hydrodynamic model. The desired horizontal resolution for the model of Palau was around 250 m so as to resolve many of the topographic features of the region while maintaining sufficient computational efficiency.

Nautical charts of Palau, produced by the U.S. Defense Mapping Agency, were acquired to provide reference depth data. These charts were primarily based on World War II era Japanese surveys and a 1969 U.S. survey. By virtue of the navigational purpose of the charts, the values stated are lowest-tide values and err towards underestimation of depth. While these provide a general shape for the Palau lagoon, the data were neither accurate enough, nor of sufficient spatial consistency for the model. In addition, some feature details may have changed during the 35 years since the most recent survey.

Further bathymetric information for the Palau lagoon was derived from Landsat imagery. These data were produced by the Special Projects Office of NOAA’s National Ocean Service. The process used to derive estimated depth for Palau is described in Newhall and Rohmann (2003) following the technique of Stumpf *et al.* (2003). The accuracy of the estimated-depth algorithm is to within 1 m in the vertical and the depth limit is 20-25 m (R. Newhall, *pers. comm.*). The Landsat images were geo-rectified and mosaicked using the Universal Transverse Mercator (UTM) grid system. The image data were transformed to estimated depths by comparing the ratios of the satellite spectral channels. The bathymetry values were calibrated using *in situ* data and observations of benthic habitat types. Bathymetry data were collected within the Palau lagoon using a dual-frequency depth sounder, mounted on a 21-foot vessel, along transects totaling more than 300 nautical miles. The spatial resolution of Landsat imagery is 28.5 m; averaging across 9×9 pixels provided the desired resolution for input to the model (256.5 m). Land boundaries were checked and corrected manually especially in locations with narrow channels that were important to the water exchange, *e.g.*, the Rock Islands. A significant portion of the lagoon was too deep for the satellite algorithm and, as such, a deepwater dataset was required to augment the bathymetry.

Large-scale bathymetric data were acquired from several databases. Following the recommendation by Marks and Smith (2006), the data of Smith and Sandwell (1997) were selected for the region surrounding Palau. The depths are derived from satellite gravity data combined with ship measurements and have resolution of two-arc-minutes (approximately 3.7 km near the equator). The dataset was re-gridded to the UTM grid and interpolated in two-dimensions at the model gridpoints. The Smith and Sandwell (1997) interpolated data were then patched into the Landsat data where the Landsat depths were greater than 20 m. The combination of the two datasets introduced some erroneous values where the datasets were joined. These values were checked and corrected manually, as were discontinuities and spikes in the combined data.

Following these refinements, there were three areas for which the bathymetry appeared to vary greatly from the navigational charts; in the western section of Kossol Passage, to the north of Ulong Island and the region immediately north of Peliliu. The first and second of these appeared to be due to loss of vertical resolution during the interpolation of the deep-water data. Faulty values were removed from the data and, where available, *in situ* measurements and navigational chart readings were inserted. The remaining vacant gridpoints were assigned depths by kriging the existing data, a process involving statistical interpolation of the data. The error to the north of Peliliu was due to an incorrect land-mask in the Landsat data. The waters of this region are shallow and the bottom surface type is either white sand or near-black seagrass. Incorrect parameterization of the bottom type causes the depth algorithm to revert to land or deepwater, respectively, for these cases. The bathymetric data were corrected manually using *in situ* measurements and chart readings. The final dataset has horizontal resolution of 256.5 m and is the most-accurate, wide-scale bathymetry of Palau in existence. Figure 5 (a) and (b) illustrates the bathymetry.

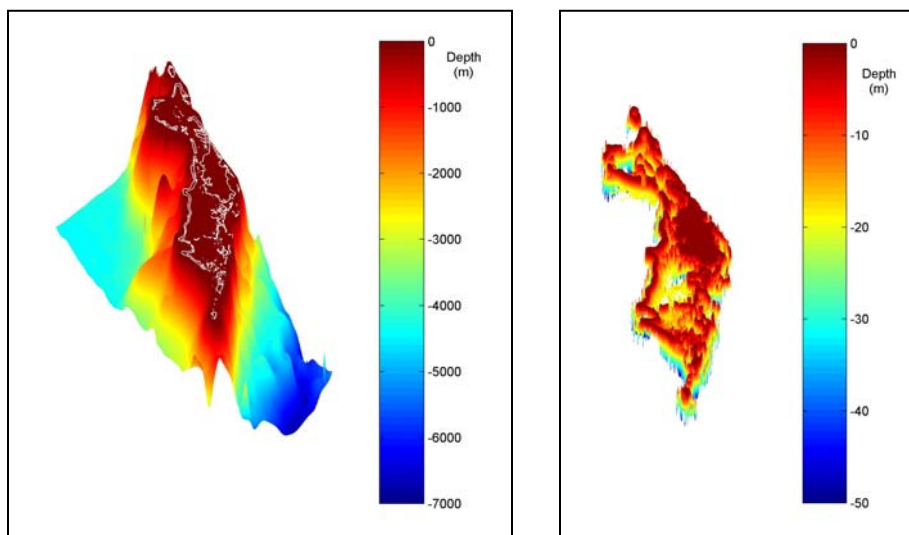


Figure 5 (a) Final bathymetry dataset for model domain. The white contour shows the land and barrier reef boundaries. (b) Bathymetry data to a depth of 50 m, showing lagoon features.

Low-Frequency Circulation

With bathymetry defined across the model domain, temporally-varying boundary conditions for the model were investigated. The first study determined low-frequency currents in the region, *i.e.*, currents varying on long time-scales. Examples of these types of currents around the world include the Kuroshio, the Gulf Stream and the East Australian Current. A literature search was undertaken for previous studies of the circulation in the immediate vicinity of Palau; no such studies were found. Due to this lack of prior information, it was necessary to include in this project a study to determine the existence of a seasonal variation in the surface currents in the western equatorial Pacific. The geographical area investigated is shown by the dotted line in Figure 6(a). A manuscript (Heron *et al.* 2006) discussing the results of this study is included in this document as Appendix 2. The results are summarized below; see Appendix 2 for further details and literature references.

Previous work in this region focused on the major currents displayed in Figure 6(b); the North Equatorial Current (NEC), the Mindanao Current (MC), the Kuroshio, the North Equatorial Counter-Current (NECC), and the Indonesian Through-Flow (ITF). Further studies investigated two major mesoscale

eddies in the region; the Mindanao Eddy (ME) and Halmahera Eddy (HE), also shown in Figure 6(b). These studies reported the high- and low-frequency variability of these features but none investigated annual patterns of the flow further to the east, near Palau.

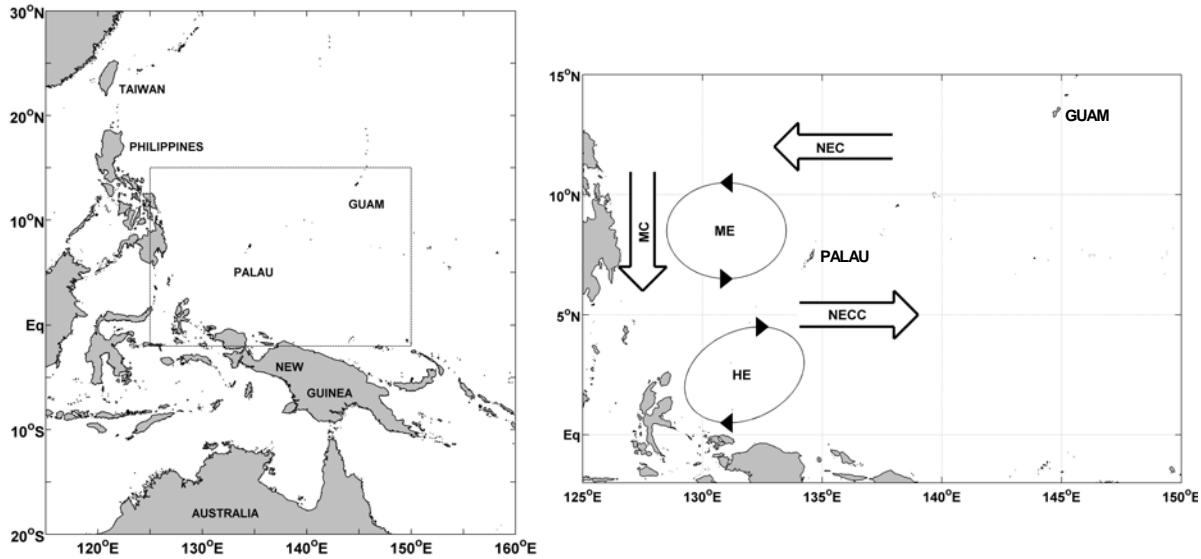


Figure 6 (a) Map of the western equatorial Pacific Ocean. The dotted line indicates the region considered in the study by Heron *et al.* (2006). (b) Schematic representation of the surface features previously reported in literature.

Data from the Ocean Surface Currents Analysis – Real-time (OSCAR) product, TRIangle Trans-Ocean buoy Network (TRITON), the Joint Archive for Shipboard Acoustic Doppler Current Profiler (JASADCP); and output from the Naval Research Laboratory Layered Ocean Model (NLOM) and were examined and compared. The JASADCP data were used to validate the NLOM output. Monthly climatologies of the surface currents from the OSCAR and NLOM datasets were examined for seasonal variations. The timing of the observed seasonality in the surface currents around Palau was consistent with the annual variation in the surface winds from the TRITON data. The existence and variability of documented surface features, previously mentioned, was verified and additional features were identified in the study region. These are shown in Figure 7 and were named the Palau Eddy (PE), Caroline Eddy (CE), the Micronesia Eddy (MiE), and the Papua New Guinea Eddies (PNGE) – a family of eddies along the north coast of Papua New Guinea. The seasonal variation of the NECC Tail, *i.e.*, the section east of 135°E, was also determined and discussed.

Low-frequency currents near Palau are driven by the major surface features; the seasonal variability of the currents follows that of the major features. North of Palau, the NEC varies only slightly in both magnitude and direction. To the south, the NECC Tail migrates seasonally and varies in magnitude; this significantly affects the fluid motion around Palau. The ME and HE are present throughout the year and vary seasonally in both extent and location. The PE exists from April to October and influences the flow to the east of Palau during this period.

Figure 8 is a schematic diagram of the annual variation in the surface currents surrounding Palau. Heron *et al.* (2006) note that the low-frequency currents are weak and disordered from July to September. This period is consistent with the timing of observations of coral bleaching events. The observed surface

currents, as described by Heron *et al.* (2006) were employed as the velocity boundary conditions for the hydrodynamic model.

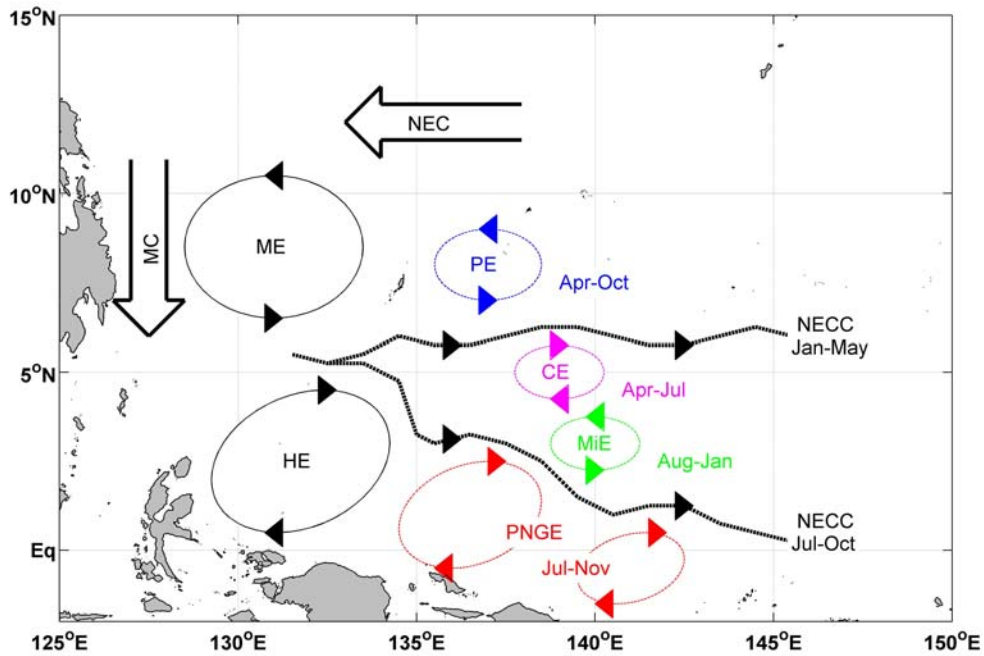


Figure 7 Surface features described by Heron *et al.* (2006). Newly described features may be identified by comparison with Figure 6(b).

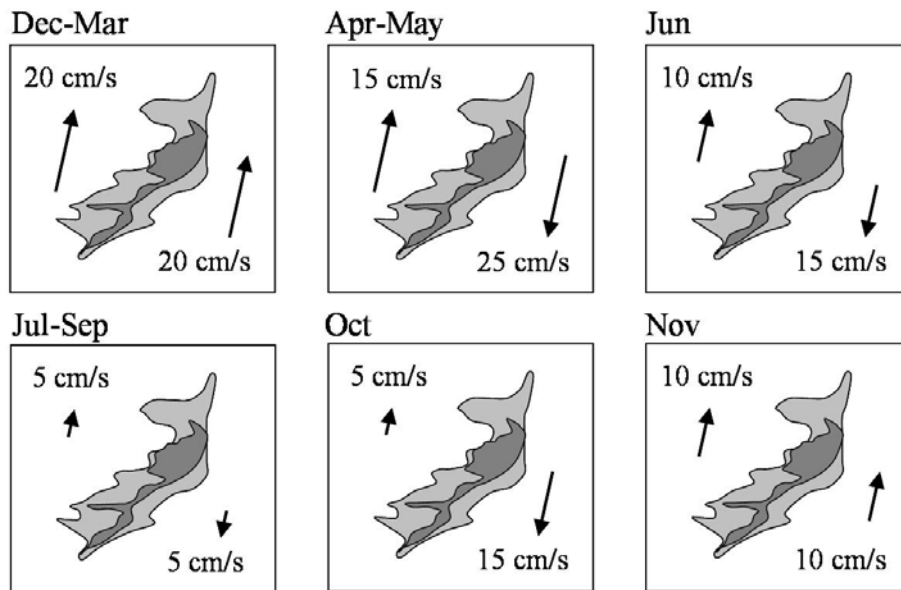


Figure 8 Schematic diagram of the seasonal variation in the currents around Palau.

Tidal Elevation

Variation in the sea-surface elevation was required as input for the numerical model. The boundaries of the model domain are located in deep-water sites where little or no tidal data have been recorded. While the determination and use of tidal constituent vectors would be preferred to constrain the tidal variation, this was virtually impossible for this study due to a lack of existing data. A sensible and suitable proxy to determine the effects of tides is to constrain values using a sea-surface elevation time-series. Again the remote location of the domain boundaries is an issue; however, in this case the extended time-series of sea-level from the Malakal Harbour Tide Gauge may be employed. This tide gauge dataset is the only extended time-series of its type in the vicinity of Palau.

A nearly continuous dataset of hourly elevations at Malakal from 1969-2004, as well as 15-minute-interval data for 1990-2001, were acquired from the Global Sea Level Observing System (GLOSS) [<http://www.bodc.ac.uk/services/glosshb/stations/gloss120.htm>]. The long-term average sea-level was determined from the data and defined as the datum for use in the model (*i.e.*, the average was set to be zero). The time-series for Malakal was adapted and used for the boundary condition for elevation, phased across the model domain from east to west. This assumed that every elevation along the eastern boundary was in-phase, similarly with the western boundary. The assumption here was based on the tidal charts of Luther and Wunsch (1975) and on a global tide model by the University of Texas' Center for Space Research [animated at <http://geodesy.eng.ohio-state.edu/tide.html>]. The phase of the tidal signal was interpolated across the northern and southern boundaries throughout the model run. The adaptation of the Malakal elevation values for the boundaries was defined so as to closely replicate the observations at the tide gauge location. Several iterations of the model were required to determine the appropriate linear relationship. This process is discussed further below.

The elevation input was taken starting at 1200 hours, 28 October 2003 for a period of thirty days. This was chosen so that the model would coincide with the majority of data collected (see Appendix 1) and encompassed a lunar month (29.5 days), the period through which the Moon returns, in phase, over each location on Earth.

Other Defined Parameters

Bleaching Weather (described above) is characterized by little-or-no wind. Applying a no-wind constraint (*i.e.*, set wind speed to zero) in the hydrodynamic model is therefore valid and simplified the model.

Bottom friction will vary with benthic habitat type; *e.g.*, coral cover would have a greater drag than sand. A coefficient of bottom friction was defined for each gridpoint and followed a logarithmic function involving the local depth, Von Karman's constant (0.4) and a roughness length. The latter of these was varied to represent difference in friction for different bottom types. Observations of the Palau lagoon showed that many shallow regions were covered by coral, while the major channels were covered by silt. To automate the definition while effectively capturing this contrast, the roughness length values were defined as a function of the water depth; shallow regions having greater roughness length than deep regions. Even though some coral-covered regions were in significantly deep water, this method proved to be effective and efficient in automating the characterization of bottom friction.

Output

The hydrodynamic model was run for thirty days including one-half day of spin-up time (to allow the solution to converge smoothly from the initial conditions). The tidal data are shown in Figure 9 with

elevations referenced to the long-term mean of the data. The period covers two spring tides (11 and 26 November) and two neap tides (03 and 18 November).

Software used to post-process the model output, *i.e.*, the production of the heat-stress map, constrained the duration of individual model runs to 1.5 days. Each subsequent 1.5-day run was continued from the final conditions of the previous run.

As stated previously, the elevation boundary conditions were defined as a function of the Malakal Harbour Tide Gauge data. The linear relation at the eastern boundary was determined by iterative comparison of the data with elevations from the co-located grid point. There is a time lag in the tidal elevation between the eastern extent of the model domain and the tide gauge location. To determine this time lag, correlation coefficients of the elevations from these locations were calculated with varying time separations. Table 1 shows the correlation coefficients for each time-lag step. As the temporal resolution of the model output is one hour, this constrains the resolution with which the time-lag of the sea-level can be defined. The correlation values in Table 1 show that the time-lag from the eastern boundary to Malakal Harbour was between two and three hours – and closer to two hours. Figure 10 shows a comparison of the model output at the tide gauge gridpoint with the measured sea-levels used to define the eastern boundary condition, with a two-hour time shift of these values. The results are for the entire simulation. A linear regression of the values gave a slope of 1.04 and intercept of 0.06 m. Figure 10 also shows the line of equity (*i.e.*, the 45° line) for reference. From this analysis it can be seen that the method of defining the elevation boundary conditions was successful.

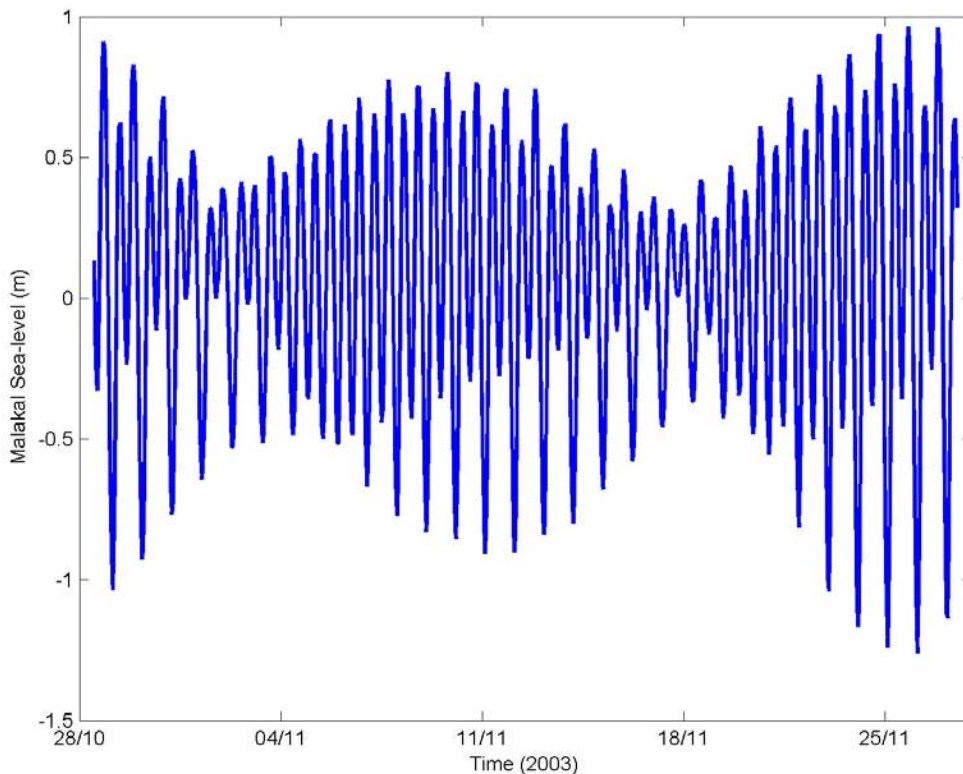


Figure 9 Time-series of sea-level measurements in Malakal Harbour used in the hydrodynamic model. The datum is the mean of measurements for the period 1985-2004.

Time Lag (hours)	Correlation Coefficient
0	0.51559
1	0.83044
2	0.97640
3	0.92102
4	0.68110
5	0.31699
6	-0.08324

Table 1 Correlations between the elevations at the Malakal Harbour Tide Gauge grid point and the eastern boundary grid point for varying time lags. The Malakal grid point lags behind the boundary grid point in each case.

The described seasonal variation in the velocity boundary condition was also applied in the model. Examination of output using different velocity constraints showed that the currents inside the Palau lagoon showed negligible variation from season to season; *i.e.*, the lagoon currents were tidally-dominated with little-to-no influence from low frequency currents outside the lagoon. For this reason, results from the thirty-day run for only one velocity boundary condition are presented, corresponding to the period July-September. This is, historically-speaking, the hottest period of the year and shows the greatest potential for coral bleaching (Bruno *et al.* 2001).

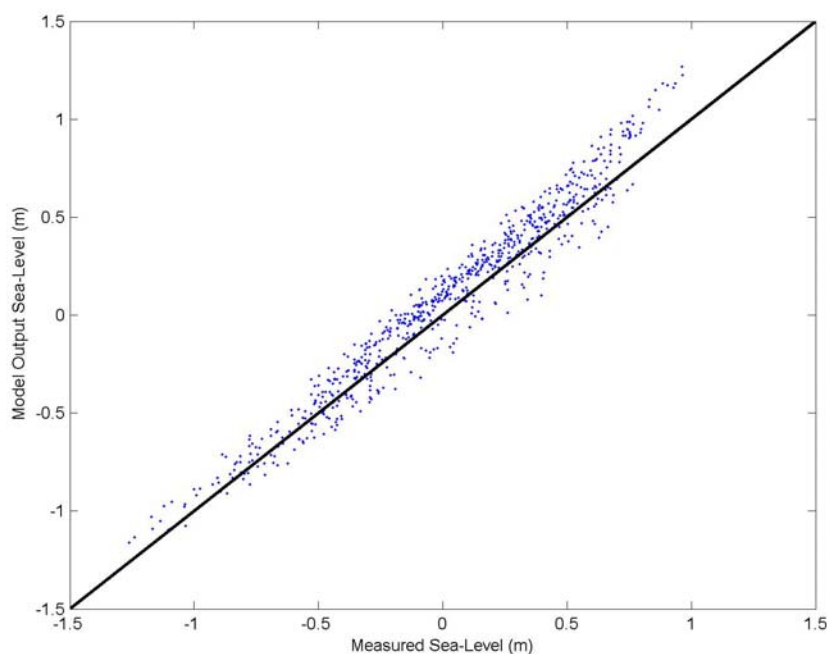


Figure 10 Scatter-plot of Malakal Tide Gauge sea-level values and model output versus measured values for a two-hour time lag in the Malakal output from the eastern boundary. The solid line is the line of equity.

Output from the Palau hydrodynamic model is illustrated in Figure 11 and Figure 12, showing currents vectors and sea-level, respectively, at the first time-step after the spin-up period (model time 0.5 days). Animation files of the model output are provided in the associated files as “PalauModel_Velocity.avi” (vel_movie) and “PalauModel_Elevation.avi” (elev_movie), respectively. The movies have a time-step of one hour, matching the output frequency of the model. For presentation purposes, the resolution of the vectors shown in Figure 12 is $1/27^{\text{th}}$ of the actual grid resolution (*i.e.*, the spacing between arrow-tails is approximately 7 km).

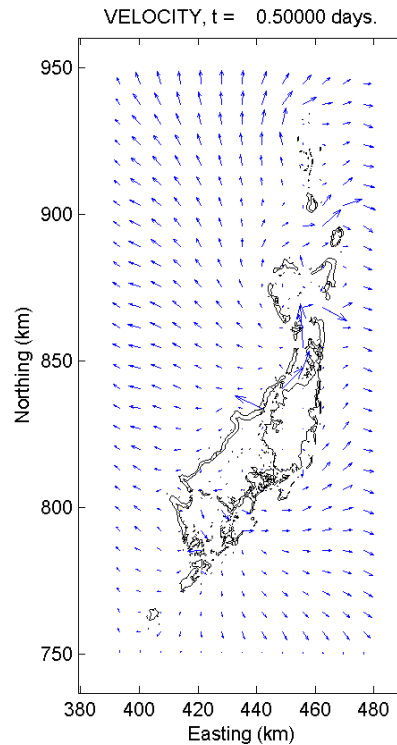


Figure 11 Surface velocity vectors at model time 0.5 days. Vectors are plotted at $1/27^{\text{th}}$ of the grid resolution.

In vel_movie the variation through the tidal cycle is reflected in the relative magnitudes of currents vectors through time. The strongest currents occur in the channels at the edges of, and within, the Palau lagoon (see also Figure 11). Notice the low magnitude of currents in the northern lagoon (the “Lagoon box” in Figure 4), while the southern lagoon (south of Ulong) has much stronger currents. The currents outside the Palau lagoon are generally stronger than those inside. Neap tidal periods coincide with the lowest-magnitude currents and spring tides with the highest currents, as expected.

In elev_movie the tidal variation is apparent, as is the phase lag of the lagoon sea-level compared with the deep-ocean water. There appears a slight phase-difference between the northern- and southern-lagoons, which can also be seen in Figure 12. This is consistent with field observations for the region. The variation in sea-level through the neap and spring periods of the tidal cycle is also evident in the animation.

While qualitative analyses of the model output suggest that it has been successful in describing the hydrodynamics of the region, further quantitative investigation is necessary to confirm the skill of the model. This was achieved by comparing data acquired during the deployment with output from

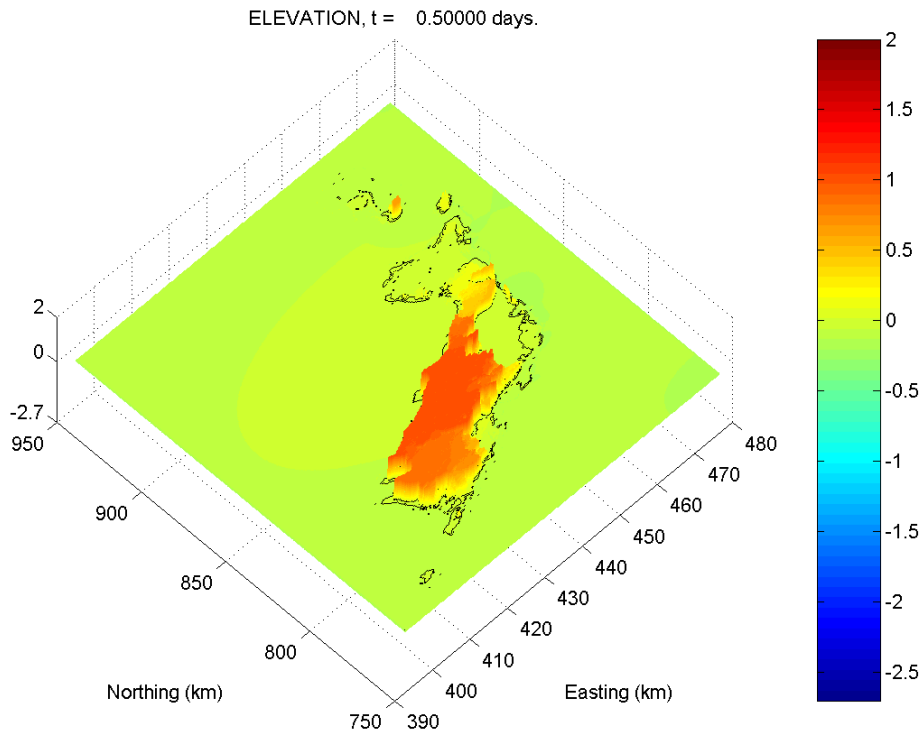


Figure 12 Sea-surface elevation, referenced to the long-term mean sea-level, at model time 0.5 days. The vertical axis and color scale have units of meters.

corresponding model gridpoints. The horizontal resolution of the numerical grid (256.5 m) was greater than the width of some channels in the Palau Lagoon. One of the defining parameters of POM is to conserve mass. As such, for a given rate of mass flow, a wide channel should have a speed of lesser magnitude as compared with a narrow channel. This effect was accounted for when comparing the model output with the data. Actual channel widths were determined using the 28.5 m-resolution Landsat bathymetry data and used to compare the volume flow rates between the model and data.

Figure 13 shows a plot of data (blue line) and model output (red cross) for the Lighthouse Channel (Toachel Ra Kesebekuu – instrument A8) from the first 1.5-day model run (including 0.5 day spin-up time). The data from the current profiler located in this channel were averaged in the vertical direction, so as to compare with the (vertically averaged) output of the 2-D model. In Figure 13 the current magnitudes from the model output are scaled by the ratio of the actual to modeled channel-widths for comparison with data values. The upper panel of Figure 13 shows the magnitudes for the scaled model output and data; the lower panel shows the directions of each.

The lower panel of Figure 13 shows that there was a slight error in the current direction. This is due to the discrete nature of the model grid structure in describing the channel – note that the currents were generally in one of two directions (into or out of the lagoon). The timing of modeled direction changes was consistent with the observations. In the upper panel of Figure 13, the current speeds output by the model showed good comparison with the measurements, with the exception of the period around midnight (0000 hours) on 29 October 2003. At this time, the current profile showed that the direction of the current was consistent throughout the water column except near the surface, where the magnitude was

also greatly reduced. This inconsistency suggests a surface event that influenced the depth-averaged measurement (*e.g.*, the wake from a boat or a wind-driven component of current). As the model did not incorporate anthropogenic or wind effects, any related effects would not be reflected in the model output.

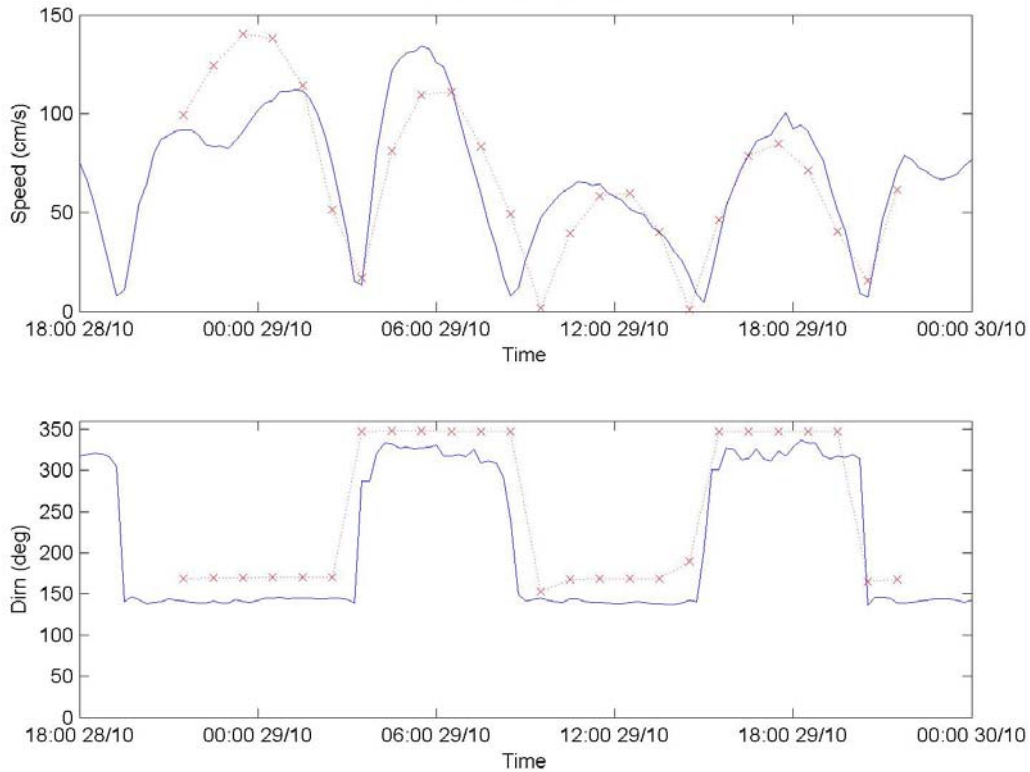


Figure 13 Scaled current speed and direction at the location of instrument A8 (Lighthouse Channel) from 28-30 October 2003. The instrument data are indicated by the blue line; the model output by red crosses.

Figure 14 shows the current speed and direction, from both model and data, for the location of instrument A13 (Toachel Mid) for a 1.5-day period towards the end of the simulation. Here it can be seen that the model was unable to describe higher-frequency variations in the speed and directions, due to the one-hour temporal resolution of the model output. However, the model provided a very good description of the low-frequency variations in the currents.

Figure 15 shows a scatter plot of scaled model output and measured current speeds at the location of instrument A8 (Lighthouse Channel) for the duration of the model. The line of equity is also shown. Here we see that the model compared well with the data through the entire simulation.

Analyses of the model output data showed it to be consistent with observations. The model output was employed directly in the production of the heat-stress map for Palau. Future improvement to the information gained from the hydrodynamic model would require an increase in resolution, both temporally and spatially. This in turn would require considerably higher-quality bathymetry and access to super-computer facilities to execute the model script.

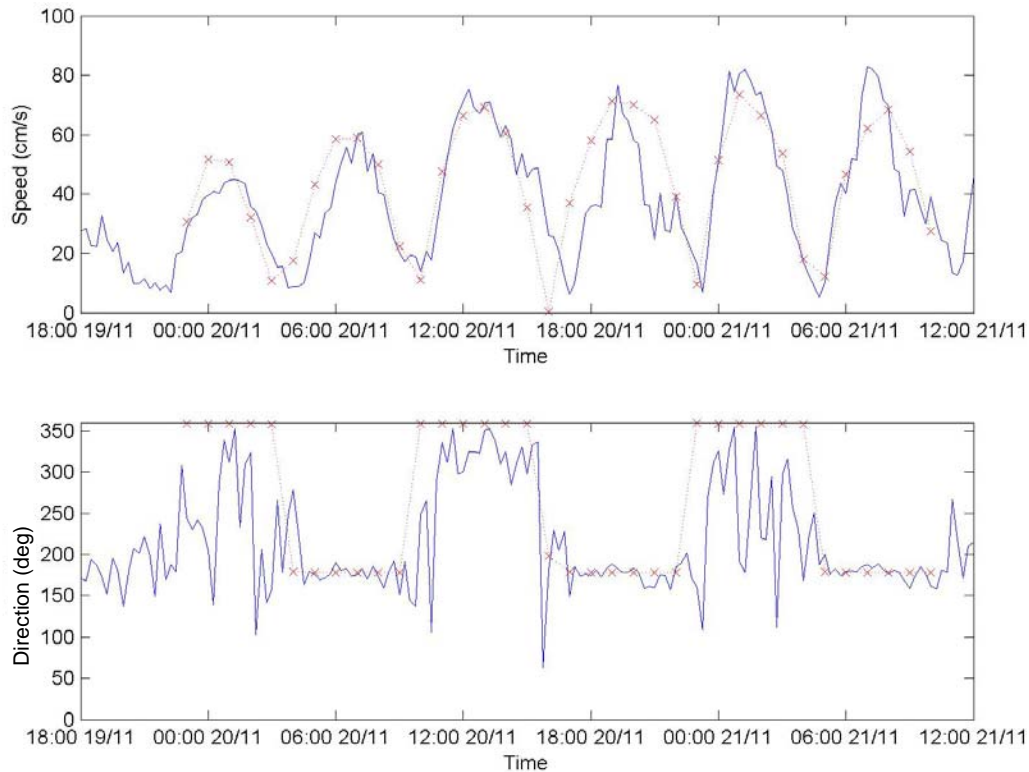


Figure 14 Scaled current speed and direction at the location of instrument A13 (Toachel Mid) for 19-21 November 2003. The instrument data are indicated by the blue line; the model output by red crosses.

Vertical Temperature Profile

The General Ocean Turbulence Model (GOTM) written by Burchard *et al.* (1999) was used here to calculate the vertical temperature distributions in Palau. GOTM simulates small-scale turbulence and vertical mixing in the ocean water column. It is a one dimensional, hydrostatic water column model which uses the Boussinesq approximation (*i.e.*, that density differences are sufficiently small to be negligible, except in the calculation of weight) when calculating the turbulent eddy viscosity.

GOTM allows the selection of a range of state-of-the-art turbulence closure schemes. A dimensionless stability function, a turbulent velocity scale, and turbulent macro length scale are all needed to calculate the Kolmogorov-Prandtl relations. Several zero-, one-, and two-equation models used to calculate the turbulent velocity and macro length scales, as well as various stability functions, are available in GOTM. Here we use the second moment closure scheme and the $k-\varepsilon$ model. Further detail on the particular turbulence schemes available in GOTM can be found in Burchard (2002).

In this application we wanted to simulate the warming of the surface waters in bleaching-like conditions to gain an understanding of how much heat would be absorbed into the water column. It is impossible to predict the exact nature of the wind and solar radiation in the next bleaching event, but we expect that it will be sunny with little to no wind. If we use maximum solar radiation (*i.e.*, assume zero cloud) and assume that it is completely still (*i.e.*, no wind), then we get a very hot layer of water in the top 2 to 3 meters of the water column and little to no heating below this.

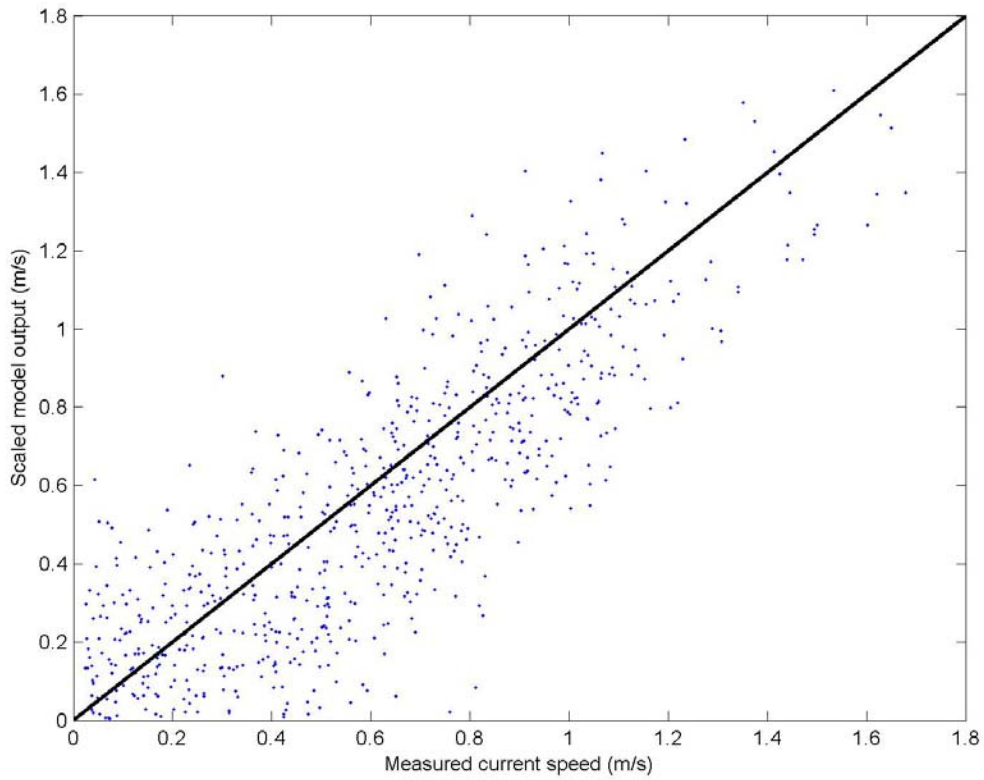


Figure 15 Scaled model output against measured current speed for location A8 (Lighthouse Channel). The solid black line is the line of equity.

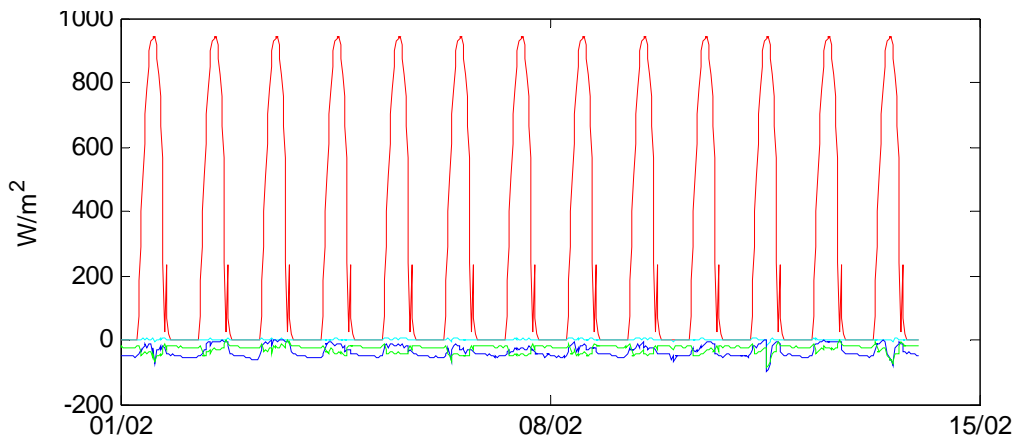


Figure 16 Plot of heat balance parameters: Red is incoming total short wave radiation, Green is longwave outgoing, Blue is the sensible heat flux, and Turquoise the Latent Heat Flux.

Experience has taught us that this is an extreme and unrealistic case. Usually it is very sunny, but it is rarely completely cloudless; often it is very still, but rarely is there absolutely no wind. After examining the small amount of information available for the Palau 1998 bleaching event it was decided to use realistic rather than extreme values of solar radiation and wind, after Bird *et al.* (2004). This meant warming the water using incoming solar radiation with a daily maximum of 940 Wm^{-2} ; an average humidity of 75% and a gentle breeze of 2.6 ms^{-1} throughout the 14 day simulation period (Figure 16). The initial condition was a linear temperature profile of $28 \text{ }^\circ\text{C}$ water at the surface to $25 \text{ }^\circ\text{C}$ at 50 m.

Figure 17 shows that over a two week period of warming, surface temperatures rose from $28 \text{ }^\circ\text{C}$ to just over $32 \text{ }^\circ\text{C}$. The depth of penetration of the heat layer was around 5 meters due mainly to the slight breezes and low tidal currents that were not able to produce bottom-friction induced turbulence that reaches the surface. The resultant temperature profile can be seen in Figure 18. This was the temperature profile used for the modeling heat-stress patterns in Palau.

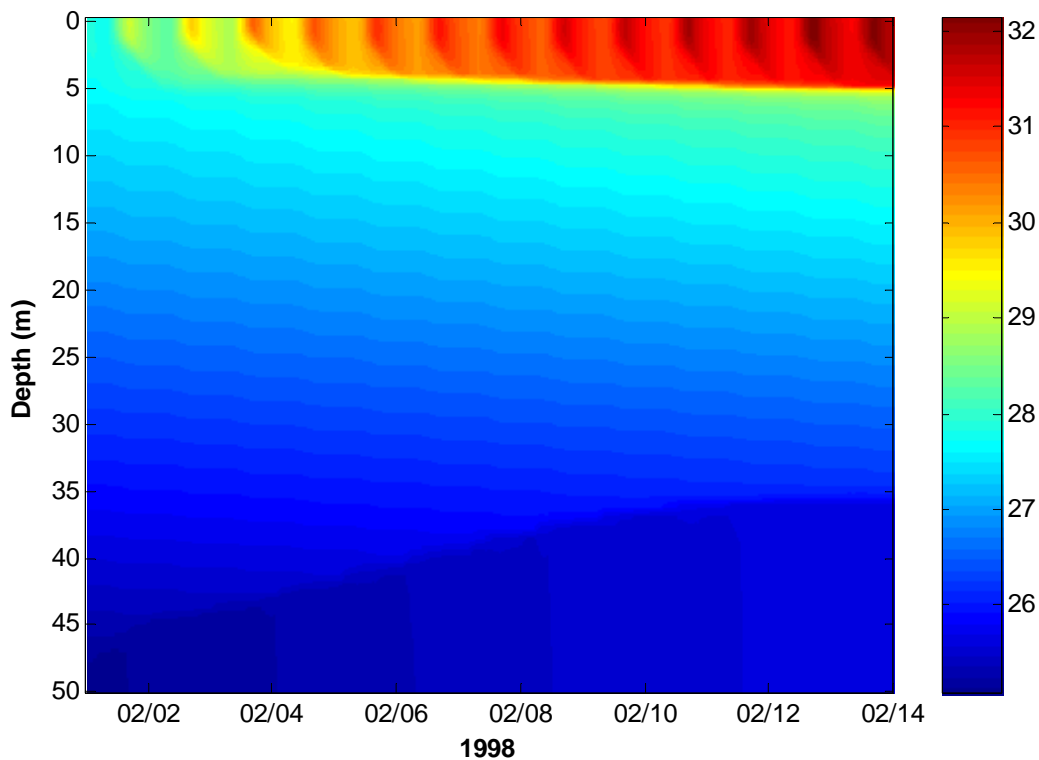


Figure 17 Development of the surface heat layer over a 14-day period.

Modeling Heat-Stress Patterns during a Bleaching Event

Simpson and Hunter (1974) provide the parameterization that was used to distinguish between stratified and well-mixed water by combining the currents with the bathymetric data (described in Heron and Skirving 2004). See the animation (PalauModel_MixingParameter.avi) of this mixing parameter over a full tidal cycle for each time step of the model.

This information was then used in conjunction with the vertical temperature profile to determine the likely spatial distribution of sea surface temperature. For well-mixed regions, the temperature of the water column (including the SST) would be the average of the vertical temperature profile values from the surface to the local depth of water. In regions where the Simpson and Hunter (1974) parameter indicated

mixing, the SST was assigned the calculated average temperature that corresponded to the local depth. All other regions were deemed to be stratified and therefore no change was made to their original 32 °C SST values.

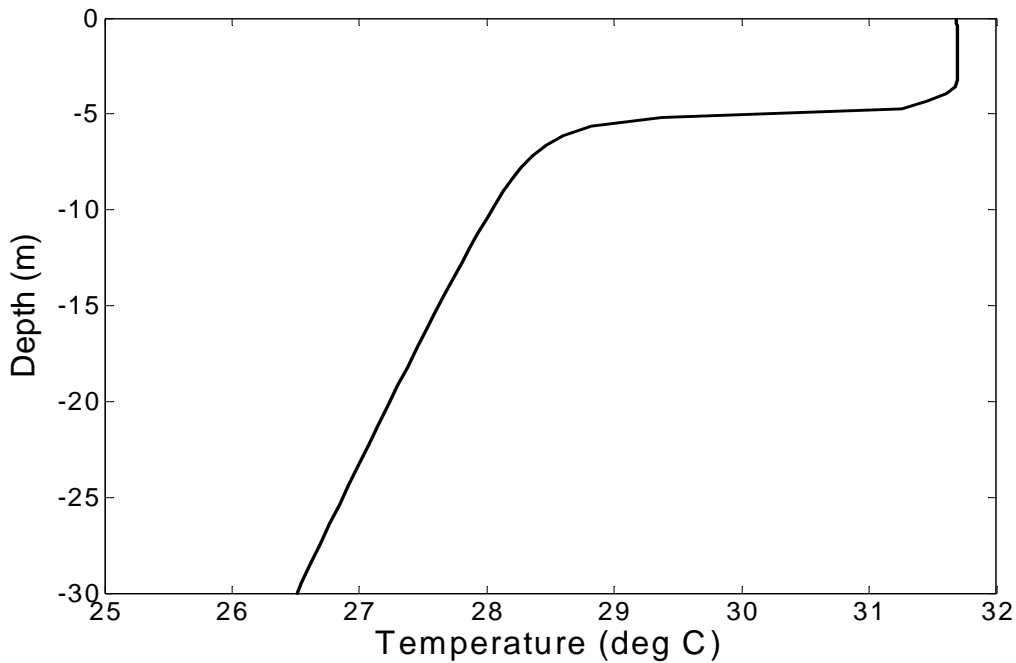


Figure 18 Vertical temperature profile on the 14th day of modeling.

The SSTs were then represented as a cooling anomaly (*i.e.*, ≤ 0 , calculated by subtracting 32 °C from each SST value). See the animation (PalauModel_CoolingIndex.avi) of this anomaly over a full tidal cycle for each time step of the model.

The anomalies at each time step of the model were then accumulated in much the same way as in the methodology used to derive the NOAA Degree Heating Week coral bleaching product (Skirving *et al.* 2006). This methodology allowed the hourly outputs from the model to be combined into a single map of thermal stress (Figure 19).

Potential use as a planning tool

Although good approximations of actual temperatures, the temperatures are better used as indications of spatial patterns of relatively cooler and warmer waters during a bleaching event. In fact, this model is better described as a measure of thermal capacitance than temperature. The warmer regions in the model have a low thermal capacitance (*i.e.*, stratified: the sun only heats up the top few meters of the water column resulting in high SST) and will heat up (and cool down) much faster than the cooler regions in the model, which have a high thermal capacitance (*i.e.*, well-mixed: the surface heating is mixed down, making it resistant to high SST).

The result of this is that the cooler regions in this model are characterized by mild thermal climatologies (*i.e.*, less thermal stress) whereas the hottest regions are those that will experience the most extreme temperatures for a region (*i.e.*, greater thermal stress). Figure 19 is an accumulation of the final product from the Palau model. It depicts the average modeled cooling effect due to mixing, accumulated over a

tidal cycle (one month). The blue regions represent the most cooling at the surface due to mixing and hence represent the regions with the lowest temperature variability and high thermal capacitance. This provides the organisms that live there with a mild climate providing greater protection against thermal stress. The red regions are the opposite, having little mixing, high temperature variability, and low thermal capacitance. These areas are at greater risk of thermal stress.

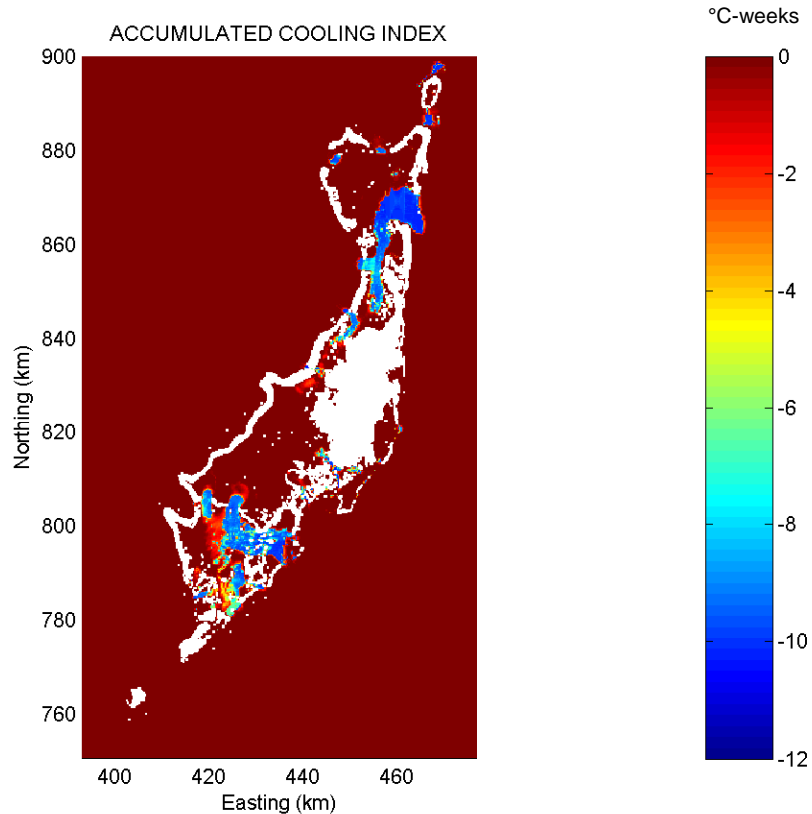


Figure 19 Final output from the Palau model of thermal capacitance, expressed as surface cooling degree-weeks (*i.e.*, how much the mixing cooled the surface temperature during the one-month period) (from Heron and Skirving 2004).

A chart of this type can be extremely useful when designing a PAN. In general, most PANs are currently designed so as to provide protection to “representative bioregions,” meaning that, as much as possible, every type of bioregion within the ecosystem of interest should be equally represented within the PAN. An ecosystem is not only made up of different species, but also has genetic variability within species that contain unique physiological characteristics. When designing a PAN, it is relatively straight forward to map bioregions on the basis of species composition; however the genetic (phenotypic) variability within each species is not represented by these techniques. With respect to a changing climate, the phenotypes that result in varied physiological characteristics are likely to correspond to different thermal capacitances throughout the region. As a result, although we may not know what these characteristics are, the relevant characteristics for resilience against climate change can be protected if a representative amount of each thermal region within the thermal capacitance map is protected. This is very important when designing a PAN to maximize resilience to climate change as it is important to both protect regions of low thermal capacitance that physically protect species from thermal stress, and to protect phenotypes that are already adapted to higher thermal stress.

Recommendations

The work described in this Technical Report represents an important new tool for Marine Protected Area (MPA) design. Prior to this project, the design of MPAs was based on species diversity alone and some socioeconomic considerations. Prior to this work, there had not been a serious attempt to include physical variables to build resilience against climate change, and in particular coral bleaching, into MPA design.

This project demonstrated that a simplistic physical model can be used to improve MPA planning to incorporate resilience against future coral bleaching events. NOAA Coral Reef Watch (CRW) are working with collaborators such as the Australian Institute of Marine Science, the University of Queensland (Australia), the University of Exeter (UK), and others to further develop this methodology so that these techniques might become common tools in the design of MPAs around the world. Three approaches are being used to improve this application of physical oceanography to MPA design:

- 1) Increased use of satellite data: For many regions of the world it is possible to replace the need for expensive hydrodynamic modeling and major deployment of oceanographic equipment with the application of high-resolution satellite data. This is possible for many places where there have been a significant number of thermal stress events and where the spatial scale of the reefs is such that sub-kilometer resolution thermal capacitance maps is not necessary. NOAA CRW is collaborating with the University of Exeter (UK) and others to investigate the use of larval connectivity models in conjunction with satellite-derived maps of thermal capacitance. A pilot project in the Bahamas has already begun.
- 2) Move from 2D to 3D: The Palau work presented in this report used a two-dimensional map of thermal capacitance. This is derived from 2D sea surface temperature patterns during bleaching conditions. As these techniques are developed, it is necessary to recognize that thermal effects and responses of corals are depth dependent and, as such, need to be described in 3D. There are three issues that need to be examined for the work in this report to be extended from 2D to 3D:
 - a. Methodologies for developing very-high-resolution 3D hydrodynamic models on coral reefs. This is the subject of a joint pilot project underway at Heron Island between NOAA CRW and AIMS.
 - b. An understanding of the three-dimensional variation in the response of corals to thermal stress; *i.e.*, the variation of thermal threshold with depth and benthic complexity. This is the subject of a joint project at Heron Island between NOAA CRW and the University of Queensland. Once complete, this project will need to be extended to include other reefs and coral species.
 - c. A methodology that allows the satellite-derived two-dimensional SSTs over coral reefs to be interpreted as three-dimensional SST. This uses an outcome of the collaborative hydrodynamic modeling at Heron Island. The very-high-resolution 3D model being developed jointly by NOAA CRW and the Australian Institute of Marine Science will be used to investigate the ability of a combination of 2D and 1D models to mimic the 3D temperature structure of a coral reef. Once developed, this methodology can be adapted for use on most coral reefs.
- 3) Include light in predictions of coral bleaching: Coral bleaching is not directly caused by temperature but results from excessive light, with the threshold modulated by temperature. By including light in the methodologies developed in the Palau MPA project, predictions of coral bleaching severity and mortality may become possible. A collaborative project led by NOAA CRW and including researchers from the Universidad Nacional Autónoma de México, the University of Exeter, and the University of Queensland has begun to develop an algorithm that combines light and temperature to produce a measure of the light stress experienced by corals.

As indicated above, preliminary work has begun for the issues mentioned above, and much of it involves work at Heron Island in the southern Great Barrier Reef. None of these efforts would be possible without collaborations between NOAA CRW and researchers from the various agencies and universities mentioned, especially collaborations between the US and Australia.

The innovative research presented in this report represents the beginning of the use of physical data from models and satellites for the management of coral reefs. It provides a glimpse of the tools that can be developed to understand and effectively manage coral reefs in a changing climate. Development of the methodologies described in this report continues; however, these efforts are limited in scope and only represent preliminary investigations. Significant funding and resources will be needed for the full potential of these methodologies to be realized.

Bibliography

- Berkelmans, R. (2002) Time-integrated thermal bleaching thresholds of reefs and their variation on the Great Barrier Reef. *Marine Ecology Progress Series* 229, 73-82.
- Berkelmans, R., G. De'ath, S. Kinimonth, and W. Skirving (2004) Coral bleaching on the Great Barrier Reef: Correlation with sea surface temperature, a handle on 'patchiness' and comparison of the 1998 and 2002 events. *Coral Reefs*, 23, 74-83.
- Bird, J.C., C.R. Steinberg, T.A. Hardy, L.B. Mason, R.M. Brinkman, and L. Bode (2004) Modeling sub-reef scale thermodynamics at Scott Reef, Western Australia to predict coral bleaching. *10th International Coral Reef Symposium*, Okinawa, Japan, July 2004.
- Blumberg, A. F. and G. L. Mellor (1987) A description of a three-dimensional coastal ocean circulation model. In: Heaps, N.S. (Ed.), *Three-Dimensional Coastal Ocean Models*, American Geophysical Union, Washington, DC, 1-16.
- Bruno, J.F., C.E. Siddon, J.D. Witman, P.L. Colin, and M.A. Toscano (2001) El Nino related coral bleaching in Palau, Western Caroline Islands. *Coral Reefs*, 20, 127-136.
- Burchard, H., K. Bolding, and M. R. Villarreal (1999) GOTM - A general ocean turbulence model: Theory, applications and test cases. European Commission Report EUR 18745 EN, 103pp.
- Burchard, H. (2002) Applied turbulence modelling in marine waters. In: *Lecture Notes in Earth Sciences, Vol. 100*, Springer, Berlin, Heidelberg, New York, 229pp.
- de Silva Samarasinghe, J.R. (1989) Transient salt-wedges in a tidal gulf: A criterion for their formation. *Estuarine, Coastal and Shelf Science*, 28, 129-148.
- Dennis, G.D. and R.I. Wicklund (1993) The relationship between environmental factors and coral bleaching at Lee Stocking Island, Bahamas in 1990. In: *Case Histories for the Colloquium and Forum on Global Aspects of Coral Reefs: Health, Hazards and History*, F15-F21.
- Downs, C.A., J.E. Fauth, J.C. Halas, P. Dustan, J. Bemiss, and C.M. Woodley (2002) Oxidative stress and seasonal coral bleaching. *Free Radical Biology and Medicine* 33, 533-543.
- Drollet, J.H., M. Faucon, S. Maritorea, and P.M.V. Martin (1994) A survey of environmental physico-chemical parameters during a minor coral mass bleaching event in Tahiti in 1993. *Marine and Freshwater Research* 45, 1149-1156.
- Eakin, C.M., J.M. Lough, and S.F. Heron (2009) Climate, Weather and Coral Bleaching. In: Lough, J. and M. Van Oppen (Eds.), *Coral Bleaching Patterns, Processes, Causes and Consequences, Ecological Studies Vol 2005*, Springer, 178pp.
- Glynn, P.W. (1993) Coral reef bleaching: ecological perspectives. *Coral Reefs*, 12, 1-17.
- Hearn, C.J. (1985) On the value of the mixing efficiency in the Simpson-Hunter h/u^3 criterion. *Deutsche Hydrographisches Zeitschrift*, 38(H.3), 133-145.

- Heron, S.F. and W.J. Skirving (2004) Satellite bathymetry use in numerical models of ocean thermal stress. *La Revista Gayana*. 68(2), 284-288.
- Heron, S.F., E.J. Metzger and W.J. Skirving (2006) Observations of the ocean surface circulation in the vicinity of Palau. *Journal of Oceanography*. 62, 413-426.
- Hoegh-Guldberg, O. (1999) Climate change, coral bleaching and the future of the world's coral reefs. *Marine Freshwater Research*, 50, 839-866.
- Jones, R.J., O. Hoegh-Guldberg, A.W.D. Larcum, and U. Schreiber (1998) Temperature-induced bleaching of corals begins with impairment of the CO₂ fixation mechanism in zooxanthellae. *Plant, Cell and Environment*, 21, 1219-123.
- Kilpatrick, K.A., G.P. Podesta, and R. Evans (2001) Overview of the NOAA/NASA advanced very high resolution radiometer Pathfinder algorithm for sea surface temperature and associated matchup database. *Journal of Geophysical Research*, 106, 9179-9197.
- Liu, G., A.E. Strong, and W.J. Skirving (2003) Remote sensing of sea surface temperatures during 2002 Great Barrier Reef coral bleaching. *EOS*, 84, 137-144.
- Luther, D.S. and C. Wunsch (1975) Tidal charts of the Central Pacific Ocean. *Journal of Physical Oceanography*, 5, 222-230.
- Marks, K.M. and W.H.F. Smith (2006) An evaluation of publicly available global bathymetry grids. *Marine Geophysical Researches*, 27(1) 19-34.
- McField, M.D. (1999) Coral response during and after mass bleaching in Belize. *Bulletin of Marine Science*, 64, 155-172.
- Newhall, R. and S. Rohmann (2003) Using Landsat and IKONOS Imagery to Create Habitat Classifications and Mosaic Maps of Pacific Freely Associated States. *Proceedings for the 30th International Symposium on Remote Sensing of Environment*, Honolulu, USA, 10-14 November 2003, CDROM.
- Simpson, J.H. and J.R. Hunter (1974) Fronts in the Irish Sea. *Nature*, 250, 404-406.
- Skirving, W.J. and J. Guinotte (2001) The sea surface temperature story on the Great Barrier Reef during the coral bleaching event of 1998. In: Wolanski, E. (Ed.), *Oceanographic Process of Coral Reefs: Physical and Biological Links in the Great Barrier Reef*, CRC Press, Boca Raton, Florida, 376pp.
- Skirving, W.J. (2004) The Hydrodynamics of a Coral Bleaching Event: The role of satellite and CREWS measurements. In: Hendee, J. (Ed.), *The effects of combined sea temperature, light, and carbon dioxide on coral bleaching, settlement, and growth*, NOAA Research Special Report, March 2004, 33-34.
- Skirving, W.J., C.R. Steinberg, and S.F. Heron (2004) The hydrodynamics of a coral bleaching event. *ASLO/TOS Ocean Research 2004 Conference*, Honolulu, Hawaii, February 2004.
- Skirving, W.J., A.E. Strong, G. Liu, C. Liu, F. Arzayus, J. Sapper, and E. Bayler (2006) Extreme events and perturbations of coastal ecosystems: Sea surface temperature change and coral bleaching. In:

L.L. Richardson, L.L. and E.F. LeDrew (Eds.), *Remote Sensing of Aquatic Coastal Ecosystem Processes*, Kluwer Publishers, Chapter 2.

Smith, W.H.F. and D.T. Sandwell (1997) Global sea floor topography from satellite altimetry and ship depth soundings. *Science*, 277, 1956-1962.

Stumpf, R.P., K. Holderied, and M. Sinclair (2003) Determination of water depth with high-resolution satellite imagery over variable bottom types. *Limnology and Oceanography*, 48, 547-556.

Wilkinson, C.R. (1998) *Status of Coral Reefs of the World: 1998*. Global Coral Reef Monitoring Network and Australian Institute of Marine Science, Townsville, Australia, 184pp.

Wilkinson, C.R. (2000) *Status of Coral Reefs of the World: 2000*. Global Coral Reef Monitoring Network and Australian Institute of Marine Science, Townsville, Australia, 363pp.

Winter A., R.S. Appeldoorn, A. Bruckner, E.H. Williams, and C. Goenaga (1998) Sea surface temperatures and coral reef bleaching off La Parguera, Puerto Rico (northeastern Caribbean Sea). *Coral Reefs* 17, 377-382.

Appendix 1

Palau Oceanographic Array Data Report: January 2003 – January 2004

Craig R. Steinberg, Scott F. Heron, William J. Skirving, Cary McLean, and Severine M. Choukroun

Abstract

Palau is an archipelago of hundreds of islands, the majority of which are surrounded by an extensive barrier reef. The major island group is located near 7° 20' N, 134° 30' E, in the Western Pacific Ocean, and is part of the Caroline Islands of Micronesia.

Coral bleaching is a global problem for coral reefs and affected large areas during 1997 and 1998. Most of Micronesia escaped damage; however, there was an unprecedented loss of coral around Palau itself. Field surveys found that on average, nearly half of 946 scleratinian taxa were totally bleached and another 15% were partially bleached. The bleaching event was relatively severe and widespread across depths, sites, habitats and coral taxa.

At the time of the bleaching event, there was no major *in situ* monitoring of water temperature around Palau. A long-term temperature monitoring program has since been instigated by Pat Colin from the Coral Reef Research Foundation (CRRF). The short-term study reported here complements the CRRF array by expanding the number of observing locations to over 60.

An extensive study of oceanographic parameters in Palauan waters was undertaken during the period August 2003 to January 2004. The period of deployment was selected to coincide with the timing of observed bleaching events. Sixty-two instruments were deployed in and near the Palau lagoon to record currents, temperatures, sea-levels, salinities and weather conditions. This number of instruments is unusually high for a region of this size, and was fueled by a desire to maximize coverage and the fortuitous availability of instruments. The deployment is the most-extensive *in situ* ocean study ever performed in Palau.

This report presents a comprehensive overview of the data collected and allows a brief view of some of the time series collected. These time series are of sufficient length to undertake a tidal current analysis for hind-casting or prediction. Raw data may be requested by contacting coralreefwatch@noaa.gov.

Citation:

Steinberg C.R., S.F. Heron, W.J. Skirving, C. McLean and S.M. Choukroun (2004) "Palau Oceanographic Array Data Report, August 2003 - January 2004. Report to The Nature Conservancy" Australian Institute of Marine Science and National Oceanic and Atmospheric Administration, 246pp.

Palau Oceanographic Array Data Report

August 2003 – January 2004



Craig Steinberg, Scott Heron, William Skirving, Cary McLean & Severine Choukroun

Australian Institute of Marine Science
National Oceanic and Atmospheric Administration
The Nature Conservancy



Disclaimer

This report has been produced for the sole use of the party who requested it. The application or use of this report and of any data or information (including results of experiments, conclusions, and recommendations) contained within it shall be at the sole risk and responsibility of that party. AIMS and NOAA do not provide any warranty or assurance as to the accuracy or suitability of the whole or any part of the report, for any particular purpose or application. Subject only to any contrary non-excludable statutory obligations neither AIMS, NOAA nor its personnel will be responsible to the party requesting the report, or any other person claiming through that party, for any consequences of its use or application (whether in whole or part).

Table of Contents

Disclaimer	ii
List of Figures.....	iv
List of Tables	iv
Acknowledgements	v
The Proposed Work.....	1
Introduction.....	2
Deployment Methodology	4
Instrument Array Summary	9
Temperature Transect and Mooring Summary.....	15
Instruments and Processing	22
Calibrations	22
Data Processing.....	23
Current Meters	24
RD Instruments ADCP	24
Nortek Aquapro current profiler	25
Nortek Aquadopp current meter	26
Nobska MAVS-3	27
Interocean S4	28
Tide Gauge.....	29
Brancker XR-420 TD.....	29
Conductivity Logger	30
SBE16	30
Temperature Loggers	31
SBE39	31
CTD Profiler	32
SBE19	32
Weather Station.....	33
Campbell Scientific.....	33
NOAA National Weather Service, Palau.....	34
Notable events.....	35
Acronyms and Instrument Notations.....	35
References.....	36
Appendix A – Daily Schedule	37
Appendix B – Tide gauge deployment information.....	41
Appendix C – Current meter deployment information.....	45
Appendix D – Temperature deployment information.....	52
Appendix E – Salinity deployment information.....	68
Appendix F – Weather station deployment information	69
Appendix G – Mooring and Transect Summary Plots.....	70
Appendix H – Time Series Plots of Current Meter Data	79
Appendix I – Time Series Plots of Tide Gauge Data	117
Appendix J – Time Series Plots of Salinity Data.....	125
Appendix K – CTD Profiles	131
Appendix L – Time Series Plots of Weather Data	234

Appendix M – Data Format & File naming conventions	238
Appendix N – Data Archive	246

List of Figures

Figure 1 Location map of Palau.....	3
Figure 2 Temperature Mooring ready for deployment.	5
Figure 3 Portable Weather station being set up by Cary McLean.	5
Figure 4 Schematic showing an in-line mooring and transect of temperature loggers.....	6
Figure 5 Cary McLean secures an SBE39 temperature logger to a coral outcrop using stainless steel wire.....	6
Figure 6 Felipe Arzayus Recovering an ADCP.....	7
Figure 7 Cary McLean securing an SBE16 Conductivity and Temperature logger.	8
Figure 8 IKONOS satellite image of Palau. The Lagoon box covers the area shown. Deployed instruments are indicated by their codes. Orientation of zoomed areas in Figure 9 and Figure 10 may be performed using these codes.....	13
Figure 9 Zoomed image of the Malakal Harbour box from Figure 8.	13
Figure 10 Zoomed image of the Rock Islands box from Figure 9.....	14
Figure 11 Typical configuration of a reef temperature transect.	15
Figure 12 T5 Mooring design.	19
Figure 13 T8 mooring design.....	21
Figure 14 Screen capture of the WinADCP data viewer	240
Figure 15 Screen capture of the WinADCP export options.....	241
Figure 16 Archival DVD-ROM directory structure.....	246

List of Tables

Table 1 Station Codes and number of instruments	9
Table 2 Instrument codes for each of the three specified regions. Co-located instruments are grouped together.	9
Table 3 Instrument codes listed by primary instrument type.....	10
Table 4 Locations of instruments and other points of interest.....	11
Table 5 List of CTD profiles taken during September 2003	131
Table 6 List of CTD profiles taken during November 2003.....	132
Table 7 Filename tags	238
Table 8 ASCII output from Pal02000.txt, illustrating format.....	242
Table 9 Example output for header from the current profiler, A5.....	243
Table 10 Example listing of attributes and units from the current profiler, A5.....	245

Acknowledgements

Steven Victor from the Palau International Coral Reef Center ensured a successful campaign and provided an excellent working base. Thanks to Pat Colin from the Coral Reef Research Foundation for guiding us, providing instrumentation and essential backup in the field. Andrew Bauman from the Office of Environmental Response and Coordination greatly supported the project and assisted with the field work. Andrew Smith and the team at The Nature Conservancy also provided excellent support and the use of their vessel. Bob Richmond from the University of Guam provided additional instrumentation. This research was funded by the Australian Institute of Marine Science, National Oceanic and Atmospheric Administration and The Nature Conservancy. Support from the Koror State Government and the Office of the President is gratefully acknowledged.

Partners

AIMS	Australian Institute of Marine Science
CRRF	Coral Reef Research Foundation
	Koror State Conservation and Law Enforcement
NOAA	National Oceanic and Atmospheric Administration
OERC	Office of the Environmental Response and Coordination & the Office of the President
PICRC	Palau International Coral Reef Center
TNC	The Nature Conservancy
UoG	University of Guam

The Proposed Work

Coral bleaching in Palau: Prediction and mapping with the use of hydrodynamic models and satellite data

Dr William Skirving*, Craig Steinberg⁺
Dr Rod Salm[#], Dr Eric Bayler* and Dr Alan E. Strong*

* NOAA/NESDIS/ORA

⁺ Australian Institute of Marine Science

[#] The Nature Conservancy

The Palau International Coral Reef Center (PICRC), the Koror State Department of Conservation and Law Enforcement and the Coral Reef Research Foundation have teamed with the US National Oceanic and Atmospheric Administration (NOAA), the Australian Institute of Marine Science (AIMS), The Nature Conservancy (TNC) and the University of Guam (UoG) to conduct the most intensive study of oceanography in Palau's history.

The project will be conducted over the next two years and will aim at developing a good understanding of the effects of water currents on coral bleaching. The aim is to model the water currents in and around Palau so that these models can be used to predict which regions are more likely and less likely to experience coral bleaching in the future.

The project has been split into five distinct sections:

- a) A study will be conducted with the use of historic environmental data (i.e. water temperatures, weather records and satellite data) to try to develop an understanding of the origin of the hot water that caused the severe bleaching during 1998.
- b) Instruments will be deployed between September 2003 and January 2004. Oceanic variables, including tidal heights, currents, water temperature and salinity; and weather variables, such as wind, air temperature and incoming solar radiation; will be recorded.
- c) IKONOS satellite imagery, in conjunction with specific hydrographic transects, will be used to derive a complete bathymetric chart of the Palau region at 4 meter resolution.
- d) A series of 1, 2 and 3 dimensional hydrodynamic models (computer simulations) will be built with the help of the bathymetric map and the field data.
- e) All of the above information will be combined to derive a map, which will describe the patterns of hot and cool water in and around Palau during a future coral bleaching event. This will be used by TNC to derive an understanding of the spatial variability of coral bleaching during a future bleaching event.

PICRC, NOAA and AIMS, with input from Koror State Dept of Conservation and Law Enforcement and TNC, have designed a plan for the deployment of instruments to measure tides, currents, water temperature and salinity. These instruments are being deployed now and will be used to calibrate and validate the computer models of water motion in and around Palau.

The modelling effort will take place at NOAA and AIMS with input from PICRC scientists. It is expected that there will be a number of spin-off projects that will build on this project and will involve PICRC, NOAA and AIMS.

This project has a number of direct benefits for Palau. For example, the bleaching information will be used to help the Federal and State Governments of Palau to design and manage their Marine Protected Areas so as to enable the sustainable use of the valuable coral reef resources in Palauan waters. The output from the models can also be used for other studies such as those concerned with sediment from rivers, fish spawning, coral spawning and gaining a general understanding of the links between one part of the reef and another.

Introduction

Palau is an archipelago of hundreds of islands, the majority of which are surrounded by an extensive barrier reef. The major island group is located near 7° 20' N, 134° 30' E, in the Western Pacific Ocean, and is part of the Caroline Islands of Micronesia.

Coral bleaching is a global problem for coral reefs and affected large areas during 1997/1998. Most of Micronesia escaped damage; however, there was an unprecedented loss of coral around Palau itself (Wilkinson, 2002). Bruno *et al.* (2001) documents the 1998 bleaching event in Palau from field surveys and found, on average, nearly half of 946 scleratinian taxa were totally bleached and another 15% were partially bleached. The bleaching event was relatively severe and widespread across depths, sites, habitats and coral taxa.

There was no major *in situ* monitoring of water temperature around Palau during the bleaching event. A long-term temperature monitoring programme has since been instigated by Pat Colin from the Coral Reef Research Foundation (Colin, 2000). The short-term study reported here complements the CRRF array by expanding the number of observing locations to over 60.

This study will attempt to explain how the corals will fair during a bleaching event by understanding the key physical processes that determine the thermal environment in which the corals live. As Palau is located near 7°N, it experiences the sun passing meridionally overhead twice a year and therefore has two peaks of solar insolation, offset from the maximum solar zenith, in March and October/November (Penland *et al.*, 2004). We were able to deploy instruments in August 2003 and recover them in January 2004 so that at least one of the hottest periods of the year was observed.

This report describes data collected from a physical oceanographic array deployed in Palau from August 2003 to January 2004. The aim was to observe bleaching-like conditions; this four-month period allowed a reasonable amount of time to experience a variety of weather events. This report presents a comprehensive overview of the data collected and allows a first look at the time series collected. Further analysis and data quality assessments will be done as the study progresses.

The data will also be useful for longer-term studies as the time series are long enough for a good tidal current analysis for hindcasting or prediction.

The [Temperature Transect and Mooring Summary](#) section displays what instruments were deployed at each site and their position in the water column or reef slope. The filenames of the raw data downloaded directly from the loggers is given together with their processed filename. The naming conventions are summarized in [Appendix M](#).

Deployment details of each instrument can be found in Appendices [B](#), [C](#), [D](#), [E](#) and [F](#). Plots of the observed data can be found in Appendices [G](#), [H](#), [I](#), [J](#), [K](#) and [L](#). The plots in these appendices are presented specifically to illustrate what data were collected; they are not intended for analysis or scientific investigation. A companion DVD-ROM to this data report is available for these purposes, the data format and layout of which are described in Appendices [M](#) & [N](#).



Figure 1 Location map of Palau.

Deployment Methodology

As coral bleaching has a high spatial variability, the best scenario would have been to position instruments to maximise the geographic coverage of Palau. However, due to time constraints and a limited number of instruments this was not possible. A region that is influenced by a wide range of oceanic conditions was selected for instrumentation, to be representative of the situation in Palau. As discussed, a planned endeavour is to use numerical models to infer oceanic information in the Palau region. Instruments were positioned so as to provide boundary conditions for such models. To this end, most major entrances or channels were assigned a current meter or tide gauge to measure flows or sealevels in order to determine the fluxes into, or out of the system. Other instrumentation was then deployed within these regions to allow model validation and observe the thermal stratification at reasonably high temporal and spatial resolution.

A small vessel from The Nature Conservancy was used and a team of SCUBA divers secured the instruments to the reef slopes or sea floor. This meant that it was more practical to instrument the region adjacent to our base at PICRC in Koror. The nearby region also had the desired large range of topographic features; for example, a reef flat, lagoons, channels, rock islands, lakes and the open ocean.

Instruments were sourced principally from AIMS and were supplemented by others from UoG and CRRF. The instruments were deployed to, in effect, bound specific regions of interest. These boxes were named Lagoon (Figure 8), Malakal Harbour (Figure 9) and the Rock Islands near Koror (Figure 10). The lagoon box extended from the Philippine Sea in the West to a deep-water mooring off Uchelbeluu in the East. Ulong Island defined the southern boundary and the Paleo channel near the western entrance, mid-way up Babeldaob, was the northernmost limit. The Malakal box is contained within the Lagoon box and adjacent to the Rock Islands box. The next section describes the locations and instrumentation deployed at each location.

A deep-water mooring was deployed seaward of the outer reef at Uchelbeluu to gain an understanding of the oceanic conditions. The mooring was designed for a water depth of 120m, however due to the rapid descent of the seafloor, the mooring was positioned at 250m, 130m deeper than anticipated. This meant that the data were collected below the main thermocline.



Figure 2 Temperature Mooring ready for deployment.

Weather:

Meteorological observations for the period from January 1994 to April 2004 were acquired from the NOAA National Weather Service station in Palau. Due to nearby obstacles, the location of the NOAA weather station led to a lack of confidence in the wind measurements. A portable weather station was installed as a part of this study to compare with the existing long-term dataset. The weather station monitored standard meteorological parameters and also included solar radiation and Photosynthetically Active Radiation (PAR) sensors to monitor the solar insolation. This station was positioned high on a promontory in the northeast of Koror to ensure the best fetch in all directions.



Figure 3 Portable Weather station being set up by Cary McLean.

Temperature measurements:

Temperature loggers were positioned either individually or as vertical profiles. Profiles were realised by placing instruments on moorings or down reef slopes. The locations of the loggers were selected to monitor regions where vertical stratification of water may occur, or conversely where turbulent mixing may occur, and also to examine possible areas of upwelling.

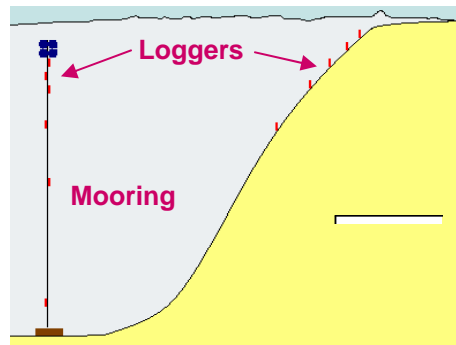


Figure 4 Schematic showing an in-line mooring and transect of temperature loggers.



Figure 5 Cary McLean secures an SBE39 temperature logger to a coral outcrop using stainless steel wire.

Current measurements:

An array of bottom mounted Acoustic Doppler Current Profilers (ADCP), as well as a number of point instruments, were deployed in reef channels, lagoons and flats to ensure a wide variety of current regimes. Current profilers monitor water movement through the entire depth of the water column using acoustic techniques and, thus, were deployed in deep channels at region boundaries. Point meters were located in shallow waters, at region boundaries and within the specified boxes.



Figure 6 Felipe Arzayus Recovering an ADCP.

Tide gauges:

While several of the temperature and current meters also contained pressure sensors, additional tide gauges were deployed to ascertain the sealevel response to weather, tides and larger scale circulation features in greater detail. Tide gauges were deployed on reef flats at region boundaries to monitor over-reef water fluxes. Tide gauges were located across the specified regions to determine the relative phase of tidal inundation across Palau. One tide gauge was positioned adjacent to the existing Malakal Harbour Tide Gauge, for a short period, to compare with the long-term dataset.

Salinity measurements:

Salinity can be determined by measuring the conductivity and temperature of water. An east-west transect of conductivity and temperature loggers was constructed to measure salinity and monitor the development of salinity fronts and hyper-saline conditions. The transect was positioned from the Philippine Sea, across the Palau lagoon, through Malakal Harbour and out to the eastern reef extreme.



Figure 7 Cary McLean securing an SBE16 Conductivity and Temperature logger.

Vertical profiles of Conductivity and Temperature with Depth (CTD):

A number of CTD profiles were measured to determine the vertical variation of water properties across the Palau region. These were performed using an instrument which measures conductivity, temperature, and pressure with a frequency of 4 Hz. The instrument was attached to a rope and lowered by hand through the water column. The speed of descent was controlled at approximately 1 m/s; the ascent of the CTD was performed at the same rate. This permitted a near-repeat measurement of the water properties.

Bathymetry measurements:

An essential input for numerical modelling is accurate bathymetry. Production of a satellite-derived bathymetry of Palau is underway at the NOAA National Ocean Service. The techniques being applied require calibration by *in situ* data. An echo-sounder was used to collect *in situ* depth measurements in a variety of regions across Palau. These data are not presented here but will be in the final bathymetry report.

Instrument Array Summary

A total of thirteen current meters, six tide gauges, five conductivity loggers, one weather station and thirty-seven individual temperature loggers were deployed in this experiment. Some instruments were positioned in two or more locations during the study; e.g., the thirteen current meters were deployed in fourteen locations.

Table 1, Table 2, Table 3 and Table 4 list the instruments, their deployment codes and geographic locations. Figure 8, Figure 9 and Figure 10 show the array locations overlaid on satellite imagery. Station coding was used to help distinguish the type of parameters measured, as shown in Table 1. Many instruments have sensing capabilities beyond their primary function listed below and thus measure additional properties (e.g., temperature is measured by the current profilers, tide gauges and conductivity probes).

Table 1 Station Codes and number of instruments

Code	Instrument	Number of Instruments
A	Current meter	13 total (9 Profiling - 2 Point S4s, 2 Point Nobskas)
B	Tide gauge	4 Brancker XR420 TD, 2 SBE39PT
C	Conductivity logger	5 SBE16CT
T	Temperature	37 SBE39, 4 SBE16CT, 1 Brancker XR420 TD, 1 RDI ADCP, 1 Nobska
WX	Weather station	1 Campbell Scientific

Table 2 lists the deployment summary ordered by the three specified regions or boxes: Lagoon, Malakal Harbour and the Rock Islands. The Malakal Harbour box completes the western boundary of the Lagoon box. Co-located instruments are grouped together in Table 2. Table 3 lists the instrument sites by the primary parameter measured; i.e., currents, sealevel, temperature and salinity.

Table 2 Instrument codes for each of the three specified regions. Co-located instruments are grouped together.

(a) Lagoon box

Code	Instrument	Serial no.	Depth	Location Description
A6	S4	564	33m	Paleo Channel - Toachel Mlengui
T6	SBE39T	<i>5 loggers</i>	20m	Philippine Sea - West reef flat
B5	SBE39PT	0760		
C1	SBE16CT	2123		
A7	Nobska	10046	14.5m	Falcon Reef - lagoon central
T1	SBE39T	<i>5 loggers</i>	to 20m	
C2	SBE16CT	2127		
A3	Nobska	10045	20m	Ulong West
A4	ADCP 300kHz	584 BT	>30m	Ulong East
T8	SBE39T	<i>5 loggers</i>	to 40m	
B4	Brancker XR420	10091	1m	
T7	SBE39T	<i>5 loggers</i>	to 18m	Central Rock Islands, Urukthapel
B3	Brancker XR420	10093	6m	
A13	Nortek Aquapro	0866 CRRF	>30m	Toachel mid

A2	S4	615	4m	Ngetalau passage (channel) outside Rock Is.
A5 T5 C5	ADCP 300kHz SBE39T SBE16CT	412 BTP <i>5 loggers</i> 2125	215m to	Uchelbeluu

(b) Malakal Harbour box

<u>Code</u>	<u>Instrument</u>	<u>Serial no.</u>	<u>Depth</u>	<u>Location Description</u>
A10	ADCP 1200kHz	1292 UoG	22m	Toachel Ra Ngel
B2	SBE39PT	0759	1.9m	Ngedarrak Reef flat
A8 T2 C4	ADCP 600kHz	3228 BTPW	30m	Lighthouse Toachel Ra Kesebekuu
A9 C3	Nortek Aquapro	0794	27.7m	Malakal Harbor Pincers
B6	Brancker XR420	10093	2m	Malakal Harbour Tide Gauge (moved from B3)

(c) Rock Islands box

<u>Code</u>	<u>Instrument</u>	<u>Serial no.</u>	<u>Depth</u>	<u>Location Description</u>
B1	Brancker XR420	10079	2.5m	RI Toirius
A11	ADCP 600kHz	1673	22m	RI northern channel entrance
A11b	ADCP 1200kHz	1292 UoG	22.6m	RI northern channel entrance
A11c	Nortek Aquapro	0866 CRRF	>30m	RI northern channel entrance
A14	ADCP 1200kHz	1292 UoG	4m	Japanese channel
A12	Nortek Aquadopp	0970 CRRF	11.4m	RI southern reef opening
A1	ADCP 1200kHz	0974	24.2m	RI mid channel
T3	SBE39T	<i>5 loggers</i>	20m	RI inside channel
T4	SBE39T	<i>5 loggers</i>	20m	RI Nikko lake

Table 3 Instrument codes listed by primary instrument type

(a) Current Profilers and Point Meters

<u>Code</u>	<u>Instrument</u>	<u>Serial no.</u>	<u>Depth</u>	<u>Location Description</u>
A1	ADCP 1200kHz	974	25m	RI mid channel
A2	S4	615	4m	Ngetalau passage outside rock is.
A3	Nobska	10045	16m	Ulong West
A4	RDI ADCP 300kHz	584 BT	30+m	Ulong East
A5	RDI ADCP 300kHz	412 BTP	126m	Uchelbeluu
A6	S4	564	30m	Paleo Channel - Toachel Mlengui
A7	Nobska	10046	25m	Falcon Reef - lagoon central
A8	RDI ADCP 600kHz	3228 BTPW	30m	Lighthouse Toachel Ra Kesebekuu
A9	Nortek Aquapro	1015	30m	Malakal Harbor Pincers
A10	ADCP 1200kHz	1292	17m	Toachel Ra Ngel
A11	RDI ADCP 600kHz	1673	25m	RI northern channel entrance
A11b	ADCP 1200kHz	1292	22.6m	RI northern channel entrance

A11c	Nortek Aquapro	0866	>30m	RI northern channel entrance
A12	Nortek Aquadopp	0970	12m	RI southern reef opening
A13	Nortek Aquapro	0866	30m	Toachel mid
A14	ADCP 1200kHz	1292	4m	Japanese channel

(b) Temperature Profiles

Code	Instruments	Other	Depth	Location Description
T1	4 SBE39s	C2	20m	Falcon Reef - lagoon central
T2	4 SBE39s	C4	20m	Lighthouse Toachel Ra Kesebekuu
T3	5 SBE39s		20m	RI inside channel
T4	5 SBE39s		18m	RI Nikko Bay
T5	5 SBE39s	C5	250m	Deep water mooring Uchelbeluu
T6	4 SBE39s	C1 B5	30m	Philippine Sea – West reef flat
T7	5 SBE39s	B3	18m	Central Rock Islands, Urukthapel
T8	4 SBE39s	B7	45m	Ulong East Channel

(c) Tide Gauges

Code	Instrument	Serial no.	Depth	Location Description
B1	Brancker XR420	10079	4m	RI Toirius
B2	SBE39PT	759	4m	Reef flat Ngedarrak Reef
B3	Brancker XR420	10093	18m	Central Rock Islands, Urukthapel
B3B	Brancker XR420	10093	4.5m	East of Blue Corner
B3C	Brancker XR420	10093	2.5m	North Babeldaup
B4	Brancker XR420	10091	30m	Ulong East
B5	SBE39PT	760	20m	Philippine Sea – lagoon side reef flat
B6	Brancker XR420	10093	2m	Malakal Harbour Tide Gauge

(d) Conductivity loggers

Code	Instrument	Serial no.	Depth	Location Description
C1	SBE16CT	2123	5.5m	Philippine Sea
C2	SBE16CT	2127	5.0m	Falcon Reef
C3	SBE16CT	2126	2.6m	Malakal Harbour Pincers
C4	SBE16CT	2124	1.5m	Lighthouse Toachel Ra Kesebekuu
C5	SBE16CT	2125	160m	Uchelbeluu

Table 4 Locations of instruments and other points of interest

(a) Instrument locations

Code	Latitude, Longitude	Location Description
A1	7,19.786,134,29.637	RI mid channel
A2	7,19.315,134,29.400	Ngetalau passage
A3	7,18.293,134,16.726	Ulong West
A4B4	7,16.617,134,18.716	Ulong East
A4	7,16.621,134,18.681	Subsurface buoy
A5T5C5	7,15.918,134,33.398	Uchelbeluu
A6	7,28.927,134,27.776	Paleo Channel – Toachel Mlengui
A7T1C2	7,22.424,134,23.231	Falcon Reef
A8T2C4	7,16.991,134,27.928	Lighthouse Toachel Ra Kesebekuu
A9C3	7,20.163,134,25.483	Malakal Harbour Pincers
A10	7,17.786,134,28.958	Toachel Ra Ngel

A11	7,19.400,134,28.949	RI northern channel entrance
A12	7,19.223,134,29.795	RI southern reef opening
A13	7,19.023,134,31.490	Toachel mid
A14	7,17.786,134,28.958	Japanese Channel
T3	7,19.570,134,29.417	RI Inside channel
T4	7,19.772,134,30.034	RI Nikko Bay
T6C1	7,24.713,134,20.258	Philippine Sea
T7B3	7,16.376,134,24.667	Urukthapel
T8	7,16.621,134,18.802	Ulong East Channel
B1	7,19.821,134,28.878	RI
B2	7,17.472,134,28.282	Ngedarrak Reef flat
B3	7, 16.376 134, 24.667	Central Rock Islands, Urukthapel
B3B	7,8.4912,134, 17.8275	East of Blue Corner
B3C	7,46.60848, 134, 35.1582	North Babeldaup
B4	07,16.621, 134,18.680	Ulong East
B5	7,24.380,134,21.065	Philippine Sea – Lagoon reef
B6	7,20.011,134,27.430	Malakal Harbour Tide Gauge
C1	7,24.713,134,20.258	Philippine Sea
C2	7,22.424,134,23.231	Falcon Reef
C3	7,20.163,134,25.483	Malakal Harbour Pincers
C4	7,16.991,134,27.928	Lighthouse Toachel Ra Kesebekuu
C5	7,15.918,134,33.398	Uchelbeluu
WXSTA	7,20.969,134,30.018	Weather Station

(b) Additional locations

<u>Code</u>	<u>Latitude, Longitude</u>	<u>Location Description</u>
L10CRRF	7,19.786,134,29.637	Lighthouse 10m CRRF
L2 CRRF	7 16.613,134,27.067	Lighthouse 2m CRRF
Falcon Reef	7 22.400,134,23.240	Falcon Reef CRRF
Malakal Hbr	7 19.008,134,27.627	Malakal Hbr CRRF
Ngaregabel Rf	7 24.725,134,27.006	Ngaregabel Reef CRRF
Ngerkul Gap	7 19.170,134,29.779	Ngerkul Gap CRRF
Nikko Bay	7 20.049,134,30.301	Nikko Bay CRRF
Ongael Basin	7 15.053,134,22.479	Ongael Basin CRRF
Ongael out	7 14.964,134,22.471	Ongael Outside CRRF
ShortDropOff	7 16.418,134,31.440	Short Drop Off CRRF
Ulong 10	7 17.425,134,14.463	Ulong Rock 10m CRRF N
Ulong 55	7 17.453,134,14.442	Ulong Rock 55m CRRF N
West Channel	7 32.560,134,28.059	West Channel CRRF
LIGHTH	7 16.927,134,27.881	Lighthouse

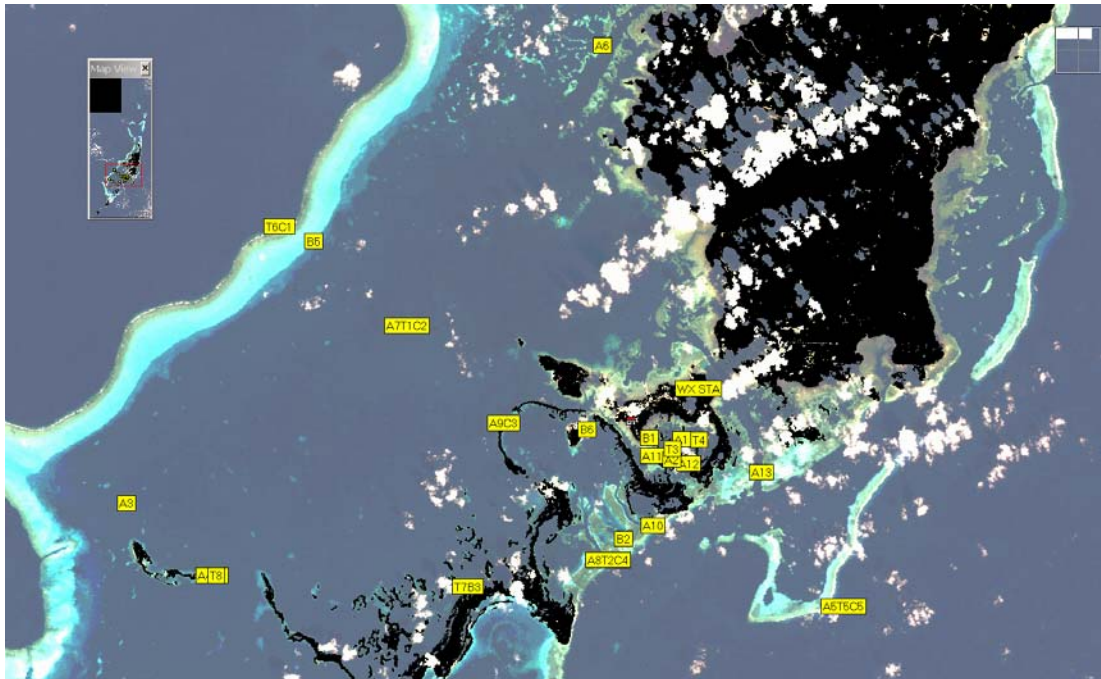


Figure 8 IKONOS satellite image of Palau. The Lagoon box covers the area shown. Deployed instruments are indicated by their codes. Orientation of zoomed areas in Figure 9 and Figure 10 may be performed using these codes.



Figure 9 Zoomed image of the Malakal Harbour box from Figure 8.



Figure 10 Zoomed image of the Rock Islands box from **Figure 9**.

Temperature Transect and Mooring Summary

The following tables summarise all of the instrumentation on each of the transects or in-line moorings. Further, instrument-specific information can be found in Appendices [B](#), [C](#), [D](#) and [E](#). Instruments are numbered from the bottom up - T1i1 indicates transect one, instrument 1 (the deepest instrument). T1i6 is the shallowest instrument in the same transect. Figure 11 depicts a typical reef transect; Figure 12 and Figure 13 illustrate the moorings deployed at locations T5 and T8, respectively.

After the tables are calculations to estimate each instrument depth relative to Lowest Astronomical Tide (LAT). The Malakal Harbour sealevel was used to estimate the tide height when observations of water depth were taken by diver pressure gauges. There were usually 2 estimates taken: one upon deployment and one at recovery. There may be missing data; however, the best estimate was included in the table proper. Deployment times are all UTC+9 hours; i.e., the local Palau time.

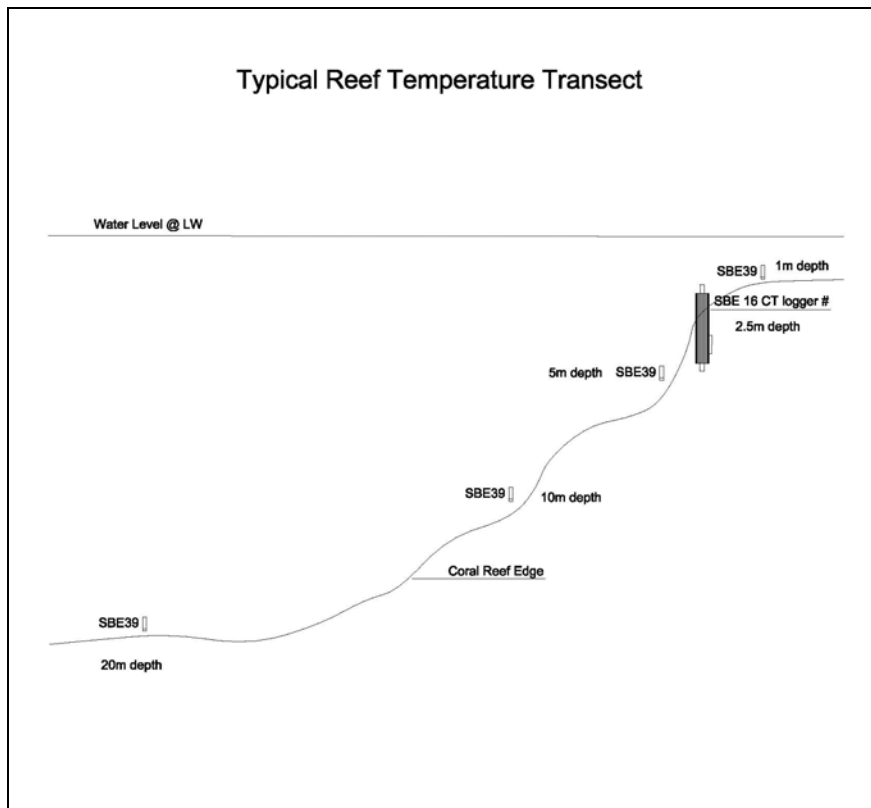


Figure 11 Typical configuration of a reef temperature transect.

T1 + A7 + C2 Falcon Reef

7° 22.424' N 134° 23.232' E 45m Total Depth

First Good: 8 Sep 2003, 14:00:00

Last Good: 3 Jan 2004, 14:30:00

	<u>Depth</u> (LAT)	<u>Instrument</u>	<u>Serial</u>	<u>Filename</u>
T1i6	1.9m	SBE39T	0935	09350401.asc
T1i5	2.9m	SBE39T	0929	09290401.asc
T1i4 C2	5.1m	SBE16CT	2127	21270401.hex
T1i3	8.2m	SBE39T	0920	09200401.asc
T1i2 A7	11.3m	Nobska	10046	10046.bin
T1i1	19.4m	SBE39T	0934	09340401.asc

		T16	T15	T14	T13	T12	T11
Deployment	depth(m)	2.5	3.5	6	9	14.5	20
Malakal slv		1.13	1.06	1.00	0.74	1.82	0.72
Recovery	depth(m)	3.7	4.7	6.9	10	13.1	21.4
Malakal slv		1.82	1.83	1.83	1.83	1.85	1.85
LAT = depth-slvs		1.9	2.9	5.1	8.2	11.3	19.4

T2 + A8 + C4 Lighthouse Toachel Ra Kesebekuu

07°16.955'N, 134°27.932'E 30m Total Depth

First Good: 31 Aug 2003, 16:00:00

Last Good: 31 Dec 2003, 08:00:00

	<u>Depth</u> (LAT)	<u>Instrument</u>	<u>Serial</u>	<u>Filename</u>
T2i6	1.3m	SBE39T	925	09250801.asc
T2i5 C4	1.5m	SBE16CT	2124	21240301.asc
T2i4	5.1m	SBE39T	933	09330801.asc
T2i3	9.2m	SBE39T	1054	10540801.asc
T2i2	21.6m	SBE39T	1052	10520801.asc
T2i1 A8	27.7m	RDI	3228	pal02000.000

		T26	T25	T24	T23	T22	T21
Deployment	depth(m)	1	2.5	5	10	20	30
Malakal slv		1	0.97	0.95	0.93	0.92	2.29
Recovery	depth(m)	3.1	2.7	6.9	11	23.4	-
Malakal slv		1.81	1.86	1.83	1.83	1.82	1.85
LAT = depth-slvs		1.3	1.5	5.1	9.2	21.6	27.7

T3 Rock Islands, inside channel

7° 19.570' N 134° 29.418 E 19m Total Depth

First Good: 29 Aug 2003, 15:30:00

Last Good: 30 Dec 2003, 15:00:00

	<u>Depth</u> (LAT)	<u>Instrument</u>	<u>Serial</u>	<u>Filename</u>
T3i5	1.0m	SBE39T	1055	10550301.asc
T3i4	1.9m	SBE39T	1058	10583112.asc
T3i3	4.3m	SBE39T	0676	06763112.asc
T3i2	8.9m	SBE39T	0675	06753112.asc
T3i1	18.9m	SBE39T	1057	10573112.asc

		T35	T34	T33	T32	T31
Recovery	depth(m)	2.6	3.5	5.9	10.5	20.5
Malakal slv		1.65	1.65	1.65	1.64	1.63
LAT = depth-slv		1.0	1.9	4.3	8.9	18.9

T4 Rock Islands, Nikko Lake

7° 22'.424 N 134° 23'.232 E 19.7m Total Depth

First Good: 30 Aug 2003, 18:00:00

Last Good: 30 Dec 2003, 15:30:00

	<u>Depth</u>	<u>Instrument</u>	<u>Serial</u>	<u>Filename</u>
T4i5	0.9m	SBE39T	1059	10593112.asc
T4i4	1.1m	SBE39T	1051	10513112.asc
T4i3	3.9m	SBE39T	1061	10613112.asc
T4i2	9.3m	SBE39T	1060	10603112.asc
T4i1	16.2m	SBE39T	1053	10533112.asc

		T45	T44	T43	T42	T41
Deployment	depth(m)	1	2.5	5	10.6	17.6
Malakal slv		1.48	1.45	1.38	1.34	1.26
Recovery	depth(m)	2.4	2.6	5.4	10.8	17.6
Malakal slv		1.52	1.51	1.50	1.50	1.49
LAT = depth-slv		0.9	1.1	3.9	9.3	16.1

T5 + A5 + C5 Uchelbeluu (deepwater mooring)

07°15.545'N 134° 33.167 E 124m Total Depth

First Good: 17 Sep 2003, 12:00:00

Last Good: 13 Jan 2004, 14:00:00

	<u>Depth</u> (LAT)	<u>Instrument</u>	<u>Serial</u>	<u>Filename</u>	
T5i6 C5	150m	SBE16	2125	21251401.hex	Bad data
T5i5	160m	SBE39PT	1062	10621401.asc	
T5i4	170m	SBE39T	931	09311401.asc	
T5i3	190m	SBE39T	923	09231401.asc	
T5i2 A5	215m	RDI	412	Pal09000.000	
T5i1	225m	SBE39T	927	09271401.asc	
		Sounder		t55	t52
Deployment	depth(m)	126m 1100	17/9/03	159.5	215
Malakal slv		1.9m		1.9	1.9
LAT = depth-slv		124		157.6	213

Uchelbeluu Mooring

Pos: 7° 15.918' N
134° 33.398' E
In water 1100 17/9/03
Depth 126m

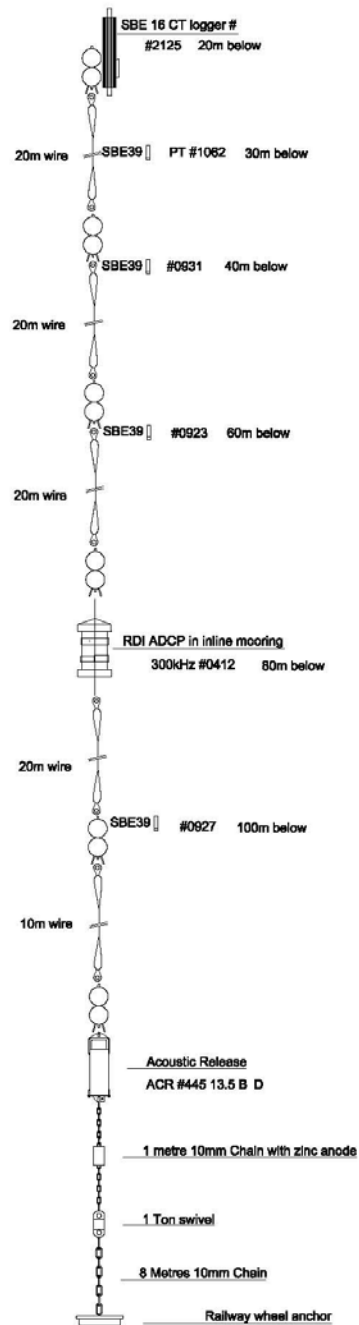


Figure 12 T5 Mooring design.

T6 + C1 Central Philippine Sea – West Reef flat

7° 16.955' N 134° 27.932' E 16 m Total Depth

First Good: 12 Sep 2003, 11:00:00

Last Good: 14 Jan 2004, 11:00:00

	<u>Depth</u>	<u>Instrument</u>	<u>Serial</u>	<u>Filename</u>		
T6i5	1m	SBE39T	1137	Not recovered		
T6i4	3m	SBE39T	928	09281401.asc		
T6i3 C1	5.5m	SBE16	2123	21231401.hex		
T6i2	10.5m	SBE39T	917	09171401.asc		
T6i1	22.5m	SBE39T	924	09241401.asc		
		T65	T64	T63	T62	T61
Deployment	depth(m)	3	4.5	7	12	24
Malakal slv		2.00	1.82	1.96	1.91	1.89
Recovery	depth(m)	-	5.3	7.5	12.5	24.5
Malakal slv		-	1.96	1.96	1.96	1.96
LAT = depth-slv		1	3	5.5	10.5	22.5

T7 + B3 Southern Rock Islands

7° 16.955' N 134° 27.932' E 16 m Total Depth

First Good: 2 Sep 2003, 10:00:00

Last Good: 2 Jan 2004, 15:30:00

	<u>Depth</u>	<u>Instrument</u>	<u>Serial</u>	<u>Filename</u>
T7i5	0.2m	SBE39T	1056	10560301.asc
T7i4	1.5m	SBE39T	0926	9260301.asc
T7i3	3.7m	SBE39T	0919	09190903.asc
T7i3b B3	3.7m	XR420	10093	100931103.dat
T7i3c	3.7m	SBE39T	0732	From T7i1
T7i2	11.3m	SBE39T	0930	09300301.asc
T7i1	16.0m	SBE39T	0732	07320401.asc

n.b., 23 Sep, 2003 SBE39 #0919 replaced with Brancker XR420 #10093

n.b., 5 Nov, 2003 Brancker XR420 #10093 replaced with SBE39 #0732 from 19m into the 3.8m position.

		T75	T74	T73	T73b	T73c	T72	T71
Deployment	depth(m)	1.5	3.0	6.0	5.0	-	12.0	18.0
Malakal slv		2.0	2.05	2.03	1.26	-	2.00	1.96
Recovery	depth(m)	2.0	3.3	5.0	-	5.5	13.2	-
Malakal slv		1.83	1.83	1.28	-	1.84	1.86	-
LAT = depth-slv		0.2	1.5	3.7	3.7	3.7	11.3	16.0

T8 Ulong East Channel

7° 16'.621 N 134° 18'.802 E 42m Total Depth

First Good: 23 Sep 2003, 09:00:00

Last Good: 13 Jan 2004, 12:30:00

	<u>Depth</u>	<u>Instrument</u>	<u>Serial</u>	<u>Filename</u>
T8i6	4m	SBE39T	918	09181401.asc
T8i5	4.2m	XR420	10092	0100921401.dat
T8i4	8m	SBE39T	932	09321401.asc
T8i3	13m	SBE39T	922	09221401.asc
T8i2	23m	SBE39T	921	09211401.asc
T8i1	43m	SBE39T	916	09161401.asc

n.b., top logger was 6m at high water from diver obs. 0818 23/9/03

Use tide gauge for final datum adjustment

	T8
Deployment depth(m)	43m 1135 22/9/03
Malakal slv	0.93
LAT = depth-slv	42m

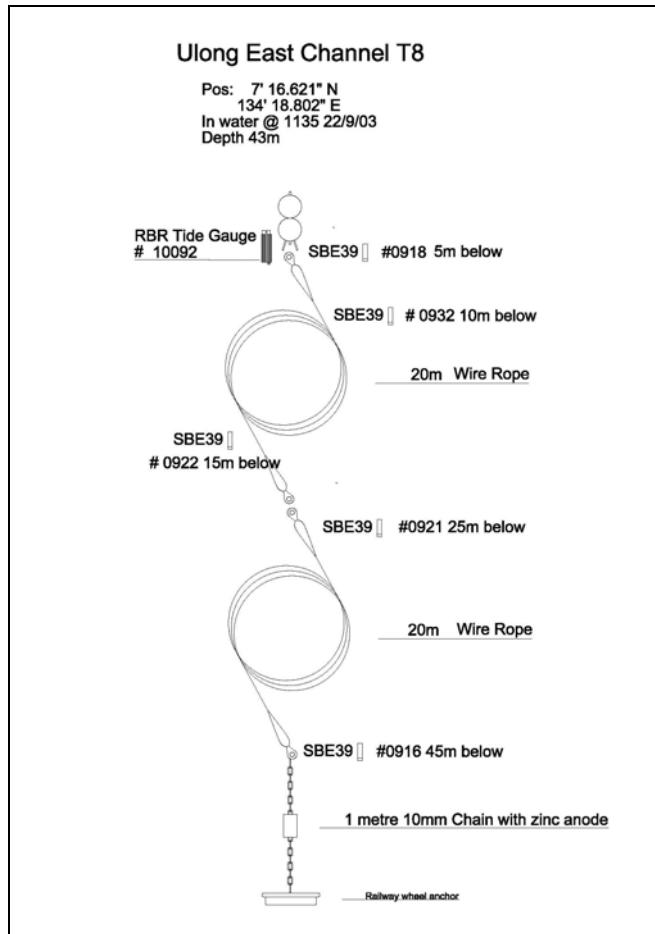


Figure 13 T8 mooring design.

Instruments and Processing

This section provides internet links to descriptions of each of the instruments by the manufacturer. Specifications and capabilities are outlined. The sheets can be obtained from the manufacturers' websites directly through the links and are also included on the companion archive DVD-ROM of this report. See [Appendix N](#) for a description of where they are located.

Calibrations

The calibration information for each instrument is contained within the headers of the binary and ASCII files directly downloaded from the instrument.

The current meters are acoustic and are difficult to calibrate in the field. The point current meters can, in general, be placed in a flow tank for calibration; however, such a facility was not available. As the Nobska point current meters had not been previously deployed, they were placed in a water bath for calibration to a zero flow reading. They were subsequently placed off the wharf at PICRC on short deployments (one tidal cycle) to gain confidence in the readings.

The tide gauges and most of the SBE39 temperature loggers were less than 12 months old and so the calibrations supplied by the manufacturer were assumed to still be valid. The Brancker tide gauges initially had unacceptably large clock drift, due to a poor batch of electronic chips. These instruments were replaced in time for the field programme.

Temperature inter-calibrations were undertaken after deployment to check the consistency of the instruments with each other. After recovery, the instruments collected that day were placed together in the ocean water outside of PICRC, usually overnight. They were then brought inside an air-conditioned room and placed in a water bath for a number of hours in order for the temperature to equilibrate. This ensured a reasonable temperature range for any linear adjustment, if found to be necessary.

Plots of all the temperatures collected from all the loggers have been made and are shown in [Appendix G](#). By grouping them from the same mooring or transect, an effective inter-calibration can be made during well-mixed periods. The best period for this was late November as the water cooled by at least one degree Celsius from near bleaching conditions. The temperatures converge and track down together until more benign weather conditions prevailed, allowing stratification to re-establish.

Of all the instruments, only two look anomalous; both were on the T2 transect. The deepest instrument, at 30.6m (red line), was the ADCP A8 and its temperature record indicates slightly higher readings than instruments above it. A linear correction in this case should be adequate. The second anomalous instrument was SBE39, serial number 1054. It was located at a depth of 9m and shows significantly higher readings than instruments above and below it. It appears a linear correction will also suffice in this case.

The SBE16CT logger called C5 and T5i6 only worked intermittently, so care should be taken when using this record. For this reason, it was not included in the consolidated mooring plot of temperatures. The data plot for this instrument is shown with the conductivity loggers in [Appendix J](#).

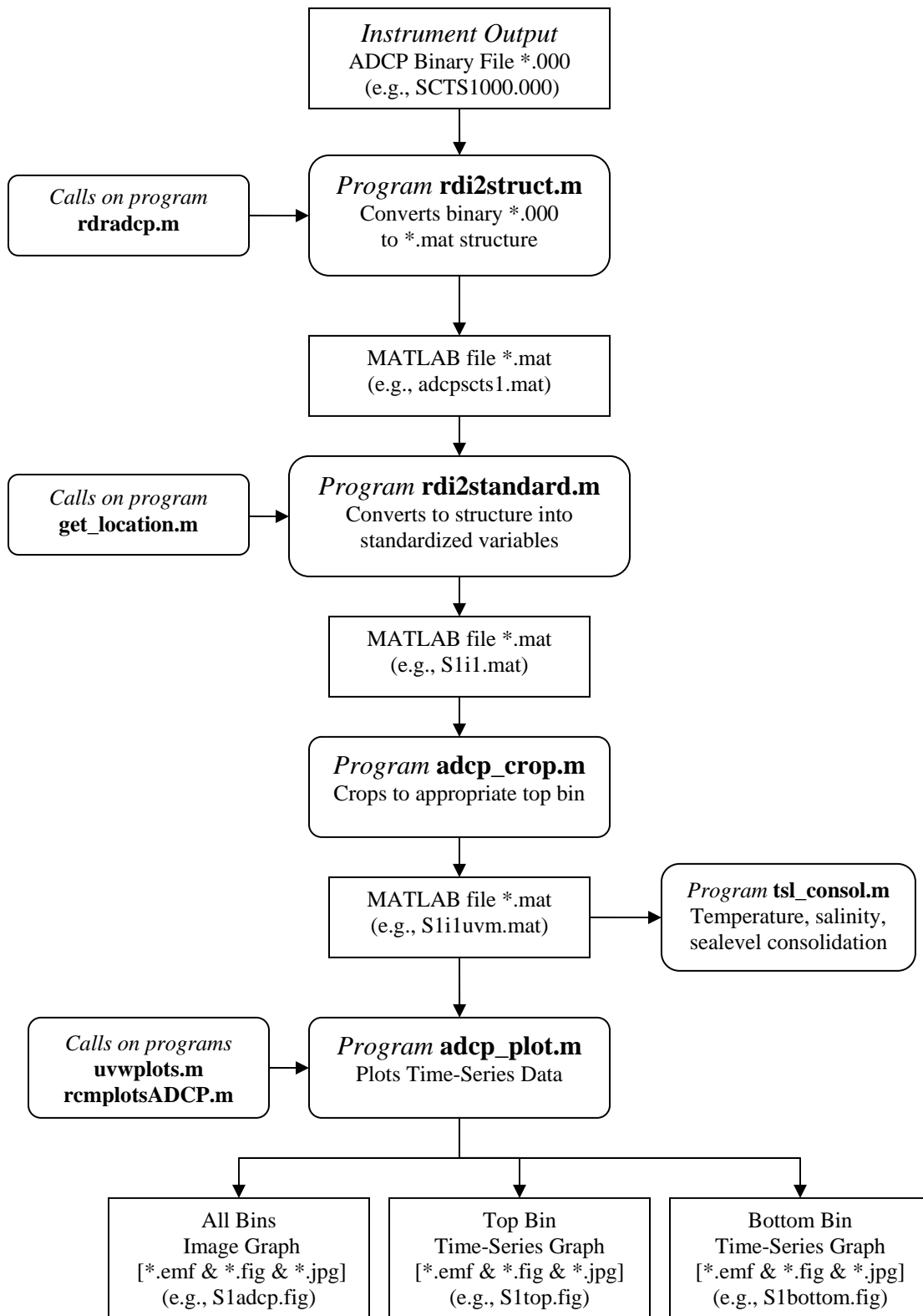
Data Processing

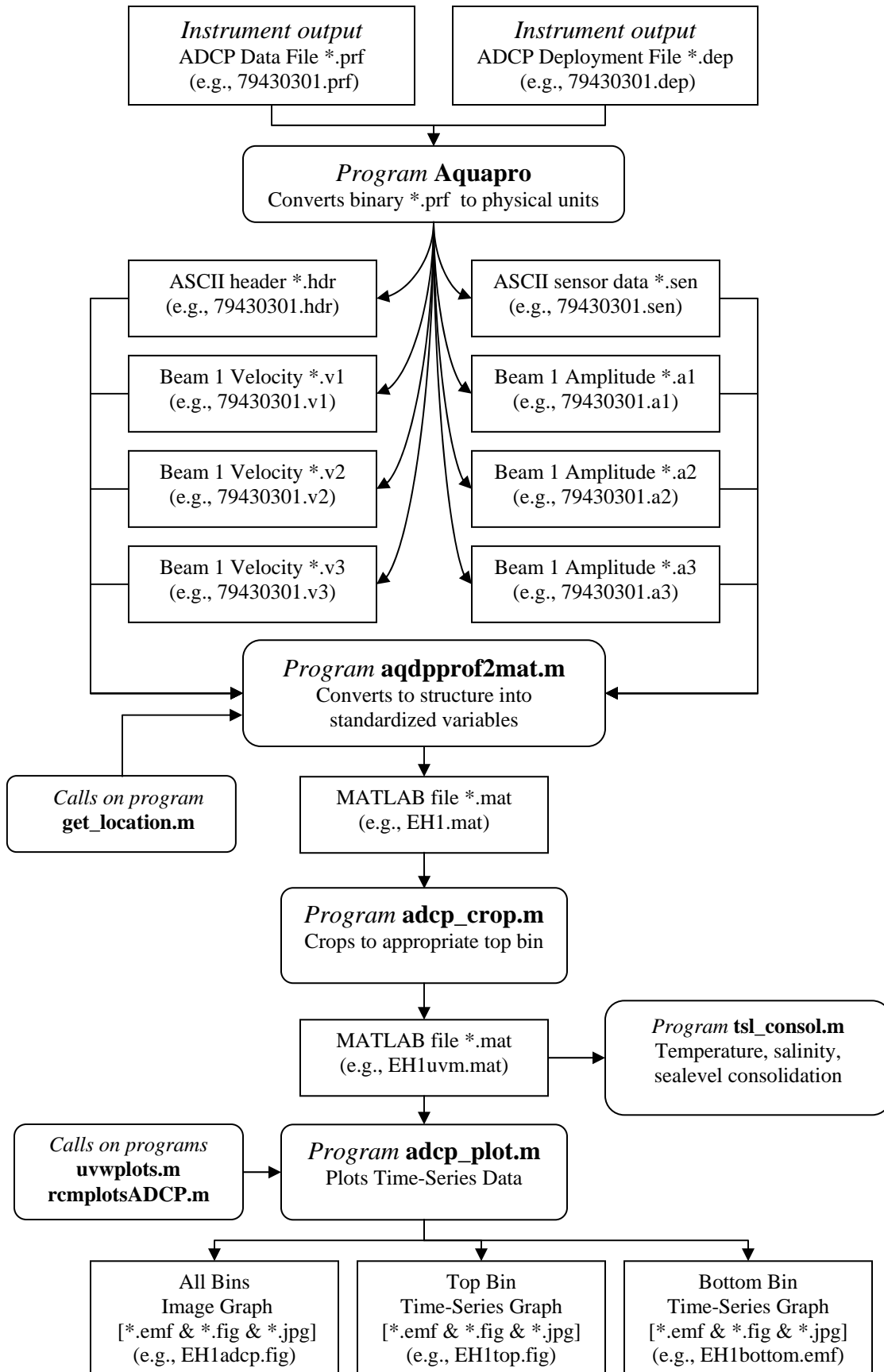
Data processing algorithms are described here using flow charts (pp. 24-34).

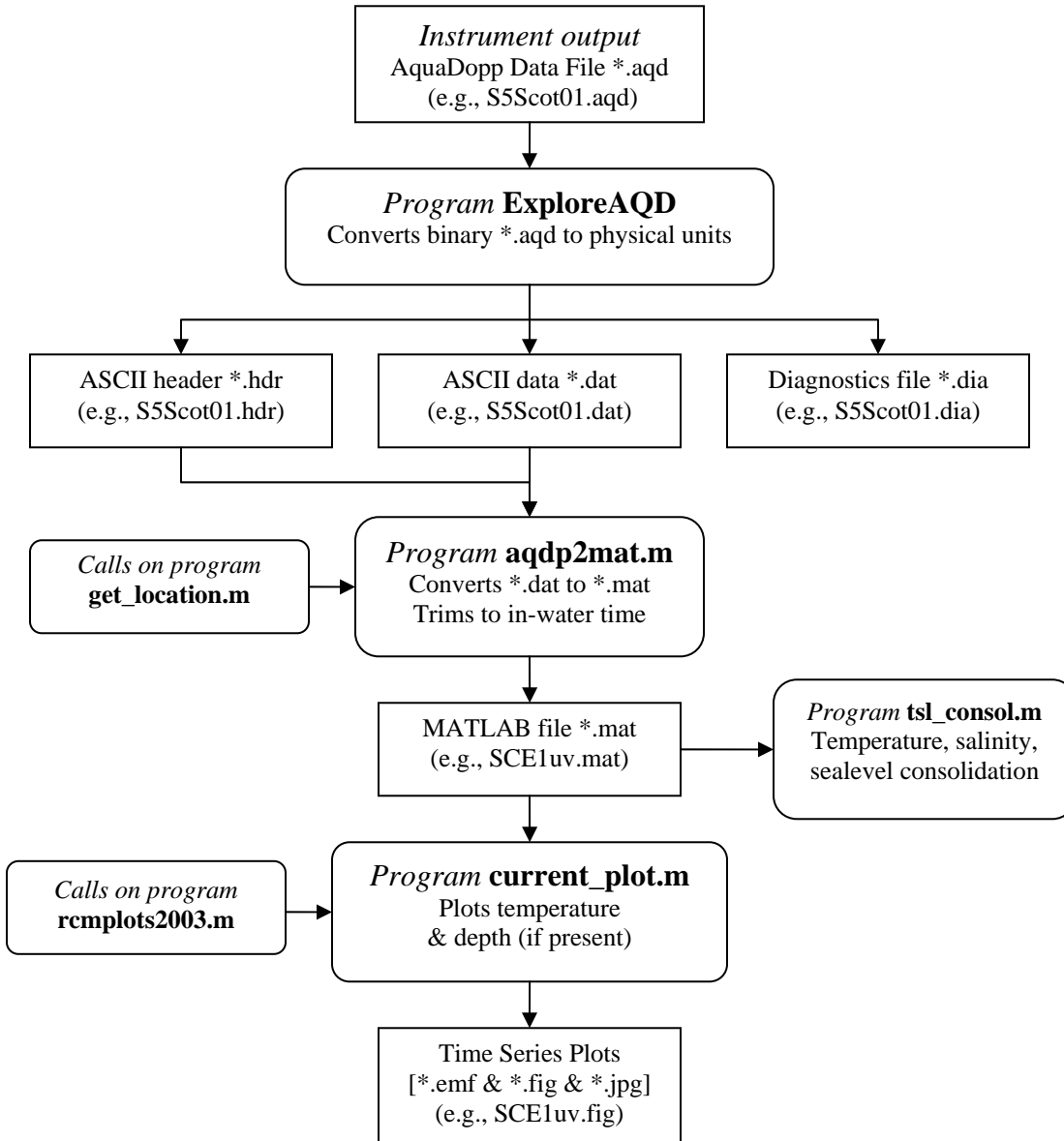
Current Meters

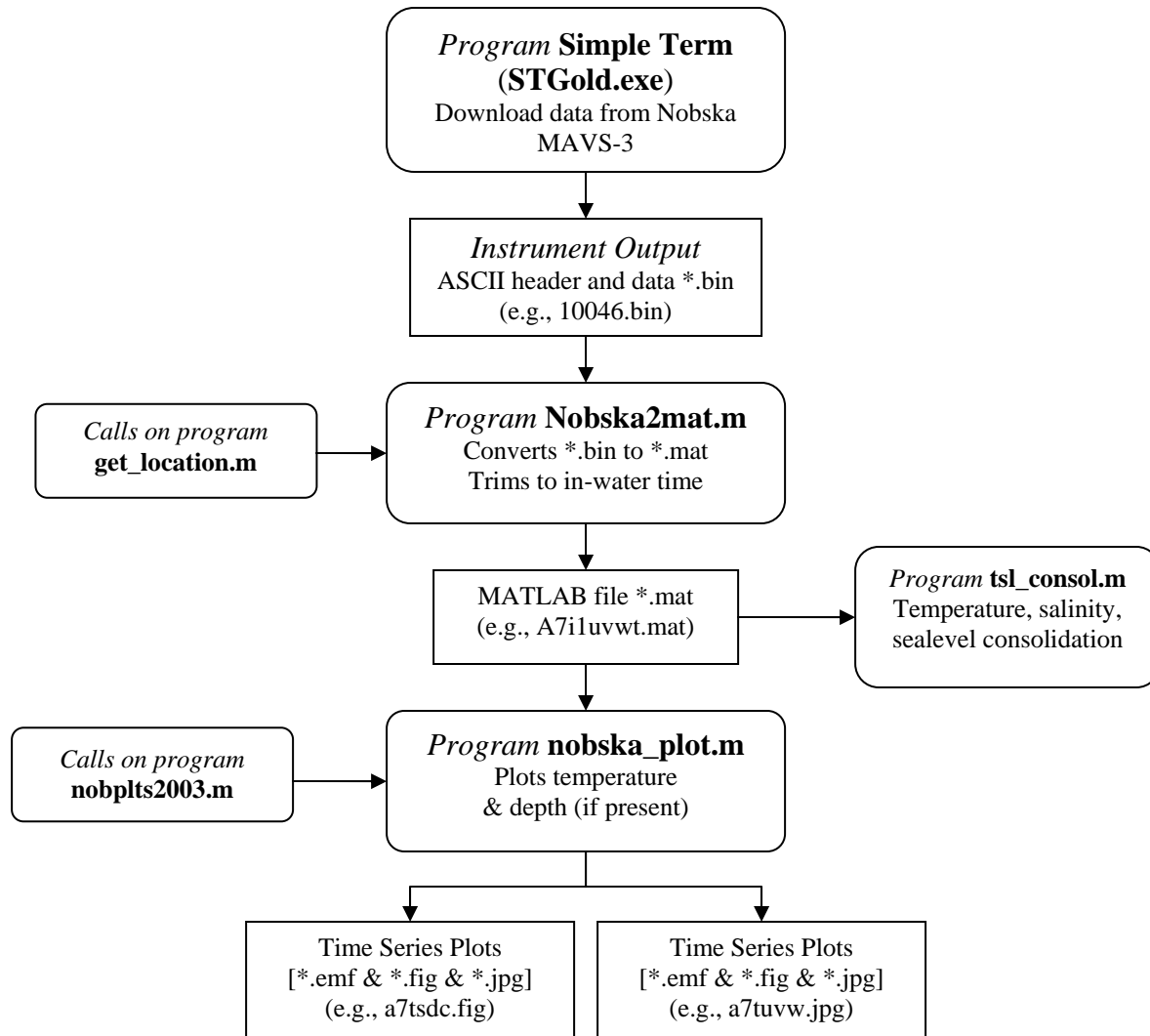
RD Instruments ADCP

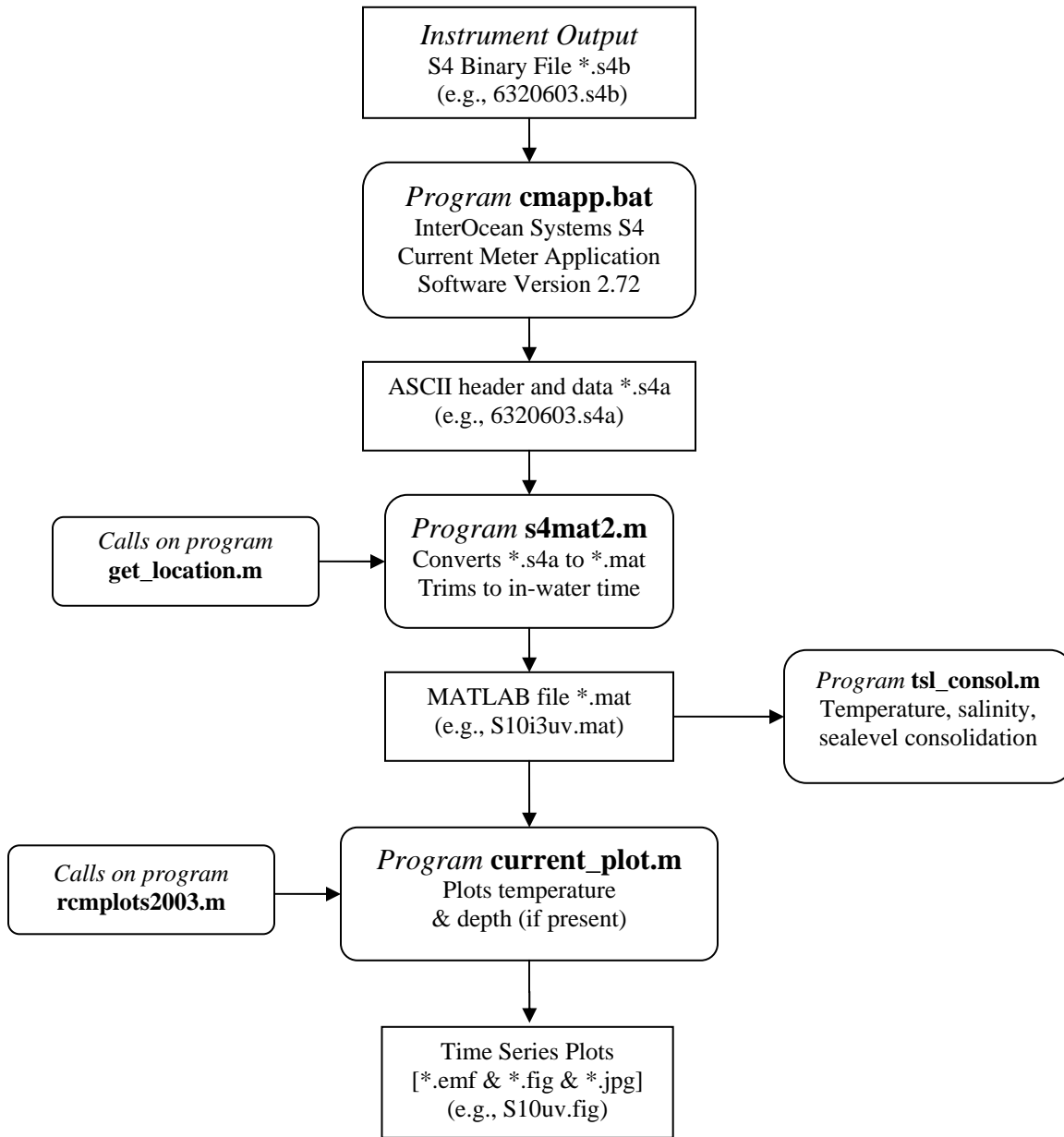
<http://www.rdinstruments.com/sen.html>







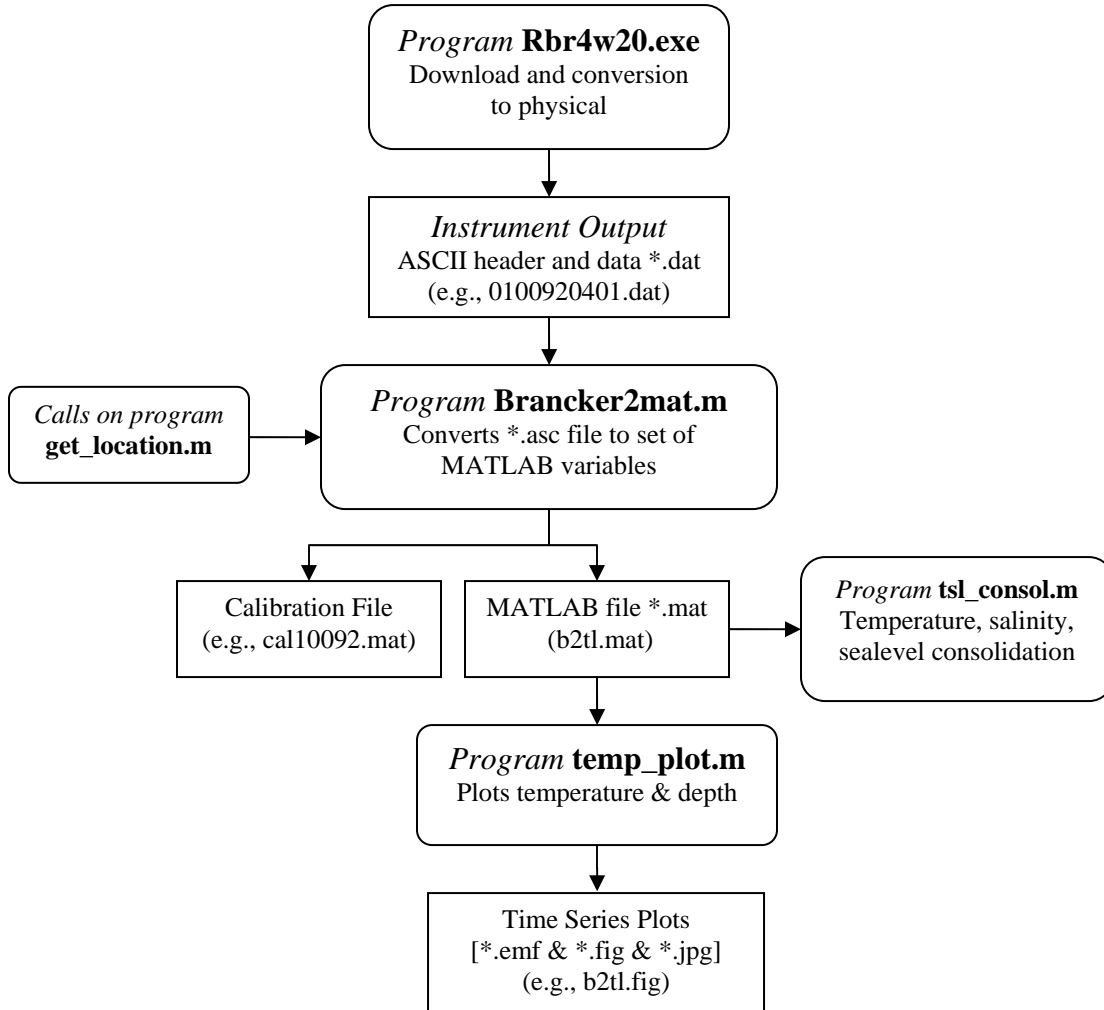




Tide Gauge

Brancker XR-420 TD

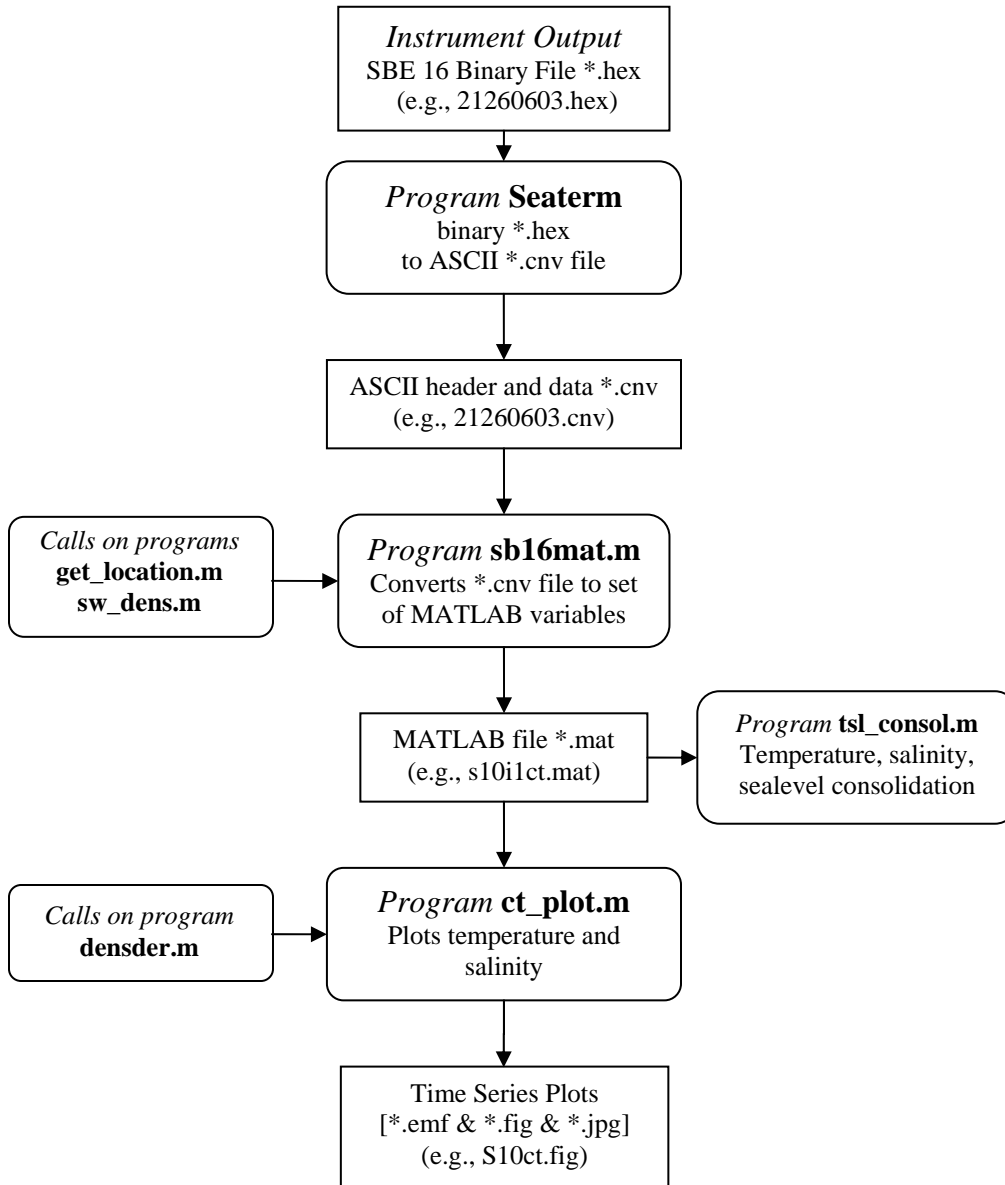
<http://www.rbr-global.com/XR-420TG.htm>



Conductivity Logger

SBE16

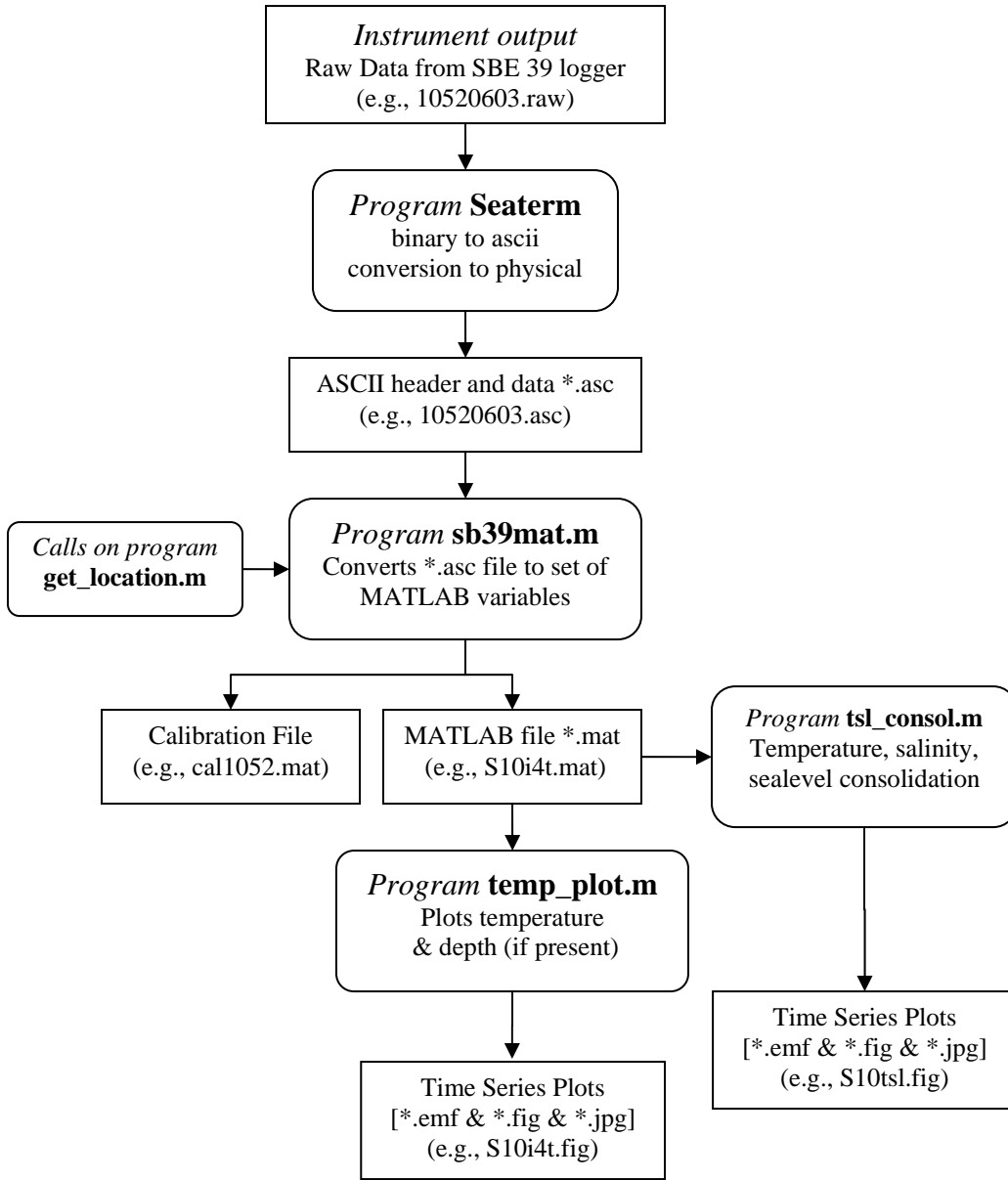
http://www.seabird.com/products/spec_sheets/16plusdata.htm



Temperature Loggers

SBE39

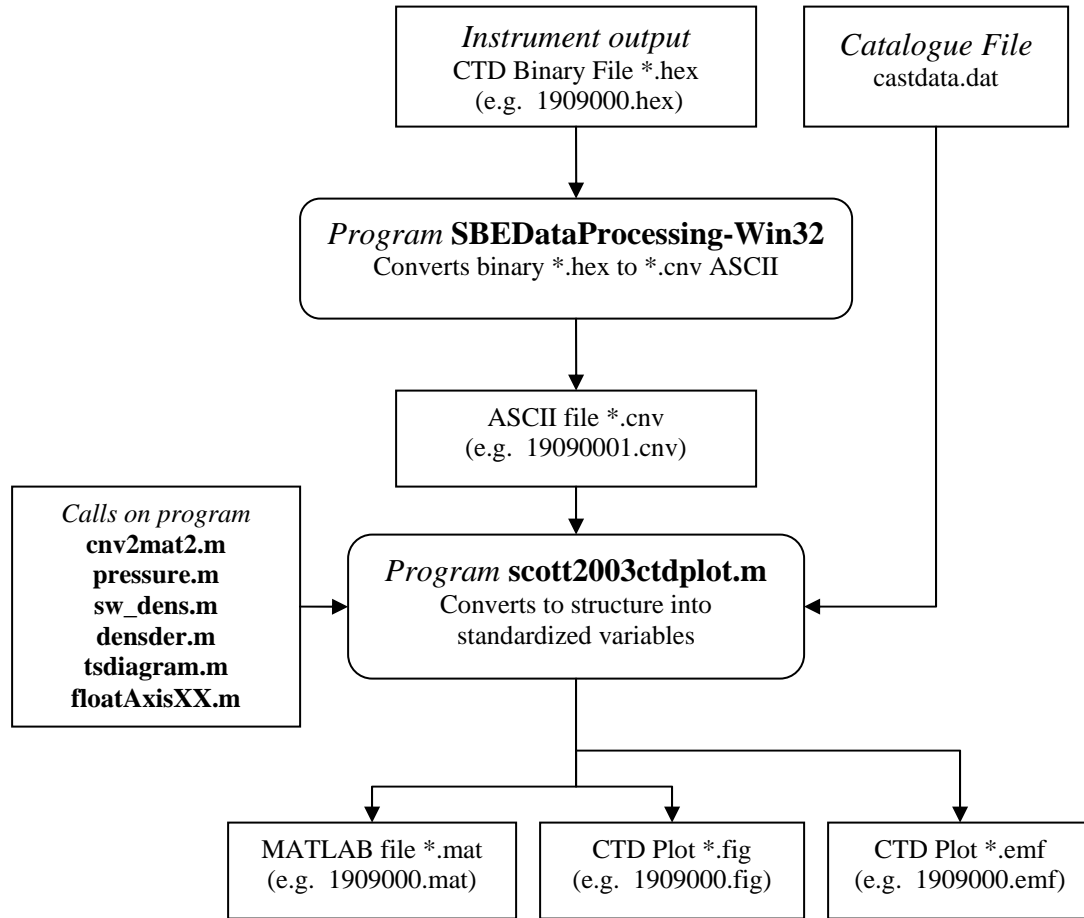
http://www.seabird.com/products/spec_sheets/39data.htm



CTD Profiler

SBE19

http://www.seabird.com/products/spec_sheets/19plusdata.htm



Weather Station

Campbell Scientific

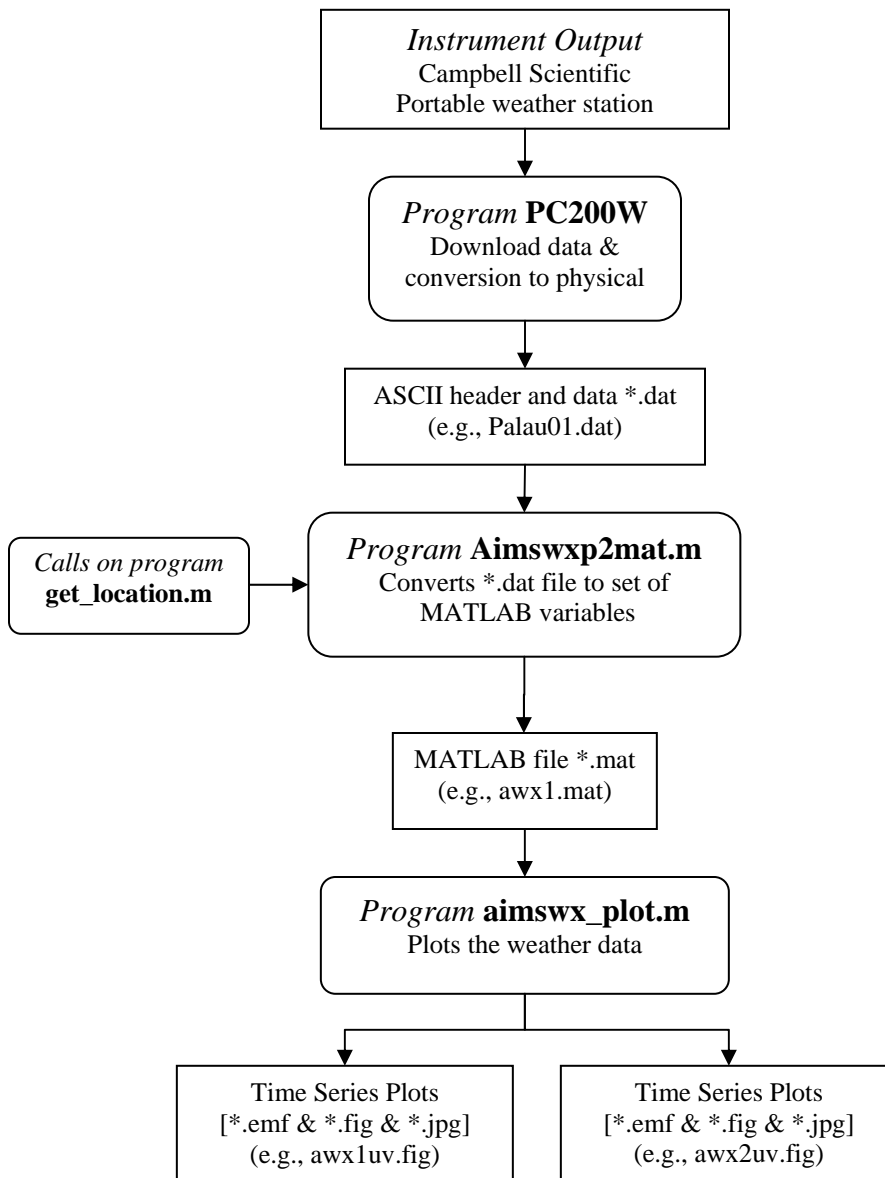
<http://www.campbellsci.com/>

This measures wind speed, direction, air temperature, photosynthetically active radiation (PAR), short wave radiation.

Relative humidity: http://www.campbellsci.com/temp_rh.html

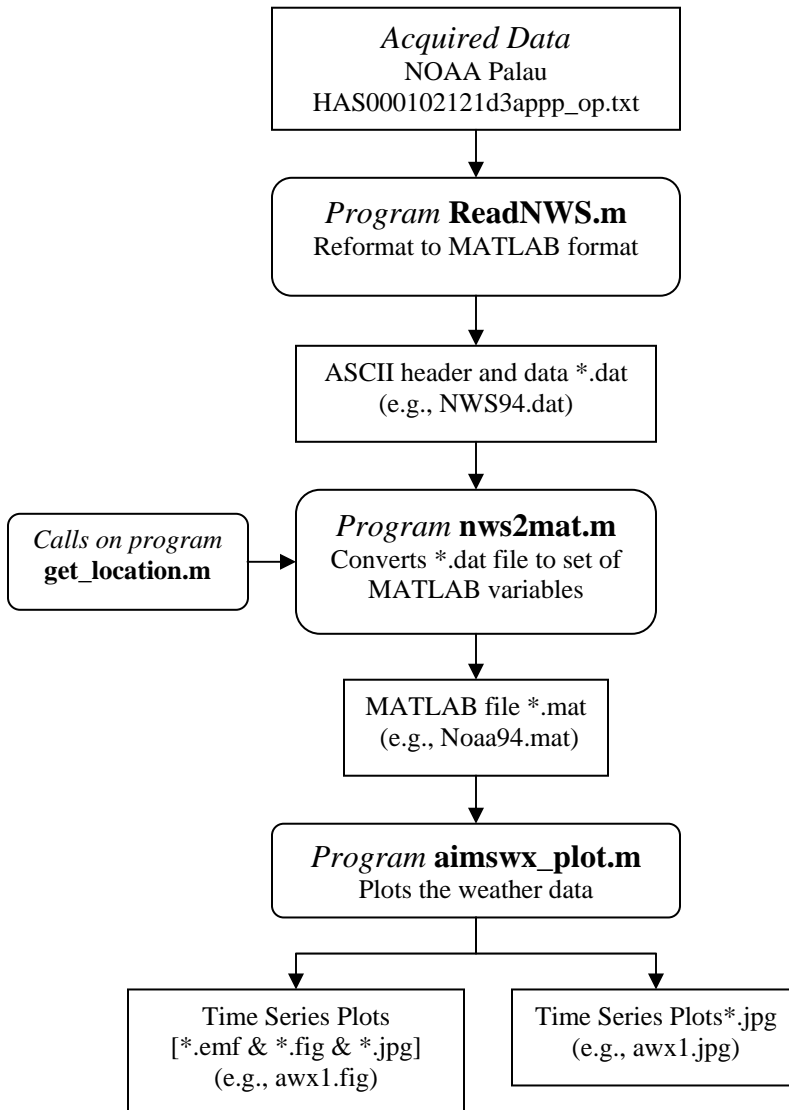
Solar radiation sensors: <http://www.campbellsci.com/solarrad.html#li190sb>

<http://env.licor.com/Products/Sensors/rad.htm>



NOAA National Weather Service, Palau

(data acquired from National Climatic Data Center, <http://www.ncdc.noaa.gov/>)



Notable events

The principle goal was to observe bleaching-like conditions whilst laying the foundation for establishing a quality observational dataset to aid in setting up numerical models. Bleaching-like conditions developed over the period between late October and late November 2003. A general warming and stratification of the waters is evident in the mooring and transect summary plots in [Appendix G](#). The plots are similar in the heating, stratification and subsequent cooling through this period. Winds were low during this warming trend, assisting the intensification of the surface warming. The winds then increased and were, in part, responsible for the subsequent cooling in late October and November.

Acronyms and Instrument Notations

A	Current meter
AIMS	Australian Institute of Marine Science
ADCP	Acoustic Doppler Current Profiler
B	Tide gauge
BT	Bottom Tracking
C	Conductivity meter
CT	Conductivity and Temperature
CTD	Conductivity, Temperature and Depth
CRRF	Coral Reef Research Foundation
LAT	Lowest Astronomical Tide
NOAA	National Oceanic and Atmospheric Administration
P	Pressure sensor
PICRC	Palau International Coral Reef Research Center
RI	Rock Islands
RDI	RD Instruments – manufacturer of ADCPs
S4	Interocean S4 current meter
S16	SBE 16 CT logger
S39	SBE 39 logger
SBE	Sea Bird Electronics
T	Temperature logger or transect
TNC	The Nature Conservancy
UoG	University of Guam
WX	Weather Station

References

- Bruno J.F., Siddon C.E., Witman J.D., Colin P.L. and Toscano M.A. (2001) El Nino related coral bleaching in Palau, Western Caroline Islands. *Coral Reefs* 20:127-136.
- Colin P.L. (2000) Water temperature on the Palauan Reef tract: Year 2000. Technical Report No. 1, Coral Reef Research Foundation, Koror, Palau.
- Penland L., Kloulechad J, Idip D., Van Woesik R. (2004) Coral spawning in the western Pacific Ocean is related to solar insolation: evidence of multiple spawning events in Palau. *Coral Reefs* 23:133-140.
- Wilkinson, C.R. (Ed.) (2002) Status of Coral Reefs of the World: 2002. Global Coral Reef Monitoring Network, Australian Institute of Marine Science. Townsville, Australia, 2002.

Appendix A – Daily Schedule

Deployment, AIMS Trip#3553 24 Aug - 18 Sep 2003

<u>Personnel</u>	Severine Choukroun, Cary McLean, Craig Steinberg (AIMS) Scott Heron, William Skirving (NOAA)				
<u>Wed 20 Aug</u>	Freight sent from AIMS				
<u>Sun 24 Aug</u>	AIMS personnel travel Townsville – Cairns NOAA personnel travel Washington DC – Guam				
<u>Mon 25 Aug</u>	AIMS personnel travel Cairns – Guam – Palau NOAA personnel travel Guam – Palau				
<u>Tue 26 Aug</u>	Pick up freight, meet and greet, find accommodation				
<u>Wed 27 Aug</u>	Setup lab				
<u>Thu 28 Aug</u>	Pat Colin, CRRF shows us around rock islands and lighthouse, check out TNC boat				
<u>Fri 29 Aug</u>	T3	5 SBE39		20m	RI inside channel
<u>Sat 30 Aug</u>	B1a	Brancker XR420	10083	4m	RI northern reef opening in 2.5m hole
	A11	ADCP 600kHz	1673	25m	RI northern channel entrance
	T4	5 SBE39		18m	RI Nikko Lake
<u>Sun 31 Aug</u>	A8	ADCP 600kHz BTPW	3228	30m	Lighthouse Toachel Ra Kesebekuu
	T2	4 SBE39		30m	Lighthouse Toachel Ra Kesebekuu
	C4	SBE16CT	2124	2.5m	Lighthouse Toachel Ra Kesebekuu
<u>Mon 1 Sep</u>	Complete A8				
	A2	S4	615	4m	Ngetalau Passage, outside Rock Islands
	Recover B1a				
	B1	Brancker XR420	10079	4m	RI northern reef opening in 2.5m hole
	Setup instruments				
<u>Tue 2 Sep</u>	T7	5 SBE39		18m	Central Rock Islands, Urukthapel
	A4	RDIADCP 300kHz BT	584	30+m	Ulong east
<u>Wed 3 Sep</u>	A12	Nortek Aquadopp CRRF	0970	12m	RI southern reef opening
	Setup instruments				
<u>Thu 4 Sep</u>	Severine departs 0145 Palau – Guam. Setup instruments and bathymetry sounder 1400 Presentation to Palau Govt & groups				
<u>Fri 5 Sep</u>	A10	ADCP 1200kHz UoG	1292	17m	Toachel Ra Ngel
	B2	SBE39PT		4m	Reef flat Ngedarrak Reef
	A13	Nortek Aquapro CRRF	0866	30m	NE channel Toachel mid
<u>Sat 6 Sep</u>	Too windy for deployment of Philippine Sea transect				
<u>Sun 7 Sep</u>	Craig departs 0030 Palau - Guam				

<u>Mon 8 Sep</u>	T1	4 SBE39		20m	Falcon Reef
	C2	SBE16CT	2127	6m	Falcon Reef
<u>Tue 9 Sep</u>	A9	Nortek Aquapro	794	27m	Malakal Harbour pincers
	C3	SBE16CT	2126	3m	Malakal Harbour pincers
<u>Wed 10 Sep</u>	Setup instruments				
<u>Thu 11 Sep</u>	William departs Perform CT calibration				
<u>Fri 12 Sep</u>	Setup Nobskas and deploy for testing at PICRC				
	T6	4 SBE39		20m	Philippine Sea – West Reef flat
	C1	SBE16	2123	7m	Philippine Sea – West Reef flat
	B5	SBE39PT	760	5m	Central Philippine Sea – East Reef
<u>Sat 13 Sep</u>	Recover Nobskas and compare data				
	A3	Nobska	10045	16m	Ulong west
<u>Sun 14 Sep</u>	Setup instruments				
<u>Mon 15 Sep</u>	A7	Nobska	10046	25m	Falcon Reef - lagoon central
	A6	S4	564	30m	Paleo Channel - Toachel Mlengui
<u>Tue 16 Sep</u>	A1	ADCP 1200kHz	974	25m	RI mid channel - Subject to Ada
	Bathymetry logging set up Prepare Deep water mooring				
<u>Wed 17 Sep</u>	A5	RDIADCP 300kHz BTP412		126m	Uchelbeluu – Deep water mooring
	T5	4 SBE39		126m	Uchelbeluu – Deep water mooring
	C5	SBE16CT		126m	Uchelbeluu – Deep water mooring
<u>Thu 18 Sep</u>	Boat maintenance				
<u>Fri 19 Sep</u>	CTD transect Blue Corner – PICRC				
<u>Sat 20 Sep</u>	Clean up Koror day				
<u>Sun 21 Sep</u>	Scott departs CTD transect A2 through SE entrance to shelf edge & north to Toachel mid channel & KB Bridge. CTD transect from A9 Pincers to central harbour				
<u>Mon 22 Sep</u>	T8	5 SBE39 + 1 XR420		43m	Ulong East Channel
	Pack up				
<u>Tue 23 Sep</u>	Recover T73				
	B4	Brancker XR420	10091	4.5m	Ulong East
	B3/T73b	Brancker XR420	10093	5m	Central Rock Islands, Urukthapel
	WX	Campbell Scientific	WX1		Shalom Etpison's residence
<u>Wed 24 Sep</u>	Cary departs				

Mid-deployment, AIMS Trip# 3585 2 – 9 Nov 2003

Personnel Cary McLean (AIMS)
William Skirving, Alan Strong (NOAA)

2-12 Nov Bathymetry validation, instrument check and CTD transects

Wed 5 Nov
Recover B3/T73b
Move T71 to T73c
B3b Brancker XR420 10093 Blue Corner, 1015-1519
Recover B3b

Fri 7 Nov B3c Brancker XR420 10093 north of Babeldaob, 0730-1437
Recover B3c (bathymetry transect 2a)

Wed 12 Nov B6 Brancker XR420 10093 2m Malakal Harbour Tide Gauge
Check WX

Recovery, AIMS Trip # 3587 27 Dec 2003 – 18 Jan 2004

Personnel Cary McLean, Craig Steinberg (AIMS)
Felipe Arzayus, William Skirving, Alan Strong (NOAA)

Mon 22 Dec Freight sent from AIMS

Sat 27 Dec Townsville 1315–1410 Cairns QF2308

Sun 28 Dec Cairns 0135-0610 Guam CO903, Guam 1940-2050 Koror CO953

Mon 29 Dec Pick up freight & preparation

Tue 30 Dec Prepare boat and gear, Recover T3, T4, A1, A2 & B1

Wed 31 Dec Recover A9, C3, B2, C2, C4 & B6

Thu 01 Jan New Year's Day

Fri 02 Jan Recover A3 & T7

Sat 03 Jan Recover A11, A7, T1 & C2

Sun 04 Jan Recover A12

Mon 05 Jan Freight urgent gear to Townsville, Felipe Arzayus arrives & has check out dive

Tue 06 Jan Blue Corner, Lighthouse channel attempt – storm.

Wed 07 Jan Deep water mooring (A5+T5+C5) recovery attempt – too rough
Recover A8+T2
Recover A10 and redeploy as A11b
A11b ADCP 1200kHz UoG 1292 23m RI Northern channel entrance

Thu 08 Jan Deep water mooring (A5+T5+C5) recovery attempt – too rough
A13 recovery attempt – found subsurface buoy. Waypoint not very good today.

Fri 09 Jan Recover A13, A4, B4 & WX
Presentations to World Bank
“Development of CRW Products: Prediction and mapping with the use of hydrodynamic models and satellite data” William Skirving, Craig Steinberg, Scott Heron, Alan Strong, Cary McLean
“NOAA’s Coral Reef Watch – An Update” Alan Strong

Sat 10 Jan Winds 20-25kts from NE. Lab day

Sun 11 Jan Winds still 20-25kts from NE. Lab day. Pat Colin arrives
Recover A11b
A11c Nortek Aquapro CRRF 0866 23m RI Northern channel entrance
A14 ADCP 1200kHz UoG 1292 4m Japanese Channel

Mon 12 Jan Recover A6 with Alma Ridep-Morris team

Tue 13 Jan Recover B5, T8, A14 & A5+T5+C5

Wed 14 Jan Recover T6 & C1
Pack up

Thu 15 Jan Felipe leaves 0230

Fri 16 Jan Freight gear

Sat 17 Jan Pack up accommodation

Sun 18 Jan Remaining personnel travel Koror 0115-0530 Guam, Guam 1955-1235 Cairns

Mon 19 Jan Cairns 1005-1100 Townsville

Thu 5 Feb Recover A11c (Pat Colin)

Appendix B – Tide gauge deployment information

B1a RI northern reef opening in 2.5m hole, off Toirius Island

Instrument: Brancker XR-420-TG, 10083
(serial no.)
Capability: Maximum depth 90m pressure sensor, temperature sensor
Location: 07°19.821'N 134°28.878'E
Sampling : 5 minute sampling interval, 60 second averaging interval

Filename : 010083test.dat
All times listed as local time UTC+9.

Switch on: 102930 30/08/03
Time check: 0839 30/08/03
In water: 1050 30/08/03
in posn : 1057 30/08/03
First good: -
Last in posn : -
Out of water : 1102 01/09/03
Switch off

Comments : Time drift of logger, gained 59 sec in 53 hours ! Withdrawn

B1 RI northern reef opening in 2.5m hole, off Toirius Island

Instrument : Brancker XR-420-TG, 10079
(serial no.)
Capability : Maximum depth 90m pressure sensor, temperature sensor
Location : 07°19.821'N 134°28.878'E
Sampling : 5 minute sampling interval, 60 second averaging interval

Filename : 0100790301.dat
All times listed as local time UTC+9.

Switch on: 102930 31/08/03
Time check: 072421 01/09/03
In water: 1050 01/09/03
in posn : 1100 01/09/03 4.1m
First good: 1100 01/09/03 01-Sep-2003 11:00:00
Last good : 03-Nov-2003 00:05:00
Last in posn :
Out of water : 1432 30/12/03
Switch off

Comments : Flat battery 3.0V, clock lost time so no time off available
5.6% memory used 18K readings, 2 months

B2 Reef flat, Ngederrak Reef

Instrument: SBE39PT Pressure & Temperature logger, #0759
(serial no.)

Capability : Pressure and Temperature, 230K samples
Location : 07°17.472'N, 134°28.282'E, 1.9m
Sampling : Sampling Interval 5 min

Filename : 07590301.asc
All times listed as local time UTC+9.
Time
Switch on: 1500 03/09/03
In water:
in posn : 1208 05/09/03 05-Sep-2003 12:30:00 1.9m
First good:
Last in posn : 0752 31/12/03 31-Dec-2003 07:30:00
Out of water :
Switch off 1055 03/01/04 35087 Samples
Logger 1 second slow
Comments : Lionfish under rock. Pressure sensor not working properly initially –
good from 21-Sep-2003 12:00:00

B3 Central Rock Islands, Urukthapel (T73b)

Instrument : Brancker XR-420-TG, 10093
(serial no.)
Capability : Maximum depth 90m pressure sensor, temperature sensor
Location : 07°16.376'N 134°24.667'E
Sampling : 5 minute sampling interval, 60 second averaging interval

Filename : 100931103.dat
All times listed as local time UTC+9.
Switch on: 00:14:30 3/9/03
In water:
in posn : 0849 23/9/03 23-sep-2003 10:00:00 5m
First good: 0900 23/9/03
Last in posn : 0900 05/11/03 05-nov-2003 09:00:00

Filename : **B3B**
Location : 7 08.4912',134 17.8275' East of Blue Corner
First good : 1015 5/11/03
Last good : 1515 5/11/03

Filename : **B3C**
Location : 7 46.60848, 134 35.1582 North Babeldaup
First good : 0730 7/11/03
Last good : 1435 7/11/03
Out of water : 1437 7/11/03
Switch Off : 1122 8/11/2003

Comments : Flat battery, clock lost time so no time off available, Clock +15 seconds, 4.1% memory
B3B
 Moved to Blue corner 5/11/03 1015-1519 wpt TIDE Region 13 transect C 7 08.4912',134 17.8275'
B3C
 Moved to north of Babeldaup 7/11/03 0730-1437 Region 2 transect A 7 46.60848, 134 35.1582; then B6 Malakal Harbour on Nov 5 2003
 Last 2 records look bad

B4 Ulong East

Instrument : Brancker XR-420-TG, 10091
 (serial no.)
Capability : Maximum depth 90m pressure sensor, temperature sensor
Location : 07°16.621'N 134°18.680'E 4.5m LAT
Sampling : 5 minute sampling interval, 60 second averaging interval

Filename : 0100911001.dat
 All times listed as local time UTC+9.

Switch on: 214430 22/09/03
In water:
in posn : 0805 23/09/03 5.5m
First good: 0805 23/09/03 23-Sep-2003 08:15:00
Last in posn : 1017 09/01/04 6.1m
Out of water : 19-Dec-2003 20:00:00
Last record: 19-Dec-2003 23:05:00
Switch off Flat battery

Comments : Flat battery, clock lost time so no time off available
 Second deployment for intercalibration with SBE39PT#732
 On @ 1513 10/1/04 Off @ 1605 11/1/04 10091calib.dat

B5 Central Philippine Sea – East Reef (Lagoon side)

Instrument : SBE39PT Pressure & Temperature logger, #0760
 (serial no.)
Capability : Pressure and Temperature, 230K samples
Location : 07°24.380'N, 134°21.065'E, 5m
Sampling : Sampling Interval 5 min

Filename : 07601401.asc
 All times listed as local time UTC+9.

	Time	Depth
Switch on:	1500 03/09/03	
In water:	1120 12/09/03	
in posn:	1125 12/09/03	
First good:	1135 12/09/03	5m 12-Sep-2003 12:00:00
Last in posn :	1030 13/01/04	5.8m
Out of water :		
Last record :		14-Jan-2004 18:44:59
Switch off :	1853 14/01/04	38351 samples

Comments : Logger 2 secs slow
Lionfish under rock.

B6 Malakal Harbour Tide Gauge

Instrument : Brancker XR-420-TG, 10093
(serial no.)
Capability : Maximum depth 90m pressure sensor, temperature sensor. 60 sec ave
Location : 07°20.016'N 134°27.429'E
Sampling : 5 minute sampling interval, 60 second averaging interval

Filename : 0100930301.dat
All times listed as local time UTC+9.

Switch on: 1230 08/11/03 From file header
Time check:
In water: 0859 12/11/03
in posn :
First good: 0915 12/11/03 12-Nov-2003 10:00:00
Last good : 20-Dec-2003 04 :00:00
Out of water : 0853 31/12/03 ~2m
Last record : 20-Dec-2003 04:45:30
Switch off

Comments : Flat battery, clock lost time so no time off available
3.7% memory used 12K readings, 1.5 months
Moved from B3 in November

Appendix C – Current meter deployment information

A1 Rock Islands, mid channel

Instrument : ADCP 1200kHz, #0974
(serial no.)
Capability : 40M card
Location : 07°19.786'N, 134°29.637'E, 24.2m
Sampling : 15min ensembles, continuous; 144 pings/ensemble, 24*1m bins, SD=0.26cm/s

Filename : pal08000.000
All times listed as local time UTC+9.

Switch on: 095230 16/09/03
In water: 1140 16/09/03
in posn : 1155 16/09/03 24.2m
First good: 1230 16/09/03 16-Sep-2003 12:30:00
Last in posn : 1614 30/12/03 30-Dec-2003 16:00:00, 23.8m
Out of water :
Switch off: 1033 31/12/03 10178 ensembles
Logger 1:04 fast

Comments :

A2 Ngetalau Passage, outside Rock Islands

Instrument : Interocean S4 current meter, #615
(serial no.)
Capability : 20 Mb RAM, high resolution pressure sensor draws 49mA no Temp
Location : 07°19.315'N, 134°29.400'E, 4m
Sampling : 1 min average every 30 minutes

Filename : 6150903.s4a setup 6150903.su
All times listed as local time UTC+9.

Switch on: 1500 01/09/03
In water: 1600 01/09/03
in posn : 1610 01/09/03 4m
First good: 1630 01/09/03 01-Sep-2003 16:30:00
Last in posn : 1642 30/12/03 30-Dec-2003 16:30:00 3.7m
Out of water :
Switch off: 1015 31/12/03
No clock drift

Comments :

A3 Ulong West

Instrument : Nobska , #10045 – UoG (Bob Richmond)
(serial no.)
Capability : UVW velocity component output, temperature, conductivity
Location : 07°18.293'N, 134°16.726'E, 20m
Sampling : 120 measurements at 2Hz averaged (1min sampling) every 15min

Filename : 10045.txt
 All times listed as local time UTC+9.
Switch on: 1030 13/09/03
In water: 1250 13/09/03
in posn : 1310 13/09/03 20m
First good:
Last in posn : 1432 02/01/04 20.7m
Out of water :
Last Read:

Comments : Subsurface buoy 5m

A4 Ulong East

Instrument : RDI ADCP 300kHz, #584 BT
 (serial no.)
Capability : 48M card Bottom tracking, No Pressure and temperature
Location : 07°16.617'N, 134°18.716'E, 30m
Sampling : 15min ensembles, continuous; 18*2m bins, SD=0.61cm/s, 6M mem – 140 days

Filename : pal03000.000
 All times listed as local time UTC+9.
Switch on: 185230 01/09/03 01-Sep-2003 19:00:00
In water: 1100 02/09/03
in posn : 1115 02/09/03 30+m
First good: 1130 02/09/03 02-Sep-2003 11:30:00
Last in posn : 1025 09/01/04 09-Jan-2004 10:00:00 33.1m
Out of water :
Last Read: 1141 10/01/04 12546 ensembles, 12530 works
 10-Jan-2004 07:15:00

 Logger 59 seconds fast
Comments : Subsurface buoy at 7°16.621'N, 134°18.680'E

A5 Uchelbeluu (deepwater mooring)

Instrument : RDI ADCP 300kHz, #412BTP
 (serial no.)
Capability : Bottom Tracking, Temperature and Pressure
Location : 07°15.545'N, 134°33.167'E, "215m" on 126m mooring
Sampling : 15min ensembles, continuous; 23*5m bins, SD=0.33cm/s, 10M mem in 170 days

Filename : pal09000.000
 All times listed as local time UTC+9.
Switch on: 082230 17/09/03
In water: 1045 17/09/03
in posn : 1100 17/09/03
First good: 1115 17/09/03 17-Sep-2003 11:30:00
Last in posn : 1445 13/01/04 13-Jan-2004 14:45:00
Popped: 1450 13/01/04

Out of water : 1505 13/01/04
Last Read: 2210 14/01/04 11479 ensembles
Logger 40 seconds slow
Comments : with T5,C5, Acoustic Release #445 (13.5 B/D)

A6 Paleo Channel – Toachel Mlengui (West Passage)

Instrument : S4, #564
(serial no.)
Capability : Temperature and pressure.
Location : 07°28.927'N, 134°27.776'E, 33m
Sampling : 1min sampling every 30 minutes

Filename : 5640104.s4a 5640903.su
All times listed as local time UTC+9.

Switch on: 1330 04/09/03
In water: 0930 15/09/03
in posn : 0938 15/09/03 30.0m
First good: 1000 15/09/03 15-Sep-2003 10:00:00
Last in posn : 1028 12/01/04 12-Jan-2004 10:00:00 32.5m
Out of water :
Last Read: 0830 05/02/04

Comments : Comms box didn't work – downloaded later in Darwin !

A7 Falcon Reef

Instrument : Nobska , #10046 – UoG (Bob Richmond)
(serial no.)
Capability : UVW velocity component output, temperature
Location : 07°22.445'N, 134°23.177'E, 14.5m
Sampling : 120 measurements at 2Hz averaged (1min sampling) every 15min

Filename : 10046.txt
All times listed as local time UTC+9.

Switch on: 1030 13/09/03
In water: 1129 15/09/03
in posn : 1145 15/09/03
First good:
Last in posn : 1507 03/01/04 13.1m
Out of water :
Last Read: Flat battery

Comments : with transect T1

A8 Lighthouse Channel

Instrument : RDI ADCP 600kHz, #3228
(serial no.)
Capability : Bottom tracking, pressure and temperature

In water: 1100 05/09/03
in posn : 1113 05/09/03 19.3m
First good: 1130 05/09/03 05-Sep-2003 11:30:00
Last in posn : 1310 07/01/04 07-Jan-2004 13:00:00
Out of water :

Last Read:

Comments : This instrument was moved to A11b and afterwards to A14

A11 Rock Islands northern channel entrance

Instrument : RDI ADCP 600kHz, #1673
(serial no.)
Capability :
Location : 07°19.400'N, 134°28.949'E, 22m
Sampling : 15min ensembles, continuous; 150 pings/ensemble, 30*1m bins,
SD=0.57cm/s, 424 Wh, 9.7m, 140 days

Filename : No Data setup pal01.whp
All times listed as local time UTC+9.

Switch on: 100730 30/08/03

In water: 1600 30/08/03

in posn : 1616 30/08/03

First good:

Last in posn : 1613 03/01/04 23.6m

Out of water :

Last Read: 1013 07/01/04 No data

Comments : No data – battery failed, put UoG ADCP#1292 in 7/1/04

A11b Rock Islands northern channel entrance

Instrument : ADCP 1200kHz, #1292 – UoG (Bob Richmond)
(serial no.)
Capability : Temperature and Pressure
Location : 07° 17.786'N, 134° 28.958'E, 22 m
Sampling : 15min ensembles, continuous; 180 pings/ensemble, 22*1m bins,
SD=0.2cm/s

Filename : pal05000.000

In water:

in posn : 1402 07/01/04 22.6m deep

First good: 1415 07/01/04

Last in posn : 1430 11/01/04

Popped: 1438 11/01/04

Out of water :

Last Read:

Comments : The above instrument was moved from A10 and afterwards to A14

A11c Rock Islands northern channel entrance

Instrument : Nortek Aquapro, #0866/784 – CRRF (Pat Colin)
(serial no.)
Capability : 50cm blanking distance
Location : 07°19.023'N, 134°31.490'E, 30+m
Sampling : 1min sampling interval every 15min, 30*1m bins

Filename : Pal1001.prf setup Pal10
All times listed as local time UTC+9.

Switch on: 125930 11/01/04

In water:

in posn : 1438 11/01/04 22.6 m

First good: 1500 11/01/04 11-Jan-2004 15:30:00

Last in posn : 1430 05/02/04 05-Feb-2004 14:30:00

Out of water :

Last Read: 125930 10/02/04 2004-02-10 13:00:00

Comments : Replaced failed current meter #1673 A11 and short A11b deployments.
21 good bins
This instrument was moved from A13

A12 Rock Islands southern reef opening

Instrument : Nortek Aquadopp, #0970/0855 – CRRF (Pat Colin)
(serial no.)
Capability : 50cm blanking distance, 5M mem
Location : 07°19.223'N, 134°29.795'E, 11.4m
Sampling : 5min sampling interval every 15min, SD=0.4cm/s, 0.3M mem, 107%
battery in 75 days

Filename : Pal0401.AQD,*.HDR & *.DAT setup pal04
All times listed as local time UTC+9.

Switch on: 151230 03/09/03

In water: 1700 03/09/03

in posn : 1715 03/09/03 11.4m

First good: 1730 03/09/03 03-Sep-2003 17:30:00

Last good : 204230 03/10/01 01-Oct-2003 20:45:00

Last in posn : 1056 04/01/04 11.2m

Out of water :

Last Read:

Switch off : 1100 07/01/04
1 sec/ 6mths specification

Comments : Battery flat as expected although should have lasted 70 days
1230 in cold box for intercalibration

A13 Toachel mid

Instrument : Nortek Aquapro, #0866/784 – CRRF (Pat Colin)
(serial no.)
Capability : 50cm blanking distance

Location : 07°19.023'N, 134°31.490'E, 30+m
Sampling : 1min sampling interval every 15min, 30*1m bins

Filename : pal0601.prf
All times listed as local time UTC+9.
Switch on: 135930 05/09/03
In water: 1510 05/09/03
in posn : 1530 05/09/03 30+m
First good: 05-Sep-2003 15:30:00
Last good : 0230 30/11/03 30-Nov-2003 02:30:00
Last in posn : 0830 09/01/04 09-Jan-2004 08:30:00
Popped: 0840 09/01/04 31.5m
Out of water :
Last Read: 1153 10/01/04
Logger 23 seconds fast
Comments : 26 good bins, shorter than deployed record – 75 days
This instrument was moved to A11c

A14 Japanese Channel

Instrument : ADCP 1200kHz, #1292 – UoG (Bob Richmond)
(serial no.)
Capability : Temperature and Pressure
Location : 07° 17.786'N, 134° 28.958'E, 22 m
Sampling : 15min ensembles, continuous; 180 pings/ensemble, 22*1m bins,
SD=0.2cm/s

Filename : pal05000.000
All times listed as local time UTC+9.
In water:
in posn : 1520 11/01/04 4m deep
First good: 1530 11/01/04
Last in posn :
Popped:
Out of water :
Switch off : 2135 14/01/04 12626 ensembles
Logger 16 seconds fast
Comments : This instrument was moved from A10 and A11b

Appendix D – Temperature deployment information

T1 Falcon Reef

T16

Instrument : SBE39T Temperature logger, #0935
(serial no.)
Capability :
Location : 07°22.424'N, 134°23.232'E, 2.5m
Sampling : Sampling Interval 5 min

Filename : 09350401.asc
All times listed as local time UTC+9.

	Time	Depth
Switch on:	1500 03/09/03	
In water:	1330 08/09/03	
in posn :	1408 08/09/03	2.5m
First good:	1410 08/09/03	
Last in posn :	1443 03/01/04	3.7m
Out of water :	1525 03/01/04	
Switch off	1601 04/01/04	

Logger 1 second fast
Comments : Long transect, 4 SBE39T & 1 SBE16CT

T15

Instrument : SBE39T Temperature logger, #0929
(serial no.)
Capability :
Location : 07°22.424'N, 134°23.232'E, 3.5m
Sampling : Sampling Interval 5 min

Filename : 09290401.asc
All times listed as local time UTC+9.

	Time	Depth
Switch on:	1500 03/09/03	
In water:	1330 08/09/03	
in posn :	1355 08/09/03	3.5m
First good:	1400 08/09/03	
Last in posn :	1448 03/01/04	4.7m
Out of water :	1525 03/01/04	
Switch off	1606 04/01/04	35438 samples

Logger 1 second fast

Comments :

T14 C2

Instrument : SBE16CT Conductivity & Temperature logger, #2127
(serial no.)
Capability :
Location : 07°22.424'N, 134°23.232'E, 6m
Sampling : Sampling Interval 5 min

Filename : 21270401.hex
All times listed as local time UTC+9.

	Time	Depth
--	-------------	--------------

Switch on: 1500 04/09/03
In water:
in posn : 1345 08/09/03 6m
First good: 1345 08/09/03 8 Sep 2003, 14:00:00
Last in posn : 1450 03/01/04 3 Jan 2004, 14:30:00 6.9m
Out of water : 1525 03/01/04
Switch off 1808 04/01/04 35170 samples

Logger 2 seconds fast

Comments :

T13

Instrument : SBE39T Temperature logger, #0920
 (serial no.)
Capability :
Location : 07° 22.445'N, 134° 23.177'E, 9m
Sampling : Sampling Interval 5 min

Filename : 09200401.asc
 All times listed as local time UTC+9.

	Time	Depth
Switch on:	1500 03/09/03	
In water:	1118 08/09/03	
in posn :	1132 08/09/03	9m
First good:	1135 08/09/03	
Last in posn :	1454 03/01/04	10.0m
Out of water :	1525 03/01/04	
Switch off	1557 04/01/04	35436 samples

Logger 1 second early

Comments : Next to CRRF logger

T12 – current meter A7

T11

Instrument : SBE39T Temperature logger, #0934
 (serial no.)
Capability :
Location : 07°22.445'N, 134°23.177'E, 20m
Sampling : Sampling Interval 5 min

Filename : 09340401.asc
 All times listed as local time UTC+9.

	Time	Depth
Switch on:	1500 03/09/03	
In water:	1118 08/09/03	
in posn :	1142 08/09/03	20m
First good:	1145 08/09/03	
Last in posn :	1509 03/01/04	21.4m
Out of water :	1525 03/01/04	
Switch off	1551 04/01/04	35435 samples

No clock drift

Comments :

T2 Lighthouse, Toachel ra Kesebekuu

T26

Instrument : SBE39T Temperature logger, #0925
(serial no.)**Capability :****Location :** 07°16.955'N, 134°27.932'E, 1m**Sampling :** Sampling Interval 5 min**Filename :** 09250801.asc

All times listed as local time UTC+9.

	Time	Depth
Switch on:	1500 30/08/03	
In water:		
in posn :	1444 31/08/03	1m
First good:	1445 31/08/03	
Last in posn :	0846 07/01/04	3.1m
Out of water :		
Switch off	1607 08/01/04	37742 samples

Logger 9 seconds fast

Comments : Transect : 4 SBE39T, 1 SBE16CT ; with A8

T25 C4

Instrument : SBE16CT Conductivity & Temperature logger, #2124
(serial no.)**Capability :****Location :** 07°16.955'N, 134°27.932'E, 3 m**Sampling :** Sampling Interval 5 min**Filename :** 21240301.asc

All times listed as local time UTC+9.

	Time	Depth
Switch on:	1230 31/08/03	
In water:		
in posn :	1452 31/08/03	2.5m
First good:	1455 31/08/03	31-Aug-2003 16:00:00
Last in posn :	0815 31/12/03	31-Dec-2003 08:00:00 2.7m
Out of water :		
Switch off	1208 03/01/04	35996 samples

Logger 6 seconds fast

Comments :

T24

Instrument : SBE39T Temperature logger, #0933
(serial no.)**Capability :****Location :** 07°16.955'N, 134°27.932'E, 5m**Sampling :** Sampling Interval 5 min**Filename :** 09330801.asc

All times listed as local time UTC+9.

	Time	Depth
Switch on:	1500 30/08/03	
In water:		

in posn : 1500 31/08/03 5m
First good: 1500 31/08/03
Last in posn : 0837 07/01/04 7.2m
Out of water :
Switch off 1558 08/01/04 37740 samples
 Logger 10 seconds fast

Comments :

T23

Instrument : SBE39T Temperature logger, #1054
 (serial no.)
Capability :
Location : 07°16.955'N, 134°27.932'E, 10m
Sampling : Sampling Interval 5 min

Filename : 10540801.asc
 List all times as local time.

	Time	Depth
Switch on:	1500 30/08/03	
In water:		
in posn :	1509 31/08/03	10m
First good:	1510 31/08/03	
Last in posn :	0834 07/01/04	11.0m
Out of water :		
Switch off	1541 08/01/04	37737 samples
	Logger 2 seconds slow	

Comments :

T22

Instrument : SBE39T Temperature logger, #1052
 (serial no.)
Capability :
Location : 07°16.955'N, 134°27.932'E, 20m
Sampling : Sampling Interval 5 min

Filename : 10520801.asc
 All times listed as local time UTC+9.

	Time	Depth
Switch on:	1500 30/08/03	
In water:		
in posn :	1516 31/08/03	20m
First good:	1520 31/08/03	
Last in posn :	0840 07/01/04	23.4m
Out of water :		
Switch off	1530 08/01/04	37737 samples
	Logger 1 second slow	

Comments :

T21 – current meter A8

T3 Rock Islands, inside channel

T35

Instrument : SBE39T Temperature logger, #1055
(serial no.)
Capability :
Location : 07°19.570'N, 134°29.418'E, 1m
Sampling : Sampling Interval 5 min

Filename : 10550301.asc
All times listed as local time UTC+9.

	Time	Depth
Switch on:	1030 29/08/03	
In water:		
in posn :	1517 29/08/03	1.0m
First good:	1520 29/08/03	
Last in posn :	1459 30/12/03	2.6m
Out of water :		
Switch off	1801 03/01/04	36667 samples
	Logger 7 seconds slow	

Comments : Transect of 5 loggers, put in at low water on cloudy day.

T34

Instrument : SBE39T Temperature logger, #1058
(serial no.)
Capability :
Location : 07°19.570'N, 134°29.418'E, 2.5m
Sampling : Sampling Interval 5 min

Filename : 10583112.asc
All times listed as local time UTC+9.

	Time	Depth
Switch on:	1030 29/08/03	
In water:		
in posn :	1510 29/08/03	2.5m
First good:	1510 29/08/03	
Last in posn :	1500 30/12/03	3.5m
Out of water :		
Switch off	1204 31/12/03	35731 samples
	Logger 2 seconds slow	

Comments :

T33

Instrument : SBE39T Temperature logger, #0676
(serial no.)
Capability :
Location : 07°19.570'N, 134°29.418'E, 5m
Sampling : Sampling Interval 5 min

Filename : 06763112.asc
All times listed as local time UTC+9.

	Time	Depth
Switch on:	1030 29/08/03	
In water:		
in posn :	1500 29/08/03	5m
First good:	1500 29/08/03	
Last in posn :	1502 30/12/03	5.9m
Out of water :		

Switch off 1135 31/12/03 35725 samples
Logger 1 second slow

Comments :

T32

Instrument : SBE39T Temperature logger, #0675
(serial no.)

Capability :

Location : 07°19.570'N, 134°29.418'E, 10m

Sampling : Sampling Interval 5 min

Filename : 06753112.asc

All times listed as local time UTC+9.

	Time	Depth
Switch on:	1030 29/08/03	
In water:		
in posn :	1444 29/08/03	10.0m
First good:	1445 29/08/03	
Last in posn :	1504 30/12/03	10.4m
Out of water :		
Switch off	1332 31/12/03	35749 samples

Logger 8 seconds fast

Comments :

T31

Instrument : SBE39T Temperature logger, #1057
(serial no.)

Capability :

Location : 07°19.570'N, 134°29.418'E, 20m

Sampling : Sampling Interval 5 min

Filename : 10573112.asc

All times listed as local time UTC+9.

	Time	Depth
Switch on:	1030 29/08/03	
In water:		
in posn :	1432 29/08/03	20m
First good:	1435 29/08/03	
Last in posn :	1506 30/12/03	20.5m
Out of water :		
Switch off	124710 31/12/03	347410 samples

Logger 9 seconds fast

Comments :

T4 Rock Islands, Nikko Bay

T45

Instrument : SBE39T Temperature logger, #1059
(serial no.)

Capability :

Location : 07°19.772'N, 134°30.034'E, 1m

Sampling : Sampling Interval 5 min

Filename : 10593112.asc

All times listed as local time UTC+9.

	Time	Depth
Switch on:	0930 30/08/03	
in posn :	1735 30/08/03	1m
First good:	1735 30/08/03	
Last in posn :	1537 30/12/03	2.4m
Out of water :		
Switch off	1153 31/12/03	35453 samples

Logger 1 second slow

Comments :

T44

Instrument : SBE39T Temperature logger, #1051
(serial no.)
Capability :
Location : 07°19.772'N, 134°30.034'E, 2.5m
Sampling : Sampling Interval 5 min

Filename : 10513112.asc

All times listed as local time UTC+9.

	Time	Depth
Switch on:	0930 30/08/03	
in posn :	1730 30/08/03	2.5m
First good:	1730 30/08/03	
Last in posn :	1540 30/12/03	2.6m
Out of water :		
Switch off	1300 31/12/03	35466 samples

Logger 6 seconds slow

Comments :

T43

Instrument : SBE39T Temperature logger, #1061
(serial no.)
Capability :
Location : 07°19.772'N, 134°30.034'E, 5m
Sampling : Sampling Interval 5 min

Filename : 1061311203.asc

All times listed as local time UTC+9.

	Time	Depth
Switch on:	0930 30/08/03	
in posn :	1720 30/08/03	5m
First good:	1720 30/08/03	
Last in posn :	1541 30/12/03	5.4m
Out of water :		
Switch off	1214 31/12/03	35457 samples

No clock drift

Comments :

T42

Instrument : SBE39T Temperature logger, #1060
(serial no.)
Capability :
Location : 07°19.772'N, 134°30.034'E, 10m

Sampling : Sampling Interval 5 min

Filename : 10603112.asc
All times listed as local time UTC+9.

	Time	Depth
Switch on:	0930 30/08/03	
in posn :	1715 30/08/03	10.6m
First good:	1715 30/08/03	
Last in posn :	1544 30/12/03	10.8m
Out of water :		
Switch off	1225 31/12/03	35460 samples

Logger 5 seconds slow

Comments :

T41

Instrument : SBE39T Temperature logger, #1053
(serial no.)

Capability :

Location : 07°19.772'N, 134°30.034'E, 17.6m

Sampling : Sampling Interval 5 min

Filename : 10533112.asc
All times listed as local time UTC+9.

	Time	Depth
Switch on:	0930 30/08/03	
in posn :	1705 30/08/03	17.6m
First good:	1705 30/08/03	
Last in posn :	1546 30/12/03	17.6m
Out of water :		
Switch off	1236 31/12/03	35462 samples

Logger 2 seconds slow

Comments :

T5 Uchelbeluu (deepwater mooring)

T56 C5

Instrument : SBE16CT Conductivity & Temperature logger, #2125
(serial no.)

Capability :

Location : 07°15.545'N, 134° 33.167'E, "150m below" on 126m mooring

Sampling : Sampling Interval 10 min, 600secs

Filename : 21251401.hex
All times listed as local time UTC+9.

	Time	
Switch on:	0810 17/09/03	
In water:	1045 17/09/03	
in posn :	1100 17/09/03	
First good:	1100 17/09/03	17 Sep 2003, 12:00:00
Last in posn :	1440 13/01/04	13 Jan 2004, 14:00:00
Out of water :	1501 13/01/04	
Switch off	1628 14/01/04	

Comments : with A5,C5, Acoustic Release #445 (13.5 B/D)
Poor data set, 50% OK

T55

Instrument : SBE39PT **Pressure & Temperature** logger, #1062
(serial no.)
Capability :
Location : 07°15.545'N, 134°33.167'E, "160m below" on 126m mooring
Sampling : Sampling Interval 5 min

Filename : 10621401.asc
All times listed as local time UTC+9.

	Time	Depth
Switch on:	1030 14/09/03	
In water:	1045 17/09/03	
in posn :	1100 17/09/03	
First good:	1100 17/09/03	
Last in posn :	1440 13/01/04	
Out of water :	1501 13/01/04	
Switch off	2233 14/01/04	35279 samples

Comments : with A5,C5, Acoustic Release #445 (13.5 B/D)

T54

Instrument : SBE39T Temperature logger, #0931
(serial no.)
Capability :
Location : 07°15.545'N, 134°33.167'E, "170m below" on 126m mooring
Sampling : Sampling Interval 5 min

Filename : 09311401.asc
All times listed as local time UTC+9.

	Time	Depth
Switch on:	1500 03/09/03	
In water:	1045 17/09/03	
in posn :	1100 17/09/03	
First good:	1100 17/09/03	
Last in posn :	1440 13/01/04	
Out of water :	1501 13/01/04	
Switch off	221212 14/01/01	28391 samples

Comments : with A5,C5, Acoustic Release #445 (13.5 B/D)
File date is worn shows wnd date 15th !

T53

Instrument : SBE39T Temperature logger, #0923
(serial no.)
Capability :
Location : 07°15.545'N, 134°33.167'E, "190m below" on 126m mooring
Sampling : Sampling Interval 5 min

Filename : 09231401.asc
All times listed as local time UTC+9.

	Time	Depth
Switch on:	1500 03/09/03	
In water:	1045 17/09/03	

In posn : 1100 17/09/03
First good: 1100 17/09/03
Last in posn : 1440 13/01/04
Out of water : 1501 13/01/04
Switch off 210955 14/01/04 38378 samples

Comments : Logger 19 seconds slow
with A5,C5, Acoustic Release #445 (13.5 B/D)

T52 – current meter A5

T51

Instrument : SBE39T Temperature logger, #0927
(serial no.)
Capability :
Location : 07°15.545'N, 134°33.167'E, "225m below" on 126m mooring
Sampling : Sampling Interval 5 min

Filename : 09271401.asc
All times listed as local time UTC+9.

	Time	Depth
Switch on:	1500 03/09/03	
In water:	1045 17/09/03	
in posn :	1100 17/09/03	
First good:	1100 17/09/03	
Last in posn :	1440 13/01/04	
Out of water :	1501 13/01/04	
Switch off	2233 14/01/04	38395 samples

Logger 7 seconds slow
Comments : with A5,C5, Acoustic Release #445 (13.5 B/D)

T6 Central Philippine Sea – West Reef flat

T65

Instrument : SBE39T Temperature logger, #1137
(serial no.)
Capability :
Location : 07°24.713'N, 134°20.258'E, 3m (high water)
Sampling : Sampling Interval 5 min

Filename : No Data
All times listed as local time UTC+9.

	Time	Depth
Switch on:	1500 03/09/03	
In water:	0955 12/09/03	
in posn :	1040 12/09/03	
First good:	1040 12/09/03	
Last in posn :		
Out of water :		
Switch off		NOT RECOVERED

Comments : Black subsurface buoy mid-transect, 4 SBE39T + SBE16CT
Wire securing logger recovered but had been cut through and had weed growth on the cut

T64

Instrument : SBE39T Temperature logger, #0928
(serial no.)
Capability :
Location : 07°24.713'N, 134°20.258'E, 4.5m (high water)
Sampling : Sampling Interval 5 min

Filename : 09281401.asc
All times listed as local time UTC+9.

	Time	Depth
Switch on:	1500 03/09/03	
In water:	0955 12/09/03	
in posn :	1028 12/09/03	
First good:	1030 12/09/03	12 Sep 2003, 11:00:00 4.5m
Last in posn :	1110 14/01/04	14 Jan 2004, 11:00:00 5.3m
Out of water :	1150 14/01/04	
Switch off	2324 14/01/04	38405 samples

Comments : Black subsurface buoy mid-transect, 4 SBE39T + SBE16CT

T63 C1

Instrument : SBE16CT Conductivity & Temperature logger, #2123
(serial no.)
Capability :
Location : 07°24.713'N, 134°20.258'E, 7m (high water)
Sampling : Sampling Interval 5 min

Filename : 21231401.hex
All times listed as local time UTC+9.

	Time	Depth
Switch on:	0750 10/09/03	
In water:	0955 12/09/03	
in posn :	1003 12/09/03	
First good:	1005 12/09/03	7m
Last in posn :	1115 14/01/04	7.5m
Out of water :	1150 14/01/04	
Switch off		

Comments : Black subsurface buoy mid-transect, 4 SBE39T + SBE16CT

T62

Instrument : SBE39T Temperature logger, #0917
(serial no.)
Capability :
Location : 07°24.713'N, 134°20.258'E, 12m (high water)
Sampling : Sampling Interval 5 min

Filename : 09171401.asc
All times listed as local time UTC+9.

	Time	Depth
Switch on:	1500 03/09/03	
In water:	0955 12/09/03	
in posn :	1010 12/09/03	

First good: 1010 12/09/03 12m
Last in posn : 1135 14/1/04 12.5m
Out of water : 1150 14/1/04
Switch off 2317 14/01/04 38404 samples
 4 seconds fast
Comments : Black subsurface buoy mid-transect, 4 SBE39T + SBE16CT

T61

Instrument : SBE39T Temperature logger, #0924
 (serial no.)
Capability :
Location : 07°24.713'N, 134°20.258'E, 24m (high water)
Sampling : Sampling Interval 5 min

Filename : 09241401.asc
 All times listed as local time UTC+9.

	Time	Depth
Switch on:	1500 03/09/03	
In water:	0955 12/09/03	
in posn :	1015 12/09/03	
First good:	1015 12/09/03	24
Last in posn :	1140 14/01/04	24.5
Out of water :	1150 14/01/04	
Switch off	2329 14/01/04	38406 samples

 Logger is 6 seconds fast
Comments : Black subsurface buoy mid-transect, 4 SBE39T + SBE16CT

T7 Southern Rock Islands

T75

Instrument : SBE39T Temperature logger, #1056
 (serial no.)
Capability :
Location : 07°16.955'N, 134°27.932'E, 1.5m
Sampling : Sampling Interval 5 min

Filename : 10560301.asc
 All times listed as local time UTC+9.

	Time	Depth
Switch on:	1500 30/08/03	
In water:		
in posn :	0957 02/09/03	1.5m
First good:	1000 02/09/03	
Last in posn :	1604 02/01/04	2.0m
Out of water :		
Switch off	1822 03/01/04	36329 samples

 6 seconds slow
Comments :

T74

Instrument : SBE39T Temperature logger, #0926
 (serial no.)
Capability :
Location : 07°16.955'N, 134°27.932'E, 3m

Sampling : Sampling Interval 5 min

Filename : 9260301.asc
All times listed as local time UTC+9.

	Time	Depth
Switch on:	1415 01/09/03	
In water:		
in posn :	0945 02/09/03	3m
First good:	0945 02/09/03	
Last in posn :	1603 02/01/04	3.3m
Out of water :		
Switch off	175640 03/01/04	35756 samples
	Logger 4 seconds fast	

Comments :

T73

Instrument : SBE39T Temperature logger, #0919
(serial no.)

Capability :

Location : 07°16.955'N, 134°27.932'E, 6m

Sampling : Sampling Interval 5 min

Filename : 09190903.asc
All times listed as local time UTC+9.

	Time	Depth
Switch on:	1415 01/09/03	
In water:		
in posn :	0940 02/09/03	5m
First good:	0940 02/09/03	02 Sep 2003, 10:00:00
Last in posn :	0845 23/09/03	23 Sep 2003, 08:45:00 5m
Out of water :		
Switch off	1134 23/09/03	6304 samples

Comments : Tide gauge B3 replaced this in late Sep and bottom logger (T71) brought up in Nov

T73b – tide gauge B3

T73c

Instrument : SBE39PT Pressure & Temperature logger, #0732
(serial no.)

Capability :

Location : 07°16.955'N, 134°27.932'E, 5m

Sampling : Sampling Interval 5 min

Filename : 07321401.asc

First good :	0915 05/11/03	05 Nov 2003, 09:15:00
Last in posn :	1601 02/01/04	02 Jan 2004, 15:30:00 5.5m
Out of water :		
Switch off	2320 14/01/04	38990 samples

Comments : Logger moved from T71

T72

Instrument : SBE39T Temperature logger, #0930
(serial no.)
Capability :
Location : 07°16.955'N, 134°27.932'E, 12m
Sampling : Sampling Interval 5 min

Filename : 09300301.asc
All times listed as local time UTC+9.

	Time	Depth
Switch on:	1415 01/09/03	
In water:		
in posn :	0930 02/09/03	12m
First good:	0930 02/09/03	
Last in posn :	1539 02/01/04	13.2m
Out of water :		
Switch off	1815 03/01/04	35761 samples
	No clock drift	

Comments :

T71

Instrument : SBE39PT Pressure & Temperature logger, #0732
(serial no.)
Capability :
Location : 07°16.376'N, 134°24.667'E ,19m 07°16.955'N, 134°27.932'E, 18m
Sampling : Sampling Interval 5 min

Filename : **07321401.asc**
All times listed as local time UTC+9.

	Time	Depth
Switch on:	1415 01/09/03	
In water:		
in posn :	0918 02/09/03	18m
First good:	0920 02/09/03	02 Sep 2003, 10:00:00
Last in posn :	0900 05/11/03	05 Nov 2003, 09:00:00
Comments :	Moved from bottom in November to 5m T73c at the same transect Temperature sub-standard for post deployment inter-calibration	

T8 Ulong East Channel

T86

Instrument : SBE39T Temperature logger, #918
(serial no.)
Capability : Temperature 300K samples
Location : 07° 16.621'N, 134° 18.802'E, 1m in 42m of water
Sampling : Sampling Interval 5 min

Filename : 09181401.asc
All times listed as local time UTC+9.

	Time	Depth
Switch on:	1500 03/09/03	
In water:		
in posn :	1135 22/09/03	
First good:	1140 22/09/03	22-Sep-2003 12:00:00

Last in posn : 1230 13/01/04 13-Jan-2004 12:30:00
Out of water :
Switch off 164034 14/1/04 38349 samples
Logger 2 seconds fast

Comments :

T85

Instrument : Brancker XR-420-TG tide gauge, #10092
(serial no.)
Capability : Temperature and pressure gauge, 60 sec ave, max depth 90m
Location : 07° 16.621'N, 134° 18.802'E, 1m in 42m of water
Sampling : Sampling Interval 5 min, 60 sec ave

Filename : 0100921401.dat
All times listed as local time UTC+9.

	Time	Depth
Switch on:	214930 22/09/03	2150 22/9/03
In water:		
in posn :	0818 23/09/03	
First good:	0830 23/09/03	23-Sep-2003 08:30:00
Last good :		
Last record :	1040 19/12/03	19-Dec-2003 06:00:00
Last in posn :	1230 13/01/04	
Out of water :		
Switch off	No power	25212 samples

Comments : Battery flat on recovery
Temp calibration
on 1555 14/1/04, 5'si 60 sec ave with 732 @1550 14/1/04 in ocean
in bath 2100 14/1/04 off @2400 14/1/04 10092calib.dat

T84

Instrument : SBE39T Temperature logger, #932
(serial no.)
Capability : Temperature 300K samples
Location : 07° 16.621'N, 134° 18.802'E, 5m in 42m of water
Sampling : Sampling Interval 5 min

Filename : 09321401.asc
All times listed as local time UTC+9.

	Time	
Switch on:	1500 03/09/03	
In water:		
in posn :	1135 22/09/03	
First good:	1140 22/09/03	
Last in posn :	1230 13/01/04	
Out of water :		
Switch off	214202 14/1/04	38385 samples

Logger 1 second fast

Comments :

T83

Instrument : SBE39T Temperature logger, #922
(serial no.)
Capability : Temperature 300K samples

Location : 07° 16.621'N, 134° 18.802'E, 10m in 42m of water
Sampling : Sampling Interval 5 min

Filename : 09221401.asc
All times listed as local time UTC+9.

	Time	Depth
Switch on:	1500 03/09/03	
In water:		
in posn :	1135 22/09/03	
First good:	1140 22/09/03	
Last in posn :	1230 13/01/04	
Out of water :		
Switch off	1741 14/01/04	38337 samples

Logger 1 second fast

Comments :

T82

Instrument : SBE39T Temperature logger, #921
(serial no.)
Capability : Temperature 300K samples
Location : 07° 16.621'N, 134° 18.802'E, 20m in 42m of water
Sampling : Sampling Interval 5 min

Filename : 09211401.asc
All times listed as local time UTC+9.

	Time	Depth
Switch on:	1500 03/09/03	
In water:		
in posn :	1135 22/09/03	
First good:	1140 22/09/03	
Last in posn :	1230 13/01/04	
Out of water :		
Switch off	1749 14/01/04	38338 samples

Logger 3 seconds slow

Comments :

T81

Instrument : SBE39T Temperature logger, #916
(serial no.)
Capability : Temperature 300K samples
Location : 07° 16.621'N, 134° 18.802'E, 40m in 42m of water
Sampling : Sampling Interval 5 min

Filename : 09161401.asc
All times listed as local time UTC+9.

	Time	Depth
Switch on:	1500 03/09/03	
In water:		
in posn :	1135 22/09/03	
First good:	1140 22/09/03	
Last in posn :	1230 13/01/04	
Out of water :		
Switch off	1727 14/01/04	38334 samples

Logger 4 seconds slow

Comments :

Appendix E – Salinity deployment information

C1 Philippine Sea – West reef flat

See T63

C2 Falcon Reef – lagoon central

See T14

C3 Malakal Harbour Pincers

Instrument : SBE16CT Conductivity & Temperature logger, #2126
(serial no.)

Capability : Conductivity and Temperature

Location : 07°20.163'N, 134°25.483'E, 3 m

Sampling : Sampling Interval 5 min

Filename : 21260301.hex

All times listed as local time UTC+9.

	Time	Depth
Switch on:	1500 04/09/03	
In water:	1615 09/09/03	
in posn :	1627 09/09/03	2.6m
First good:	1630 09/09/03	09-Sep-2003 16:30:00
Last in posn :	0732 31/12/03	31-Dec-2003 07:30:00 2.1m
Out of water :		
Switch off	1112 03/01/04	34803 Samples
	Logger 5 seconds fast	
Comments :	with A9	

C4 Lighthouse Toachel Ra Kesebekuu

See T25

C5 Uchelbeluu

See T56

Appendix F – Weather station deployment information

WX

Instrument : Campbell Scientific WX1
(serial no.)

Capability : Wind Speed and direction RM Young
Air temperature
Pyranometer Kipp & Zonen CM3 #026233 $22.24e-6$ V/Wm⁻²
PAR Licor Quantum Q31622

Location : 07°20.969'N 134°30.018'E, 210m Shalom Etpisons residence

Sampling : 5 minute sampling interval, 60 second averaging interval

Filename : 0100930301.dat
All times listed as local time UTC+9.

Switch on:
in posn :

First good: 1350 23/09/03

Last in posn : 1430 09/01/04

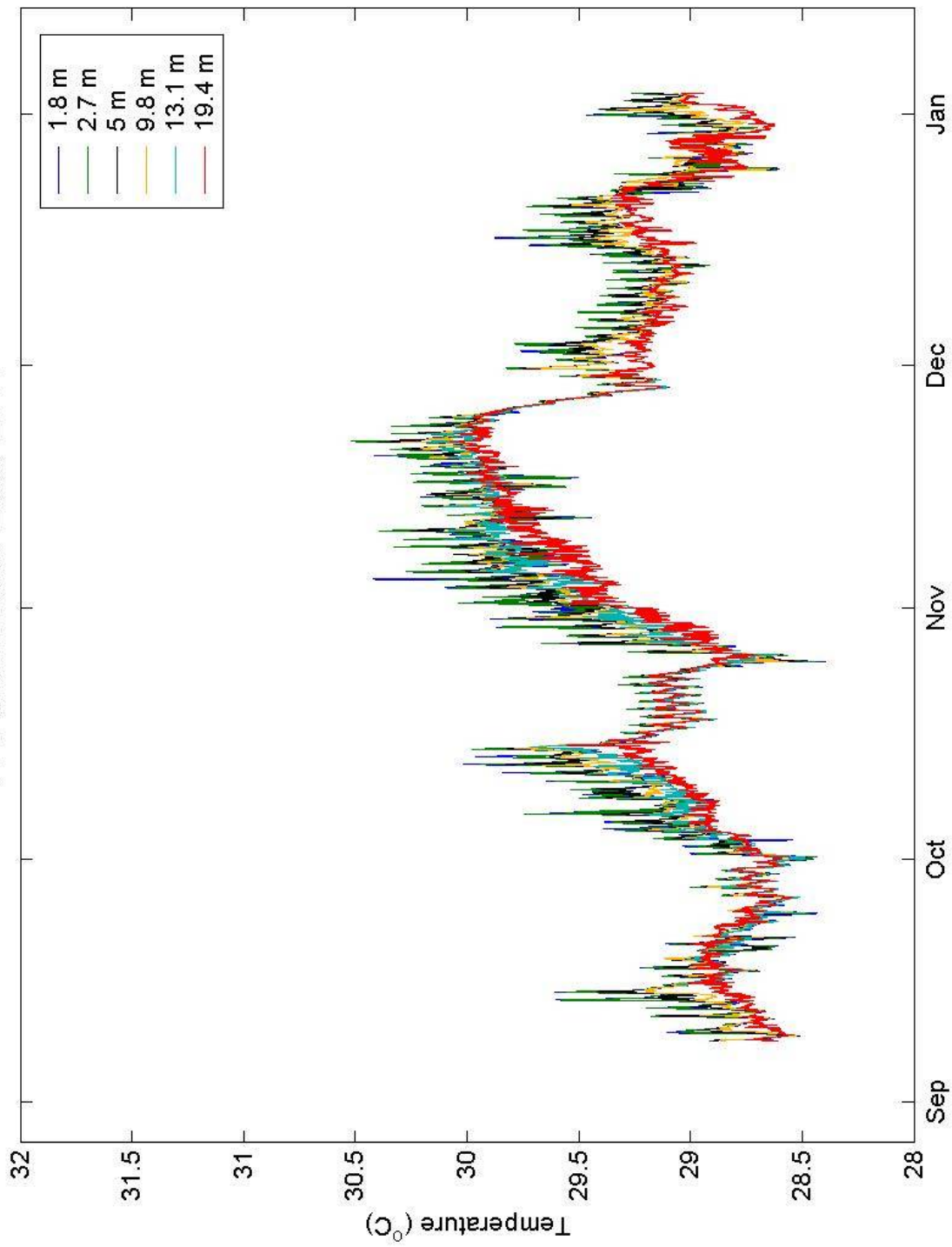
Switch off

Comments : Flat battery – gap

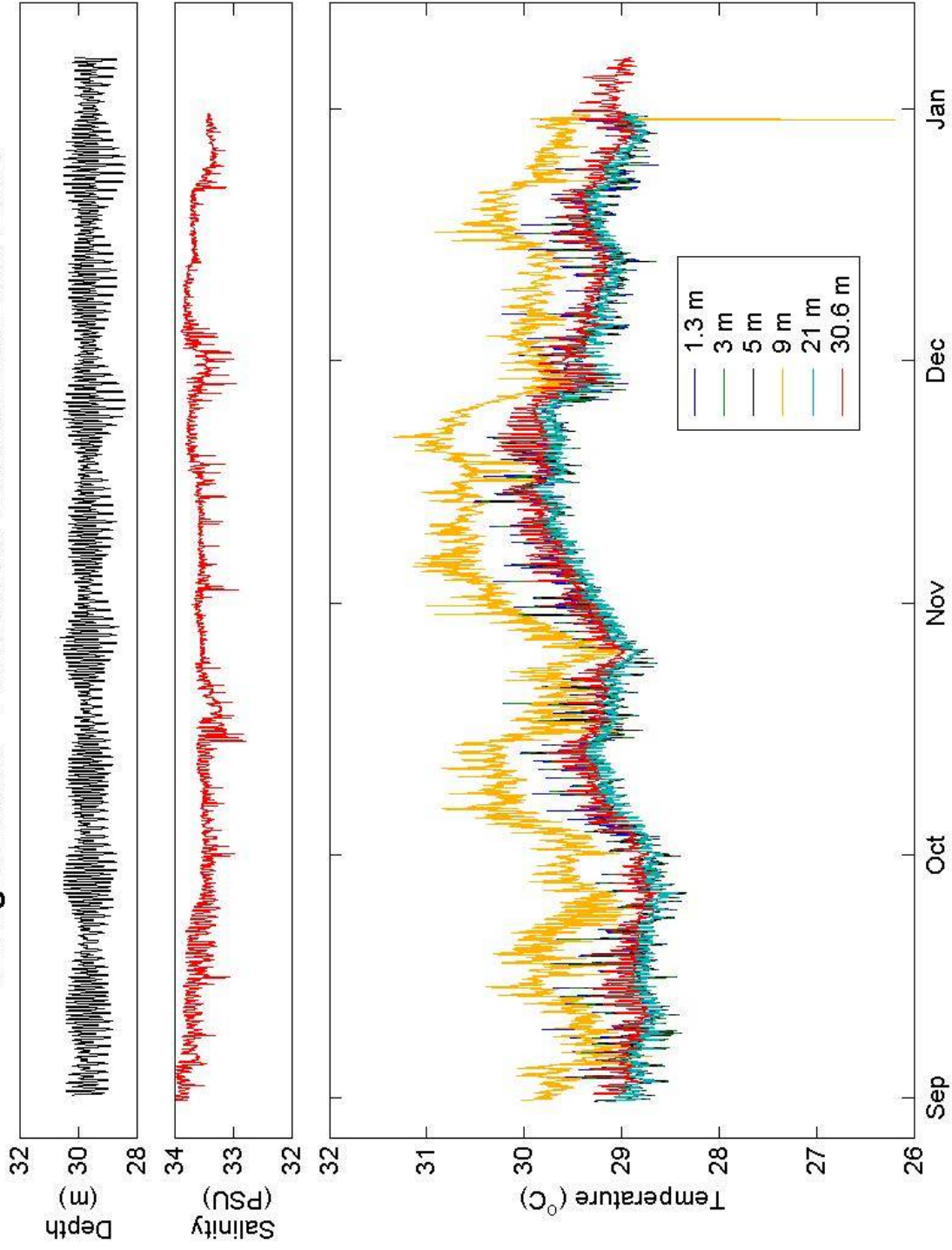
Appendix G – Mooring and Transect Summary Plots

Summary plots from the moorings and transects of temperature loggers are presented for observation of temperature variations with depth. Where available, depth and salinity data are also shown for each location.

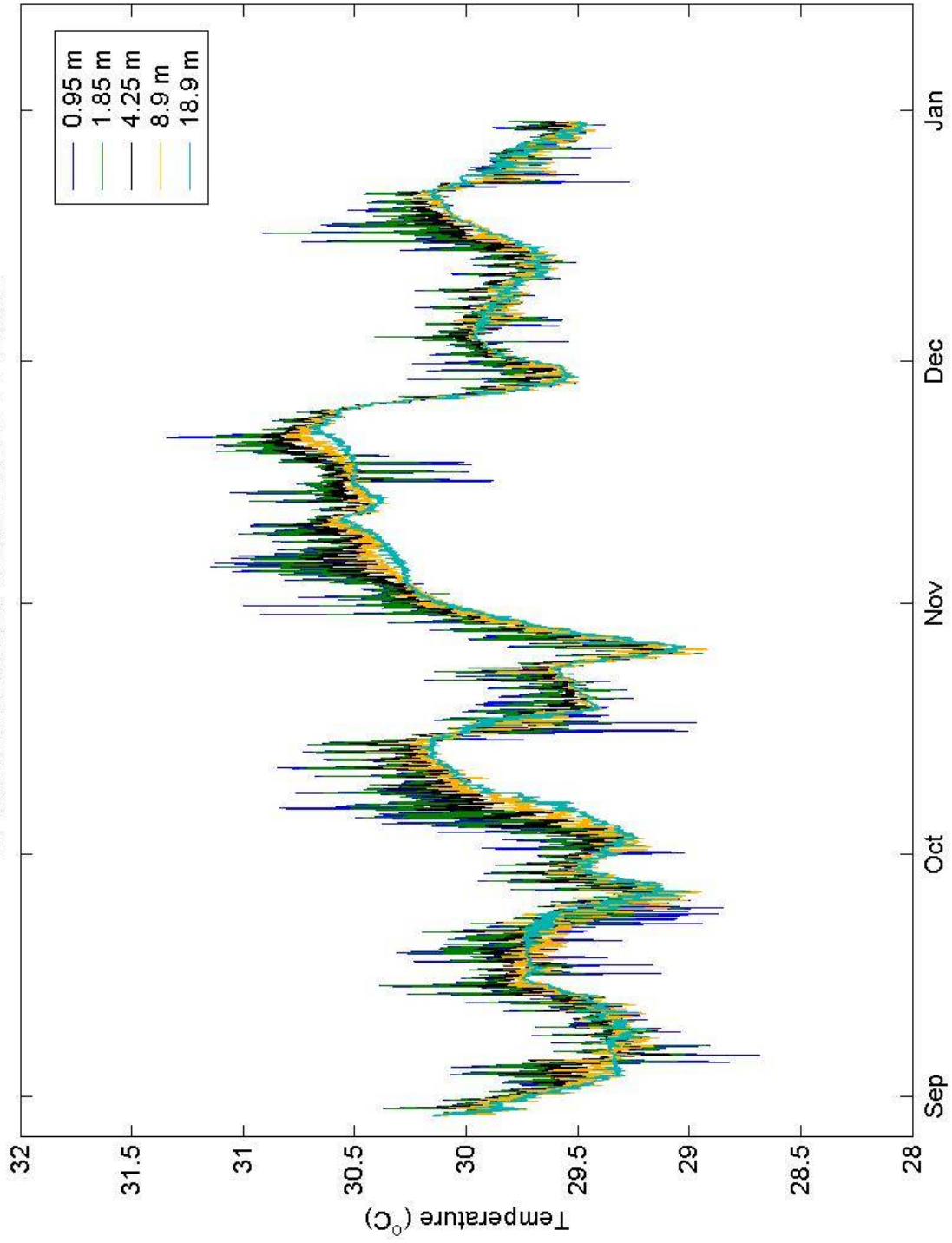
T1 Falcon Reef 2003-2004



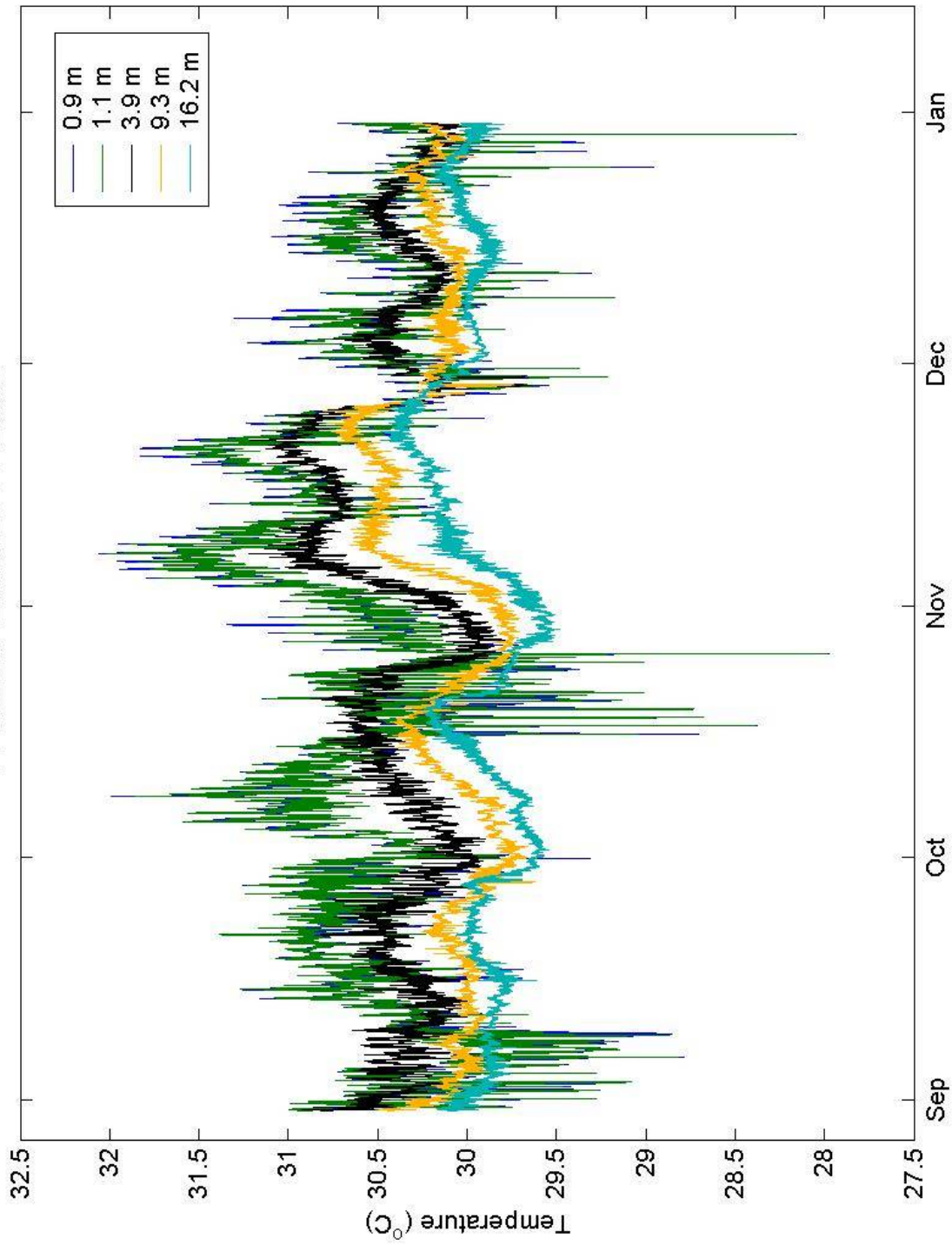
T2 Lighthouse - Toachel Ra Kesebekuu 2003-2004



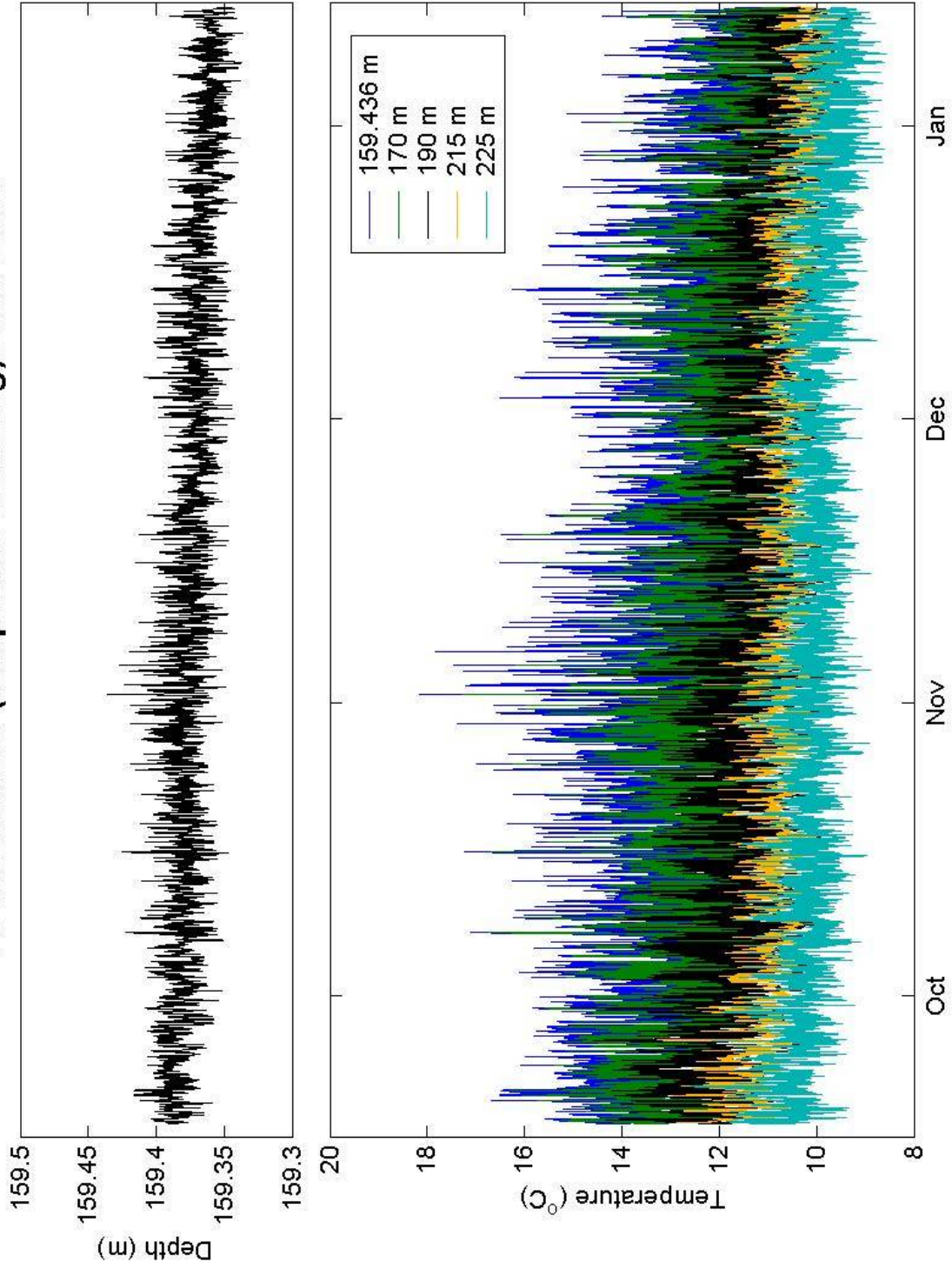
T3 Rock islands channel 2003-2004



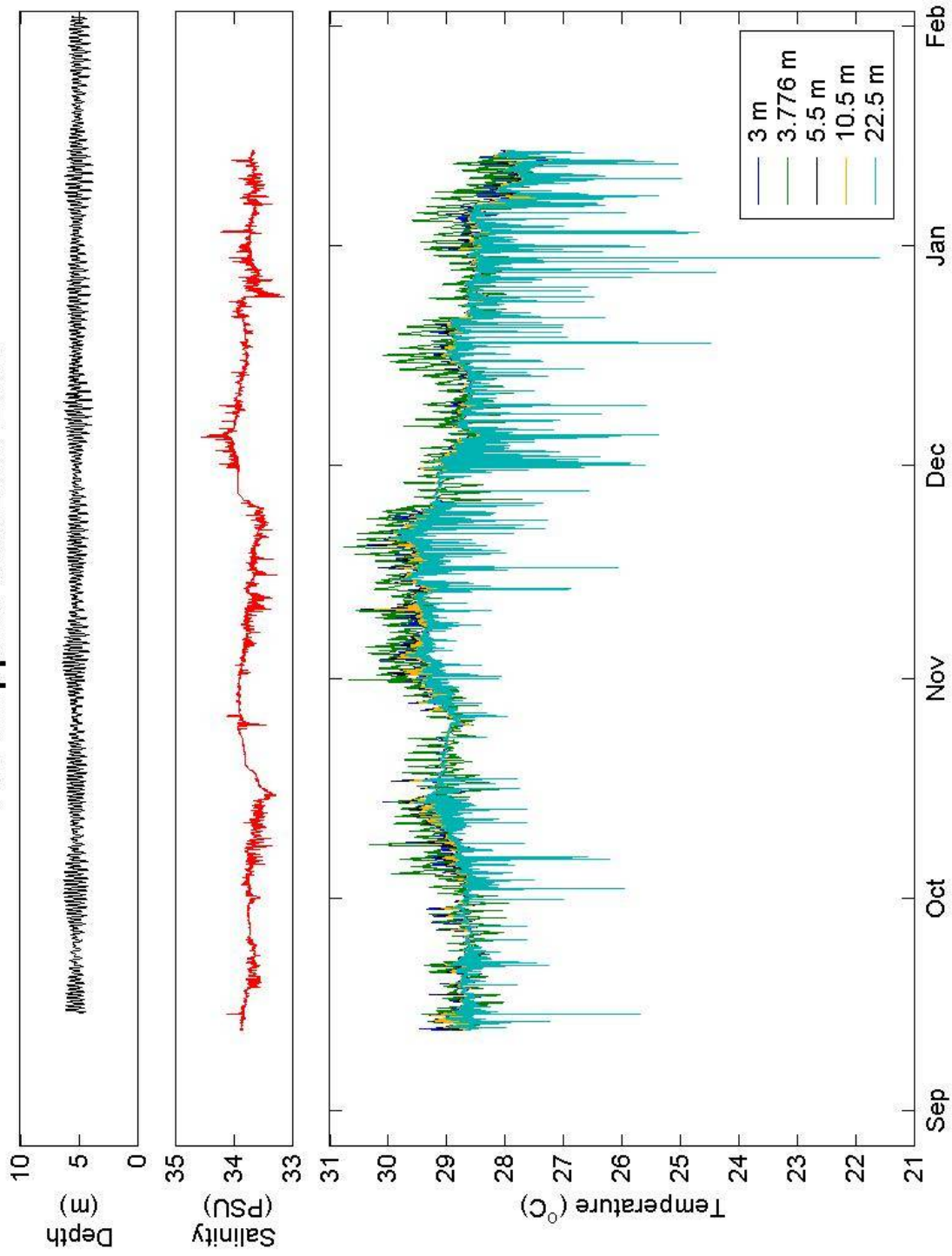
T4 Nikko Lake 2003-2004



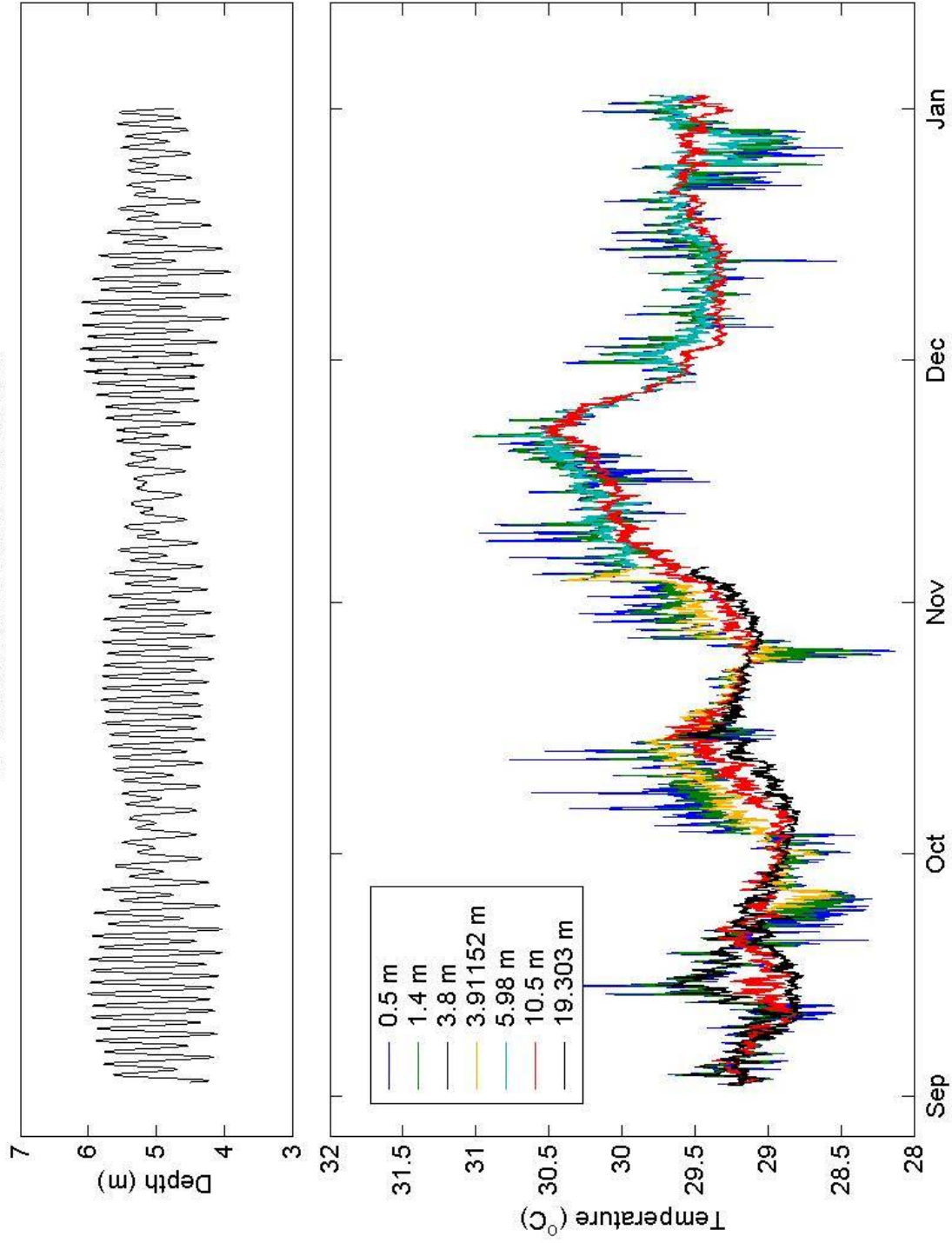
T5 Uchelbeluu (deepwater mooring) 2003-2004



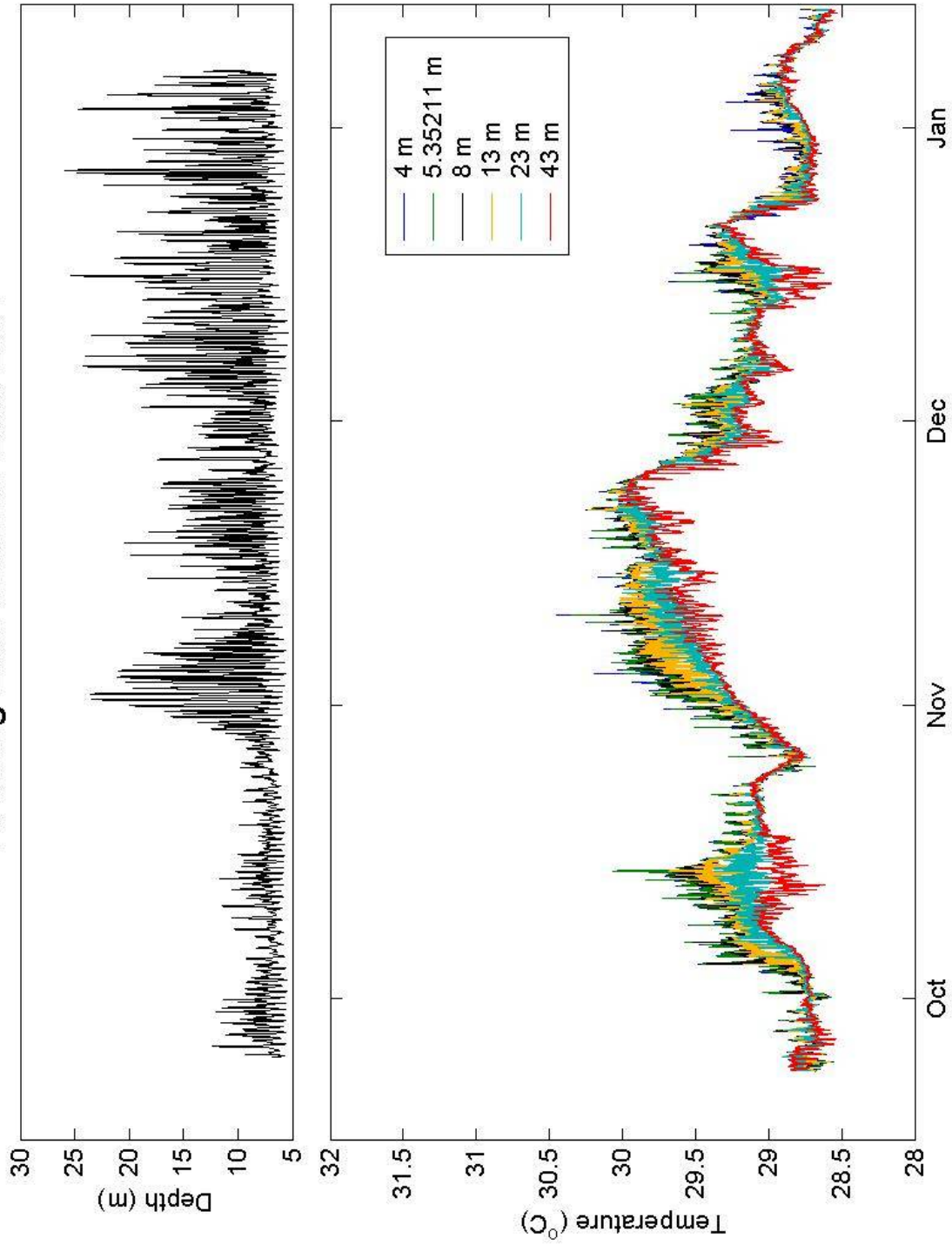
T6 Philippine Sea 2003-2004



T7 Southern Rock Islands



T8 Ulong East Channel 2003-2004



Appendix H – Time Series Plots of Current Meter Data

The following data plots vary according to the type of instrument used to record the currents.

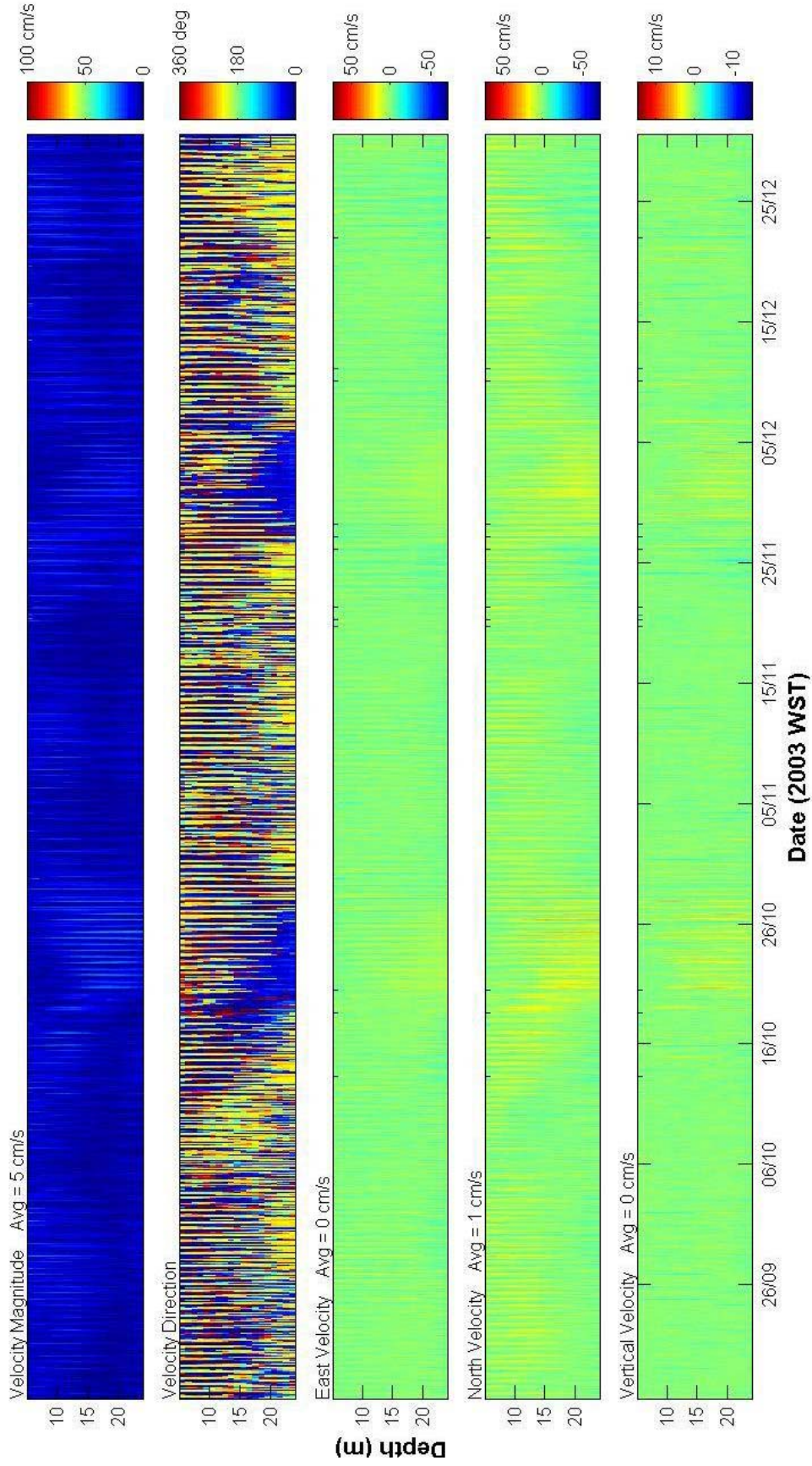
ADCP data (A1, A4, A5, A8, A9, A10, A11b, A11c, A13, A14) are presented using three figures. The first of these provides plots of current magnitude, direction and components (east, north and vertical) for all depth bins and throughout the deployment. The second and third figures show time series from the top and bottom bins of the vertical profile (i.e., nearest to the ocean surface and nearest to the instrument, respectively). These figures provide plots of temperature, depth (where available), current speed, current direction and a quiver plot of the currents. The quiver plot representation draws a line segment, originating at the axis, whose length is proportional to the current speed and whose direction represents that of the current (north and east directions are along the ordinate and abscissae, respectively). The scale on the ordinate axis reflects the current speed, as represented by the length of the line segment.

S4 current meter data (A2, A6) are presented in a single figure with time series plots of temperature (where available), depth, current magnitude, current direction and the quiver plot of currents, as described previously.

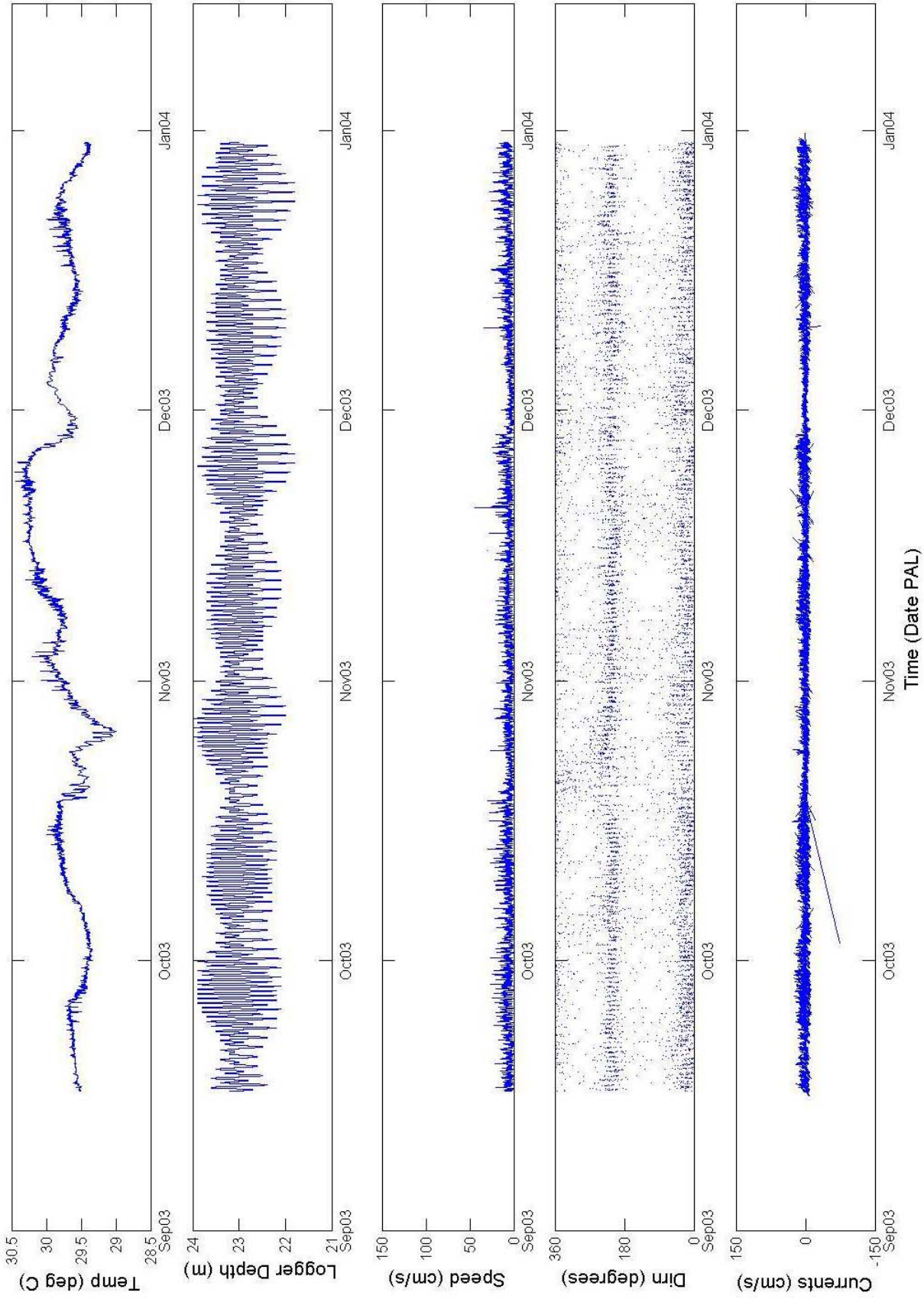
Nobska current meter data (A3, A7) are presented in two figures. The first of these shows time series of temperature, pressure in depth units (where available), current speed, current direction and the quiver plot of currents, as described previously. The second figure repeats the temperature plot accompanied by plots of conductivity (where available) and current components (east – u; north – v; and vertical – w).

No data were recorded for deployments A11 and A12.

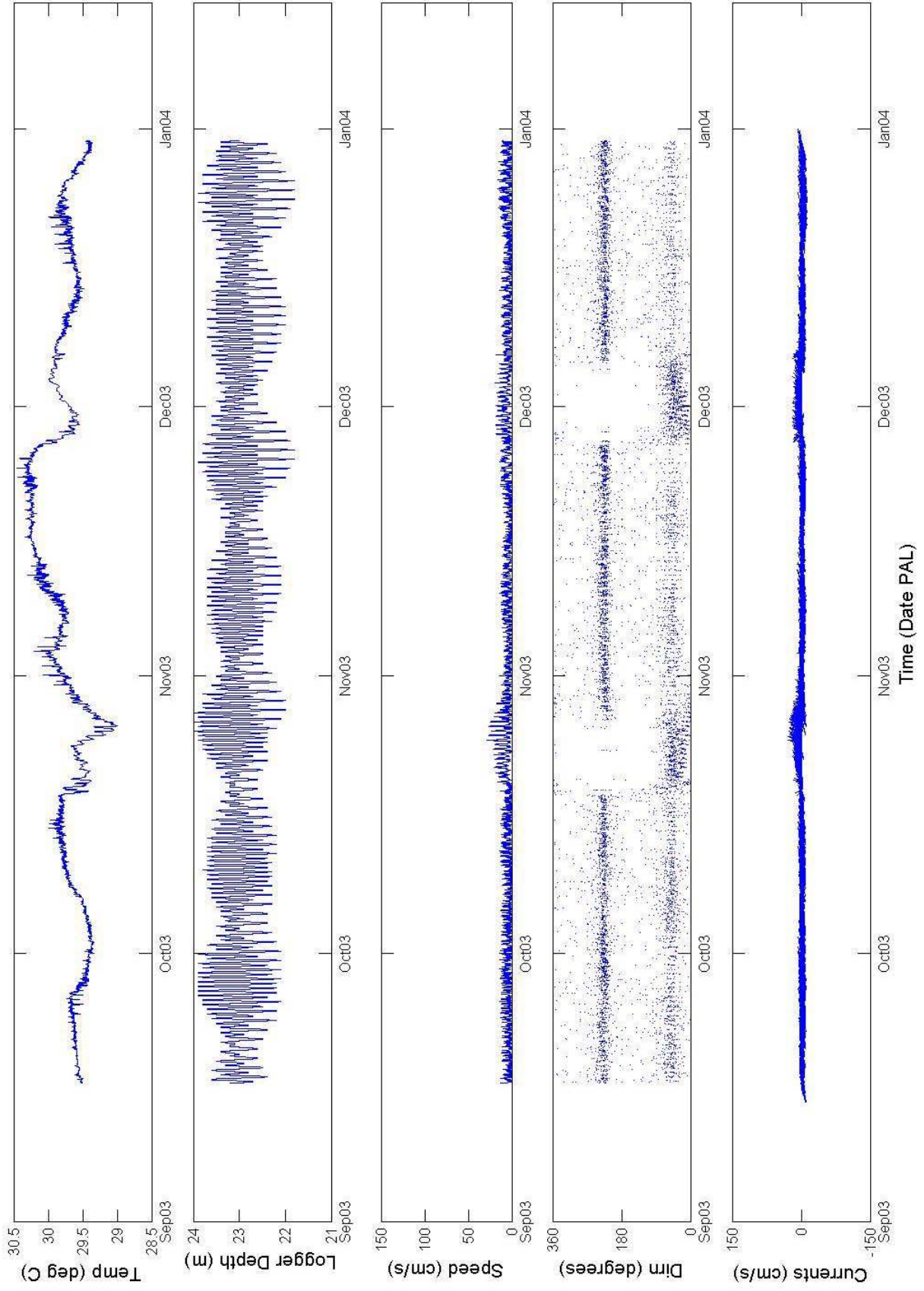
**A1 Palau
RDI/ADCP 974**



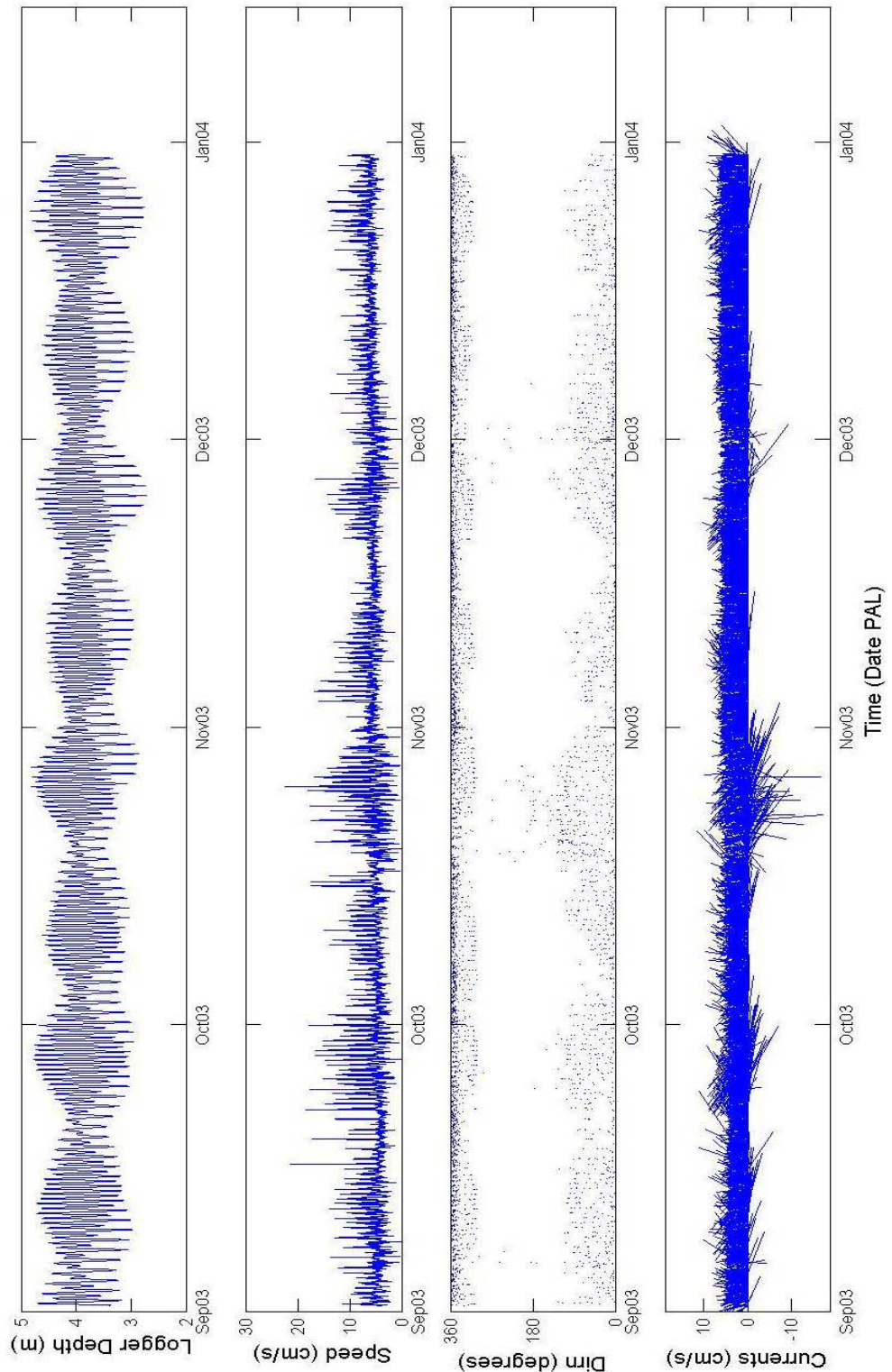
A1 - Top Bin - Palau



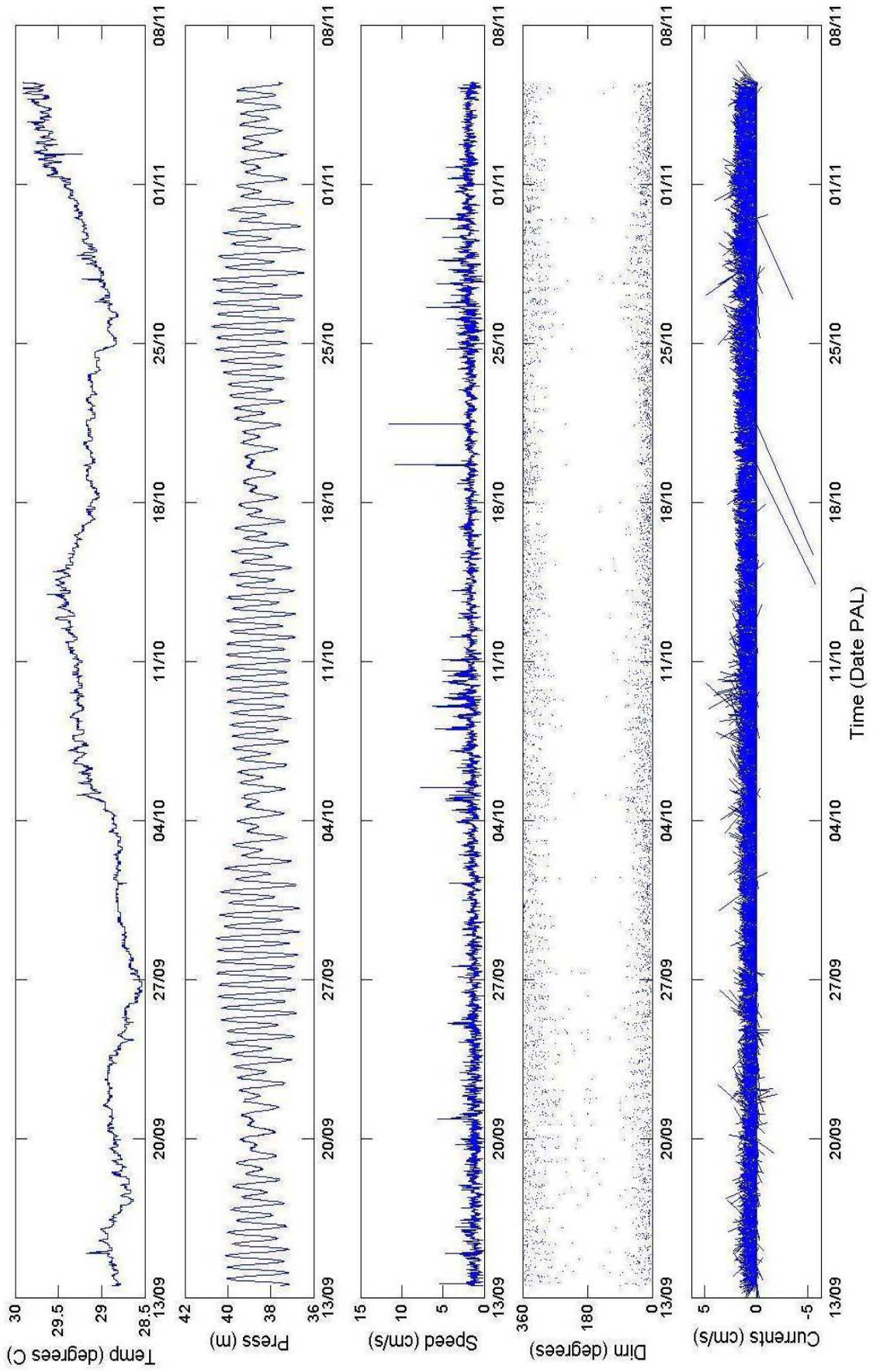
A1 - Bottom Bin - Palau



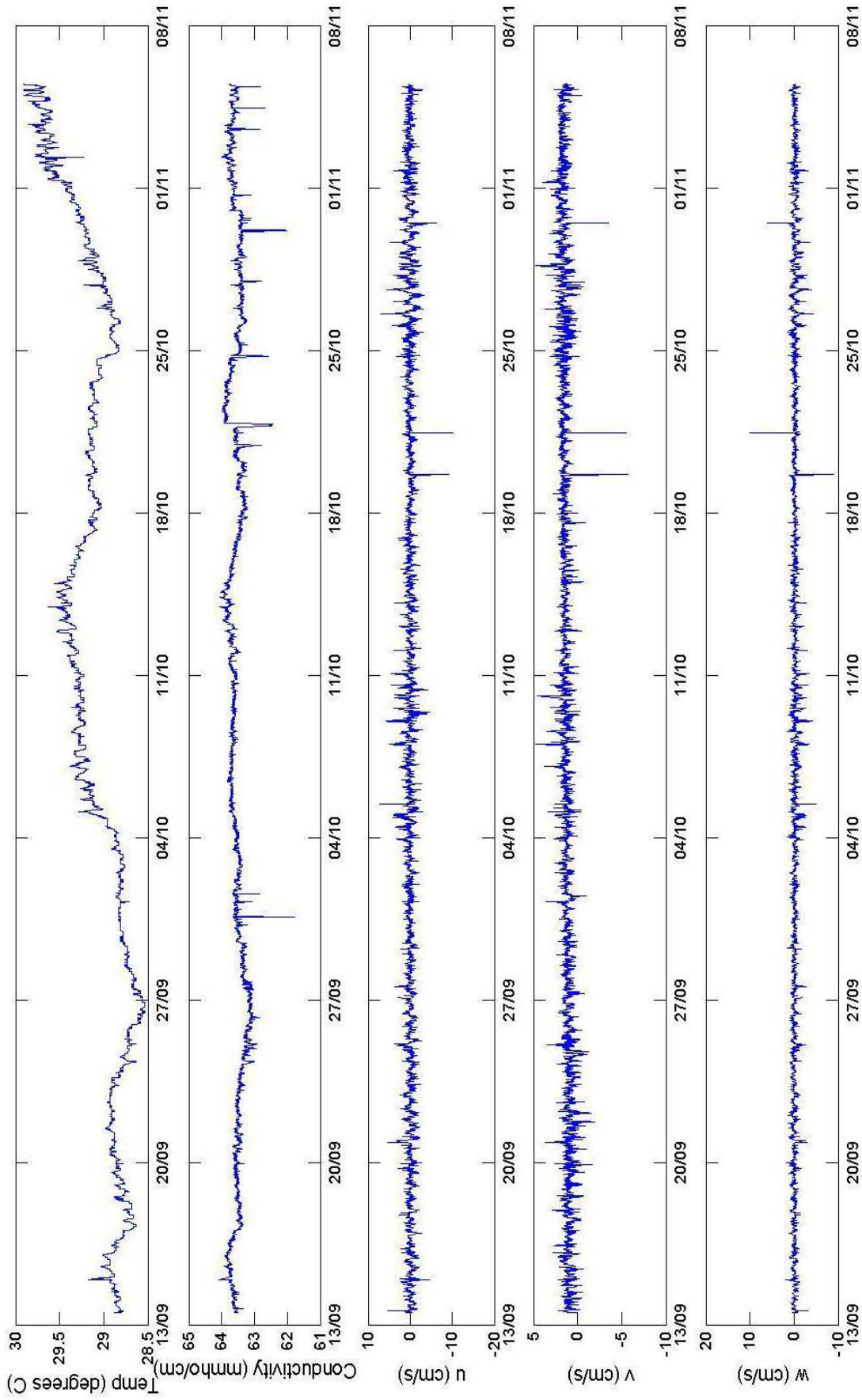
A2 - Palau



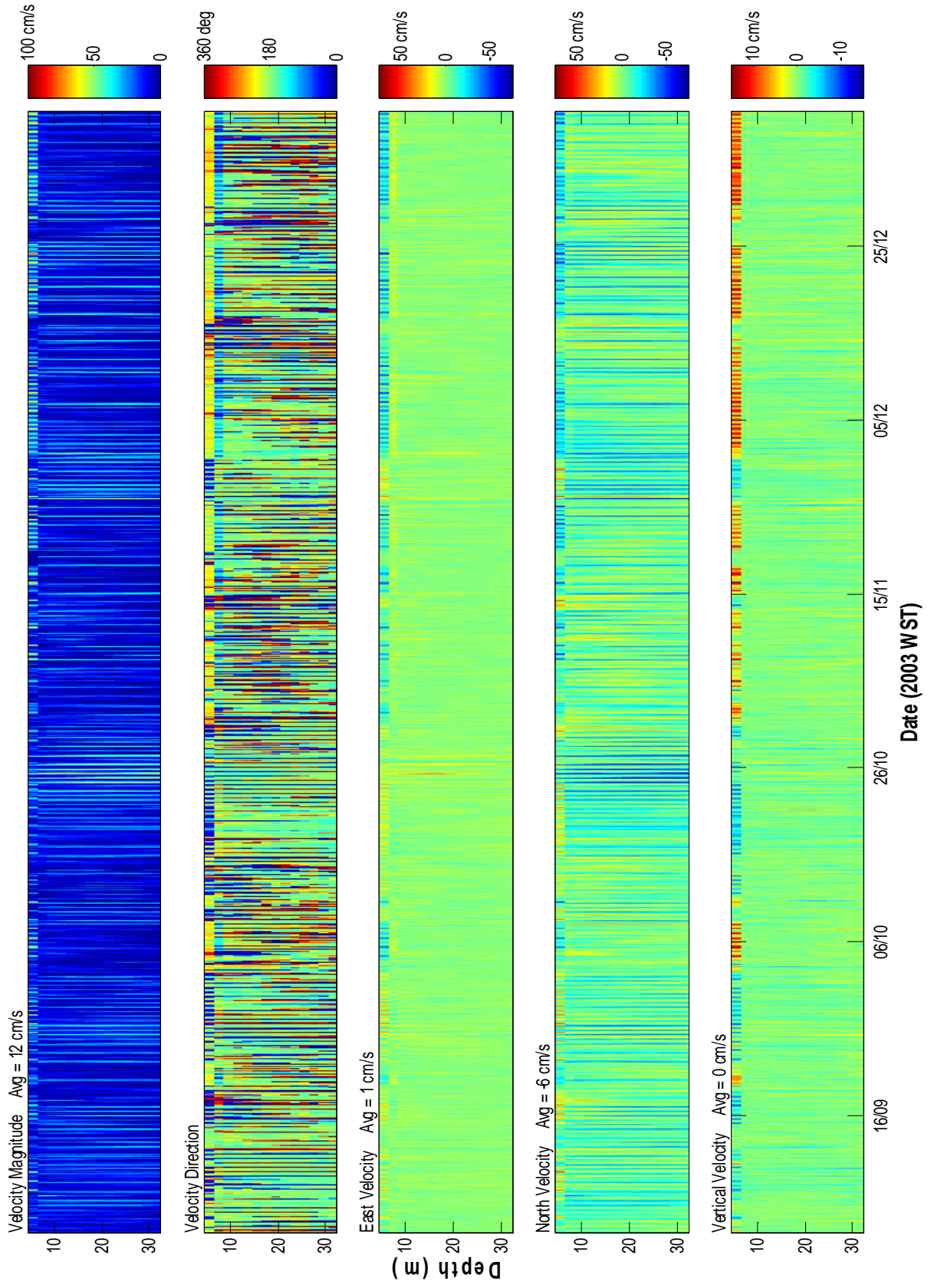
A3 - Palau



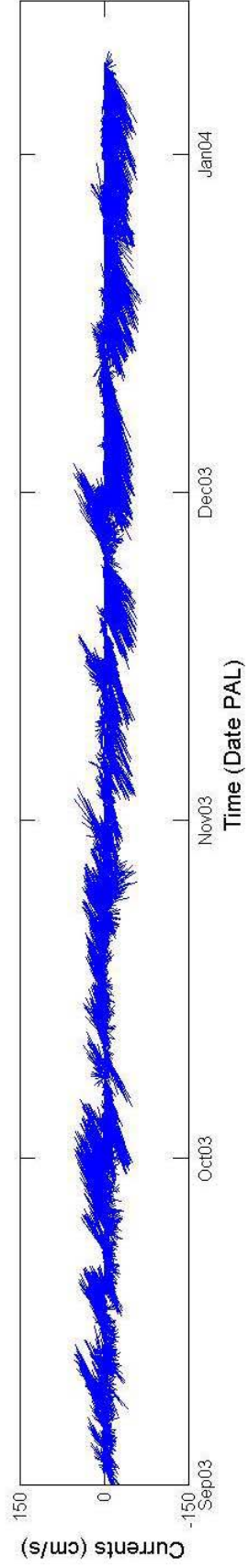
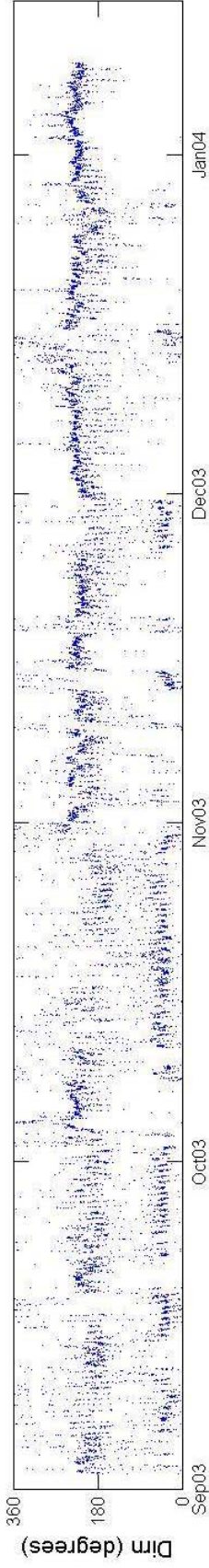
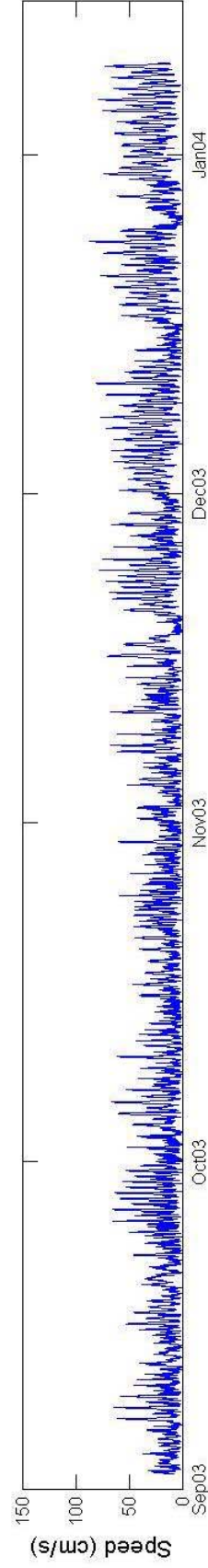
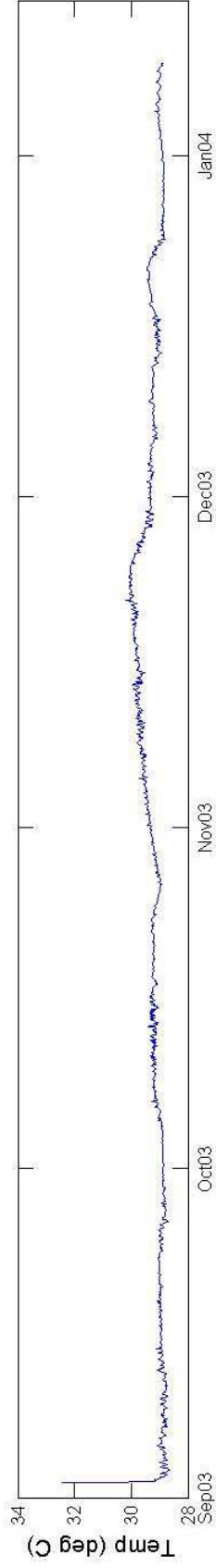
A3 - Palau



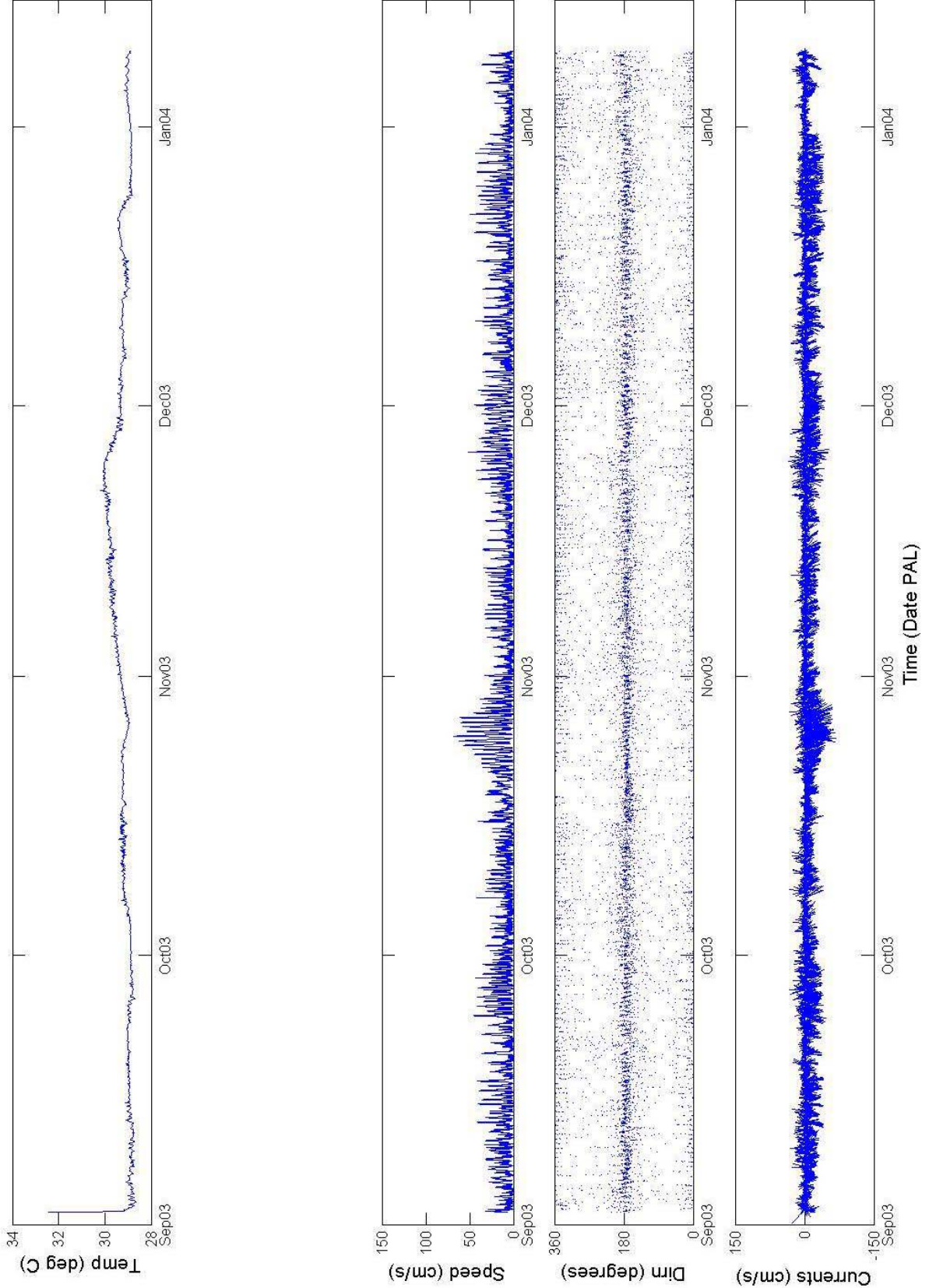
A4 Palau
RDI ADCP 584



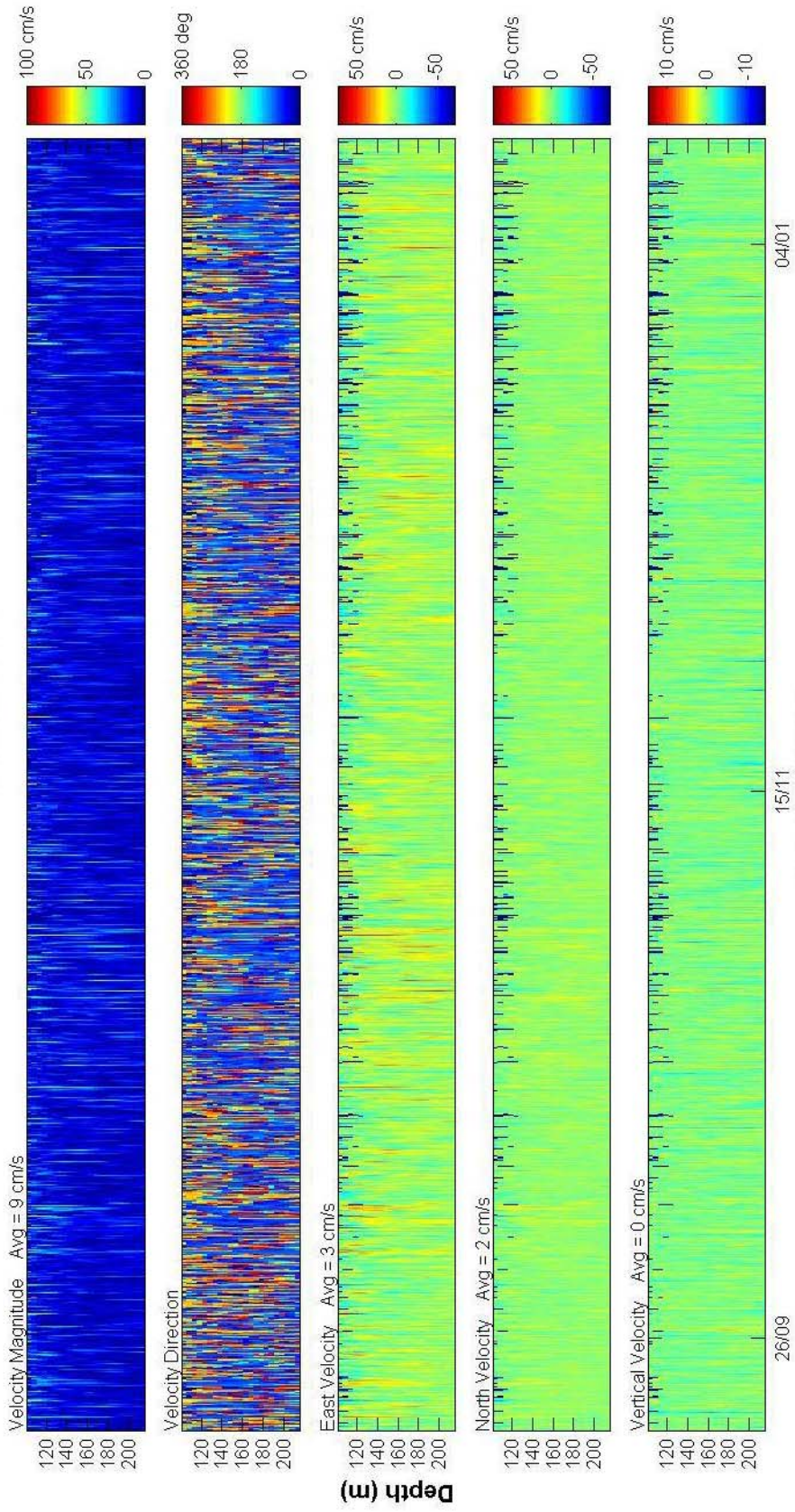
A4 - Top Bin - Palau



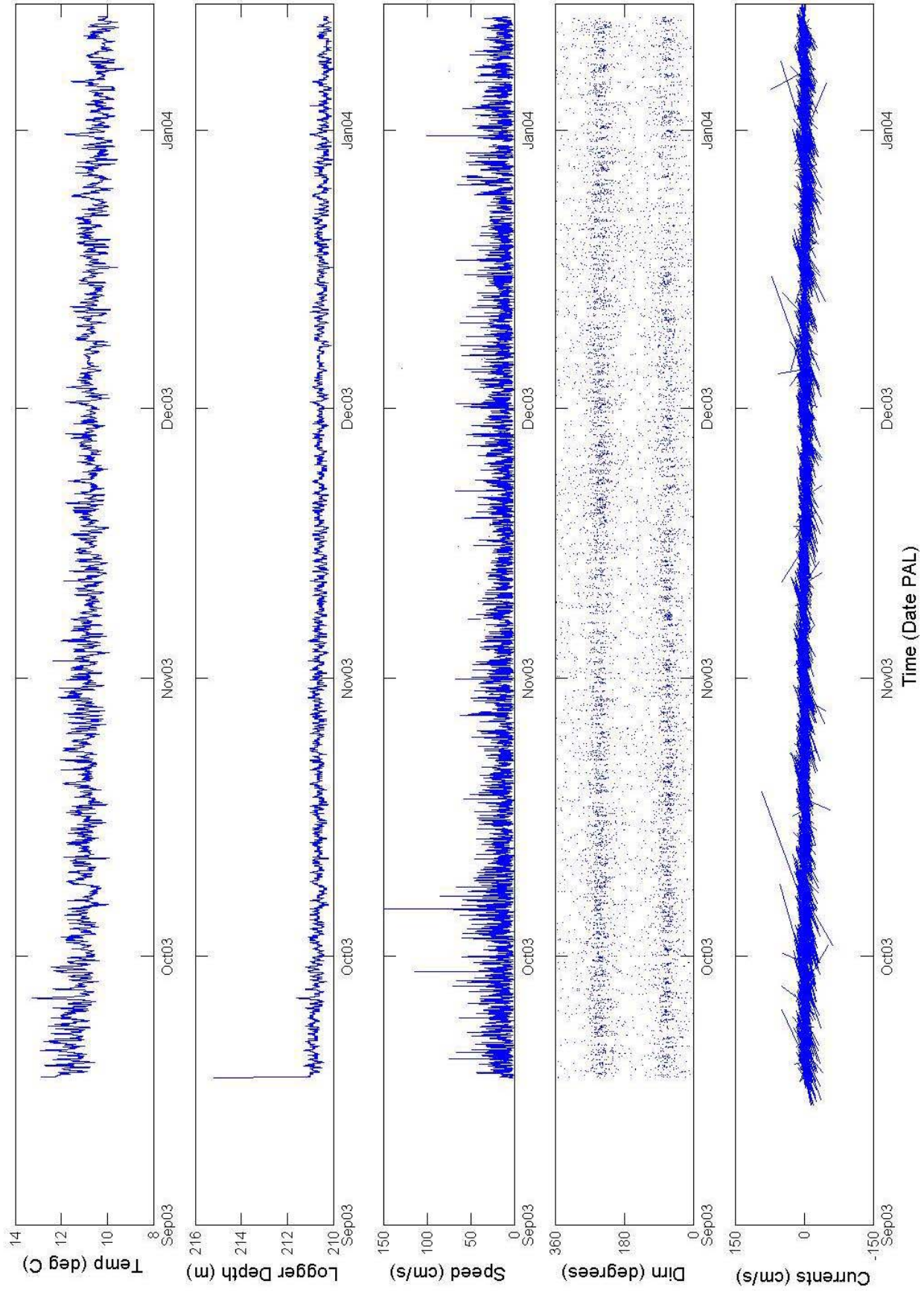
A4 - Bottom Bin - Palau



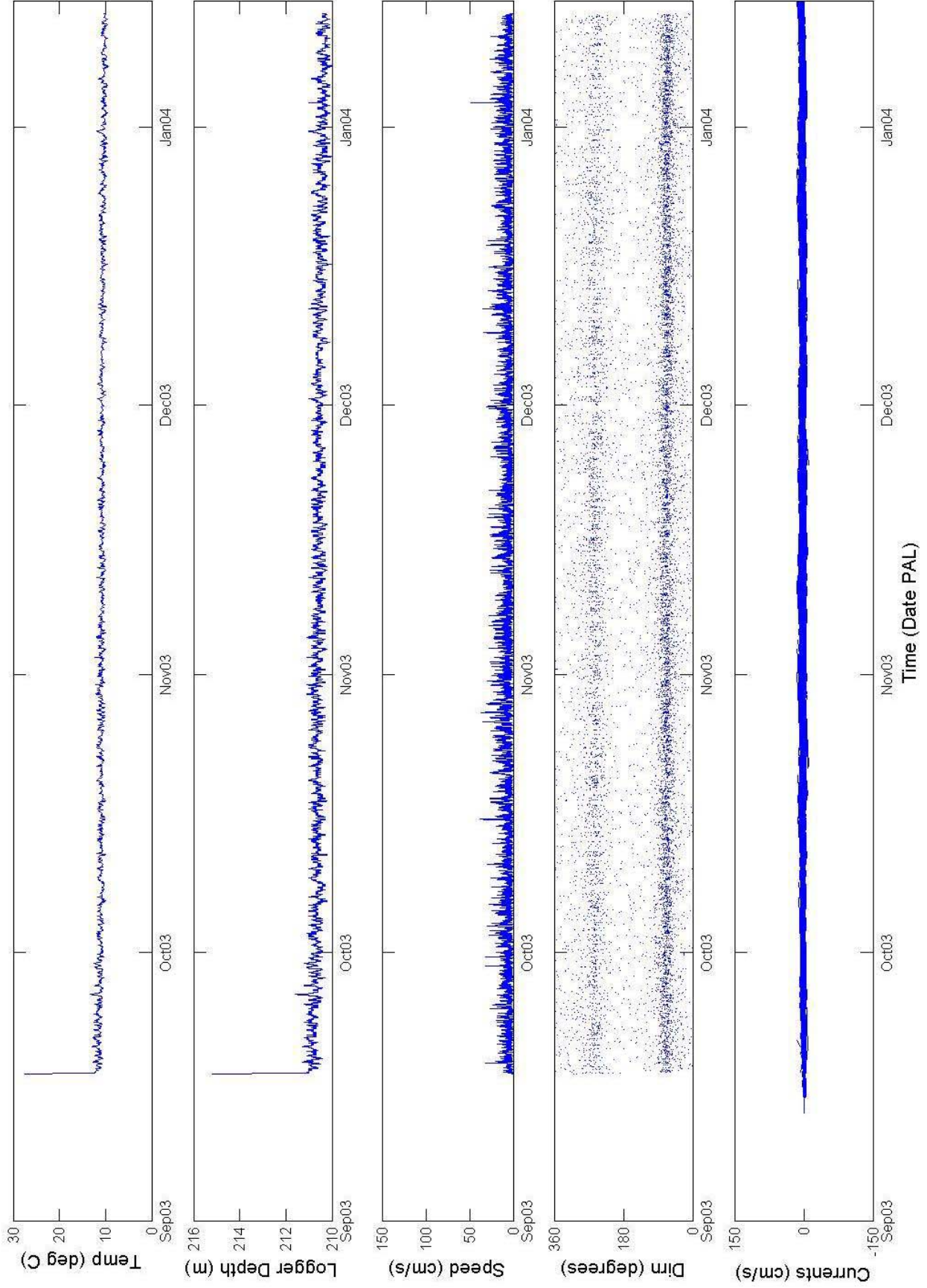
**A5 Palau
RDI ADCP 412**



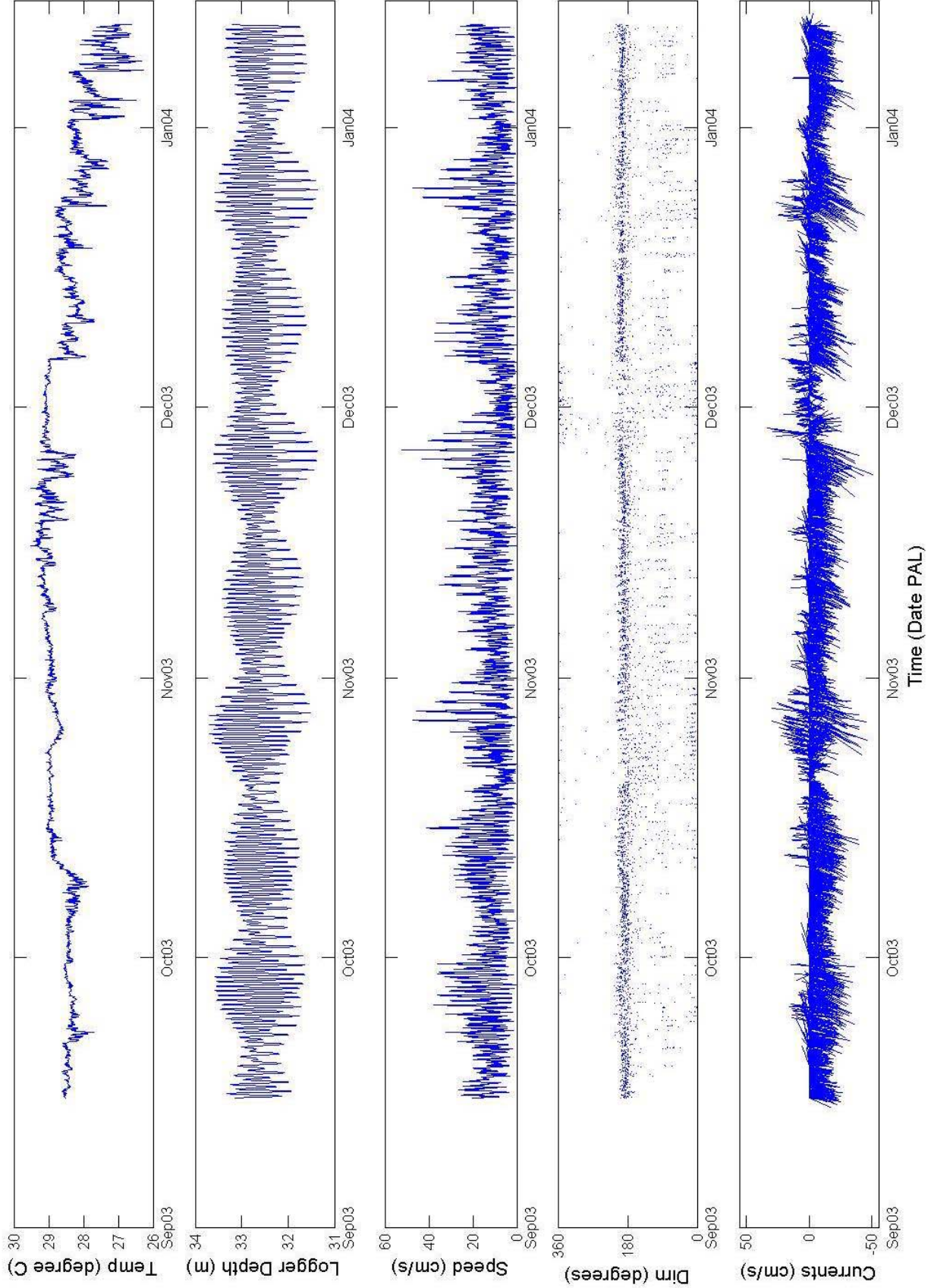
A5 - Top Bin - Palau



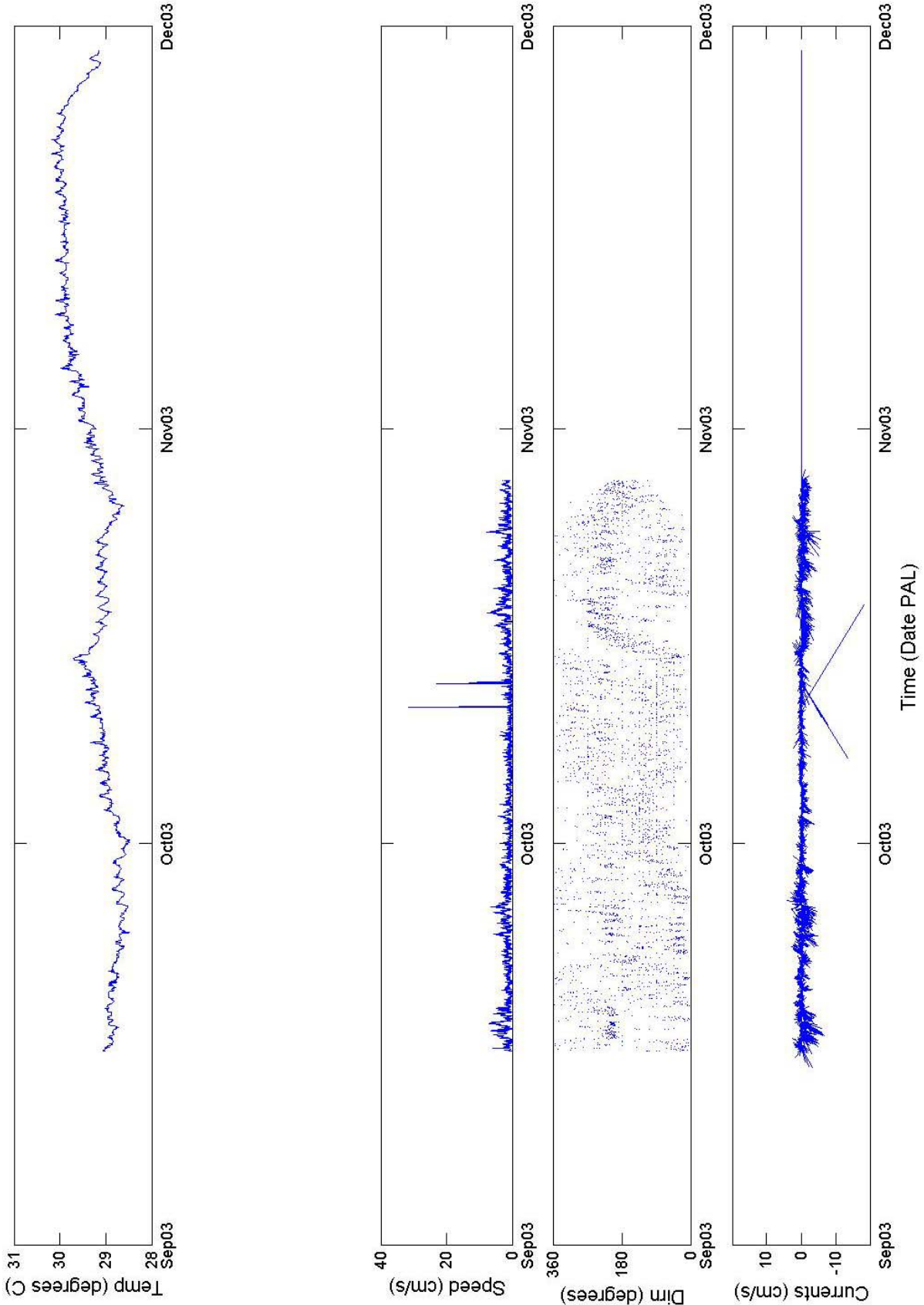
A5 - Bottom Bin - Palau



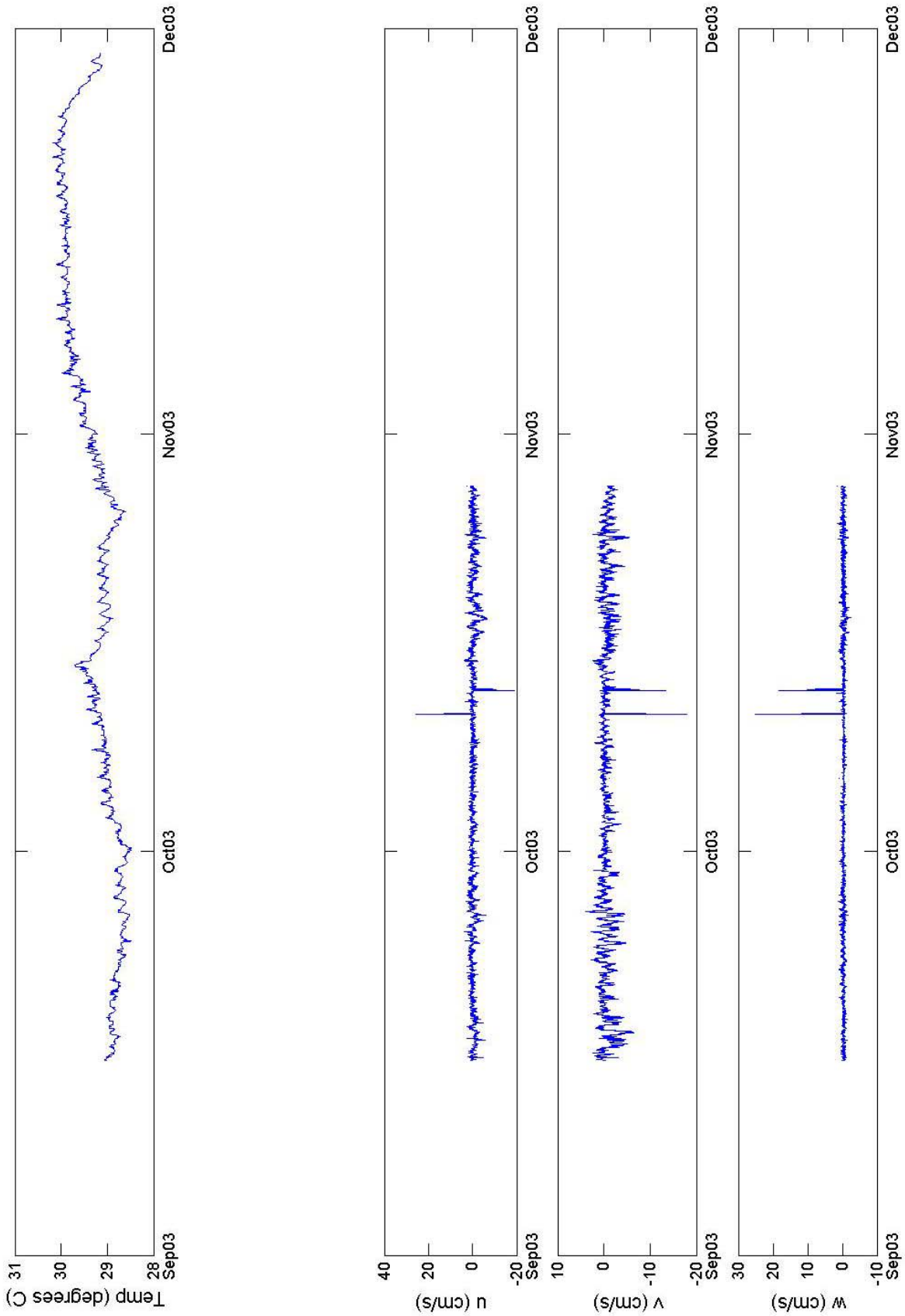
A6 - Palau



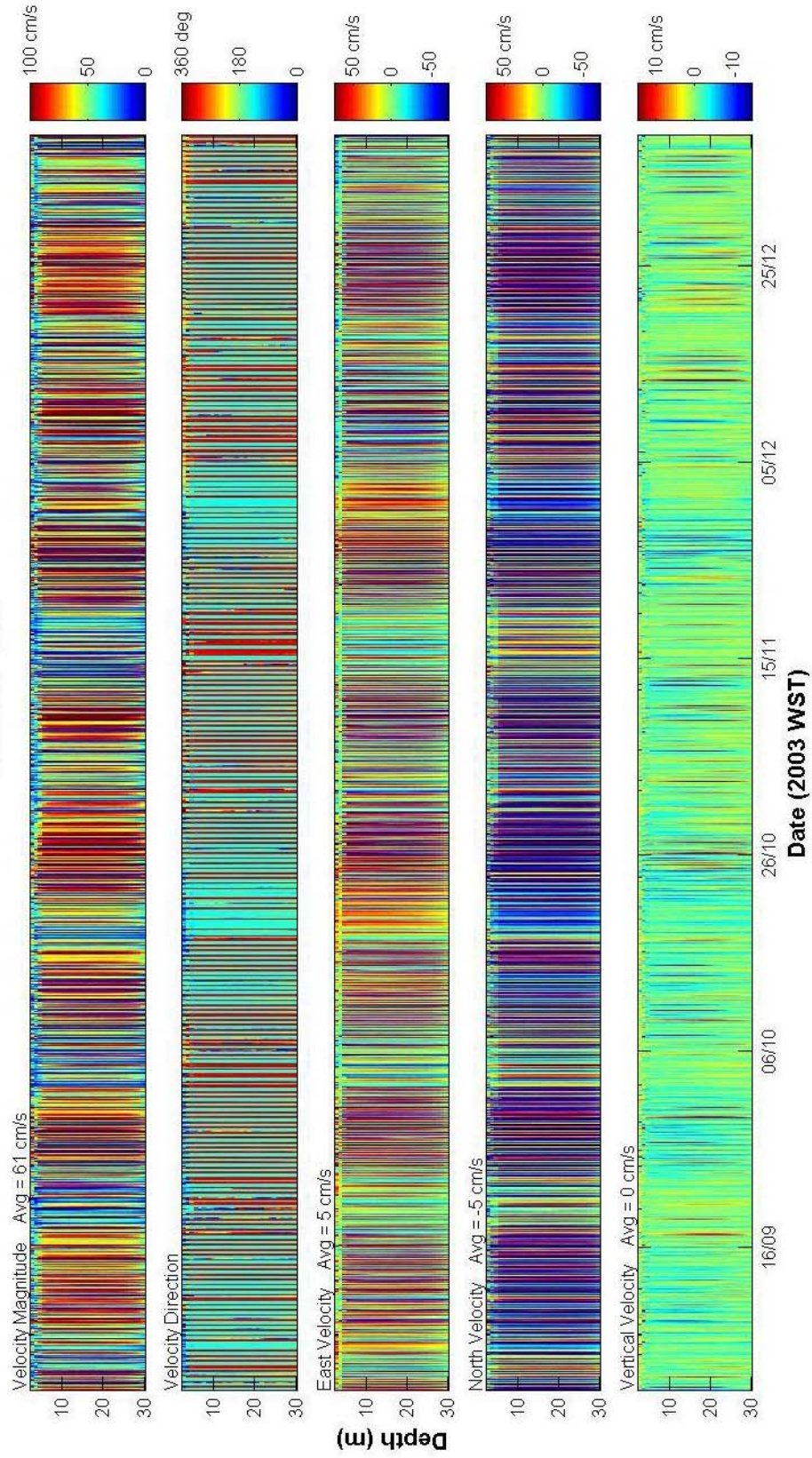
A7 - Palau



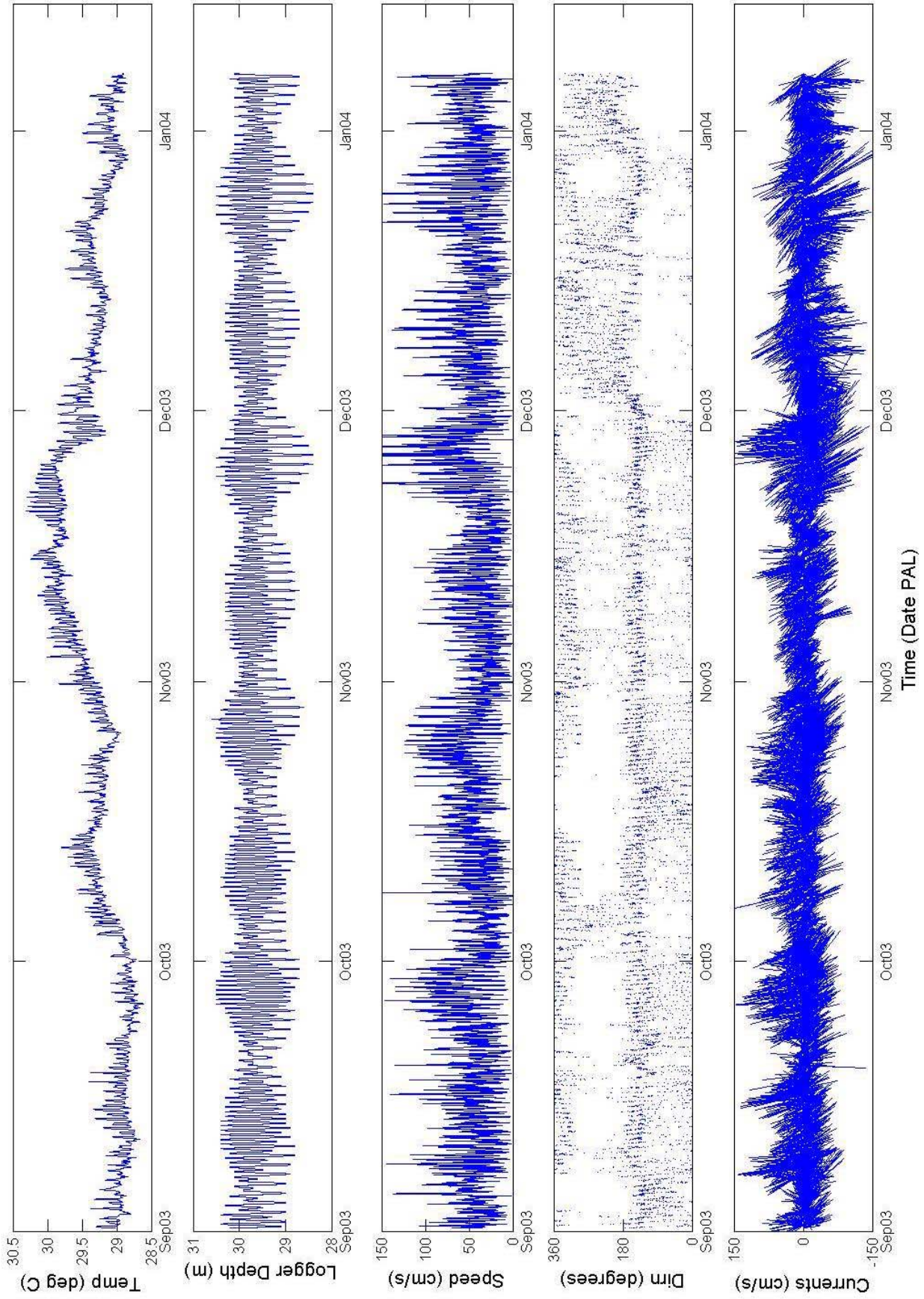
A7 - Palau



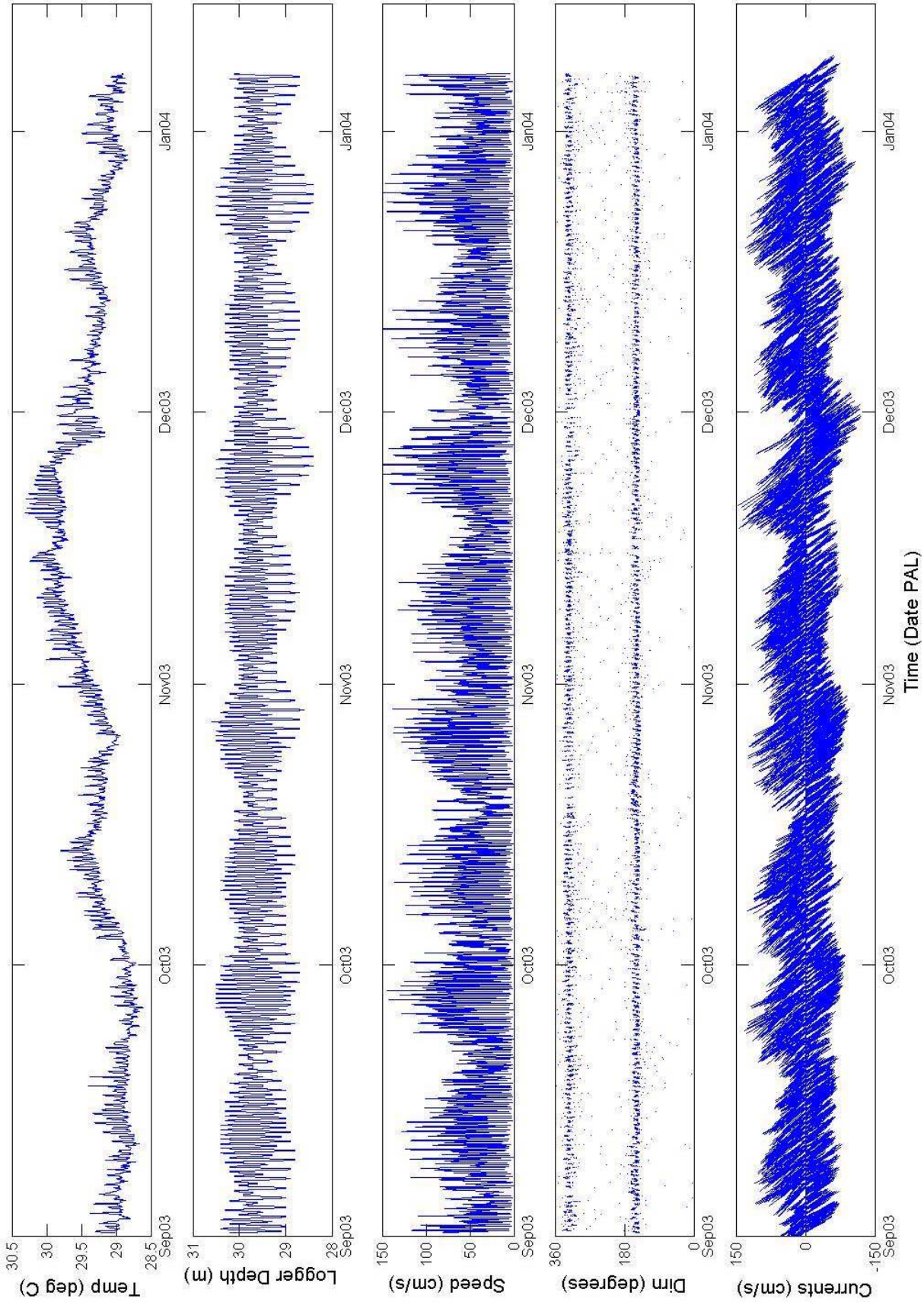
**A8 Palau
RDI ADCP 3228**



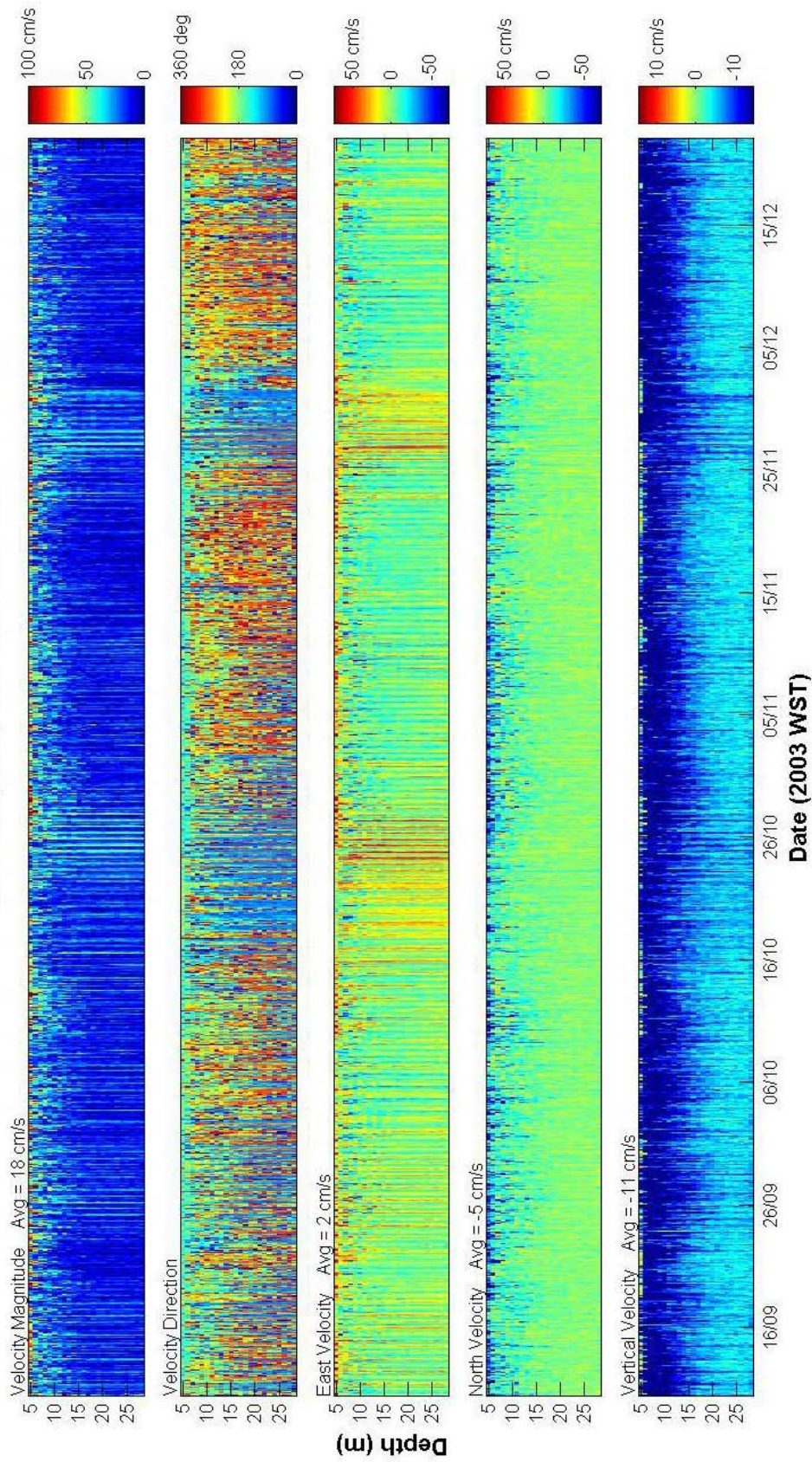
A8 - Top Bin - Palau



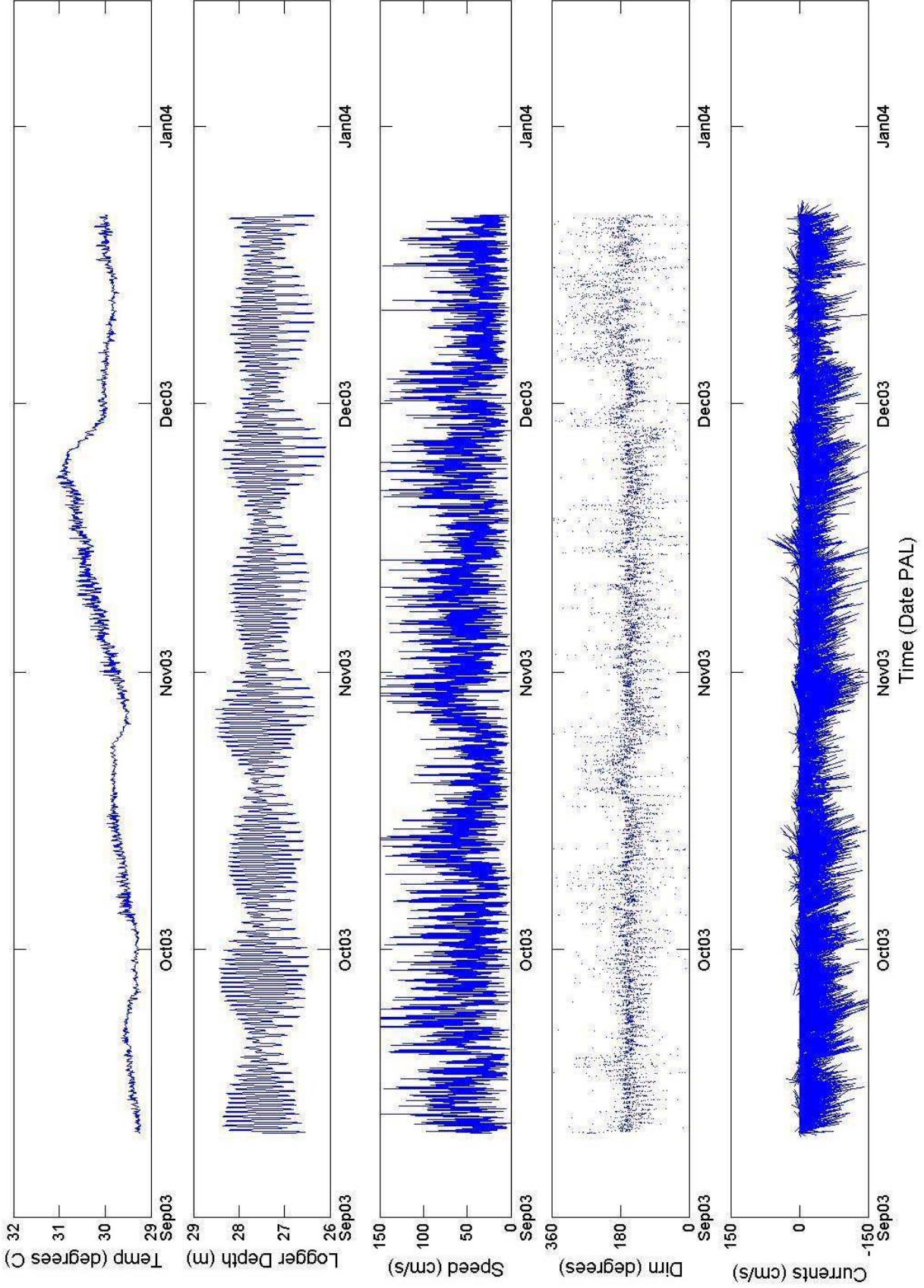
A8 - Bottom Bin - Palau



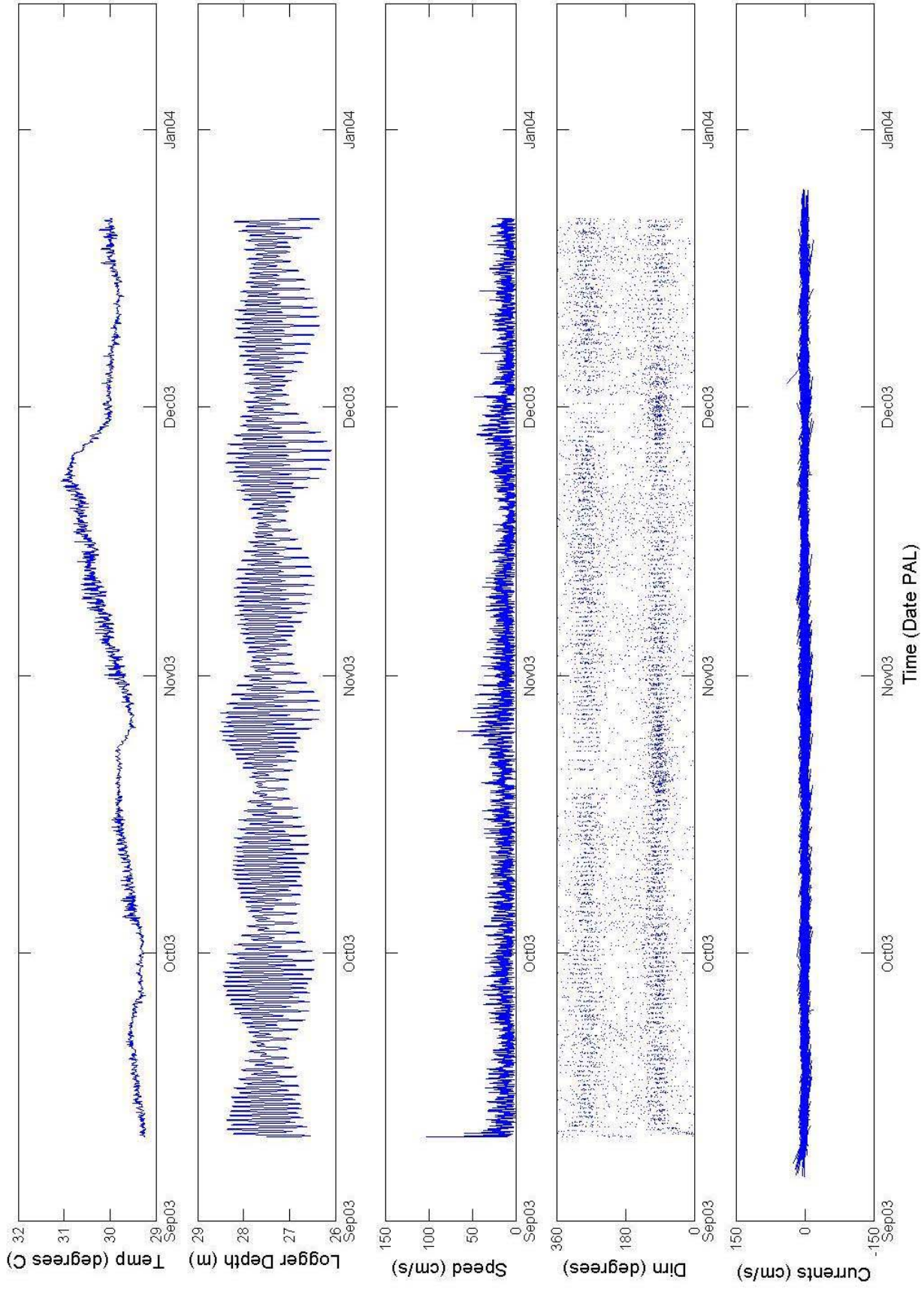
**A9 Palau
Nortek Aquadop Current Profiler 794**



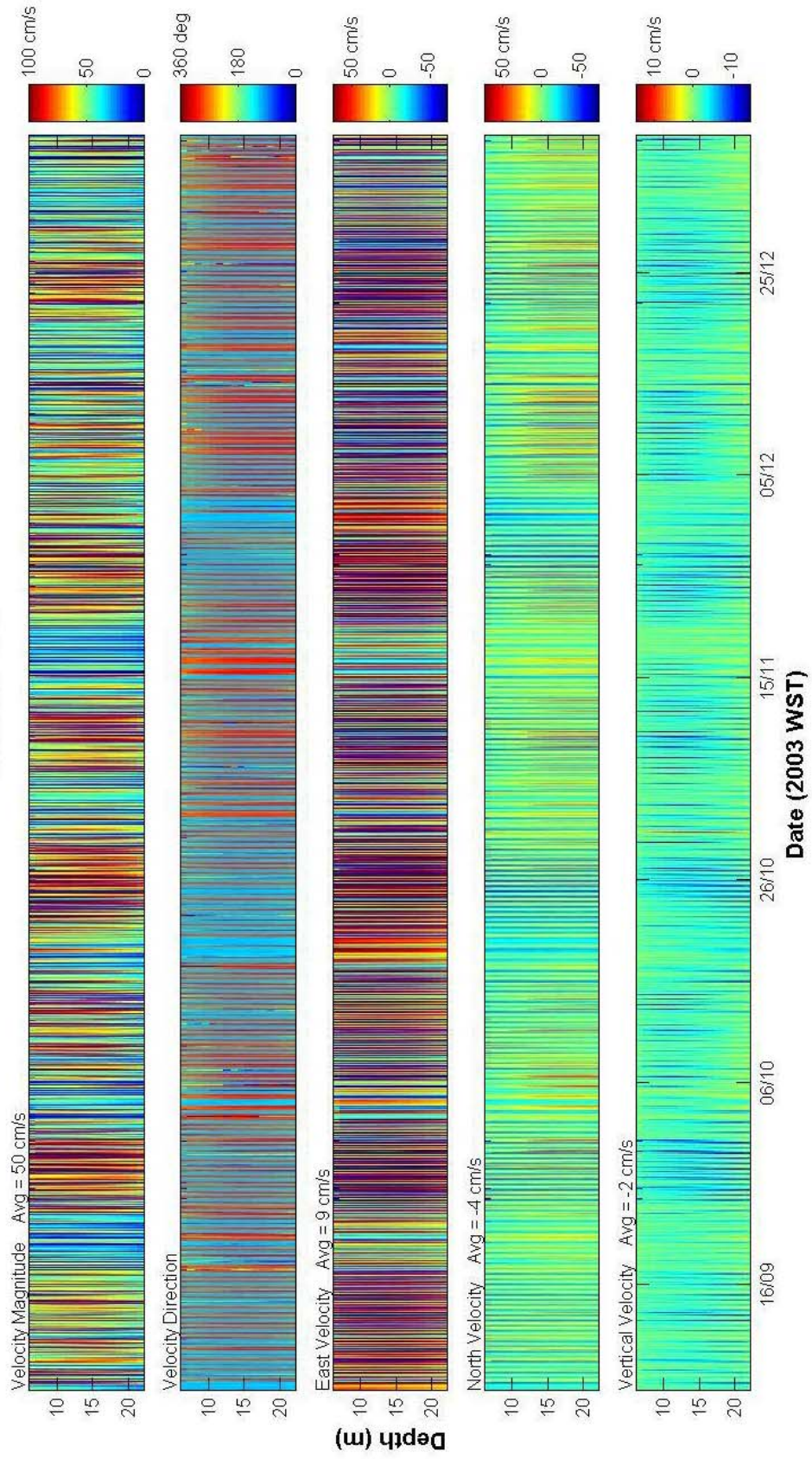
A9 - Top Bin - Palau



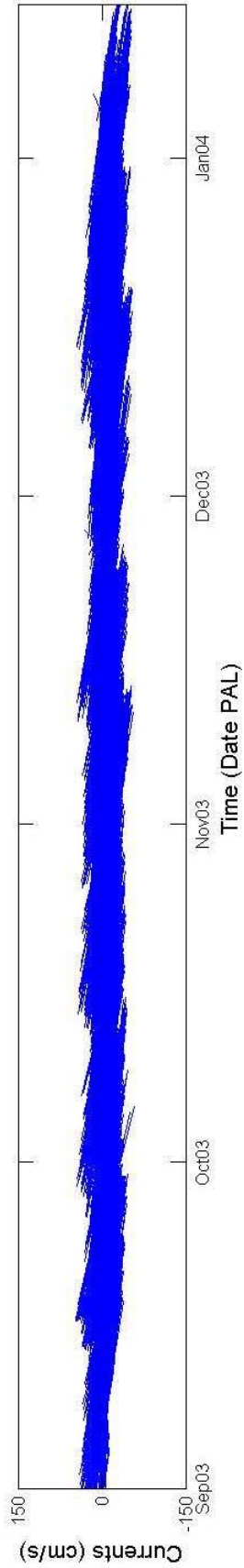
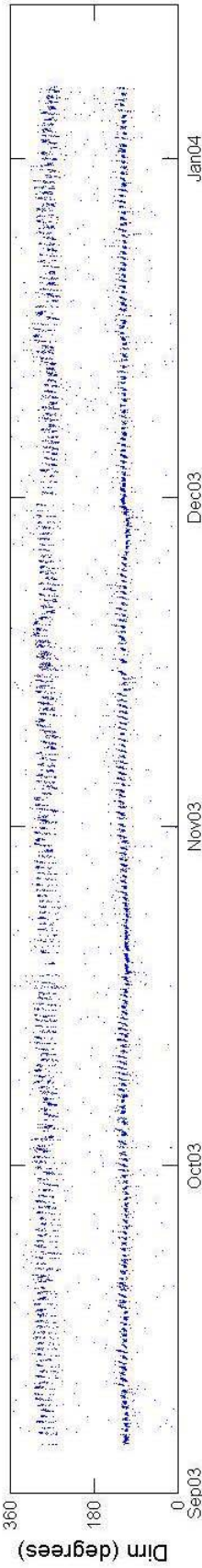
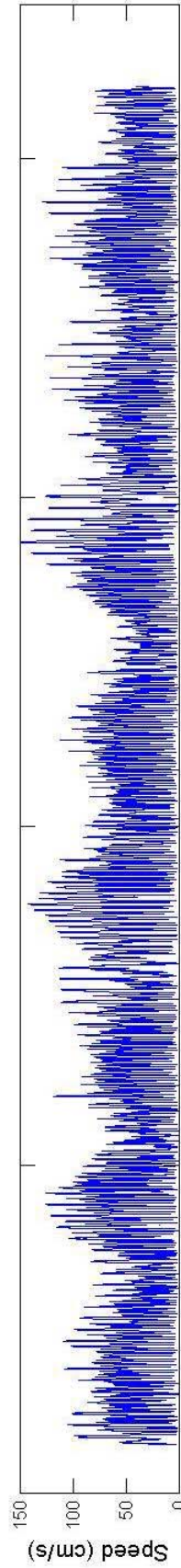
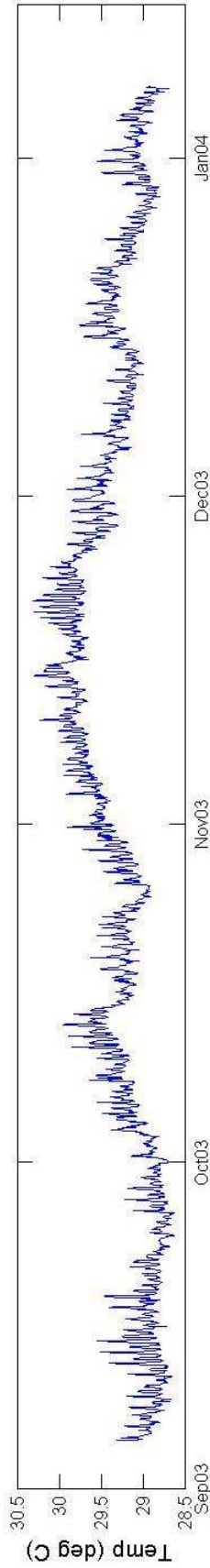
A9 - Bottom Bin - Palau



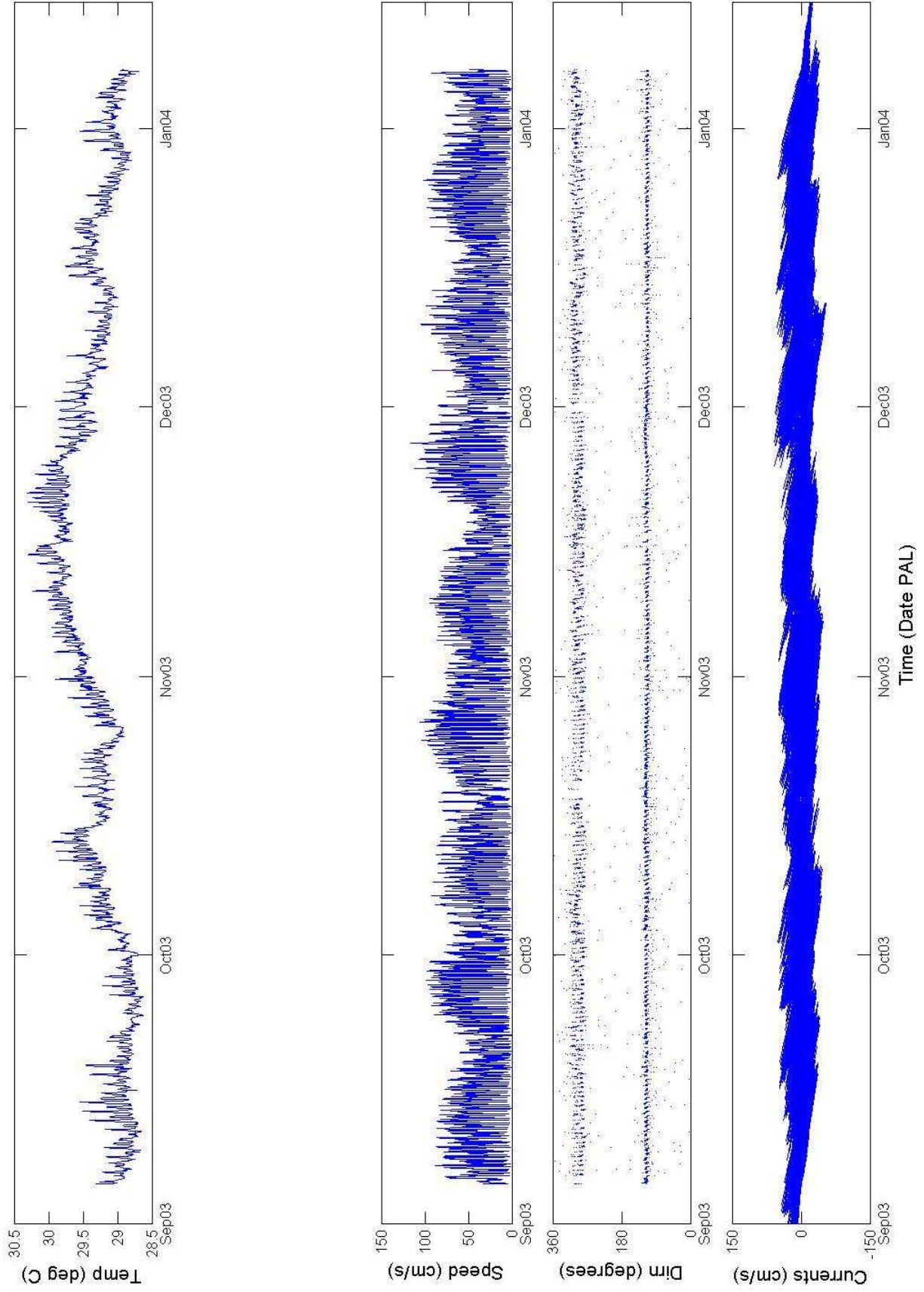
**A10 Palau
RDI ADCP 1292**



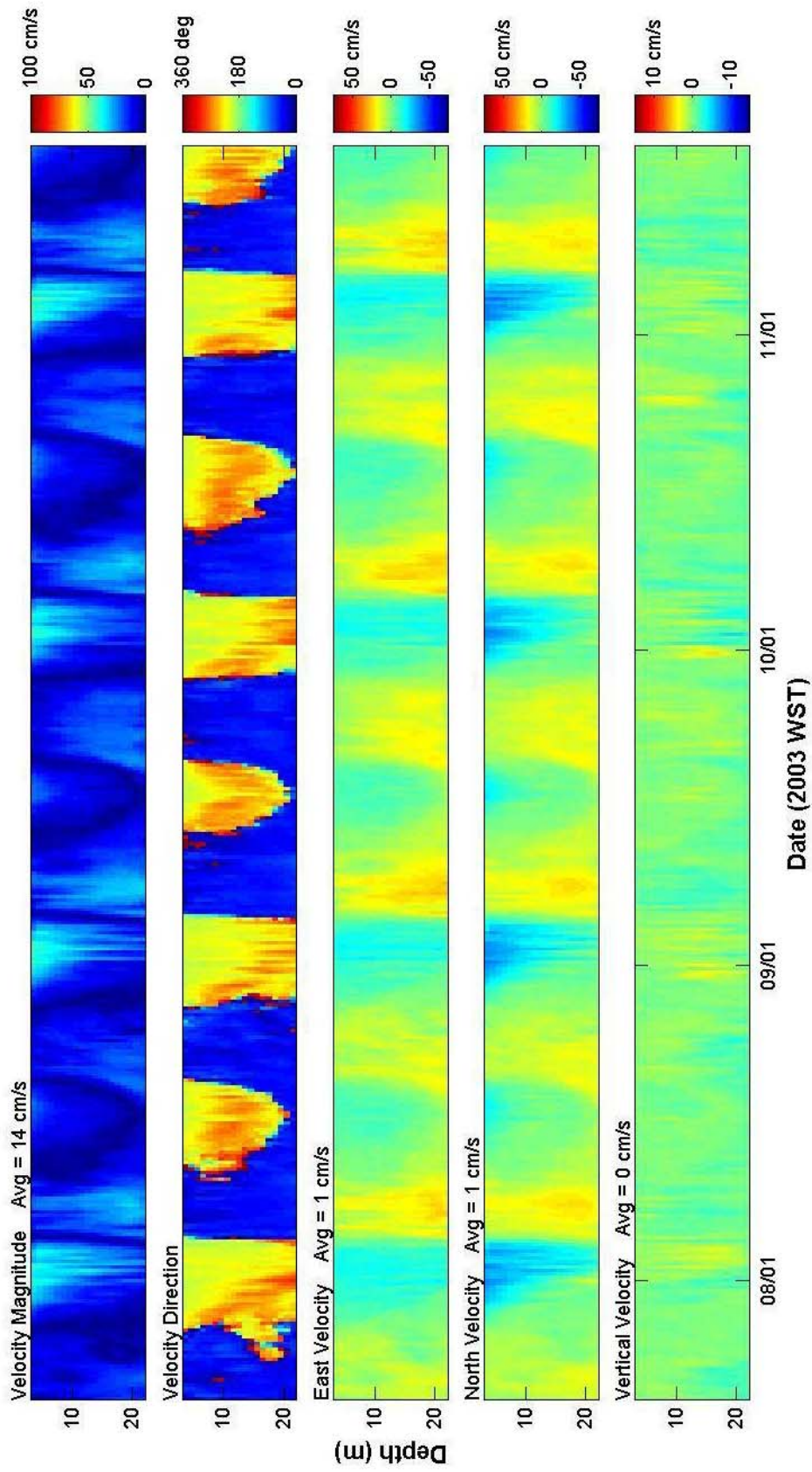
A10 - Top Bin - Palau



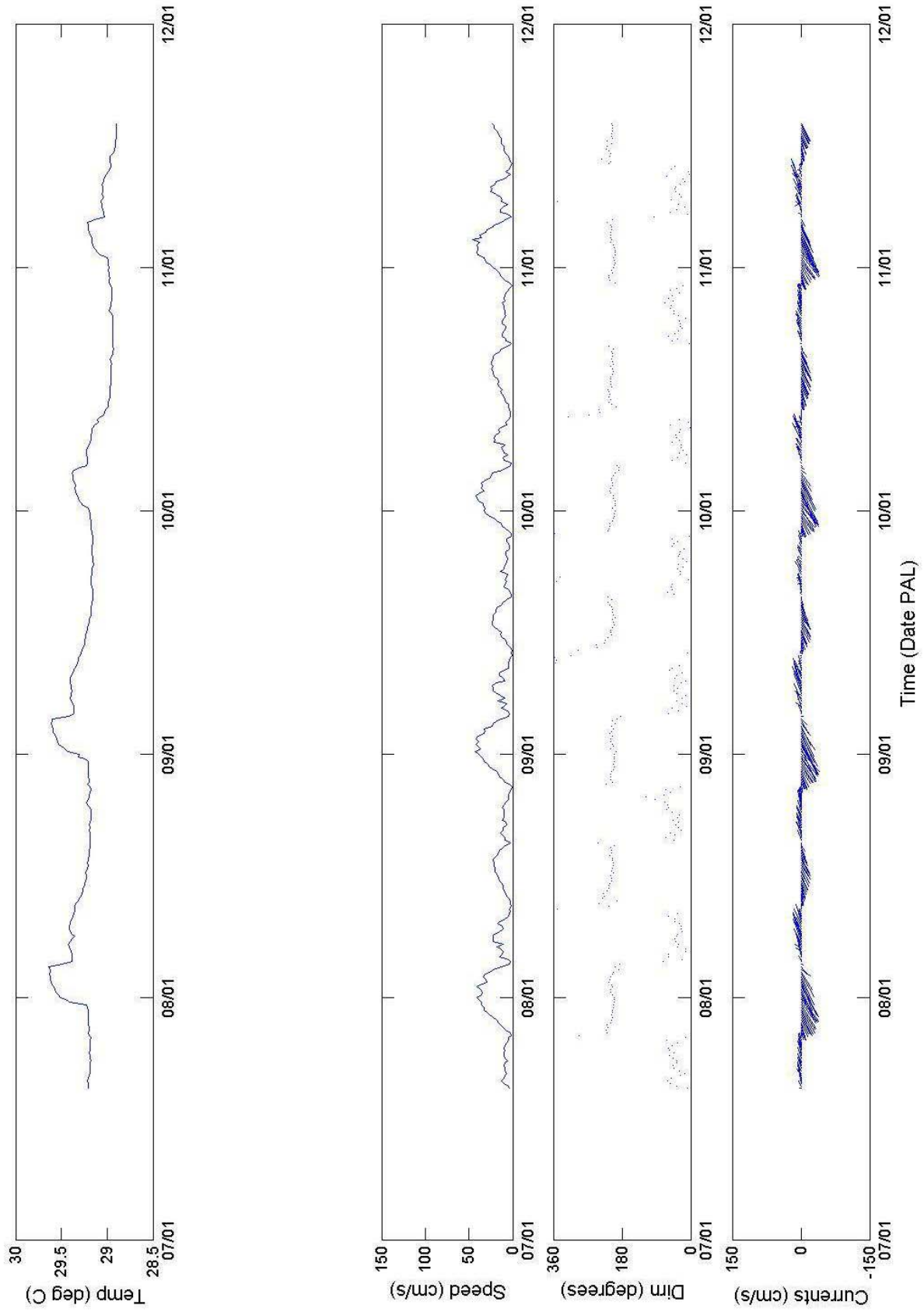
A10 - Bottom Bin - Palau



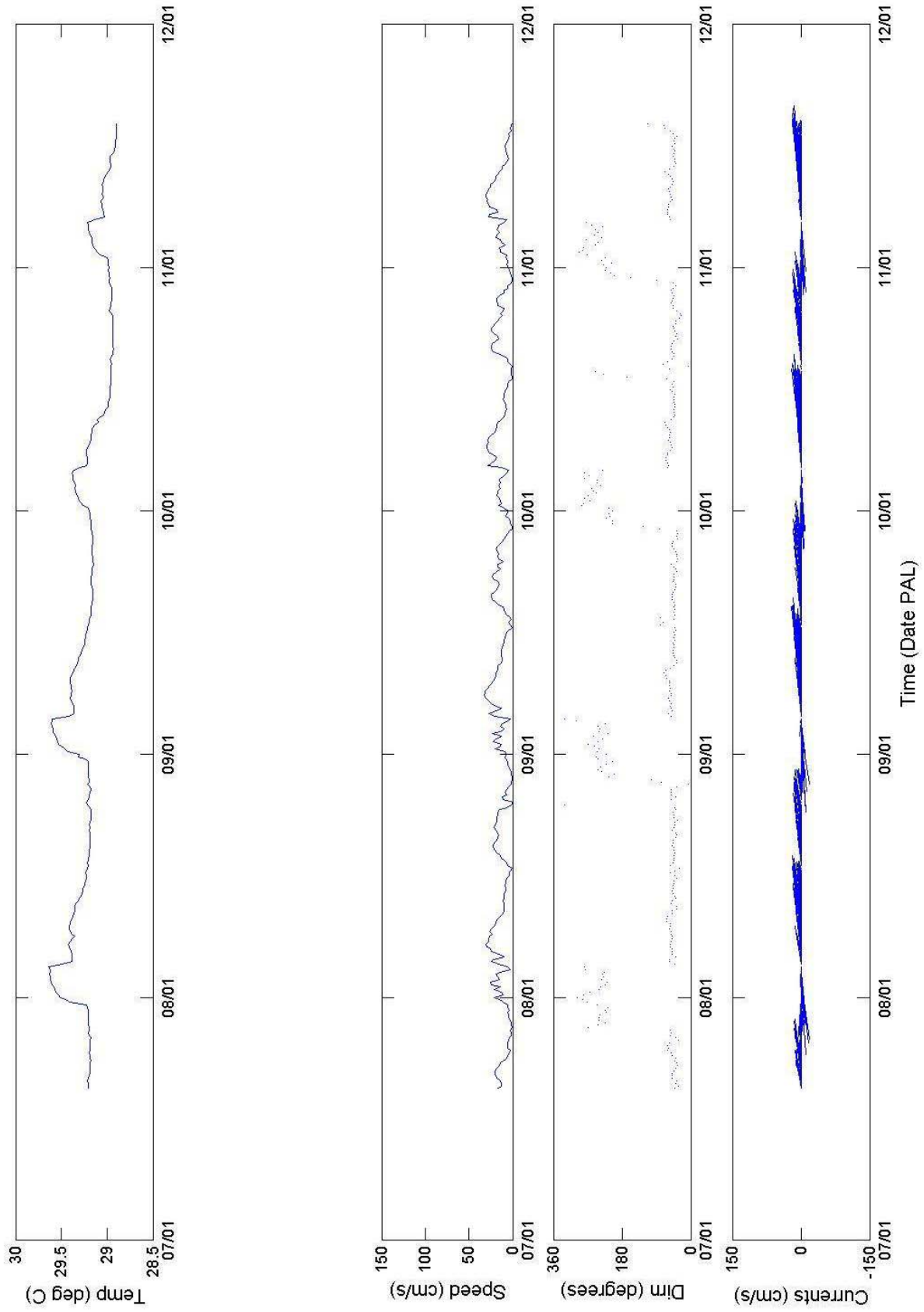
A11b Palau
RDI ADCP 1292



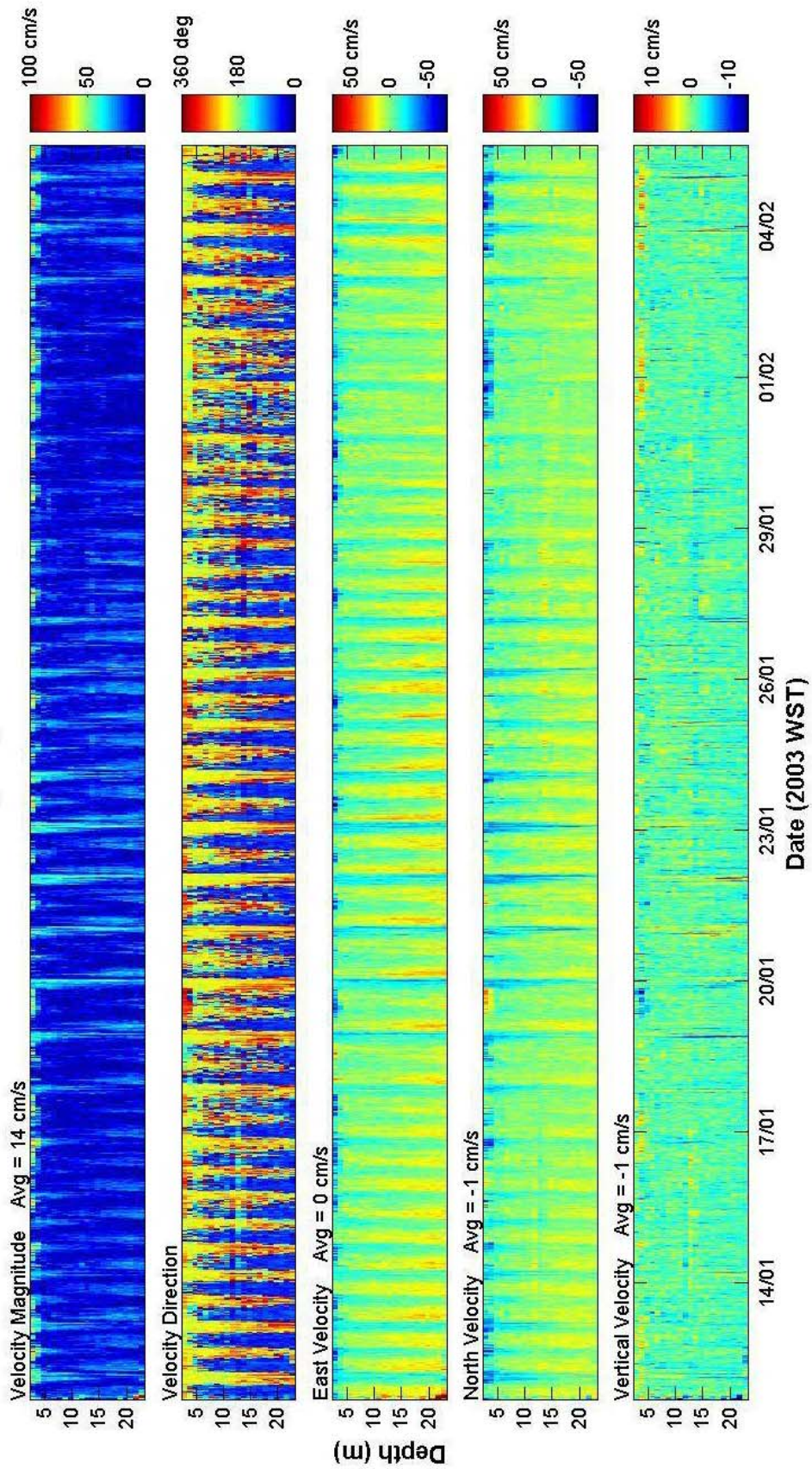
A11b - Top Bin - Palau



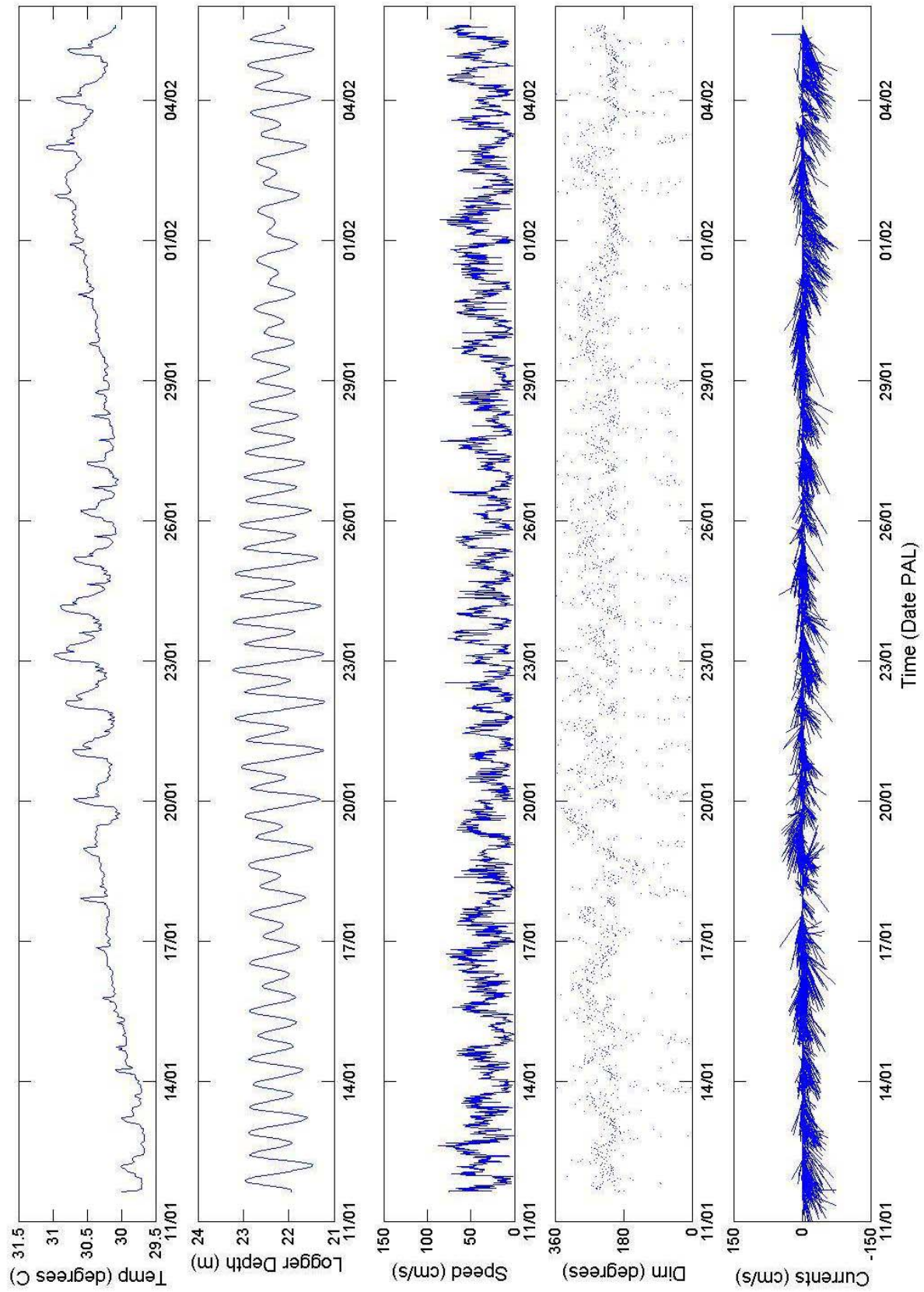
A11b - Bottom Bin - Palau



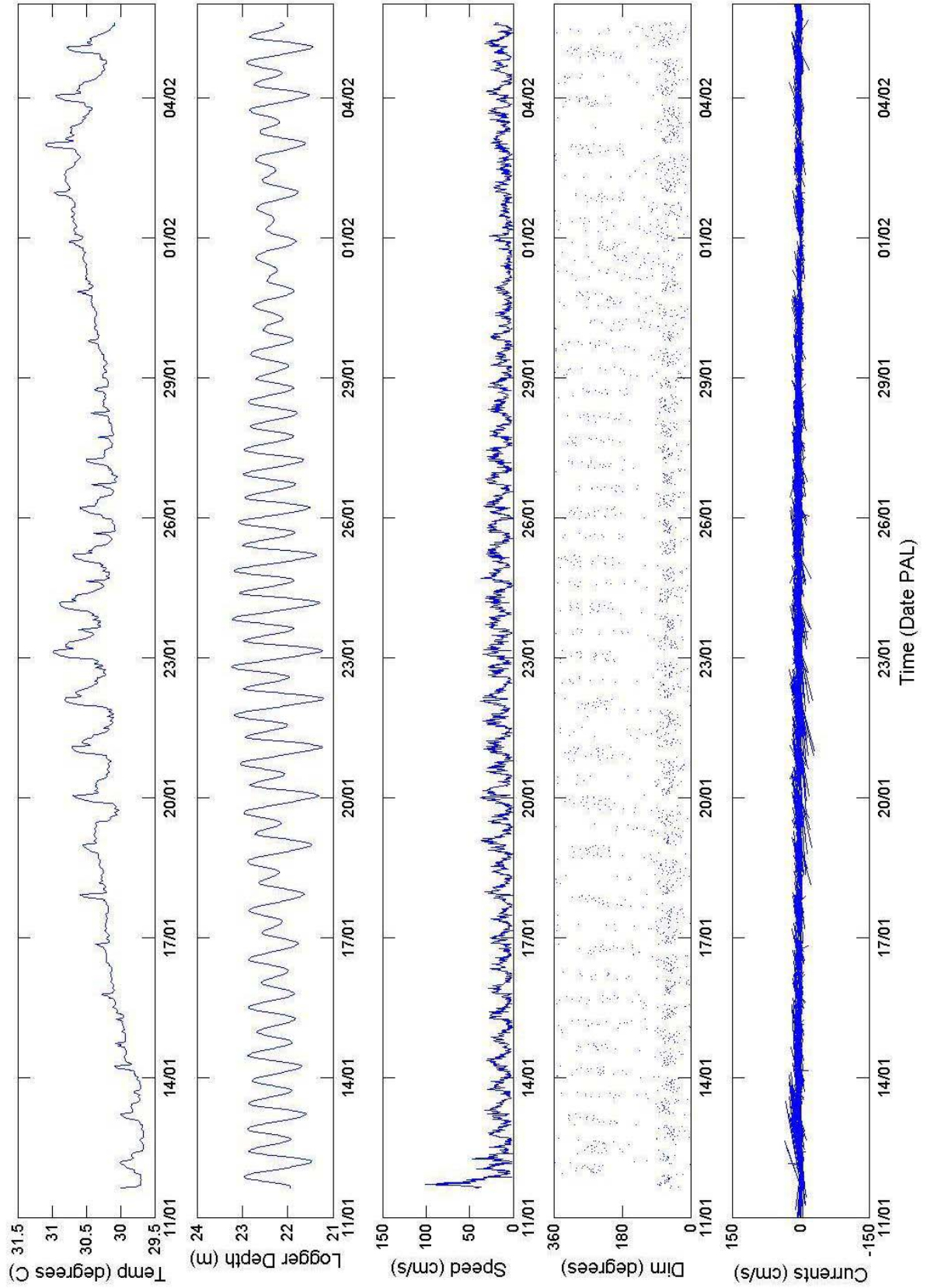
A11c Palau
Nortek Aquadop Current Profiler 866



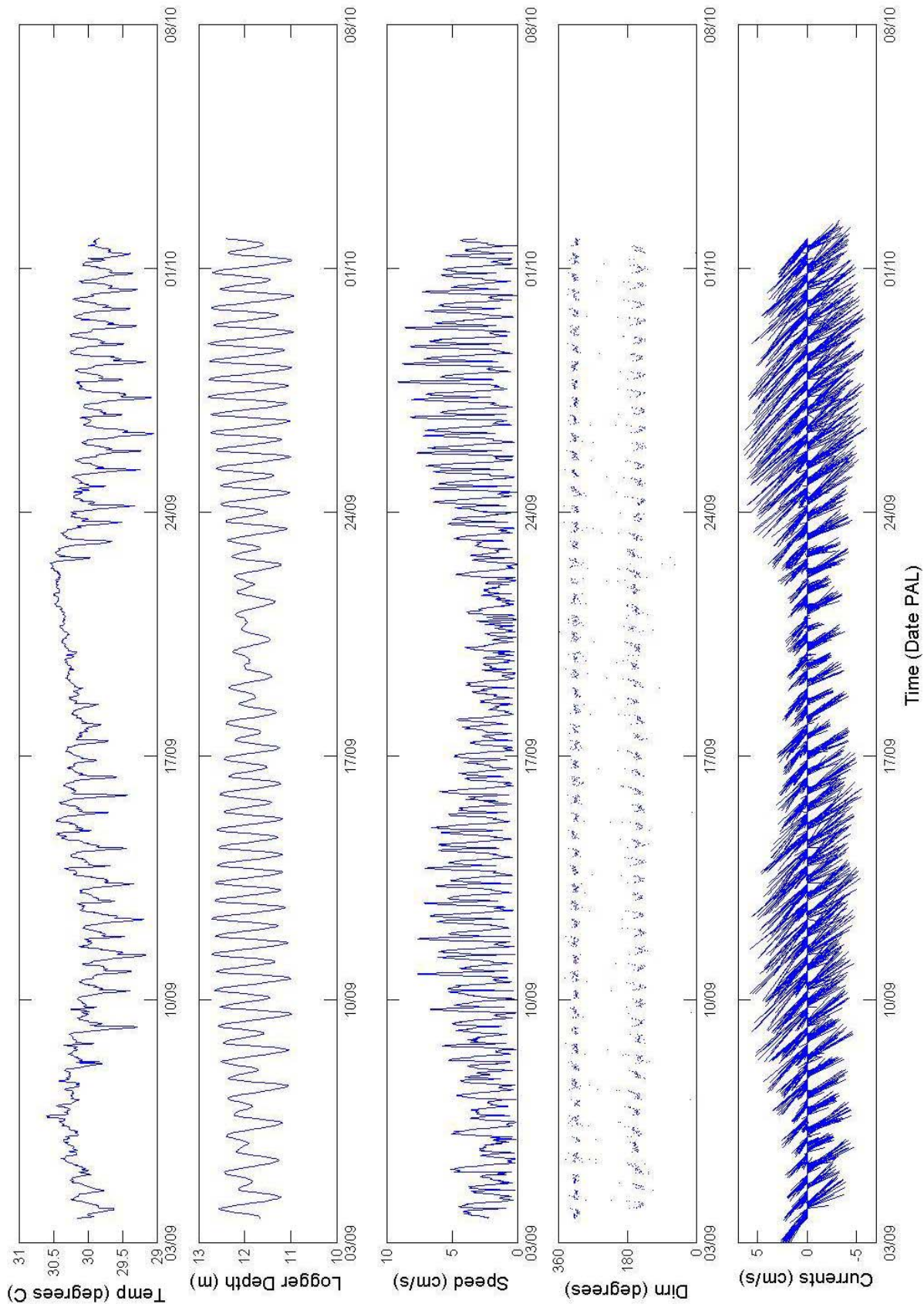
A11c - Top Bin - Palau



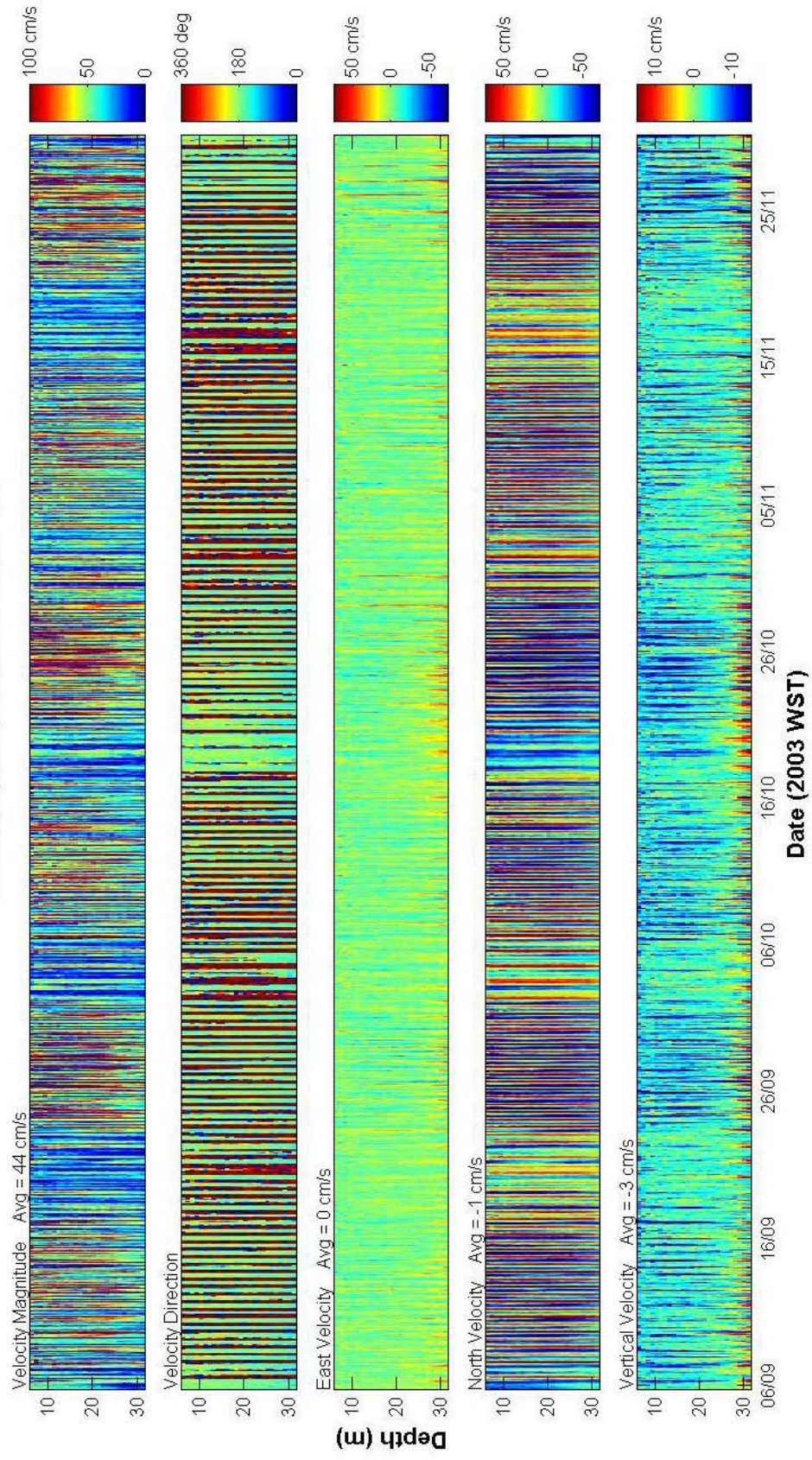
A11c - Bottom Bin - Palau



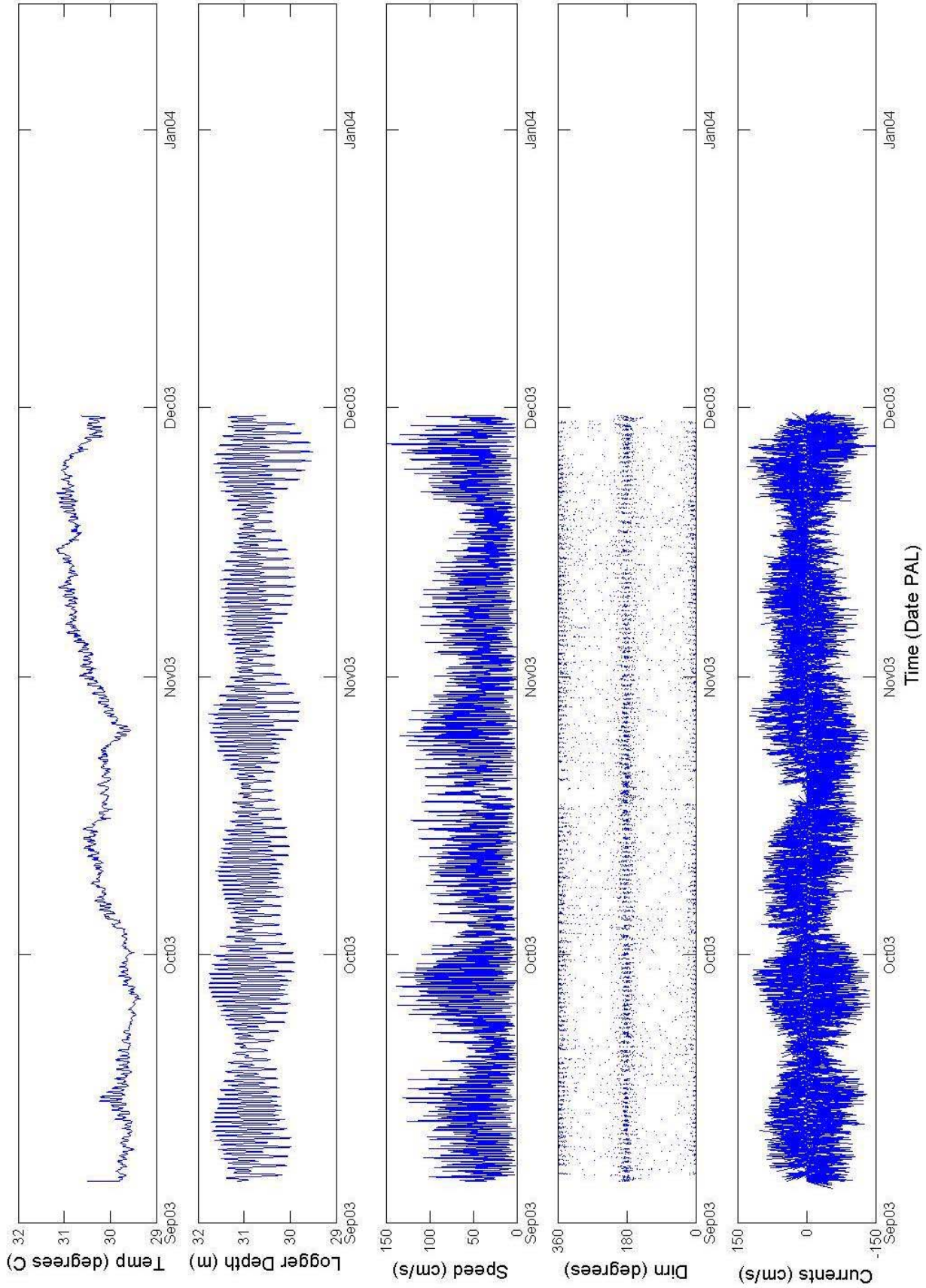
A12 - Palau



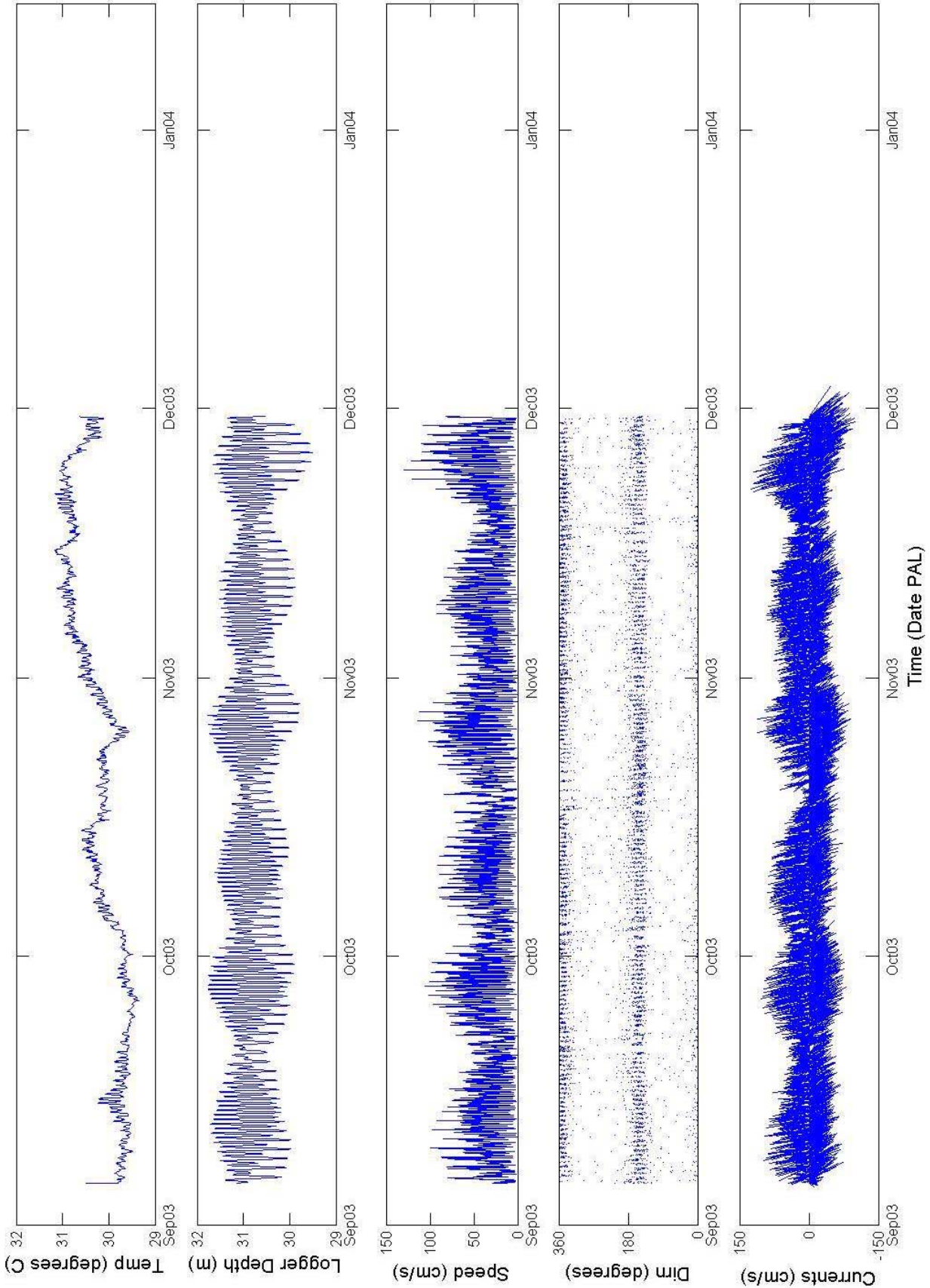
**A13 Palau
Nortek Aquadop Current Profiler 866**



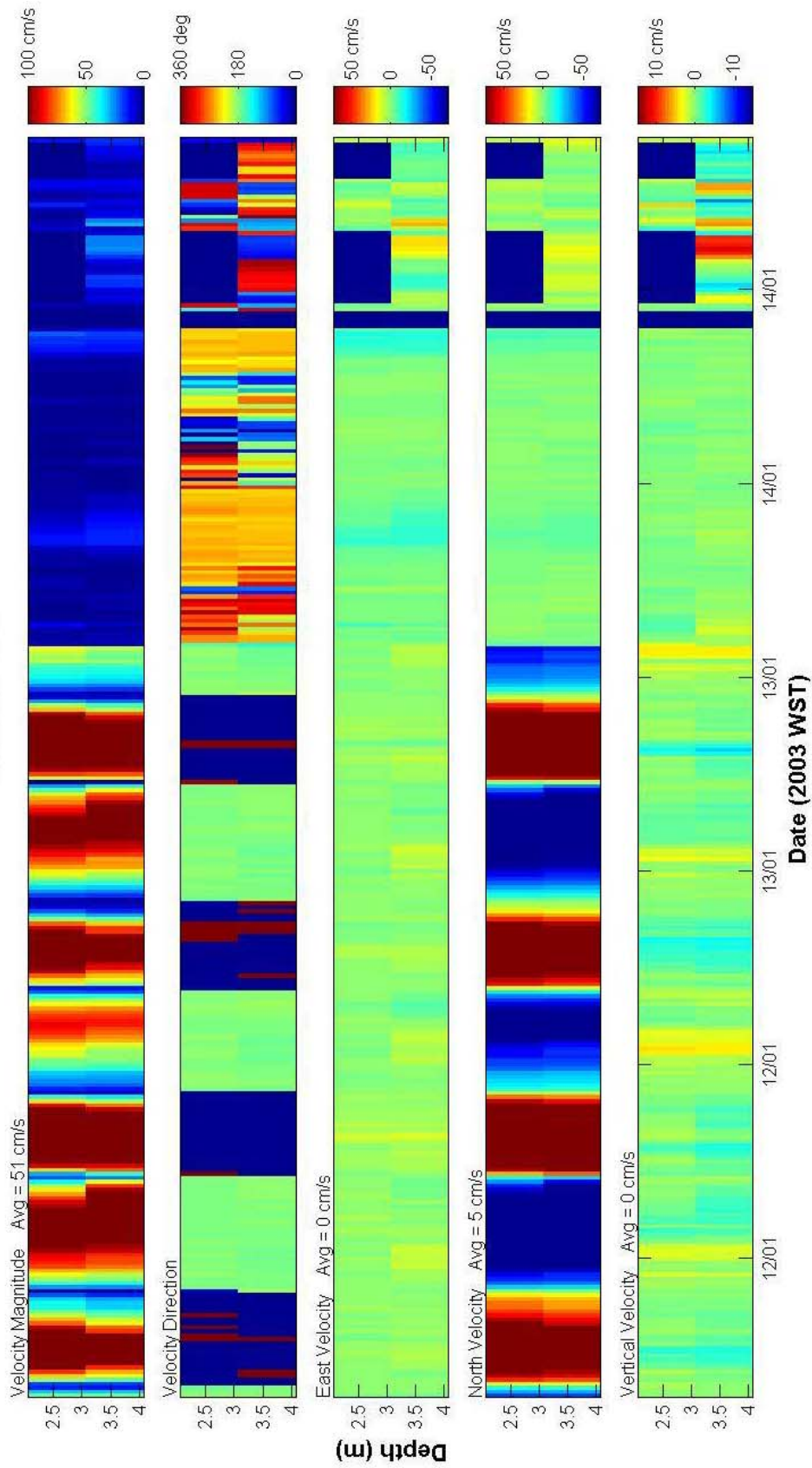
A13 - Top Bin - Palau



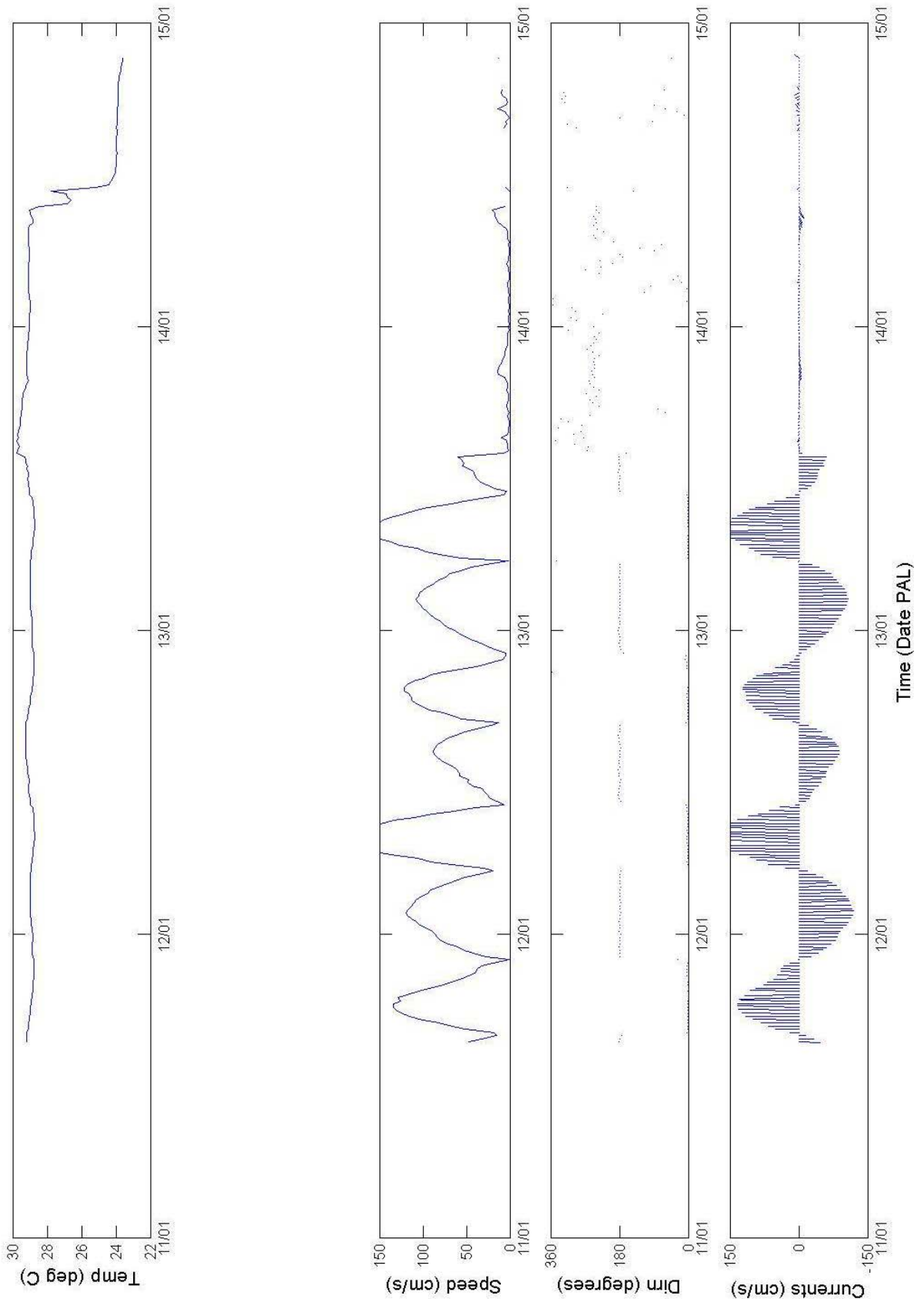
A13 - Bottom Bin - Palau



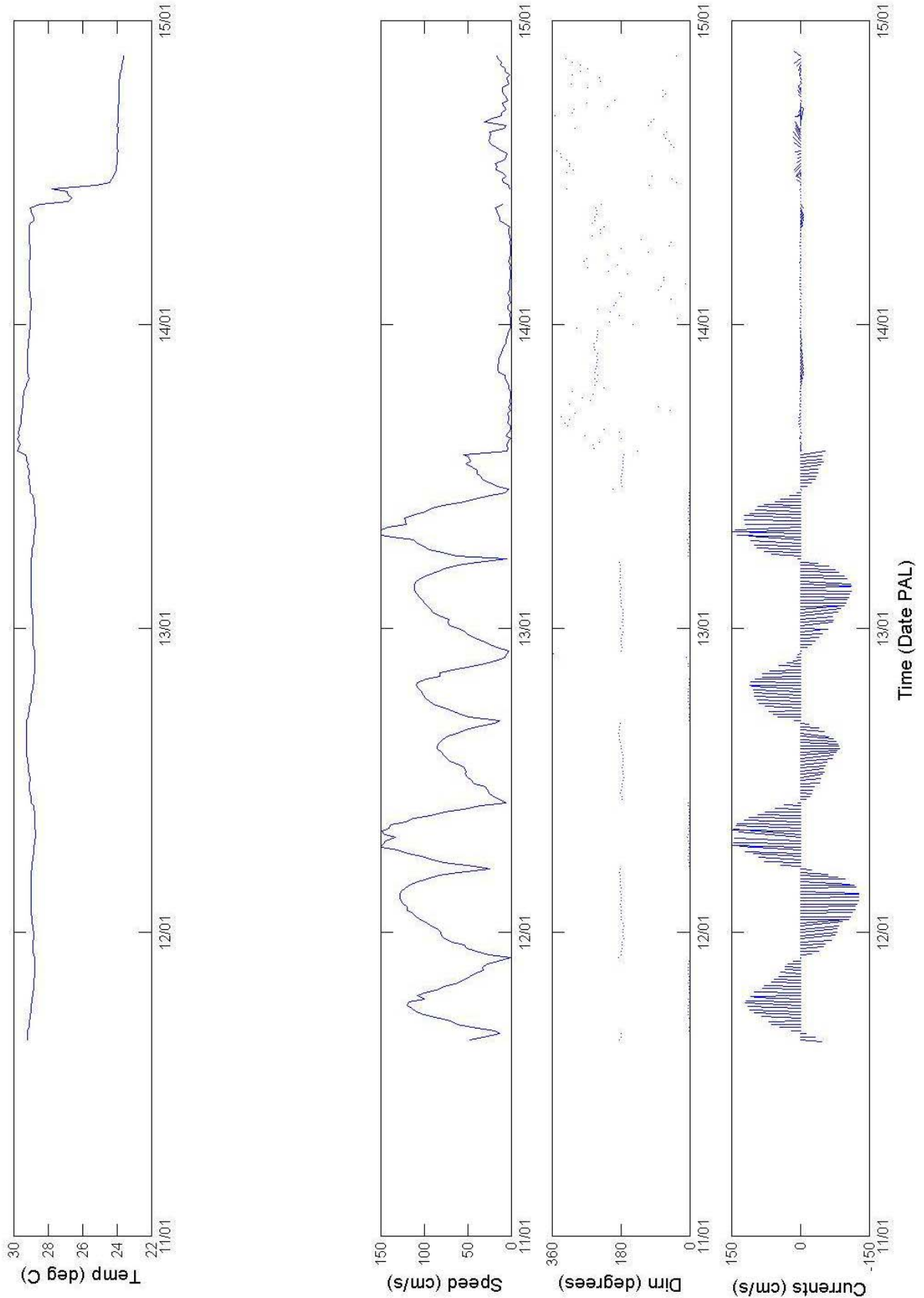
**A14 Palau
RDI ADCP 1292**



A14 - Top Bin - Palau



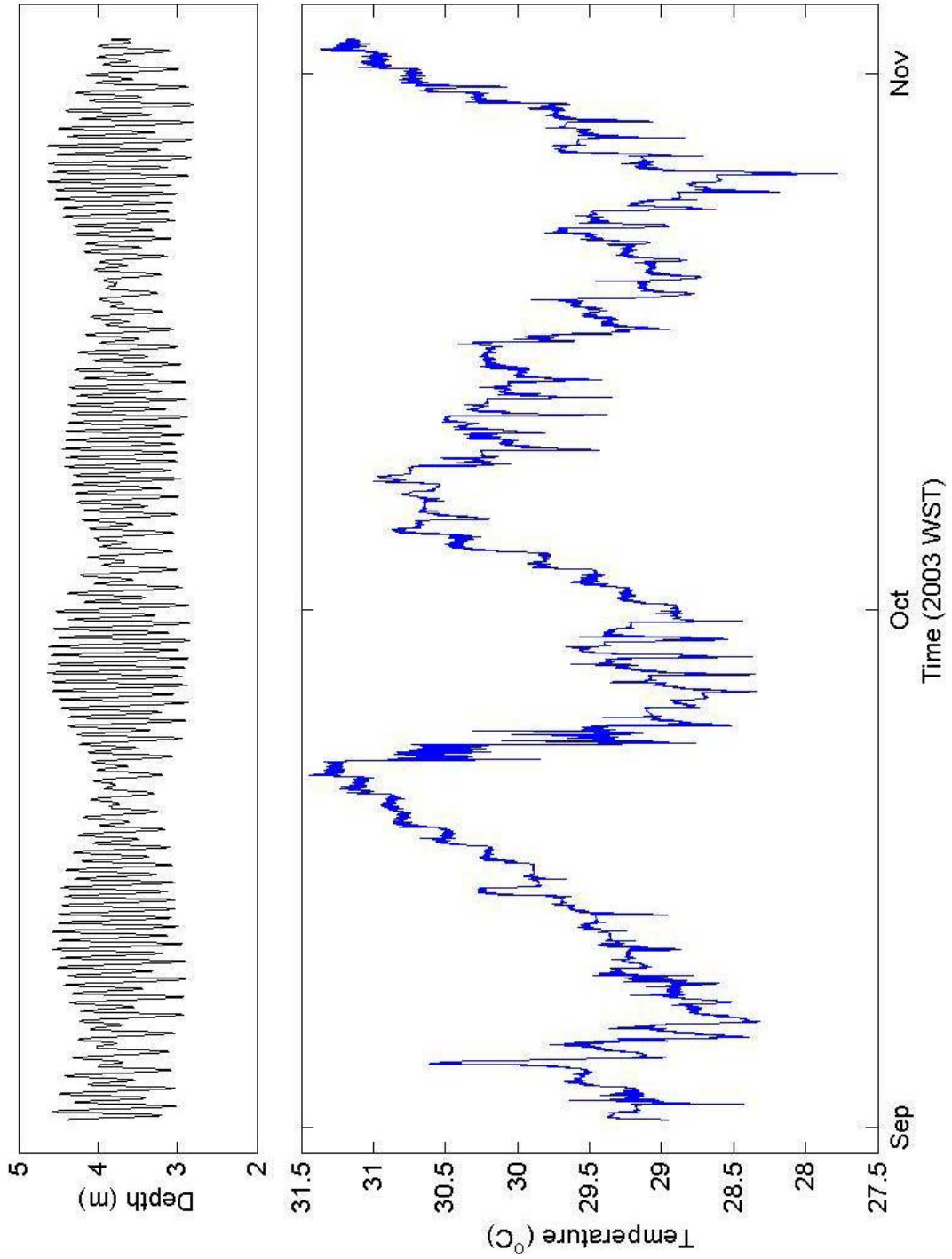
A14 - Bottom Bin - Palau



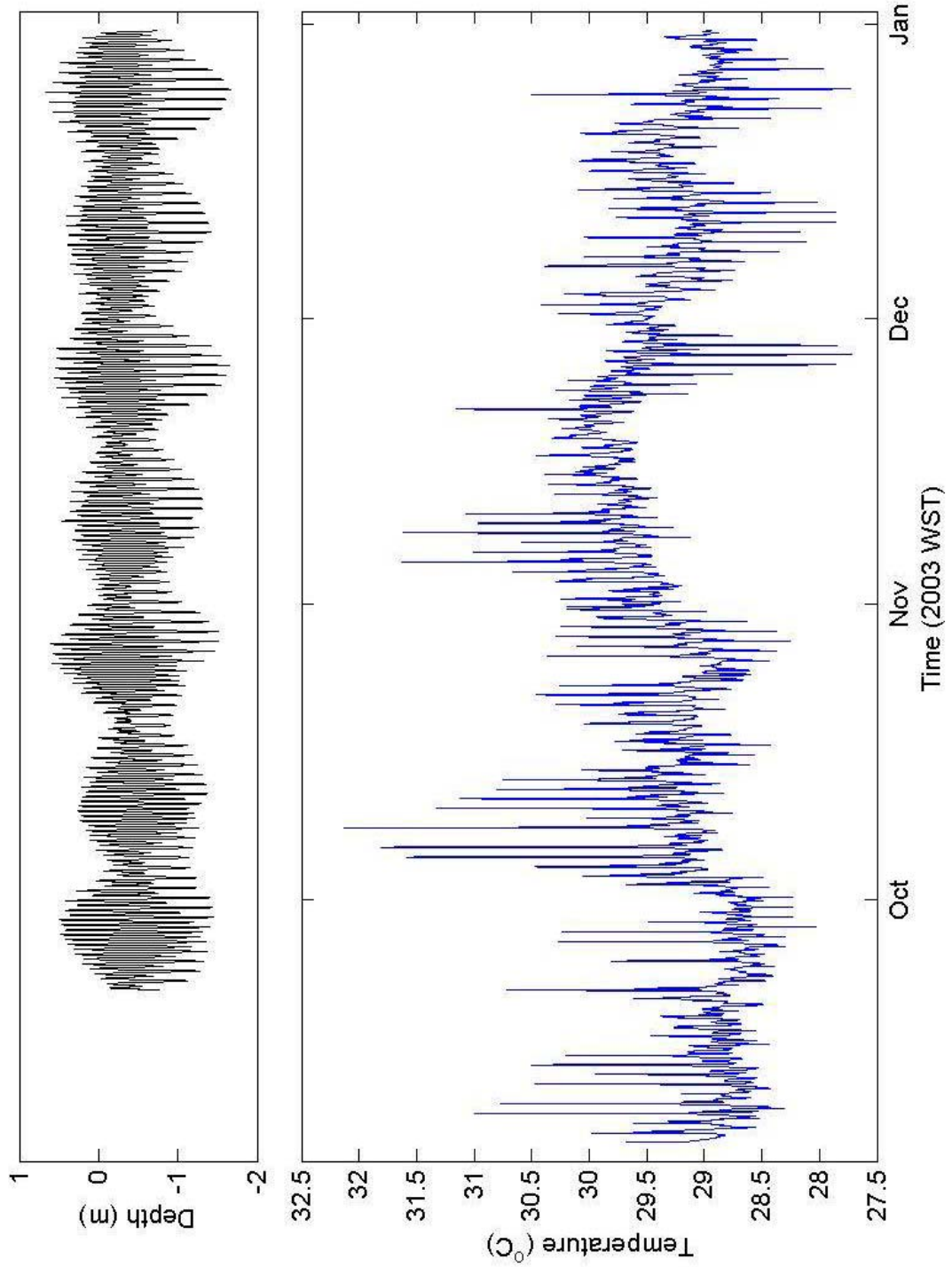
Appendix I – Time Series Plots of Tide Gauge Data

Tide gauge data are presented as plots of depth and temperature for each deployment. Note that deployments B3b and B3c are presented as a single graph. The two deployments can be clearly seen from the depth graph by observing the surface-interval between them.

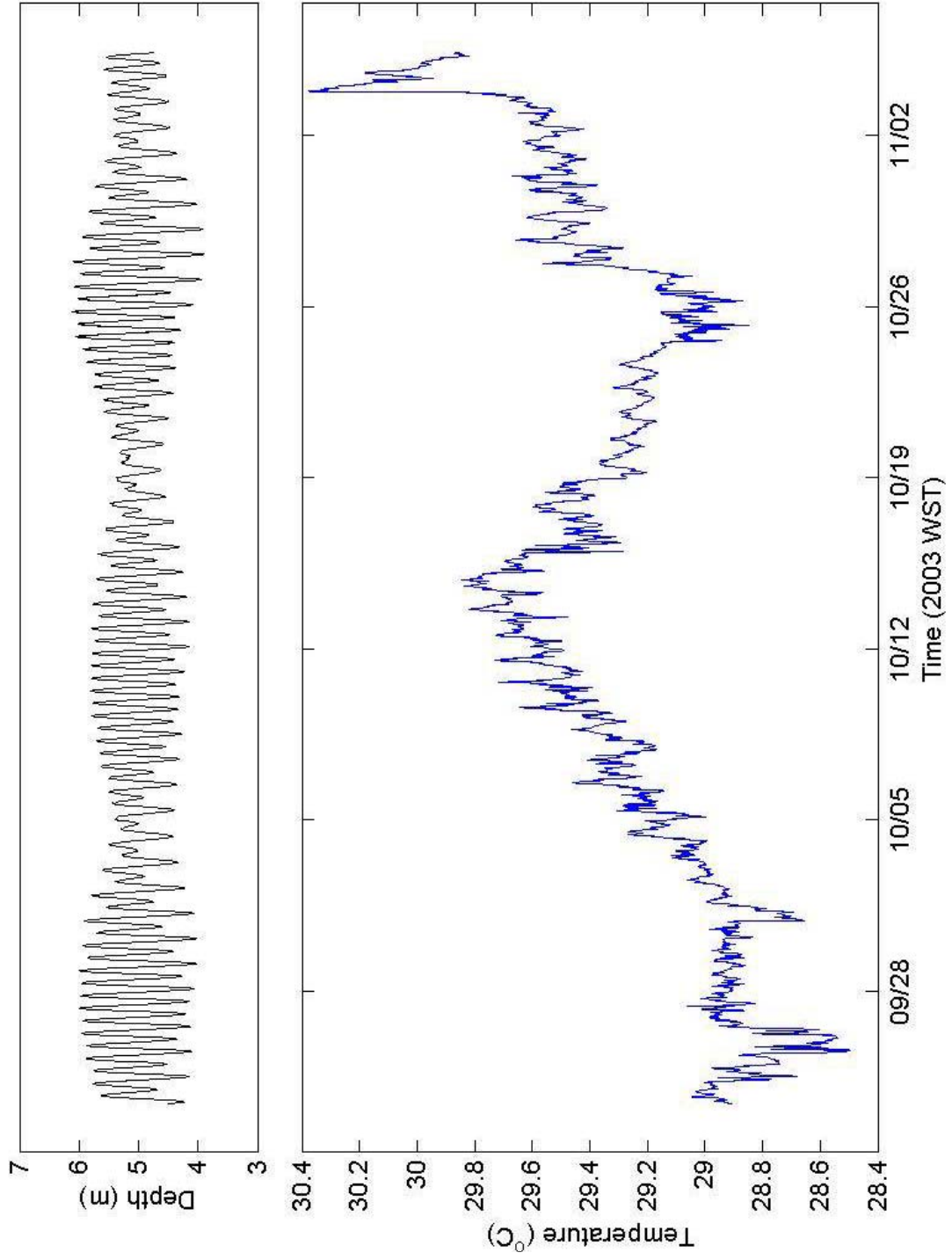
B1 - Palau b11ti



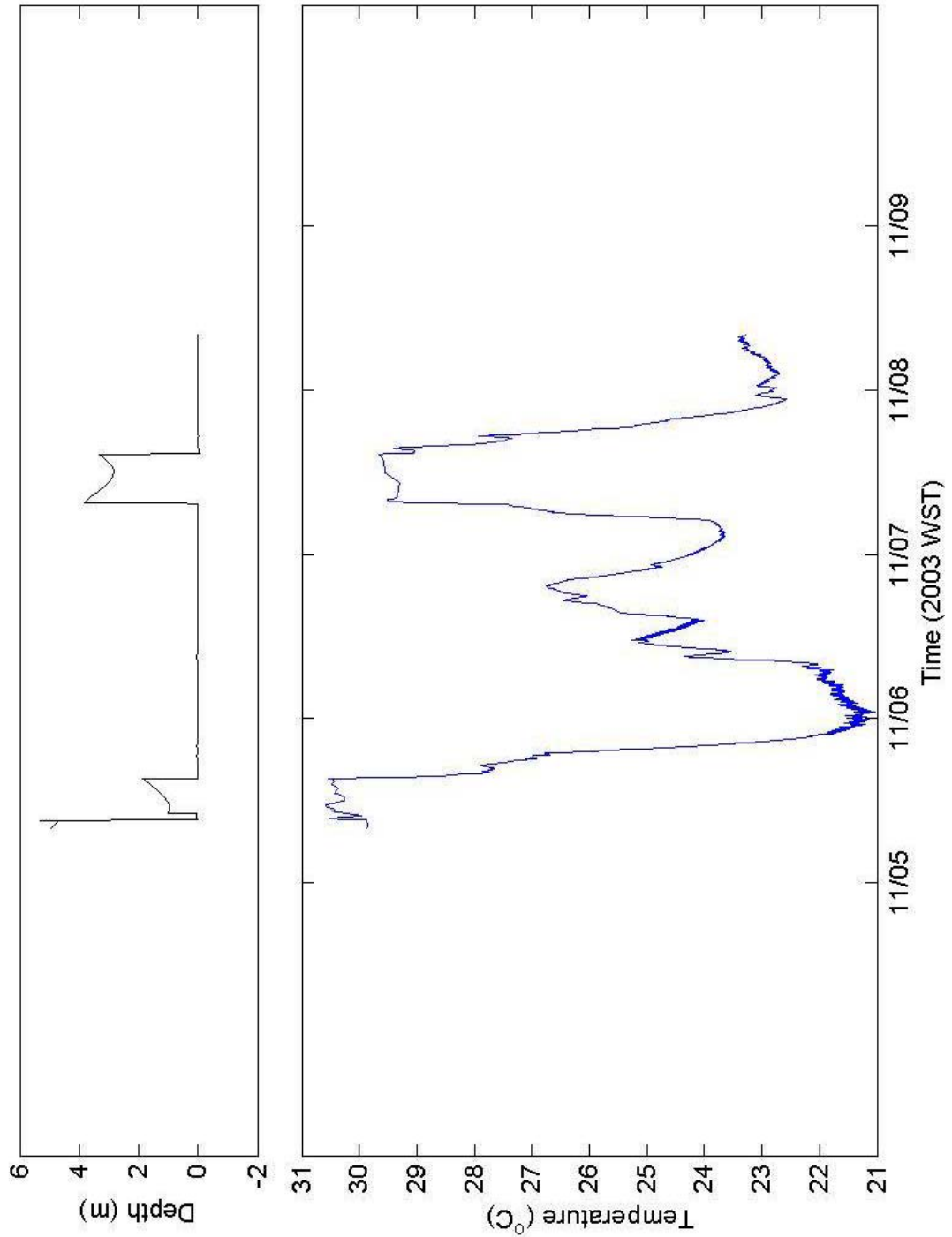
B2 - Palau b2tl



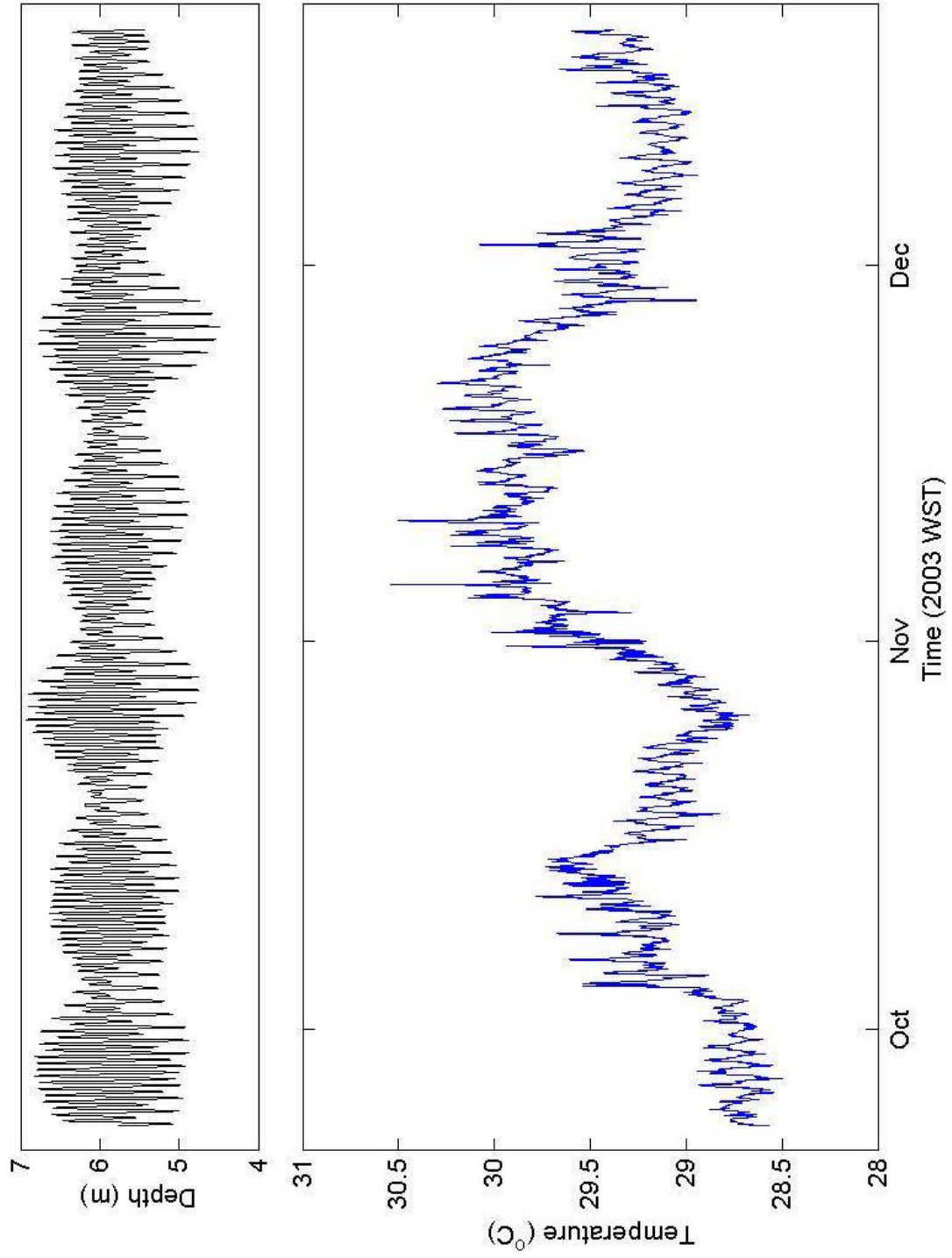
B3 - Palau b3tl



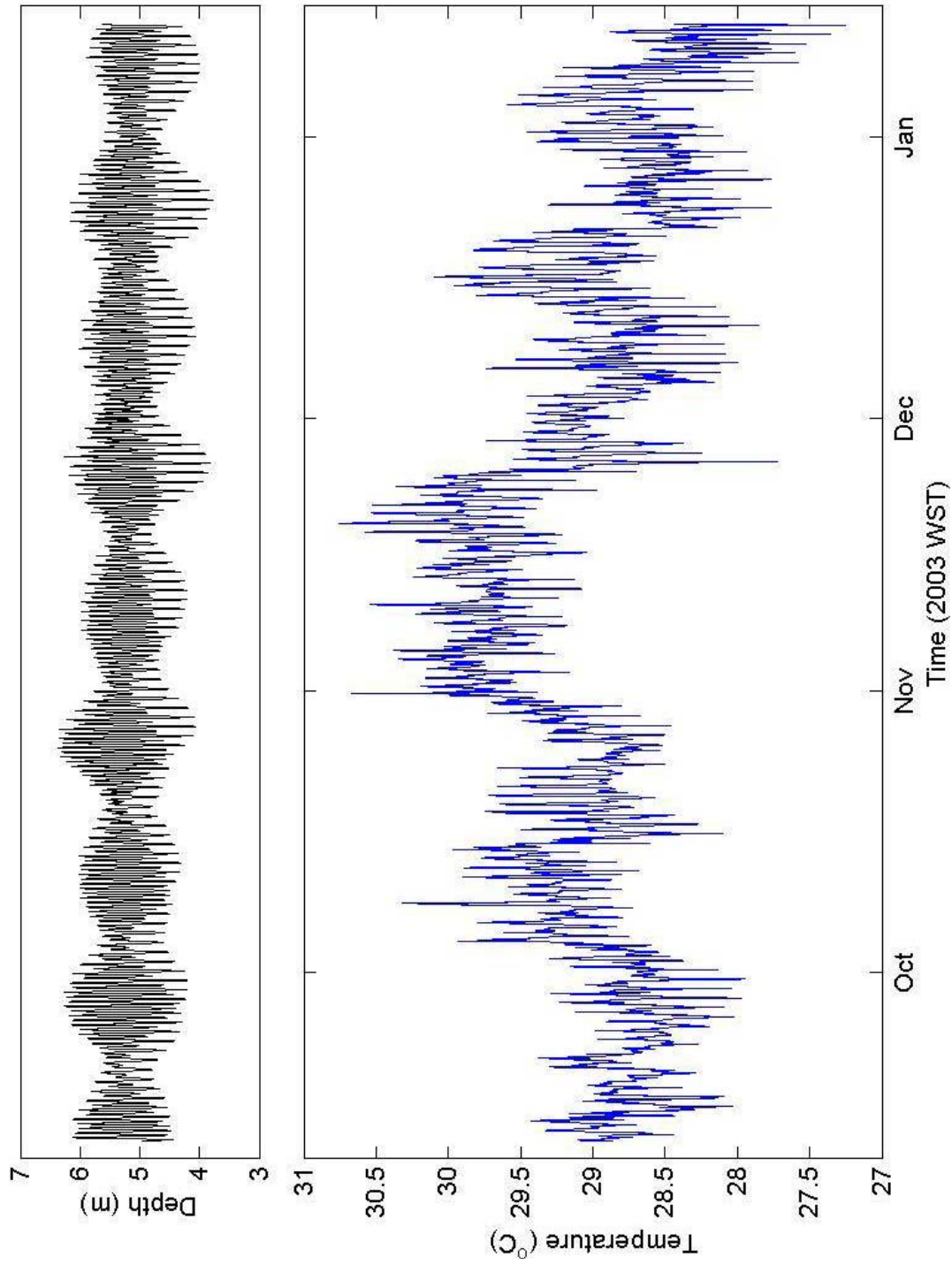
B3 - Palau b3bct1



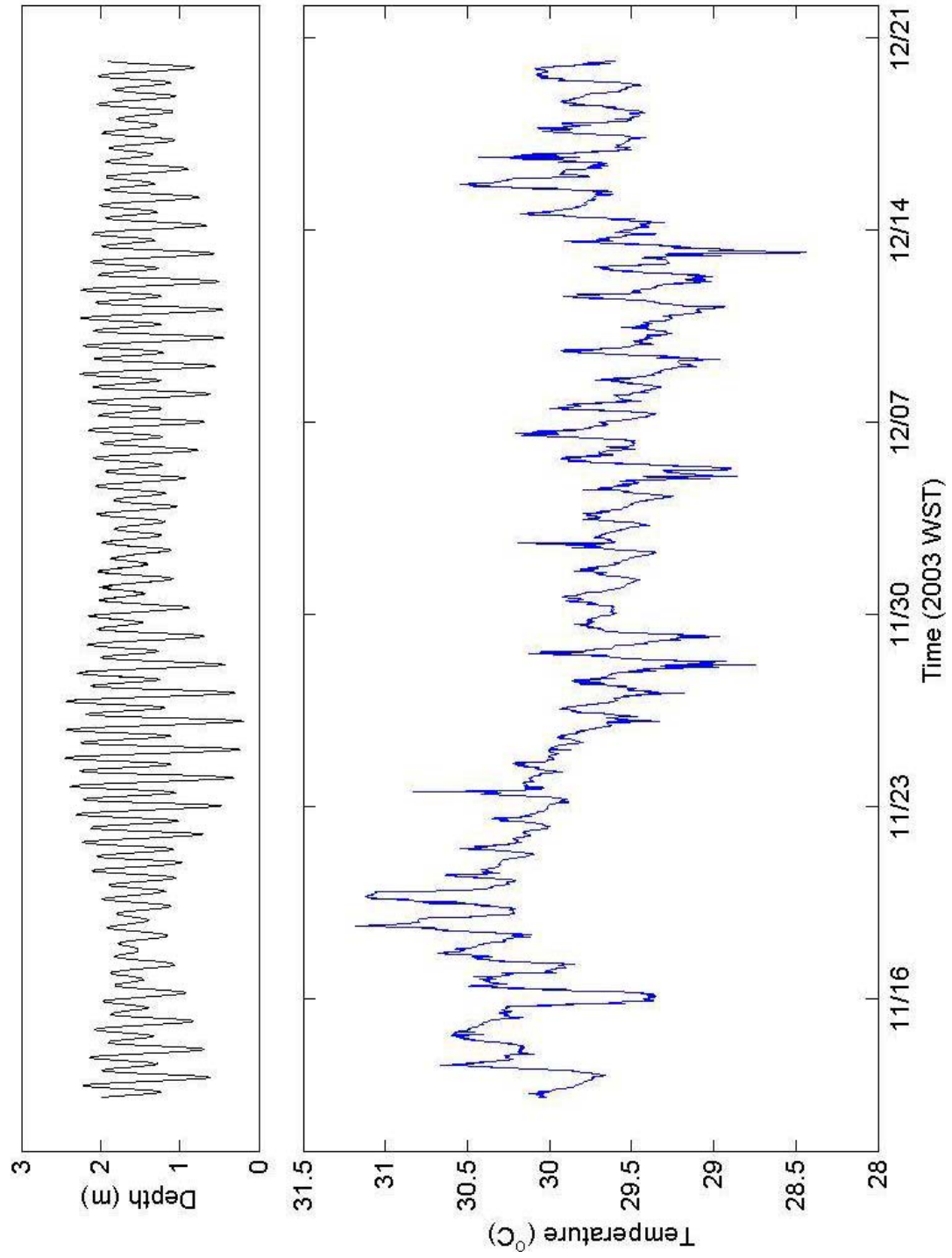
B4 - Palau b4tl



B5 - Palau b5tl



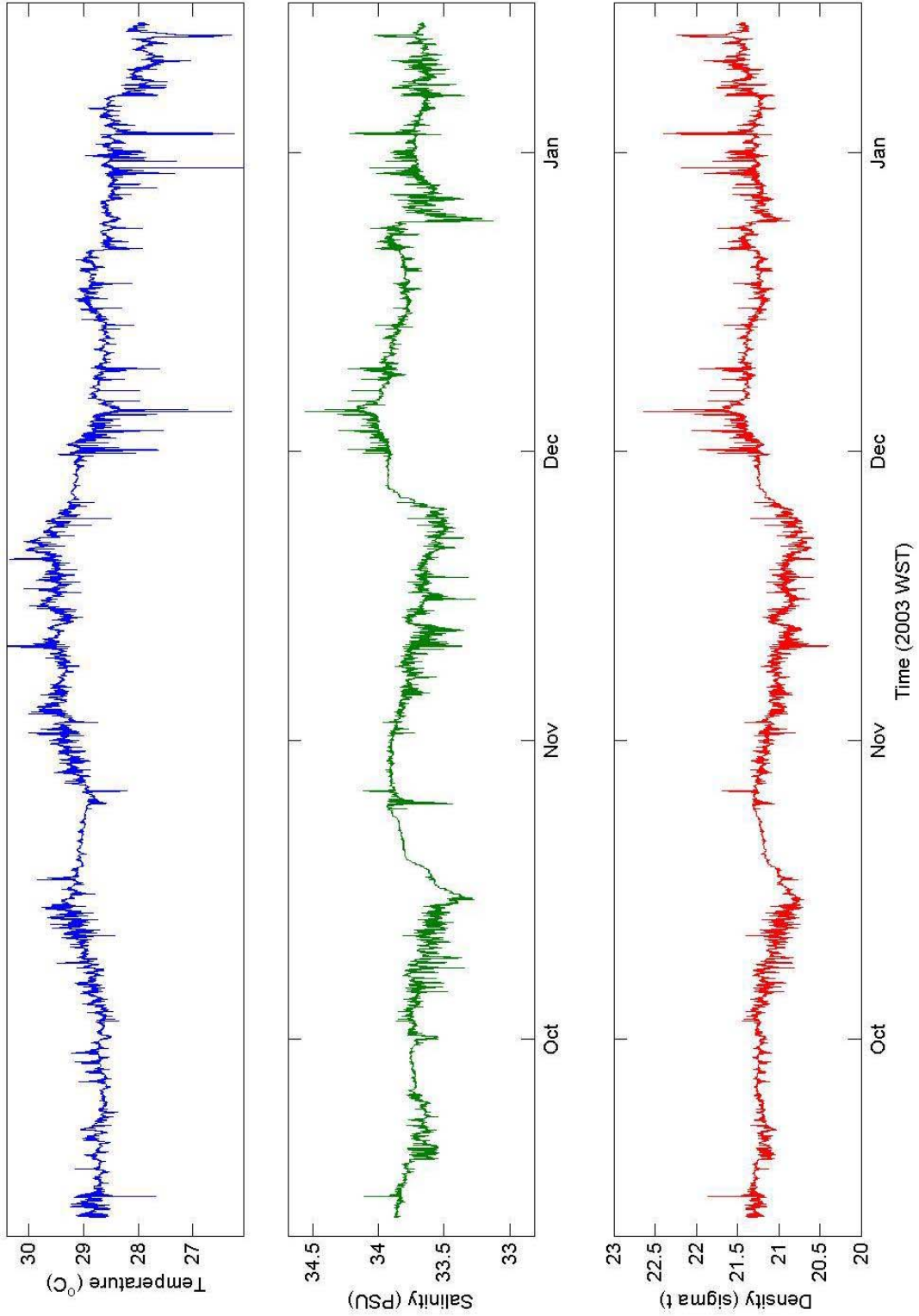
B6 - Palau b6tl



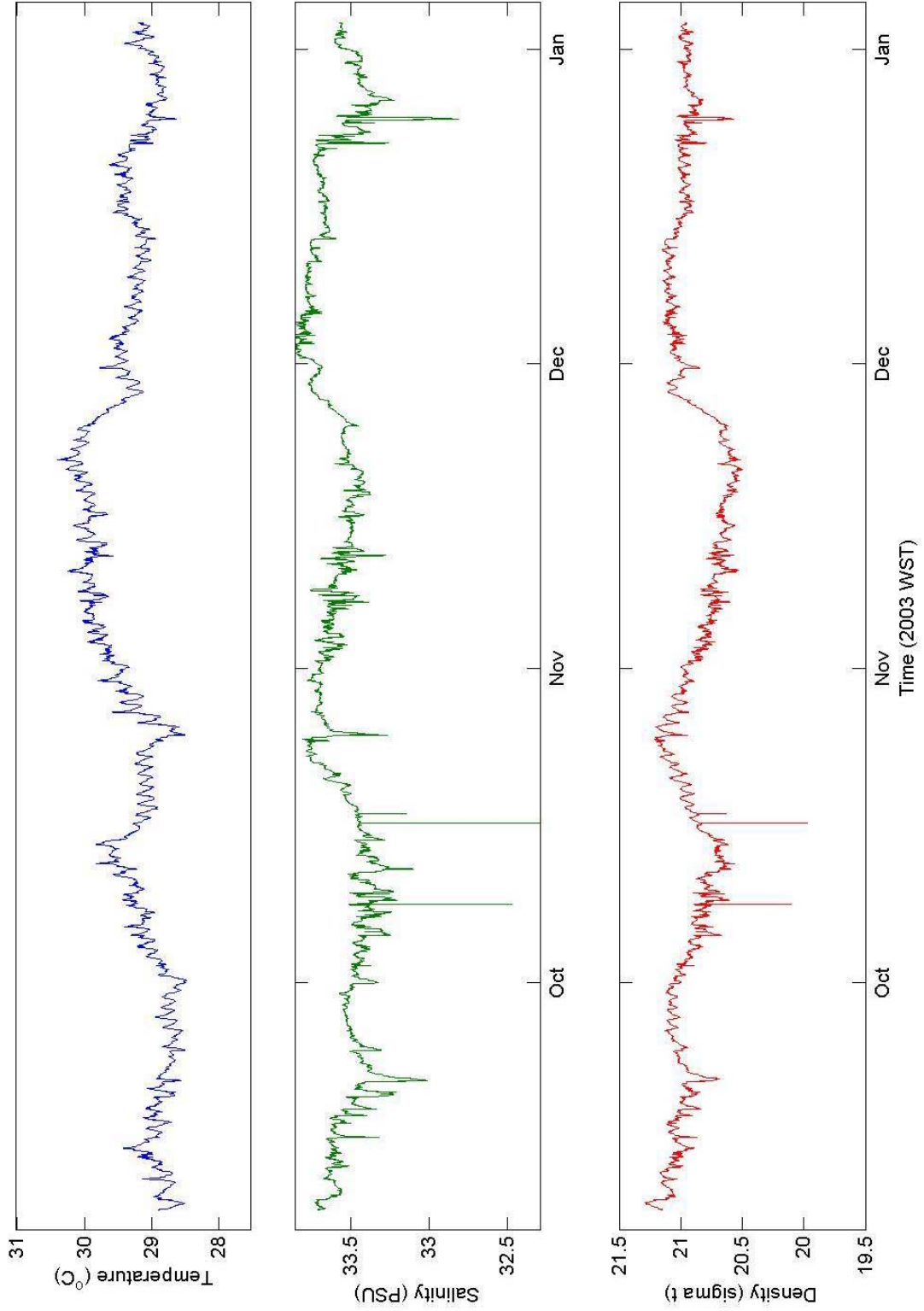
Appendix J – Time Series Plots of Salinity Data

Salinity values were determined from measurements of conductivity and temperature. The density anomaly (σ_t), the increase in the density of the sea-water sample from that of fresh-water (1000 kg.m^{-3}), can be derived from the temperature and salinity. Three time-series plots (temperature, salinity and density anomaly) are presented for each instrument.

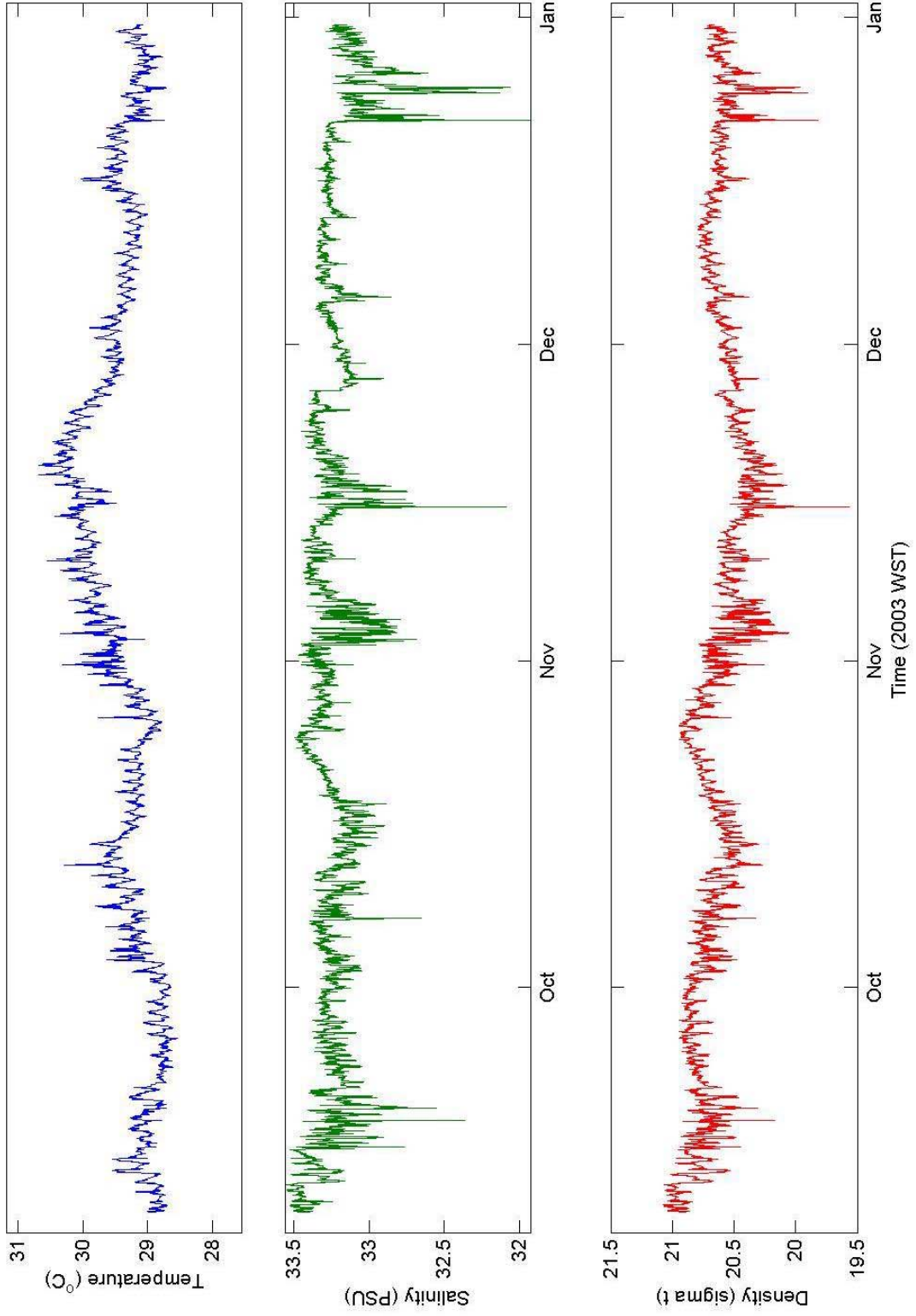
C1 - Palau cfts



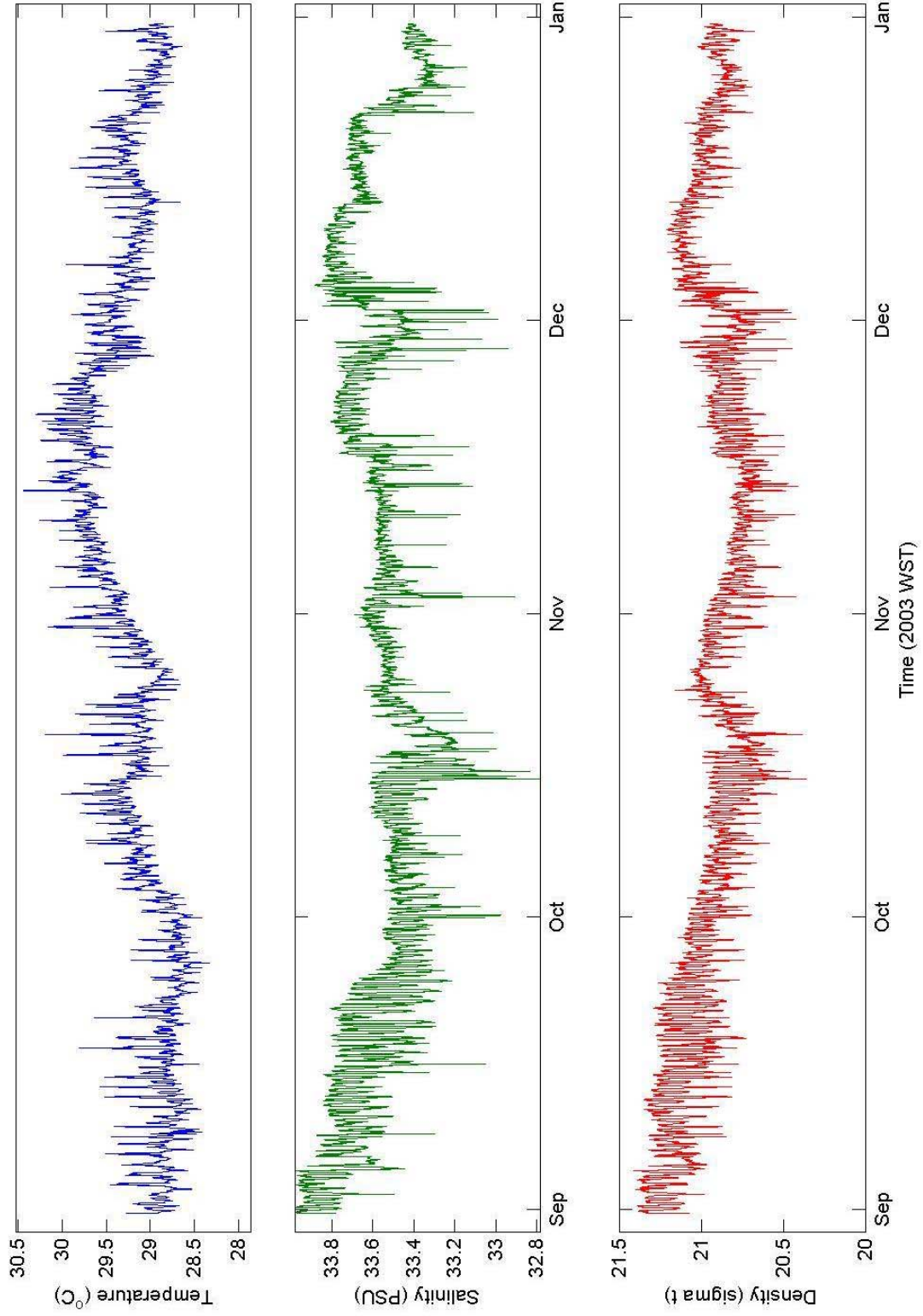
C2 - Palau c2ts



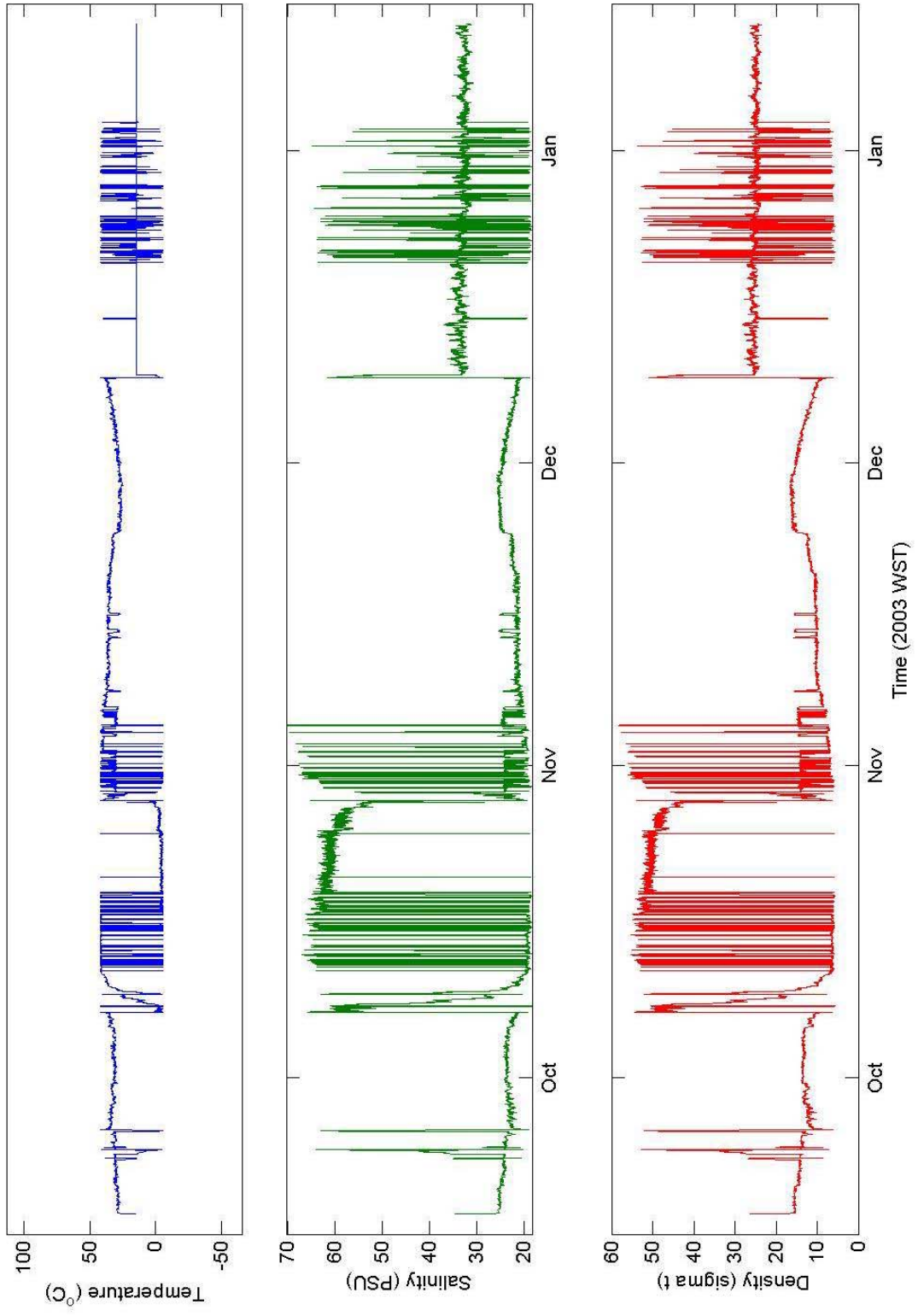
C3 - Palau c3ts



C4 - Palau c4ts



C5 - Palau c5ts



Appendix K – CTD Profiles

Conductivity Temperature and Depth (CTD) Cast Summary

CTD casts are named using the following naming convention: ddmmnnn, with dd being the day, mm the month and nnn being the cast number starting from zero. Data were processed from raw *.hex files to *.cnv using the manufacturer software. They were then edited to in-water values.

The tables below summarise the cast locations from each survey in September and November 2003. The *Site* column identifies the CTD location. If the profile was recorded near deployed instruments, the site is referenced by the instrument code; e.g., cast 2109000 was taken near temperature profile T4. The information is contained in the ASCII file castdata.dat.

MATLAB uses this information to process the data into *.mat files and produce figures (*.emf). The data from each cast are presented here in two plots. The time, locations and depths, obtained from the original file header information, are included in the title. The first plot illustrates the variation with depth of the temperature, salinity and density anomaly. The second plot combines these three variables (contours of density anomaly are shown on the axes) on a two-dimensional graph. In this representation, a grouping of data indicates a specific type of water.

As an example, the second plot from cast 1909001 (page 136) is analysed. Two distinct water types are observed; to the right of the diagram, water with near-constant salinity (33.7 psu) and density anomaly (21.12) shows a temperature range of 28.88 – 28.91°C; on the left of the diagram, water with near-constant temperature (28.89°C) has variable salinity (33.5 – 33.6 psu) and density anomaly (20.99 – 21.07).

Table 5 List of CTD profiles taken during September 2003

Cast	Site	Lat [°]	Lat [min]	Lon [°]	Lon [min]	Cast Depth
1909000	018	7	6.857	134	15.937	24.5
1909001	019	7	8.073	134	17.910	15.8
1909002	020	7	9.686	134	19.861	25
1909003	021	7	10.880	134	21.754	26
1909004	022	7	12.783	134	23.249	18.5
1909005	023	7	13.054	134	26.643	27
1909006	026	7	15.351	134	27.651	28
1909007	025	7	16.966	134	27.922	22
1909008	026	7	17.672	134	27.459	13.8
1909009	027	7	18.653	134	27.605	14.7
1909010	028	7	19.858	134	27.887	29.5

1909011	029	7	20.230	134	27.941	13
2109000	T4	7	19.772	134	30.034	15
2109001	A2	7	19.315	134	29.400	13
2109002	031	7	19.071	134	29.707	20
2109003	032	7	18.689	134	30.115	1.9
2109004	033	7	18.493	134	30.627	1.4
2109005	034	7	18.557	134	31.463	32
2109006	A13	7	19.034	134	31.459	33
2109007	036	7	20.033	134	31.250	33
2109008	037	7	20.430	134	31.025	26
2109009	038	7	21.106	134	30.723	29
2109010	KB	7	21.757	134	30.253	27.5
2109011	040	7	20.309	134	25.685	31
2109012	041	7	19.958	134	26.143	27.5
2109013	042	7	19.249	134	27.220	31
2209000	043	7	16.733	134	19.770	7.8
2209001	044	7	16.700	134	19.451	27
2209002	045	7	16.674	134	19.018	28
2209003	A4	7	16.621	134	18.807	20
2209004	048	7	17.468	134	16.796	9
2209005	049	7	17.426	134	16.410	15
2209006	050	7	17.487	134	16.000	13.8
2209007	051	7	17.378	134	15.676	3.7
2209008	052	7	16.579	134	20.219	24
2209009	053	7	15.444	134	21.278	29.7
2209010	054	7	15.959	134	22.529	26
2209011	055	7	15.839	134	23.821	22
2209012	T7	7	16.382	134	24.664	32
2209013	056	7	17.285	134	25.216	28
2209014	057	7	18.796	134	25.321	15

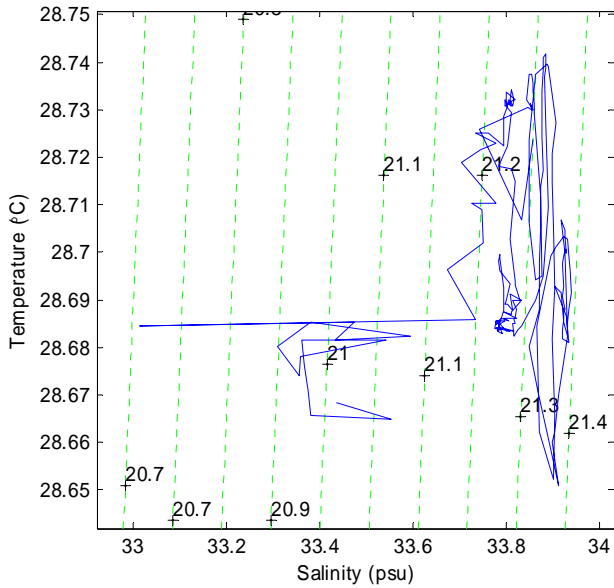
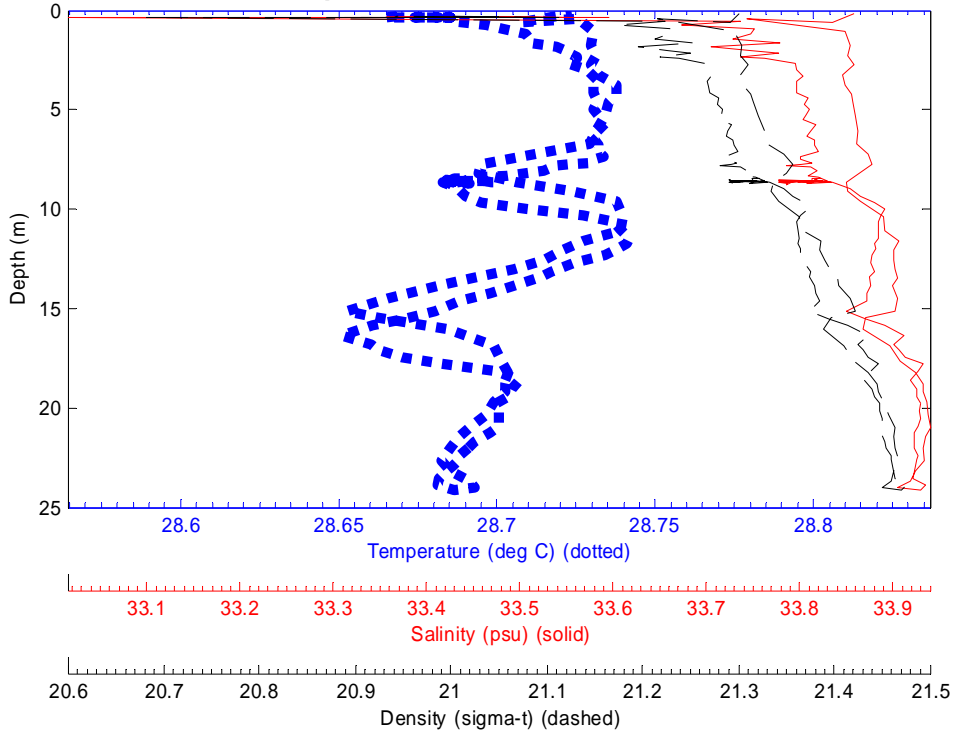
Table 6 List of CTD profiles taken during November 2003

Cast	Site	Lat [°]	Lat [min]	Lon [°]	Lon [min]	Cast Depth	Sounder Depth
0311000	11b	7	18.8864	134	27.3167	29	33
0411000	CTD0	7	14.0504	134	27.0888	15	14.6
0411001	CTD1	7	14.0386	134	27.0801	20	14.8
0411002	CTD2	7	14.0366	134	27.0790	24	14.2
0411003	CTD3	7	12.6739	134	26.8814	27	134.5
0411004	CTD4	7	12.6008	134	25.3299	25	17.9
0411005	CTD5	7	12.5031	134	23.9171	3.2	0
0411006	CTD6	7	09.3991	134	25.0446	13.8	12.3

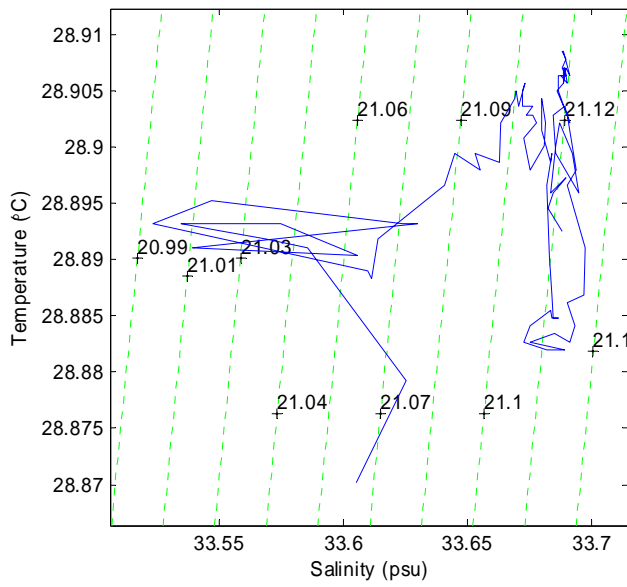
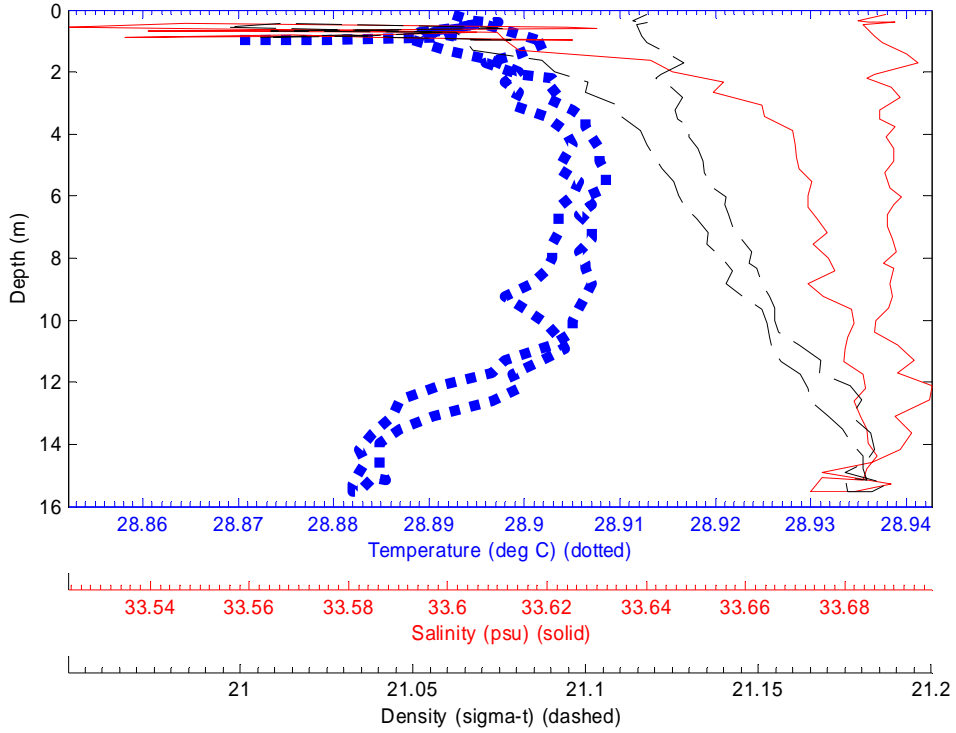
0411007	CTD7	7	12.7256	134	25.0439	21	21
0411008	CTD8	7	15.6579	134	24.9592	5.5	5.9
0411009	CTD9	7	16.1055	134	25.7940	6	5.8
0411010	CTD10	7	12.6050	134	25.8862	22.5	20.1
0411011	CTD11	7	09.4580	134	25.8855	27	282.8
0411012	CTD12	7	16.4348	134	26.6251	10	9.4
0411013	CTD13	7	17.3838	134	27.5574	14.9	14
0411014	CTD14	7	18.1537	134	28.3293	17	16.3
0511000	Tide	7	08.4912	134	17.8275	1	17.9
0511001	C2	7	08.4912	134	17.8275	19	17.9
0511002	CTD2	7	08.5862	134	16.1945	5.2	4.3
0511003	C1	7	08.6464	134	15.1383	7	8
0511004	CTD4	7	07.6638	134	15.0724	5.7	5.7
0511005	CTD5	7	08.9591	134	15.7566	5.5	10.2
0511006	CTD6	7	09.5599	134	16.0855	16	-
0511007	CTD7	7	09.8933	134	15.2803	17	16.5
0511008	CTD8	7	08.8731	134	16.4170	13.8	5.3
0511009	CTD9	7	08.0643	134	17.4009	4.2	4.2
0511010	CTD10	7	19.2354	134	21.0854	27.5	38
0511011	CTD11	7	21.5479	134	19.6039	26	24
0511012	CTD12	7	23.2839	134	18.4827	27	167.1
0511013	CTD13	7	26.8286	134	21.3439	27	111.8
0511014	CTD14	7	22.5419	134	23.2218	21	20.2
0511015	CTD14	7	21.7790	134	23.7905	27	28.1
0611000	CTD0	7	28.6144	134	23.7271	0.5	1.7
0611001	CTD1	7	29.5474	134	24.9141	15.5	14.6
0611002	CTD2	7	30.6139	134	26.1717	1.4	1.5
0611003	CTD3	7	31.0064	134	23.1289	0.5	3.1
0611004	CTD4	7	29.5404	134	25.0558	12.9	12.9
0611005	CTD5	7	29.5404	134	25.0558	27	-
0711000	CTD0	7	46.3574	134	35.6308	14.5	15.4
0711001	CTD1	7	50.7233	134	32.5500	12.7	11.9
0711002	CTD2	7	54.8317	134	30.2406	3.5	5
0711003	CTD3	7	56.3801	134	38.1900	28	29.5
0711004	CTD4	7	58.5619	134	40.2784	8	7.3
0711005	CTD5	7	59.5498	134	41.3447	1.1	1.1
0711006	CTD6	7	52.7399	134	39.9645	17	15.5
0711007	CTD7	7	50.9388	134	38.4327	22.5	21.9
0711008	CTD8	7	49.0609	134	36.6004	24	23.5
0711009	CTD9	7	46.3673	134	35.2366	13	10.7
0711010	CTD10	7	44.6621	134	34.6736	8.2	7.4
0711011	CTD11	7	43.5478	134	34.8441	2	2
0911000	11C1	7	16.9557	134	30.1576	17.7	27
0911001	11C2	7	15.8782	134	28.9070	21	20.1
0911002	11C3	7	14.8337	134	27.9863	19.3	18

0911003	10A1	7	20.6072	134	34.3320	27	37.3
0911004	CTD4	7	22.0578	134	35.9943	27	1.5
1111000	6A	7	36.5044	134	31.3058	29	35.2
1111001	6Af	7	37.6915	134	33.0635	28	36.6
1111002	5As	7	39.6513	134	37.4472	6.9	1.1
1111003	5Af	7	38.1567	134	35.4293	24.5	33.5
1111004	5bs	7	37.7145	134	36.1149	19.5	19.5
1111005	5bf	7	40.6068	134	36.9029	26	0.9

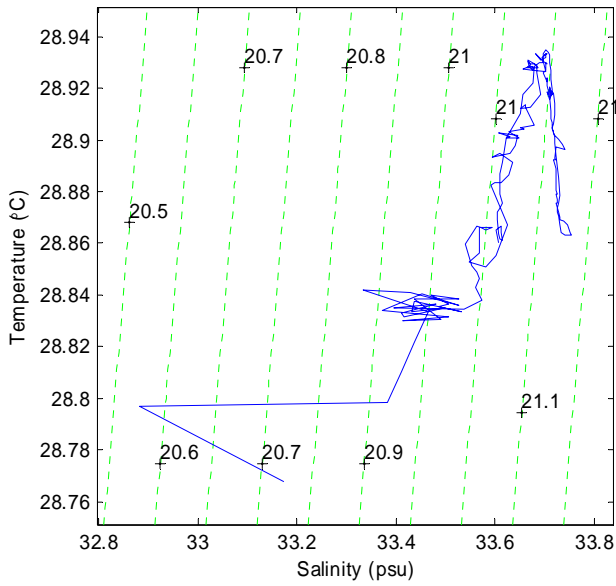
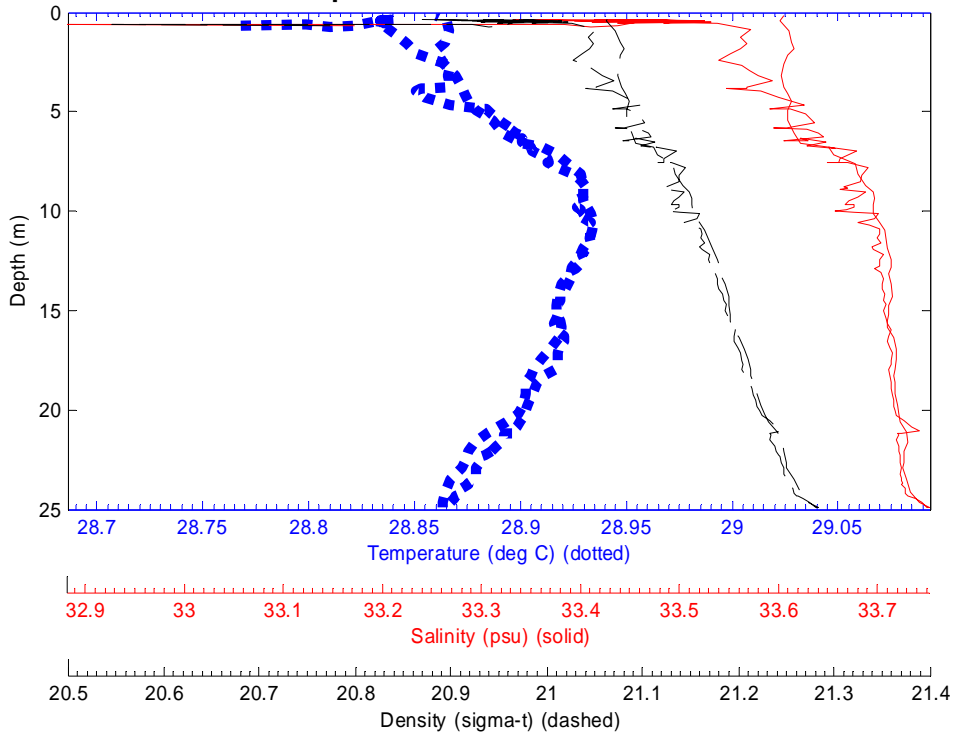
File: 1909000 19-Sep-2003 11:48:26 S7.1143 E134.2656 Site: 018



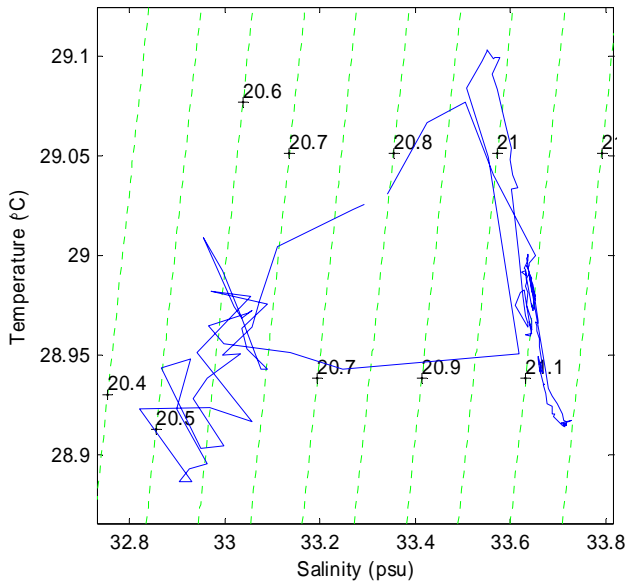
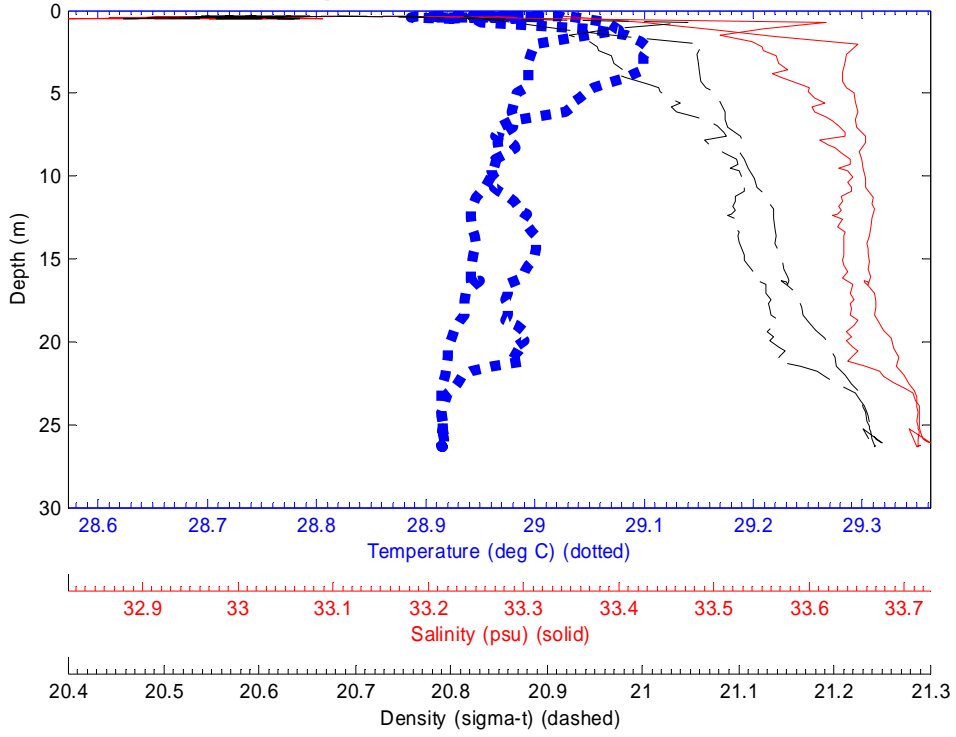
File: 1909001 19-Sep-2003 11:59:35 S7.1345 E134.2985 Site: 019



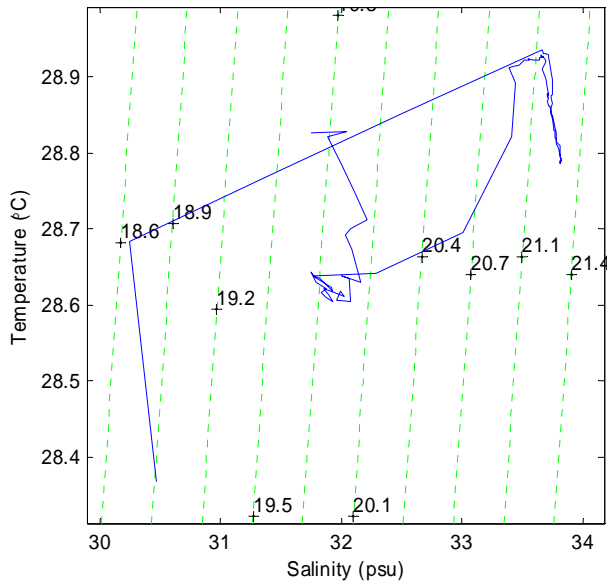
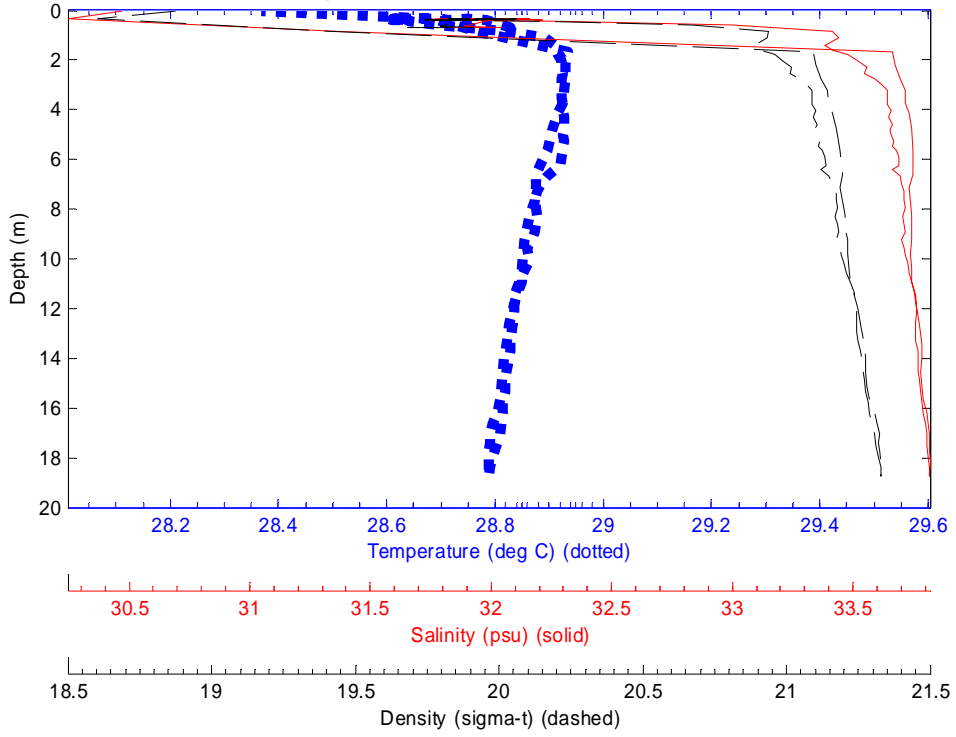
File: 1909002 19-Sep-2003 12:12:40 S7.1614 E134.331 Site: 020



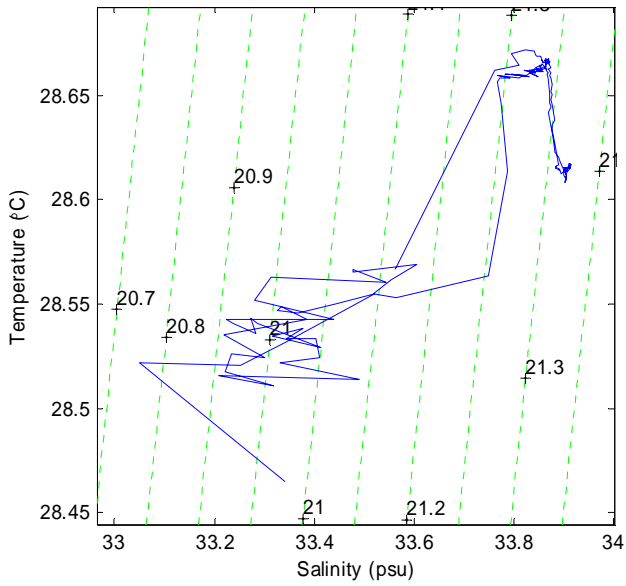
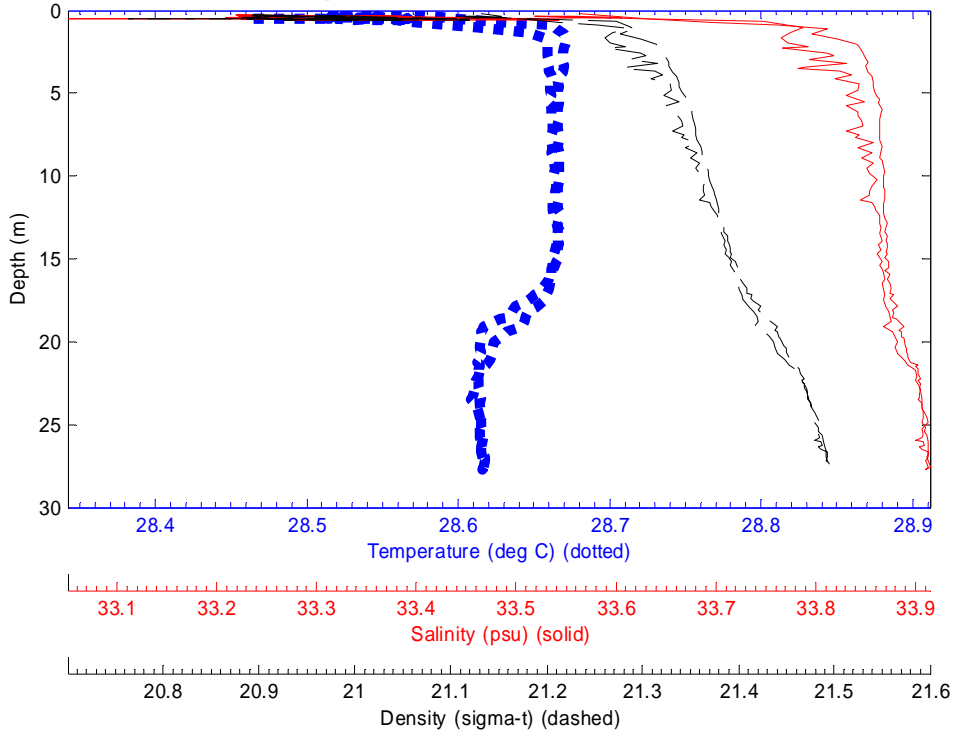
File: 1909003 19-Sep-2003 12:25:47 S7.1813 E134.3626 Site: 021



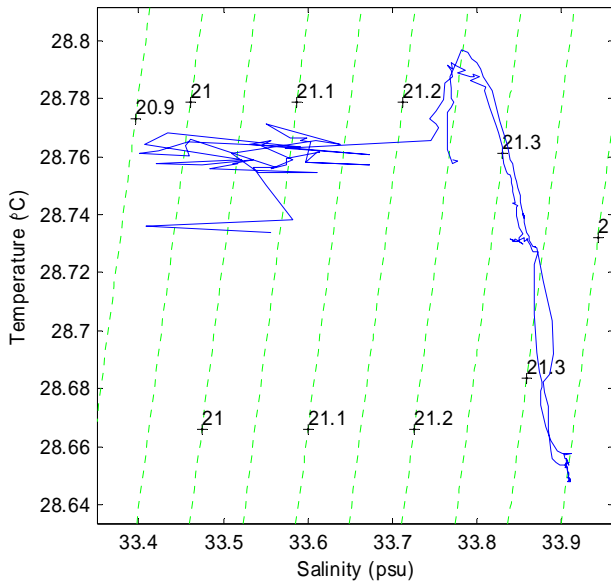
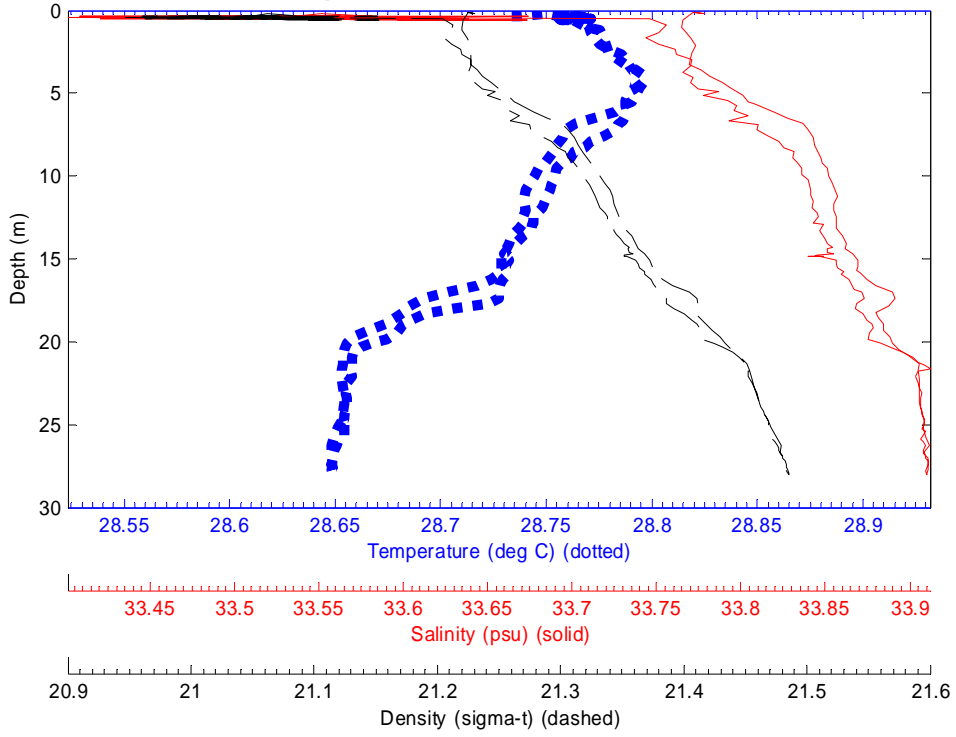
File: 1909004 19-Sep-2003 12:38:18 S7.2131 E134.3875 Site: 022



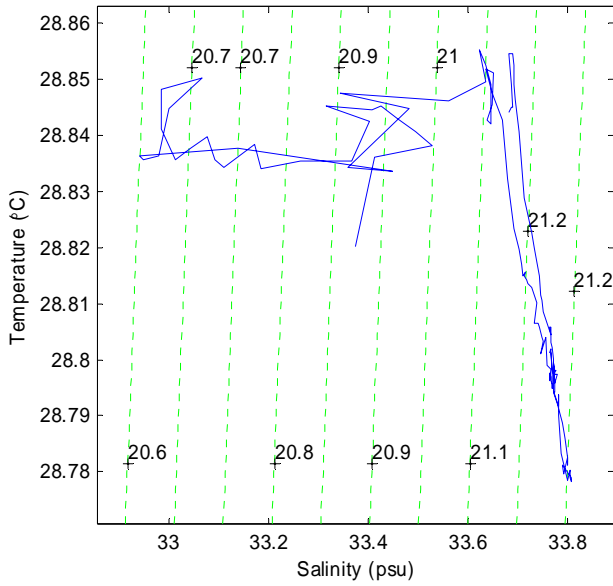
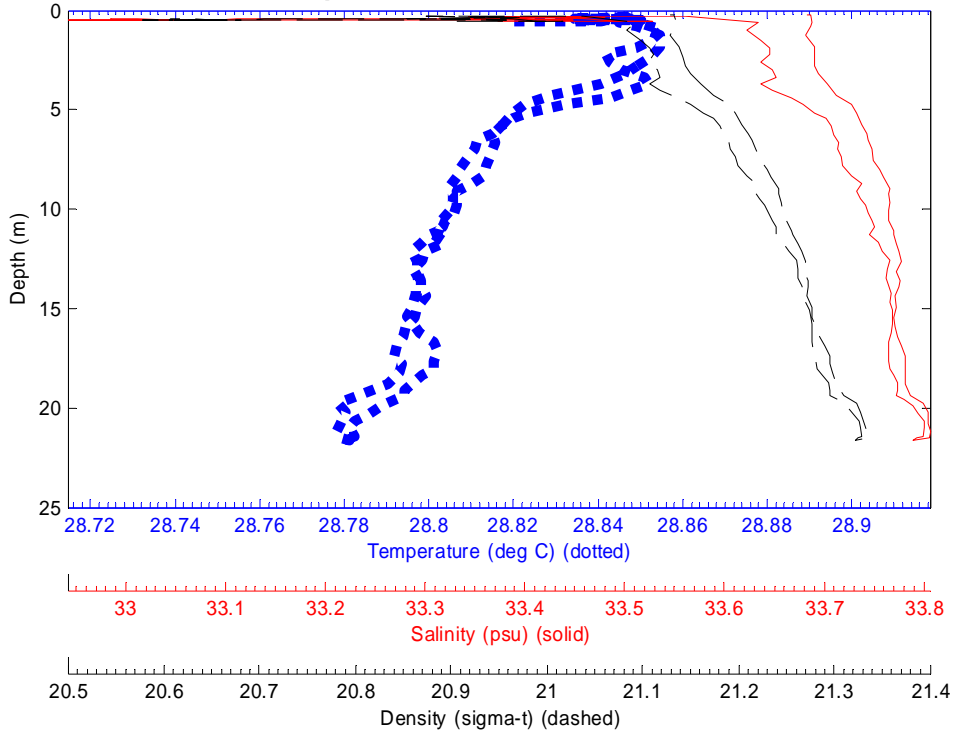
File: 1909005 19-Sep-2003 12:52:48 S7.2176 E134.4441 Site: 023



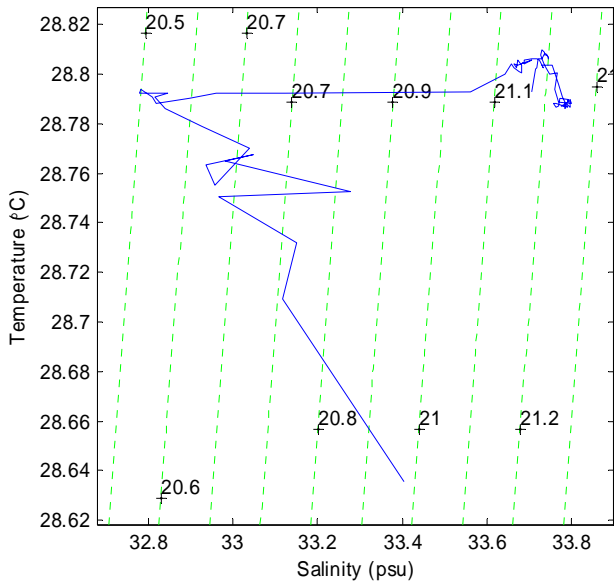
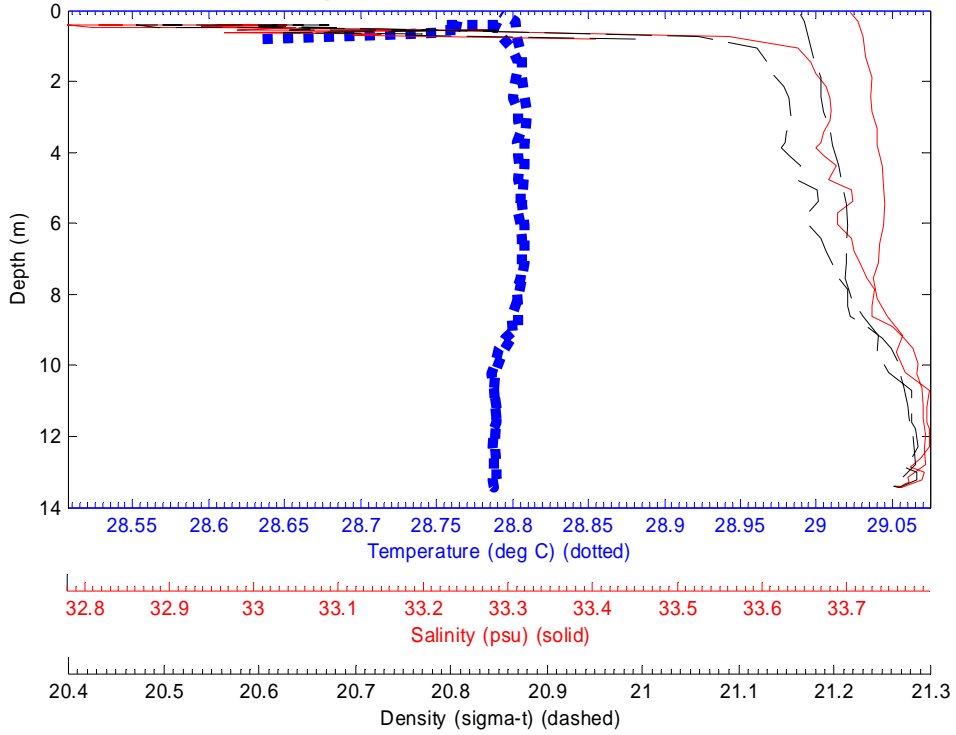
File: 1909006 19-Sep-2003 13:04:30 S7.2558 E134.4608 Site: 026



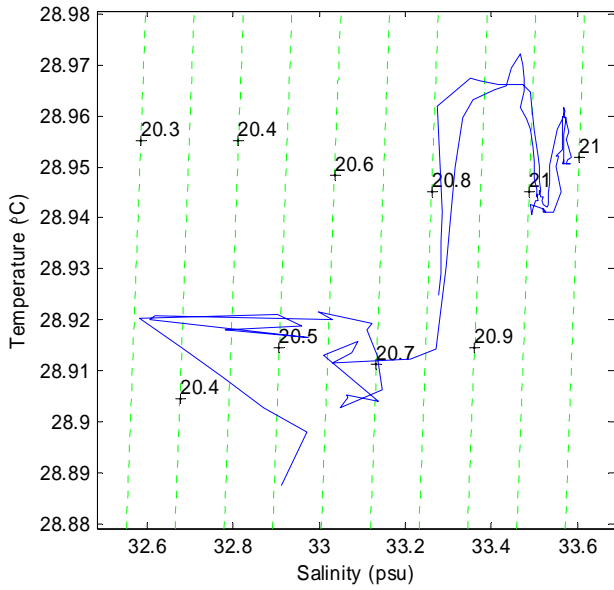
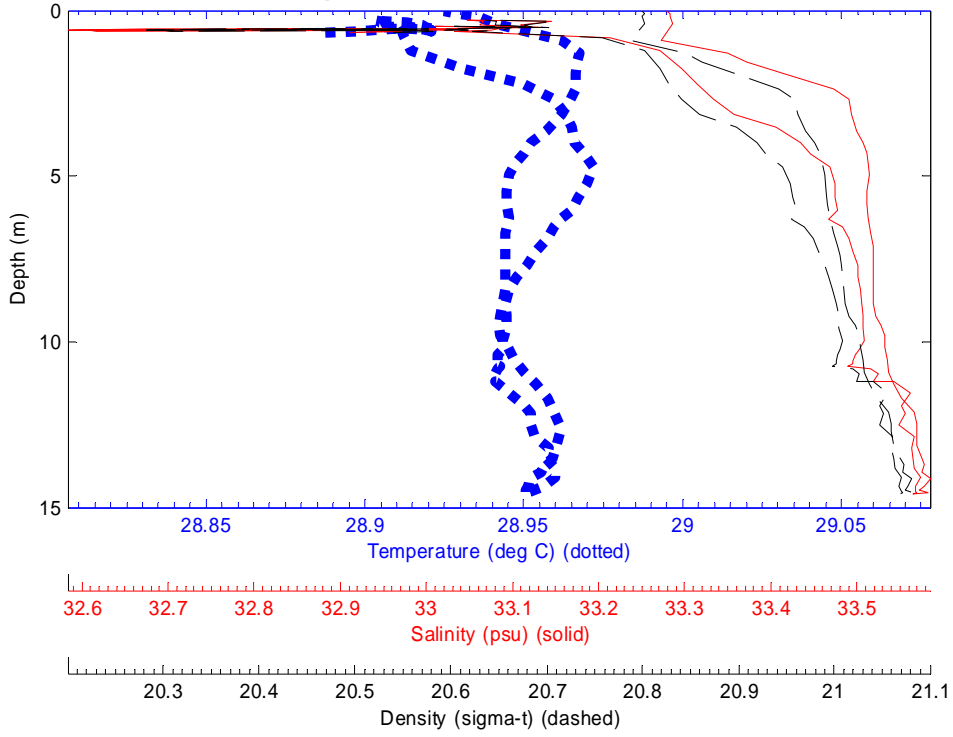
File: 1909007 19-Sep-2003 13:14:29 S7.2828 E134.4654 Site: 025



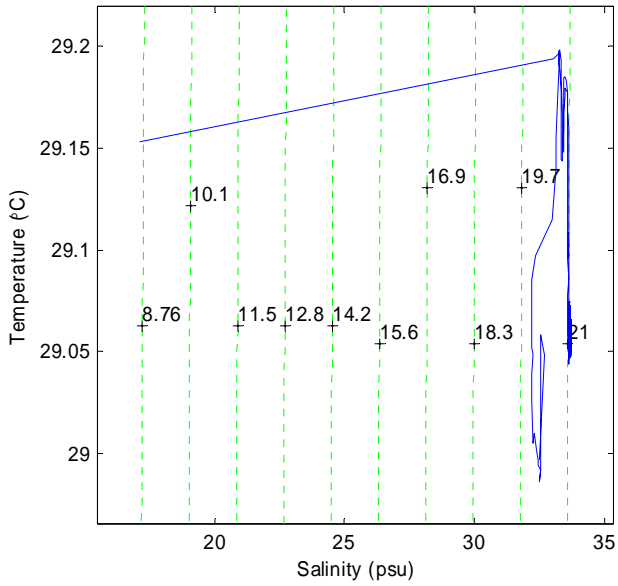
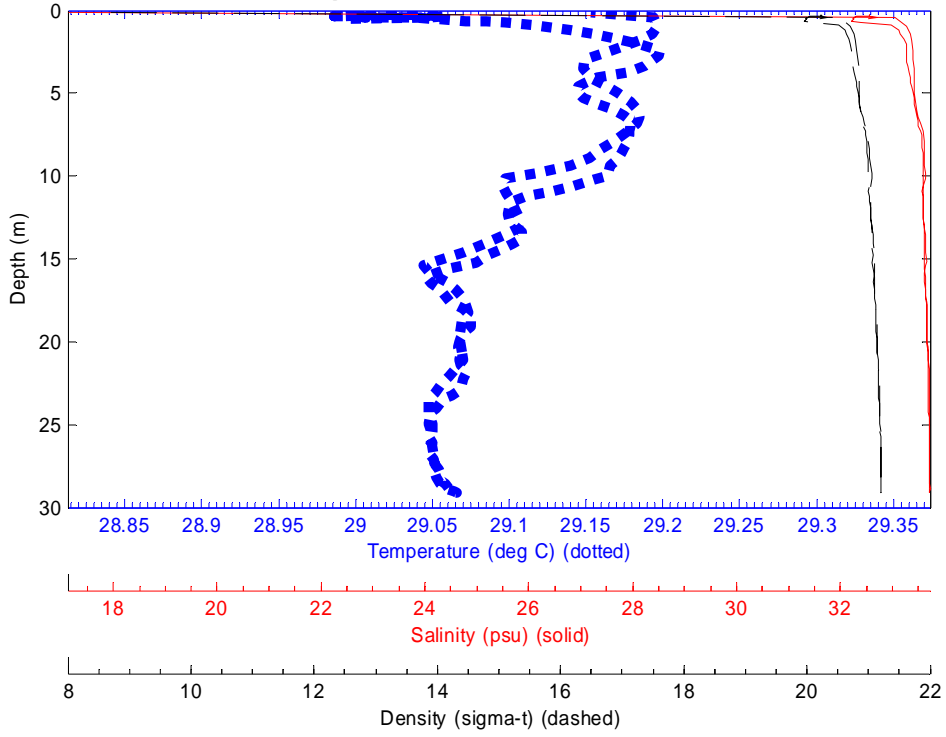
File: 1909008 19-Sep-2003 13:19:07 S7.2945 E134.4577 Site: 026



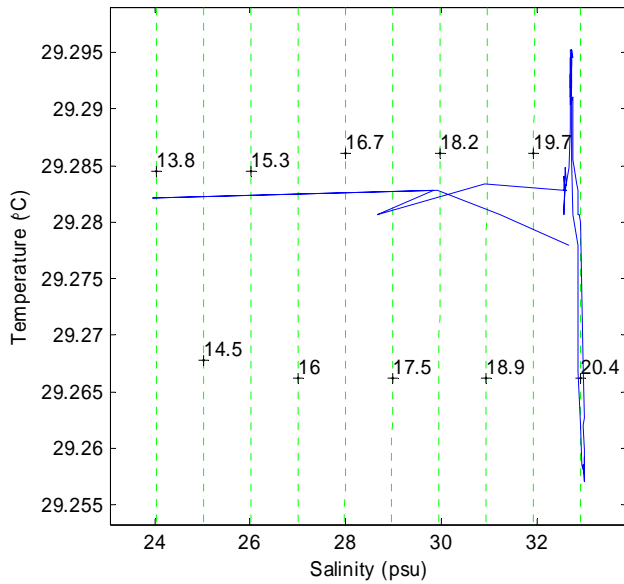
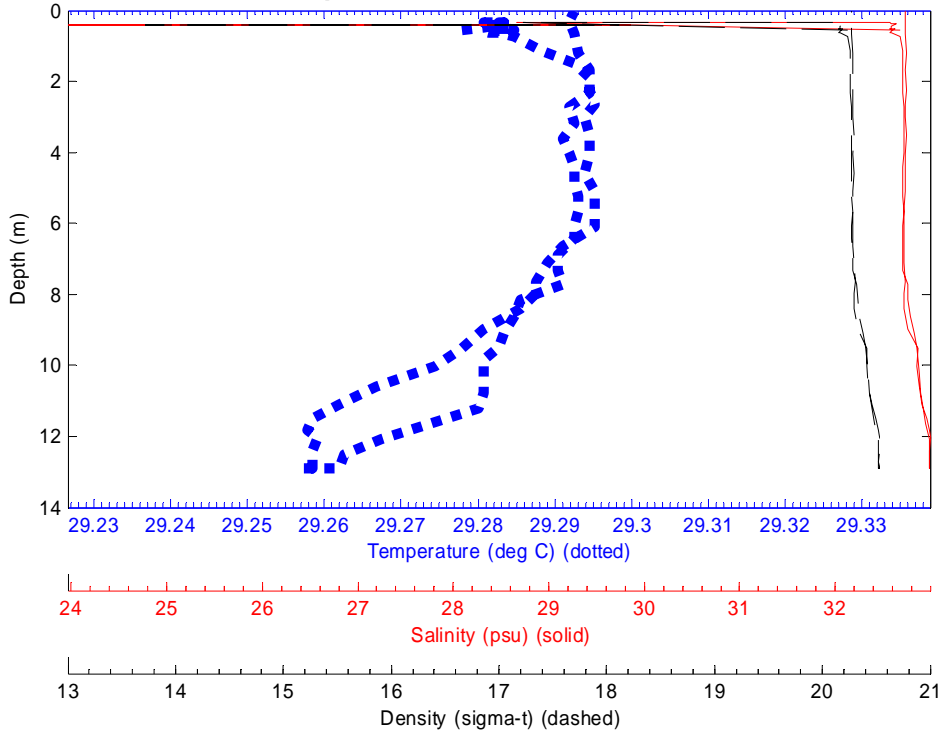
File: 1909009 19-Sep-2003 13:23:27 S7.3109 E134.4601 Site: 027



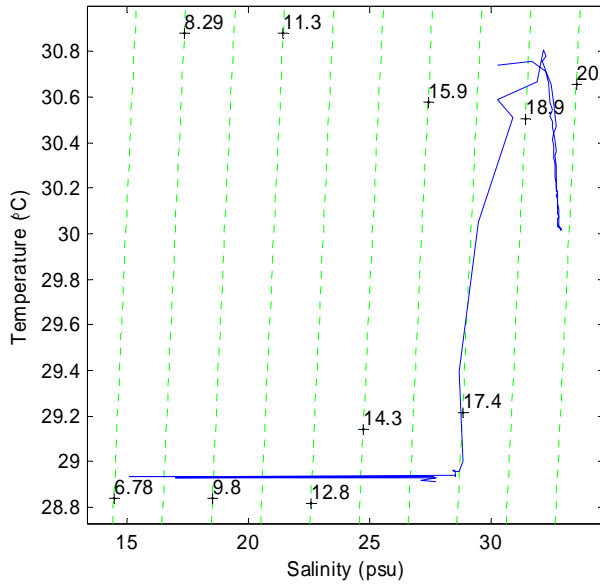
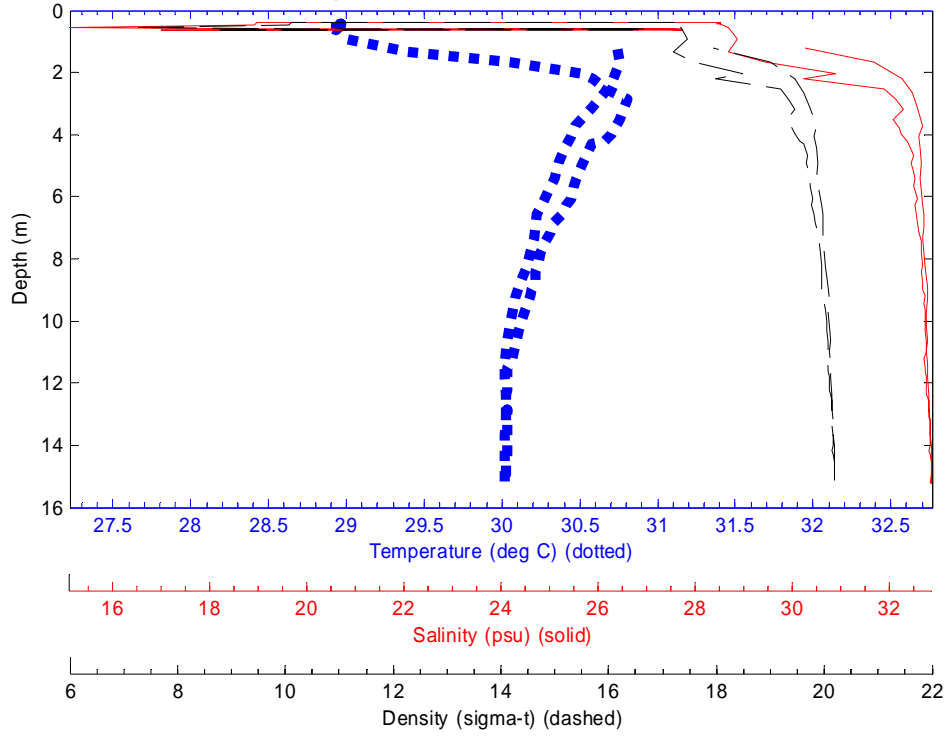
File: 1909010 19-Sep-2003 13:28:43 S7.331 E134.4648 Site: 028



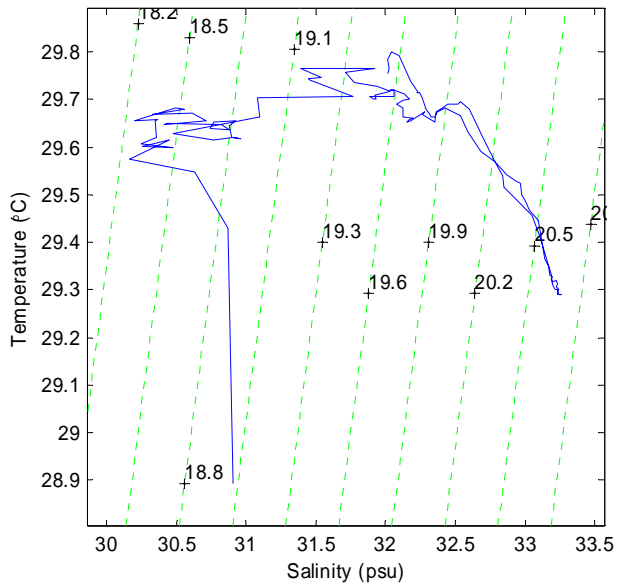
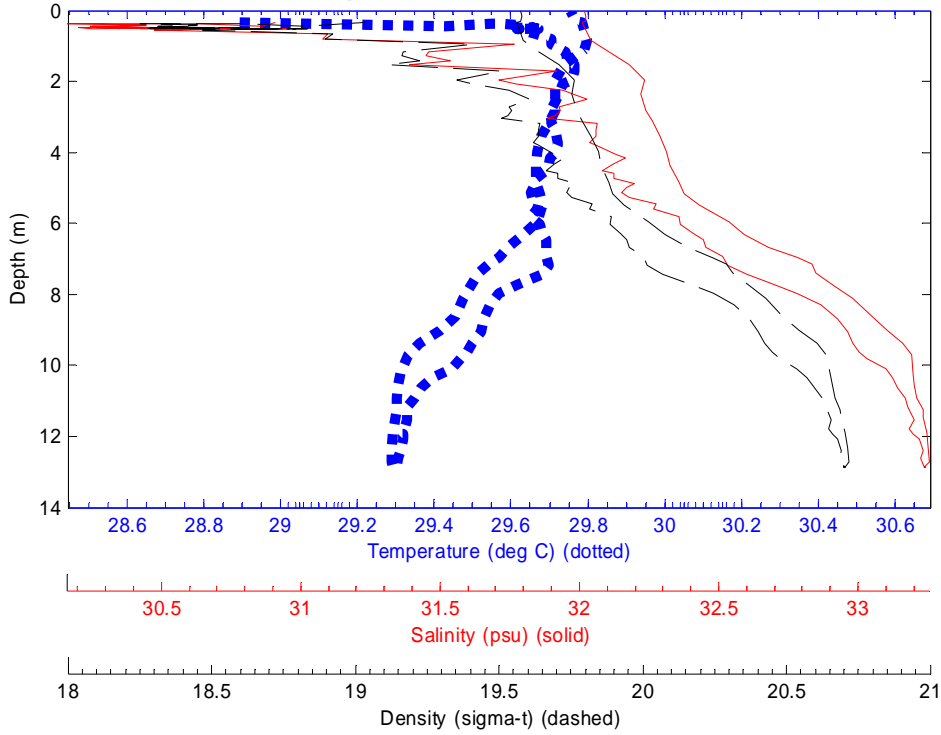
File: 1909011 19-Sep-2003 13:32:23 S7.3372 E134.4657 Site: 029



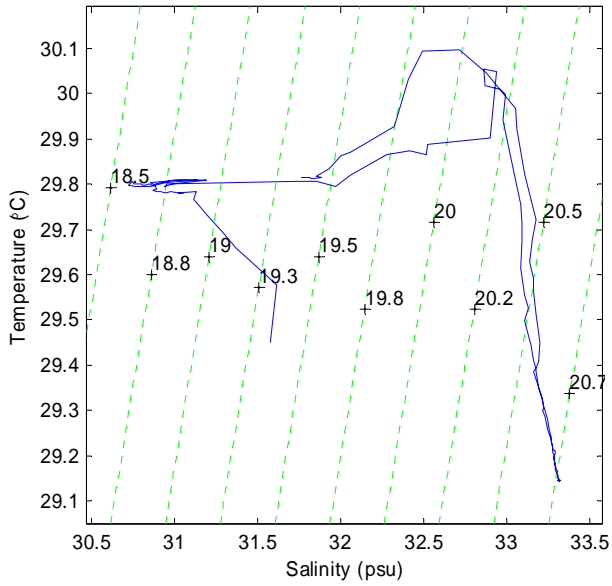
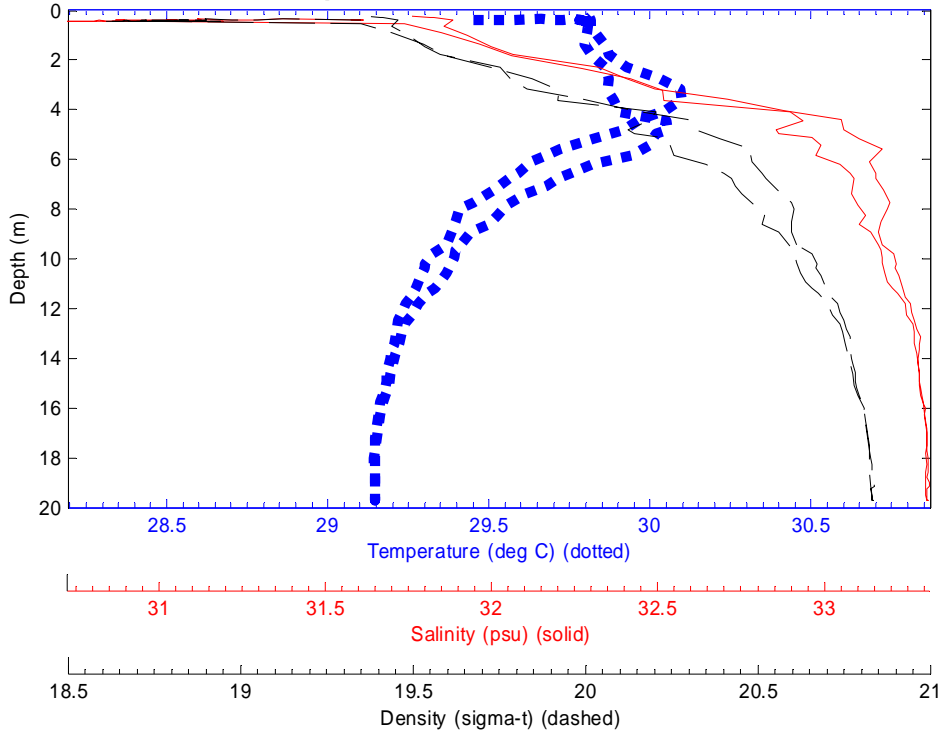
File: 2109000 21-Sep-2003 13:13:05 S7.3295 E134.5006 Site: T4



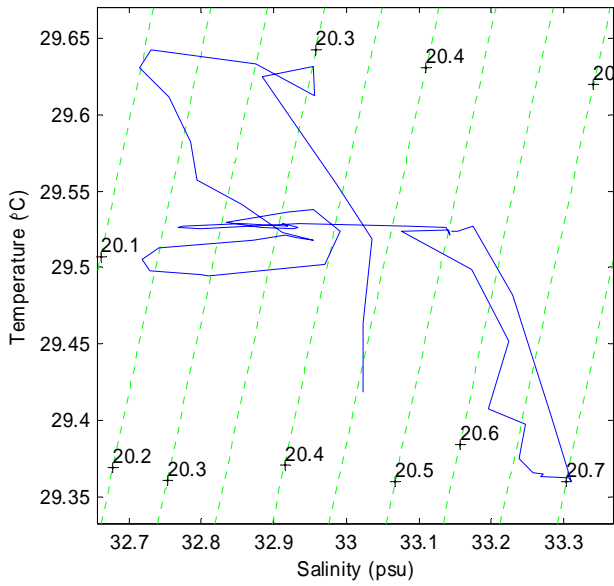
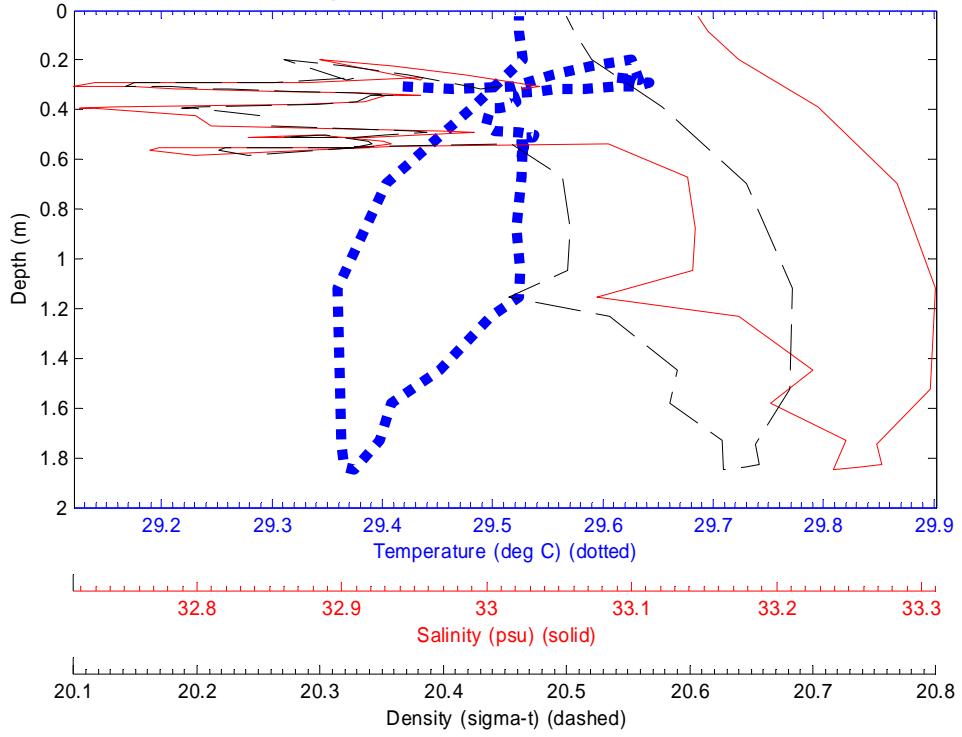
File: 2109001 21-Sep-2003 13:46:00 S7.3219 E134.49 Site: A2



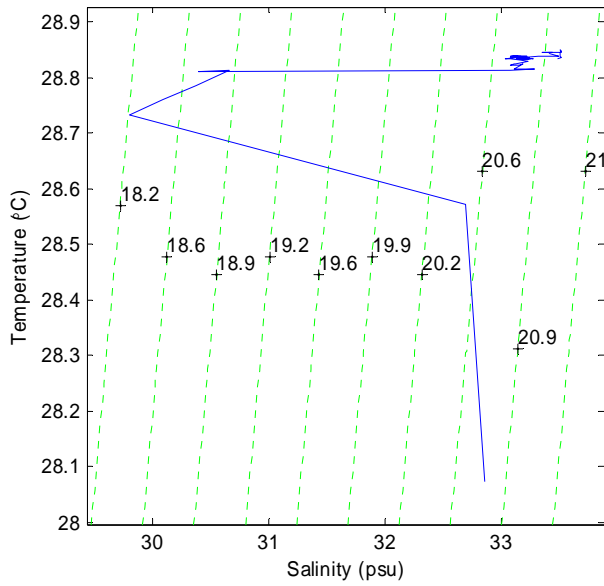
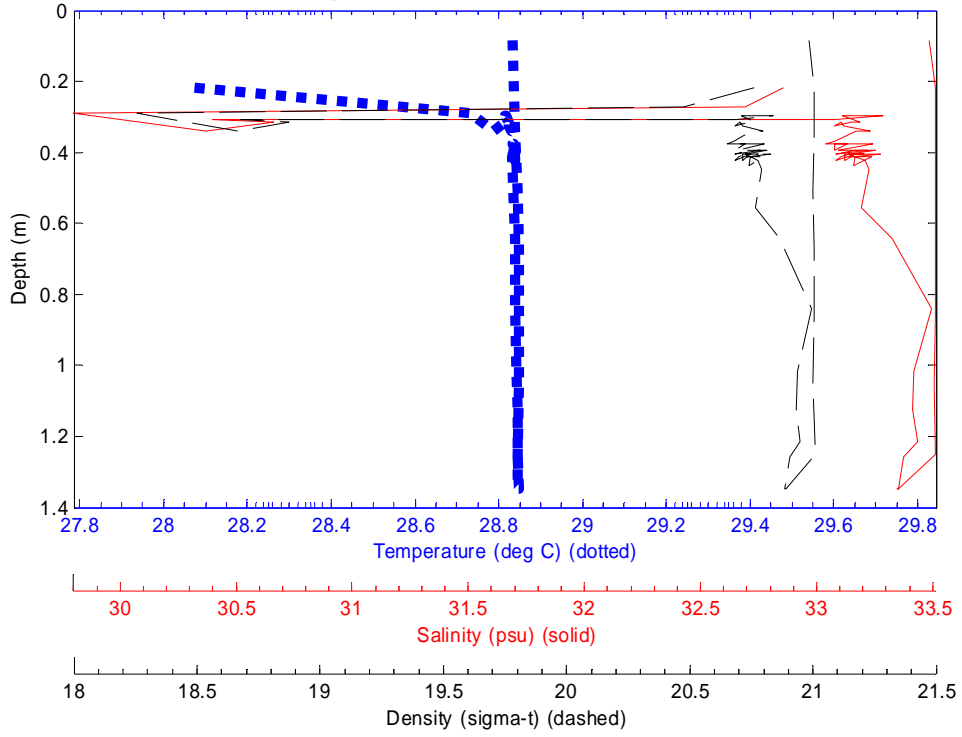
File: 2109002 21-Sep-2003 13:53:23 S7.3179 E134.4951 Site: 031



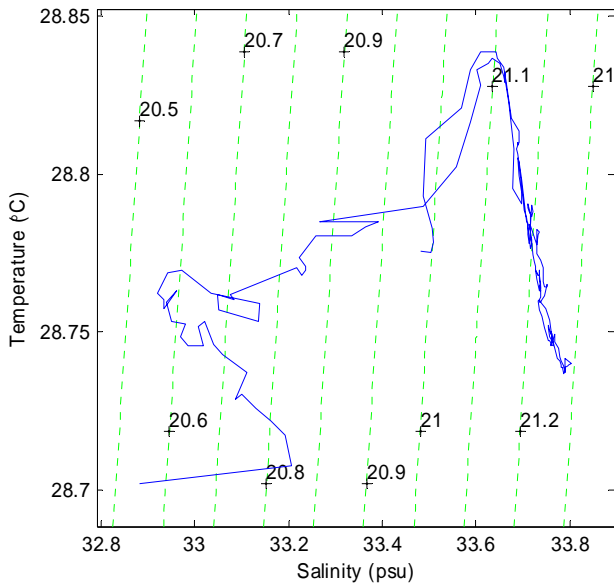
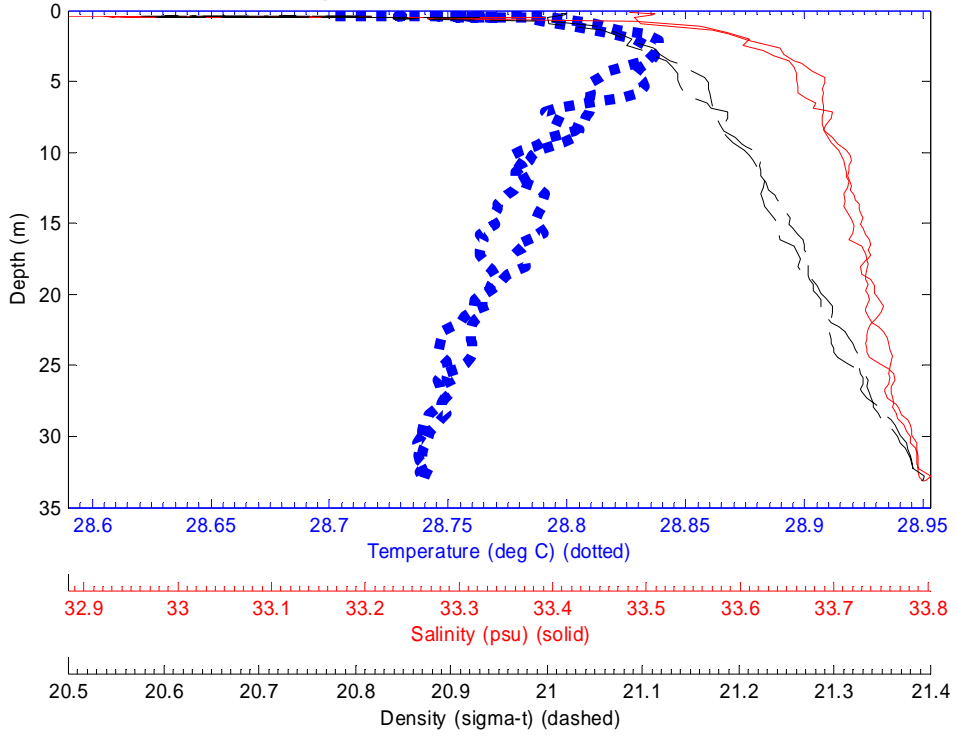
File: 2109003 21-Sep-2003 14:01:30 S7.3115 E134.5019 Site: 032



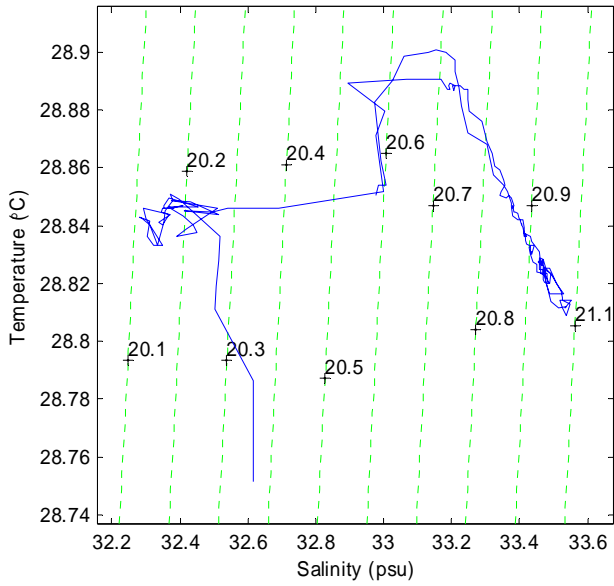
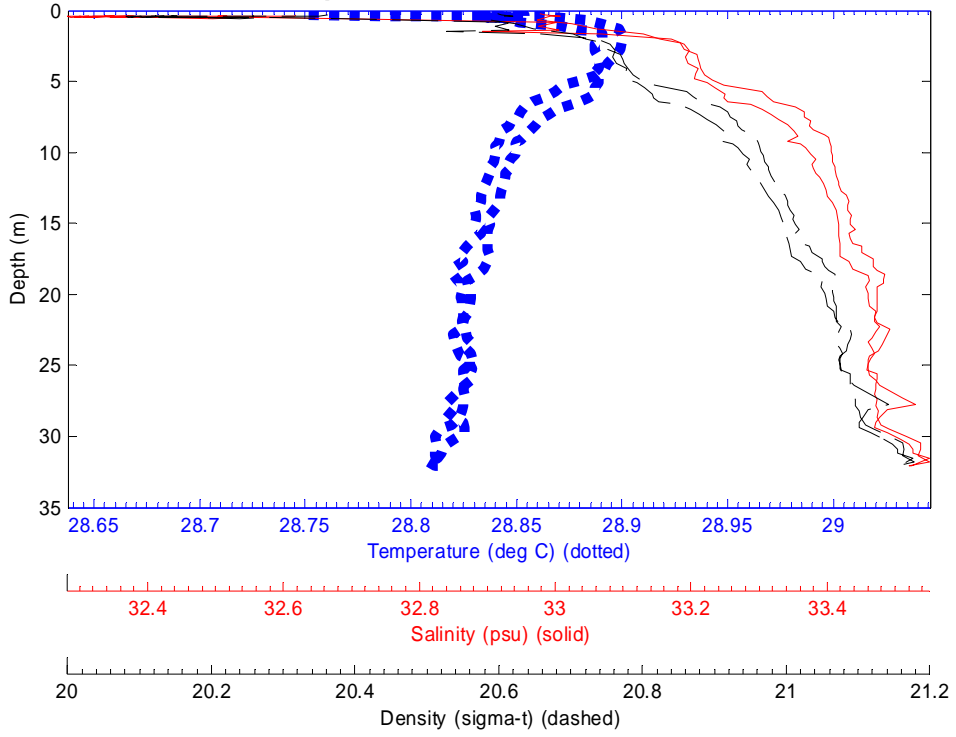
File: 2109004 21-Sep-2003 14:09:02 S7.3082 E134.5104 Site: 033



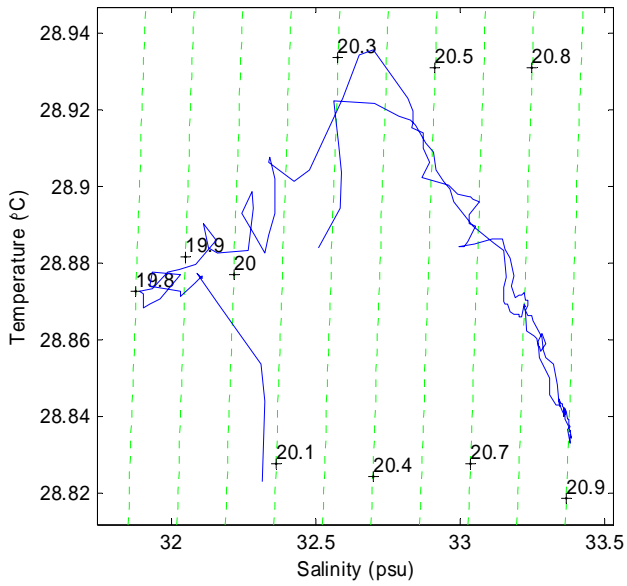
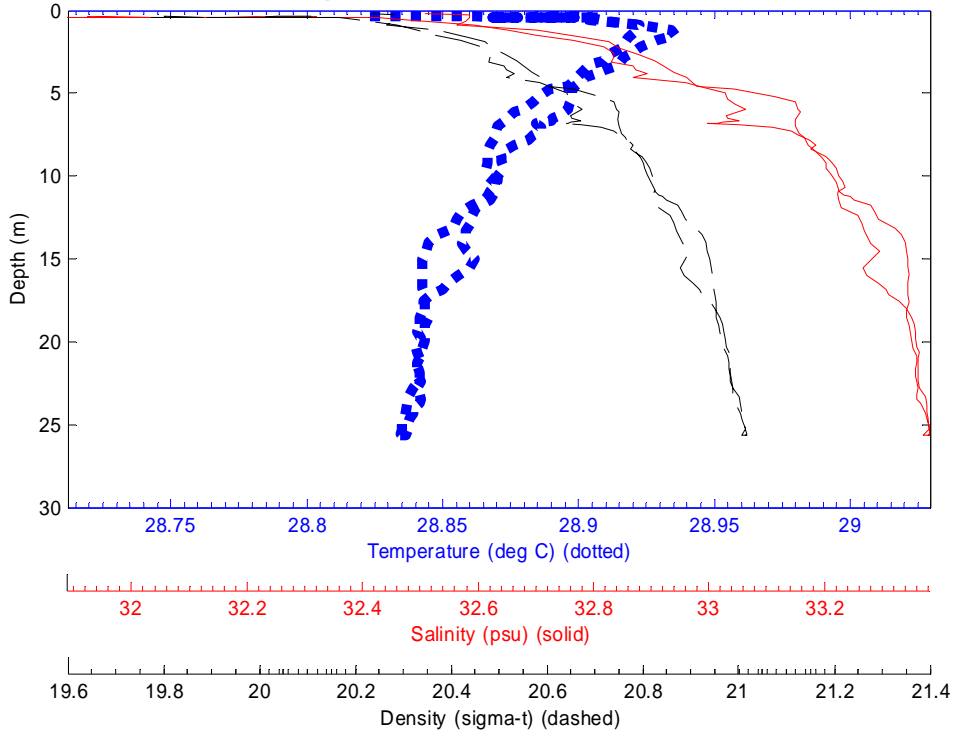
File: 2109006 21-Sep-2003 14:17:39 S7.3172 E134.5243 Site: A13



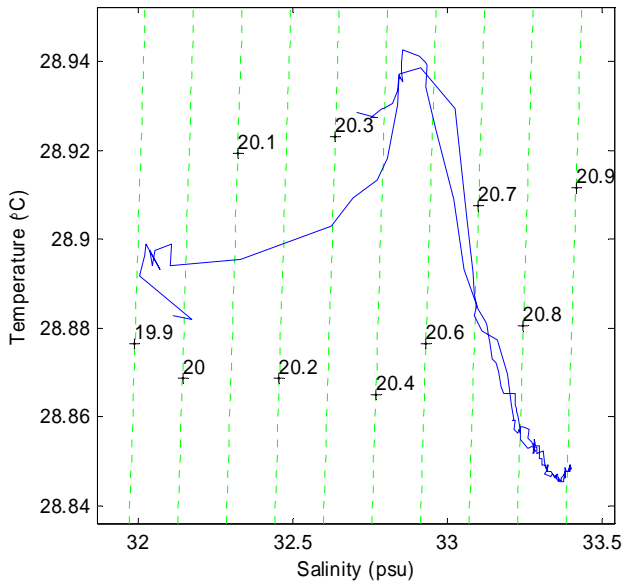
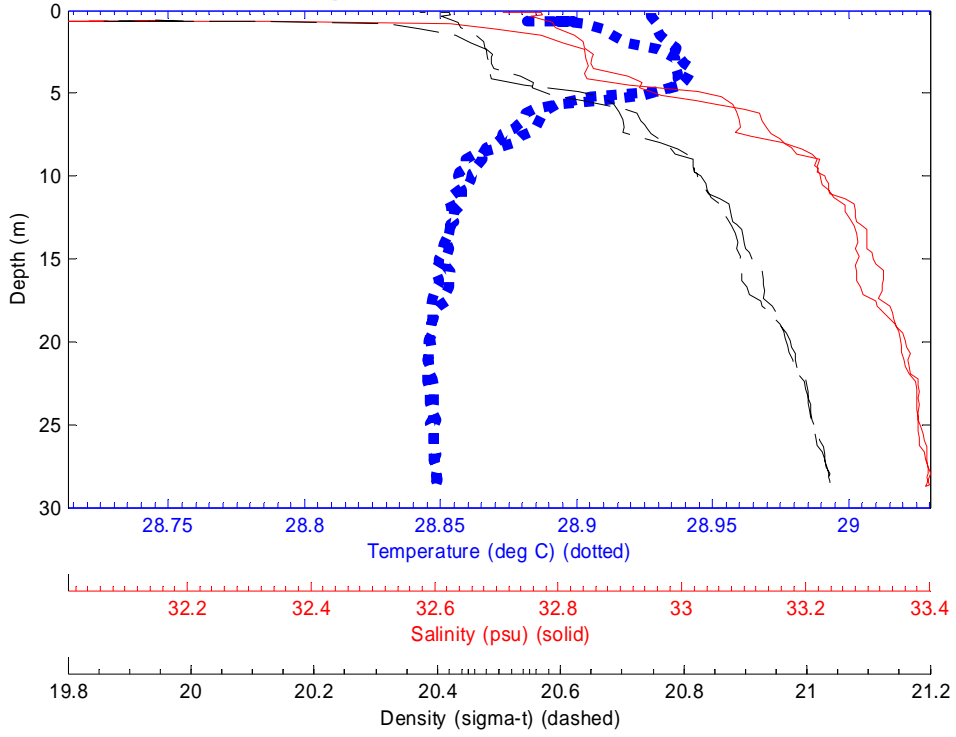
File: 2109007 21-Sep-2003 14:23:28 S7.3339 E134.5208 Site: 036



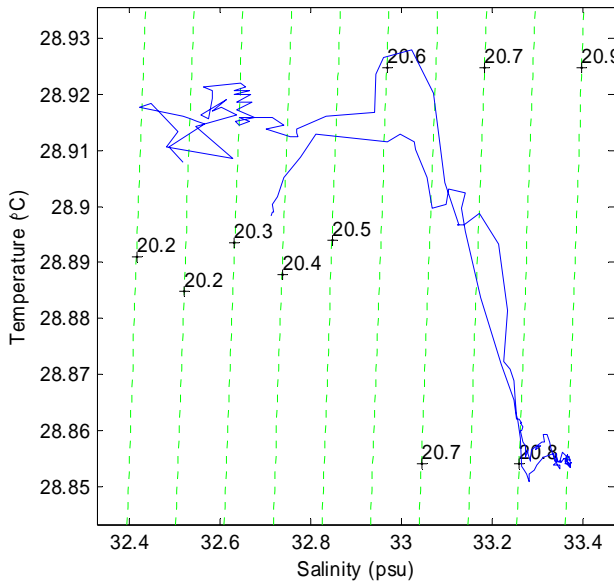
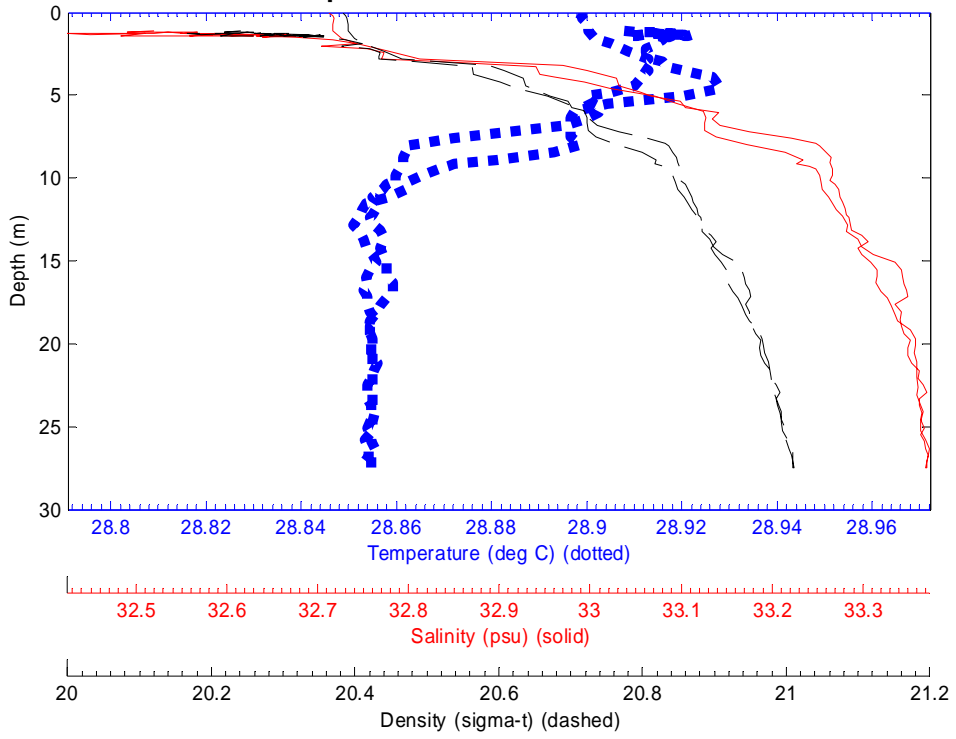
File: 2109008 21-Sep-2003 14:40:24 S7.3405 E134.5171 Site: 037



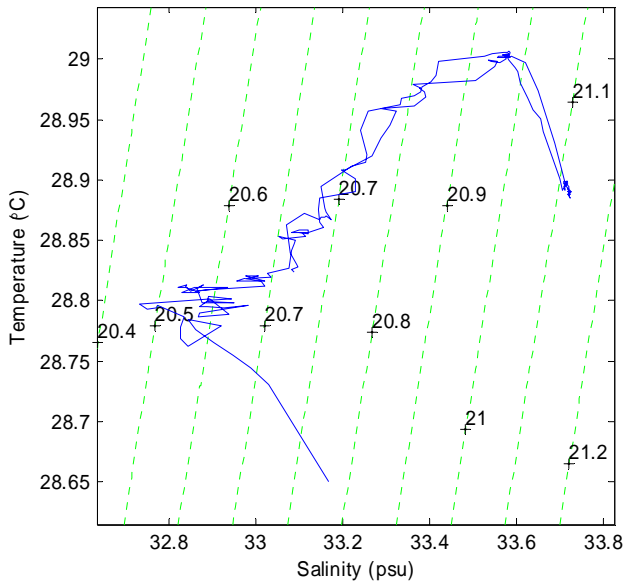
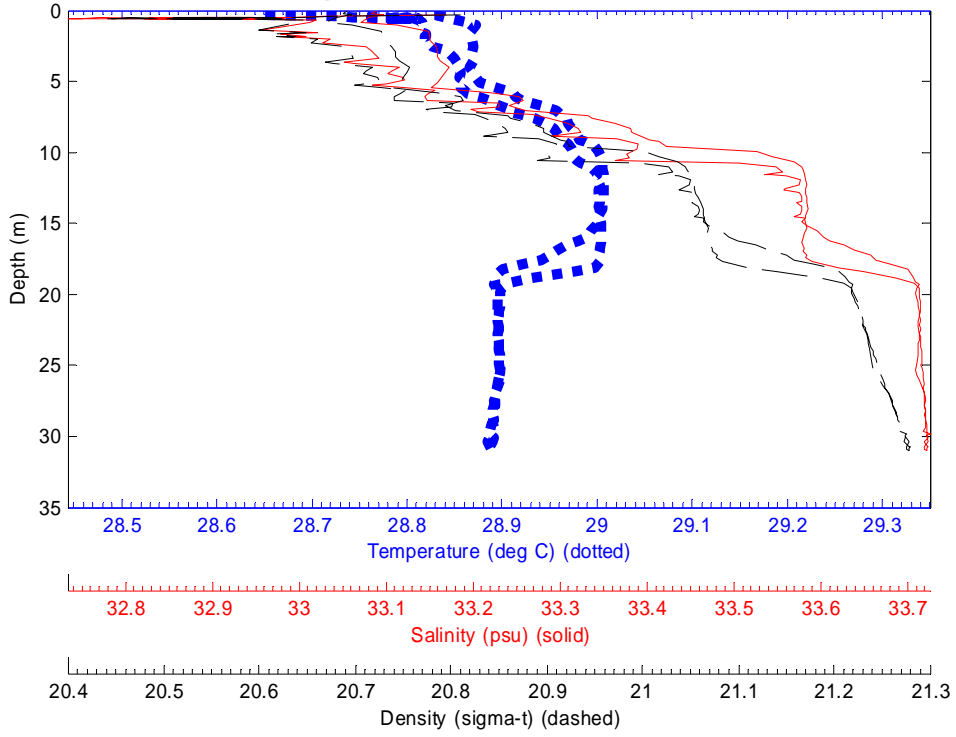
File: 2109009 21-Sep-2003 14:47:42 S7.3518 E134.512 Site: 038



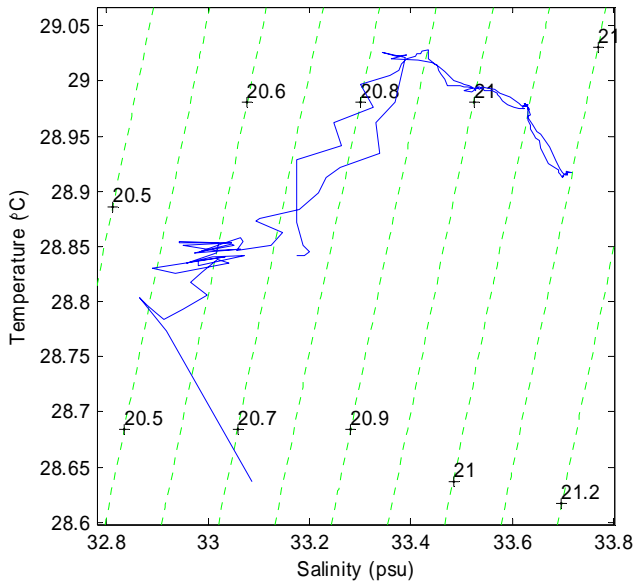
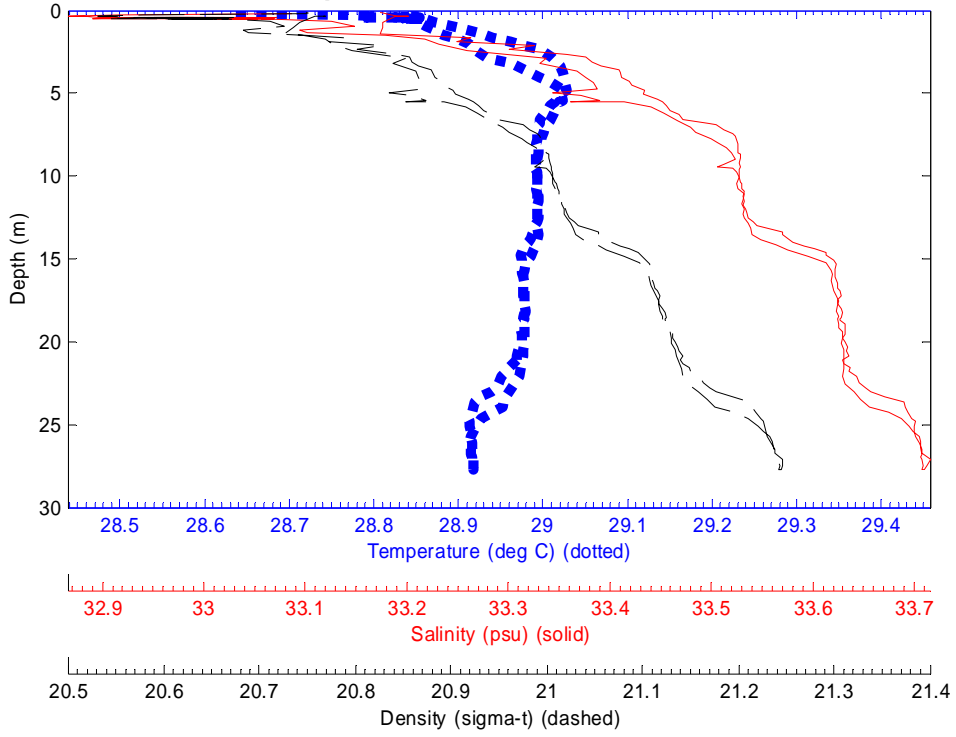
File: 2109010 21-Sep-2003 14:53:18 S7.3626 E134.5042 Site: KB



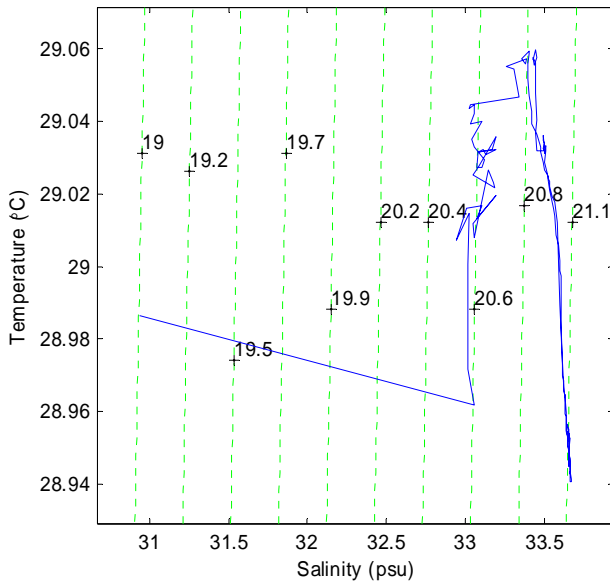
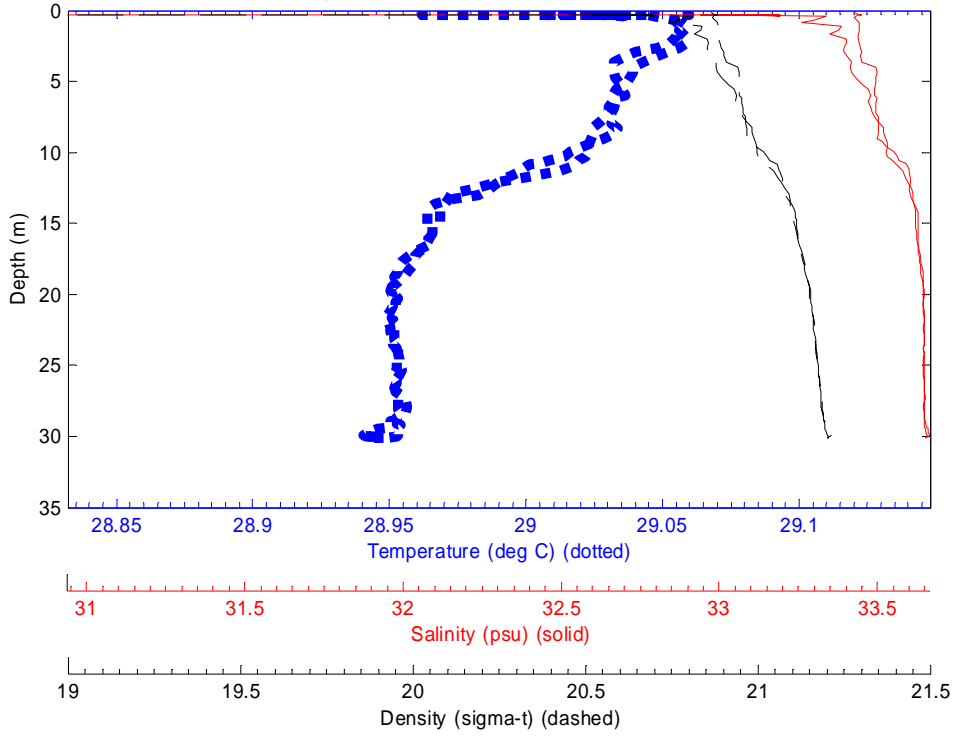
File: 2109011 21-Sep-2003 16:57:13 S7.3385 E134.4281 Site: 040



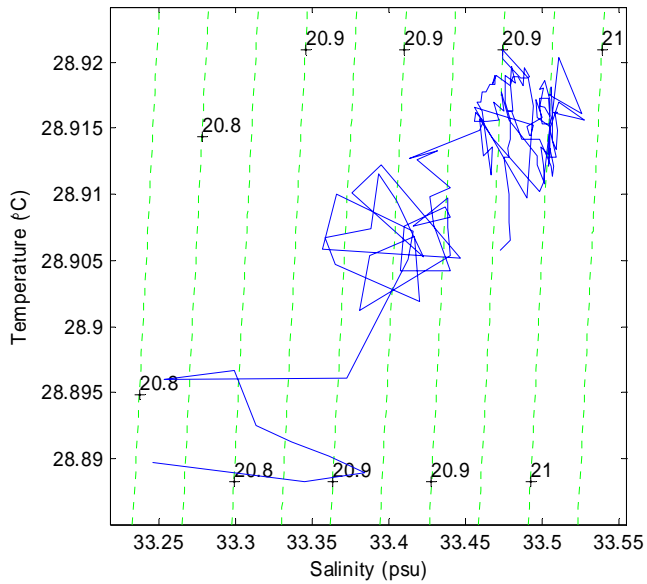
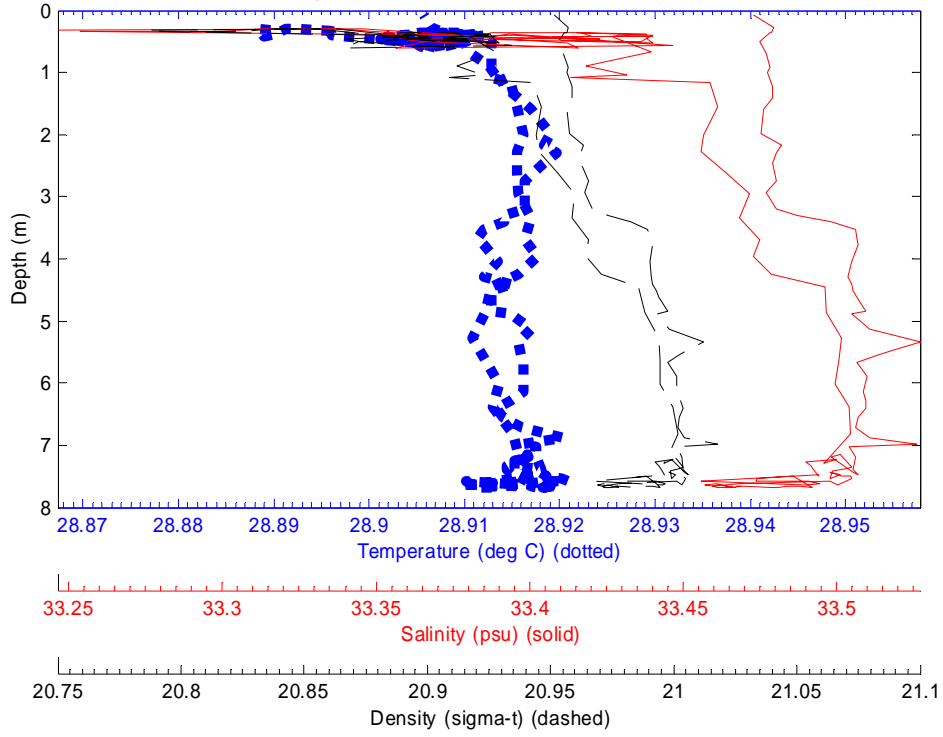
File: 2109012 21-Sep-2003 17:03:29 S7.3326 E134.4357 Site: 041



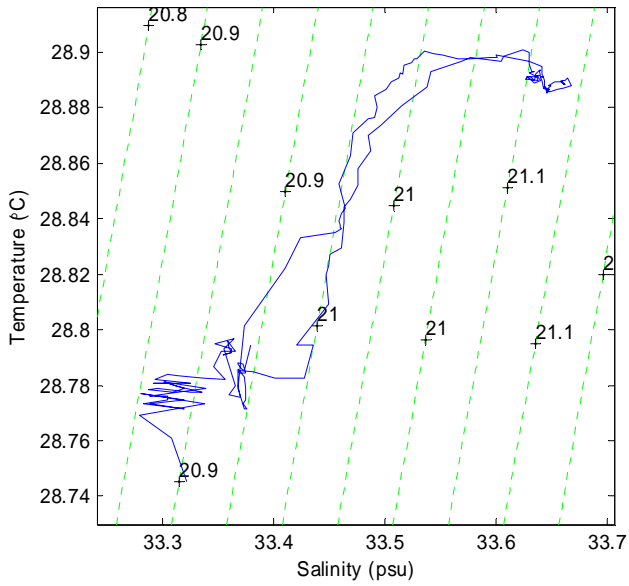
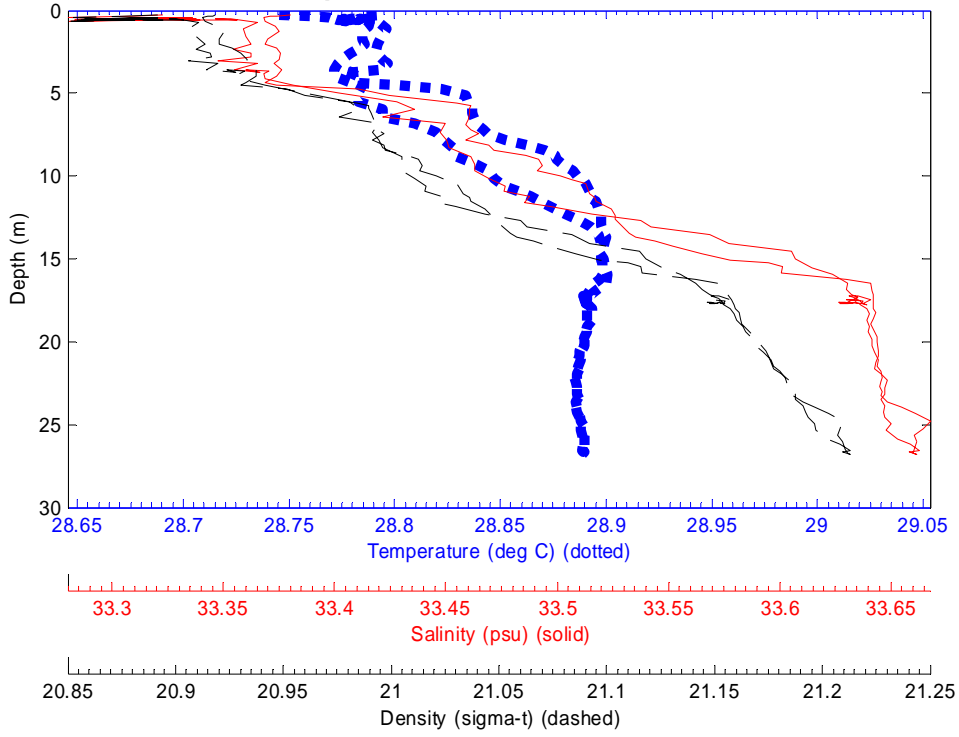
File: 2109013 21-Sep-2003 17:09:01 S7.3208 E134.4537 Site: 042



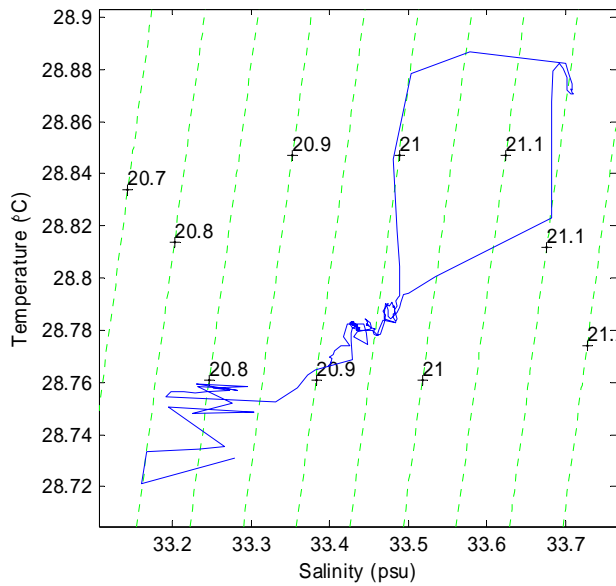
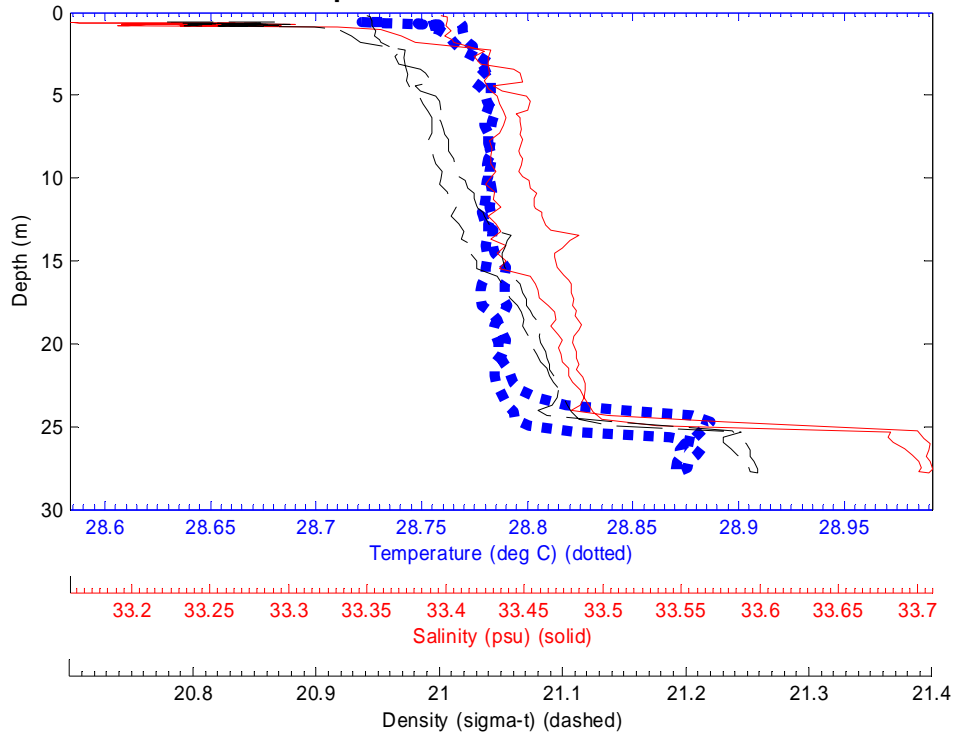
File: 2209000 22-Sep-2003 10:21:01 S7.2789 E134.3295 Site: 043



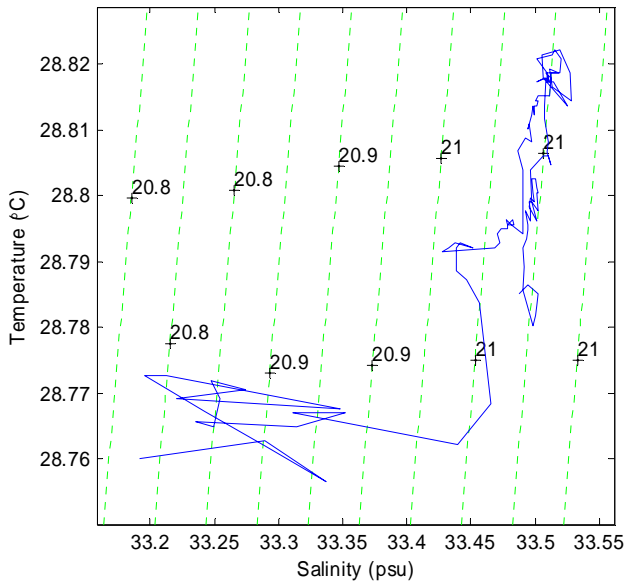
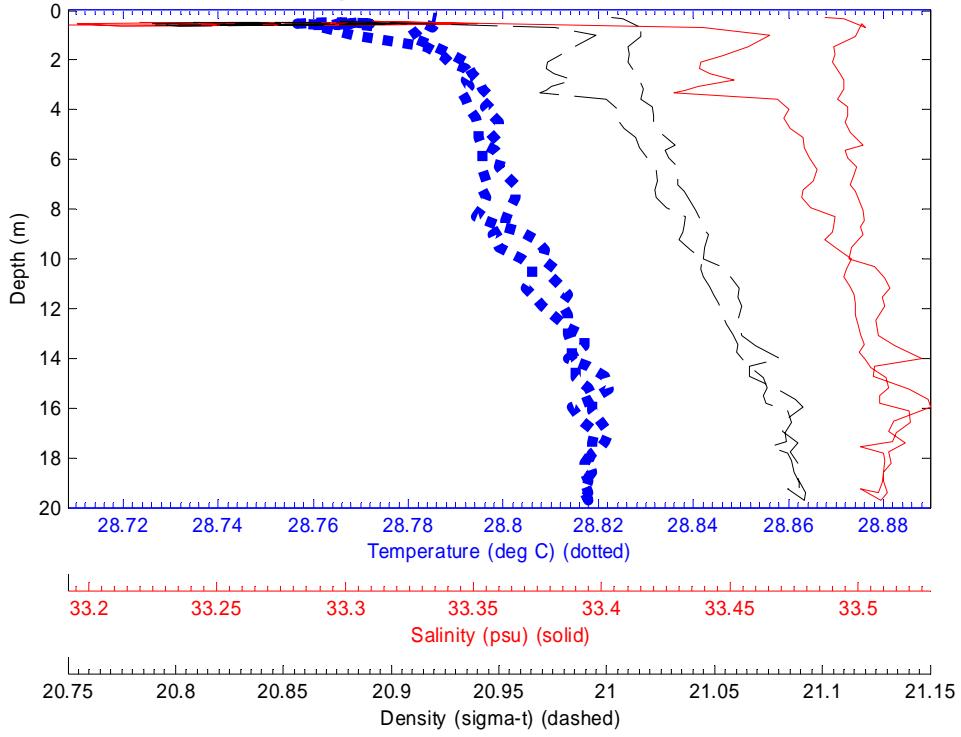
File: 2209001 22-Sep-2003 10:24:43 S7.2783 E134.3242 Site: 044



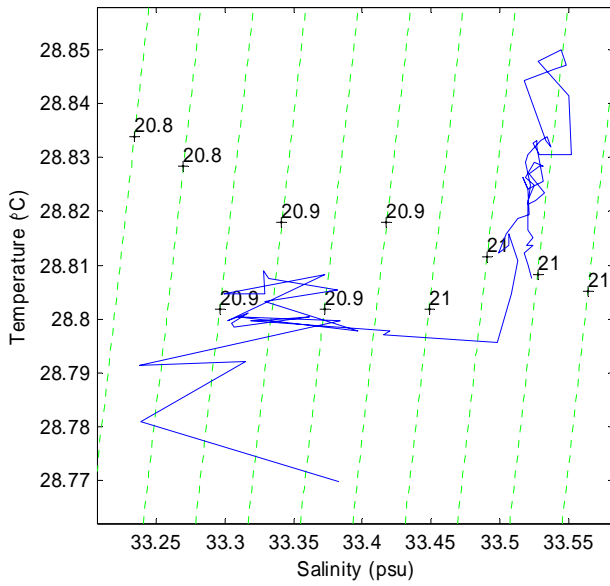
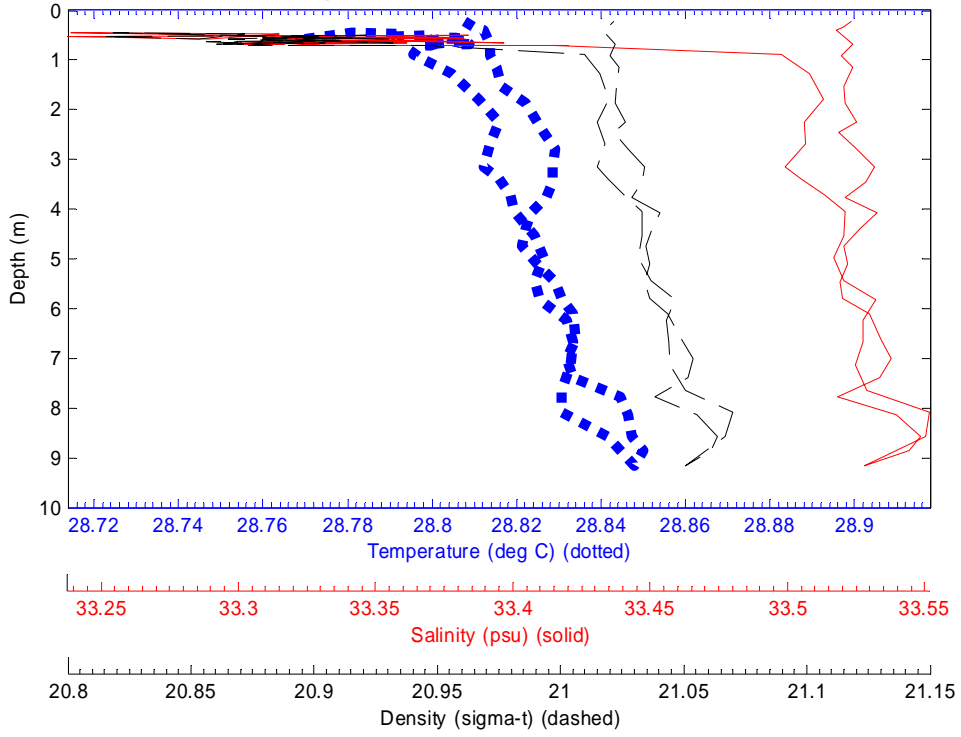
File: 2209002 22-Sep-2003 10:29:29 S7.2779 E134.317 Site: 045



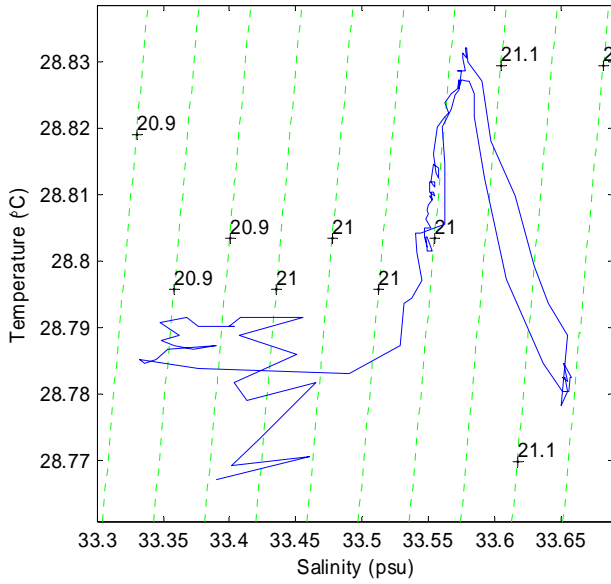
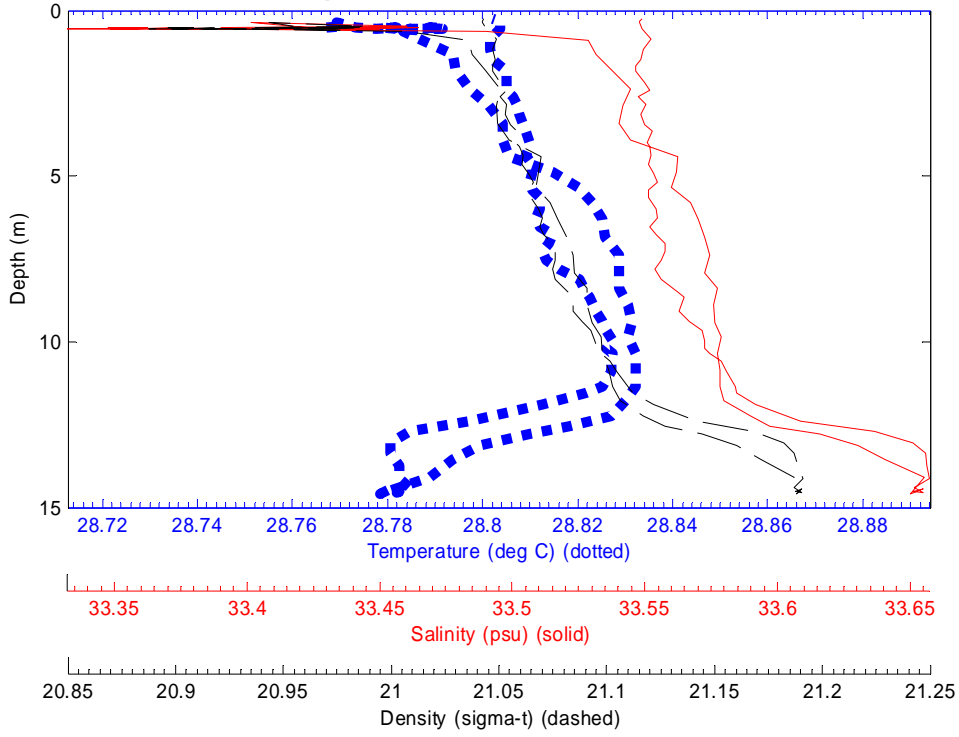
File: 2209003 22-Sep-2003 10:36:24 S7.277 E134.3134 Site: A4



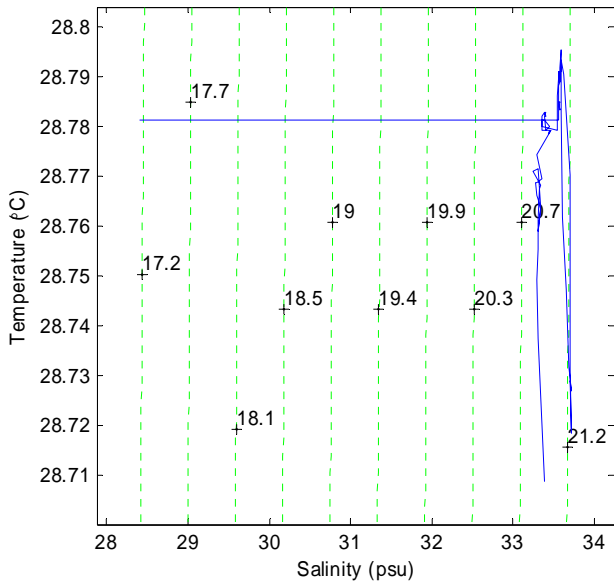
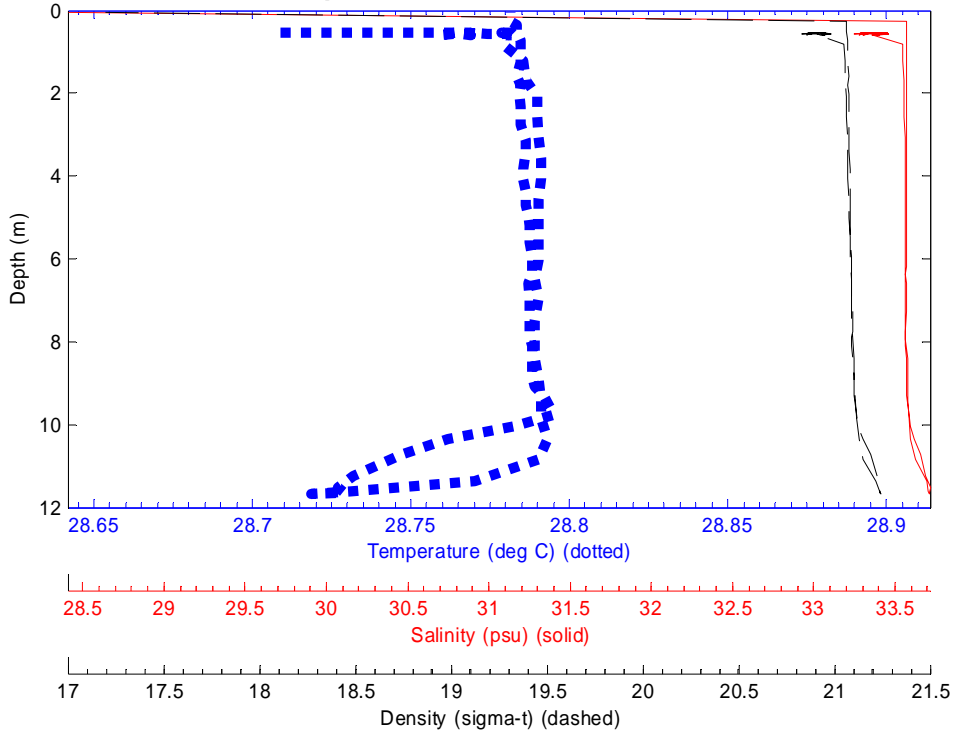
File: 2209004 22-Sep-2003 11:49:22 S7.2911 E134.2799 Site: 048



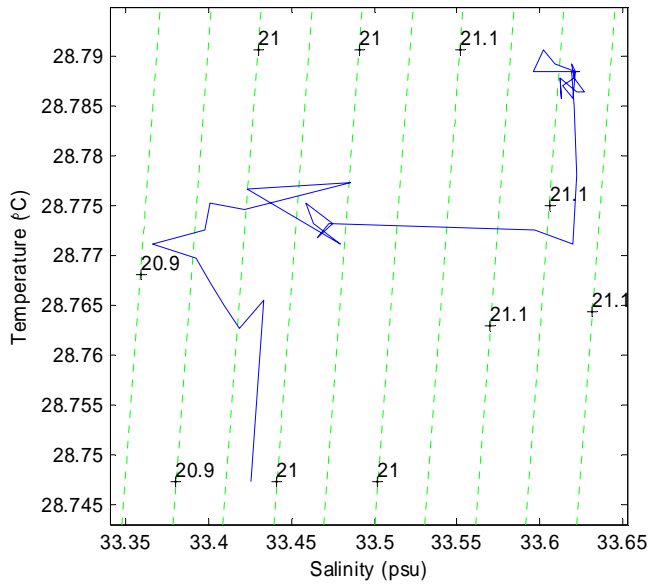
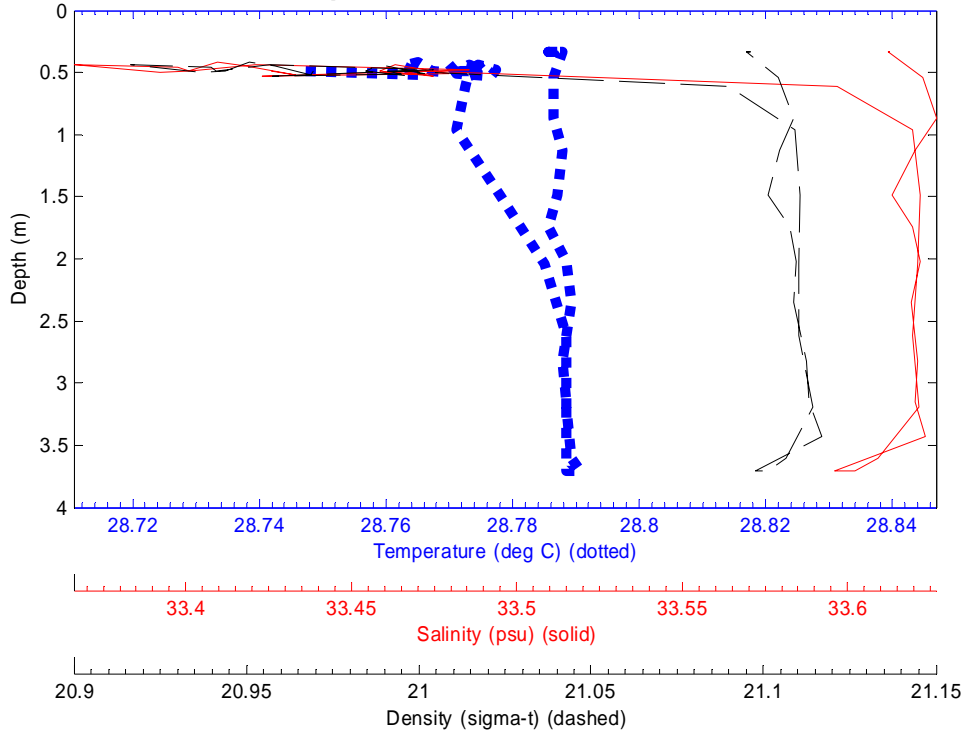
File: 2209005 22-Sep-2003 11:52:43 S7.2904 E134.2735 Site: 049



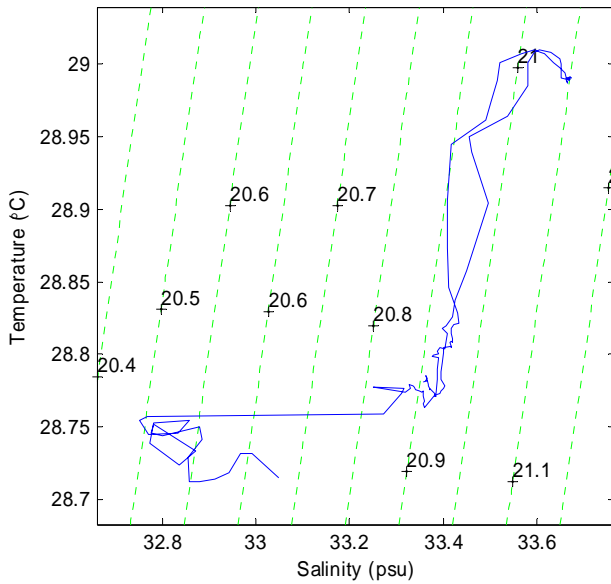
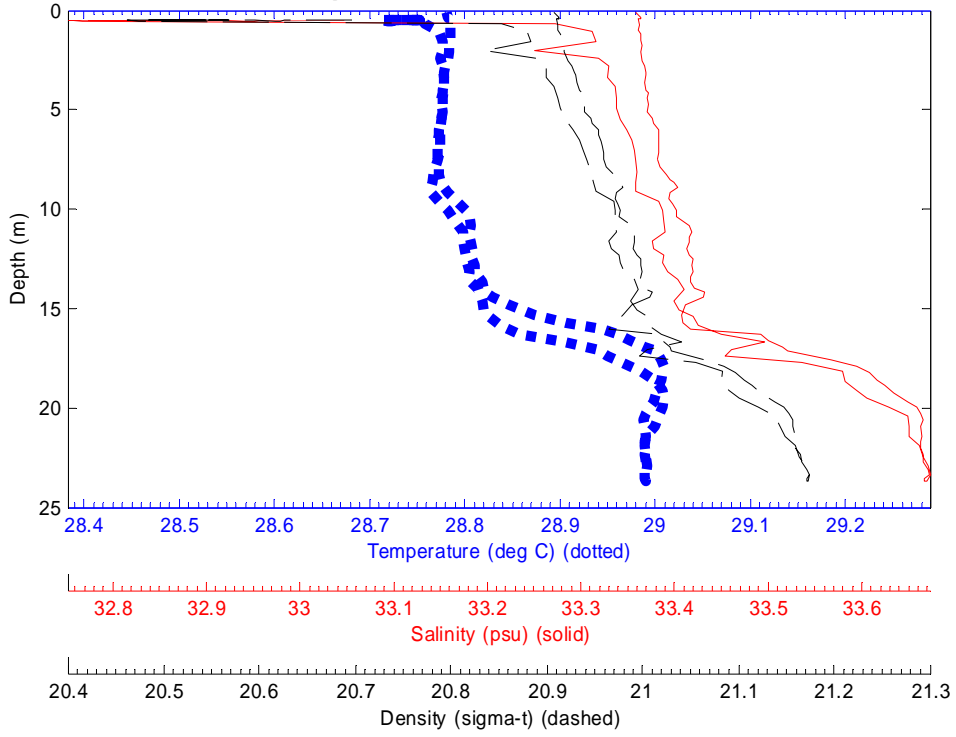
File: 2209006 22-Sep-2003 11:56:23 S7.2915 E134.2667 Site: 050



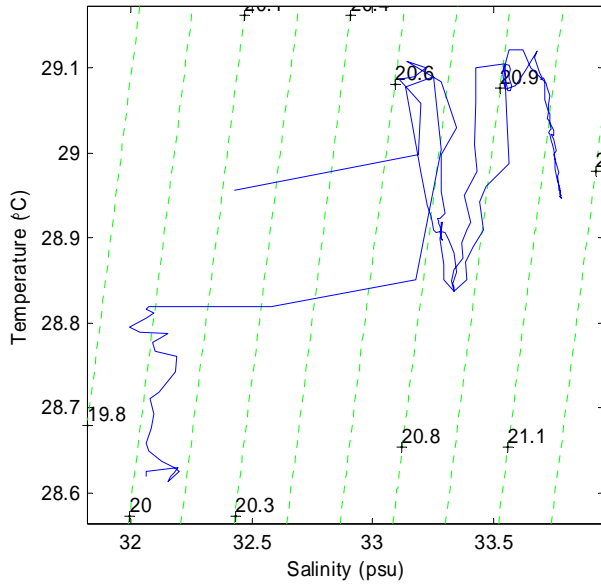
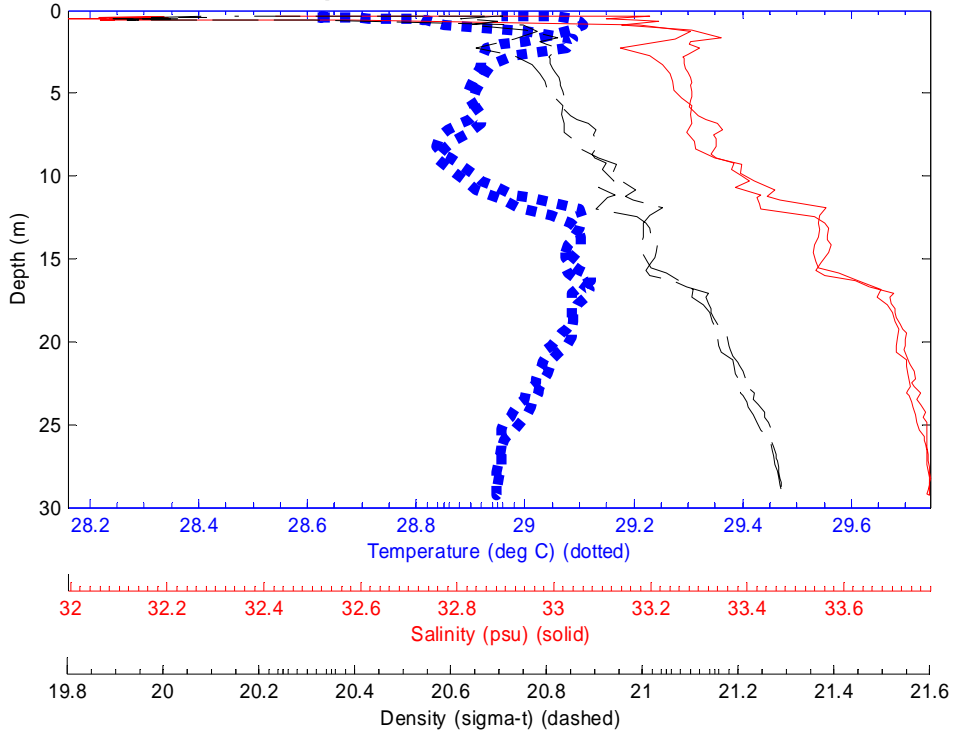
File: 2209007 22-Sep-2003 12:00:14 S7.2896 E134.2613 Site: 051



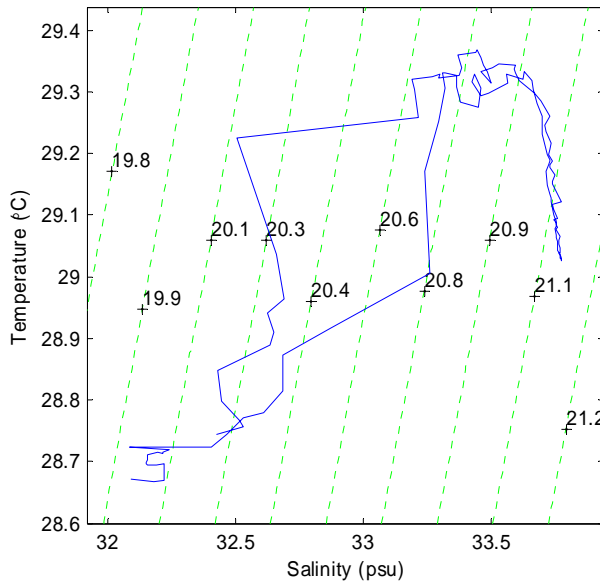
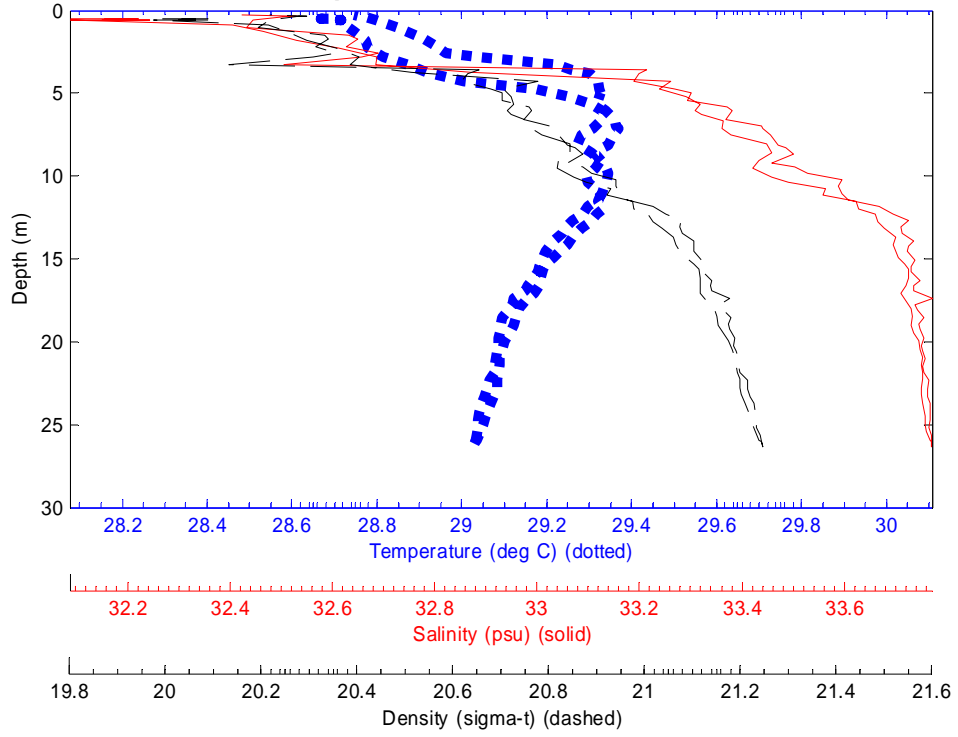
File: 2209008 22-Sep-2003 12:24:19 S7.2763 E134.337 Site: 052



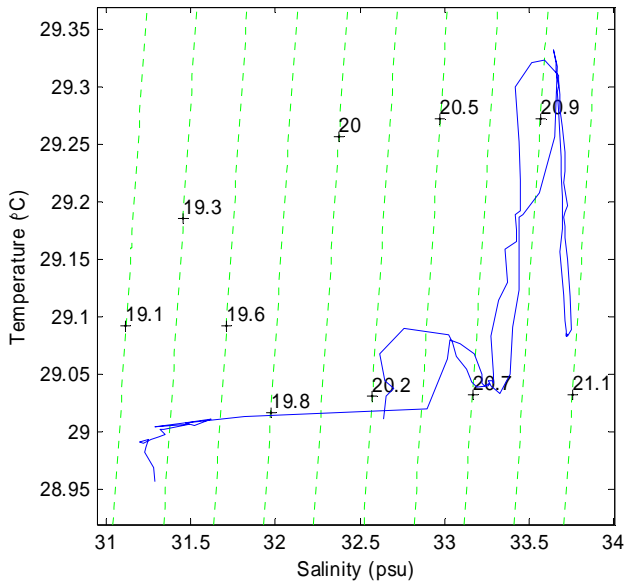
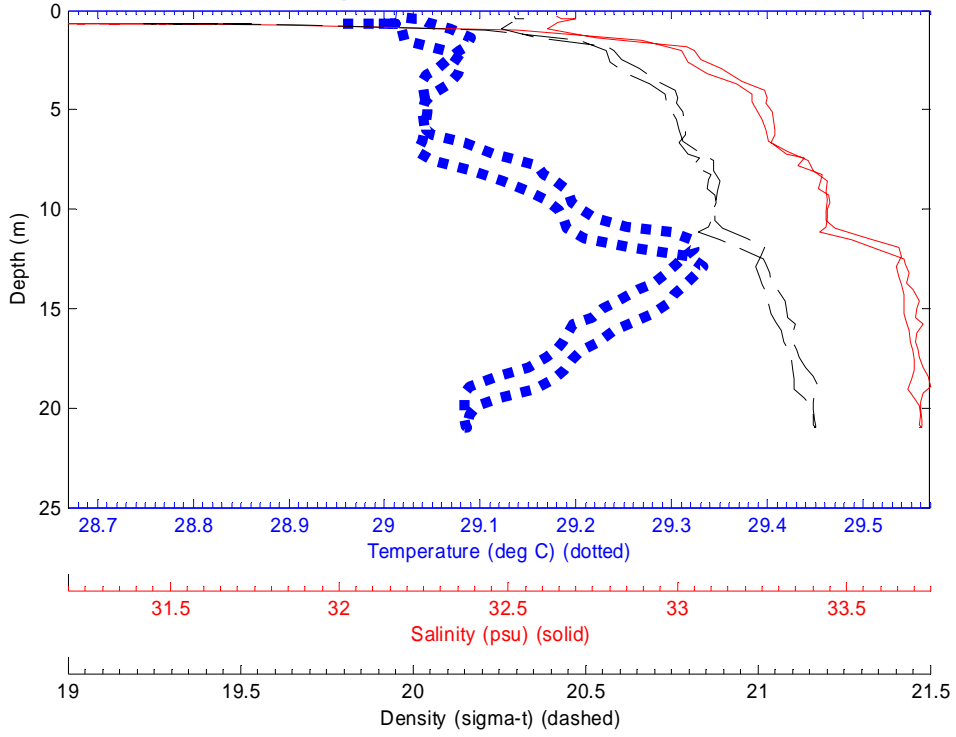
File: 2209009 22-Sep-2003 12:31:50 S7.2574 E134.3546 Site: 053



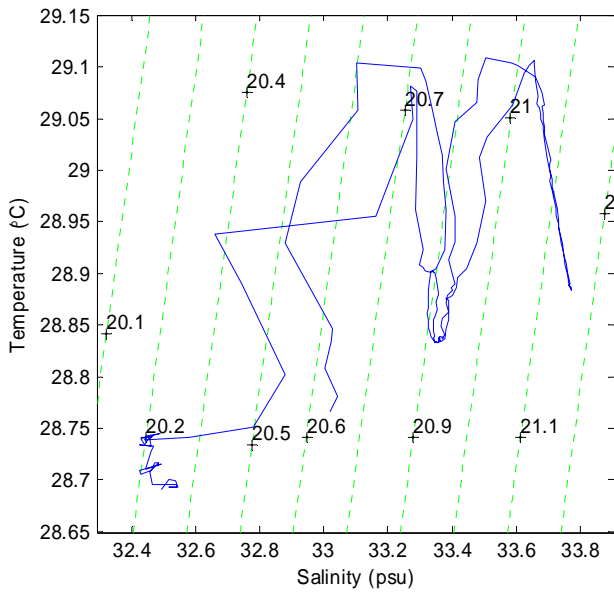
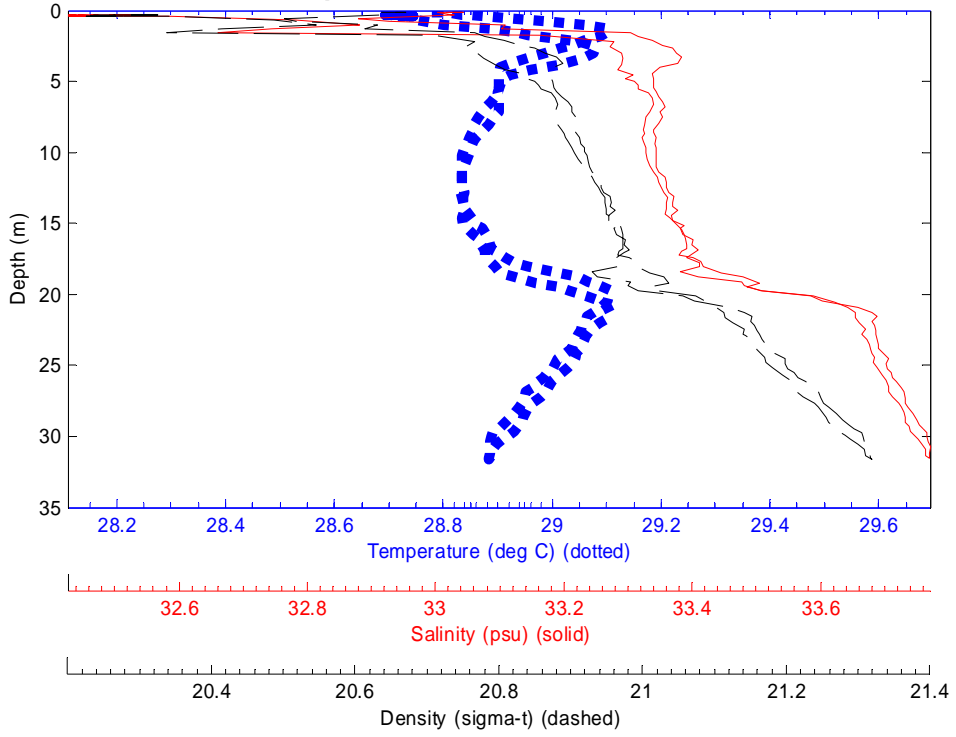
File: 2209010 22-Sep-2003 12:39:48 S7.266 E134.3755 Site: 054



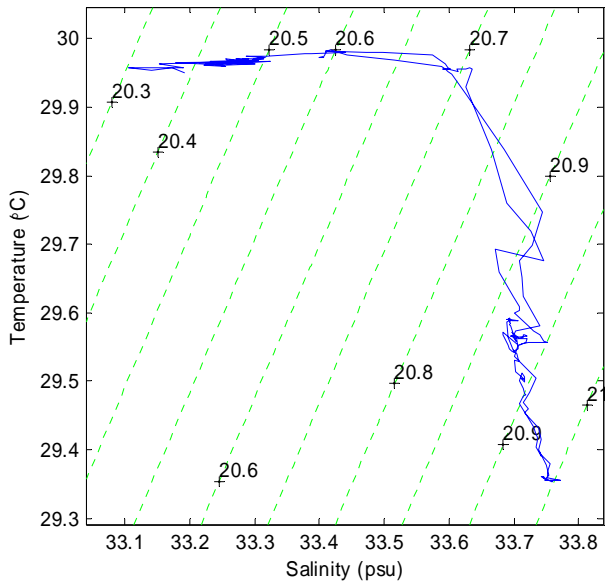
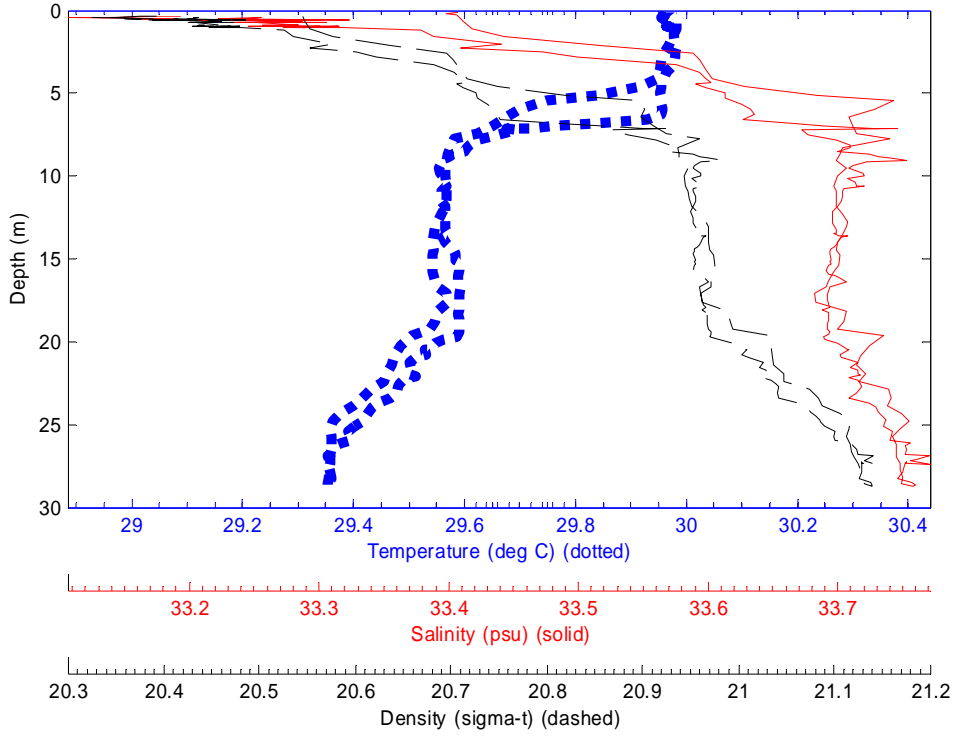
File: 2209011 22-Sep-2003 12:47:11 S7.264 E134.397 Site: 055



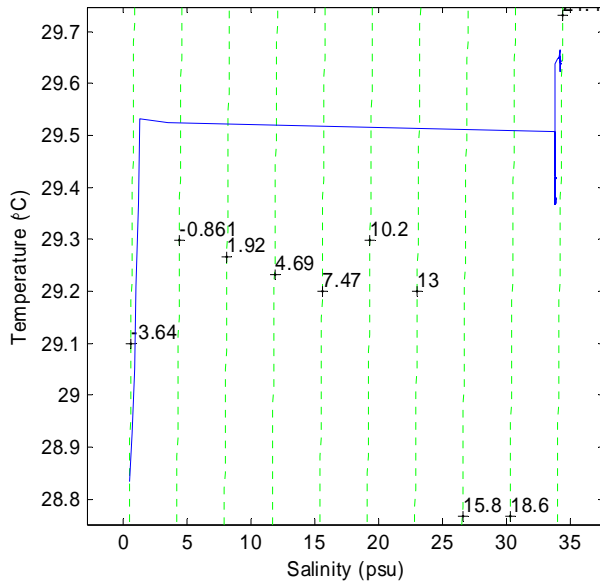
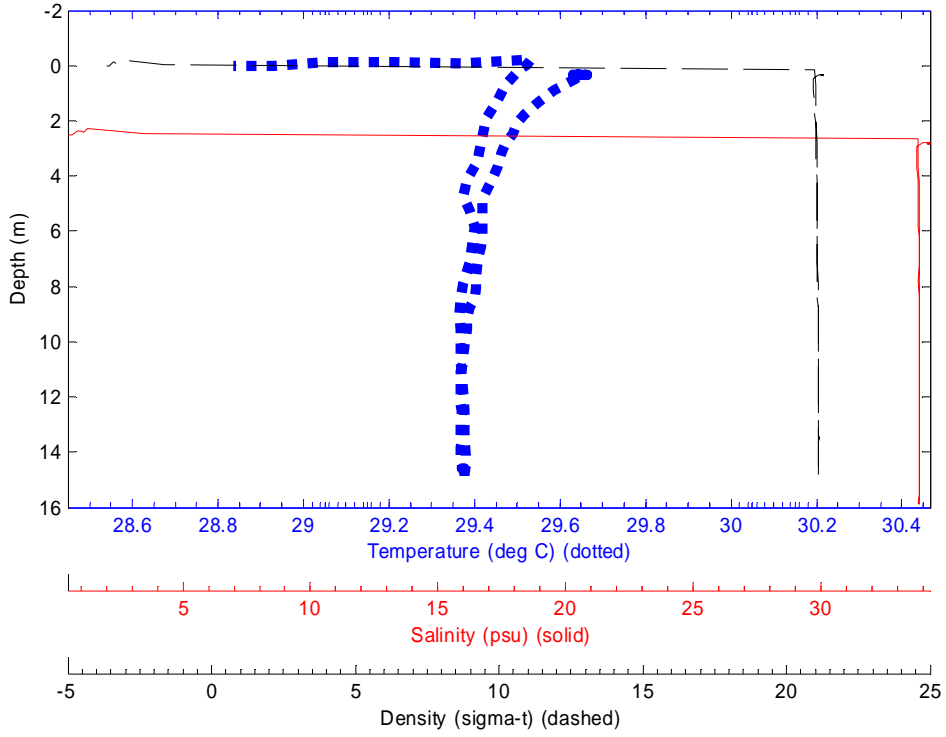
File: 2209013 22-Sep-2003 15:06:41 S7.2881 E134.4203 Site: 056



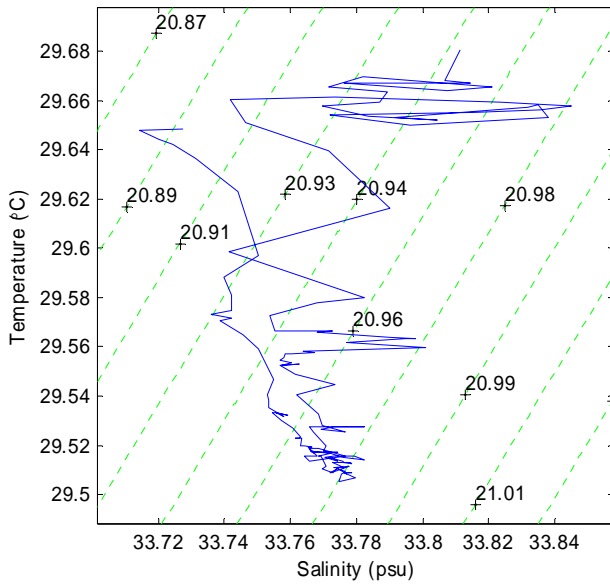
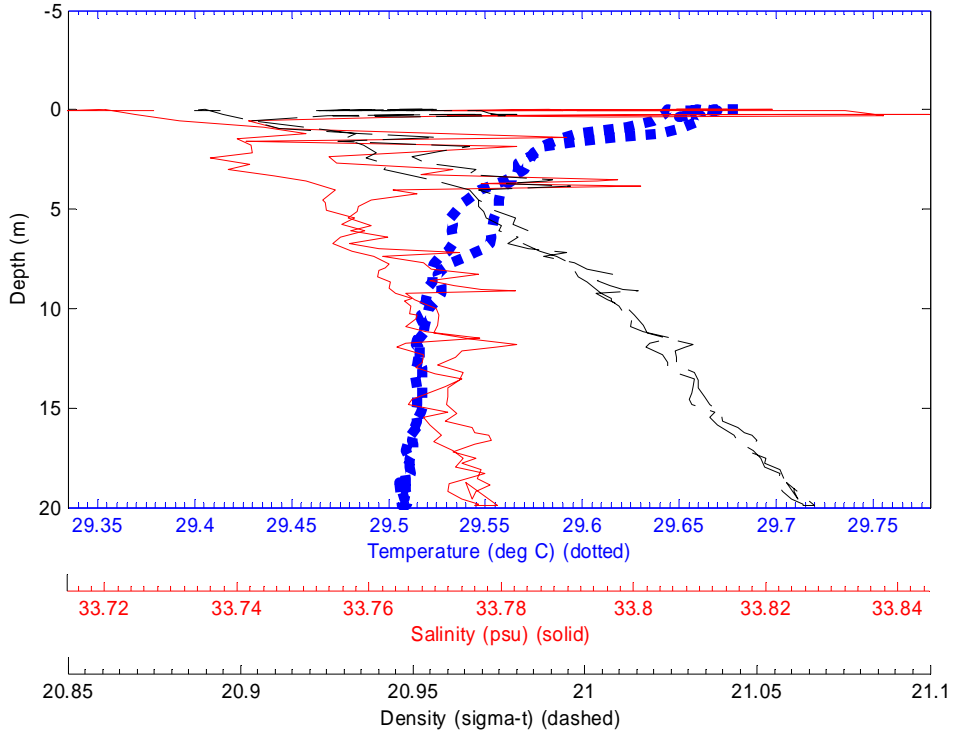
File: 0311000 03-Nov-2003 17:20:23 S7.3148 E134.4553 Site: 11b



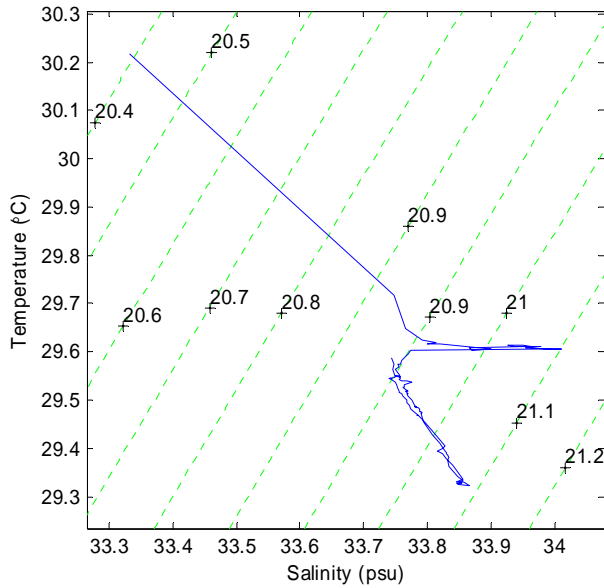
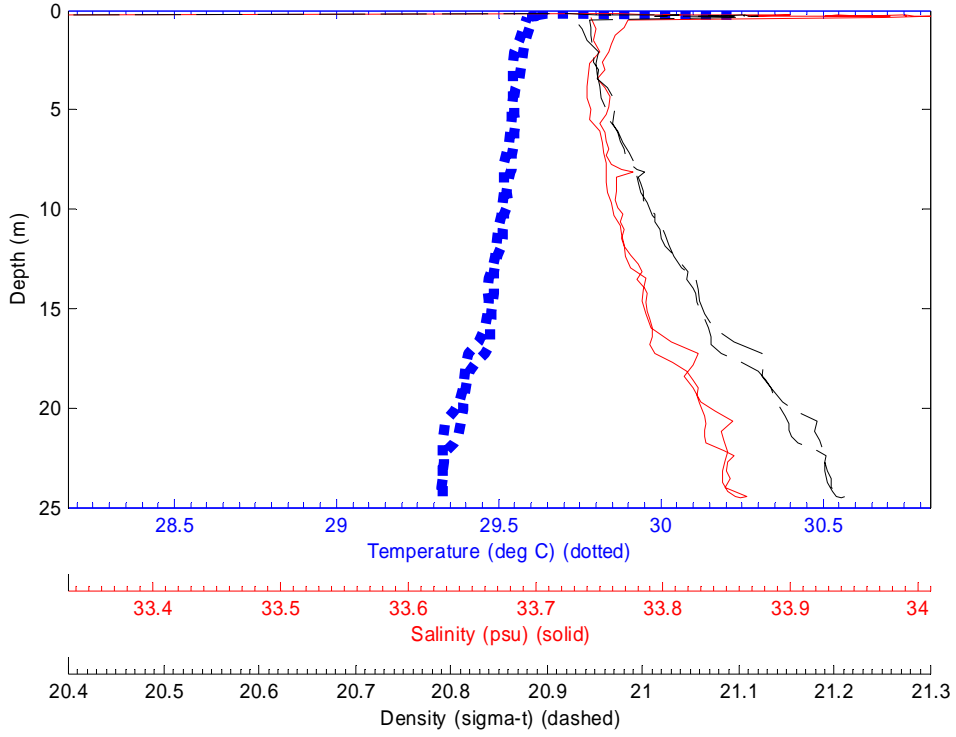
File: 0411000 04-Nov-2003 09:00:29 S7.2342 E134.4515 Site: CTD0



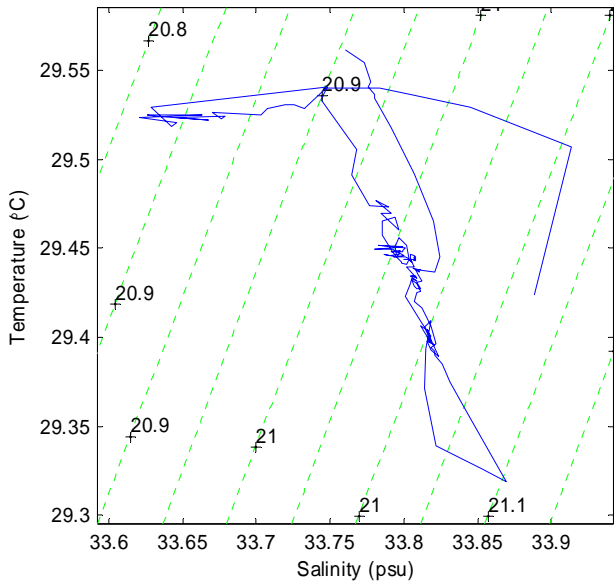
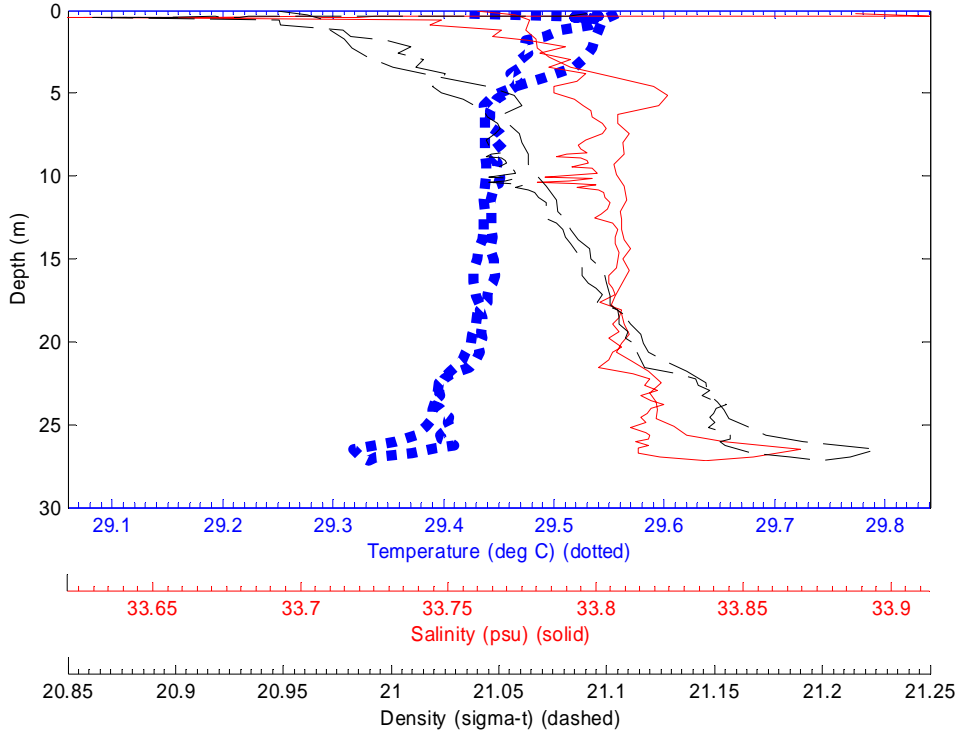
File: 0411001 04-Nov-2003 09:25:53 S7.234 E134.4513 Site: CTD1



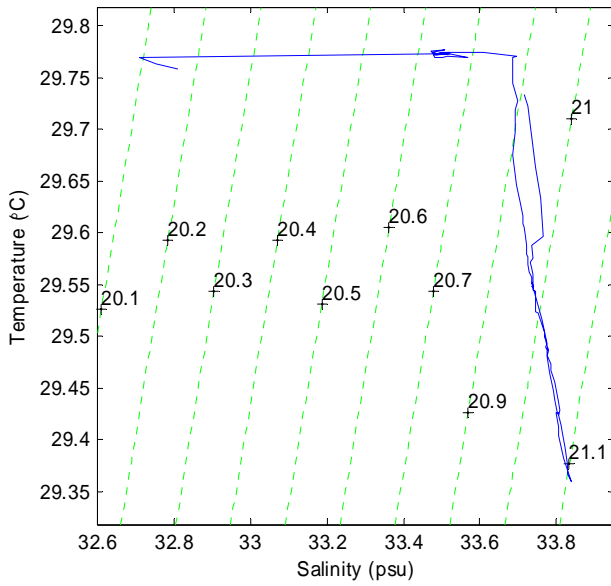
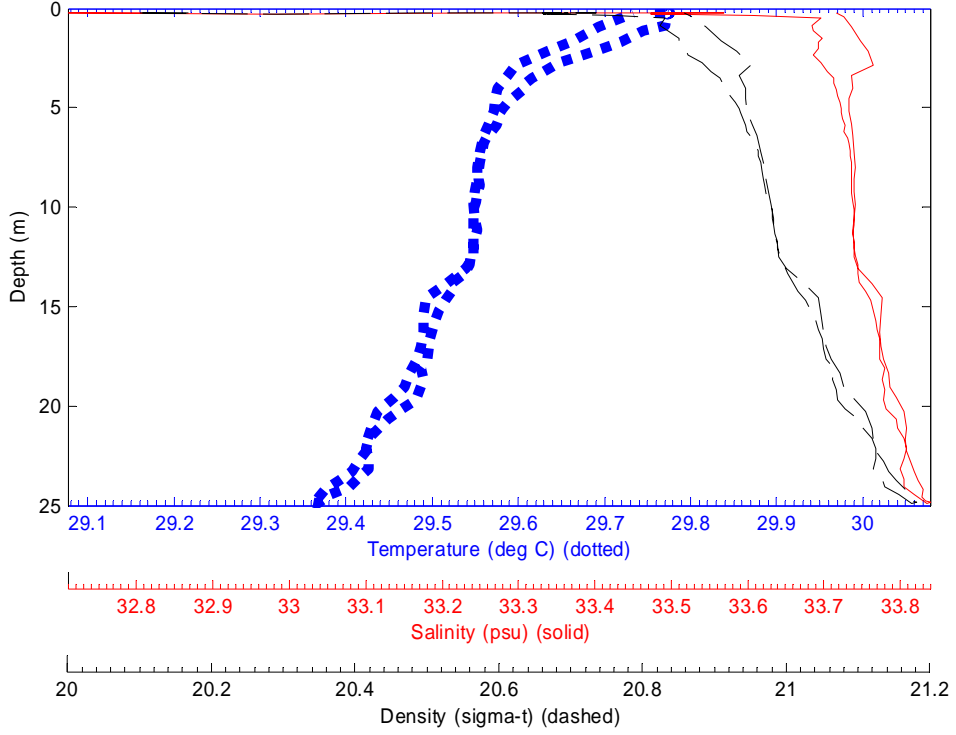
File: 0411002 04-Nov-2003 09:49:20 S7.2339 E134.4513 Site: CTD2



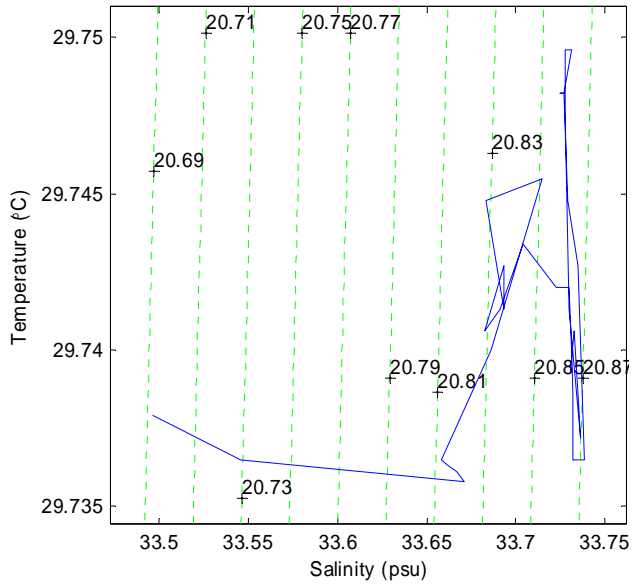
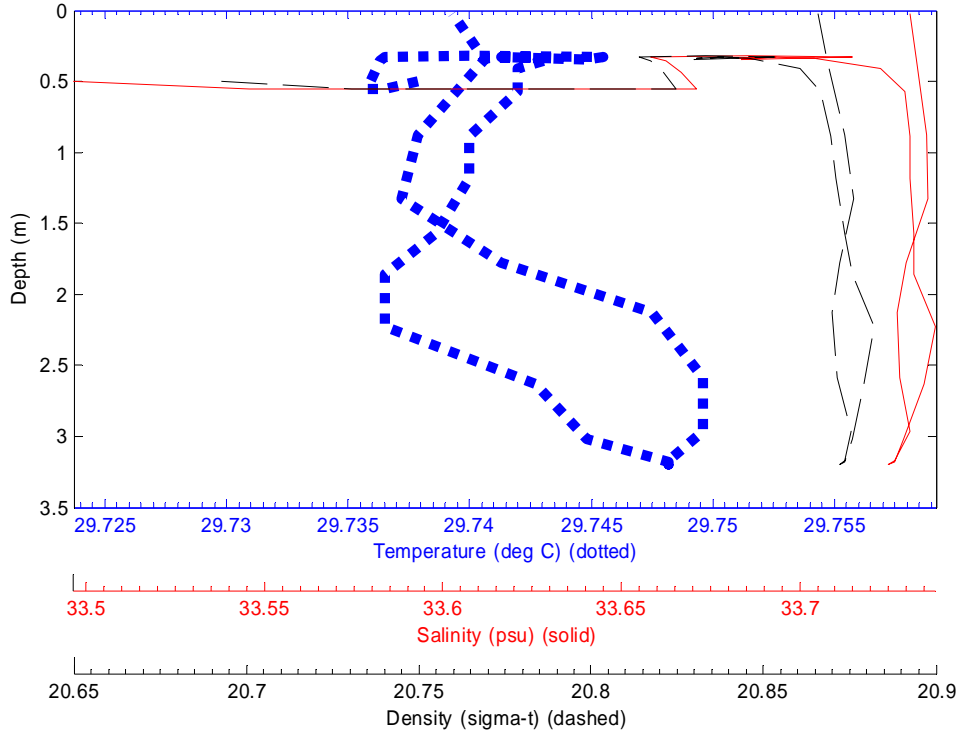
File: 0411003 04-Nov-2003 10:04:51 S7.2112 E134.448 Site: CTD3



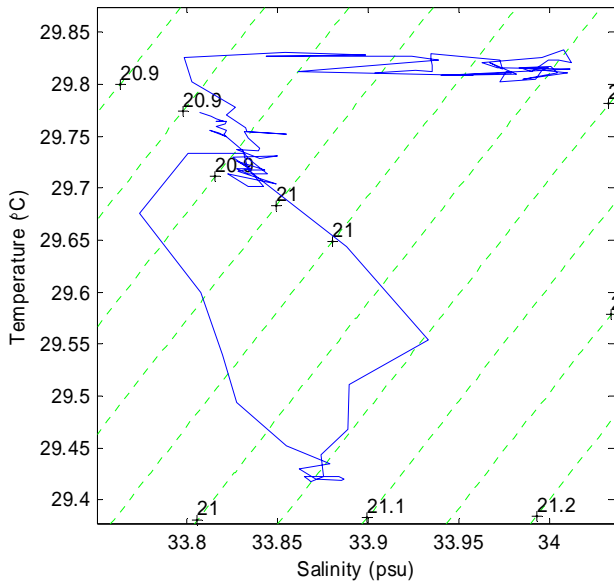
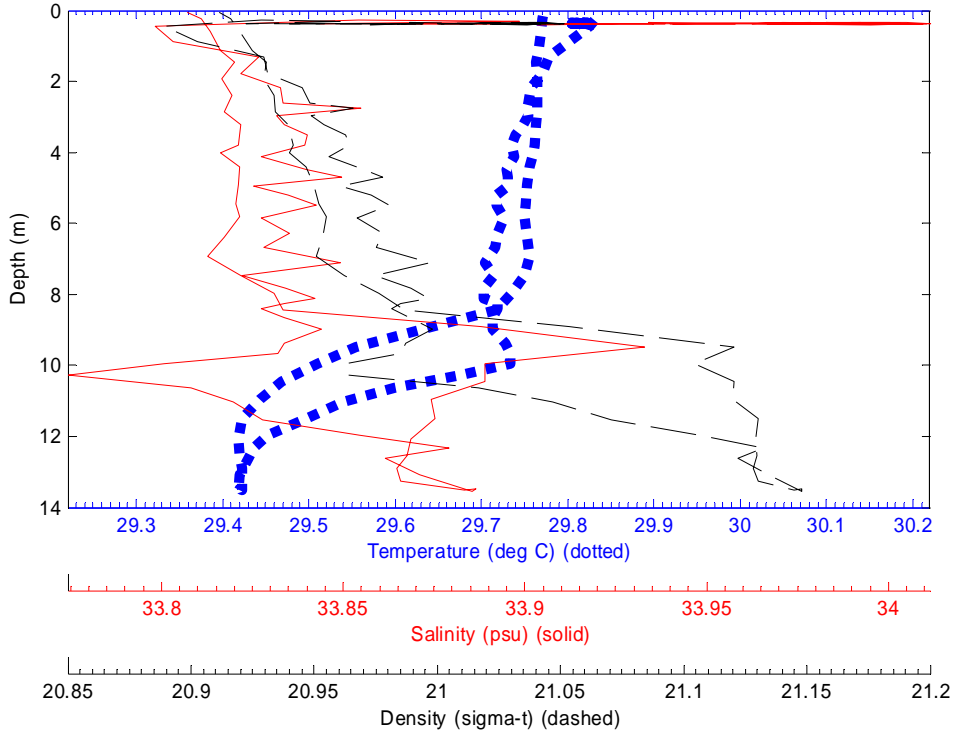
File: 0411004 04-Nov-2003 10:36:46 S7.21 E134.4222 Site: CTD4



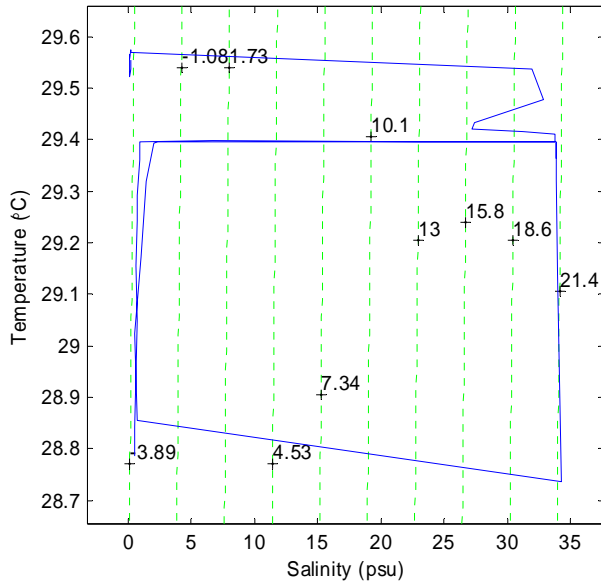
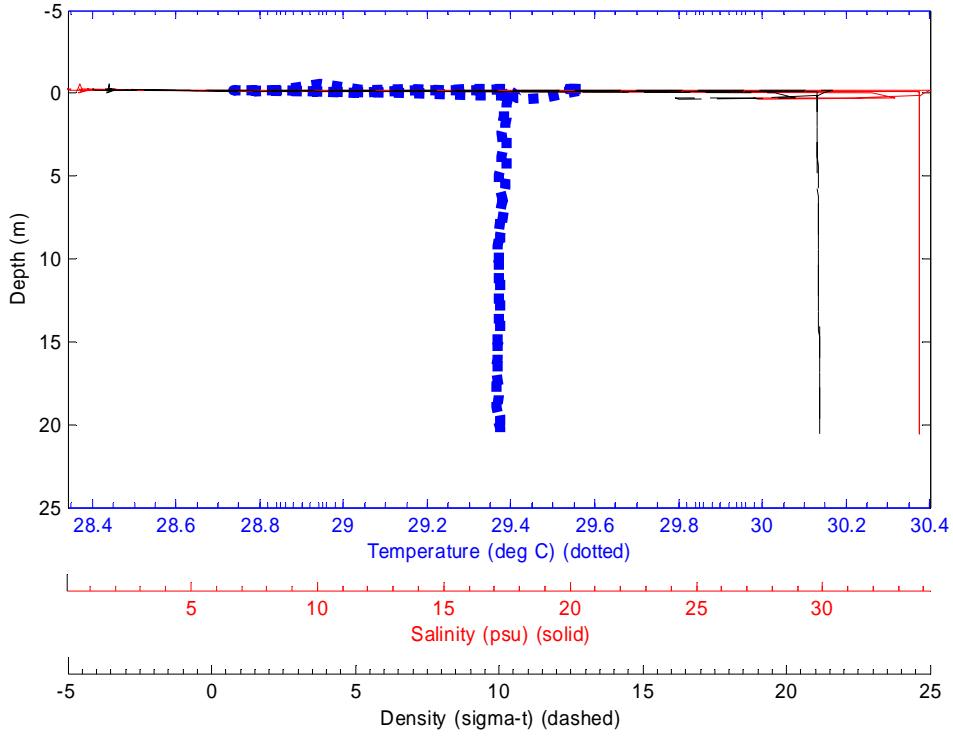
File: 0411005 04-Nov-2003 10:55:43 S7.2084 E134.3986 Site: CTD5



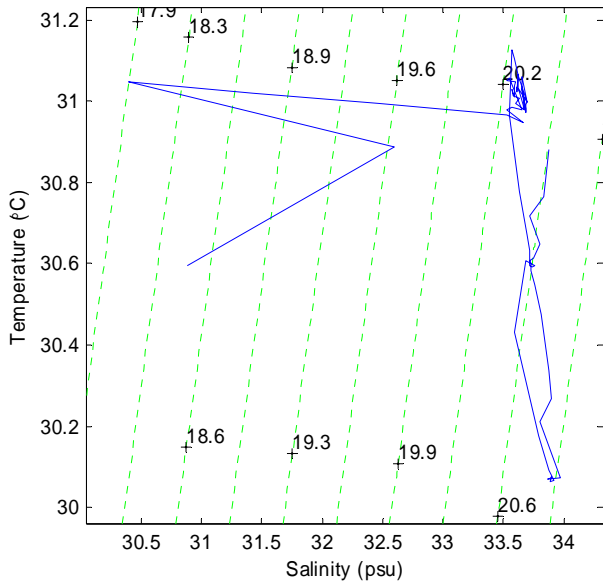
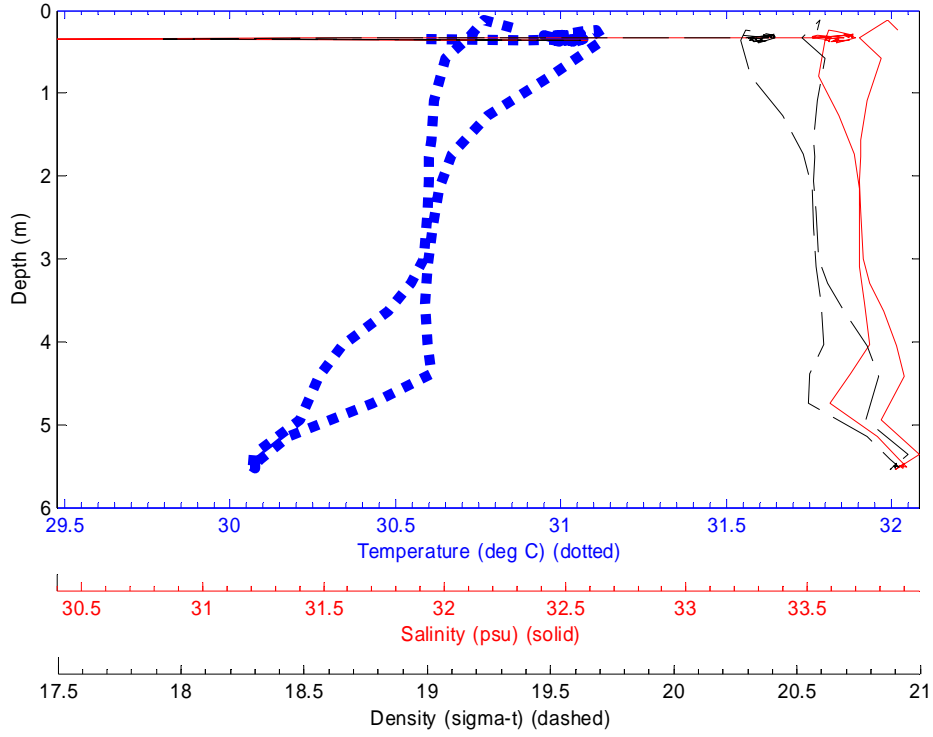
File: 0411006 04-Nov-2003 12:40:39 S7.1567 E134.4174 Site: CTD6



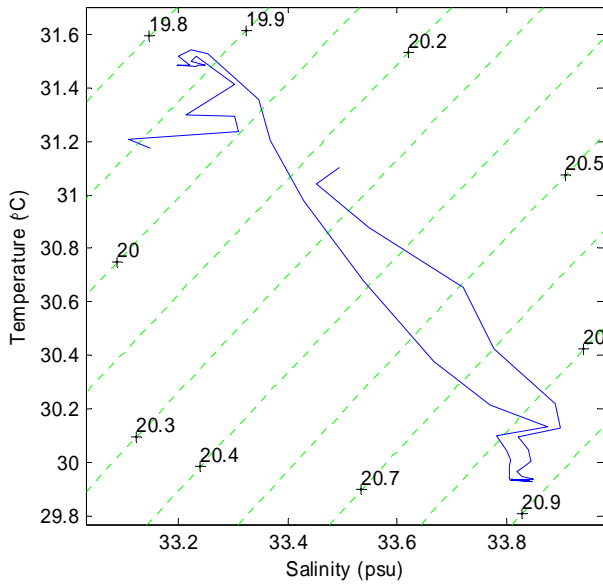
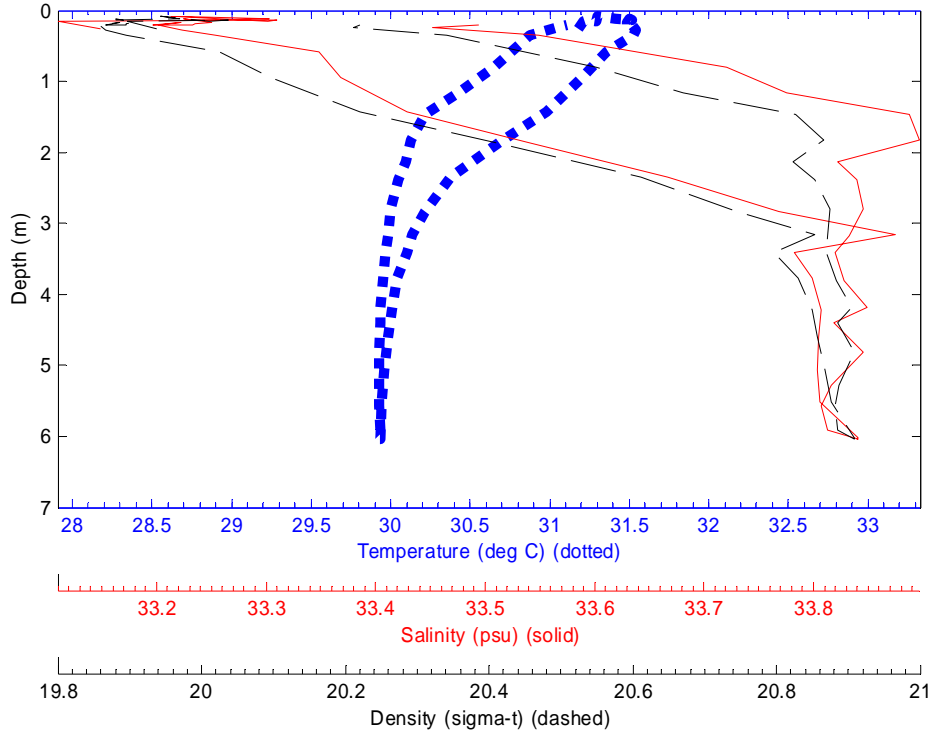
File: 0411007 04-Nov-2003 13:23:11 S7.2121 E134.4174 Site: CTD7



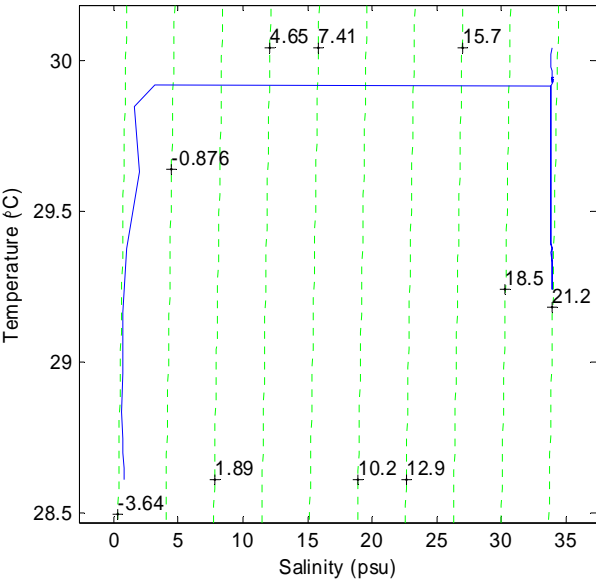
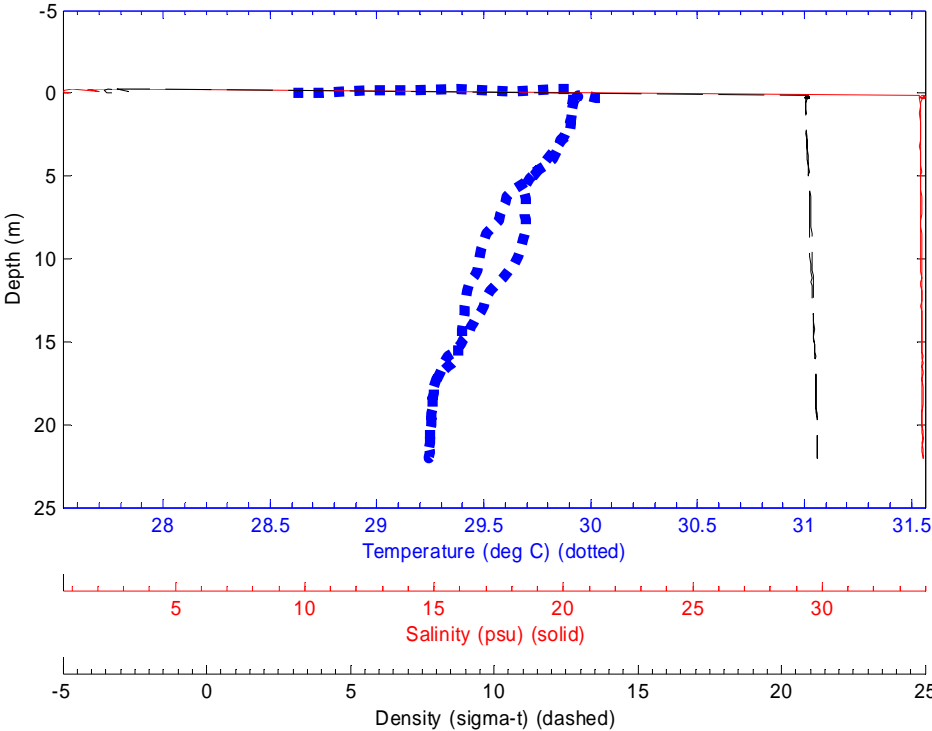
File: 0411008 04-Nov-2003 13:57:24 S7.261 E134.416 Site: CTD8



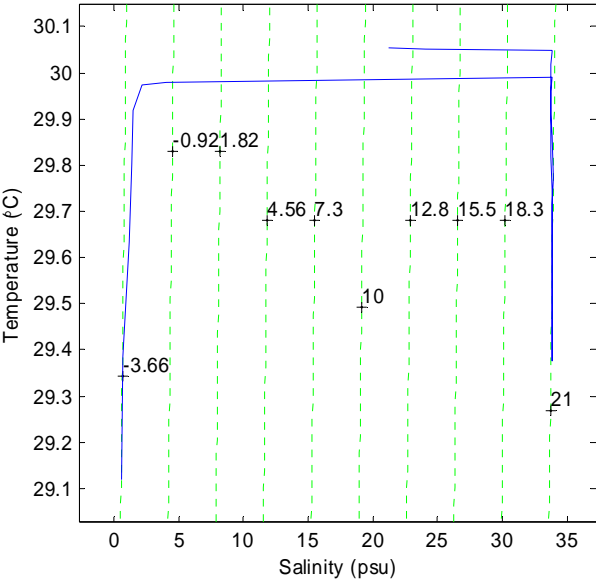
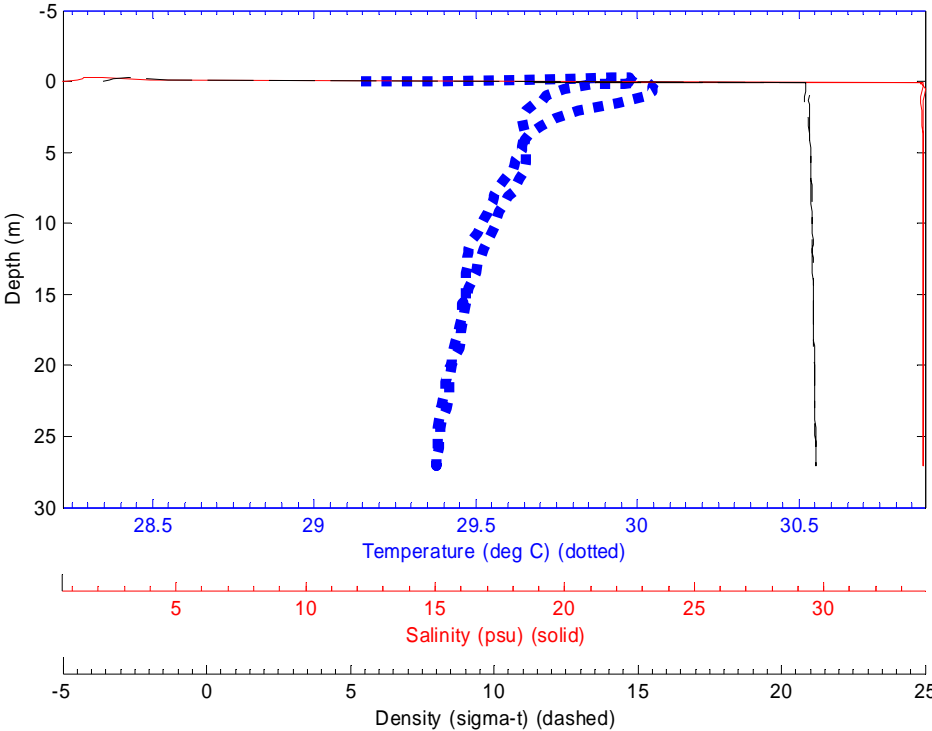
File: 0411009 04-Nov-2003 15:03:50 S7.2684 E134.4299 Site: CTD9



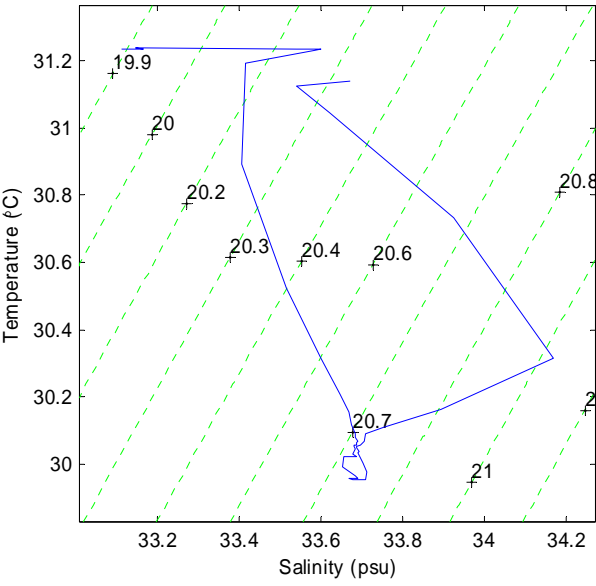
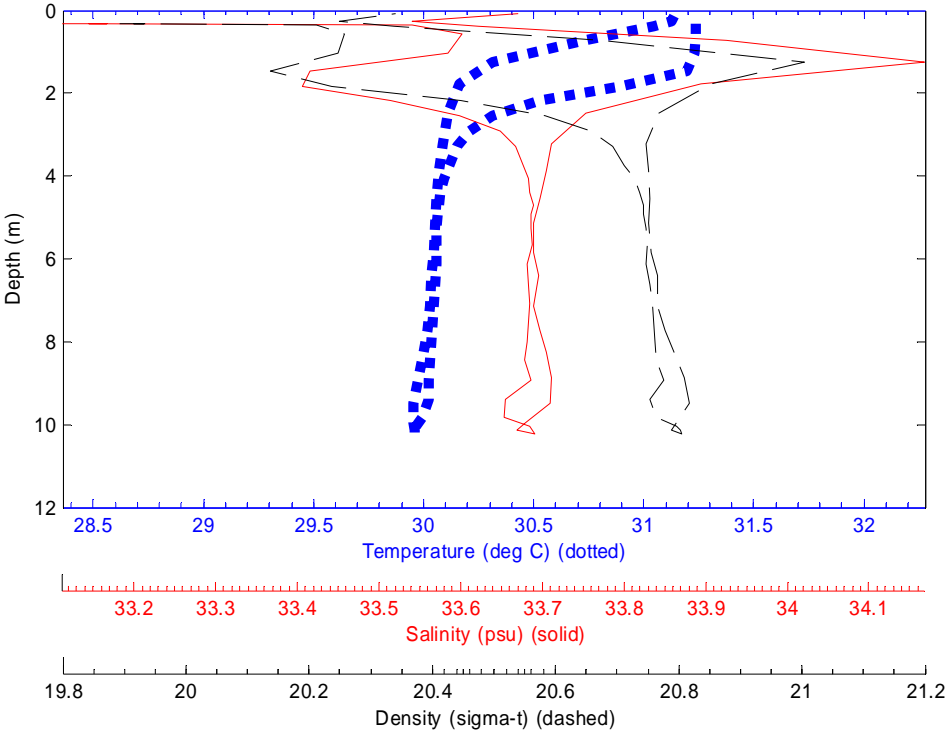
File: 0411010 04-Nov-2003 15:45:25 S7.2101 E134.4314 Site: CTD10



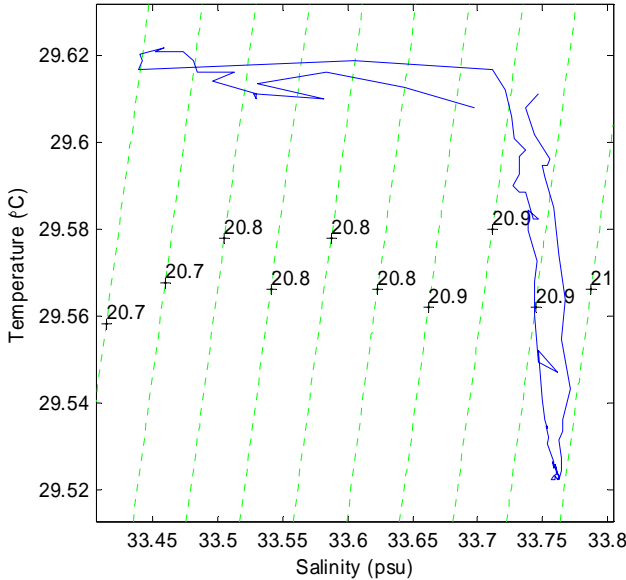
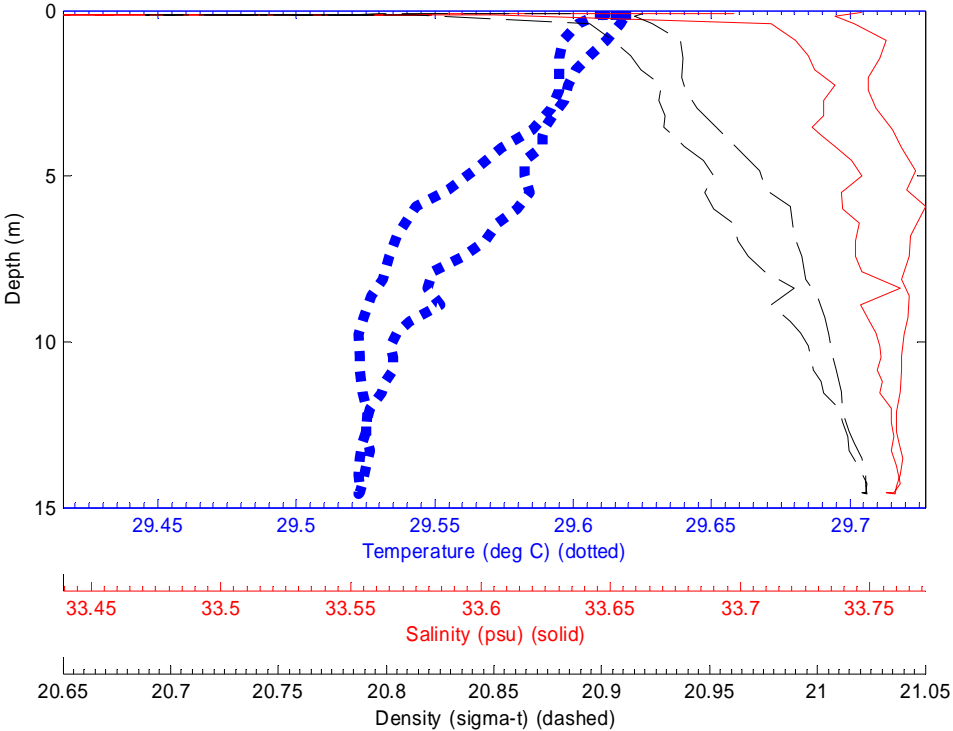
File: 0411011 04-Nov-2003 16:26:20 S7.1576 E134.4314 Site: CTD11



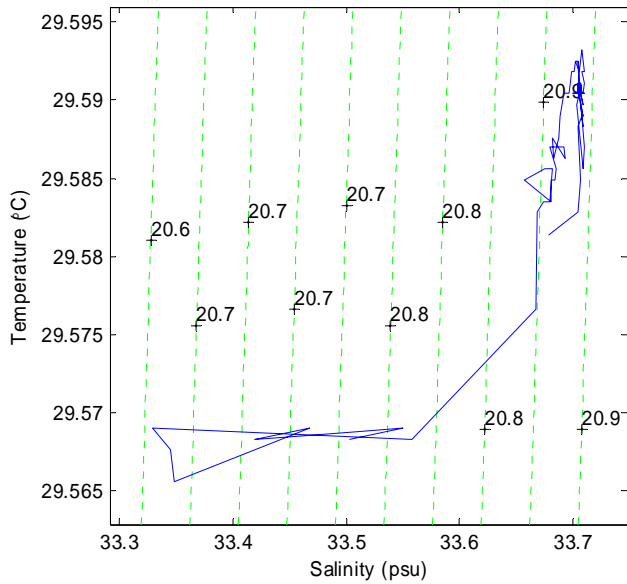
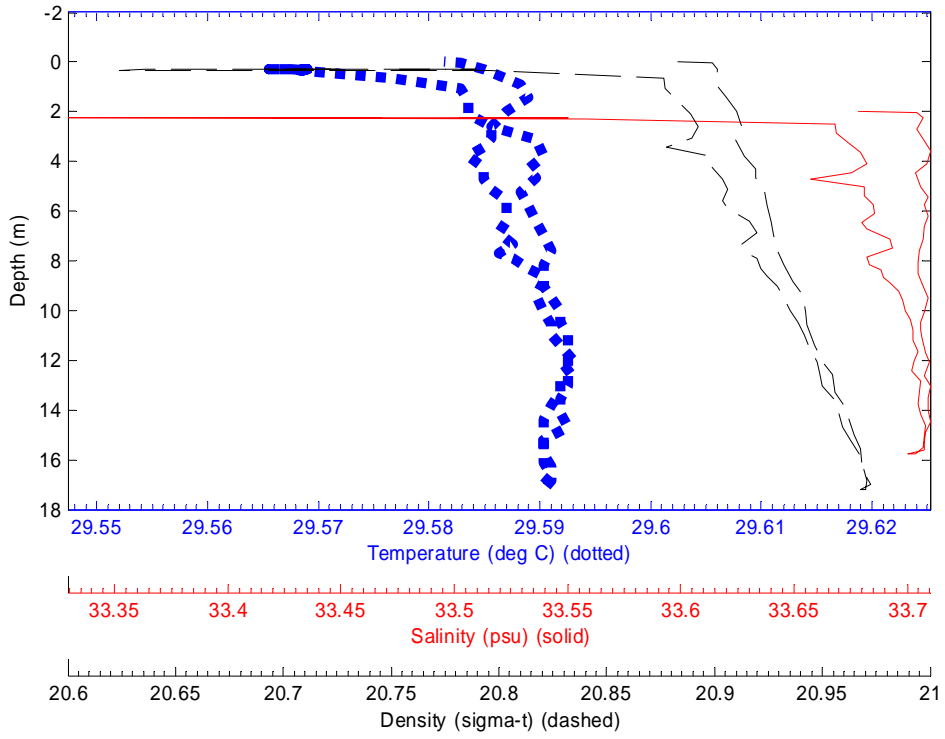
File: 0411012 04-Nov-2003 16:57:41 S7.2739 E134.4438 Site: CTD12



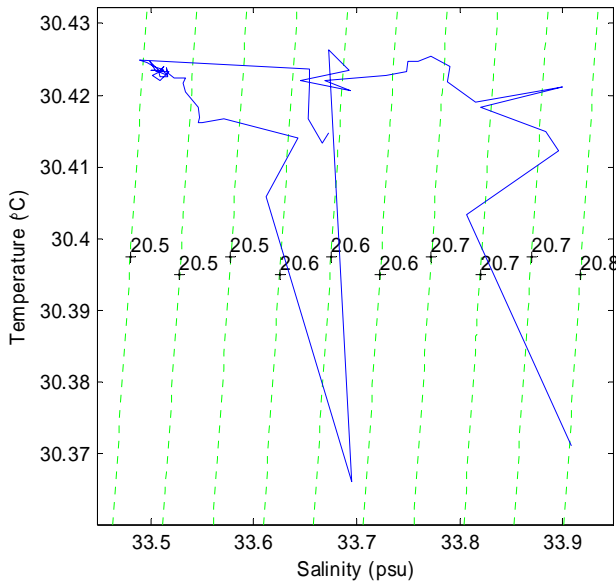
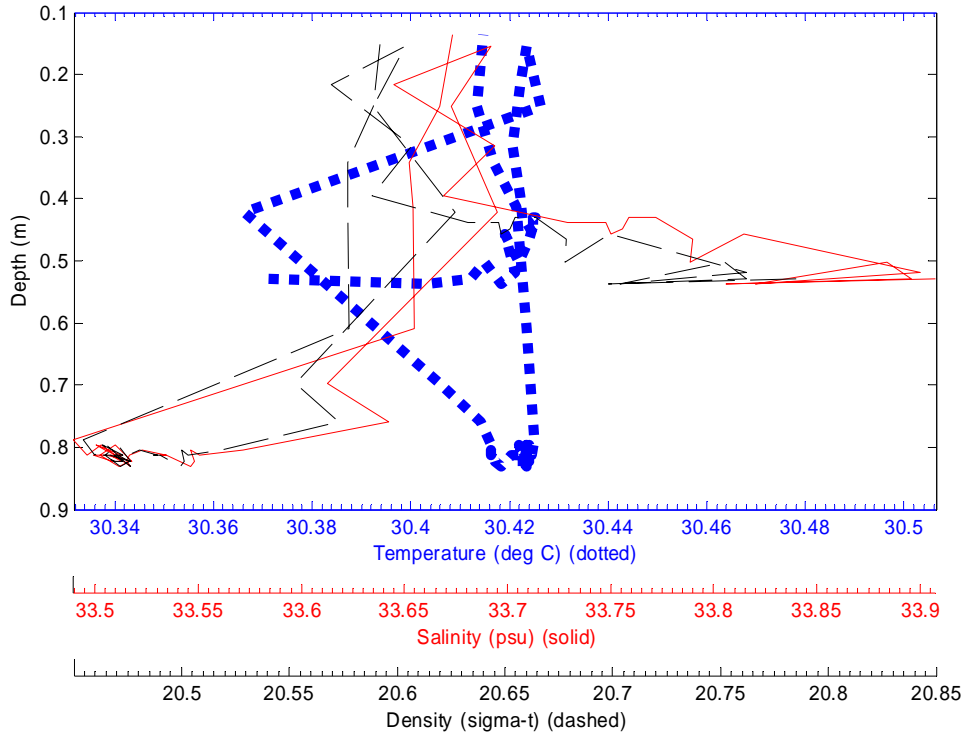
File: 0411013 04-Nov-2003 17:16:10 S7.2897 E134.4593 Site: CTD13



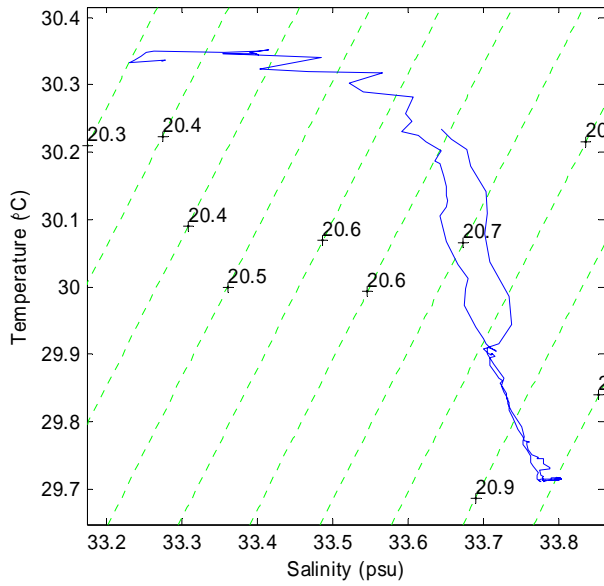
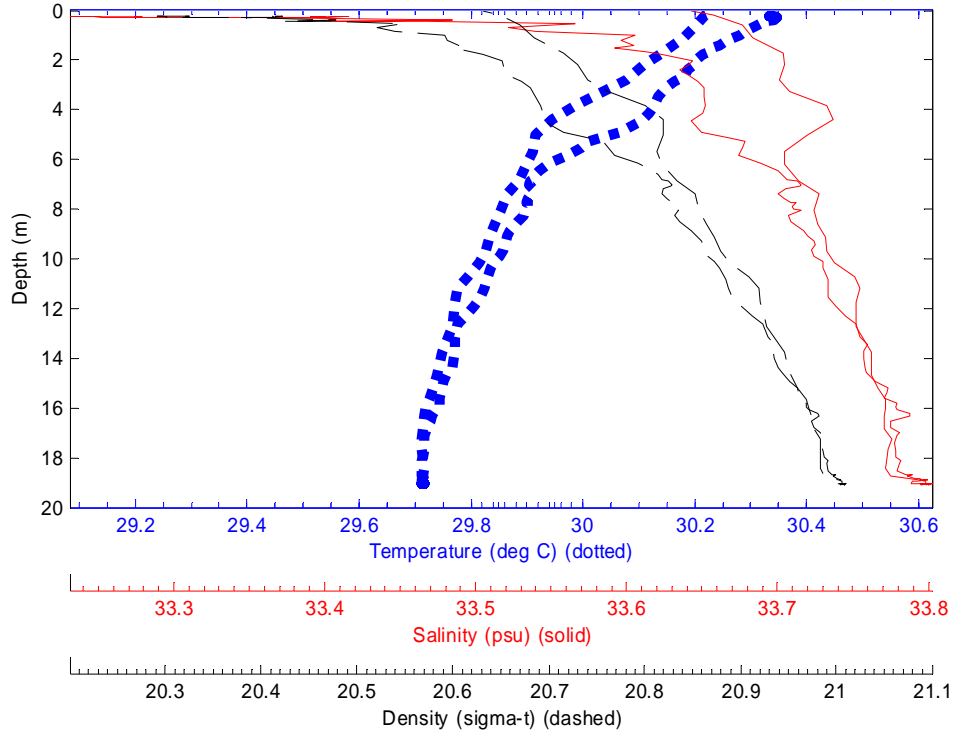
File: 0411014 04-Nov-2003 17:34:03 S7.3026 E134.4722 Site: CTD14



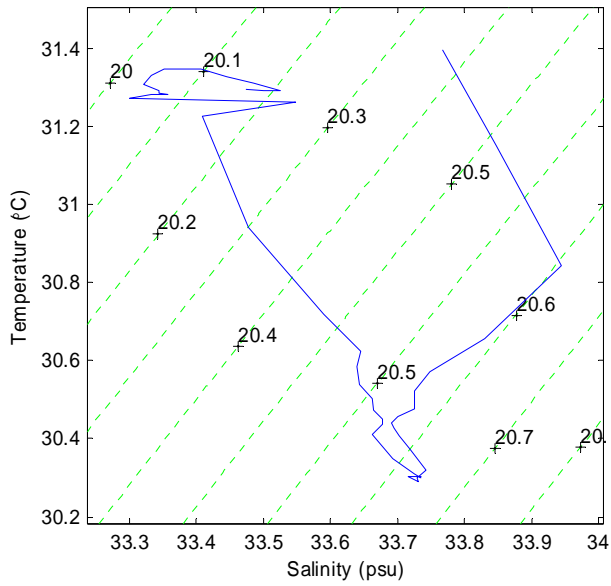
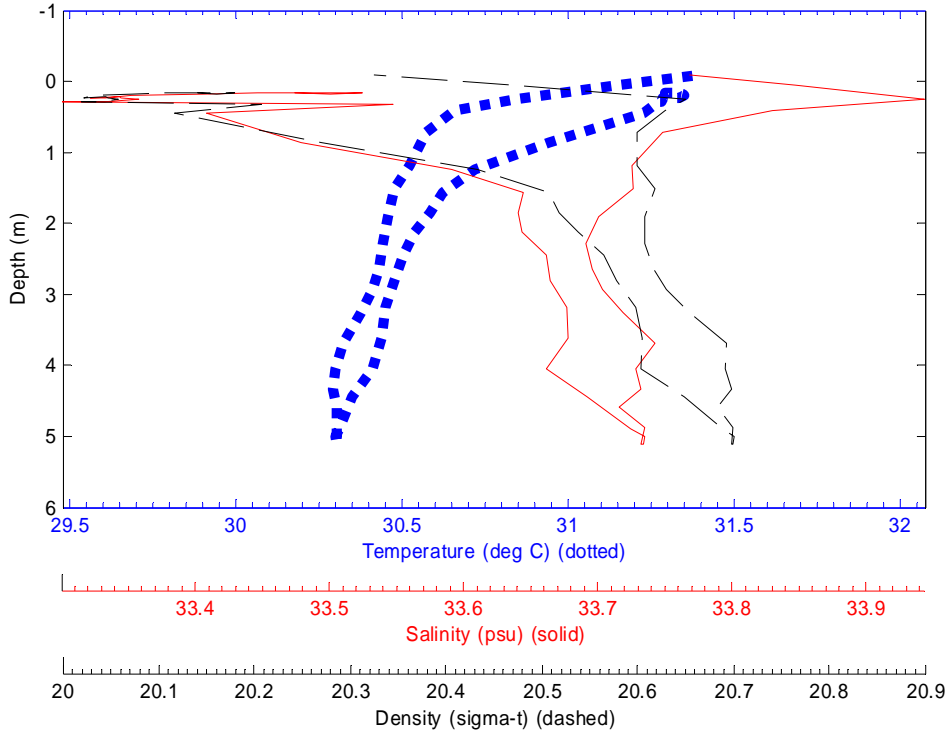
File: 0511000 05-Nov-2003 10:12:50 S7.1415 E134.2971 Site: Tide



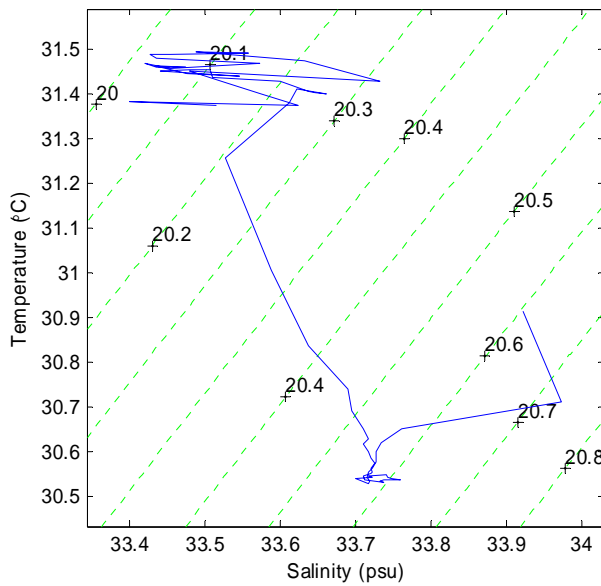
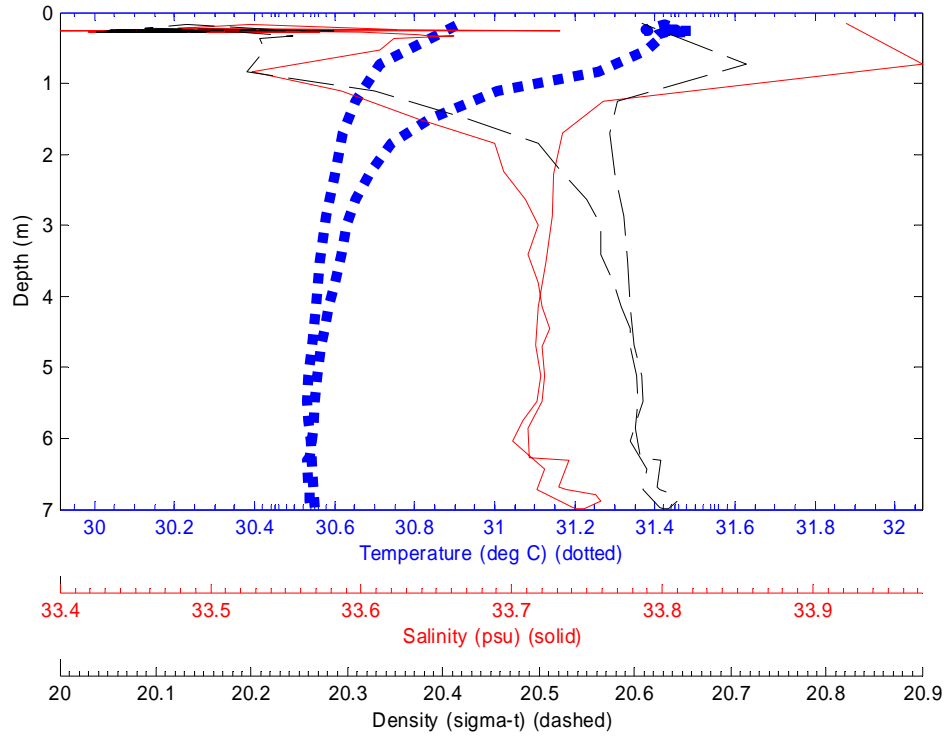
File: 0511001 05-Nov-2003 10:20:07 S7.1415 E134.2971 Site: C2



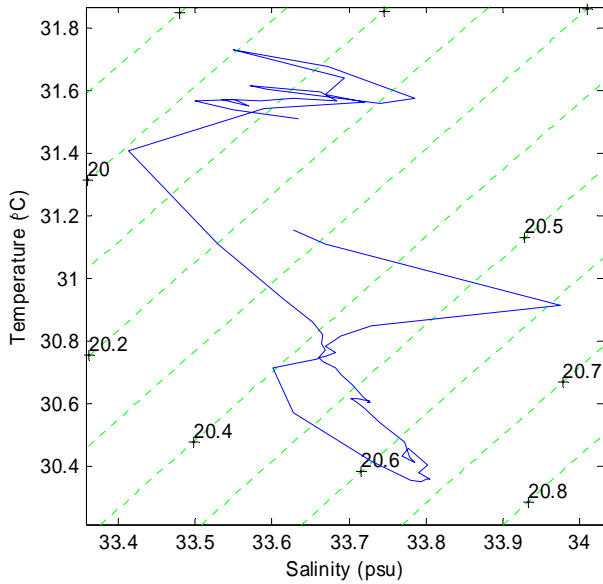
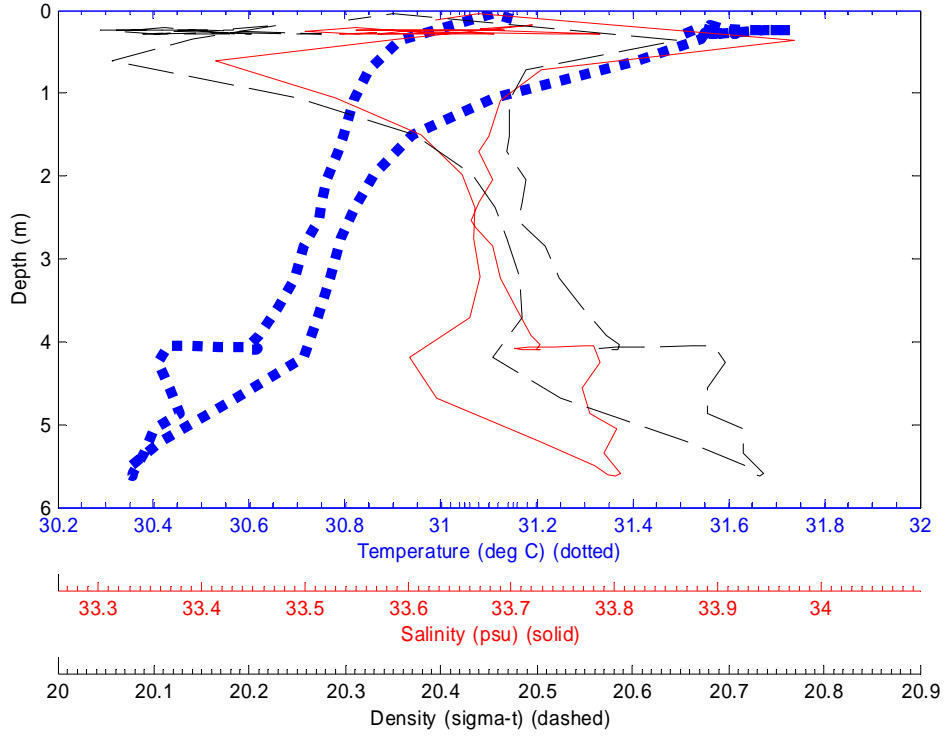
File: 0511002 05-Nov-2003 10:41:59 S7.1431 E134.2699 Site: CTD2



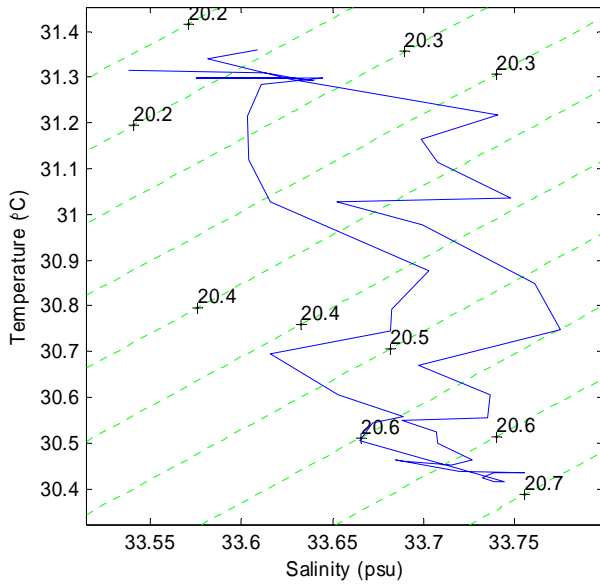
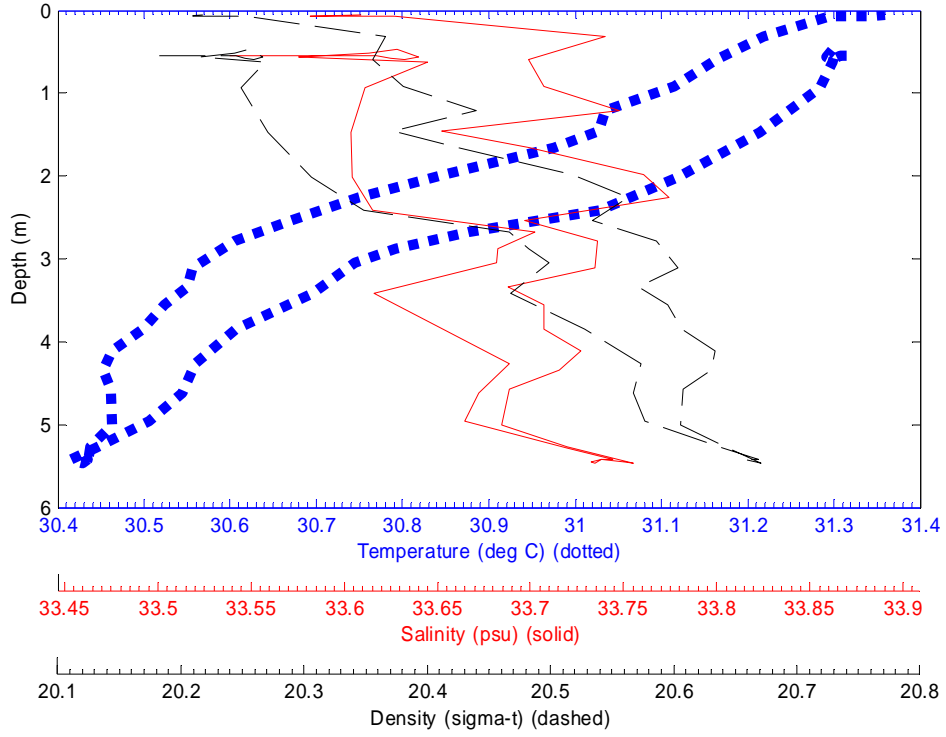
File: 0511003 05-Nov-2003 11:00:43 S7.1441 E134.2523 Site: C1



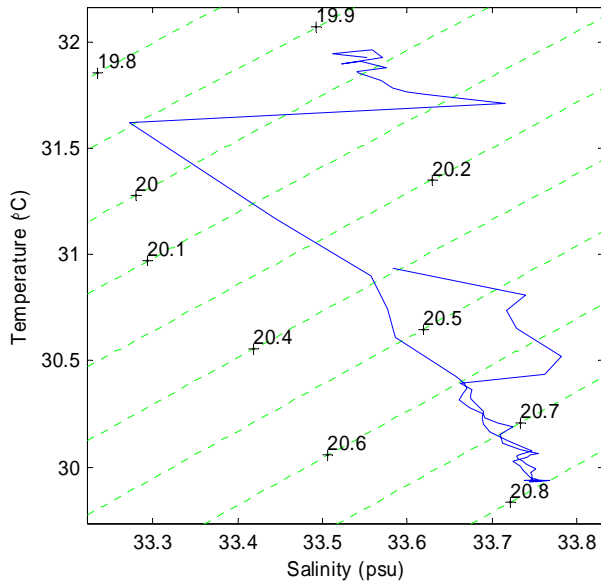
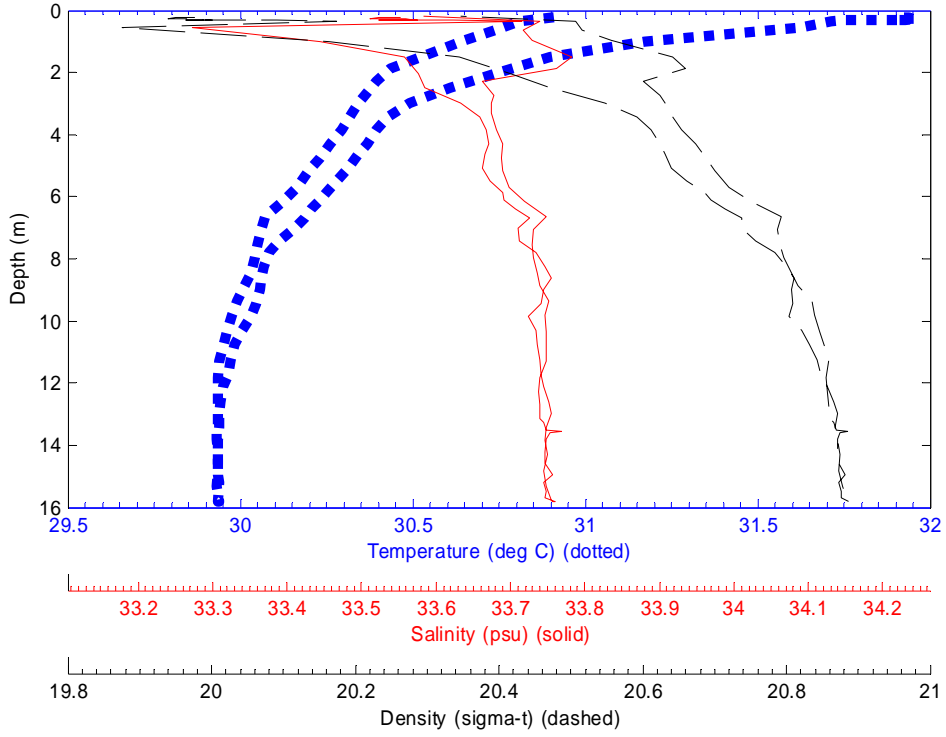
File: 0511004 05-Nov-2003 11:23:12 S7.1277 E134.2512 Site: CTD4



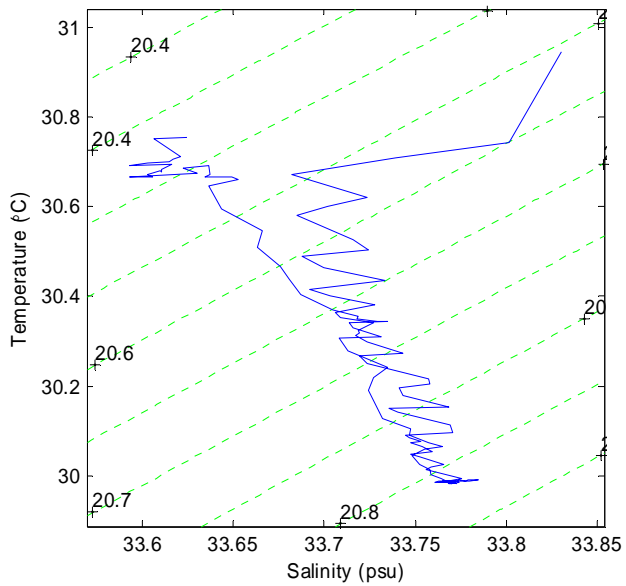
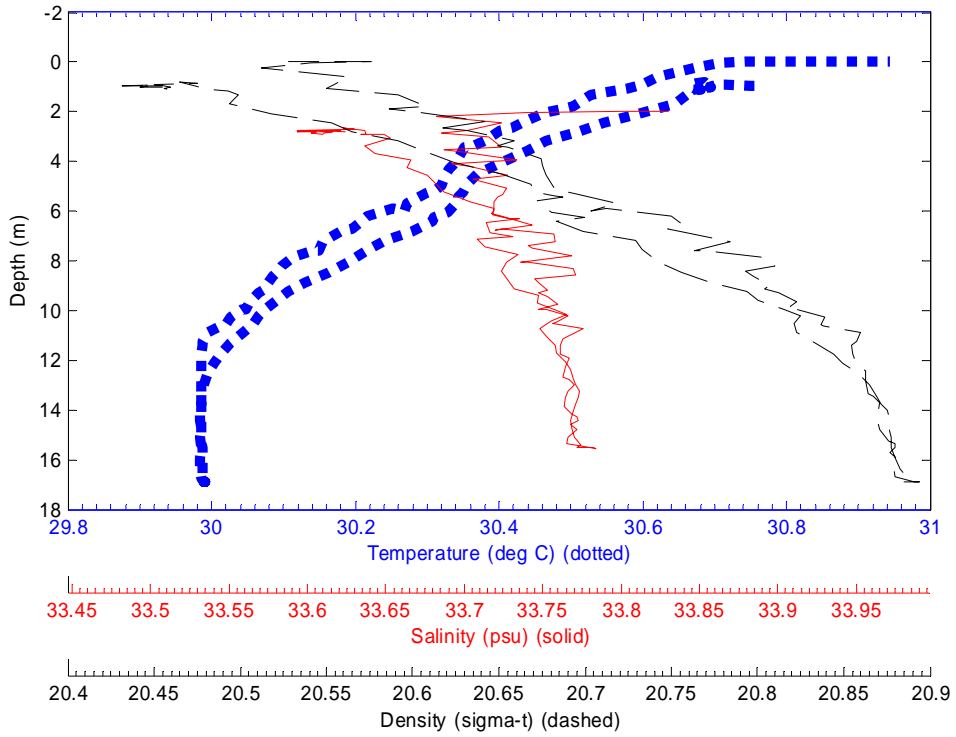
File: 0511005 05-Nov-2003 11:48:04 S7.1493 E134.2626 Site: CTD5



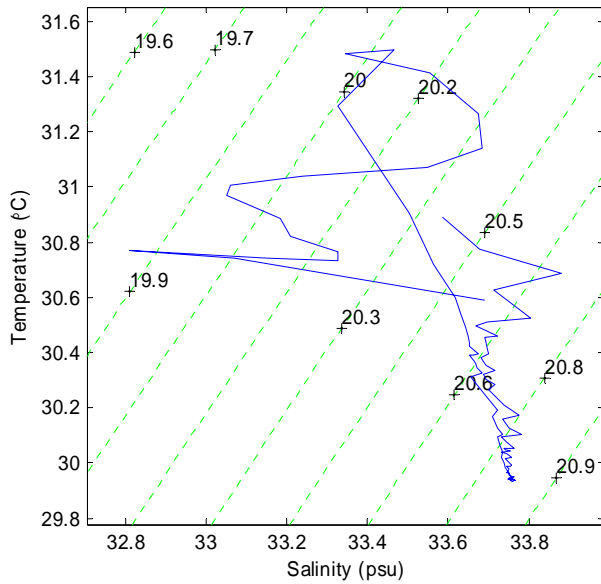
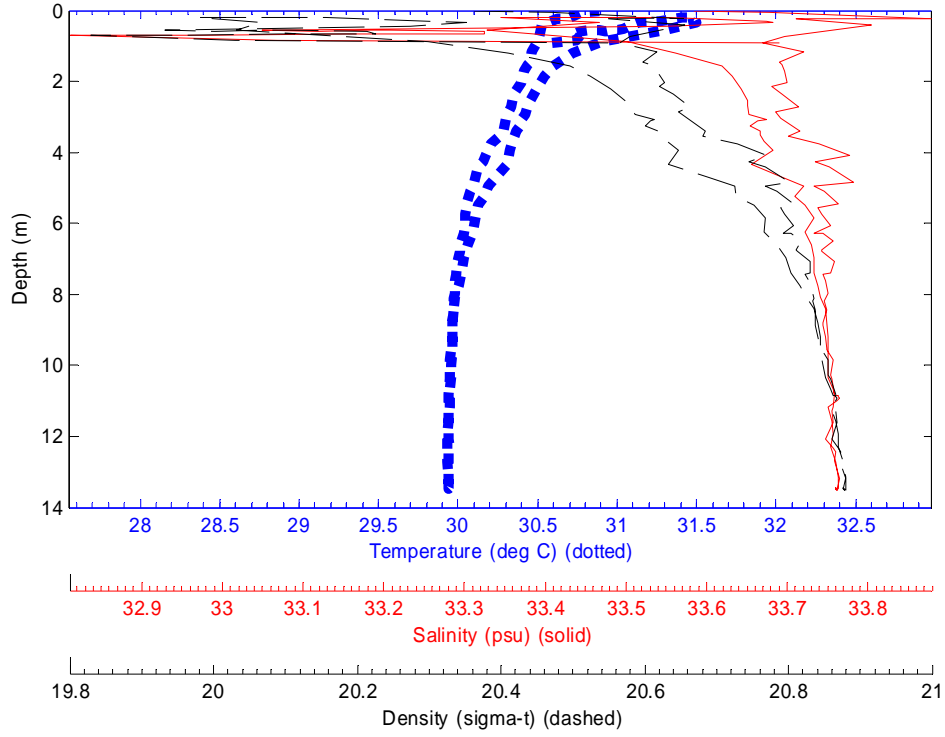
File: 0511006 05-Nov-2003 11:58:55 S7.1593 E134.2681 Site: CTD6



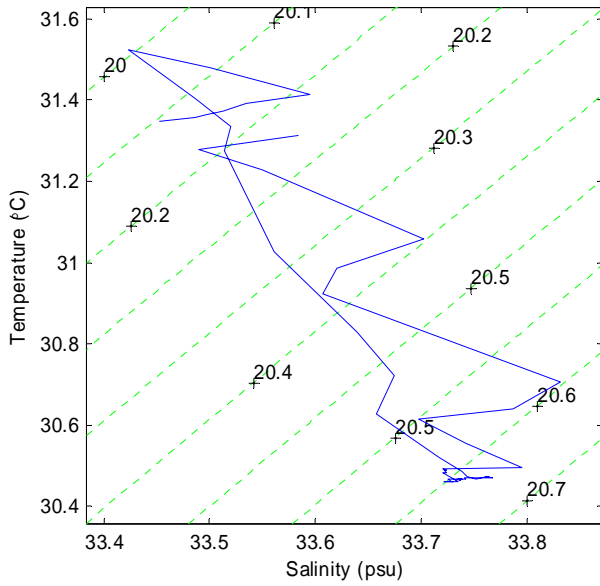
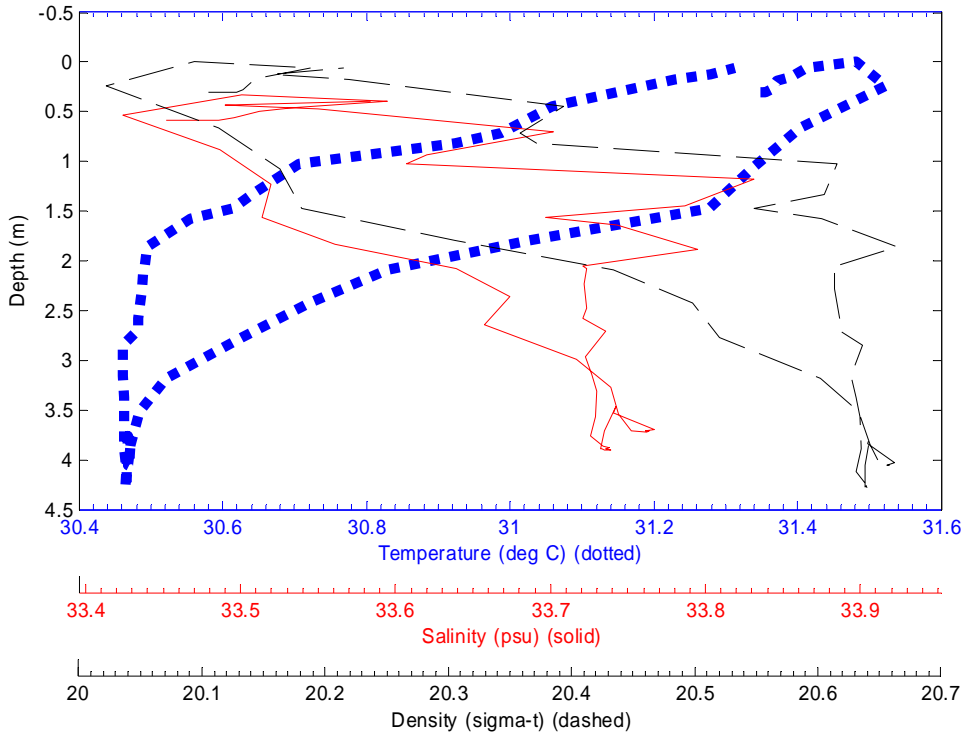
File: 0511007 05-Nov-2003 12:18:07 S7.1649 E134.2547 Site: CTD7



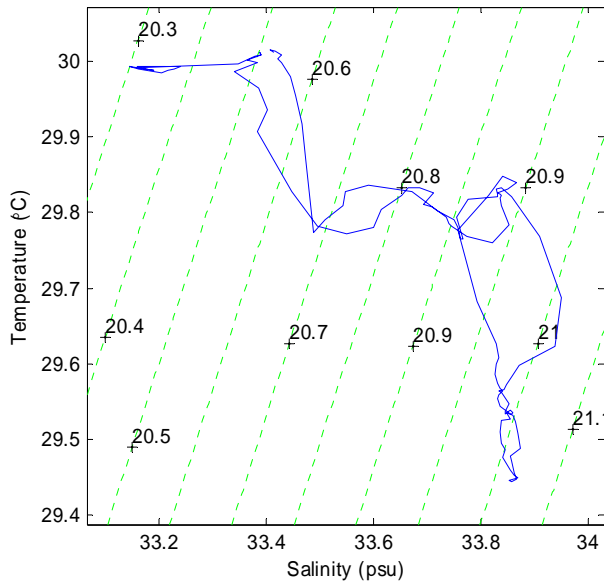
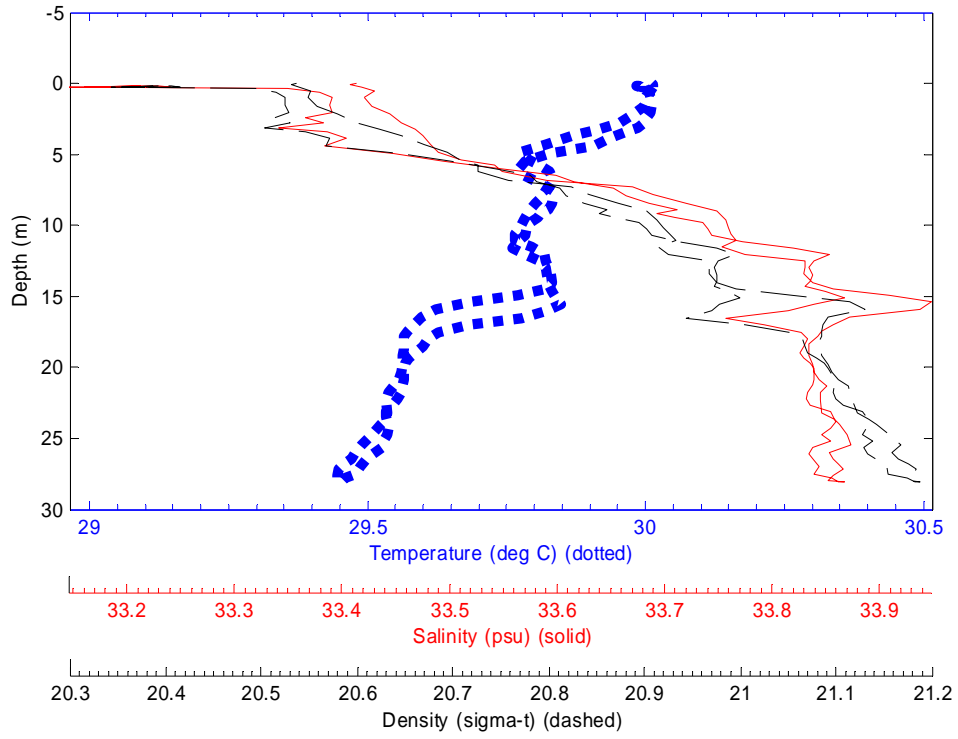
File: 0511008 05-Nov-2003 12:39:10 S7.1479 E134.2736 Site: CTD8



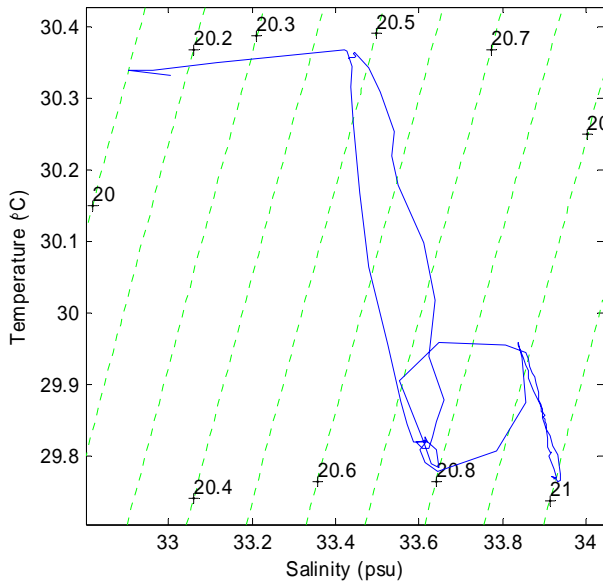
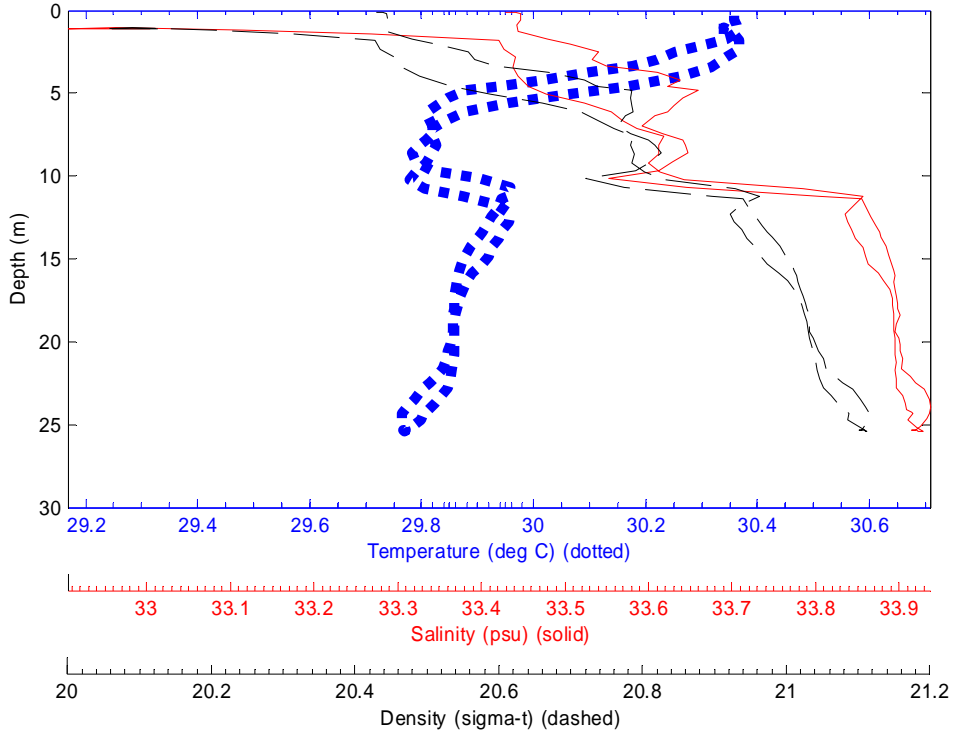
File: 0511009 05-Nov-2003 12:55:42 S7.1344 E134.29 Site: CTD9



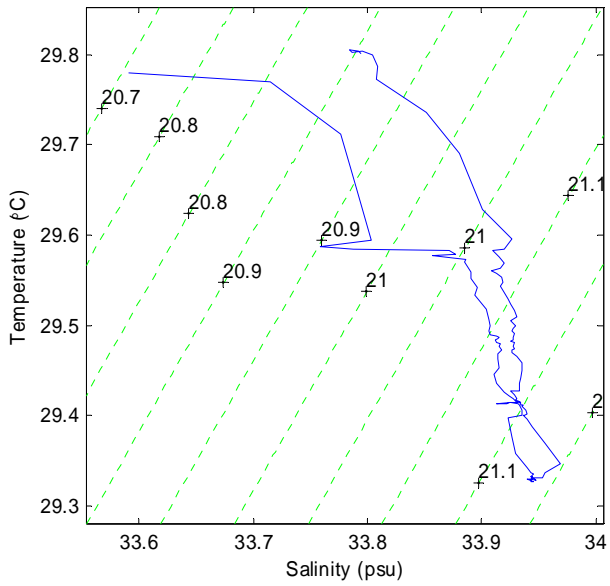
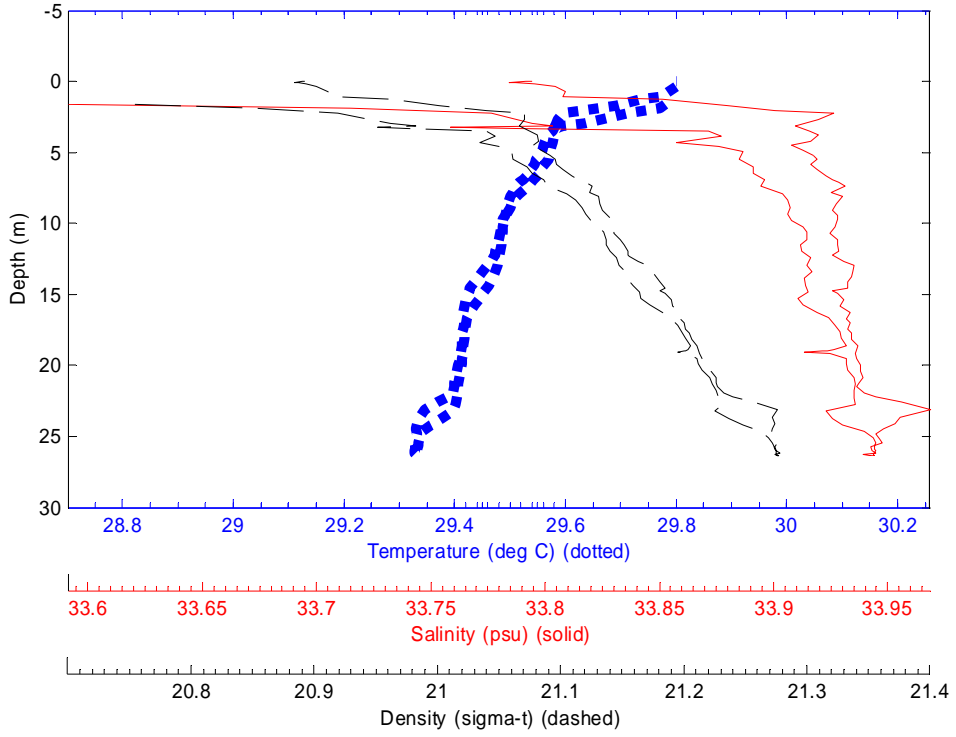
File: 0511010 05-Nov-2003 16:09:03 S7.3206 E134.3514 Site: CTD10



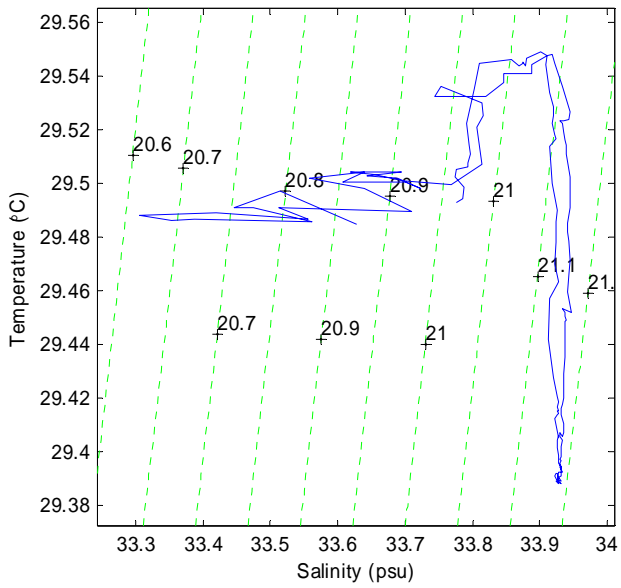
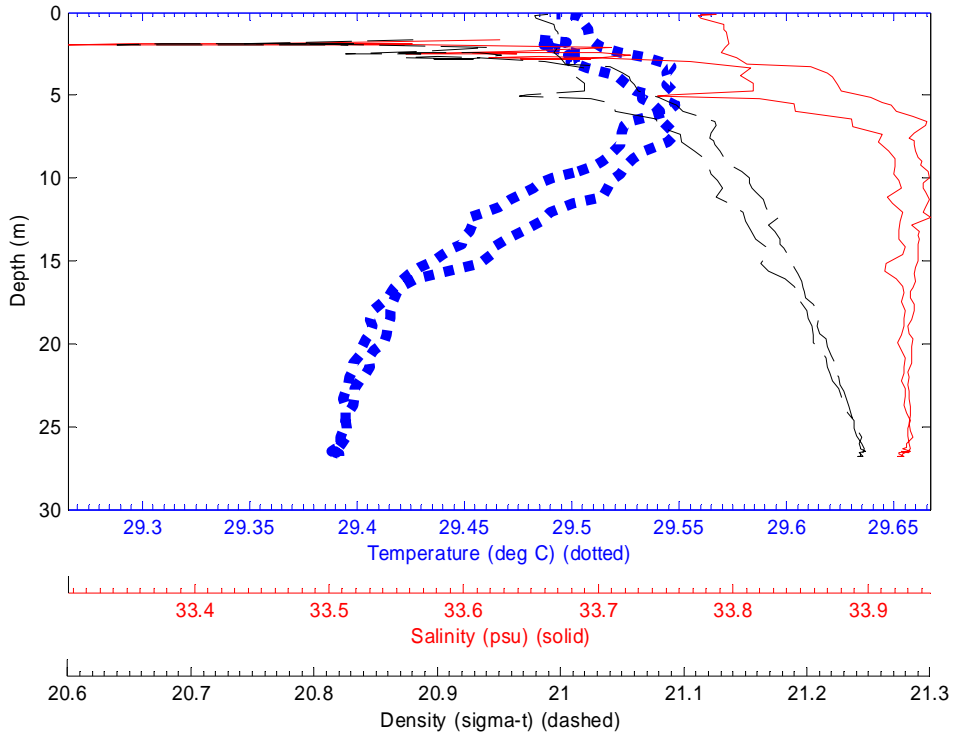
File: 0511011 05-Nov-2003 16:42:34 S7.3591 E134.3267 Site: CTD11



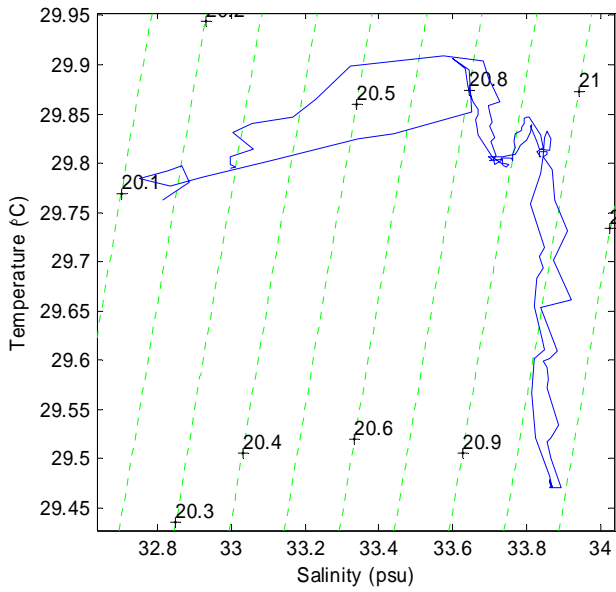
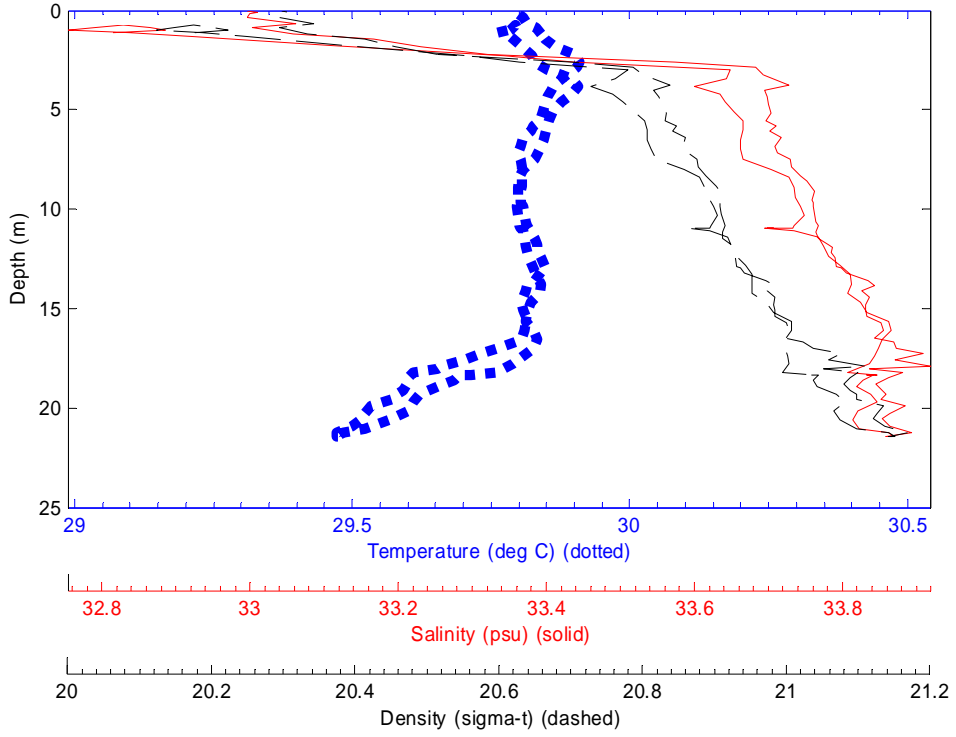
File: 0511012 05-Nov-2003 17:06:14 S7.3881 E134.308 Site: CTD12



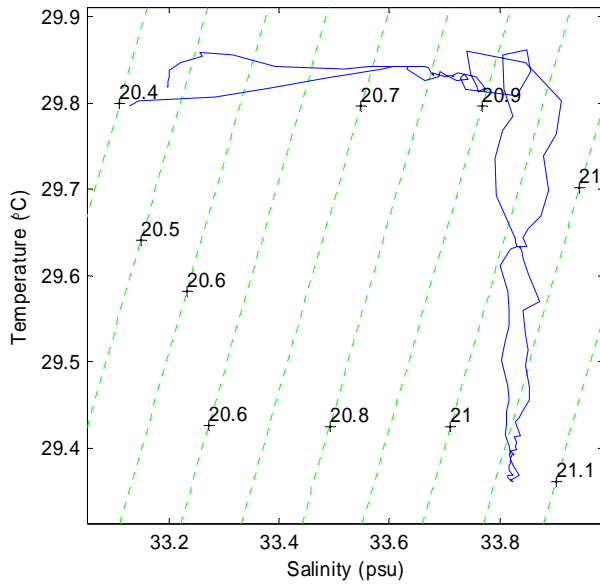
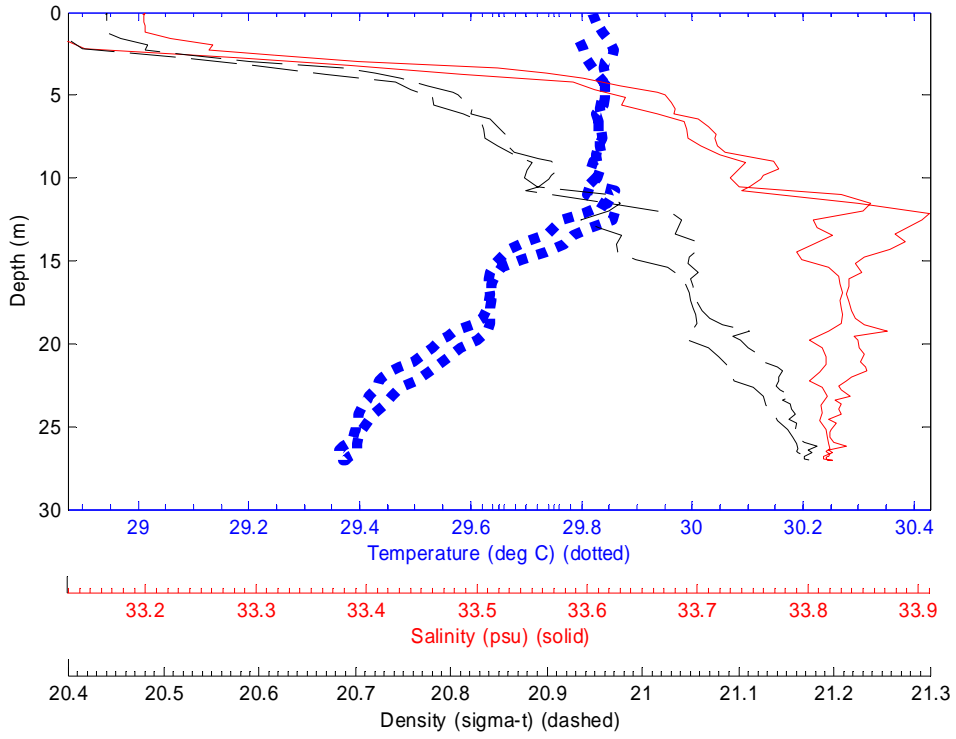
File: 0511013 05-Nov-2003 17:22:59 S7.4471 E134.3557 Site: CTD13



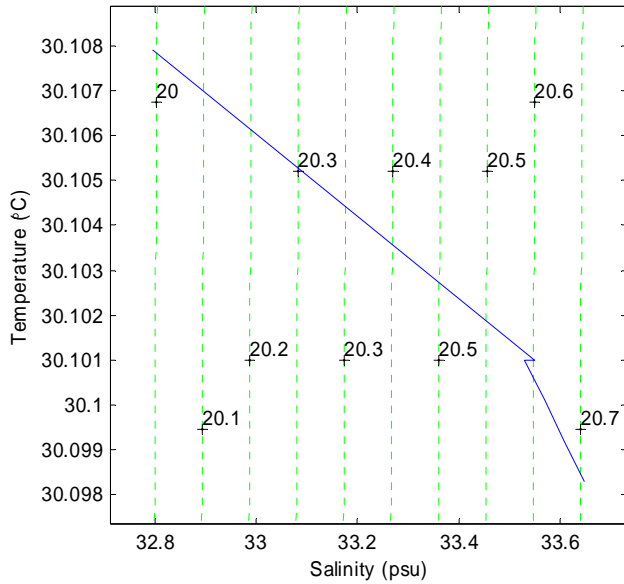
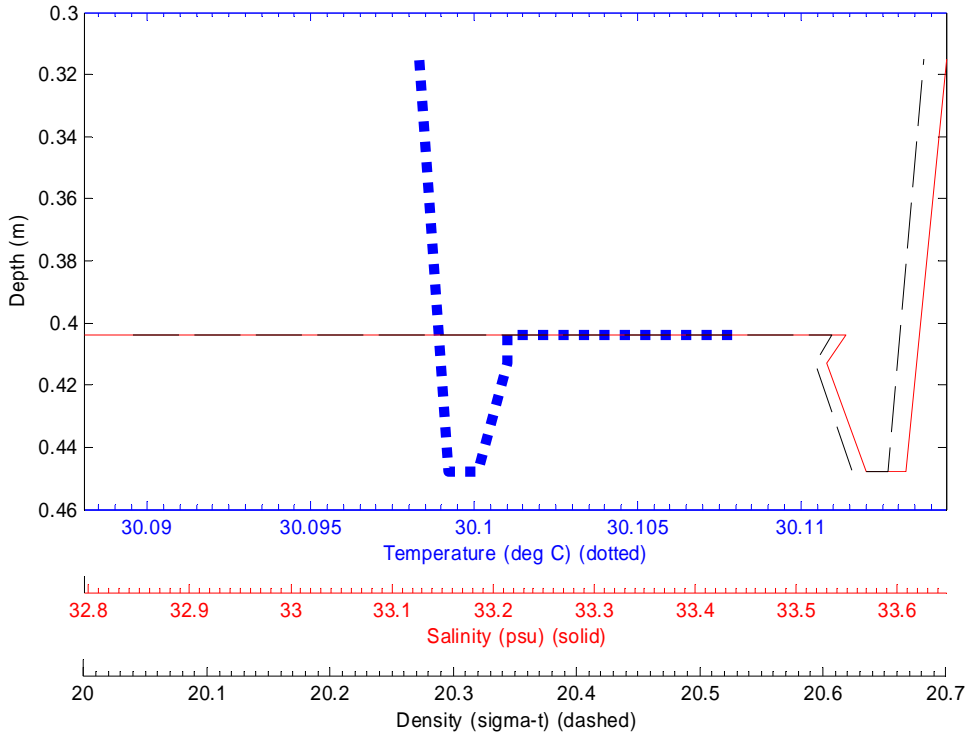
File: 0511014 05-Nov-2003 18:17:36 S7.3757 E134.387 Site: CTD14



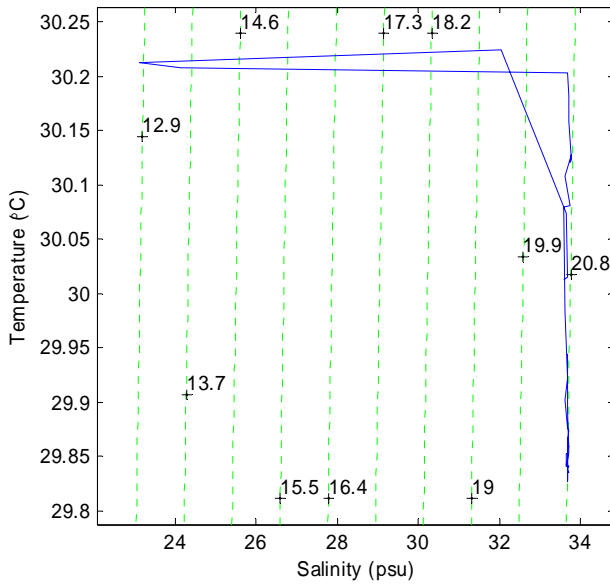
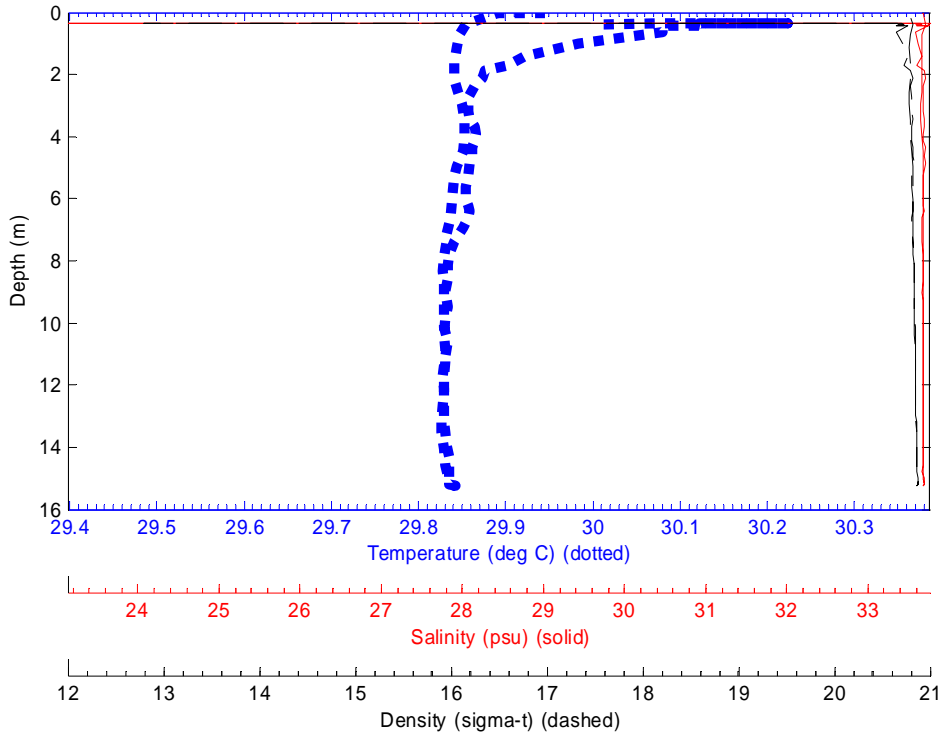
File: 0511015 05-Nov-2003 18:31:29 S7.363 E134.3965 Site: CTD14



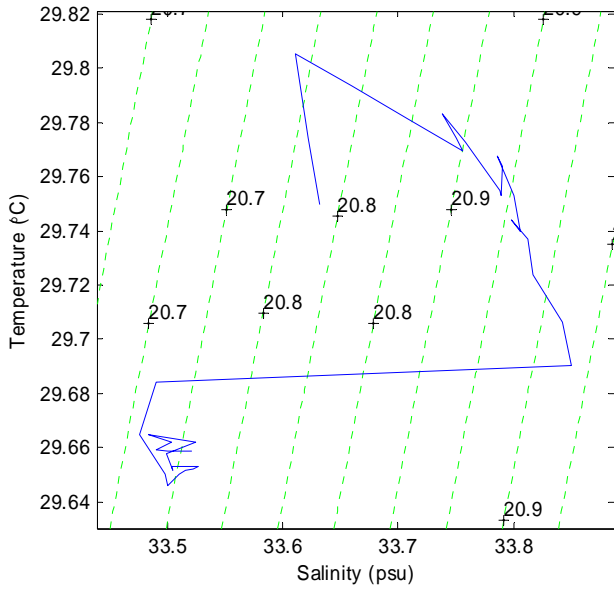
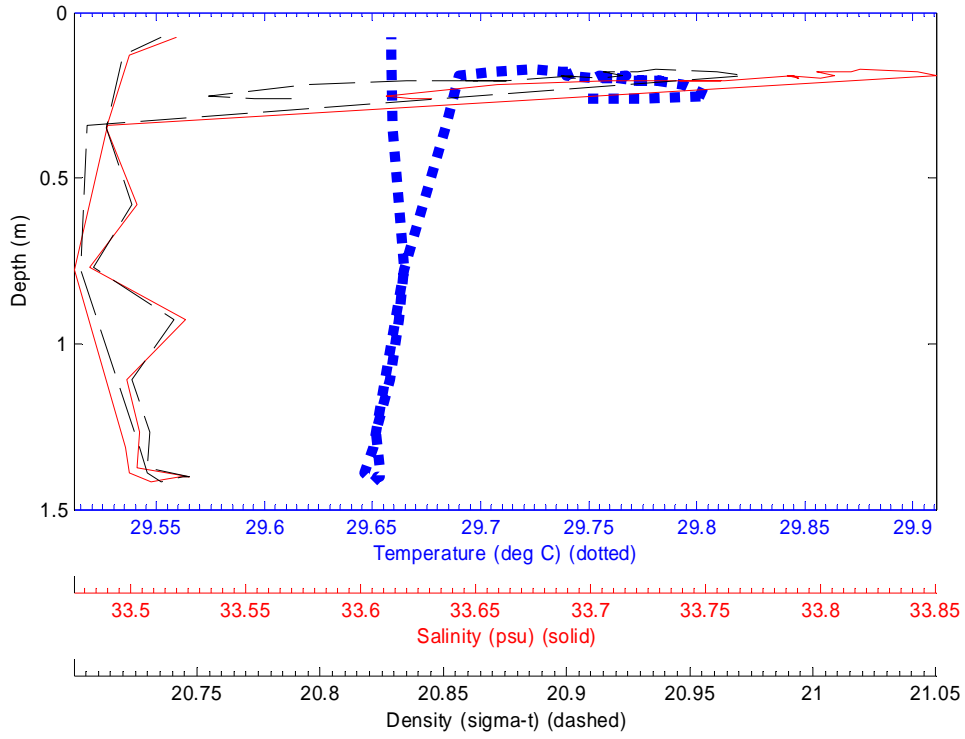
File: 0611000 06-Nov-2003 10:01:57 S7.4769 E134.3955 Site: CTD0



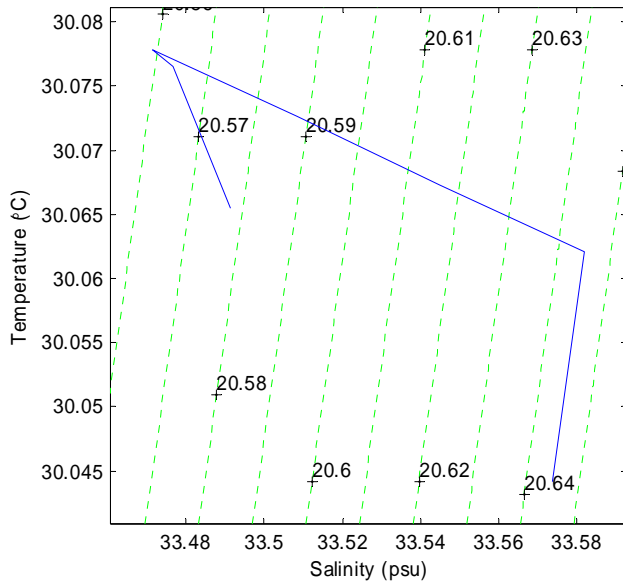
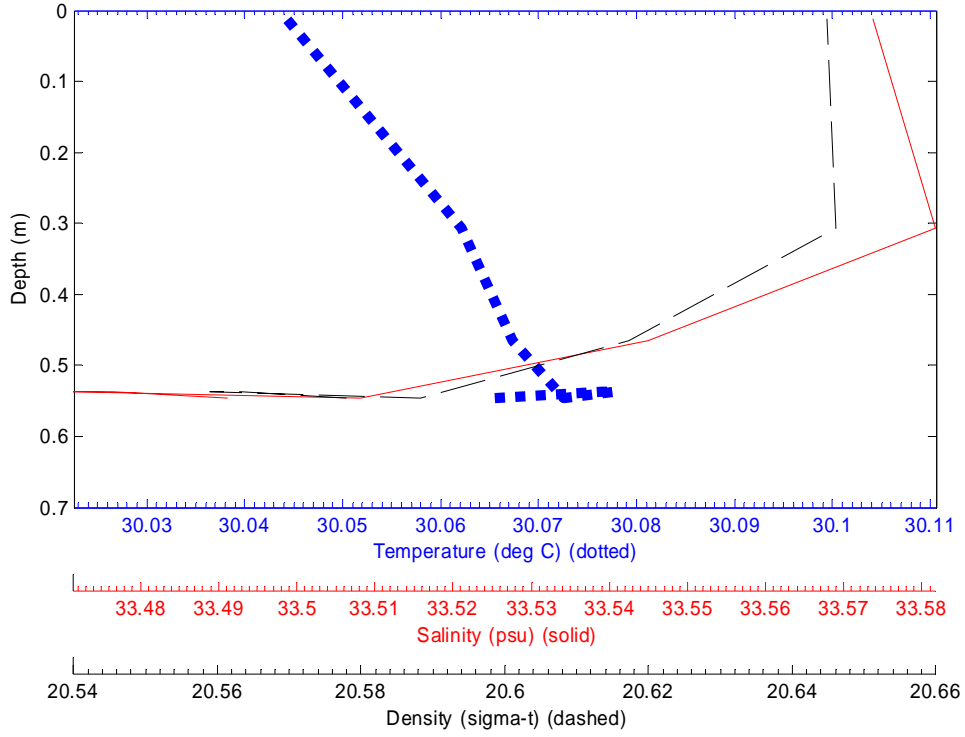
File: 0611001 06-Nov-2003 10:22:25 S7.4925 E134.4152 Site: CTD1



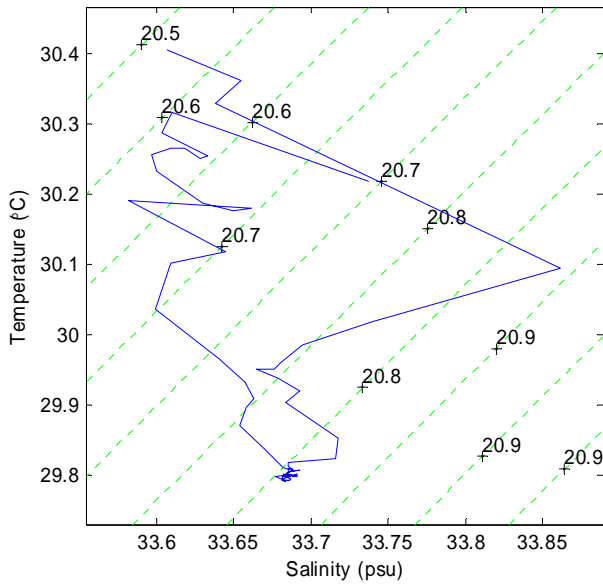
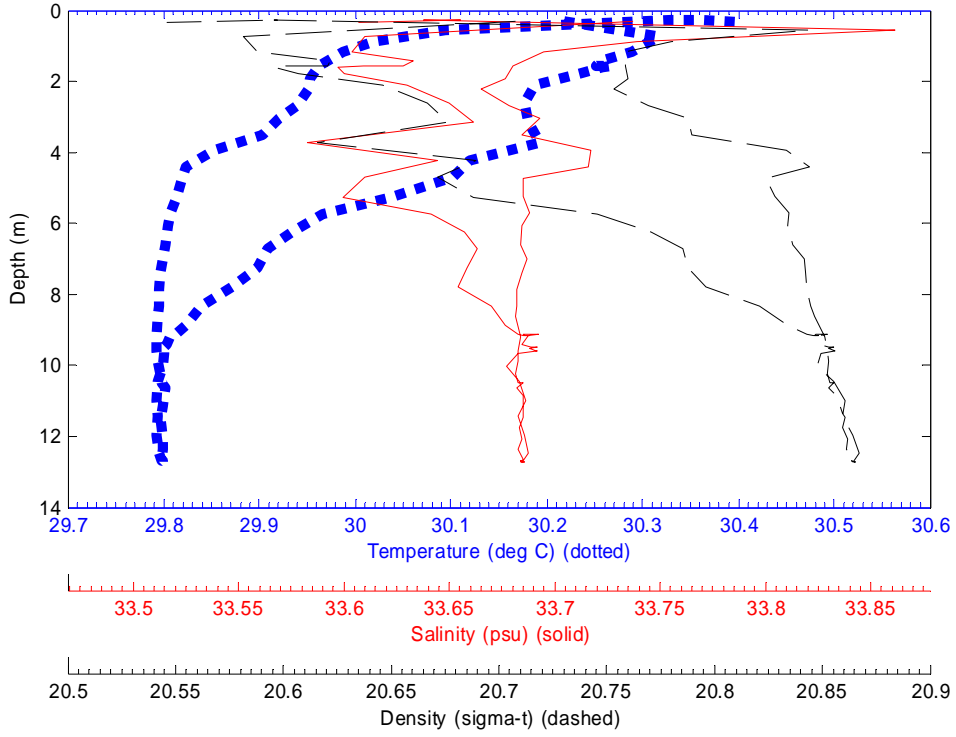
File: 0611002 06-Nov-2003 10:43:17 S7.5102 E134.4362 Site: CTD2



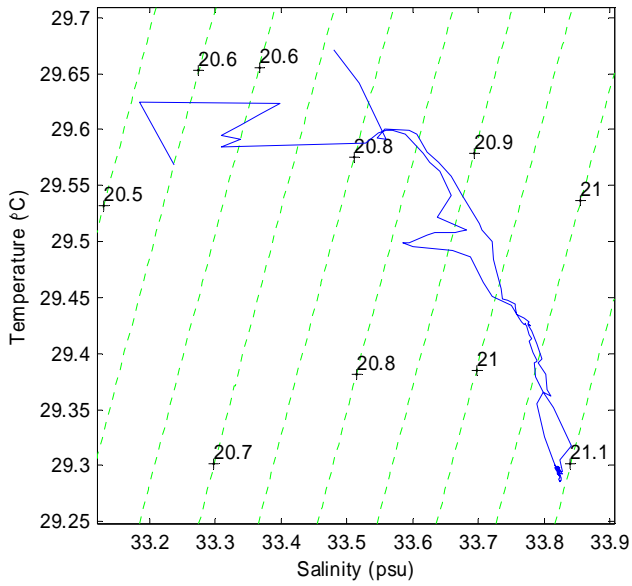
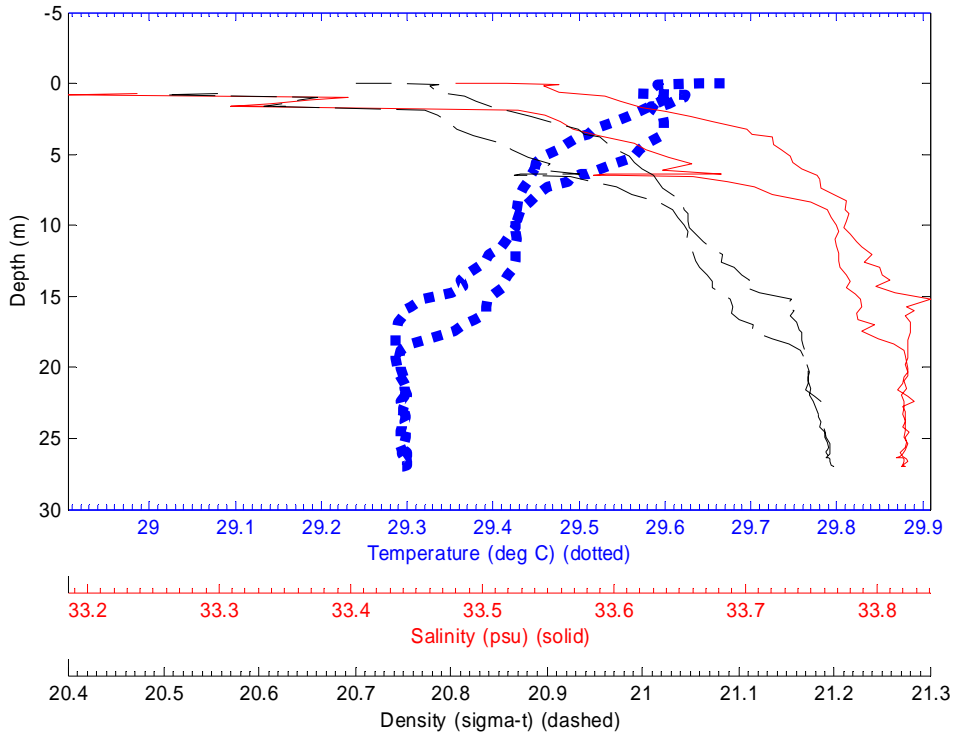
File: 0611003 06-Nov-2003 11:05:42 S7.5168 E134.3855 Site: CTD3



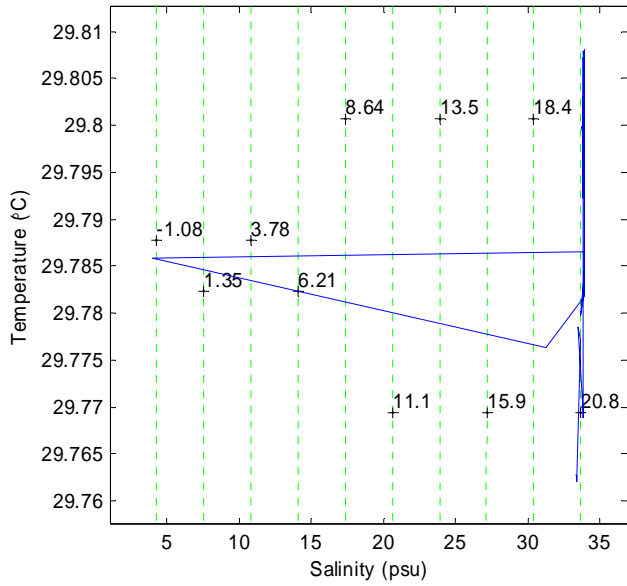
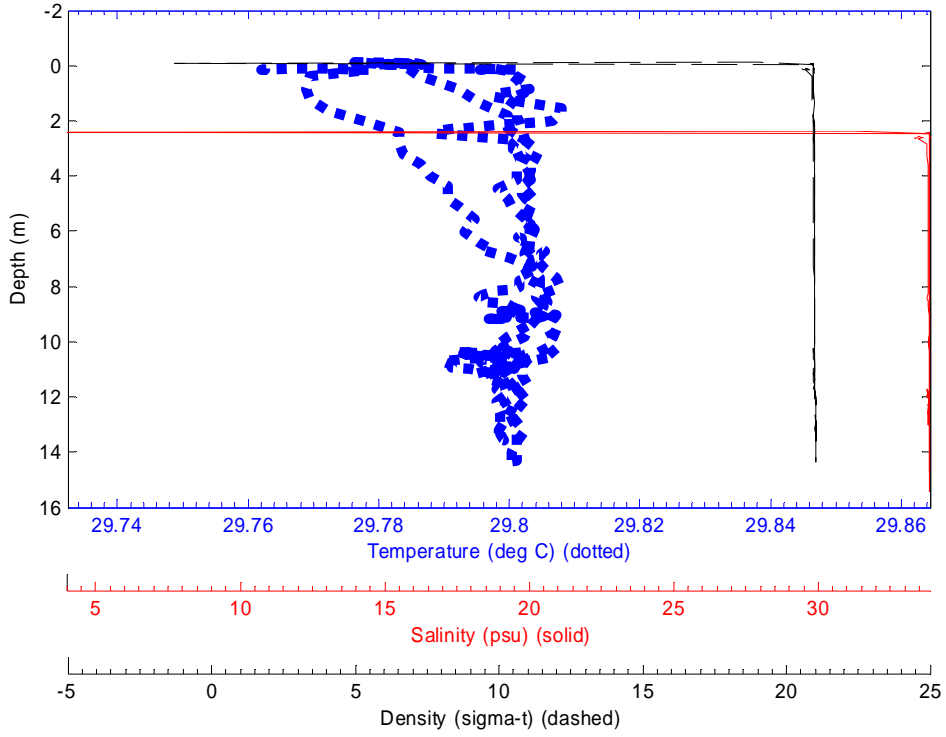
File: 0611004 06-Nov-2003 11:36:03 S7.4923 E134.4176 Site: CTD4



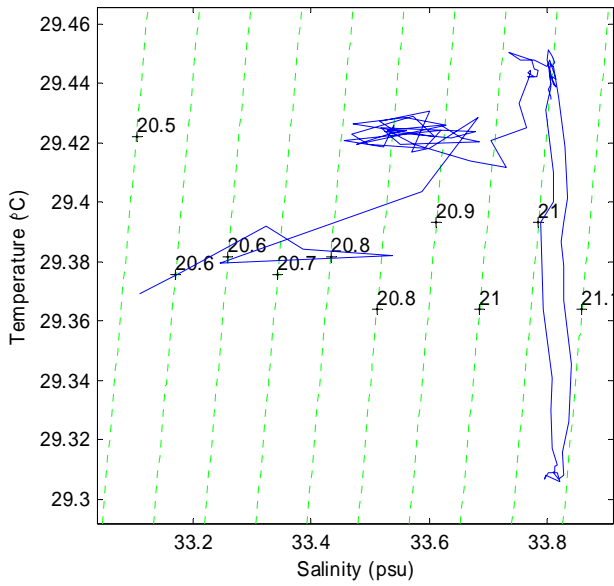
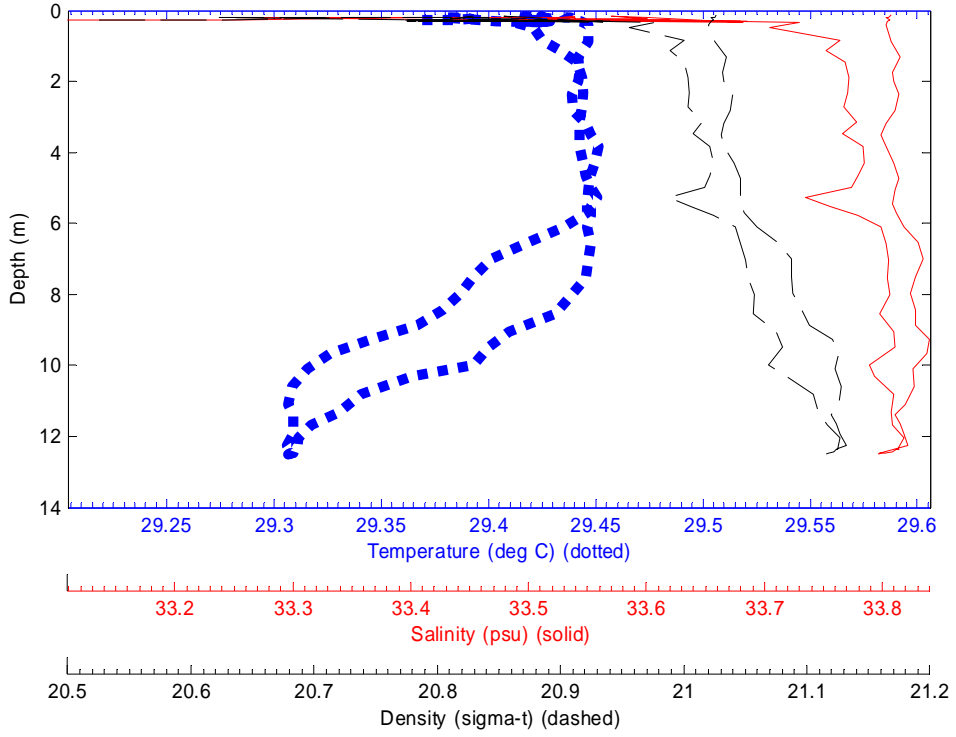
File: 0611005 06-Nov-2003 12:05:49 S7.4923 E134.4176 Site: CTD5



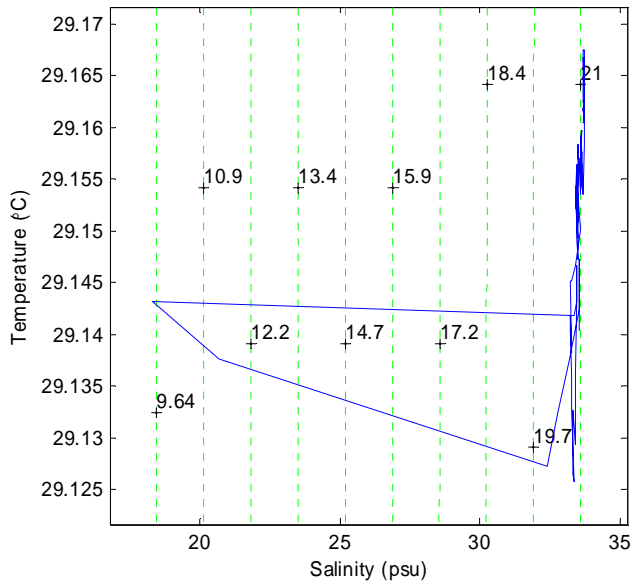
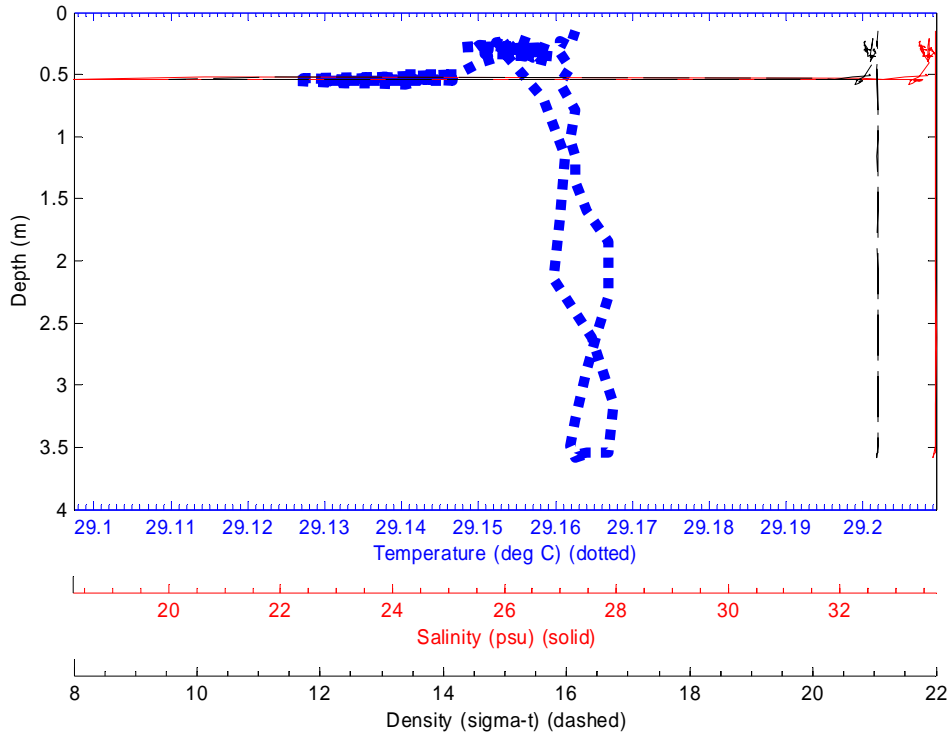
File: 0711000 07-Nov-2003 07:12:59 S7.7726 E134.5938 Site: CTD0



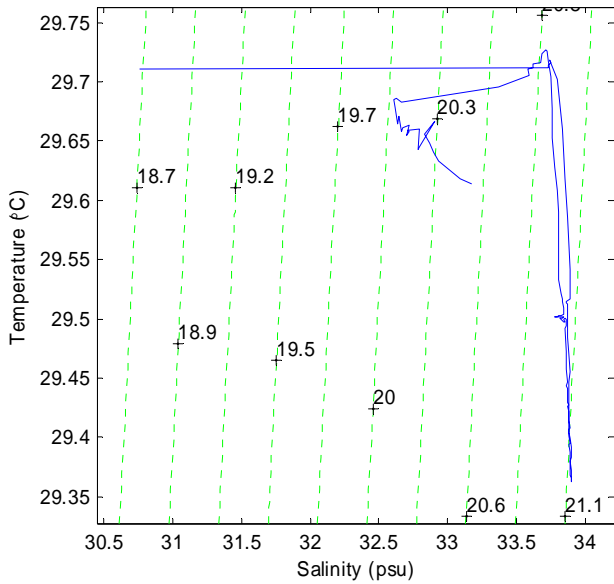
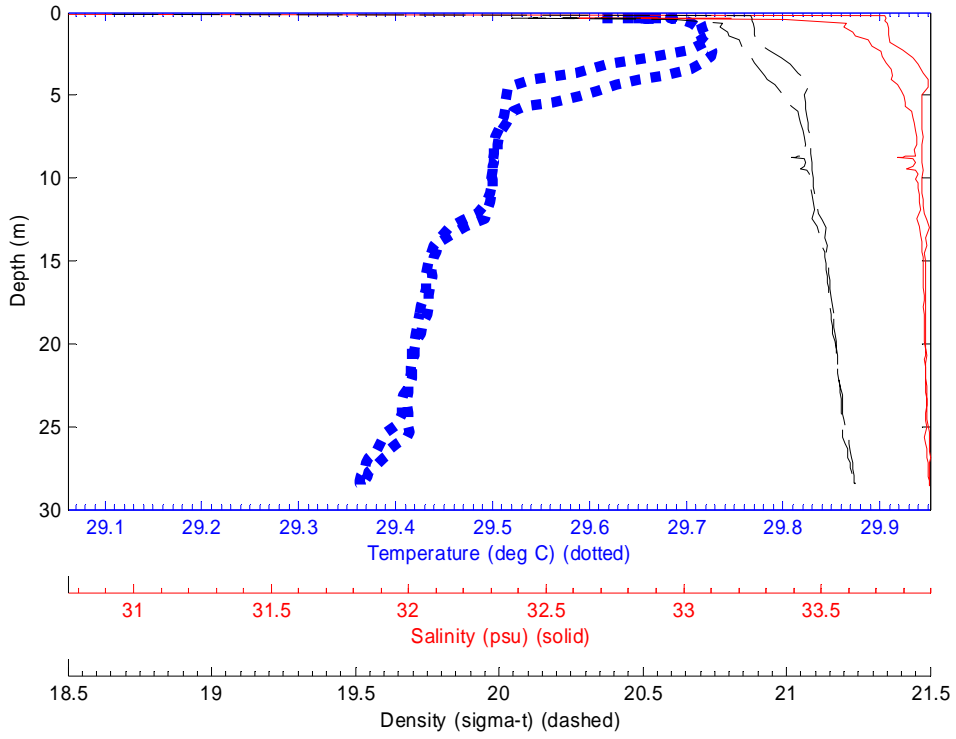
File: 0711001 07-Nov-2003 08:31:36 S7.8454 E134.5425 Site: CTD1



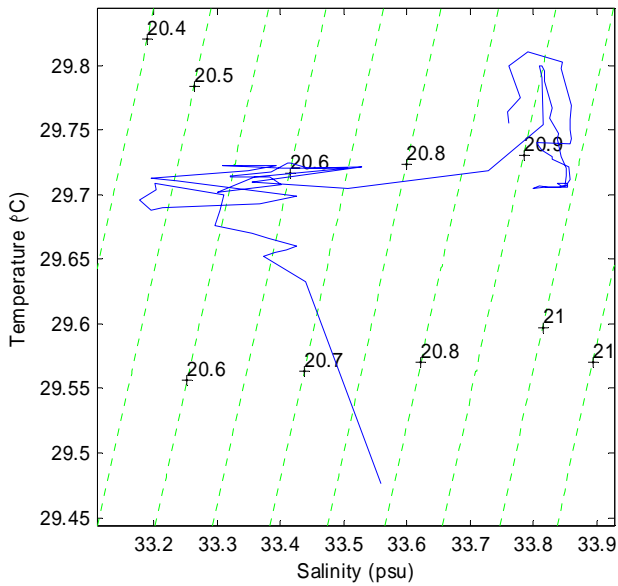
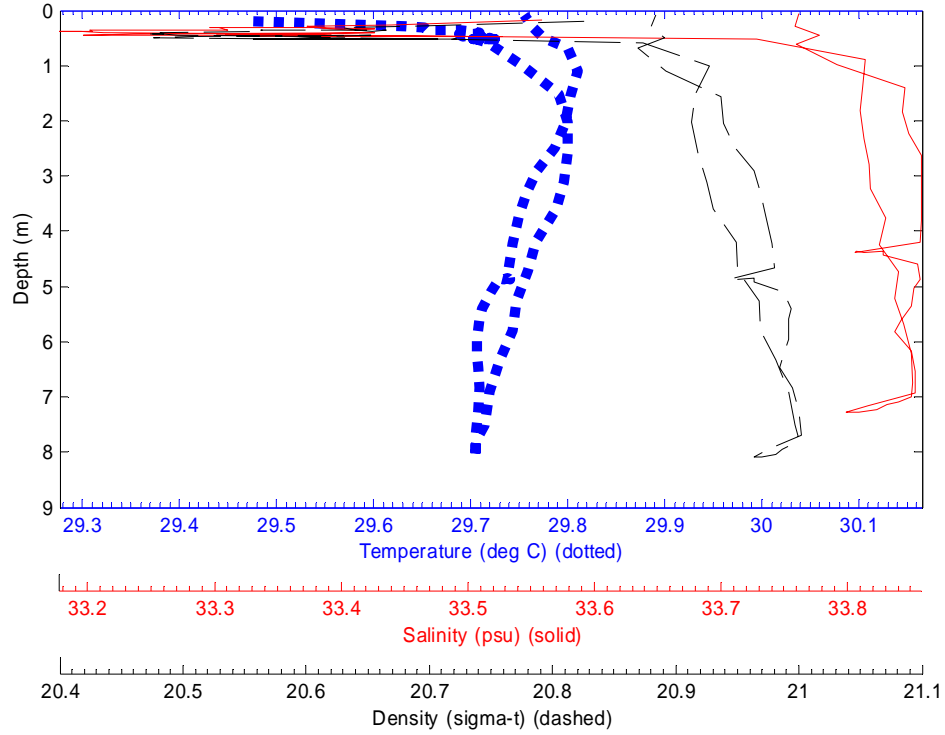
File: 0711002 07-Nov-2003 09:27:51 S7.9139 E134.504 Site: CTD2



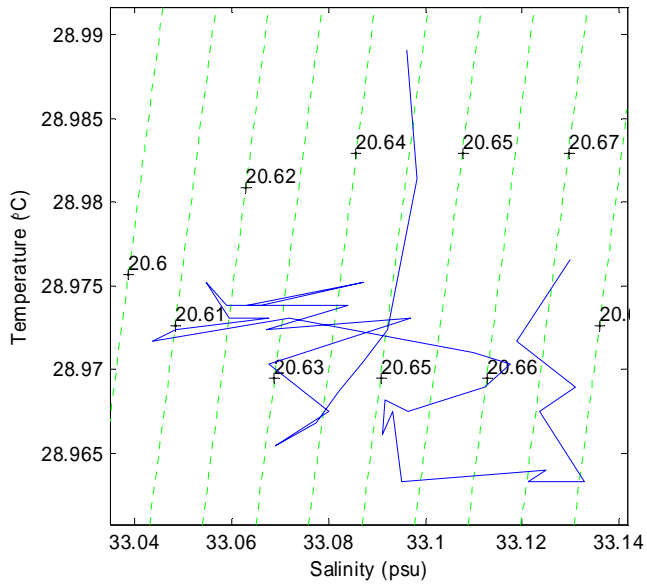
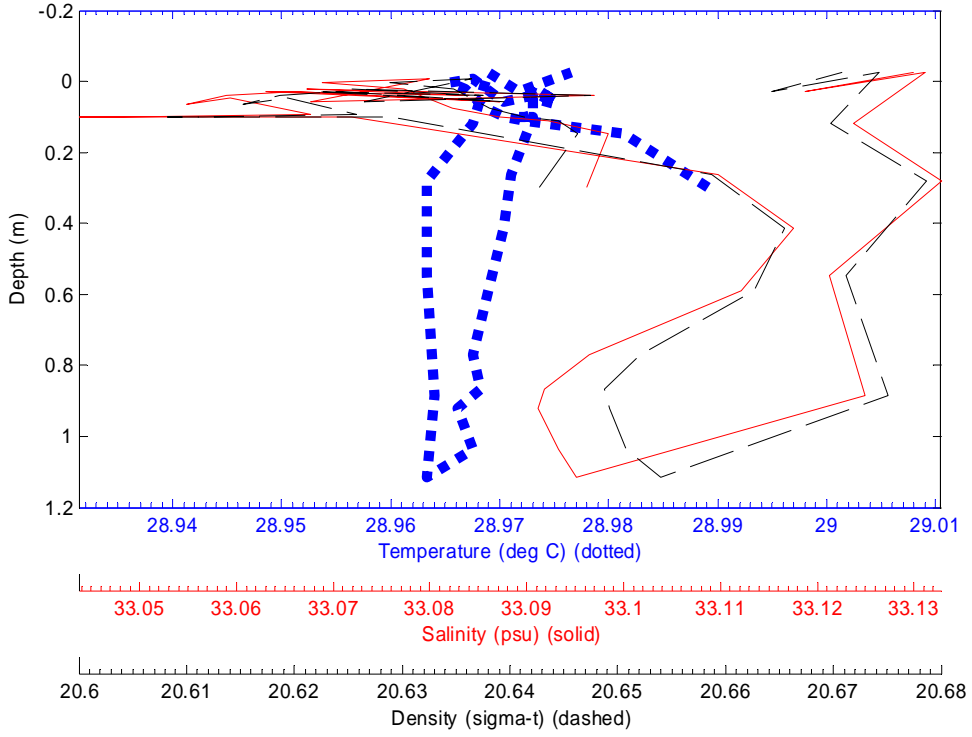
File: 0711003 07-Nov-2003 11:38:38 S7.9397 E134.6365 Site: CTD3



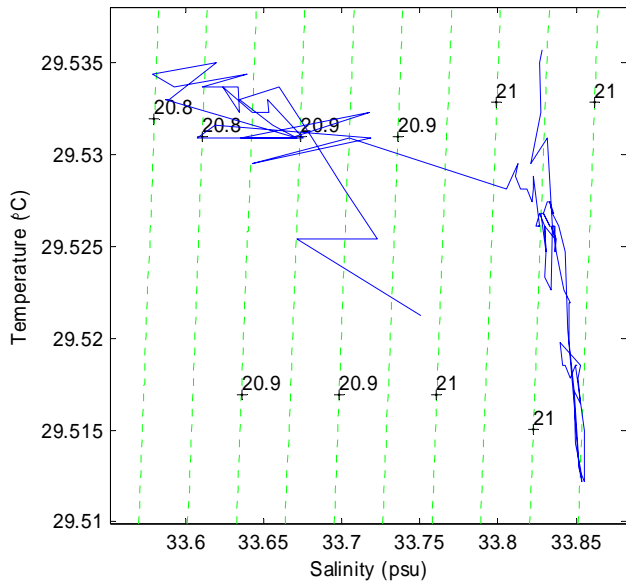
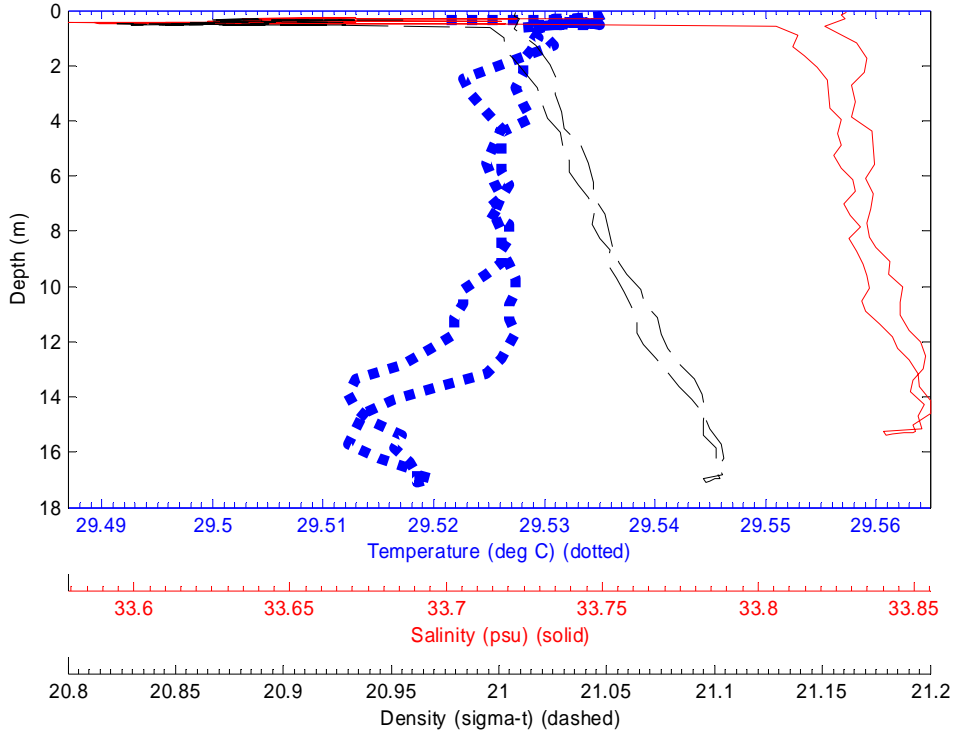
File: 0711004 07-Nov-2003 12:19:53 S7.976 E134.6713 Site: CTD4



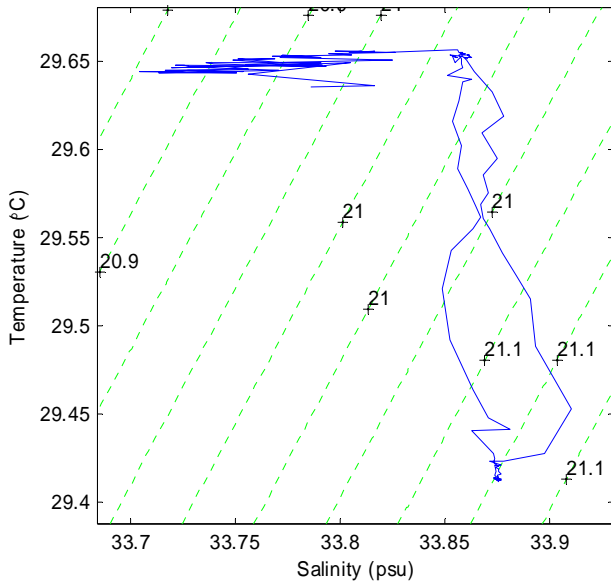
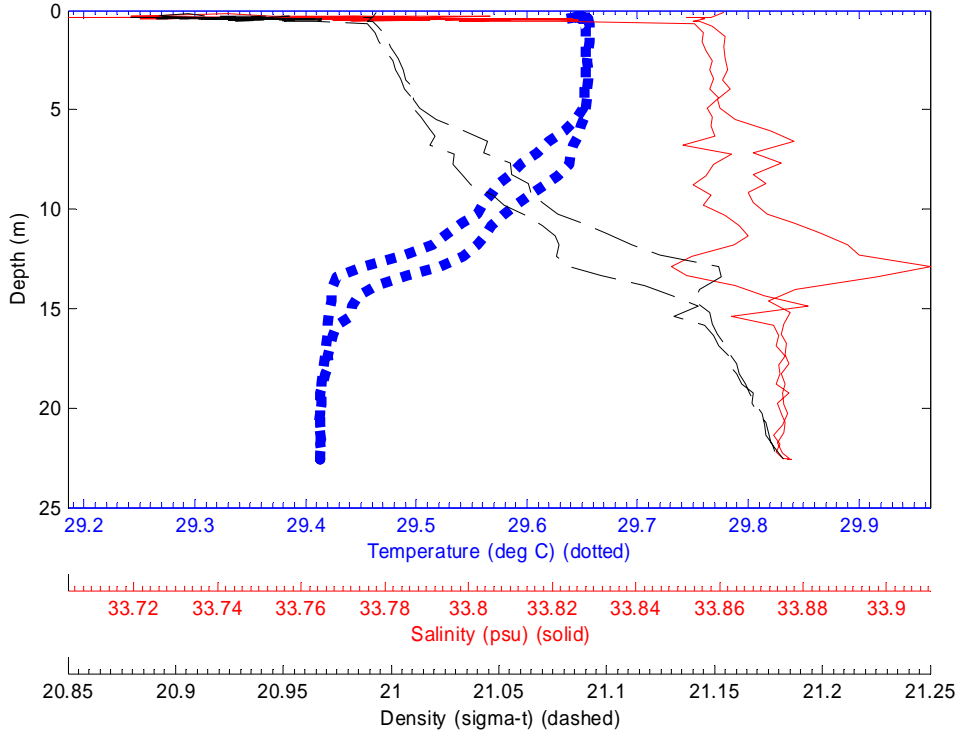
File: 0711005 07-Nov-2003 12:43:20 S7.9925 E134.6891 Site: CTD5



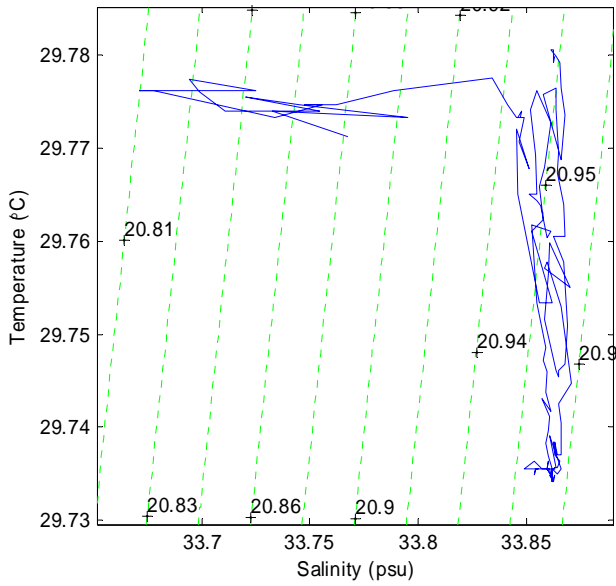
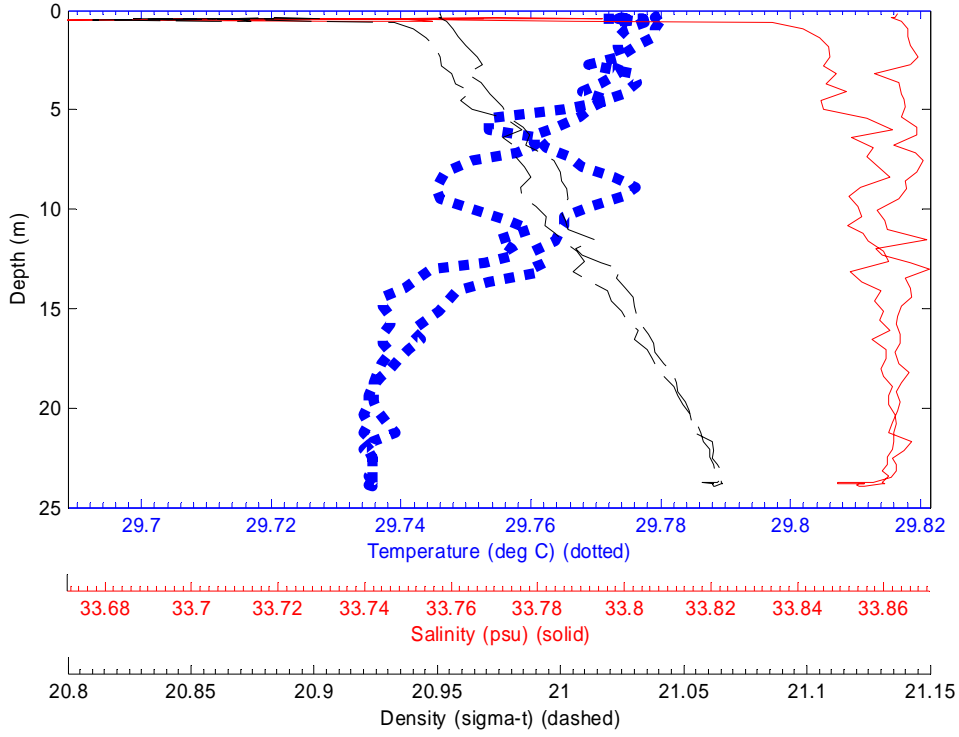
File: 0711006 07-Nov-2003 13:22:33 S7.879 E134.6661 Site: CTD6



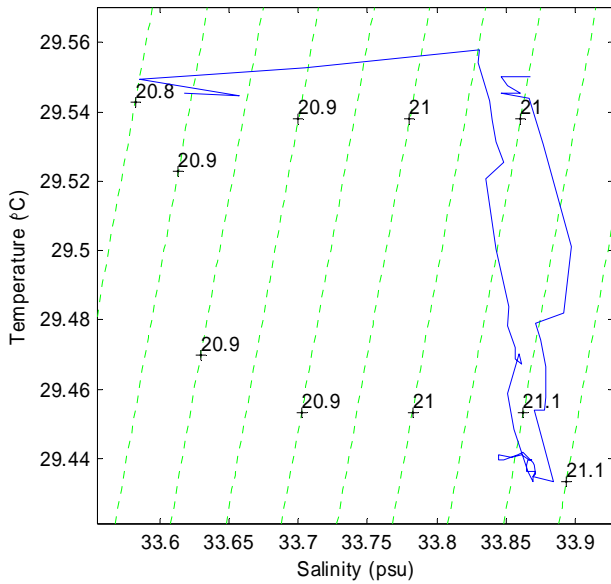
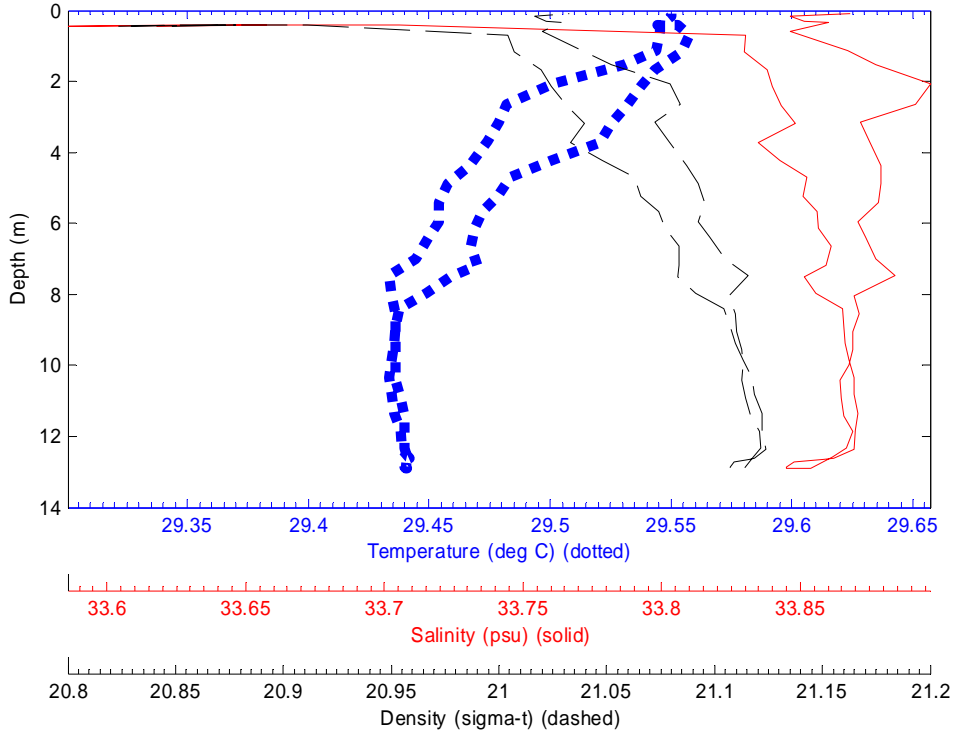
File: 0711007 07-Nov-2003 13:52:10 S7.849 E134.6405 Site: CTD7



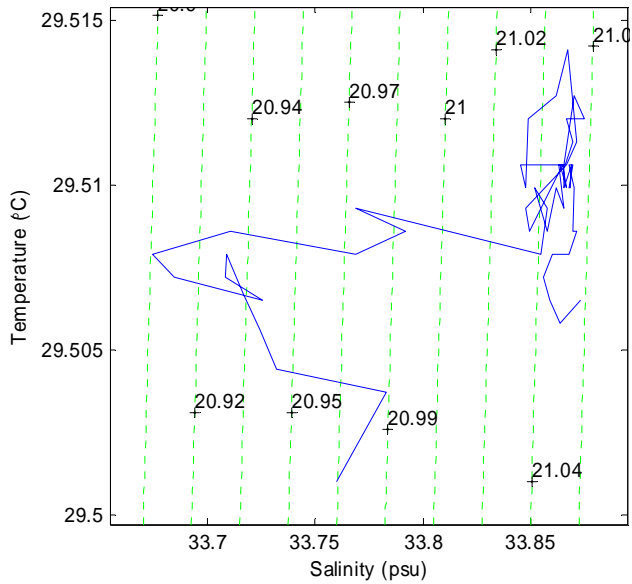
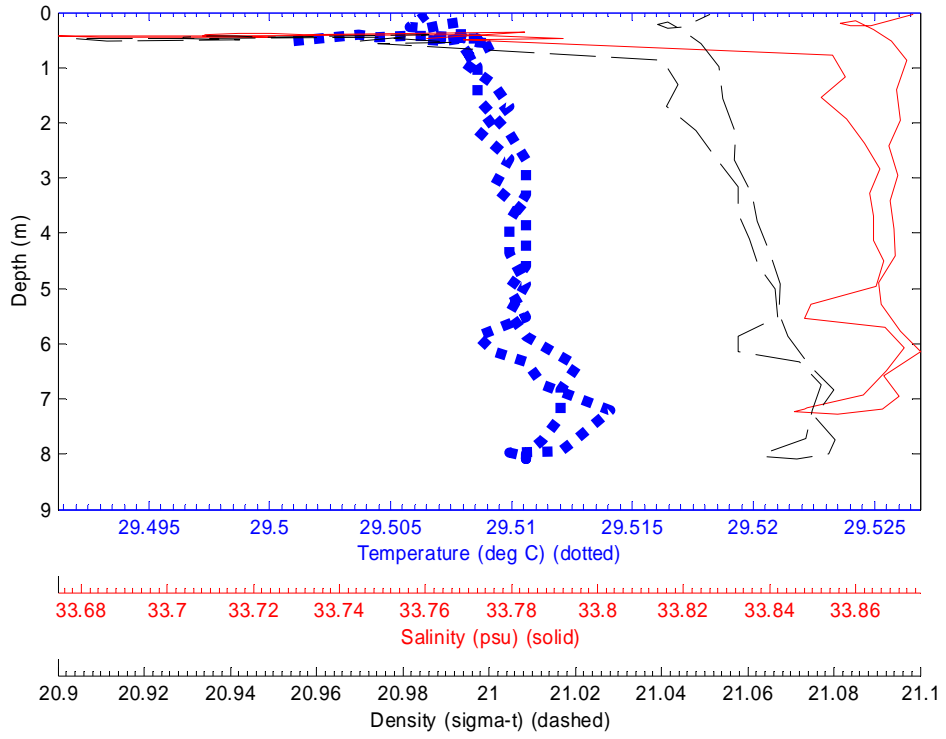
File: 0711008 07-Nov-2003 14:21:58 S7.8177 E134.61 Site: CTD8



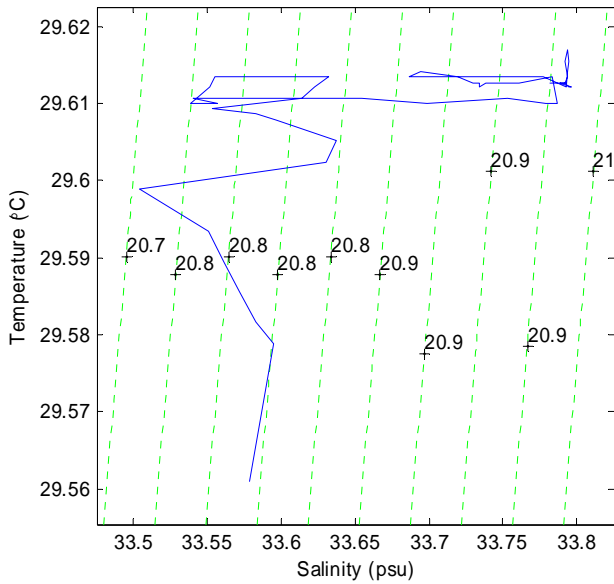
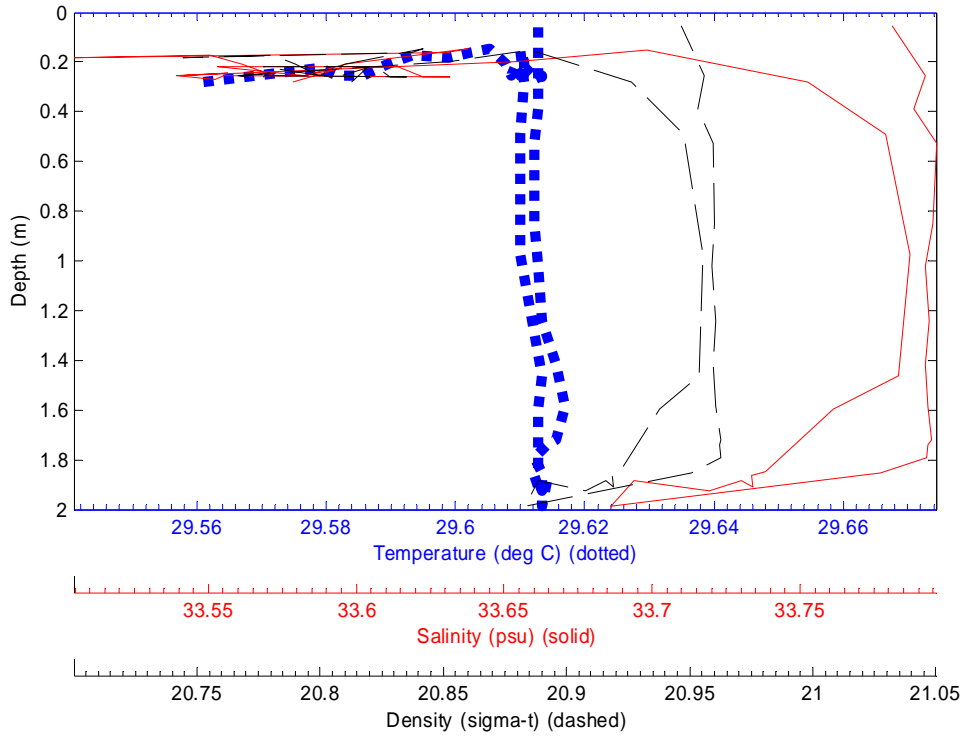
File: 0711009 07-Nov-2003 14:50:19 S7.7728 E134.5873 Site: CTD9



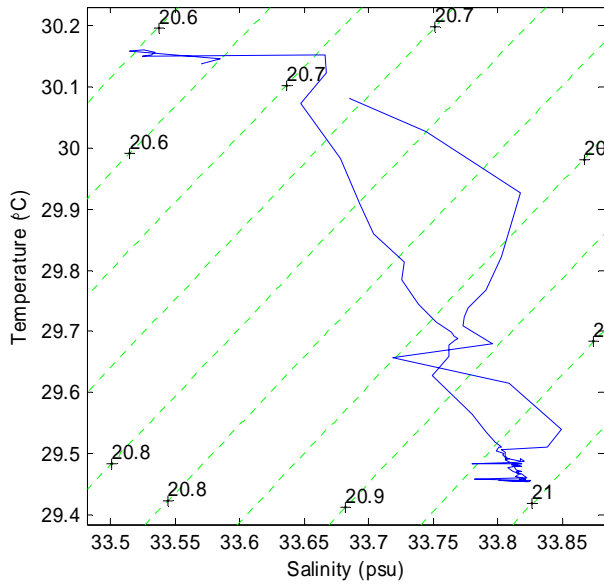
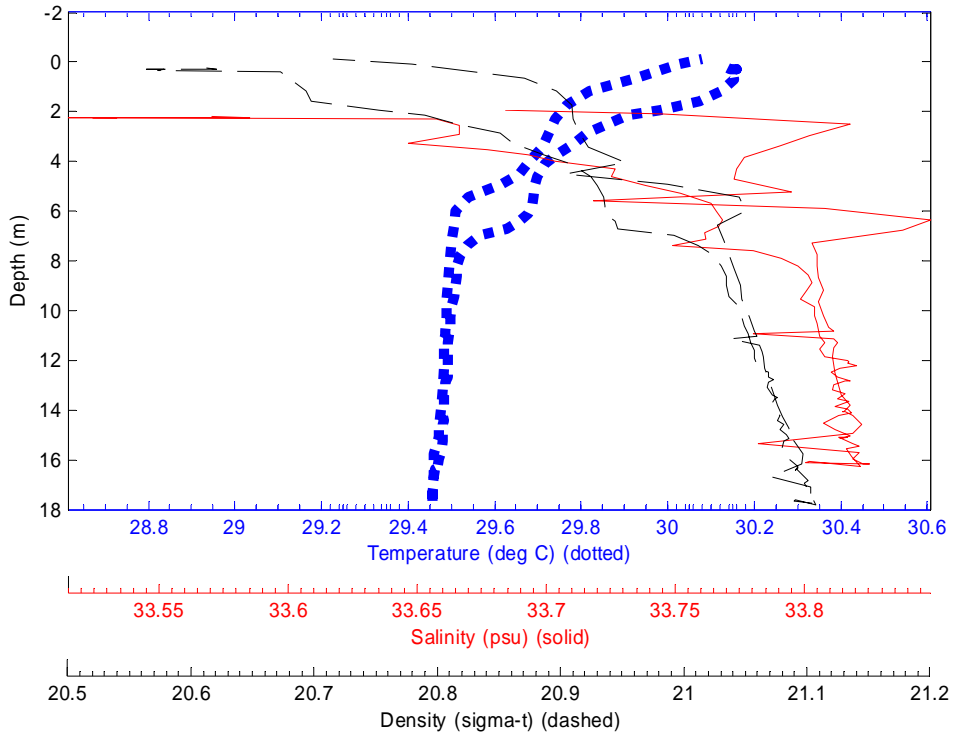
File: 0711010 07-Nov-2003 15:14:18 S7.7444 E134.5779 Site: CTD10



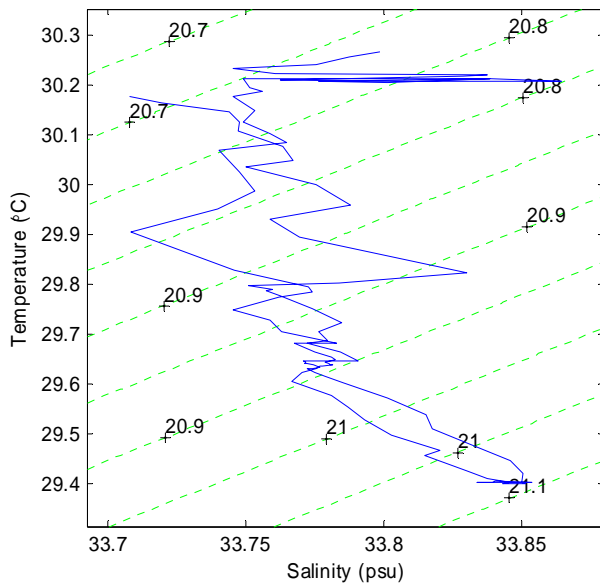
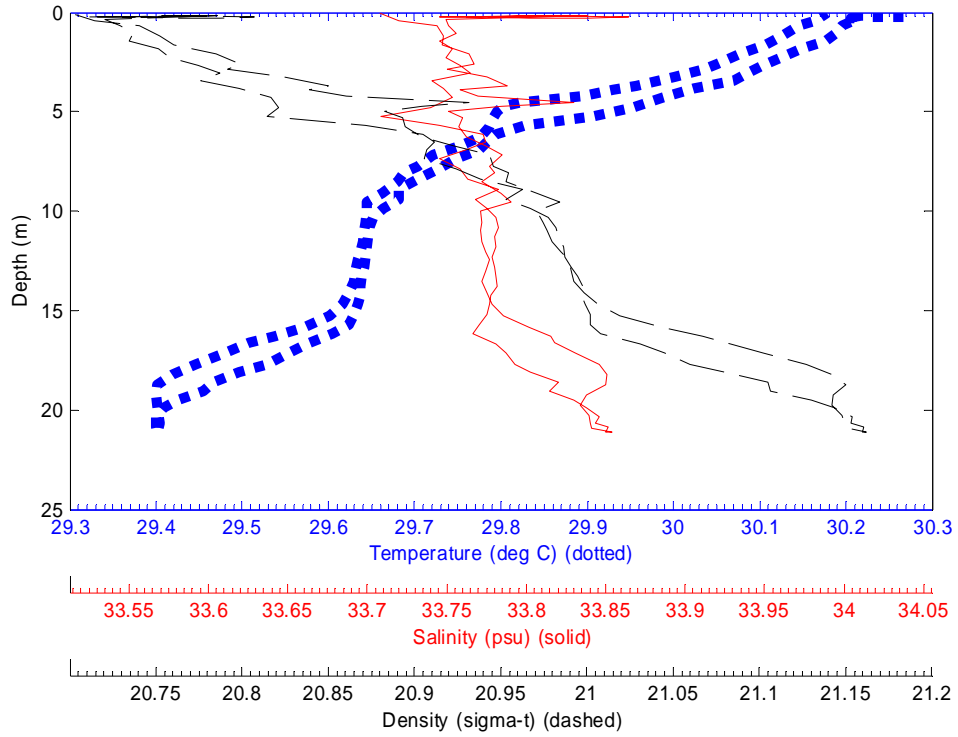
File: 0711011 07-Nov-2003 15:30:45 S7.7258 E134.5807 Site: CTD11



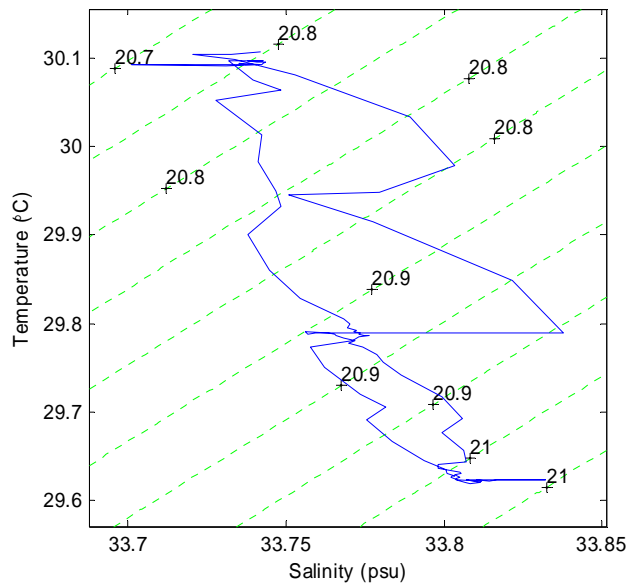
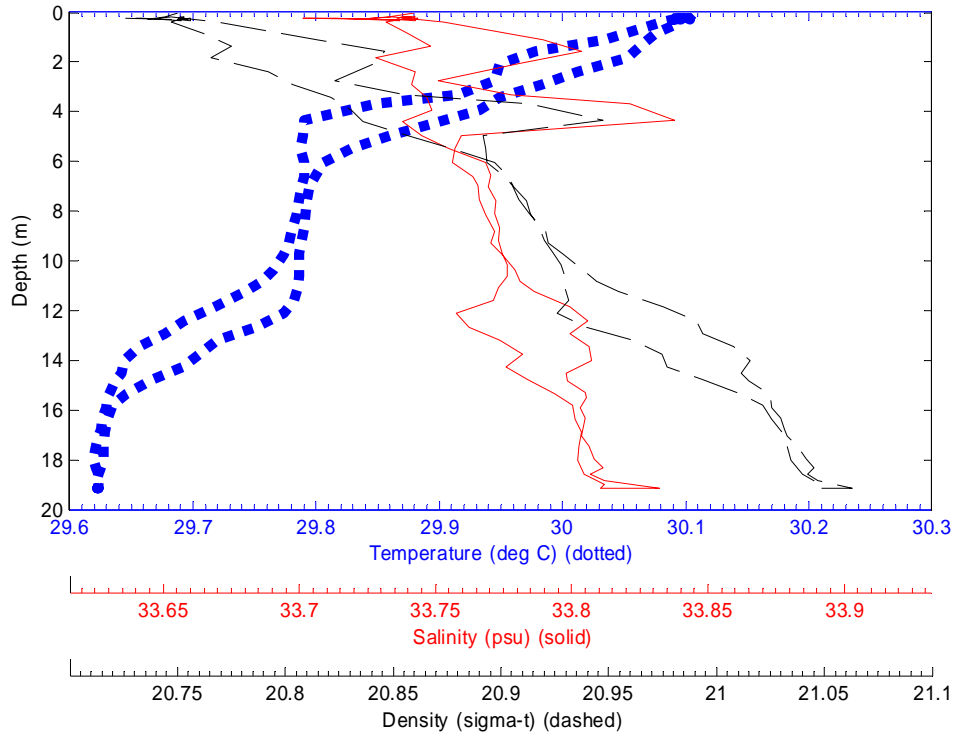
File: 0911000 09-Nov-2003 15:15:25 S7.2826 E134.5026 Site: 11C1



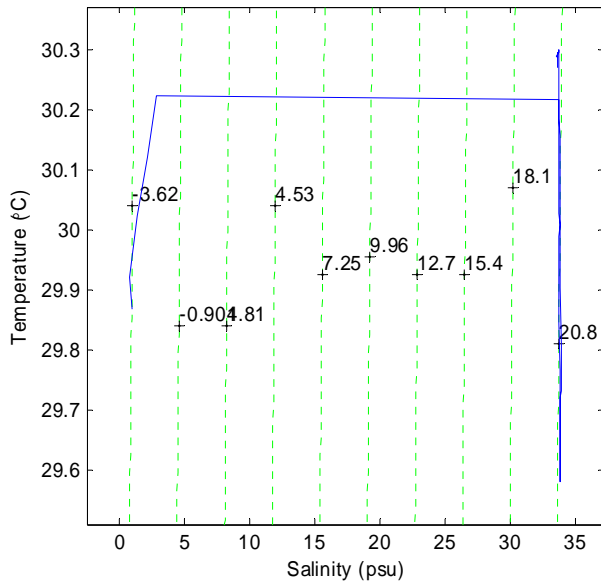
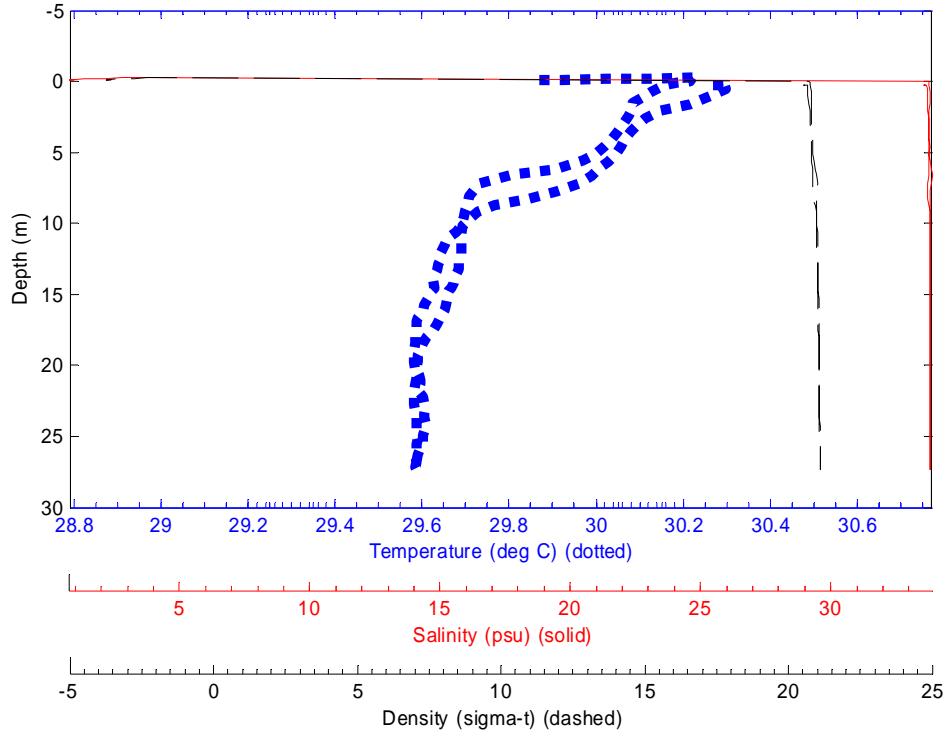
File: 0911001 09-Nov-2003 15:37:48 S7.2646 E134.4818 Site: 11C2



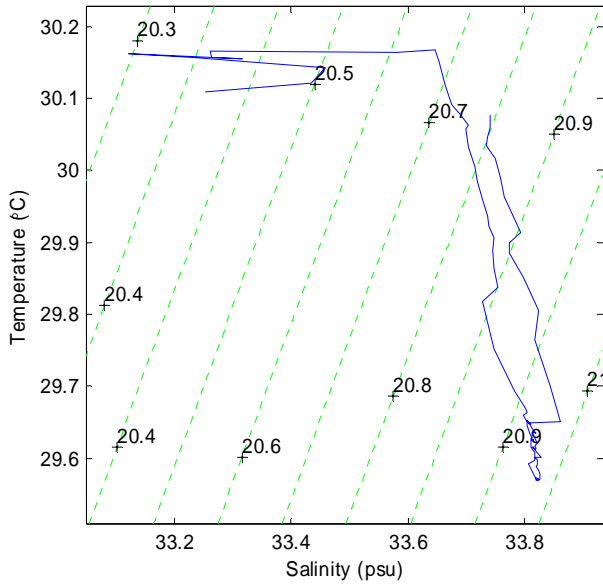
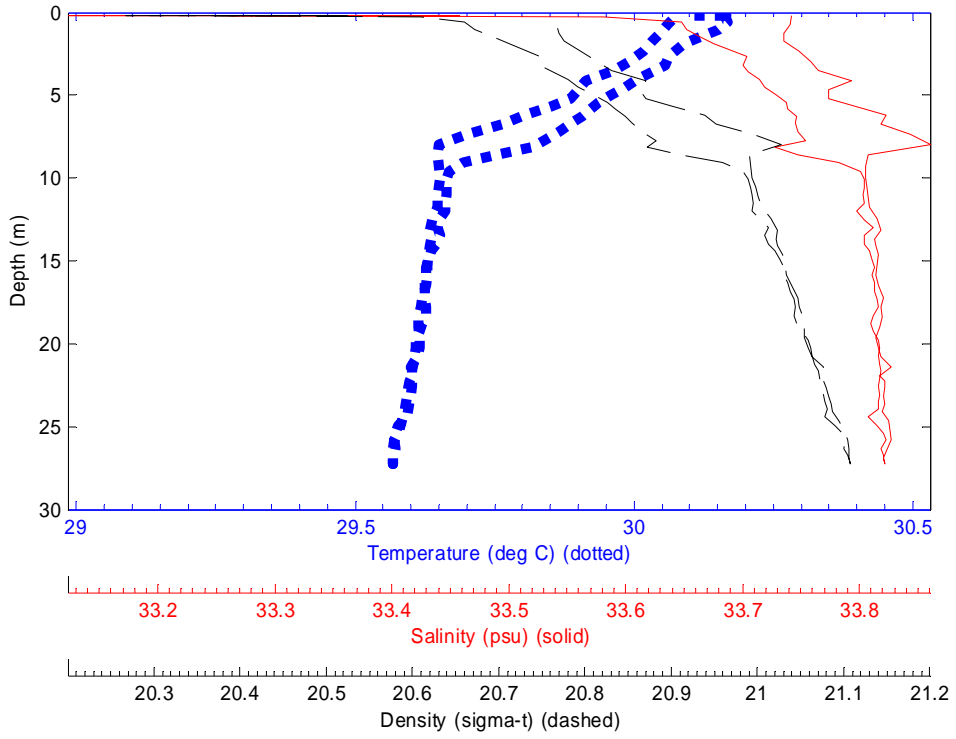
File: 0911002 09-Nov-2003 15:56:01 S7.2472 E134.4664 Site: 11C3



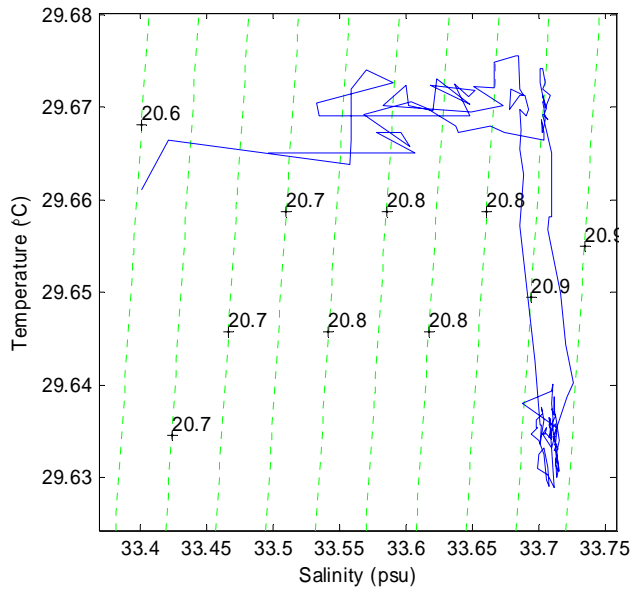
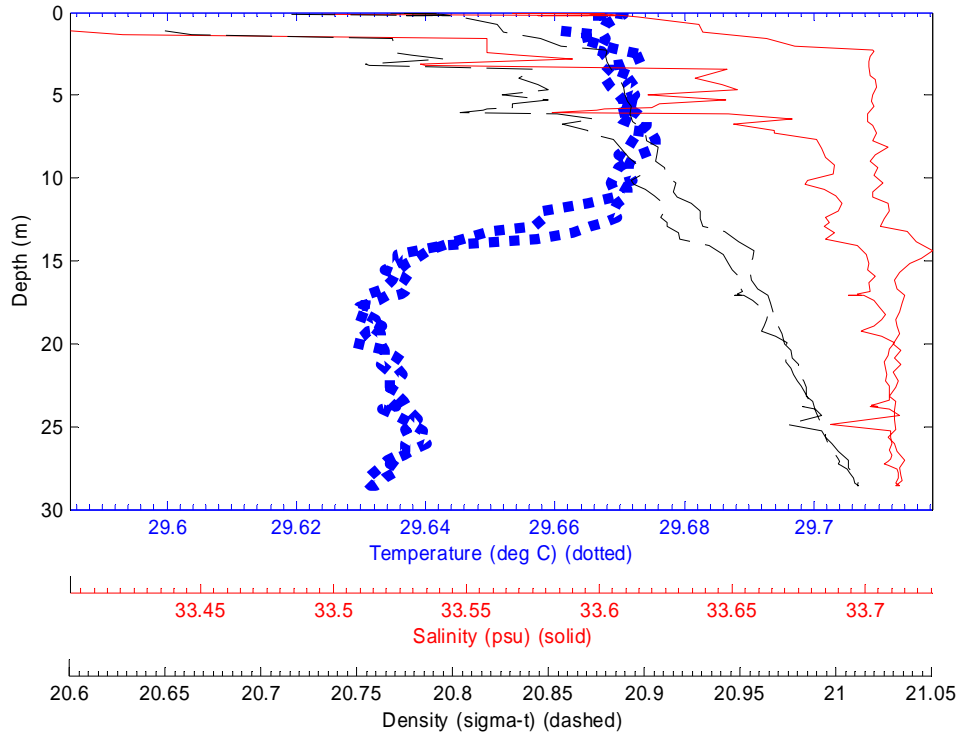
File: 0911003 09-Nov-2003 16:35:46 S7.3435 E134.5722 Site: 10A1



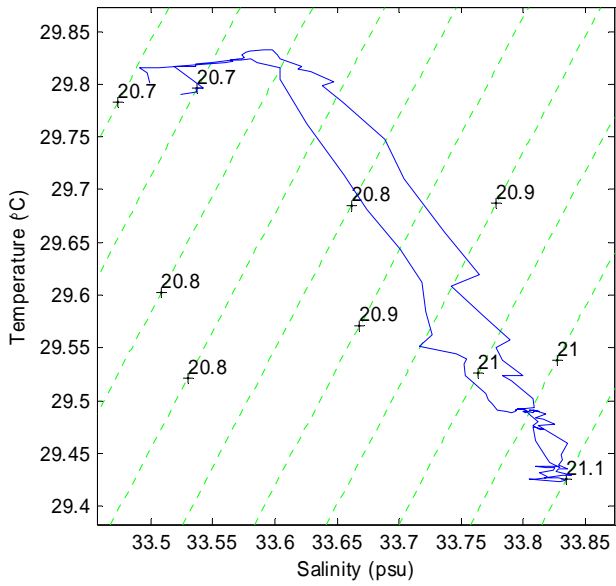
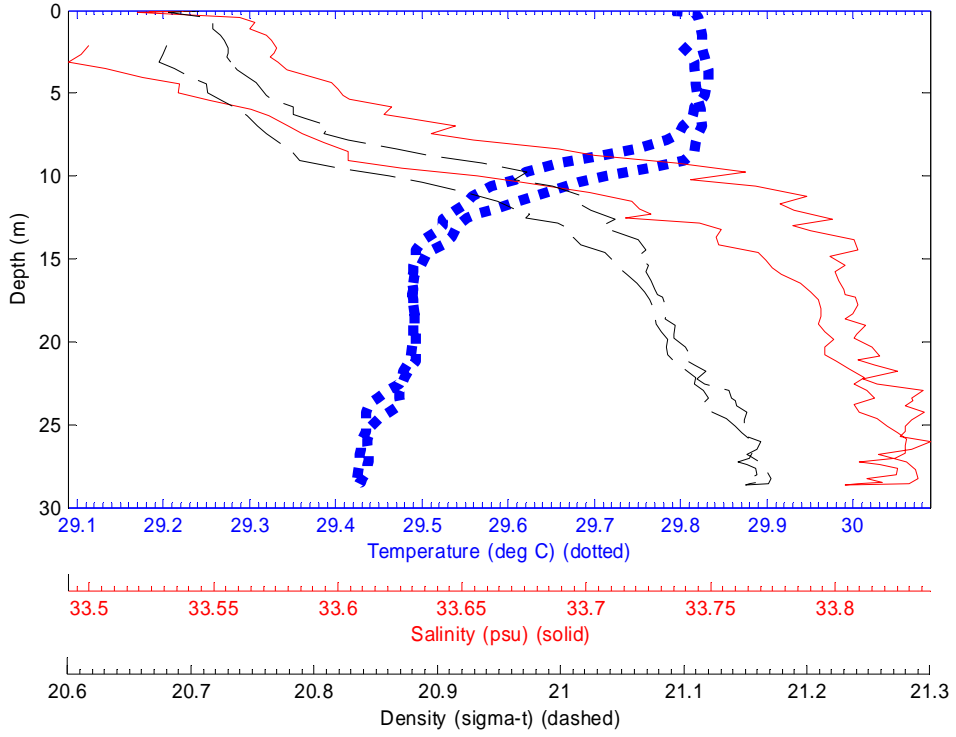
File: 0911004 09-Nov-2003 17:33:09 S7.3676 E134.5999 Site: CTD4



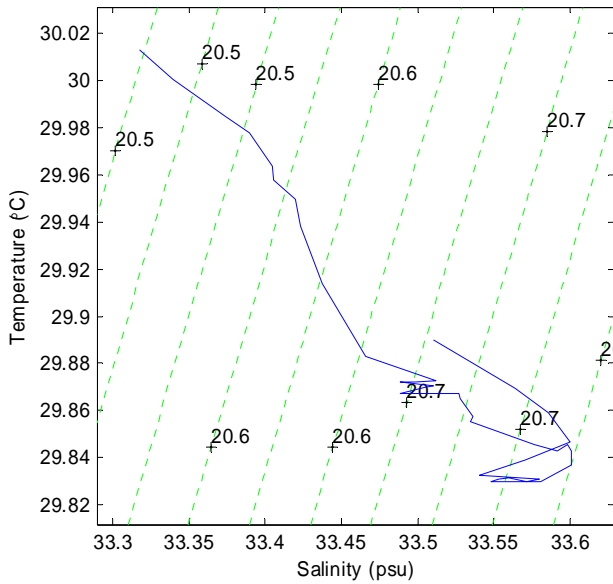
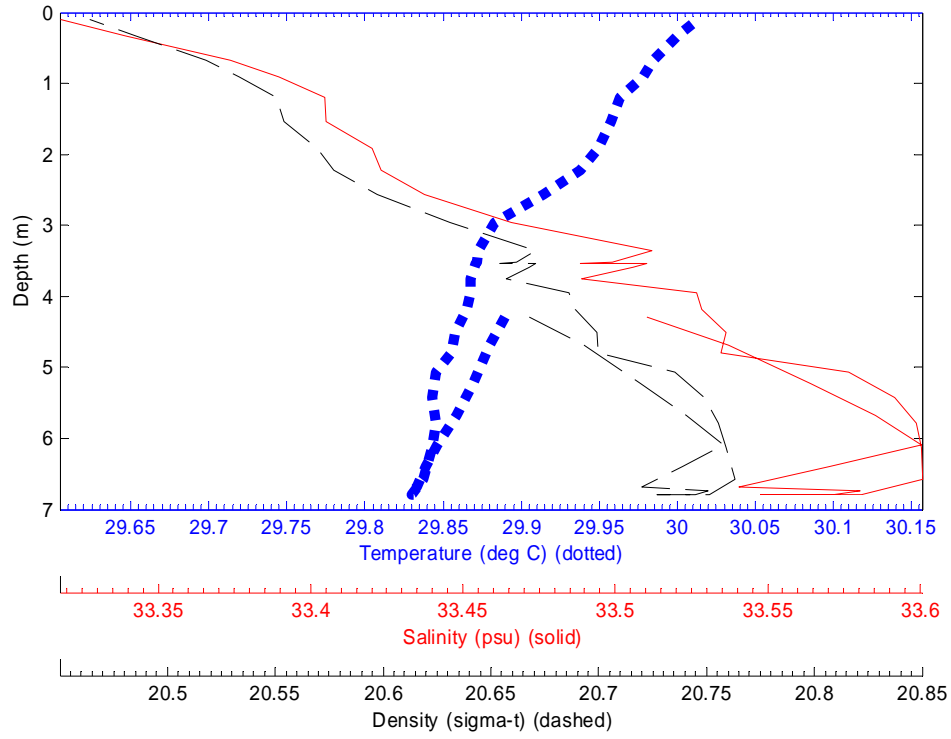
File: 1111000 11-Nov-2003 09:31:36 S7.6084 E134.5218 Site: 6A



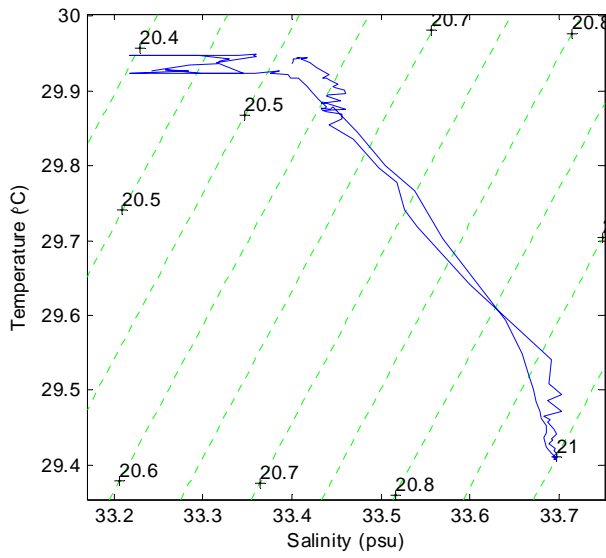
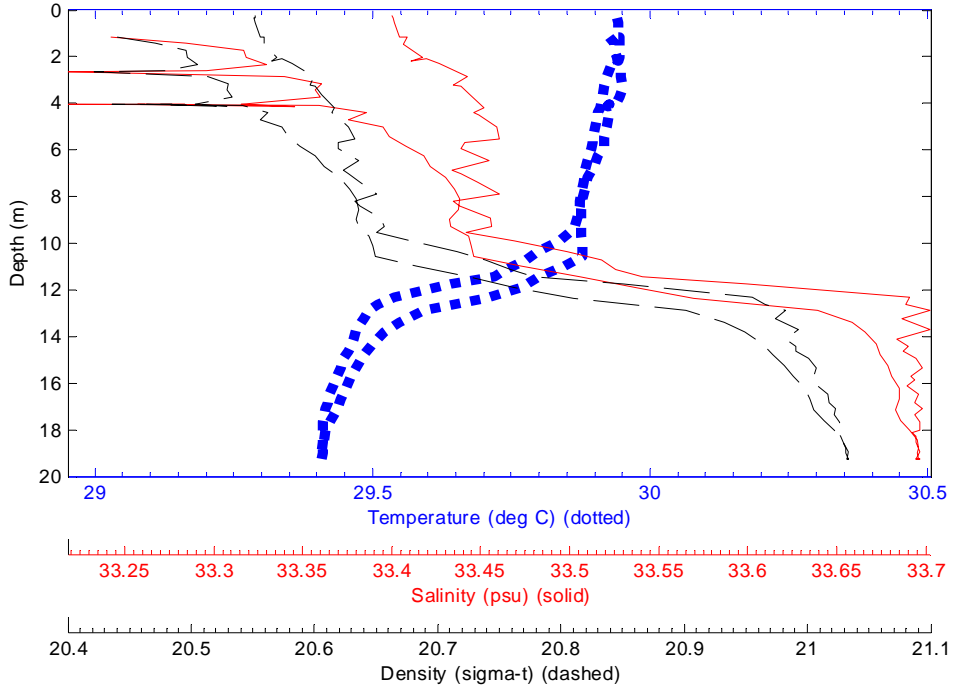
File: 1111001 11-Nov-2003 10:11:45 S7.6282 E134.5511 Site: 6Af



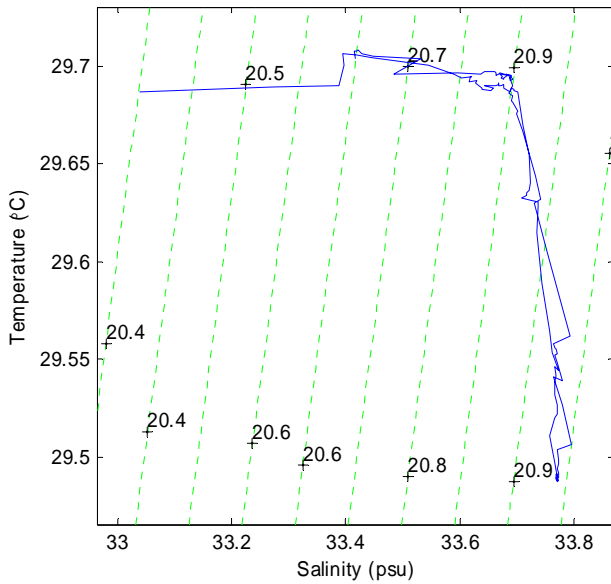
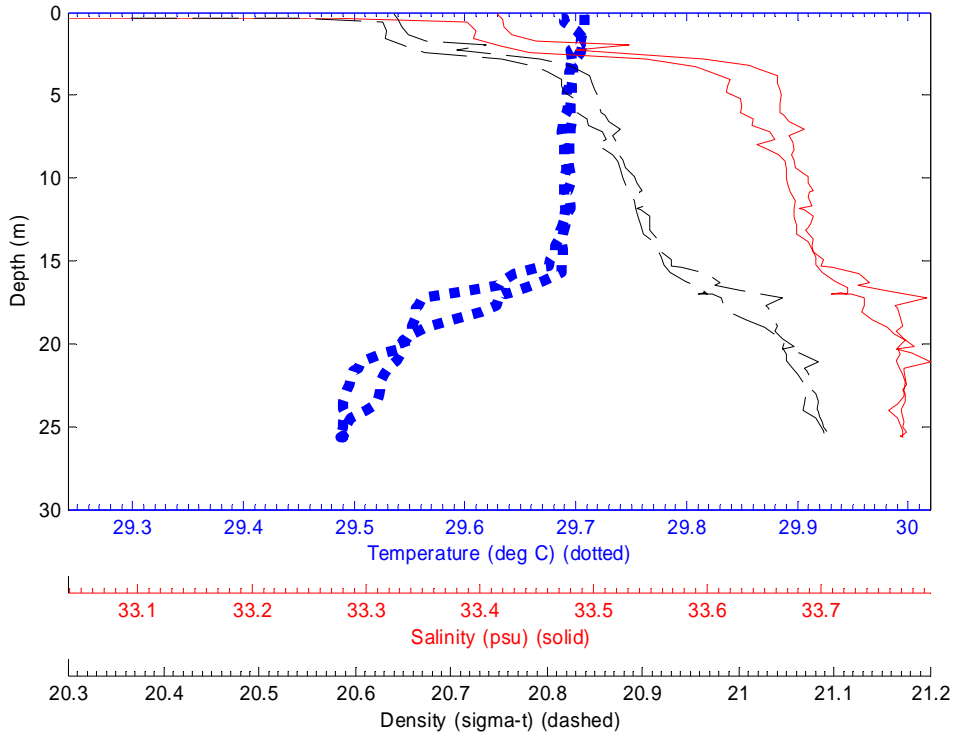
File: 1111002 11-Nov-2003 10:47:05 S7.6609 E134.6241 Site: 5As



File: 1111004 11-Nov-2003 12:19:38 S7.6286 E134.6019 Site: 5bs



File: 1111005 11-Nov-2003 13:07:23 S7.6768 E134.615 Site: 5bf



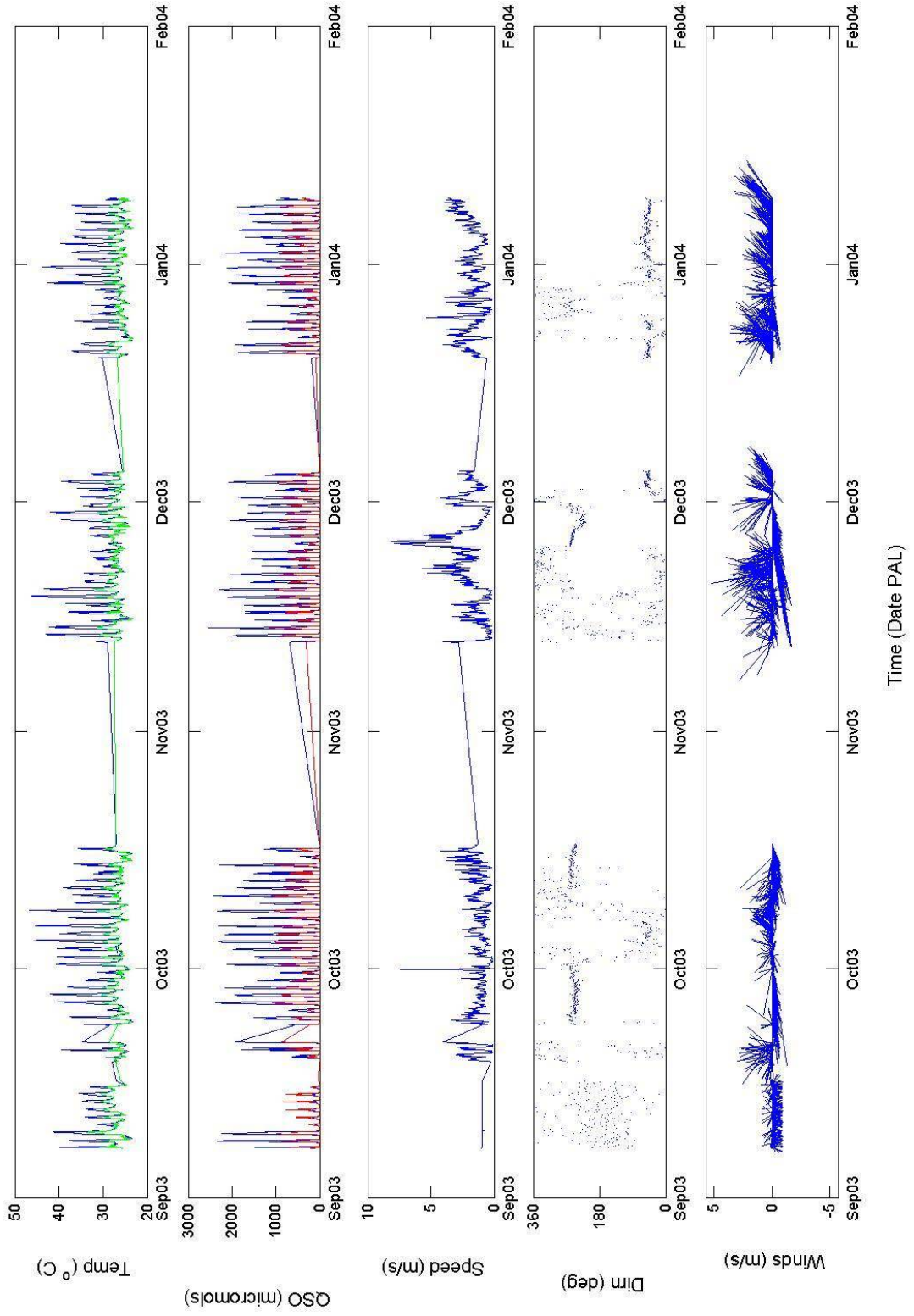
Appendix L – Time Series Plots of Weather Data

Two figures are presented for the portable weather station (WXSTA) data; the first shows the entire deployment and the second is zoomed to the Sep-Oct period. On each of these figures, two air temperatures (direct sunlight – blue; shaded – green) are presented together on the first plot, with axis label “Temp”. The data from two radiation measurements (Short-Wave Radiation – red; Photosynthetically Active Radiation (PAR) – blue) are shown on the second plot; the axis label, QSO, stands for Quantum Sensor Output. The two radiation measurements, although plotted together, differ in their units. The PAR has units of $\mu\text{mol}\cdot\text{m}^{-2}\cdot\text{s}^{-1}$, whereas short wave radiation is in units of Wm^{-2} . Wind speed and direction are shown on the third and fourth plots. The fifth plot represents the wind data as a quiver plot, as described in [Appendix H](#) for ocean currents.

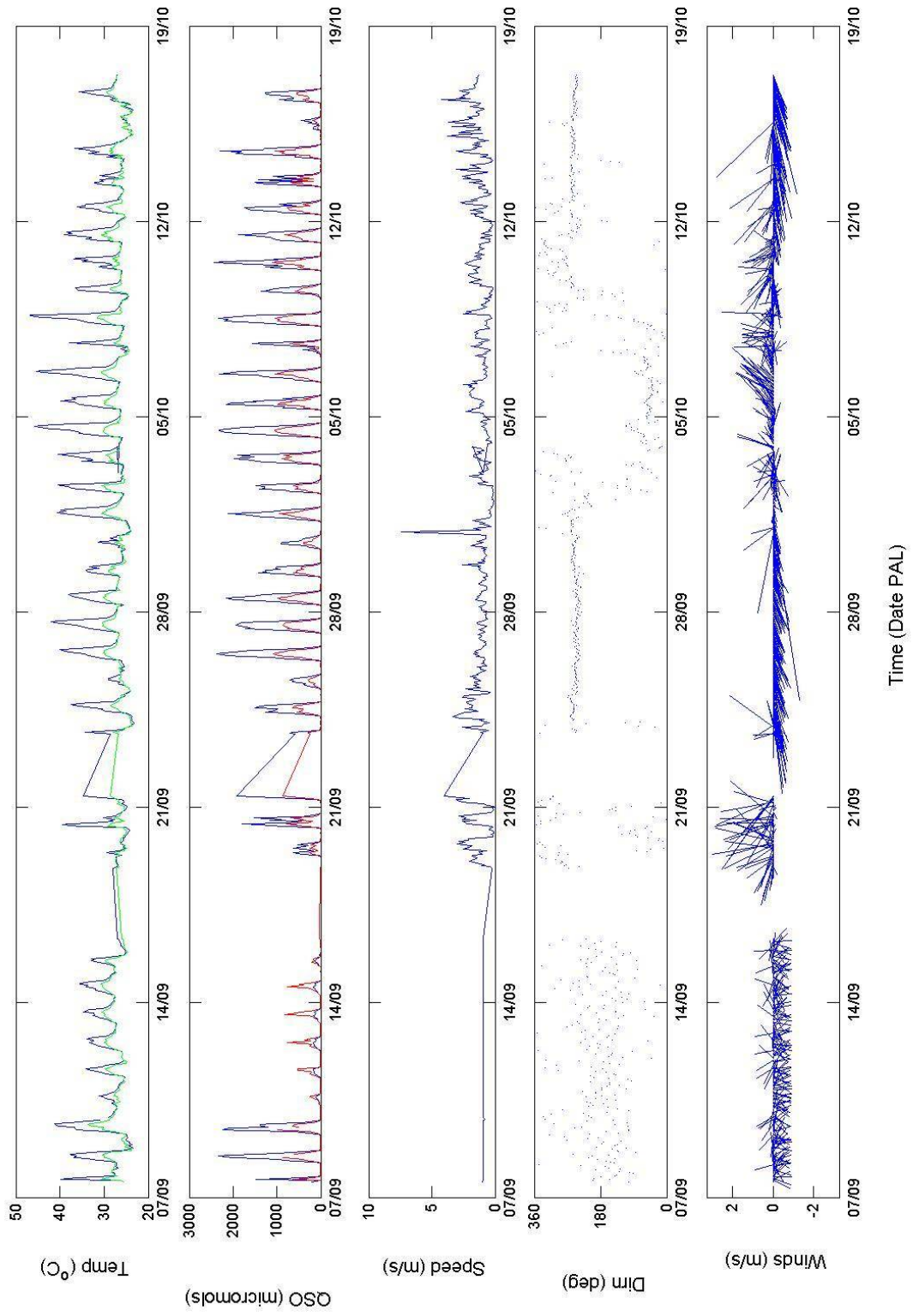
The NOAA data are presented in a single figure with plots of temperature, atmospheric pressure, wind speed, wind direction and the quiver plot of winds.

Unit Conversions for PAR: $1 \mu\text{Einstein} = 6.02 \times 10^{17} \text{ photons s}^{-1} \text{ m}^{-2} = 1 \mu\text{mols m}^{-2} \text{ s}^{-1}$

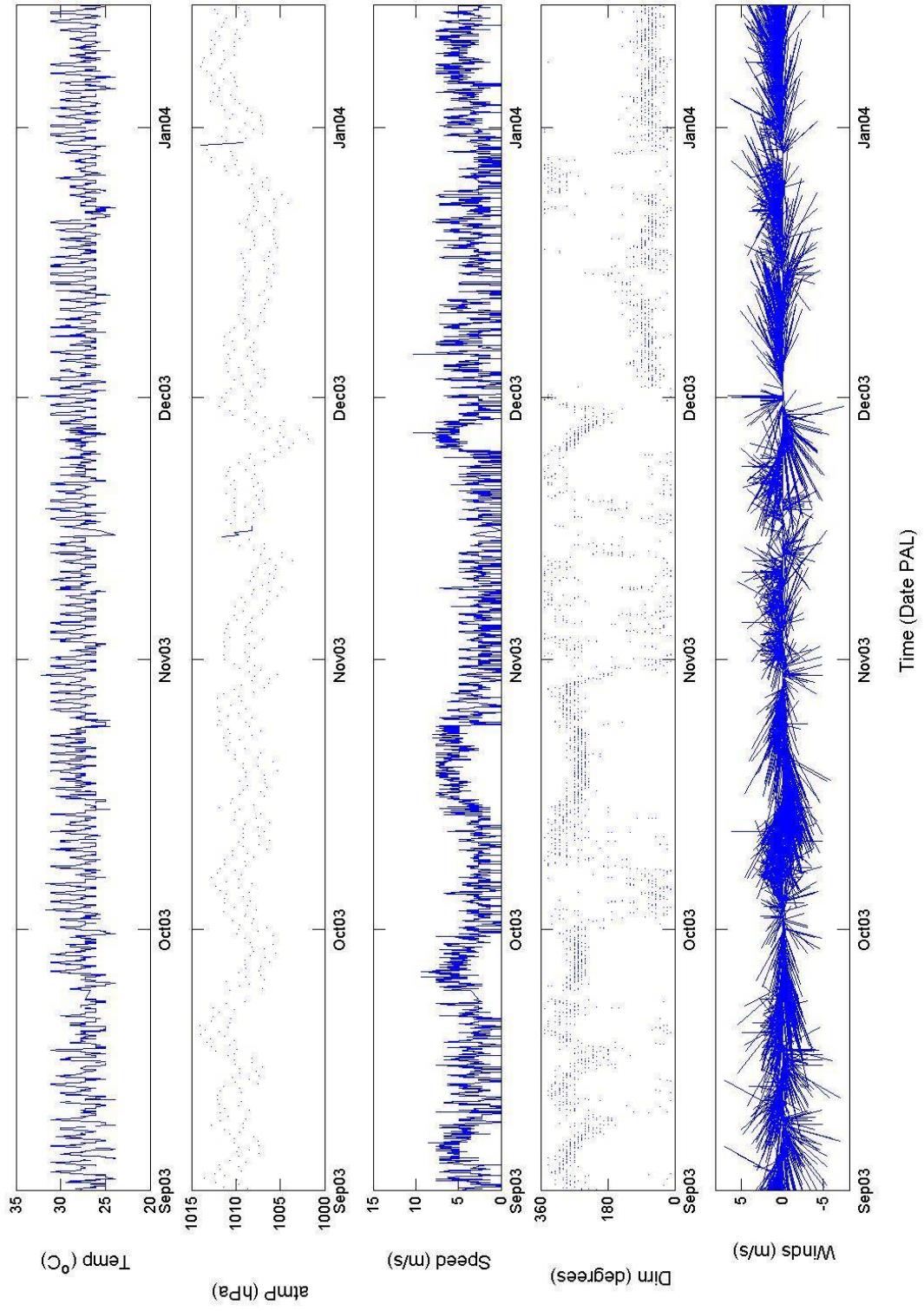
WXSTA - Palau



WXSTA - Palau, Sep-Oct 2003



NOAA NWS - Palau



Appendix M – Data Format & File naming conventions

Each instrument’s output data has its own, often manufacturer-specific, format when downloaded. From these, a standard file format is produced utilising MATLAB, a widely-used analysis package. The MATLAB data are binary; however, they can easily be reformatted to alternative formats, such as ASCII, from within the MATLAB environment.

File naming convention

File names are attributed according to the naming conventions associated with each particular project. The file prefix is made up of a 2 or 3 character instrument type and site number, and a 2 character position code, with further characters appended to help understand what type/s of data the file contains and what processing has been performed. The MATLAB files have a default filename extension ‘.mat’.

Example names are A10i1uv.m.mat and T4i3t.mat

Table 7 Filename tags

Instrument Type Processing	Site Number	Position	Parameter
A – current meters p,r,o,l,h	1-14	i1-7	uv, uvw, uvm
B – tide gauges	1-6	i1	tl
C – salinity	1-5	i1	tc
T – Temperature transect	1-8	i1-7	t,tl

Instrument Type and **Site Number** codes can be found in the [Instrument Array Summary](#) section in the main part of this document. The tables in that section cross reference to actual location names, and a later table lists their geographic position coordinates.

Position codes indicate an instrument’s vertical position, as listed in The [Temperature Transect and Mooring Summary](#) section. The letter “i” precedes a number where 1 is the deepest instrument at the site and each higher instrument is given a consecutively higher number. If two loggers are located at the same depth, they are given the same number. Therefore the deepest instrument position on mooring A10 would be A10i1 or for transect T4 – T4i1.

Parameter codes, the final tag/s, indicate what variables are being measured by the instrument. Multiple tags are used to classify loggers with more than one sensor. Thus the instrument at mooring A10, which measured current profiles, has the codename A10i1uv.m. The “m” indicates a matrix of data instead of a vector from single point measurements. The temperature (t) and water level (l) are sometimes suppressed for the current meters.

Processing codes are used to indicate level of data processing, specifically:
p – prediction, r – residual, o – observed, l – low passed, h – high passed

CTD casts are named using the following naming convention: ddmmnnn, with dd being the day, mm the month and nnn being the cast number starting from zero. Data were processed from raw *.hex files to *.cnv using the manufacturer software. They were then edited to in-water values.

ASCII Data Format

Most data were downloaded from the instruments in a binary or hexadecimal format. Manufacturer’s software was then used to convert to American Standard Code for Information Interchange (ASCII) prior to ingestion into MATLAB for visualisation and analysis. ASCII is potentially the most easily-read format for this data where MATLAB is not available. These files can simply be inspected in any common text file viewer and most are self-explanatory.

ASCII files for individual instruments are listed in the instrument deployment tables in Appendices [B](#), [C](#), [D](#), [E](#) and [F](#). For instruments deployed in transects or on moorings, the file names are summarised in the [Temperature Transect and Mooring Summary](#) section. The original instrument output files were archived by instrument type in the “Raw Data” folder ([Appendix N](#)). A description of the ASCII-output format from the RDI ADCP instruments is provided here due to the complexity of the data file.

RDI ADCP data were converted to ASCII using the manufacturer software package, WinADCP. Due to their size, these files were compressed (*.zip) for inclusion in the DVD archive. While the ASCII files are provided with this report, it is recommended that the manufacturer’s software be obtained by individual users as it provides a method to view and export the data. The software is available at the RDInstruments website (<http://www.rdinstruments.com/>); while the package is free-of-charge, registration is required for download. To register, select “Customer Support” from the option column at the left of the screen and then follow the “Request Registration” link in the text. Fill in the required fields; for the type of ADCP, enter “300-kHz Workhorse Sentinel”. After submitting the form, RDI will provide access information via email. Upon receipt of this information, the downloading process requires, as input, parameters from one instrument. The necessary parameters from the instrument deployed at location A5 are:

ADCP Serial number – WH 412
Frequency – 300 kHz
Type – Real time fixed

An example of the use of the WinADCP software is provided here. RDI ADCP binary data files for this study have a filename of the form “PAL02000.000”. To open a binary file from WinADCP go to the “File” menu and select “Open”. In the pop-up window select the data file to be opened and click “Open”. Binary data files output by BroadBand and WorkHorse ADCP instruments may be accessed by this process. Figure 14 is a screen-capture of the WinADCP workspace displaying data from the file PAL02000.000. A summary of the setup of the instrument and logging parameters is

shown in the upper-left sub-window, labelled “WinADCP Information”; the full dataset is displayed in the upper-right sub-window, labelled “Whole Set”; and a zoomed image of data from the first 64-hours of the deployment is shown in the bottom sub-window, labelled “Sub Set”.

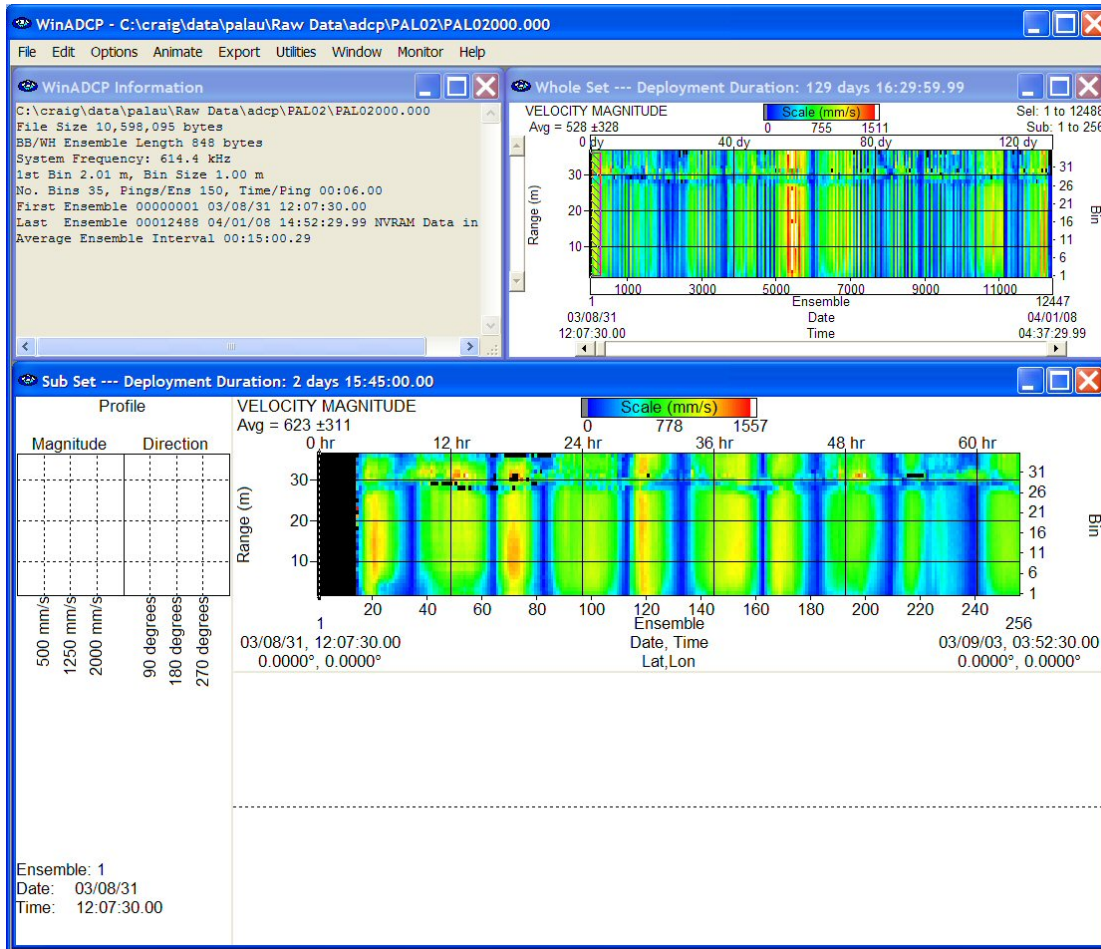


Figure 14 Screen-capture of the WinADCP data viewer

To export data from WinADCP click on the “Export” menu; this opens the Export Options control box (Figure 15). In the “Series/Ancillary” tab, select the output file type (text or MATLAB); the required bins; the time-series data desired; the ancillary data desired; and which ensembles (i.e., timesteps of data) are required for downloading.

Selecting the items as shown Figure 15 will replicate the ASCII data supplied on the accompanying DVD. The format for the text output is shown in Table 8. General header information is listed, followed by the matrix of data. The number of columns in the matrix depends on the export options chosen; each column header containing short-forms of the variable name and units. Each row in the matrix represents one ensemble average; i.e., one time period of measurement. For the deployment shown, a total of 12488

ensemble averages were made. The first column lists the ensemble number and the subsequent eight columns show the ancillary data (as selected from Figure 15). The remaining columns contain time series data for each selected variable, grouped by the number of bins in the vertical profile (thirty-five in this case). The first thirty-five of these columns contain data of the first variable; the second set of thirty-five columns contains data of the second variable; etc. For compactness, only the values from the first bin (nearest the instrument) are presented here. The variables shown in Table 8 reflect those selected in the export options window; i.e., the average of the 4-beam echo amplitudes (EAA); the correlations for each bin (C1); the east component of velocity; the north component of velocity; the vertical component of velocity; the error in the magnitude of velocity; the velocity magnitude; and the velocity direction.

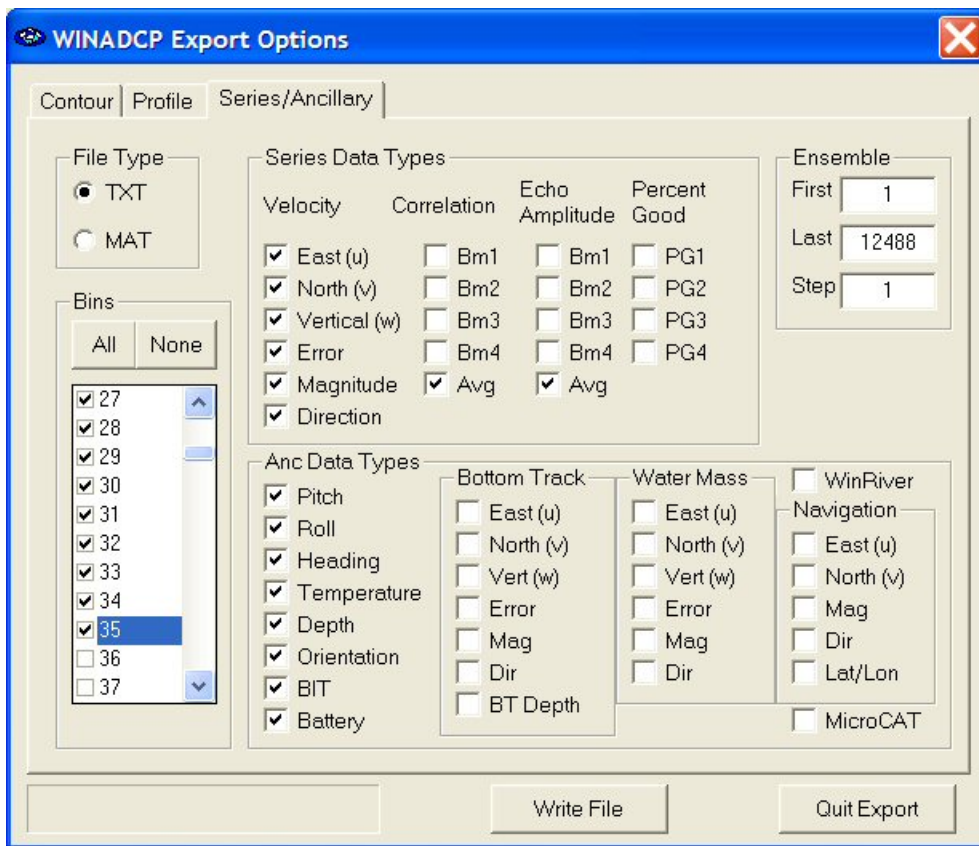


Figure 15 Screen-capture of the WinADCP export options

MATLAB Data Format

MATLAB is a commonly-used scientific programming language with high-level visualisation capabilities. For this reason, the data collected in this study have been archived using the MATLAB format. Metadata are contained within the MATLAB data files. After loading a data file, the program “hdrmat.m” displays a summary of the information. An example for the current profiler A5 is shown in Table 9.

Table 9 Example output for header from the current profiler, A5

```
>> load a5iluvmt
>> hdrmat

Palau A5 RDI ADCP 412
Instrument Depth 215 m

start          finish          si      tz
17-Sep-2003 11:30:00 13-Jan-2004 14:45:00 15      -9

Time series statistics
Variable      Min           Max           Mean          Units
Temp          9.30000      13.27000     10.82724     deg C
Depth         210.00000    215.20000    210.58688     m
Dirn          0.00000      359.61467    140.72883    degrees
Speed         0.00000      293.48284     9.29600      cm/s
U             -98.20000    291.70000     3.24222      cm/s
V            -138.80000   193.30000     1.63225      cm/s

>> whos
Name          Size          Bytes  Class

attributes    1x1           2028   struct array
depth         1x11342       90736  double array
dirn          23x11342     2086928 double array
speed         23x11342     2086928 double array
temp          1x11342       90736  double array
time          1x11342       90736  double array
u             23x11342     2086928 double array
units         1x1           1714   struct array
v             23x11342     2086928 double array
w             23x11342     2086928 double array
z             23x1         184    double array
```

Variables

The MATLAB file associated with each instrument contains the variable names listed in the adjacent table, as appropriate to the sensors. Each data point is placed into a vector based on its data type and sample number. In addition, the time when each data point is sampled is written to the time vector element with the corresponding sample number. Time, temperature (temp), instrument depth (depth), salinity (sal), and density (sigma_t) are always vectors.

Currents, however, can be measured at either a particular location (point current meter) or at several locations throughout the water column (current profiler). If the logger measures at only one location, as is the case with an S4 current meter, the velocity data are stored in four, one-dimensional vectors: eastward velocity (u), northward velocity (v), magnitude (speed), and direction (dirn). If several currents are measured at different depths, the data are stored in several matrices (or arrays). The currents are placed into bins (in accordance with the instrument setup) based on their depth. The data from each bin occupy a row of the matrix. Additionally, the column vector, z, identifies the height of the bins. Thus the depth of the fourth bin from the bottom is tabulated as the fourth element of column vector, z. The northward currents measured at this depth are recorded in the fourth row of the matrix, v. Current profiler instrument files have a vertical velocity (w) matrix in addition to the eastward velocity (u), northward velocity (v), magnitude (speed), and direction (dirn) matrices. For Nortek Aquadopp Current Profilers, the count of measured particles at each bin for each sampling interval is also recorded. These values are arranged in the matrices au, av, and aw and correspond to the matrices u, v, and w respectively.

time
temp
depth
speed
dirn
sal
sigma_t
z
u
v
w
au
av
aw
attributes
units

The final two parameters are attributes and units. Unlike the other variables which are all vector based, these are structure arrays. They contain pertinent information regarding the instrument and the units for each of the variables. Thus, every data file will contain both the *attributes* and *units* variables. Table 10 lists the *attributes* and *units* fields and values for the Uchelbeluu deepwater current profiler (A5).

Attributes

Information, such as the instrument make and serial number, are stored as fields in the *attributes* structure array. All instrument files have the same core of attributes listed in Table 10. A standard core of attributes allows MATLAB scripts to easily retrieve information among different instruments. Profiler data contain additional attribute fields which describe how the bins are set up.

Units

Like *attributes*, *units* are also structure arrays. The *units* field names are the same as *variable* and *attribute* names, such as temp and instrument_depth. However, the values are all strings describing the units of the named parameter. The number of fields in a *units* structure array vary from instrument to instrument and depend on which variables are measured.

Table 10 Example listing of attributes and units from the current profiler, A5

```
attributes =  
  
    tz: 9  
    si: 900  
ensemble_period: 900  
  project: 'Palau'  
    lat: 7.2653  
    lon: 134.5566  
    site: 'A5'  
  serial: '412'  
    make: 'RDI ADCP'  
instrument_depth: 215  
  cell_size: 5  
blanking_distance: 1.7600  
  bin_depth: [1x23 double]  
  top_bin: 23
```

```
units =  
  
    time: 'serial date'  
    si: 'seconds'  
    u: 'cm/s'  
    v: 'cm/s'  
    w: 'cm/s'  
    temp: 'deg C'  
    depth: 'm'  
instrument_depth: 'm'  
  cell_size: 'm'  
blanking_distance: 'm'  
    speed: 'cm/s'  
    dirn: 'degrees'  
    z: 'm'
```

Other computing languages

MATLAB binary files can be read directly into other programming languages (Fortran, C). Programs to access data are provided in each of these languages at the Mathworks web site:

http://www.mathworks.com/access/helpdesk/help/techdoc/matlab_external/matlab_external.html.

Appendix N – Data Archive

Data are stored on a companion DVD-ROM and is structured as shown in Figure 16. This document, “Palau Oceanographic Array Data Report.doc”, is contained in the Documents subdirectory.

The Raw Data have been organised by instrument type; whereas, the processed data are organised by variable type – Currents, CTD, Salinity, Sealevels, Temperatures and Weather. Temperature mooring and transect data were consolidated and placed in the Tempprofiles subdirectory. The summary data plots can also be found under each of variable type as shown below for currents.

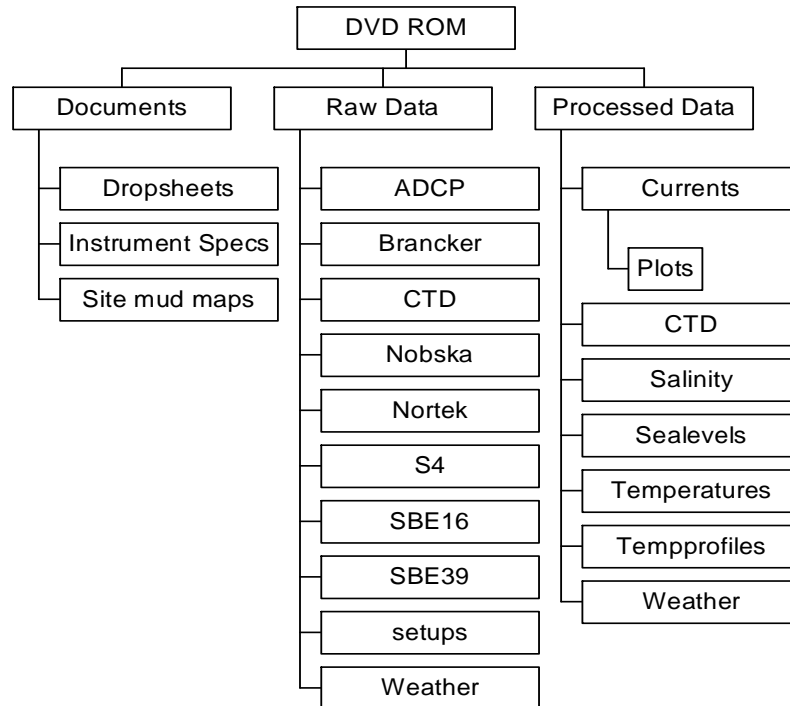


Figure 16 Archival DVD-ROM directory structure

Appendix 2

Seasonal Variations of the Ocean Surface Circulation in the Vicinity of Palau

Scott F. Heron, E. Joseph Metzger, and William J. Skirving

Abstract

The surface circulation in the western equatorial Pacific Ocean is investigated with the aim of describing intra-annual variations near Palau (134°30' E, 7°30' N). *In situ* data and model output from the Ocean Surface Currents Analysis—Real-time, TRIangle Trans-Ocean buoy Network, Naval Research Laboratory Layered Ocean Model and the Joint Archive for Shipboard ADCP are examined and compared. Known major currents and eddies of the western equatorial Pacific are observed and discussed, and previously undocumented features are identified and named (Palau Eddy, Caroline Eddy, Micronesian Eddy). The circulation at Palau follows a seasonal variation aligned with that of the Asian monsoon (December–April; July–October) and is driven by the major circulation features. From December to April, currents around Palau are generally directed northward with speeds of approximately 20 cm/s, influenced by the North Equatorial Counter-Current and the Mindanao Eddy. The current direction turns slightly clockwise through this boreal winter period, due to the northern migration of the Mindanao Eddy. During April–May, the current west of Palau is reduced to 15 cm/s as the Mindanao Eddy weakens. East of Palau, a cyclonic eddy (Palau Eddy) forms producing southward flow of around 25 cm/s. The flow during the period July to September is disordered with no influence from major circulation features. The current is generally northward west of Palau and southward to the east, each with speeds on the order of 5 cm/s. During October, as the Palau Eddy reforms, the southward current to the east of Palau increases to 15 cm/s. During November, the circulation transitions to the north-directed winter regime.

Citation:

Heron, S.F., E.J. Metzger and W.J. Skirving. (2006). Observations of the ocean surface circulation in the vicinity of Palau. *Journal of Oceanography*, 62, 413-426.

The text of this article is reprinted in this document with permission from *The Journal of Oceanography*, The Oceanographic Society of Japan, Tokyo, Japan. Please use the above citation for any information in this article.

Seasonal Variations of the Ocean Surface Circulation in the Vicinity of Palau

SCOTT F. HERON^{1*}, E. JOSEPH METZGER² and WILLIAM J. SKIRVING¹

¹*Coral Reef Watch, NOAA/NESDIS/ORA, E/RA31, SSMCI,
1335 East-West Highway, Silver Spring, MD 20910, U.S.A.*

²*Naval Research Laboratory, Stennis Space Center, MS 39529-5004, U.S.A.*

(Received 2 August 2005; in revised form 17 January 2006; accepted 18 January 2006)

The surface circulation in the western equatorial Pacific Ocean is investigated with the aim of describing intra-annual variations near Palau (134°30' E, 7°30' N). *In situ* data and model output from the Ocean Surface Currents Analysis—Real-time, TRiangle Trans-Ocean buoy Network, Naval Research Laboratory Layered Ocean Model and the Joint Archive for Shipboard ADCP are examined and compared. Known major currents and eddies of the western equatorial Pacific are observed and discussed, and previously undocumented features are identified and named (Palau Eddy, Caroline Eddy, Micronesian Eddy). The circulation at Palau follows a seasonal variation aligned with that of the Asian monsoon (December–April; July–October) and is driven by the major circulation features. From December to April, currents around Palau are generally directed northward with speeds of approximately 20 cm/s, influenced by the North Equatorial Counter-Current and the Mindanao Eddy. The current direction turns slightly clockwise through this boreal winter period, due to the northern migration of the Mindanao Eddy. During April–May, the current west of Palau is reduced to 15 cm/s as the Mindanao Eddy weakens. East of Palau, a cyclonic eddy (Palau Eddy) forms producing southward flow of around 25 cm/s. The flow during the period July to September is disordered with no influence from major circulation features. The current is generally northward west of Palau and southward to the east, each with speeds on the order of 5 cm/s. During October, as the Palau Eddy reforms, the southward current to the east of Palau increases to 15 cm/s. During November, the circulation transitions to the north-directed winter regime.

Keywords:

- Ocean surface circulation,
- seasonal variation,
- western equatorial Pacific,
- Palau.

1. Introduction

The western equatorial Pacific Ocean is a key region of the world for climate studies that is difficult to describe due to its highly variable nature. Descriptions of the general circulation in the western equatorial Pacific Ocean that have focused on the major current systems of the North Equatorial Current (NEC), the Mindanao Current (MC), the Kuroshio, the North Equatorial Counter-Current (NECC) and the Indonesian Through-Flow (ITF) include the work of Toole *et al.* (1988), Lukas (1988), Lukas *et al.* (1991), Qu *et al.* (1998) and Qu and Lukas (2003). Two major mesoscale eddies reported in this region are the Mindanao Eddy (ME) and

Halmahera Eddy (HE). Specific studies have examined the high- and low-frequency variability of these features (e.g., Lukas, 1988; Arief and Murray, 1996; Qiu and Lukas, 1996; Kashino *et al.*, 2001; Yaremchuk and Qu, 2004). Circulation studies in basins adjacent to the western Pacific have also been undertaken, e.g., the South China Sea (Metzger, 2003), and the Celebes and Maluku Seas (Kashino *et al.*, 2001). Lukas *et al.* (1991) described observations of current measurements from the Western Equatorial Pacific Ocean Circulation Study (WEPOCS) III conducted in the middle of 1988. Surface drifter and acoustic Doppler current profiler (ADCP) data were combined to produce a map of ocean currents that clearly showed the MC, ME, HE, NECC and portions of the ITF. Metzger *et al.* (1992) used these data as validation in a global ocean model. The model generated the same features from the WEPOCS III data with good effect and supplied further circulation detail in data-barren regions.

* Corresponding author. E-mail: Scott.Heron@noaa.gov

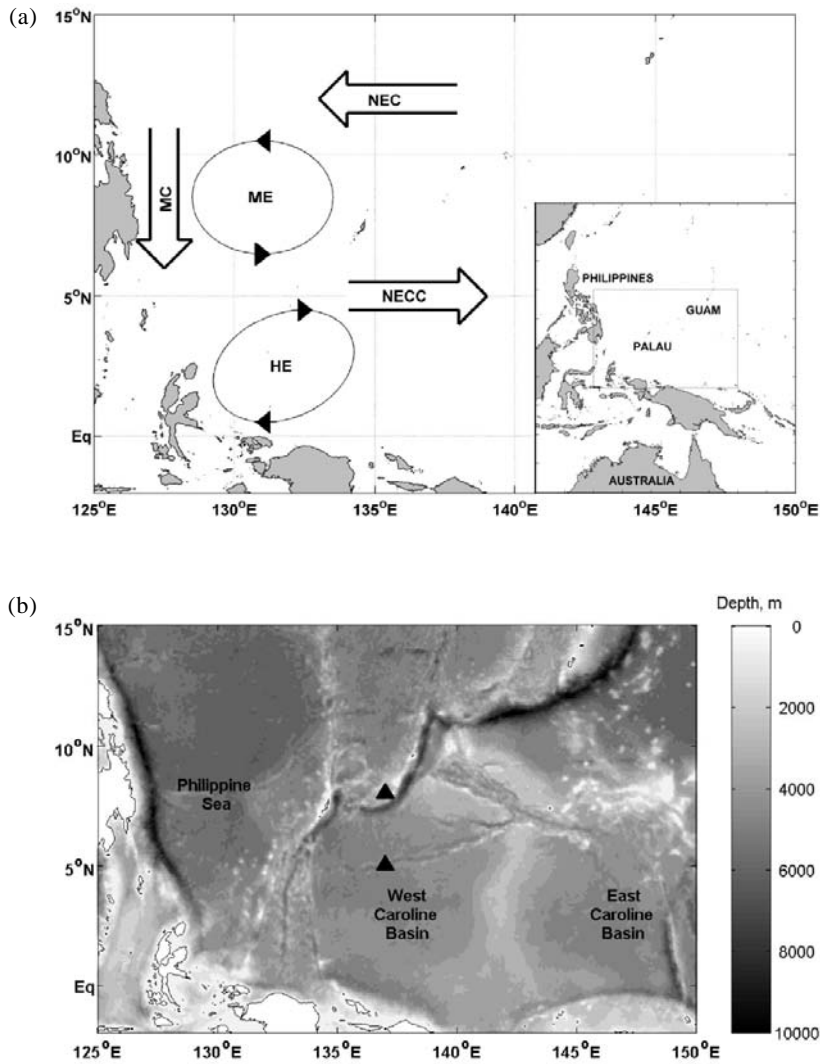


Fig. 1. (a) Schematic of the major ocean circulation features within the study area. Inset shows the geography of the western equatorial Pacific Ocean, with the study area indicated by the dashed box. (b) Smith and Sandwell (1997) bathymetry of study area. Triangles indicate the locations of TRITON buoys from which data are used.

However, to our knowledge, no existing investigations have focused on the circulation patterns in the immediate vicinity around Palau. The western equatorial Pacific is of significant interest in global ocean dynamics and the transport of waters in this region is important in understanding mass, heat and salt exchange. Physical connectivity of the remote Micronesian islands is an important factor for biological development; coral distribution and fish migration and reproduction are examples of biological processes that depend on physical ocean parameters.

The major islands of Palau are grouped together in the western Pacific Ocean 850 km east of the Philippine island of Mindanao, near 7°30' N, 134°30' E. Figure 1(a) shows the location of Palau and schematically illustrates the reported oceanographic features previously men-

tioned. These islands are at the peak of a topographic ridge that stretches to the SSW where the smaller island groups of Palau are found. This ridge separates the waters surrounding Palau into the Philippine Sea to the west of Palau, and the West Caroline Basin. Figure 1(b) shows the bathymetry of the western equatorial Pacific from the two-minute resolution data of Smith and Sandwell (1997). A rapid drop-off from the Palau Ridge to depths greater than 4000 m can be seen immediately to the east and west.

This work investigates seasonal characteristics of the ocean surface circulation in the region surrounding Palau. Existing satellite-derived and *in situ* data are collated and examined to identify general circulation features. Due to the spatially and temporally sparse nature of oceanographic data, particularly in the western equatorial Pa-

cific, output from a numerical model is also studied. To describe the ocean circulation near Palau, it is pertinent to first examine the larger scale features that may influence the Palauan waters. Thus, this study includes the ocean region bounded by 125–150°E and 2°S–15°N, as illustrated in Fig. 1(a).

The sources from which data were acquired to study the surface circulation are described in Section 2. The observations from each data source are summarized in Section 3 and then compared in Section 4 to determine consistency in the flow description. Section 5 summarizes the seasonal variations observed in surface waters around Palau.

2. Data Sources

2.1 Ocean Surface Currents Analyses—Real-time (OSCAR)

The Ocean Surface Currents Analyses—Real-time (OSCAR) derives sea surface currents from satellite observations for the global ocean, as described in Bonjean and Lagerloef (2002). Altimeter-derived sea surface height (SSH) and winds from scatterometer data are the primary input sources to OSCAR, with sea surface temperature (SST) data used as a secondary source. The SSH is gridded to 1° resolution, smoothed and then used to calculate geostrophic motion. This is linearly combined with the wind-driven (Stommel/Ekman) component. The accuracy of the OSCAR system is still under investigation. Surface current data were downloaded from the OSCAR website, <http://www.oscar.noaa.gov>. The time resolution is defined by the repeat period of the satellites, the minimum of which is 10-days for Jason-1. The database spanned eleven complete years, 1993–2003.

2.2 TRIangle Trans-Ocean buoy Network (TRITON)

The TRIangle Trans-Ocean buoy Network (TRITON) is a series of eighteen buoys deployed in the equatorial regions of the Pacific and Indian Oceans (<http://www.jamstec.go.jp/jamstec/TRITON/>). Mounted instruments provide information on the upper-ocean and surface meteorology. Surface wind data recorded by two TRITON buoys, located in the vicinity of Palau, were accessed from the TRITON website. The TRITON buoys located at 8°N, 137°E and 5°N, 137°E (Fig. 1(b)) provide the only *in situ*, extended observational data record near to Palau. However, the datasets from these buoys only span the periods of September 2001 to June 2003 and September 2001 to November 2003, respectively. The wind speed and direction were measured at a height of 4 m from the ocean surface and were sampled once every 5 seconds for a period of two minutes. The two-minute averages were recorded every ten minutes. Six such records were then averaged and published on the website as hourly means. To examine seasonal variability in the wind field,

the hourly mean data were smoothed to eliminate high-frequency components.

2.3 NRL Layered Ocean Model (NLOM)

Output from the Naval Research Laboratory (NRL) Layered Ocean Model (NLOM) is also examined for the study region. NLOM is part of a real-time, eddy-resolving, nearly global ocean nowcast/forecast system (http://www7320.nrlssc.navy.mil/global_nlom) running daily at the Naval Oceanographic Office. It has a horizontal resolution of 1/16° and seven layers in the vertical, including a Kraus-Turner type bulk mixed layer. The model is forced with winds and heat fluxes from the Fleet Numerical Meteorology and Oceanography Center (FNMOC) Navy Operational Global Atmospheric Prediction System. It assimilates SST from satellite infrared data and SSH from satellite altimeter (TOPEX/POSEIDON, ERS-2 and Geosat Follow-On) data. Velocity fields are updated using a geostrophic correction calculated from pressure changes, but not within 5° of the equator. Between 5–8°, the correction is gradually increased to full strength using a hyperbolic tangent function. The entire system has been described in detail by Smedstad *et al.* (2003). The output used here is not from the operational model itself, but from a simulation system nearly identical to it. A hindcast reanalysis experiment was performed over the period 1993–2000 making use of all available satellite altimeter data.

2.4 Joint Archive for Shipboard ADCP Data (JASADCP)

ADCP data were downloaded from the Joint Archive for Shipboard ADCP website (<http://ilikai.soest.hawaii.edu/sadcp>) and collated for use as validation against the NLOM output. Thirty-one cruises passed through the region of interest from 1985–2000; sixteen of these during the 8-year span of NLOM data (1993–2000). For each cruise, the currents recorded at the shallowest depth were extracted from the archive to be representative of the surface layer currents. These depths ranged from 20–50 m. Currents sampled from NLOM represent an upper layer average with a typical thickness of ~70 m in this region. They do not contain an Ekman component and thus should be comparable to the ADCP-derived currents. Datasets were averaged into one-half- or one-quarter-degree bins for presentation, depending on the data density.

3. Results

3.1 OSCAR

OSCAR surface current plots are compiled for the region of interest. Monthly means based on eleven years of data are shown in Fig. 2. The strong westward flow of the NEC north of 10°N is consistent with the generally

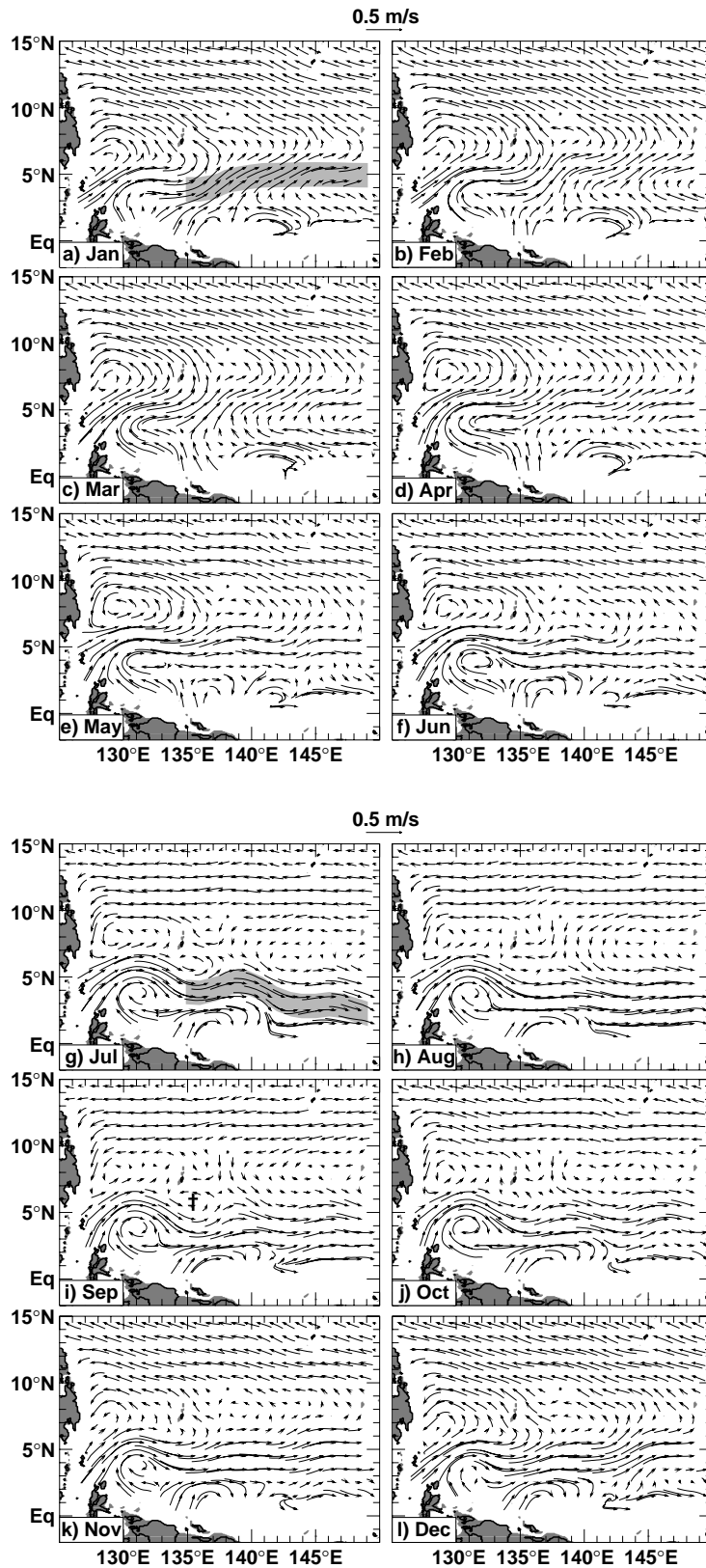


Fig. 2. Monthly mean surface currents from OSCAR plotted on the NLOM topography. Data are averaged over the period 1993–2003. (a) January, (b) February, etc. Approximate location of the MiE is identified in the September plot by the dagger (†) symbol.

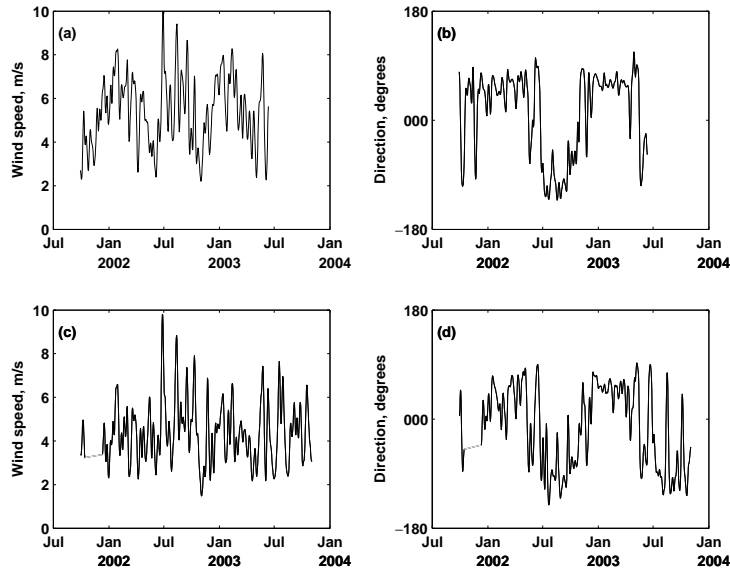


Fig. 3. TRITON buoy time series for locations: 137°E, 8°N—(a) wind speed and (b) direction. 137°E, 5°N—(c) wind speed and (d) direction.

accepted position (Gorshkov, 1976; Bramwell, 1977) with a maximum speed of 30–35 cm/s from November to March, declining to around 20–25 cm/s for July to October. During the boreal winter, there is a significant northward component to the surface current, up to 10–15 cm/s. This meridional component is reduced through spring and summer, turning southwards in late summer, and returning northwards and strengthening in winter. The timing of each of these variations is consistent with the descriptions by Yaremchuk and Qu (2004) and also that of the Asian monsoonal winds; strongest and from the northeast in winter (December–March), from the southeast during summer (June–September) (Tomczak and Godfrey, 2002).

The eastward flow of the NECC “Tail” (defined here as the section of the NECC east of 135°E) varies in position following the seasonal trend of the Asian Monsoon season (approximate positions for January and July are gray in Figs. 2(a) and (g)). From January–May, the NECC Tail is located around 5°N, consistent with literature descriptions (Tomczak and Godfrey, 2002), with maximum speeds of the order of 45 cm/s. The NECC Tail moves southward during the boreal summer to 2–5°N and is strongest (70 cm/s) during July–October when it is located at its southernmost latitudes, consistent with the findings of Toole *et al.* (1988).

During the period from December to February the cyclonic Mindanao Eddy may have developed near the Philippine coast; however, discussion of both the ME and the Mindanao Current is limited by the spatial scope of OSCAR data. From March–June the circulation of the ME

is clearly seen west of Palau. The center of the eddy moves northward from 7°N in December to 8°N in July and increases its zonal dimension during this time. The ME appears to weaken from July to November, as suggested from model data by Masumoto and Yamagata (1991); as a result the zonal extent is reduced.

The spatial scope of the OSCAR system does not cover the region south of 2°N and west of 134°E, i.e., in the vicinity of Halmahera Island, and so the discussion of the Halmahera Eddy presented here is incomplete. However, the seasonal variation of HE can be deduced from the available data. During the period March–May, the eddy appears to be weakly formed. As the NECC Tail moves southwards in June, the HE becomes more clearly defined and continues to strengthen as it moves northwards, through to October. From November–February, the HE weakens and returns southwards. This annual variation is phased with the seasonality of the NECC Tail and the ME, and with that of the Asian Monsoon. The correlation in the timing of these events supports the suggestion by Toole *et al.* (1988) that the major surface currents of the western equatorial Pacific are wind-dominated. No discussion of the New Guinea Coastal Current (NGCC) can be undertaken due to the limited spatial scope of the OSCAR data near the equator.

Of note is the trace of a cyclonic eddy centered to the southeast of Palau at 136°E, 6°N during the July–September period. This previously undescribed formation, here named the Micronesian Eddy (MiE), is bounded on the south by the NECC, and the approximate location is shown by the dagger symbol in Fig. 2(i).

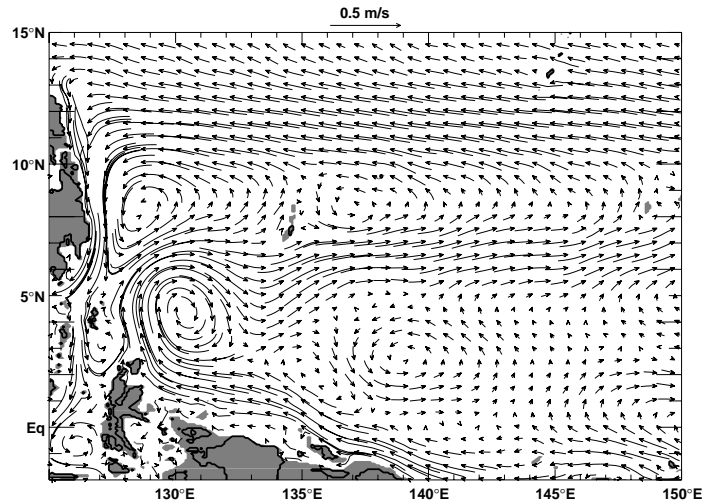


Fig. 4. NLOM annual upper layer currents averaged over the period 1993–2000. The ME is centred at 129°E, 8°N, the HE at 130°E, 4°N and the PE at 137°E, 9°N.

3.2 TRITON

Toole *et al.* (1988), Masumoto and Yamagata (1991) and Tomczak and Godfrey (2002) all assert that the major surface currents in the western equatorial Pacific are dominated by winds. Thus, wind data from the TRITON buoys are examined for periodic fluctuations to compare with the currents. Figure 3 shows wind speed and direction time-series from the buoys located at 8°N, 137°E and 5°N, 137°E. The wind direction data of the two buoys are synchronized in their seasonal variation, directed from the northeast from December to April, and from the southwest during July–October. This seasonal variation is consistent with that of the Asian monsoon (Tomczak and Godfrey, 2002). Between these dominant wind events (i.e., during May and June, and again in November), there are some short-term fluctuations in the wind direction. These times of variable wind direction generally coincide with low wind speeds. If the surface currents are wind-dominated then this observed seasonal cycle in the wind field should be reflected in the seasonality of ocean surface features.

While the OSCAR and TRITON data provide insight into the circulation in the western equatorial Pacific, more detailed information requires higher spatial (and temporal) resolutions. Numerical modelling of the ocean circulation provides a method that satisfies these requirements.

3.3 NLOM

The NLOM output is initially verified by observing the accepted western equatorial Pacific features; i.e., the NEC, ME, HE and NECC. These can be seen in the NLOM annual upper layer current climatology shown in Fig. 4. The westward-directed NEC is clearly seen north of 10°N

turning southward to form the Mindanao Current around 127°E (at the Philippine coast). Part of the MC turns eastward to become the NECC, which is located at approximately 6°N. The ME, bounded by these three currents, has its dome close to the Philippine coast and extends eastwards towards Palau. The NECC is also composed of NGCC water from the southeast that has rotated around the HE, centered near 130°E, 4°N. The locations and sizes of the ME and HE, and the meandering nature of the NECC compare well with observations during WEPOCS III by Lukas *et al.* (1991) and the OSCAR data.

Figure 5 illustrates the monthly climatology from NLOM and the seasonal variations in the circulation features are observed. The description of the NEC from NLOM is generally consistent with the description from OSCAR. The NEC is located generally north of 10°N with surface current maximum speed greatest in the boreal winter (43 cm/s) and least during summer and early autumn (28 cm/s). While the maximum speeds are slightly greater than suggested by OSCAR, due perhaps to the difference in resolution, the seasonal variation is aligned. The meridional component of the NEC is greatest and northward from December to March, and turns southward during July to September.

The NECC Tail (east of 135°E) also compares favorably with the descriptions from the OSCAR data, both in magnitude and path variation; the approximate positions of the NECC Tail for January and July are gray in Figs. 5(a) and (g). The maximum surface currents for the summer and winter periods and the annual variation in the flow-rate are generally consistent with those given by OSCAR. However, the northernmost variation of the NECC Tail reaches higher latitudes (6–7°N) than those

described by OSCAR during the late winter and spring, and slightly lower latitudes (1–2°N) during late-summer/autumn. In the October–November monthly climatologies, while it appears that the NECC bifurcates at 135°E, this is not the case. Examination of each year's current maps shows that the transition between summer and winter positions can occur during October or November: the apparent bifurcation is an artifact of averaging.

In January, the ME extends southwards towards Halmahera and circulates close to the Mindanao coast, consistent with a topographic survey presented in Lukas (1988). By April, the ME has strengthened and is located adjacent to Mindanao; the meridional extent has decreased while the eddy now extends zonally to Palau. The ME begins to weaken in June and is weakest during August–September, again consistent with the annual variation suggested by the OSCAR data.

The seasonal variations in the ME seen in both NLOM and OSCAR are in contrast to the description of Wyrski (1961), i.e., the ME is close to Mindanao in May and weakest and centered near Palau in January. This difference may be explained by the sparse data, both spatially and temporally, available to Wyrski (1961); however, it is also possible, though seemingly unlikely, that there has been a shift in the circulation regime. The consistency between OSCAR and NLOM descriptions provide confidence in the present study.

Associated with the ME, and due to the increased spatial coverage of the model at the Philippine coast, variability of the Mindanao Current can be examined. The MC is the south-directed current produced by the bifurcation of the NEC, near the Philippine coast at $14.3 \pm 0.7^\circ\text{N}$ (Yaremchuk and Qu, 2004). While the NEC bifurcation may be inferred from Fig. 5, the study region does not cover these coastal waters; as such, discussion of neither the bifurcation latitude nor the meridional variation of the MC is undertaken. The zonal position of the MC is observed to vary little through the year, remaining within approximately 1° of longitude from the Mindanao coast. The speed varies from a maximum value of 1.4 m/s during the winter to 1.2 m/s during the April to November period. The MC width and surface speed are consistent with those measured by Cannon (1970) as 70–80 km and 1.1–1.3 m/s, respectively. The relatively small variation in speed through the year is consistent with the findings of Lukas (1988) that the current anomaly was in the range ± 10 cm/s and with the annual variation in timing and magnitude of the MC transport described by Yaremchuk and Qu (2004). The consistency of the MC with previous studies lends further support to the reliability of the NLOM results.

The New Guinea Coastal Current between 130°E and 140°E is directed westwards for most of the annual cycle, gaining strength through May to July as a result of

the increase in the South Equatorial Current (SEC) (Tomczak and Godfrey, 2002). The NGCC reaches its maximum speed in the period August to October and then diminishes through November. During December and January the NGCC reverses its direction, following the seasonal cycle of the Asian monsoon.

The Halmahera Eddy is greatly influenced by the influx of the NGCC, intensifying and increasing in size as it moves northwards during the May to September period. The HE flow dominates the waters southwest of Palau during this period. The HE begins to diminish through October and November—the same period through which the ME begins to strengthen. The HE then weakens rapidly in December with the reversal of the NGCC. This development cycle of the HE is also linked with the zonal movement of the NECC Tail, described previously.

In addition to these well-documented features, the NLOM output suggests other circulation features that influence the waters of the western equatorial Pacific. A cyclonic eddy, named the Palauan Eddy (PE), develops in April to the northeast of Palau, near 137°E, 8°N (the approximate location is shown in Fig. 5(d) by the cross symbol). The PE is bounded to the north and south by the NEC and NECC, respectively. The PE appears to be strongly correlated with the position of the NECC Tail and the abatement of the ME. The PE is strengthened during May with the northernmost attitude of the NECC Tail, and then weakens through June and July with the NECC Tail's southward migration. There is evidence of a weak regeneration of the eddy, with the return to the NECC's northern meander, from October to December. However, the PE is not visible during the January to March quarter.

An anticyclonic eddy forms in April centered near 139°E, 5°N and is designated here the Caroline Eddy (CE). The approximate location of the CE is shown in Fig. 5(d) by the plus symbol. This eddy is bounded at the north by the NECC and moves west and south in May and June as the NECC Tail migrates southwards; the CE disappears by July. Examination of each year's plots for March–June showed this feature appearing every year and propagating westward. However, as the eddy exists south of the NECC, it has no direct influence on currents near Palau and was therefore not investigated further.

A third eddy forms weakly in August and September at a meander of the NECC Tail, near 140°E, 3°N. It may be synonymous with the Micronesian Eddy (MiE) described in the OSCAR data. This cyclonic eddy strengthens in October, maintaining its position through the migration of the NECC Tail, and is present until January. Examination of each year's output for August–January showed the appearance of this feature in most, but not all, years. When formed, the eddy characteristically propagated westward. It is also important to note that the eddy

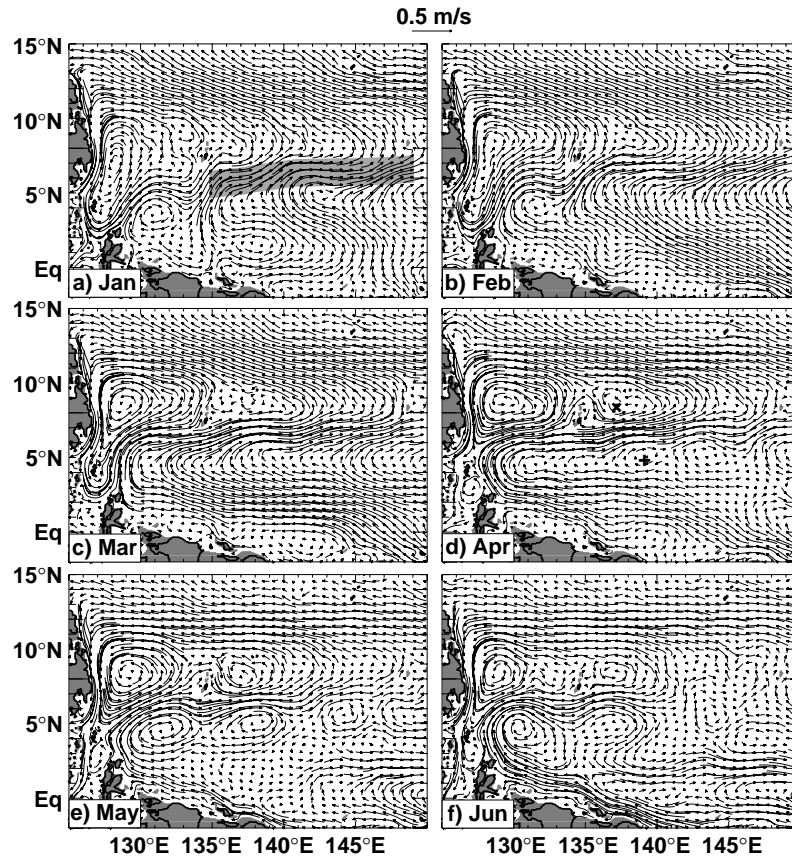


Fig. 5. Monthly mean upper layer currents from NLOM averaged over the period 1993–2000. (a) January, (b) February, etc. Approximate locations of the PE and CE are identified in the April plot by the cross (×) and plus (+) symbols, respectively.

described here may not be the same as the MiE identified in the OSCAR data. While it is located in a similar position, the spatial coverage and resolution of the OSCAR data do not permit a clear comparison. Additional studies are necessary to examine the nature and relationship of these features. As this feature is not in the vicinity of Palau, it was not investigated further.

A family of temporary eddies are also seen to form along the coast of New Guinea from July to November, between the NECC Tail and the NGCC. The formation of these eddies coincides with the greatest strength of HE, also bounded by the NECC and NGCC.

Each of the new eddies described here could be formed as a barotropic instability of the zonally-directed flows (NEC, NECC). Characteristically such instabilities propagate westwards (Rossby waves), as observed for the CE and MiE. The PE is topographically trapped by the Palau ridge (Fig. 1(b)), maintaining its position and increasing in extent and influence over the Palau waters.

While the NLOM model succeeds qualitatively in describing the surface circulation, comparison with ADCP data provides further verification.

3.4 JASADCP

Sixteen ADCP datasets with cruise tracks across the domain of interest were recorded during the 8-year span of NLOM output (1993–2000). Figure 6 shows the currents of all sixteen cruises averaged to a $0.5^\circ \times 0.5^\circ$ grid. The MC, ME, HE and NECC are identifiable in the sparse data and their locations compare well with the NLOM annual climatology (Fig. 4). Comparison of individual ADCP datasets with the NLOM output at the time of the cruise (i.e., not climatology) provides a more rigorous validation of the NLOM output in the western equatorial Pacific.

4. Discussion

The effects of the major currents and eddies, and their annual variations, on the circulation near Palau are summarized based on the information from OSCAR, TRITON, NLOM and the Joint Archive for Ship-based ADCP.

The OSCAR mean dynamic topography (MDT) was recently updated from a dataset that did not coincide with the 1993–2003 time period (derived from Levitus *et al.*, 1994; Levitus and Boyer, 1994) to a more rigorously de-

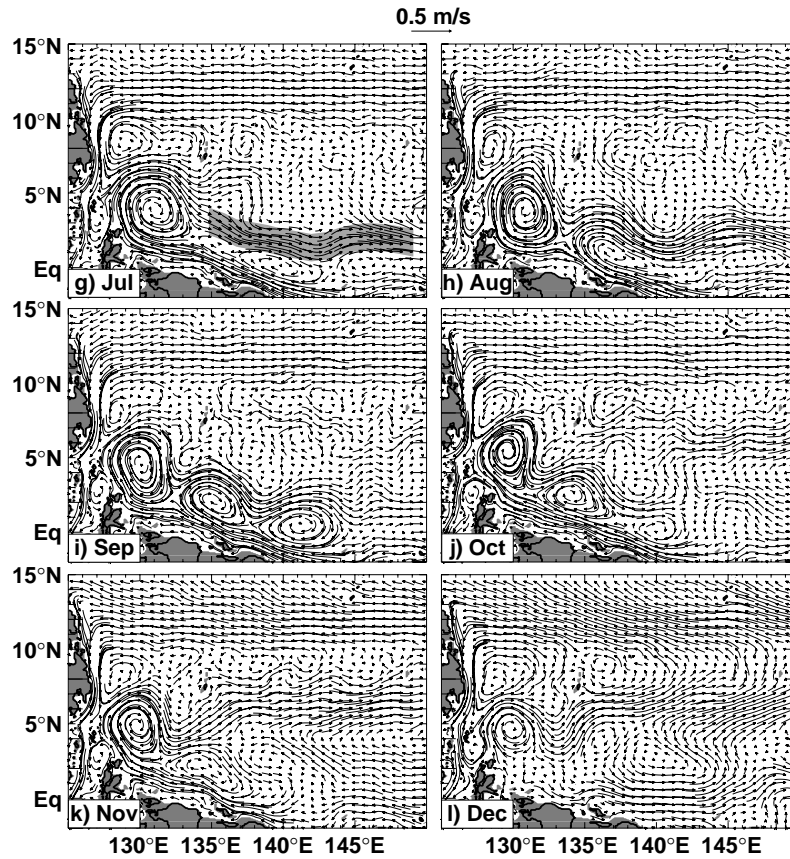


Fig. 5. (continued).

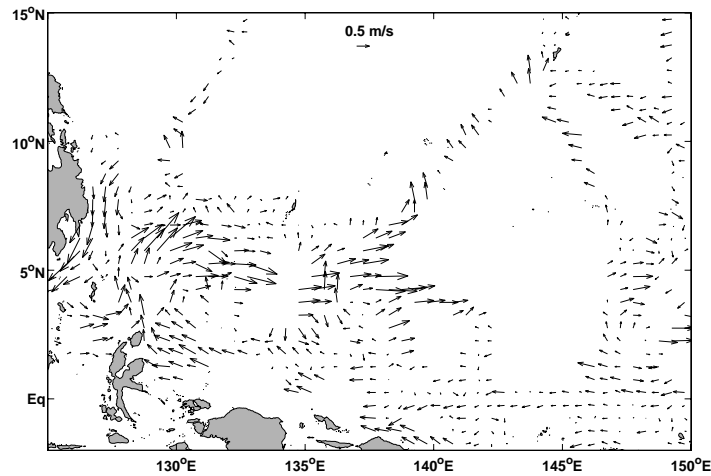


Fig. 6. Surface layer currents from ADCP measurements for the period 1993–2000. Data are averaged into $0.5^\circ \times 0.5^\circ$ bins.

finer MDT that was representative of the period of OSCAR data (F. Bonjean, 2004, personal communication). This change caused a significant alteration to the vector fields and consequently to the position and extent

of the major ocean features. Prior to the update, the OSCAR currents did not instill much confidence and the choice to favor the NLOM output was clear. The post-update OSCAR output showed significant visual improve-

Table 1. Vector correlation coefficients between NLOM monthly mean upper layer current climatologies and each of the pre- and post-update OSCAR monthly mean surface current climatologies.

	NLOM vs. pre-update OSCAR	NLOM vs. post-update OSCAR
Jan	0.67	0.66
Feb	0.71	0.68
Mar	0.69	0.68
Apr	0.67	0.65
May	0.63	0.58
Jun	0.62	0.57
Jul	0.62	0.63
Aug	0.62	0.65
Sep	0.52	0.53
Oct	0.48	0.43
Nov	0.55	0.52
Dec	0.62	0.64

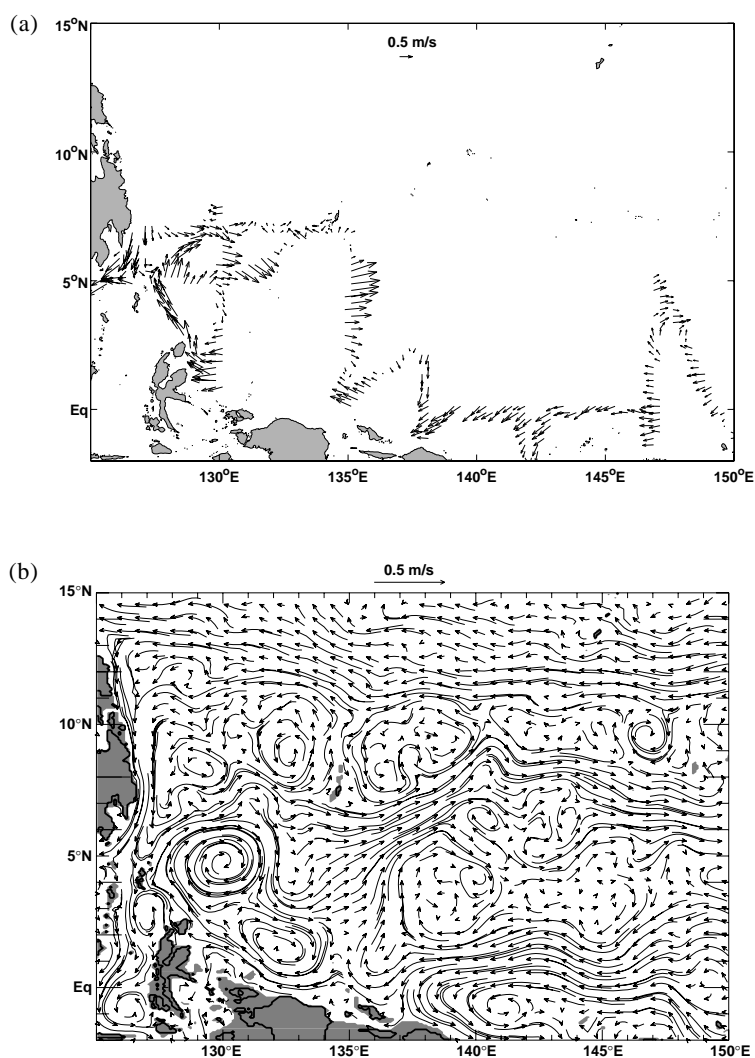


Fig. 7. (a) ADCP surface currents measured during cruise 517 (October–November 1999), averaged into $0.25^\circ \times 0.25^\circ$ bins. (b) NLOM mean upper layer currents corresponding to ADCP data for cruise 517 (October–November 1999).

Table 2. Vector correlation coefficients between ADCP data and NLOM output from the same time period.

Cruise identifier	Cruise dates	Correlation with NLOM output
86	24 Jan–22 Feb 1993	0.64
138	05 Oct–09 Nov 1993	0.59
36	11 Apr–11 May 1994	0.42
535	21 Dec 1994–11 Jan 1995	0.26
483	13 Jan–23 Jan 1995	0.56
509	01–14 Jul 1995	0.74
510	23 Jan–21 Feb 1996	0.43
464	17 Jun–02 Jul 1996	0.68
511	07 Jul–04 Aug 1996	0.30
512	26 Jan–27 Feb 1997	0.28
513	29 Jul–28 Aug 1997	0.55
514	03–29 Jan 1998	0.47
515	08 Aug–08 Sep 1998	0.26
516	26 Jan–28 Feb 1999	0.69
517	21 Oct–23 Nov 1999	0.71
518	31 Aug–30 Sep 2000	0.70

ment as compared with literature studies and is the dataset presented here. In comparing the two OSCAR datasets (pre- and post-update) with the NLOM output, the new dataset appears considerably closer to that of NLOM. However, vector correlation between NLOM monthly climatologies and that of each of the OSCAR datasets resulted in very similar results. Table 1 shows the correlation coefficients; the averages of the pre- and post-update correlation coefficients are nearly identical, as are the annual variations of each. While the statistics do not reflect an improvement, the visual correlation between the post-update OSCAR and NLOM lends confidence in the more recent dataset. While it is unlikely that either of the NLOM and (post-update) OSCAR datasets are completely correct, the convergence of the information suggests they are both approaching a true representation of the western equatorial Pacific flow and that the truth is likely to lie somewhere between them.

Figures 7(a) and (b) show the ADCP data (averaged into 0.25° bins) and NLOM output, respectively, for October–November 1999. A visual comparison suggests that the model successfully replicates the position and dimension of surface features inferred from the data. The daily NLOM output was interpolated to the locations of the ADCP data points and a vector correlation between these calculated to be 0.71. Vector correlations were performed for each of the sixteen ADCP datasets and are shown in Table 2. The correlation coefficients were within the range 0.26–0.74, with a mean of 0.52. Nine values were above the mean with a further three greater than one standard deviation below the mean. Figures 8(a) and (b) shows the comparison for January–February 1997, for which a correlation coefficient of 0.28 was calculated. The NECC

Tail at the longitude of Palau appears to be too far north in the NLOM output, as does the eastward flow of the NGCC. The data along the 138°E meridional transect in Fig. 8(a) may represent the eddy centered at 140°E , 2°N in the accompanying NLOM plot. For those NLOM output with poor correlations to the ADCP data, visual comparison suggests that the major features of the flow are present in the NLOM output but are displaced from the locations observed in the ADCP data. While the spatial shifting of such features is significant, the pattern of the flow given by NLOM is consistent with the ADCP data.

Of note in Fig. 8 are the strong east-directed currents at the equator. The monthly climatologies in Fig. 5 show that eastward, equatorial flow exists more weakly in the December–January climatologies and has ceased by February. While it can be postulated that this anomalous current may be related with onset of the 1997–98 ENSO event, it certainly illustrates the high variability in the western equatorial Pacific region.

While it can only be postulated that this anomalous current may be generated by west-directed winds, prior to or during the onset of the 1997–98 ENSO event, it certainly illustrates the high variability in the western equatorial Pacific region.

5. Conclusion

A seasonal variation of the currents in the waters surrounding the main islands of Palau is supported by both NLOM and OSCAR outputs. The seasonality in the TRITON wind data (i.e., December–April and July–October) is mirrored by the circulation around Palau.

During the period December to April, the currents at Palau are influenced by the NECC and the ME. The posi-

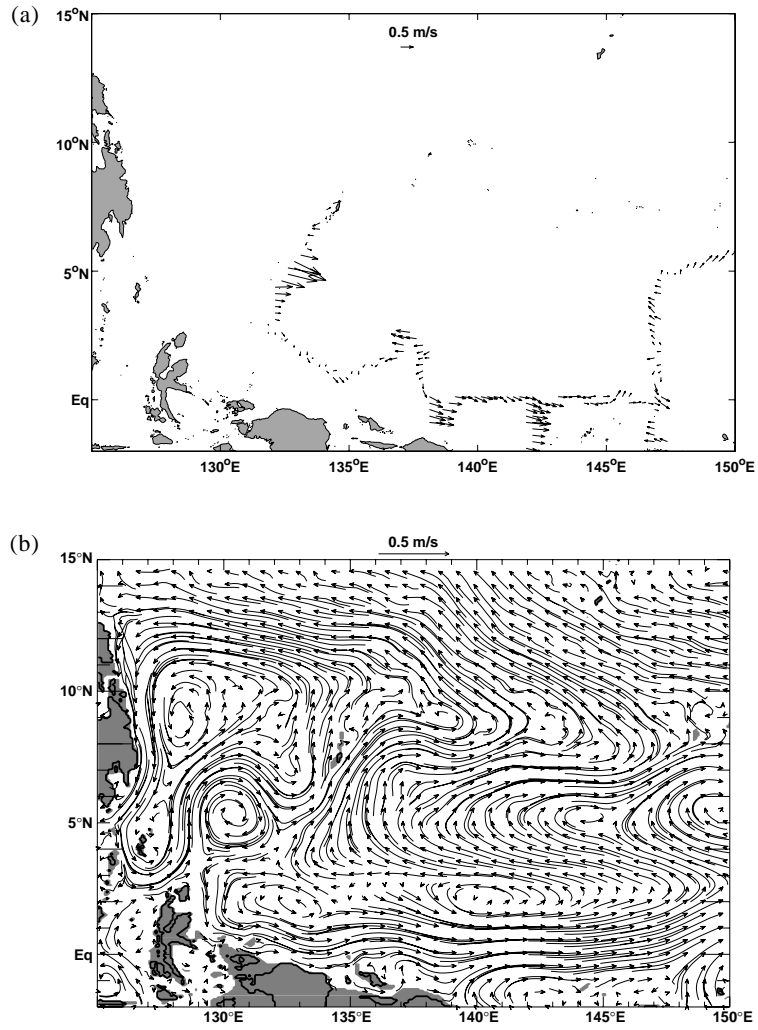


Fig. 8. As Fig. 7, except for cruise 512 (January–February 1997).

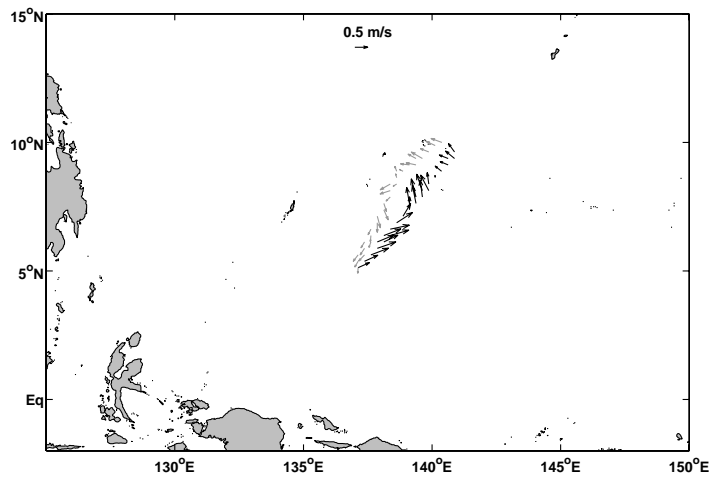


Fig. 9. ADCP surface currents measured during cruise 036 (April–May 1994, black) and cruise 037 (April–May 1992, gray) in the vicinity of the Palau Eddy (cf. Fig. 4). Data from each cruise is averaged into $0.25^\circ \times 0.25^\circ$ bins.

tions of the ME and NECC Tail are generally farther north in the NLOM output than that given by OSCAR. The Palauan currents described by NLOM are dominated by the NECC and are directed more towards the northeast; OSCAR currents are dominated by the ME and thus deflect more towards the northwest. The direction of the TRITON wind data for this period is from the northeast. Accounting for the Ekman-shift between wind and current directions, this suggests that the surface water transport will be directed towards the north and northwest. Combining these pieces of information suggests that the current is generally directed to the north in this period. The speed of the current for this period, according to both NLOM and OSCAR, is around 20 cm/s.

Both data sets indicate the effect of the ME upon the currents to the west of Palau through the December to April period. The currents curve with the shape of the ME, from northeast to northwest, with increasing latitude. As the ME migrates northwards through this period, the directions of the currents turn clockwise. As the ME decreases in its meridional extent (from April onwards), its effect on the Palauan currents is reduced.

The NLOM output suggests the formation of the PE in April; however, this eddy is not observed in the OSCAR output. This may be due to the lower spatial resolution of OSCAR. The existence of the PE would affect the currents along the east coast of Palau through significant portions of the year. ADCP data for April–May 1992 and April–May 1994, shown in Fig. 9, supports the existence of a cyclonic circulation (the PE) at a similar location as indicated by the NLOM climatology (Fig. 4).

During April and May, the PE directs currents along the east coast of Palau to the south with speeds up to 25 cm/s. With the southward migration of the NECC Tail in June, the currents east of Palau are less directionally defined and reduced in magnitude to less than 15 cm/s. West of Palau the ME continues to weaken, resulting in north-directed currents of approximately 10–15 cm/s.

During the period July to September, the major surface features do not affect the waters around Palau and the circulation becomes somewhat disordered. The flow shows a tendency to the north along the west coast and to the south along the east coast. The magnitude of the currents is around 5 cm/s. With the regeneration of the PE in October, the south-directed current along the east coast increases to 15 cm/s. In November the currents begin the transition to their north-directed winter pattern with the return of the NECC Tail to its northern path.

The seasonal variation of the surface circulation in the western equatorial Pacific is linked to the Asian monsoon cycle and is dependent upon the major surface features of the region. Observational data were used to validate numerical model output in the region and, together, these have confirmed the locations and annual

variations of the established surface features. Previously undescribed, transient eddies (named here the Palau Eddy, Caroline Eddy and Micronesian Eddy) have been identified and their seasonality discussed. The flow in the immediate vicinity of Palau is affected by many of these features.

This description of the currents is the first known study of the variability of circulation around Palau and thus forms a basis for oceanographic studies of Palauan waters. The currents described provide insight into studies of biological connectivity and may be applied as far-field boundary conditions for high resolution numerical models of Palau. The identification of transient eddies, in both location and seasonal duration, from the model output provides a sensible guide for future studies to obtain *in situ* data.

Acknowledgements

OSCAR data were provided by NOAA/NESDIS under the National Oceanographic Partnership Program. Thanks to the TRITON Project Office (Dr. Yoshifumi Kuroda, Director) for the buoy data and to the JASADCP for the ADCP data archive. This work was performed as part of the 6.1 Dynamics of Low Latitude Western Boundary Currents project under program element 601153N sponsored by the Office of Naval Research. The numerical simulation was performed using a grant of computer time from the Department of Defense High Performance Computing Modernization Office on the Cray T3E computer at the Naval Oceanographic Office, Stennis Space Center, Mississippi. Thanks to Tamara Townsend (NRL) who performed the NLOM simulation used here. This work was funded, in part, by The Nature Conservancy, including a contribution from the Michael and Andrea Banks Nature Fund. Thanks to Al Strong and Eric Bayler whose comments improved the manuscript.

References

- Arief, D. and S. P. Murray (1996): Low-frequency fluctuations in the Indonesian throughflow through Lombok Strait. *J. Geophys. Res.*, **101**, 12455–12464.
- Bonjean, F. and G. S. E. Lagerloef (2002): Diagnostic model and analysis of the surface currents in the tropical Pacific Ocean. *J. Phys. Oceanogr.*, **32**, 2938–2954.
- Bramwell, M. (ed.) (1977): *The Atlas of the Oceans*. Mitchell Beazley Publishers Ltd, London, p. 162–163.
- Cannon, G. A. (1970): Characteristics of waters east of Mindanao, Philippine Islands, August 1965. p. 205–211. In *The Kuroshio, A Symposium on the Japan Current*, ed. by J. C. Marr, East-West Center Press, Honolulu.
- Gorshkov, S. G. (ed.) (1976): *World Ocean Atlas, Volume 1—Pacific Ocean*. Pergamon Press, Oxford, p. 204–207.
- Kashino, Y., E. Firing, P. Hacker, A. Sulaiman and Lukiyanto (2001): Currents in the Celebes and Maluku Seas, February 1999. *Geophys. Res. Lett.*, **28**, 1263–1266.

- Levitus, S. and T. P. Boyer (1994): *World Ocean Atlas 1994. Vol. 4, Temperature*. NOAA Atlas NESDIS 4, NOAA, Washington, D.C., 117 pp.
- Levitus, S., R. Burgett and T. P. Boyer (1994): *World Ocean Atlas 1994. Vol. 3, Salinity*. NOAA Atlas NESDIS 3, NOAA, Washington, D.C., 99 pp.
- Lukas, R. (1988): Interannual fluctuations of the Mindanao Current inferred from sea level. *J. Geophys. Res.*, **93**, 6744–6748.
- Lukas, R., E. Firing, P. Hacker, P. L. Richardson, C. A. Collins, R. Fine and R. Gammon (1991): Observations of the Mindanao Current during the Western Equatorial Pacific Ocean Circulation Study. *J. Geophys. Res.*, **96**, 7089–7104.
- Masumoto, Y. and T. Yamagata (1991): Response of the Western Tropical Pacific to the Asia Winter Monsoon: The generation of the Mindanao Dome. *J. Phys. Oceanogr.*, **21**, 1386–1398.
- Metzger, E. J. (2003): Upper ocean sensitivity to wind forcing in the South China Sea. *J. Oceanogr.*, **59**, 783–798.
- Metzger, E. J., H. E. Hurlburt, J. C. Kindle, Z. Sirkes and J. M. Pringle (1992): Hindcasting of wind-driven anomalies using a reduced gravity global ocean model. *Mar. Technol. Soc. J.*, **26**(2), 23–32.
- Qiu, B. and R. Lukas (1996): Seasonal and interannual variability of the North Equatorial Current, the Mindanao Current, and the Kuroshio along the Pacific western boundary. *J. Geophys. Res.*, **101**, 12315–12330.
- Qu, T. and R. Lukas (2003): The bifurcation of the North Equatorial Current in the Pacific. *J. Phys. Oceanogr.*, **33**, 5–18.
- Qu, T., H. Mitsudera and T. Yamagata (1998): On the western boundary currents in the Philippines Sea. *J. Geophys. Res.*, **103**, 7537–7548.
- Smedstad, O. M., H. E. Hurlburt, E. J. Metzger, R. C. Rhodes, J. F. Shriver, A. J. Wallcraft and A. B. Kara (2003): An operational eddy resolving 1/16° global ocean nowcast/forecast system. *J. Mar. Sys.*, **40–41**, 341–361.
- Smith, W. H. F. and D. T. Sandwell (1997): Global sea floor topography from satellite altimetry and ship depth soundings. *Science*, **277**, 1956–1962.
- Tomczak, M. and J. S. Godfrey (2002): *Regional Oceanography: An Introduction*. Online publication (<http://www.es.flinders.edu.au/~mattom/regoc/pdfversion.html>).
- Toole, J. M., E. Zou and R. C. Millard (1988): On the circulation of the upper waters in the western equatorial Pacific Ocean. *Deep-Sea Res.*, **35**, 1451–1482.
- Wyrtki, K. (1961): *Naga Report, Volume 2—Physical Oceanography of the Southeast Asian Waters*. Scripps Institution of Oceanography, La Jolla, U.S.A., 195 pp.
- Yaremchuk, M. and T. Qu (2004): Seasonal variability of the large-scale currents near the coast of the Philippines. *J. Phys. Oceanogr.*, **34**, 844–855.

Appendix 3

Satellite Bathymetry Use in Numerical Models of Ocean Thermal Stress

Scott F. Heron and William J. Skirving

Abstract

Techniques for deriving estimated bathymetry from satellite data are well established; however, use of this product in complex terrains is limited. Accurate bathymetry is essential in the construction of hydrodynamic models and satellite derived bathymetry is a strong candidate for use in coastal and shallow waters. A case study of Palau is presented which uses satellite-derived bathymetry as input to a hydrodynamic model. Palau underwent widespread coral bleaching during 1998, thought to be due to thermal stress, and existing satellite products observed anomalous increases in temperature. The numerical model is used to evaluate sea surface temperature patterns during such a bleaching event. Comparisons between the model and thermal indicators derived from satellite data are made, and the results used to suggest improvements for satellite monitoring of thermal stress events.

Citation:

Heron, S.F. and W.J. Skirving. (2004) Satellite bathymetry use in numerical models of ocean thermal stress. *La Revista Gayana*, 68, (2) 284-288.

The text of this article is reprinted in this document with permission from *La Revista Gayana*, Universidad de Concepción, Casilla 160-C Correo 3. Concepción. Chile S.A. Please use the above citation for any information in this article.

SATELLITE BATHYMETRY USE IN NUMERICAL MODELS OF OCEAN THERMAL STRESS

S.F. Heron & W.J. Skirving

Coral Reef Watch
National Environmental Satellite Data Information Service
National Oceanographic and Atmospheric Administration
Scott.Heron@noaa.gov

ABSTRACT

Techniques for deriving estimated bathymetry from satellite data are well established; however, use of this product in complex terrains is limited. Accurate bathymetry is essential in the construction of hydrodynamic models and satellite-derived bathymetry is a strong candidate for use in coastal and shallow waters. A case study of Palau is presented which uses satellite-derived bathymetry as input to a hydrodynamic model. Palau underwent widespread coral bleaching during 1998, thought to be due to thermal stress, and existing satellite products observed anomalous increases in temperature. The numerical model is used to evaluate sea surface temperature patterns during such a bleaching event. Comparisons between the model and thermal indicators derived from satellite data are made, and the results used to suggest improvements for satellite monitoring of thermal stress events.

INTRODUCTION

Coral bleaching is the process by which a coral polyp, under environmental stress, expels its symbiotic zooxanthellae. The affected coral colony appears bleached. Severe bleaching can cause death of the coral colony. In September 1998, coral reefs across Palau were observed to be severely affected by bleaching (Wilkinson, 1998). A large proportion of the region (70-80%) underwent widespread bleaching and incurred high mortality rates; however, other regions appeared less affected.

One of the major environmental stresses that causes bleaching of corals is heightened water temperature (Berkelmans & Willis, 1999). Increased water temperatures, and hence bleaching events, are linked to weather events, which in turn may or may not be linked to climate events (e.g., El Niño). Mass bleaching occurs when there is an extended summer period of calm, sunny conditions that coincide with weak currents.

Over 98% of solar radiation energy is absorbed within the top 4 metres of the water column. This heat remains at the top of the water column unless there is a mechanism to mix it with the cooler water below. Vertical mixing occurs in regions of relatively strong horizontal currents, which can be associated with surface winds, large scale currents (e.g., North Equatorial Current) and tides. Therefore, extended periods of sustained cloudless summer days with low winds and low currents will likely induce bleaching events.

Hydrodynamic models can be used to describe oceanographic currents and from these predict SST patterns for future, severe, mass coral bleaching events. Hydrodynamic modelling can also assist in the investigation of other issues that relate to the coral reef ecosystem; connectivity with biological events (e.g., coral/fish spawning) and anthropogenic interactions (e.g., sewage outfall, pollution accidents) can be monitored and/or predicted.

One of the most important inputs to a high resolution hydrodynamic model is the bathymetry. The effect of incorrect bathymetry on computational fluid dynamic models can be significant and, as such, the accuracy of bathymetry can be crucial to the success of the numerical model (a detailed discussion is given in Gille *et al.*, 2004). For remote geographic locations, where in situ data are limited, remote sensing techniques can provide such bathymetry.

Lyzenga (1978) developed a theoretical basis for describing water depth by passive remote sensing upon which many others have expanded. Stumpf *et al.* (2003) applied this knowledge to investigate shallow regions with low bottom-albedo and variable bottom-types (e.g., sand, coral, algae, seagrass) using satellite data and developed a new algorithm for estimating water depths to 25 m and beyond.

In this work, satellite-derived bathymetry data are used as input for a numerical model to study the surface currents near Palau. From the model output, regions of vertical mixing are identified and the subsequent reduction in surface temperature for these waters is calculated. Patterns in the modelled temperature distribution are compared with satellite-derived Sea Surface Temperature (SST) data.

METHOD

Historical bathymetric data for Palau were measured primarily by Japanese ships prior to the Second World War; however, little in-situ data has been published since 1969. Newhall & Rohmann (2003) derived estimated-depths for the region surrounding Palau from LandSat imagery to use in classifying benthic habitat. The method used followed that described in Stumpf *et al.* (2003), an algorithm which is accurate to an approximate depth of 25 metres. The estimated-depth values were determined at the grid resolution of the LandSat image; i.e., 28.5 m. As the desired resolution for the numerical model was approximately 250 m, the estimated depth values were averaged across 99 points to produce a 256.5 m resolution data set. To describe the bathymetry beyond the depth-scope of the LandSat data (~20 m), the two-arc-minute-resolution data of Smith & Sandwell (1997) were interpolated to a 256.5 m grid aligned with the LandSat-derived data. Some smoothing was undertaken to combine the datasets. In addition, corrections were made to the data near to land, known coral reefs and in regions of obvious discrepancy, determined by comparison of the data with nautical charts and depth soundings (C. McLean, *unpublished data*). The corrections were incorporated by removing incorrect values, inserting replacement values where available and kriging the data to fill any remaining gridpoints. Initial output from the computational model gave further indications of short-comings in the bathymetry, deduced by the presence/absence of observed currents, and further corrections were made.

The numerical study was undertaken using the Princeton Ocean Model (POM) as described by Blumberg & Mellor (1987). POM is a terrain-following (s-coordinate) model that has been used in a variety of oceanic and coastal applications (e.g., Chang & Isobe, 2003). The surface currents around Palau were modelled on a two-dimensional rectangular grid of 764328 points at 256.5 m resolution. Model land was defined by a 2.5 m isobath. Surface current velocities were defined at the open boundaries according to Heron *et al.* (in prep.) for the December to March season. The sea-surface elevations at these boundaries were defined as a function of tide gauge data collected in the Palau lagoon (Malakal Harbour). The boundary conditions were defined so as to reproduce the recorded elevations at the nearest model grid-point as closely as possible. No wind stress was applied in the model, as per the conditions for mass coral

bleaching events. The model was ramped to the stated boundary conditions for 0.5 days and then run for 29.5 days. Model validation was performed using data collected during Aug 2002–Jan 2003, described in Steinberg *et al.* (in prep.).

The currents output from the computational model can be used to determine whether there is vertical mixing, due to bottom friction, throughout the water column. Simpson & Hunter (1974) examined the energy required for full vertical mixing and deduced a parameter to describe the position of fronts between mixed and stratified waters in the Irish Sea. This parameter (h/u^3 , where h is the water depth and u is the surface velocity) was determined at each model timestep across the numerical domain. The value suggested by Simpson *et al.* (1982) for complete vertical mixing was employed here; i.e.

$$\log_{10}[h/u^3] \leq 2.7$$

As mass bleaching events are related to temperature stress, an estimate of temperature variations, due to vertical mixing, was calculated. A vertical profile of the water temperature was determined by modelling the diurnal insolation of an initially uniform-temperature water column for a period of two weeks. The profile was then mixed from the surface to a specified depth to determine the reduction in temperature at the sea surface for a fully-mixed water column of that depth. This temperature-reduction was calculated for the range of water depths observed in the Palau lagoon, thus providing an indication of the temperature of the water column for any regions that are fully mixed. Advection of cooled waters is not presented here but will likely expand any areas cooled by the mixing mechanism. The temperature distribution across the Palau lagoon due to mixing was compared with satellite-derived Sea Surface Temperature (SST) data acquired during the widespread bleaching event in late 1998. SST values from the Pathfinder 4km SST database for the period 01 May 1998–28 Feb 1999 were examined to compare with the results from the model output. The daily data selected were for the night-time descending pass of the satellite so as to eliminate diurnal heating effects. For the region corresponding to the model domain, the quality tests imposed upon the 4km SST data discounted more than 80% of the values. The analysis of Kilpatrick *et al.* (2001) uses two tests to determine if an SST value is of sufficient quality. The first test compares the SST value with a value derived from the weekly SST data described by Reynolds & Smith (1994). Kilpatrick *et al.* (2001) indicate that this comparison may be biased in coastal zones and in regions with large SST gradients (spatial or temporal). The second discrimination identifies pixels contaminated with cloud. Failure to meet the conditions of either of these tests causes the data to be considered as poor quality. Due to the coastal location and variable-temperature nature of this study, the "poor-quality" pixel data were also considered.

RESULTS

Surface currents derived in the Palau model during the advent of the highest high-tide of the 30-day modelled period are shown in Figure 1. The surface currents in the lagoon exceeded 1.4 m/s during the spring tides. The surface currents in the Palau region are tidally-dominated (Heron *et al.*, in prep.). As such, the currents, and therefore the vertical mixing, are maximised during times of greatest tidal range. Figure 2 illustrates the minimum value of the Simpson-Hunter parameter across the domain, corresponding to the greatest mixing that occurs for each location. From this it can be seen that very few regions of the Palau lagoon undergo complete vertical mixing. The determined mixing-induced temperature variations are referenced to a maximum temperature of 32.6°C and the resultant temperature values are shown in Figure 3. The temperature range in Figure 3 was matched to the satellite observation, discussed below, for ease of comparison.

Imagery from the Pathfinder SST 4 km dataset were examined for comparison with the modelled temperature distribution. The daily image for which the highest SST was measured (32.6°C) was selected;

the data were collected on 09 Sep 1998. This was one of only four images from the study period for which greater than 70% of the pixels passed the quality tests. In the selected image, some pixels surrounding the largest island of Palau were flagged as poor data. Examination of the quality masks indicated that the data were flagged by the first quality test described above. As this test is known to be biased against coastal regions, the "poor quality" SST values were included. The SST image for this day is shown in Figure 4, overlaid with the model land for ease of comparison. White pixels indicate land and coloured pixels indicate the SST value in degrees Celsius. The pixels with grey hash-strokes are those flagged by the quality testing as poor data. The average measured SST value (high-quality only) across the illustrated domain was 31.6°C.

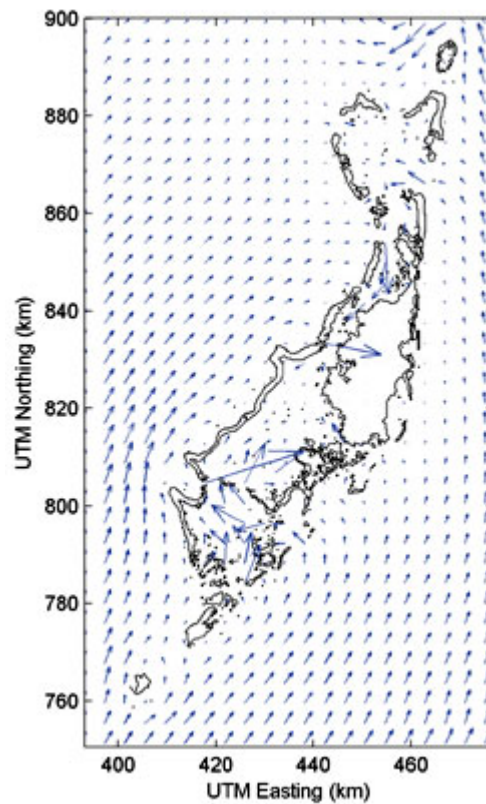


Figure 1. Currents around Palau output from numerical model. Horizontal resolution of vectors is approximately 4 km (16 gridpoints) for presentation purposes. Maximum current shown is 1.33 m/s. Axis scales in Universal Transverse Mercator (135 E) coordinates.

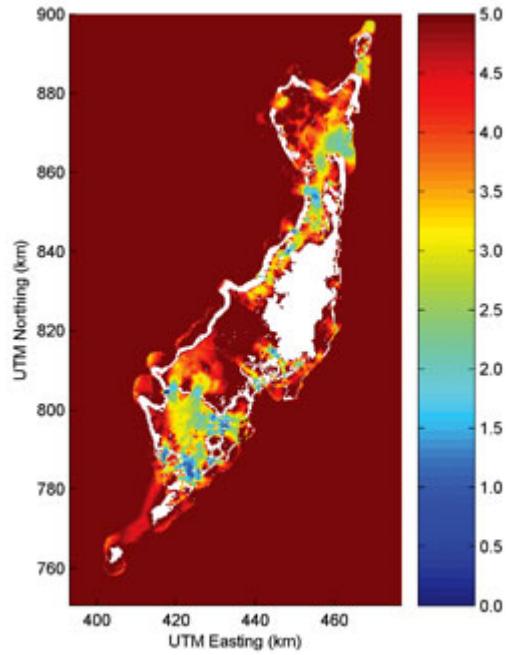


Figure 2. Minimum value of Simpson-Hunter parameter during 30 day model-run. The colour scale is in dimensionless units of $\log_{10}[h/u^3]$. A value below 2.7 indicates complete vertical mixing.

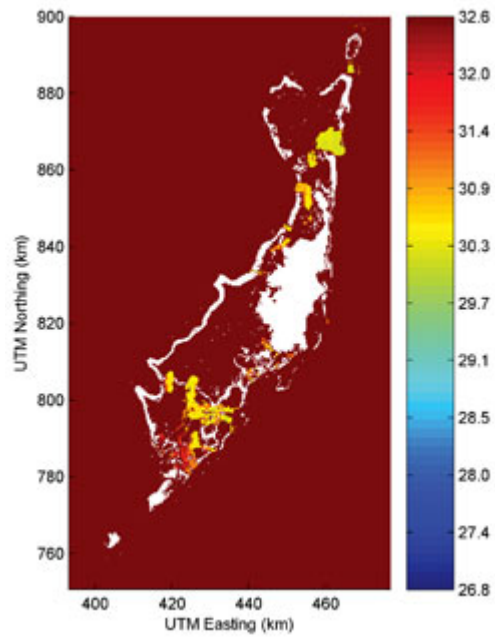


Figure 3. Modelled sea surface temperature due to vertical mixing. The values are reduced from a maximum value of 32.6°C.

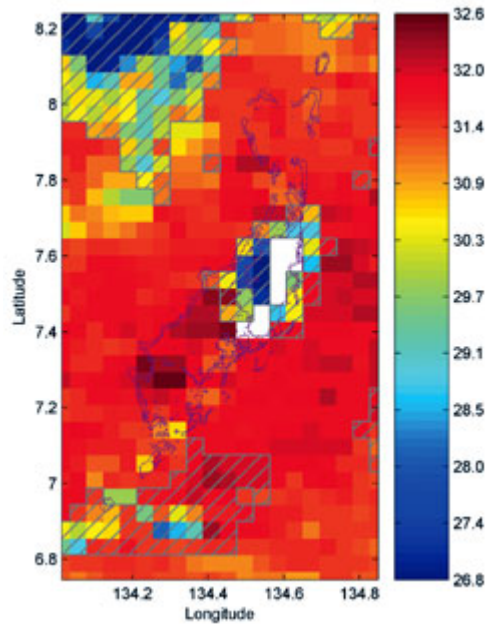


Figure 4. Pathfinder 4km SST values for the Palau region on 09 Sep 1998. White pixels represent land; coloured pixels represent SST in °C; grey hash-lines indicate data flagged as poor-quality. The model land is shown in purple for ease of comparison with previous figures.

DISCUSSION

Figure 3 shows two main areas of reduced temperature; the southern lagoon and a region in the north (near [445km E, 860 km N], known to be a grouper spawning zone (Johannes *et al.*, 1999). Comparison of the water temperatures across the lagoon is somewhat limited by the resolution of the satellite data; however, temperature patterns may be observed and discussed. The extreme low temperatures of some "poor-quality" pixels in the top-left and at the centre of Figure 4 appear to have been correctly flagged as poor; however, many of the pixels in the regions designated as poor appear to display credible temperatures.

At the locations of predicted vertical mixing (Fig. 2), slight reductions in the measured SST, compared with surrounding pixels, can be observed (Fig. 4). In the southern lagoon, two relatively-cooler pixels are observed near [134.30°E, 7.15°N] and a further two near [134.38°E, 7.23°N]. These pixels correspond with predicted locations of mixing-induced cooling. In the grouper spawning region in northern Palau, the model predicts regions of cooling. The SST data in this location are indeed cooler than those in the surrounding, non-mixed waters. However, near [134.32°E, 7.27°N], the hottest temperature pixel for the domain is located in a region for which significant mixing (and therefore cooling) was predicted.

The overall patterns in the datasets suggest that vertical mixing of water columns, and the subsequent decrease in SST, may be a significant mechanism for surface cooling in the Palauan lagoon. Further work on the model output is required to incorporate the effects of advection of cooled waters. As coral reefs are primarily located in shallow, coastal regions, improvements to the monitoring of thermal stress on corals using satellite platforms requires SST algorithms to perform with greater stability in coastal areas. Increased horizontal resolution is a first step for this; however, consistently producing data of sufficient

quality in these regions is a necessity. Derivation of at-depth temperatures from satellite data will aid in further understanding of thermal impacts on corals throughout the water column.

ACKNOWLEDGEMENTS

Craig Steinberg is thanked for his input to the development of the vertical mixing algorithm. The Pathfinder 4km SST data were obtained from the NOAA/NESDIS/NODC ftp site at:
<ftp://data.nodc.noaa.gov/pub/data.nodc/pathfinder/Version5.0/>.

REFERENCES

- Berkelmans, R. & B.L. Willis (1999) "Seasonal and local spatial patterns in the upper thermal limits of corals on the inshore Central Great Barrier Reef", *Coral Reefs*, vol.18, pp.219-228.
- Blumberg, A.F. & G.L. Mellor (1987) "A description of a three-dimensional coastal ocean circulation model" *Three-Dimensional Coastal Ocean Models*, Coastal and Estuarine Sciences, 4, N.S. Heaps, ed., American Geophysical Union, pp.1-16.
- Chang, P.-H. & A. Isobe (2003) "A numerical study on diluted water in the Yellow and East China Seas" *Journal of Geophysical Research. C. Oceans*, vol. 108.
- Gille, S.T., E.J. Metzger & R. Tokmakian (2004) "Seafloor Topography and Ocean Circulation", *Oceanography*, volume 17, no. 1, pp.47-54.
- Heron, S.F., E.J. Metzger & W.J. Skirving (in prep.) "Observations of the ocean surface circulation in the vicinity of Palau".
- Johannes, R.E., L. Squire, T. Granam, Y. Sadovy & H. Renguul (1999) Spawning aggregations of groupers (*Serranidae*) in Palau. Marine Conservation Research Series Publication #1, The Nature Conservancy. 144 pp.
- Lyzenga, D.R. (1978) "Passive remote sensing techniques for mapping water depth and bottom features" *Applied Optics*, vol.17, pp.379-383.
- Newhall, R. & S. Rohmann (2003) "Using Landsat and IKONOS Imagery to Create Habitat Classifications and Mosaic Maps of Pacific Freely Associated States" Proceedings for the 30th International Symposium on Remote Sensing of Environment . Honolulu, USA, 10-14 November 2003, CDROM.
- Reynolds, R.W., & T.M. Smith (1994) "Improved global sea surface temperature analyses using optimum interpolation" *Journal of Climate*, vol.7, pp929-948.
- Simpson, J.H. & J.R. Hunter (1974) "Fronts in the Irish Sea" *Nature*, vol.250, pp.404-406.
- Simpson, J.H., P.B. Tett, M.L. Argote-Espinoza, A. Edwards, K.J. Jones & G. Savidge (1982) "Mixing and phytoplankton growth around an island in a stratified sea" *Continental Shelf Research*, vol.1, pp.15-31.

Smith, W.H.F. & D.T.Sandwell (1997) "Global Sea Floor Topography from Satellite Altimetry and Ship Depth Soundings" *Science*, vol.277, pp. 1956-1962.

Steinberg, C., W. Skirving, C.McLean, S.Heron & S. Choukroun (in prep.) "Palau Oceanographic Array Data Report" Technical Report, Australian Institute of Marine Science and National Oceanic and Atmospheric Administration (USA).

Stumpf, R.P., K. Holderied & M. Sinclair (2003) "Determination of water depth with high-resolution satellite imagery over variable bottom types" *Limnology and Oceanography*, vol.48, pp.547-556.

Wilkinson, C. (1998) "The 1997-1998 mass bleaching event around the world" in *Status of Coral Reefs of the World:1998*, C. Wilkinson (ed.), Australian Institute of Marine Science. Retrieved from: <http://www.aims.gov.au/pages/research/coral-bleaching/scr1998/scr-00.html>

United States Department of Commerce
Gary Locke
Secretary

National Oceanic and Atmospheric Administration
Dr. Jane Lubchenco
Under Secretary of Commerce for Oceans and Atmospheres

National Ocean Service
David Kennedy
Acting Assistant Administrator for Ocean Service and Coastal Zone Management

